Laboratory Dissolution of Blast Hole Samples of Duluth Complex Rock from the South Kawishiwi Intrusion: Twenty-four year laboratory experiment

February 2014

Minnesota Department of Natural Resources
Division of Lands and Minerals
500 Lafayette Road, Box 45
Saint Paul, MN 55155-4045

Laboratory Dissolution of Blast Hole Samples of Duluth Complex Rock from the South Kawishiwi Intrusion: Twenty-four year laboratory experiment

February 2014

Chev Kellogg
Kim Lapakko
Michael Olson
Ethan Jenzen
David Antonson

Minnesota Department of Natural Resources
Division of Lands and Minerals
500 Lafayette Road, Box 45
St. Paul, MN 55155-4045

Table of Contents

List of Tables

List of Figures

List of Appendices

A1. Appendix 1—Solid Phase Characterization and Mineralogical Analyses
A2. Appendix 2—Laboratory Methods
A3. Appendix 3—Drainage Quality
A4. Appendix 4—Cumulative Mass Release
A5. Appendix 5—Weekly Release and Mineral Dissolution Rates
A6. Appendix 6—Quality Assurance
A7. Appendix 7—Additional Data Analysis

0. EXECUTIVE SUMMARY

The *research reported will be applied* in the environmental review and permitting of future nonferrous mines in Minnesota, particularly those in the Duluth Complex. These regulatory activities require prediction of solute release from waste rock during mine operation and in the decades and centuries following mine closure. As a foundation for such predictions, the reactions occurring in waste rock stockpiles and variables affecting these reactions must be understood. This knowledge and a description of the proposed method of waste rock disposal are necessary to 1) design appropriate tests for predicting the release of potential pollutants from waste rock, 2) extrapolate results of such tests to field conditions, and 3) if necessary, implement mitigation measures that will ensure that water resources are not adversely impacted. In the present project, laboratory studies were conducted to examine solute release and variables affecting this release from waste rock from the South Kawishiwi intrusion (SKI) of the Duluth Complex. This study provides scientific and technical information necessary to address questions inherent to environmental review and permitting of nonferrous metal mines. The project also provides empirical data describing up to 24 years of rock dissolution for comparison with and extrapolation of data submitted for environmental review and permitting by companies proposing mining in the Duluth Complex.

The *objectives* of the study were as follows.

1) Determine the variation of laboratory drainage pH with solid-phase sulfur content of Duluth Complex samples.
2) Based on the aforementioned relationship, categorize solids based on sulfur content and associated drainage pH.
3) Determine the variation of major ion release rates with solid-phase sulfur content and dissolution time.
4) Determine the empirical neutralization potentials of solids producing acidic drainage and compare these values to those determined by solid-phase analysis.
5) Determine rates of sulfide and silicate mineral dissolution as a function of dissolution time and drainage pH.

To *summarize the methods*, dissolution tests were conducted on fairly fine ($0.053 < d < 0.149$ mm; $0.18 \leq \%S \leq 1.71$) rock samples that were characterized with respect to chemical composition, mineral content, and mineral chemistry. Tests on ten SKI rock samples (and four Virginia formation samples) from Dunka Mine blast holes were initiated in February 1989 and on four more of these samples in September 1990. These samples were blasted 9 to 64 week prior to experimentation. Dissolution tests on six additional SKI rock samples that had been stored for at least 20 years were initiated subsequently. Some of the tests remain in progress and the following report presents data generated through week 1252. Leached rock samples from terminated tests were examined for dissolution features. This report summarizes drainage quality results, categorizes samples based on sulfur content and minimum drainage pH, and estimates dissolution rates for pyrrhotite, plagioclase, augite, olivine, hypersthene, and biotite.

Dependence of drainage quality on sulfur content of the rock and time was assessed based on dissolution test results. These results indicated that, in general, drainage pH tended to decrease and release rates of heavy metals (copper, nickel, cobalt, zinc) and major cations (calcium, magnesium, sodium, potassium) tended to increase with increasing sulfur content. Based on this observation, samples were divided into three groups based on sulfur content and corresponding drainage quality: Group I, 0.18, 0.22 %S; Group II, $0.40 \leq \%S \leq 0.70$; and Group III, $0.70 < \%S \leq 1.64$. Drainage pH for the Group I samples was generally above 6.0. The minimum drainage pH values for Groups II and III were 3.8 and 3.0, respectively. Minimum pH values and corresponding maximum sulfate release values were typically attained after 300 to 400 weeks (6 to 8 years) of dissolution. The maximum time to minimum pH was roughly 800 weeks, emphasizing the fact that short term drainage quality results do not necessarily reflect long-term trends. The decreasing sulfate release following attainment of maximum values was attributed to development of coatings on the sulfide mineral surface, and this was supported by photographs of leached sulfide grains. Diminishing sulfide mineral content over time contributed, to a lesser extent, to the decrease in sulfate release.

Neutralization potentials (NP) are a measure of the capacity of a sample to neutralize acid, and this capacity was determined empirically based on the drainage quality observed in dissolution tests. The empirical neutralization potential (ENP) was used for comparison with results from three methods used to determine NP based on solid-phase analysis. ENP values typically fell between 0.5 and 2 kg $CaCO_3$/t rock. NP calculated using carbon dioxide analysis to estimate total calcium plus magnesium carbonate content were closest to the ENP values (<0.7 to 2.5 kg $CaCO_3$/t rock), therefore the best estimate of the capacity of these samples to neutralize acid. Values determined on a subset of samples by a direct titration technique (Lapakko 1994a) yielded values roughly 1 to 3 kg $CaCO_3$/t rock higher than the observed values. Values determined by one common method (Sobek et al. 1978) almost always fell between 12 and 21 kg $CaCO_3$/t rock, substantially higher than the observed values. These results indicate that caution must be exercised when selecting solid-phase methods for determining NP and interpreting the results generated.

Mineral dissolution rates were calculated for an iron sulfide mineral and five silicate minerals. The iron sulfide (pyrrhotite) oxidation rates were based on sulfate release and, at circumneutral pH, were in reasonable agreement with rates reported for laboratory tests on pyrrhotite alone (i.e. in the absence of other minerals). These rates were higher under conditions of low pH and tended to increase after 300 to 400 weeks of dissolution, following a period of low pH and high sulfate release. Silicate dissolution rates calculated using four different models were generally in fair agreement. There did not appear to be strong dependence of rates on pH, with the exception of augite dissolution rates, and generally little dependence on time of dissolution. These estimates are intended to facilitate extrapolation of results from the rock samples examined to rock of varying mineral content within the Duluth Complex.

In summary these results demonstrate the 1) dependence of sulfide mineral oxidation (as reflected by sulfate release) and the attendant acid production on the amount of sulfide minerals present; 2) importance of sulfide mineral oxidation as a driving force for release of sulfate, acid, heavy metals and major cations; 3) importance of long-term dissolution tests in obtaining a technically defensible empirical foundation for mine waste drainage quality prediction; 4) caution that must be exercised when assessing the capacity of rock to neutralize acid based on solid-phase analyses; and 5) potential for determining mineral dissolution rates from laboratory test results and thereby extrapolating results to variable compositions of Duluth Complex rock.

Practical implications of these results for environmentally sound management of waste rock generated by mining in Minnesota include the potential for managing waste rock based on sulfur content, a relatively simple analytical assessment. Based on drainage pH alone, disposal of waste rock in Group I ($\%S \leq 0.22$ %) would probably require no rigorous reclamation. Potential impacts of sulfate, copper, nickel, cobalt, and zinc release from rock in this range of sulfur content would require consideration. In order to meet water quality standards, waste rock producing drainage pH values similar to Group III samples ($0.70 < \%S \leq 1.64$) would require the most rigorous control measures of the samples tested. Elevated release of sulfate and heavy metals from these groups would likely require mitigation as well. The results have implications of substance to mine waste drainage quality prediction. First, caution that must be exercised when assessing the capacity of rock to neutralize acid based on solid-phase analyses designed to quantify NP. Second, results generated from short-term dissolution tests do not necessarily simulate long-term drainage quality. Emphasizing this point, drainage pH from one sample was circumneutral for 800 weeks and then acidified, reaching a minimum pH of 3.8. Third, tests conducted on samples that had been stored for 8 to 20 years yielded lower rates of sulfate release and higher drainage than samples within about one year of excavation. Therefore, samples used for mine waste drainage quality prediction should be tested as close to the time of their excavation as possible.

Additional work should be conducted to further the benefits generated to date. This includes continued dissolution testing to confidently define long-term trends, analysis of leached solids to increase understanding of chemical reactions controlling solute release (e.g. chemical precipitation and adsorption), and more detailed analysis of the present data, including calculation of mineral dissolution rates. Furthermore, the methods for calculating mineral dissolution rates and approaches for other aspects of data analysis developed for this project should be applied to experiments examining dissolution of Partridge River Intrusion rocks.

1. INTRODUCTION

Tailings and waste rock, as well as the mine itself, are components of metal mining operations that remain long after ore removal has ceased. These mine wastes can be contacted by precipitation, ground water, or surface water. The quality of water exiting mine wastes spans a wide range, with some drainage producing little adverse impact on natural waters. In contrast, some drainage can adversely affect water quality long after mining operations have ceased. Acidic drainage, for example, was observed in 1977 at a Norwegian mine abandoned in 1833, nearly 150 years after termination of mining activities (Iversen and Johannessen, 1987). Dependent upon size and severity of the problem, remediation of mining impacts can cost hundreds of millions of dollars (Biggs, 1989). This potential for long-term impacts has led to regulations requiring post-closure care of mine wastes (Ciccarelli et al., 2009; Jerz and Rimstidt, 2000; Lapakko, 1990).

Regulations governing the mitigation of potentially problematic mine waste drainage and any associated financial liability have been developed. Plans and costs for closure and post-closure care of mine wastes are an important part of these policies and must be submitted prior to mine development (e.g. Lapakko, 1990). Any mine waste reclamation costs can then be associated with other mining expenses during assessment of mineral recovery costs.

Prediction of the quality and quantity of drainage generated by flow through waste rock lithologies excavated to access ore is integral to developing effective and economically efficient waste rock management plans. Based on these predictions and their associated impacts, mitigation techniques for individual mine waste units can be tailored to the potential for adverse impact. The best indicators of drainage quality for specific waste lithologies are existing data from similar geologic units, subjected to similar mining and mineral processing methods, and exposed to similar environmental conditions. Because data of this nature are rarely available, it is often necessary to use other means to predict the quality of drainage data, such as compositional characterization and dissolution testing.

Minnesota's Precambrian rocks, specifically the Duluth Complex and Archean metavolcanics and metasedimentary formations, have potential for base and precious metal development. The Duluth Complex is a composite series of massive gabbroic intrusions in northeastern Minnesota, some of which contain low-grade copper and nickel sulfides, titanium oxides, and platinum group elements (PGE's). In the present study 25 rock samples from the Duluth Complex and underlying Virginia Formation were characterized (physical, chemical, mineralogical) and subjected to laboratory dissolution testing. The intent of this testing was to generate data that would assist in the environmentally sound management of Duluth Complex waste rock generated during mining. The general approach was to determine the dependence of drainage quality on solid-phase composition of troctolitic/gabbroic Duluth Complex rocks and dissolution time. By establishing such a relationship, solid-phase composition of these rocks would provide beneficial insight on their dissolution behavior in the field. Dissolution rates of major minerals present were also calculated to aid in extrapolation of results on the solids examined to rocks with different amounts of the major minerals. Mineral dissolution rates might also be helpful in extrapolation of laboratory rates to field settings.

2. OBJECTIVES

The general objective of this study is to correlate drainage quality with rock composition. More specifically, the following objectives are addressed in the present report.

1) Determine the variation of laboratory drainage pH with solid-phase sulfur content of Duluth Complex samples.
2) Based on the aforementioned relationship, categorize solids based on sulfur content and associated drainage pH.
3) Determine the variation of major ion release rates with solid-phase sulfur content and dissolution time.
4) Determine the empirical neutralization potentials of solids producing acidic drainage and compare these values to those determined by solid-phase analysis.
5) Determine rates of sulfide and silicate mineral dissolution as a function of dissolution time and drainage pH.

The data generated by the study will be used to assist in environmentally sound management of Duluth Complex waste rock. The present report describes the laboratory dissolution of 25 rock samples, 21 Duluth Complex and 4 with a large Virginia Formation component, containing 0.18% to 5.44% sulfur for periods varying from 78 to 1252 weeks

3. BACKGROUND

3.1. Mine Waste Dissolution

The following discussion focuses on mineral dissolution reactions that influence mine waste drainage quality. The reactions presented result in acid production, acid neutralization, and trace metal release. Within the discussion, several solid phases of interest in mine waste characterization are identified. Detailed discussion of aqueous geochemistry fundamentals and geochemistry of acid mine drainage is presented by Nordstrom (1999), Nordstrom and Alpers (1999), Smith (1999) and Smith and Huyck (1999).

3.1.1. Acid Production

There are three general types of acid generation from mine wastes: iron sulfide oxidation, dissolution of soluble iron sulfate minerals, and dissolution of less soluble sulfate minerals of the alunite/jarosite series. Oxidation of iron sulfide minerals common in intrusive mafic complexes (e.g., Duluth Complex), such as pyrite (FeS_2, reaction 1) and pyrrhotite ($Fe_{1-x}S$, $0 \leq x \leq 0.2$, reaction 2), are responsible for most acid production by mine wastes (Stumm and Morgan 1981).

$$FeS_2(s) + (15/4)O_2(aq) + (7/2)H_2O = Fe(OH)_3(s) + 2SO_4^{2-}(aq) + 4H^+(aq) \qquad \mathbf{(1)}$$

$$Fe_{1-x}S(s) + [(9-3x)/4]O_2(aq) + [(5-3x)/2]H_2O =$$

$$(1-x)Fe(OH)_3(s) + SO_4^{2-}(aq) + 2H^+(aq) \qquad \mathbf{(2)}$$

In addition to acid production, sulfate is also released to solution, and its presence in mine waste drainage is typically the first indicator of sulfide mineral oxidation. The iron product presented is ferric hydroxide ($Fe^{3+}(OH^-)_3$, although formation of intermediate aqueous ferric hydroxyl species (e.g. $Fe(OH)_2^+(aq)$, $Fe(OH)_3(aq)$) will also result in acid production.

Ferric iron can also oxidize sulfide minerals (reactions 3, 4). The amount of acid generated as a result of iron sulfide oxidation is the same as that for oxidation by oxygen. The additional acid generated is due to precipitation of the aqueous ferric iron (left side of equation) as ferric hydroxide (equation 5).

$$FeS_2(s) + 14Fe^{3+}(aq) + (19/2)H_2O + 15/4O_2(aq) =$$

$$15Fe(OH)_3(s) + 2SO_4^{2-}(aq) + 46H^+(aq) \qquad \mathbf{(3)}$$

$$Fe_{1-x}S(s) + (8-2x)Fe^{3+}(aq) + [(9-3x)/4]O_2(aq) + [(53-15x)/2]H_2O =$$

$$(9-3x)Fe(OH)_3(s) + SO_4^{2-}(aq) + (26-6x)H^+(aq) \qquad \mathbf{(4)}$$

$$Fe^{3+}(aq) + 3H_2O = Fe(OH)_3(s) + 3H^+(aq) \qquad \mathbf{(5)}$$

The rate of iron sulfide oxidation and attendant acid production is dependent on solid-phase composition and microbial activity, as well as the availability of oxygen and water. Oxidation rates vary among sulfide minerals, with reactivity decreasing as follows: marcasite > pyrrhotite > pyrite (e.g. Kwong and Ferguson 1990). However, variations in the reactivity of iron sulfide minerals have been reported. Reactivity may be a function of reaction conditions, trace element concentrations, and crystal-morphology characteristics, among other factors (Jambor 1994; Plumlee 1999).

Mineral surface area also plays a role in rates of acid production. For any sulfide mineral, oxidation rates increase with available surface area. Consequently, acid production by a given mass of framboidal pyrite (high associated surface area) is much more than that resulting from oxidation of a comparable mass of euhedral pyrite (low associated surface area) (Pugh et al. 1984; White and Jeffers 1994). Mineral grain coatings (Janzen et al. 2000) and sulfur-depleted outer grain layers can also reduce oxidation rates (Belzile et al. 2004).

Abiotic oxidation rate is also pH dependant. Whereas the abiotic rate of pyrite oxidation by oxygen declines slightly as pH decreases, the overall abiotic rate increases as pH declines below about 4.5. This occurs due to ferric iron becoming the dominant oxidant (Williamson and Rimstidt 1994). Nordstrom (1982) reported, "as pH decreases to 4.5, ferric iron becomes more soluble and begins to act as an oxidizing agent." As pH further decreases, bacterial oxidation of ferrous iron becomes the rate limiting step in the oxidation of pyrite by ferric iron (Singer and Stumm 1970), which is the only significant oxidizing agent in this pH range (Nordstrom 1982; Singer and Stumm 1970; Kleinmann et al. 1981). In laboratory tests, pyrrhotite oxidation at pH 3.5 - 4.05 was roughly six to seven times that at pH 5.35 - 6.1. Rate increases were attributed to bacterially mediated oxidation (Lapakko and Antonson, 1994). It has also been indicated that bacterially mediated pyrite oxidation by ferric iron at pH 2 is roughly two to three orders of magnitude faster than abiotic oxidation (Nordstrom and Alpers 1999).

The combination of sulfide mineral characteristics and weathering reactions produce acidic, iron- and sulfate-rich waters which can 1) further react with sulfide minerals to accelerate oxidation, 2) evaporate partially or totally to precipitate hydrated iron-sulfates and other minerals, and/or 3) contact host rock minerals, which react to neutralize some or all of the acid. Acidic flow that is not neutralized within the mine waste will exit as acid rock drainage (ARD).

In some cases, flow events (rain or snow-melt) can result in ARD. Hydrated iron-sulfate and trace-metal sulfate minerals will precipitate out during the evaporation of acidic, metal- and sulfate-rich water within mine-waste materials, as will any heavy metals released during sulfide mineral oxidation. The precipitated materials can be reoxidized by additional flow through the precipitated waste (e.g. rain events, snow melt). The more common hydrated iron-sulfate minerals that occur as efflorescent salts on the surfaces of weathering pyrite include melanterite, rozenite, szomolnokite, romerite and copiapite ($FeSO_4 \bullet 7H_2O$, $FeSO_4 \bullet 4H_2O$, $FeSO_4 \bullet H_2O$, $[Fe^{2+}(Fe^{3+})_2(SO_4)_4 \bullet 14H_2O]$, and $[Fe^{2+}(Fe^{3+})_4(SO_4)_6(OH)_2 \bullet 20H_2O]$, respectively; Alpers et al., 1994). These efflorescent salts are highly soluble and provide an instantaneous source of acidic water upon dissolution and hydrolysis (Nordstrom, 1982; Cravotta, 1994). They may be partially responsible for increased acidity and metals loadings in the receiving environment during rain events. The storage and incremental release of these salts may help explain lag from mine-waste placement to AMD-formation, particularly in arid climates.

As an example, reactions 6, 7 and 8 summarize the step-wise dissolution of melanterite, a hydrated iron-sulfide mineral that can be deposited through evaporation and precipitation. The net result of equations 6 – 8 is summarized in equation 9, which shows net production of two moles of acid for each mole of melanterite dissolved. (Cravotta 1994) showed that a similar aqueous dissolution of romerite produced six moles of acid for each mole of romerite dissolved.

$$FeSO_4 \bullet 7H_2O\mathit{(s)} = Fe^{2+}\mathit{(aq)} + SO_4^{2-}\mathit{(aq)} + 7H_2O\mathit{(aq)} \qquad \textbf{(6)}$$

$$Fe^{2+}\mathit{(aq)} + (1/4)O_2\mathit{(g)} + H^{+}\mathit{(aq)} = Fe^{3+}\mathit{(aq)} + (\tfrac{1}{2})H_2O\mathit{(aq)} \qquad \textbf{(7)}$$

$$Fe^{3+}(aq) + 3H_2O(aq) = Fe(OH)_3(s) + 3H^+(aq) \qquad \textbf{(8)}$$

$$FeSO_4{\bullet}7H_2O(s) + (1/4)O_2(g) = Fe(OH)_3(s) + SO_4^{2-}(aq) + (9/2)H_2O + 2H^+(aq) \qquad \textbf{(9)}$$

The alunite-jarosite mineral group consists of sulfate minerals that are less soluble than the efflorescent sulfate salts. The evaporative concentration of efflorescent iron sulfates leads to the precipitation of the more common iron minerals such as goethite and jarosite (Nordstrom 1982). Similar reaction of efflorescent aluminum sulfates will produce alunite. Alpers et al. (1994) reported that jarosite is slightly soluble and can, therefore, contribute acid according to equation 10. Lapakko and Berndt (2003) demonstrated that the rate of acid production from potassium jarosite is markedly slower than that from samples of similar sulfur content in which the sulfur occurs as pyrite. Consistent with data presented in the aforementioned paper, preliminary leach studies on natural and synthetic jarosites conducted by the U.S. Bureau of Mines showed a drop in pH from 6 to the range of 3 to 4 after contact with the jarosites (White 2000). It should be noted, however, that there are a wide variety of alunite and jarosite minerals, as well as mineral properties, and consequently, reactivities can also vary. For example, Alpers (2000) speculated that a pure jarosite or hydronium jarosite might buffer pH in the range of 1.5-3, and this is supported by data presented by Lapakko and Berndt (2003).

$$KFe_3(SO_4)_2(OH)_6(s) = K^+ + 3FeOOH(s) + 2SO_4^{2-}(aq) + 3H^+(aq) \qquad \textbf{(10)}$$

3.1.2. Acid Neutralization

The balance between the rates of acid production by iron-sulfide mineral oxidation and host-rock mineral neutralization will determine the acidity of mine-waste drainage. The most effective minerals for neutralizing acid are those containing calcium carbonate and magnesium carbonate, including calcite ($CaCO_3$), magnesite ($MgCO_3$), dolomite ($CaMg(CO_3)_2$), and ankerite ($Ca\ (Fe, Mg, Mn)(CO_3)_2$). Reaction 11 represents the dominant acid-neutralizing reaction of calcite ($CaCO_3$) above pH 6.4, whereas reaction 12 is the dominant reaction below pH 6.4 (Drever, 1988):

$$CaCO_3(s) + H^+(aq) = HCO_3^-(aq) + Ca^{2+}(aq) \qquad \textbf{(11)}$$

$$CaCO_3(s) + 2H^+(aq) = H_2CO_3(aq) + Ca^{2+}(aq) \qquad \textbf{(12)}$$

Of the carbonate minerals, calcite ($CaCO_3$) dissolves most rapidly (Busenberg and Plummer 1986). Relative to calcite, the rate of dolomite [$(Ca,Mg)CO_3$] dissolution is about an order of magnitude slower (Busenberg and Plummer 1982) and the rate of magnesite ($MgCO_3$) dissolution is about four orders of magnitude slower (Chou et al. 1989). The rate of siderite ($FeCO_3$) dissolution under anoxic conditions is reported to be three orders of magnitude slower than that of calcite (Greenberg and Tomson 1992). Iron and manganese carbonates do not provide net acid neutralization under oxidizing conditions, due to acid production from hydrolysis and precipitation of oxidized iron or manganese (e.g. reactions 7, 8).

Dissolution of silicates such as plagioclase-feldspars (e.g. anorthite in equation 13, from Busenberg and Clemency 1976) and olivine (e.g. forsterite in equation 14, from Hem 1970) can also neutralize acid. However, their rates of dissolution and consequent acid neutralization are slow relative to the carbonate minerals (Nesbitt and Jambor 1998). For example, at near neutral pH, the dissolution rate of calcite is approximately 7 orders of magnitude faster than the dissolution of plagioclase feldspar (White et al., 1999). Nonetheless, silicate mineral dissolution can maintain neutral conditions if the rate of acid production is quite slow (Lapakko and Antonson 1993; Lapakko et al. 1997; Lapakko and Antonson 2002). The effectiveness of silicate minerals in neutralizing acid rises with increasing mineral surface area, which increases with elevated mineral cation content and decreasing grain size.

$$CaAl_2Si_2O_8(s) + 2H^+(aq) + H_2O(aq) = Ca^{2+}(aq) + Al_2Si_2O_5(OH)_4(s) \tag{13}$$

$$Mg_2SiO_4(s) + 4H^+(aq) = 2Mg^{2+}(aq) + H_4SiO_4(aq) \tag{14}$$

The dissolution of plagioclase in the neutral range (above approximately pH 4.3) produces kaolinite ($Al_2Si_2O_5(OH)_4(s)$, equation 13), which produces gibbsite (equation 15, from Stumm and Morgan 1981).

$$Al_2Si_2O_5(OH)_4(s) + 5H_2O = 2H_4SiO_4 + Al_2O_3 \bullet 3H_2O(s) \tag{15}$$

As aluminum becomes increasingly soluble near pH 4, gibbsite dissolution increases considerably, and is capable of neutralizing 6 moles of acid. So, with every mole of Ca released from plagioclase, there is a potential additional neutralization from gibbsite dissolution. This assumes that the alteration rate of kaolinite to gibbsite is faster than neutral range plagioclase dissolution. This situation presents the possibility that gibbsite could limit pH minima to approximately 4, if sulfur oxidation was slowed before gibbsite was depleted. Sulfide mineral oxidation could either be slowed by depletion of minerals in low-sulfur samples, or by coating of sulfide grains in higher-sulfur samples. This mechanism of acid neutralization would ultimately be limited by the rate of plagioclase dissolution. After the gibbsite is depleted, neutralization would be dependent on silicate mineral dissolution exclusively.

3.1.3. Trace Metal Release by Trace Metal Sulfide Oxidation

Trace metals are metals that occur at low average concentrations in the earth's crust but can be present in higher concentrations in mineralized areas. Trace metals can occur in sulfide minerals, from which they can be released by oxidation (e.g. reaction 16). Once released to solution, the migration of these metals can be influenced by a number of factors. At a regional scale, generalizations frequently can be used to estimate broad trends in metal mobility. However, as the scale becomes increasingly finer, estimating metal behavior generally becomes increasingly difficult (Smith and Huyck 1999).

$$ZnS(s) + 2O_2(aq) = Zn^{2+}(aq) + SO_4^{2-}(aq) \tag{16}$$

In general, metals may remain in solution or be removed in secondary phases. For removal from solution, trace metals may precipitate as oxides, hydroxides, or carbonates, be adsorbed by surfaces such as iron oxyhydroxides (Smith 1999), or co-precipitate with other solid phases. In acidic solutions trace metal removal is limited, and elevated trace metal concentrations are often associated with these solutions. However, circumneutral drainages can also contain elevated concentrations of trace metals such as nickel, copper, cobalt (Lapakko 1993c), zinc, manganese (Smith and Huyck 1999), molybdenum (Brown 1989), arsenic, and antimony. Concentrations of molybdenum, arsenic, and antimony in particular can be elevated even as pH increases above 7.

Oxidation of arsenic and antimony sulfides can produce acid, as can oxidation of the iron sulfide fraction of mixed sulfide minerals such as chalcopyrite (Plumlee 1999). Other trace metal sulfide oxidation will produce acid if and only if the metal released hydrolyzes (reaction 17) or precipitates as a hydroxide, oxide, or carbonate (reaction 18). For most trace metals this will occur only at pH levels above 6, and as pH decreases below this level the secondary phases will dissolve. Consequently, they do not generally contribute to acid production observed at lower pH levels.

$$Zn^{2+}(aq) + H_2O(aq) = Zn(OH)^+(aq) + H^+(aq) \tag{17}$$

$$Zn^{2+}(aq) + 2H_2O(aq) = Zn(OH)_2(s) + 2H^+(aq) \tag{18}$$

3.1.4. Key Solid-Phase Factors Controlling Mineral Oxidation and Dissolution

Whereas the balance of the acid producing and acid-neutralizing minerals influence mine waste drainage quality, there are several mineralogical factors that substantially influence drainage quality. Individual minerals may be entirely liberated from the rock matrix, occur interstitial to other minerals (partially liberated), or as inclusions within other minerals. The extent of liberation affects availability for reaction. In addition, acid-producing or acid-neutralizing minerals present as inclusions within unreactive minerals (e.g. quartz) will be essentially unavailable for reaction.

Oxidation of sulfide minerals and dissolution of some carbonate minerals are surface reactions and, therefore, the rates of these reactions are dependent on the reactive surface area. Reactivity decreases as mineral surfaces are covered by non-reactive reaction byproducts, such as iron oxyhydroxides (precipitants from iron sulfide oxidation), whereas the concentration of lattice defects increases mineral surface area, and therefore tends to increase reactivity. Mineral surface area is also dependent on the extent to which the mineral is liberated from the rock matrix, mineral grain size, and the "roughness" of the mineral surface.

3.1.5. Common Minerals and Specific Factors Controlling Mineral Oxidation and Dissolution

3.1.5.1. Sulfide Minerals

The most common sulfide mineral in these samples was pyrrhotite. Pyrrhotite has a chemical formula of $Fe_{1-x}S$, where $0 \leq x \leq 0.2$. Thus the pyrrhotite formula may range from FeS to Fe_7S_8. Pyrrhotite has a specific gravity of 4.58-4.65 and a hardness of 4 (Klein and Hurlbut 1985). The FeS end member has an orthorhombic structure. $Fe_{1-x}S$ such as Fe_8S_9, Fe_9S_{10} and $Fe_{10}S_{11}$, have hexagonal structures and Fe_7S_8 is monoclinic. Pyrrhotite is typically found as mixtures of hexagonal and monoclinic phases. These different crystal structures are thought by some researchers to have effects on oxidation rates (see equation 2 for oxidation reaction). However, Janzen (1996) found that the literature on this topic gave conflicting reports of the effect of crystal structure on oxidation rate. Furthermore, in his own experiment, Janzen found no correlation between pyrrhotite oxidation rates and crystal structure in the presence of dissolved oxygen or ferric iron.

3.1.5.2. Silicate Minerals

Typical silicate minerals in these samples were labradorite from the plagioclase feldspar group, forsterite as a reasonable representative of the olivine group, biotite from the mica group, as well as augite and bronzite (as a substitute for hypersthene) from the pyroxene group. Each of these minerals have published research on dissolution rates available, as well as information on physical factors that affect dissolution rate, such as specific gravity, hardness and surface roughness. Research available on these minerals in 2001, as well as six other silicate minerals present in the Duluth Complex, was compiled in a literature survey (Phillips et al. 2001). The rest of the material in this section is taken from that report, which has a more detailed treatment of this topic available.

Plagioclase feldspar forms a solid solution series from albite ($NaAlSi_3O_8$), the sodium-rich end member, to anorthite ($CaAl_2Si_2O_8$), the calcium-rich end member. Labradorite ($An_{50-70}Ab_{30-50}$; notation indicates 50-70% anorthite and 30-50% albite) was the plagioclase feldspar selected as representative for these samples. It has a specific gravity of 2.71 and a hardness of 6 (Klein and Hurlbut 1999). No data for surface roughness were available, but bytownite (An_{70-90}) had a range of 6.6-27.1 and a mean of 12.6 (Blum 1994). Blum and Stillings (1995) express the overall feldspar weathering process as the alteration of feldspar to common clay minerals (reaction 19).

$$2NaAlSi_3O_8(s) + 2H^+(aq) + 9H_2O(aq) = 2Na^+(aq) + Al_2Si_2O_5(OH)_4(s) + 4H_4SiO_4(aq) \qquad \mathbf{(19)}$$

Olivine forms a solid solution series from forsterite (Mg_2SiO_4) to fayalite (Fe_2SiO_4). Olivine has a specific gravity of 3.27-4.37 and a hardness of 6.5-7.0 (Klein and Hurlbut 1999). A surface roughness factor of 85 is reported for olivine (Sverdrup 1990). The weathering of forsteritic olivine is expressed by reaction 14 (Hem 1970).

Biotite ($K(Mg,Fe)_3(AlSi_3O_{10})(OH)_2$) is a phyllosilicate with a specific gravity of 2.8-3.2 and a hardness of 2.5-3.0 (Klein and Hurlbut 1999). Sverdrup (1990) reported a surface roughness factor of 17. The first stage of biotite weathering in which biotite is converted to vermiculite is expressed by reaction 20 (Acker and Bricker 1992).

$$3K_2(Mg_3Fe_3)\ (Al_2Si_6O_{20})(OH)_4(s) + 8H_2O + 12H_2CO_3 + 6H^+(aq) + 3/2O_2 = 2[(Mg_3Fe_3)(Al_3Si_5O_{20})(OH)_4\bullet 8H_2O] + 6K^+ + 3Mg^{2+} + 3Fe^{2+} + 12H_2CO_3^- + 8\ SiO_2 + 3H_2O \qquad \mathbf{(20)}$$

Pyroxenes are inosilicates, or silicates that form chain structures by sharing oxygen atoms. The pyroxenes form single chain structures that can be divided into two groups, orthopyroxene and clinopyroxene, based on their crystal systems. Orthopyroxenes form in the orthorhombic crystal system and include hypersthene. Clinopyroxenes form in the monoclinic crystal system and include augite.

Hypersthene has only limited research into its dissolution, so bronzite was used as a substitute. Both are orthopyroxenes, with hypersthene having 50-70% Mg and bronzite having 70-88% (Klein and Hurlbut 1985). Hypersthene and bronzite ($(Mg,Fe)SiO_3$) have specific gravities of 3.3-3.5 and hardnesses of 5-6 (Klein and Hurlbut 1999). Sverdrup (1990) reported a surface roughness factor of 17.

Augite ($(Ca,Na)(Mg,Fe,Al)(Si,Al)_2O_6$) is a clinopyroxene with a specific gravity of 3.2-3.4 and a hardness of 5-6 (Klein and Hurlbut 1999). Sverdrup (1990) reported a surface roughness factor of 50.

3.2. Duluth Complex Geology

3.2.1. General Description

The Duluth Complex is one of the largest mafic intrusive complexes in the world. It covers roughly 6500 km^2, ranging from the Duluth, MN area northward 240 km and is over 50 km wide at some points (Figure 1, Miller et al, 2001). Geologic contacts on the north and west are easily recognized, where the mafic intrusives and volcanics of the Duluth Complex form the headwall of the contact, and metagreywackes and slates of the Animike Group form most of the footwall of the contact. The Animike Group is composed primarily of the Virginia Formation and Biwabik Iron Formation that dominate the Animike metasediments near the contact. The Virginia Formation is a well-bedded sequence of argillaceous siltstone, carbonaceous shale, mudstone, fine-grained feldspathic greywacke, and minor limey-cherty interbeds variably contact metamorphosed to hornfels facies by the Duluth Complex. The Biwabik Iron Formation is a well bedded, iron-bearing strata of alternating cherty intervals also variably contact metamorphosed by the Duluth Complex. The Giants Range Batholith, predominantly late Archean quartz monzonite, granite and monzodiorite, also forms a portion of the western footwall (Figure 1).

The Duluth Complex has been classified into four major series of intrusions on the basis of age, lithology, internal structure, and structural position (Weiblen & Morey, 1980). These series (in order of emplacement) are the Felsic series, the Early Gabbro series, the Anorthositic series, and the Layered Series. The Layered Series hosts all known sulfide mineralization, including the South Kawishiwi and Partridge River Intrusions, and has the highest potential for undiscovered mineralized zones (Severson, 1994).

The South Kawishiwi is a southeast-dipping, layered igneous intrusion forming part of the northwestern margin of the Duluth Complex. It is predominantly composed of troctolitic (plagioclase-olivine) cumulates with local concentrations of anorthositic rock and volcanic hornfels inclusions.

3.2.2. Mineralization

Sulfide and platinum group element (PGE) mineralization occurs near the basal contact between the country rock and the intrusive complex. Four distinct types of magmatic mineral deposits are recognized. The first two deposit types include (1) large-low grade disseminated Ni-Cu concentrations, and (2) localized high-grade zones of massive Ni-Cu sulfides, both with some local PGE enrichment. These two types occur only at or very near the basal contact zone, and are the types found near the Dunka Mine (Figure 2, Miller et al, 2005). Other types include (3) strata-bound reefs with PGE enrichment, and (4) oxide-rich ultramafic plugs, possible sources of titanium and vanadium. These types can be found both in the basal contact zone and stratigraphically higher in the complex.

Several sulfide deposits are associated with the basal contact of the Duluth Complex with the Animike Group and the Giants Range Batholith. Identified deposits include the Dunka Mine and the Babbitt/Mesaba deposit, among other sulfide mineral deposits (Figure 3). The Dunka Mine lies on the contact of the Giants Range Batholith, the Animike Group, and the Duluth Complex. South Kawishiwi Intrusion rock was excavated to mine the underlying Biwabik Iron Formation, and comprises much of the waste rock at the mine. The dominant Duluth Complex lithology at the mine is olivine gabbro with occurrences of norite and olivine norite. Sulfide mineralization is concentrated within these rocks, especially those near the contact with the underlying rocks. The footwall of the contact with the South Kawishiwi intrusion is composed of Virginia Formation along most of its length, but borders the Biwabik Iron Formation and the Giants Range batholith along strike to the northeast and down dip to the southeast (Figure 2).

The Babbitt/Mesaba deposit is located five miles southwest of the Dunka Mine and is situated within very similar lithologies. Sulfide bearing rocks are found in a very similar setting in the Partridge River Intrusion, a layered cogenetic mafic layered intrusion of the Duluth Complex south of the South Kawishiwi Intrusion (Figure 1). The Partridge River intrusion is composed of a complex assemblage of gabbroic to troctolitic rocks, basaltic hornfels, and olivine gabbro, all of which are cross cut by heterogeneous troctolitic rocks ascribed to the upper Partridge River intrusion. Extensive exploratory drilling has defined the Babbitt/Mesaba copper-nickel-PGE sulfide deposit along the basal contact zone of the Partridge River intrusion. Additional information on prospects and deposits within the Duluth Complex is available in publications by the Natural Resources Research Institute (2013).

3.3. Previous Work

Experimental results after 150 weeks of laboratory dissolution were described previously (Lapakko 1993b; Lapakko and Antonson 1993), and included results for four Dunka mine blast hole samples (2.06%S □S_{TOT} □ 5.44%S) for which testing was terminated after 78 weeks. The results from this laboratory testing displayed similarities to those from field test piles of Duluth Complex rock (Lapakko 1994b, 1993c). An earlier dissolution experiment of shorter duration was conducted on 14 drill-core samples and a test-shaft sample from the Duluth Complex. Observations related to the rock chemistry, mineralogy, and surface area were made and initial results pertaining to the oxidation of sulfide minerals, the dissolution of silicate minerals, and associated effects on drainage chemistry were reported (Lapakko 1993a, 1988). In addition, experimental results after 8-10 years of laboratory dissolution on Partridge River Intrusion waste rock and tailing samples were recently reported and provide a comparison with the South Kawishiwi Intrusion samples discussed in this report (Lapakko et al. 2013a, 2013b).

4. METHODS

4.1. Materials

This laboratory experiment examined the effects of Duluth Complex and Virginia Formation rock dissolution on water quality. Twenty-five crushed rock samples ($0.053 \leq d \leq 0.149$ mm), ranging from 0.18-5.44% sulfur content (Table 1), were subjected to weekly rinses of deionized water. Nineteen samples, each replicated twice, were initiated on February 1989 (14 samples, reactors 1-28) and September 1990 (5 samples, reactors 29-38). These samples originated from blasts between December 1988 and October 1989 and were stored for 9 to 64 weeks prior to initiation of dissolution tests. Even numbered experimental reactors from 1-38 contained the same rock sample as the preceding odd numbered reactor. Fifteen of these samples were from the Duluth Complex and four contained a substantial fraction of metamorphosed rock from the underlying Virginia Formation. Six additional samples in the middle range of sulfur content were added in August 1997. These samples originated mostly from core drilled between 1974 and 1977 and were stored for at least 20 years prior to initiation of dissolution tests. These final six samples were analyzed more frequently, thoroughly based on what was learned from prior samples, and were not replicated. All samples were chosen for low metal concentrations, so metal concentrations were in a narrow range for all samples.

The Duluth Complex samples came from three locations. All seventeen Dunka blast hole samples were from the South Kawishiwi intrusion near Babbitt, Minnesota, and the one ARIMETCO and the three AMAX samples came from the Babbitt/Mesaba deposit of the Partridge River intrusion.

The four Virginia Formation samples (Reactors 21-28, 2.06 □□%S □□5.44) were terminated after 78 weeks of operation (August 1990). The data at this time indicated that waste rock with sulfur content in this range would produce drainage in need of rigorous environmental controls. It was concluded that testing of rock with lower sulfur contents would provide information more beneficial to environmental mine waste management planning than continuation of the higher sulfur samples already known to produce strongly acidic drainage. Drainage quality from first 15 Duluth Complex samples replicated well (see section 5.2.1), so even numbered reactors in the ranges 2-20 and 30-38 were discontinued after 247-328 weeks to save time and resources. The 1.71% S sample introduced in 1997 was terminated after 144 weeks. All other reactor data presented in this report were for periods ranging from 360-1252 weeks (Table 1).

4.2. Reactor Design and Operation

All rock samples begun in 1989 and 1990 (reactors 1-38) were reduced by hand, through the use of a bucking maul, or mechanically, with a pulverizor in 1989. The solids were then crushed to particles with diameters from 0.053 to 0.149 mm (-100/+270 mesh) and analyzed for sulfur content. The maximum diameter was selected to ensure sufficient liberation of the sulfide minerals present (Lapakko, 1988). These solids were then sieved and placed in reactors. Samples with 1.12, 1.16, 1.40, 1.44, and 1.64%S were wet-sieved, while the remaining samples were dry-sieved (Lapakko, 1988).

Samples begun in 1997 (reactors 39-44) were stage crushed with a jaw crusher. After each crushing step the sample was wet-sieved to obtain the –100/+270 fraction. This was continued until an adequate sample mass was obtained. These samples received initial crushing prior to storage. Reactor 39 was crushed to –1.9 cm and stored in 1996. All other samples crushed to –0.64 cm prior to storage. Reactors 40 and 43 were crushed in 1989, reactors 42 and 44 in 1977, and reactor 41 in 1976.

Seventy-five grams of crushed rock were placed into the upper segment of a two-stage filter unit (Figure

4). The solids were placed on a glass fiber filter that rested on a perforated plastic plate near the bottom of the reactor. At the inception of the experiment, each reactor was rinsed three times to remove any oxidation products that accumulated between sample crushing and onset of the experiment. Each week thereafter, two hundred milliliters of distilled-deionized water was added, and remained in contact with the solids for four to seven minutes, and then vacuum-pumped from the upper stage through a 0.45-micron filter on top of the lower stage of the filter unit. This procedure changed slightly beginning in July 2002. During weeks where no sample was collected, the reactors were filled with water as before, but were then gravity drained. The procedure remained the same as before for weeks during which samples were collected.

Between rinses, the solids remained within the reactors, allowing evaporation of retained rinse water and continuous oxidation. The reactors were stored in individual cubicles that formed a rectangular matrix within a topless housing with a perforated base. The cells were stored in a temperature and humidity controlled room (8.5 x 10.5 x 9.5 ft).

4.3. Analyses

4.3.1. Replication, Environmental Conditions, and Water Retention

4.3.1.1. Analysis of Humidity and Temperature Control

Between sampling, reactors were stored in a room with a thermostatically controlled heater (Lakewood 750). A Holmes HM 3500 humidifier and Sears Kenmore dehumidifier, both controlled by Honeywell humidistat, maintained humidity. From February 14, 1989 to February 11, 2013 temperature and relative humidity were measured three to four times weekly with a Taylor wet-bulb, dry-bulb hygrometer, and mean weekly values were determined. Range, mean and standard deviation of temperature and humidity of the average weekly values were determined to assess effectiveness of environmental controls in the testing chamber.

4.3.1.2. Testing for Differences between Replicates

All samples initiated in 1989 or 1990 were replicated. Average releases of calcium (Ca), magnesium (Mg) and sulfate (SO_4), as well as minimum pH measurements were compared between the two replicates of these 19 samples. These measurements were determined only for the period of record in which both replicate reactors were running (78-328 weeks). Differences between replicates were tested using the paired t-test in Systat 10.2. Details of drainage analysis are presented in section 5.2.1.

4.3.1.3. Analysis of Water Retention and Evaporation of Samples

In a six-week trial during 2003, eight samples were weighed daily, with the exception of weekends, to measure water retention in the sample and evaporation rate of the retained water. Mean amount of water retained and mean rate of evaporation were determined.

4.3.1.4. Analysis of Effect of Rinse Volume on Drainage pH

The effect of rinse water volume on drainage pH of samples was testing using two volumes: 10 and 200 ml. This was done in sixteen reactors by separately collecting the first approximately 10 ml of drainage water to leave the reactor. After the first 10 ml was collected, the vacuum pump was briefly turned off to allow another sample vessel to be positioned to collect the remaining leachate. The pH for each 10 ml sample was determined, before adding this volume to the rest of the drainage and determining pH for the entire volume. All reactors chosen had a relatively stable pH for eight weeks prior to this experiment (Table 20). pH from different volume drainages was compared using a paired Student's t test.

4.3.2. Characterization of Solid Samples

4.3.2.1. Particle Size

Effects of particle size were assessed in two ways using an electron microprobe. First, the perimeter to area ratio for a large number of grains in each sample was determined as an overall indicator of particle size. Second, the extent of small particles adhering to the surface of larger particles was assessed by comparing washed and unwashed grains.

Selected samples were analyzed to determine the extent of grains finer than that intended by sieving (-100/+270 mesh or 49-153 microns). As an indicator of particle size, three images of multiple grains (two for 0.40%S unleached and 0.58%S leached, four for 1.16%S leached) were analyzed from leached and unleached samples with 0.22-1.71%S (Table 17). These images were processed using *NIH ImageJ* software to analyze the total number of particles, their area and circumferences. From these data, a single value was calculated to give the cumulative perimeter to area ratio (McSwiggen and Associates, P.A., Saint Anthony MN). This ratio was used as a surrogate for particle size to compare among samples and to assess the effects of leaching. These data were also used to determine average particle diameter by assuming spherical particles and applying the formula specified in Table 17.

Cleaned and uncleaned grains of unleached and leached samples containing 0.22 and 0.40%S were imaged. To clean the samples, mineral grains were placed in distilled alcohol for five minutes, and then placed in an ultrasonic cleaner for an additional five minutes before analysis. Images of these grains allowed a qualitative comparison of the amount of fine particulates on the surface of leached and unleached samples.

4.3.2.2. Chemistry

4.3.2.2.1. Whole Rock Chemical Composition

Initial sulfur content was determined with a LECO furnace (Lerch Brothers, Inc., Hibbing, MN) using ASTM 395 (ASTM 2000). ACTLABS, Inc. (Tucson, AZ) determined SO_4 and evolved carbon dioxide. SO_4 was determined for leached samples only using ASTM E-1915-97 (ASTM 2000). Evolved carbon dioxide was analyzed using ASTM E350-89C (ASTM 2000). A 10% hydrochloric acid solution was used to dissolve the carbonate minerals, and the carbonate present was quantified as the difference between total carbon in the initial sample and that in the residue. Whole rock oxide percentages were determined using a lithium tetraborate fusion modified from ASTM E886-94 (ASTM 2000) and analysis by inductively coupled plasma-atomic emission spectroscopy (ICP-AES) using a Thermo Jarrell-Ash ENVIRO II ICP (ACTLABS, Inc., Ancaster, ON). Chemex Labs (Sparks NV) also conducted similar whole rock chemistry on a subset of these samples. These results are not discussed in the text, but are presented in Appendix 1, Attachment A1.4.

Concentrations of Ag, Cd, Cu, Ni, Pb, Zn, and Bi were determined using a total digestion modified from Crock et al. (1983), with analysis by ICP-AES (ACTLABS, Inc., Ancaster, ON). Other trace elements were determined using instrumental neutron activation analysis (Hoffman 1992) (ACTLABS, Inc., Ancaster, ON).

4.3.2.2.2. Solid-Phase Acid Production and Neutralization Potential

Acid production potential was determined mathematically as %S x 31.18. This calculation was based on production of 2 moles of acid per mole of S, and expressing this value as kg $CaCO_3$ equivalents/ton rock.

Two methods were used to determine neutralization potential for the initial nineteen samples (those started in 1989 and 1990). The first was the Standard ABA Sobek method, in which the sample was crushed to pass a 60-mesh screen (diameter <0.25 mm). Approximately 0.5 g of crushed sample was placed on aluminum foil with one or two drops of one part hydrochloric acid (HCl) to three parts deionized water. Based on extent of “fizzing” in this test, the volume and concentration of HCl were selected and 2 g of crushed rock was combined with the HCl solution in a 250-mL Erlenmeyer flask. The rock-acid mixture was boiled until the reaction ceased, as indicated by the termination of the production of bubbles. The solution was diluted to 125 ml using distilled water, boiled for 1 min and cooled to room temperature. The mixture was then titrated to pH 7.0 with sodium hydroxide (NaOH) to determine the amount of acid neutralized by the sample (as $CaCO_3$). The NP (acid neutralization per unit mass rock) was expressed in units of kilograms of $CaCO_3$ per metric ton of mine waste (kg $CaCO_3$/MT)

The second method used was the Modified ABA determination of neutralization potential (Lawrence 1990). The acid/rock mixture was prepared as above and digested at room temperature for 24 hours, at which time pH was measured. If pH was not in the range of 1.5-2.0, the digestion was rerun with an adjusted acid addition, based on the observed pH, until the pH range of 1.5-2.0 was attained. After the pH criterion was met, the amount of acid neutralized by the rock was determined by titrating the acid/rock mixture NaOH until a pH endpoint of 8.3 was maintained for at least 30 seconds. The NP of the lithology is then recorded in kg $CaCO_3$/MT.

A third method, a slight modification of the NP(pH6) method (Lapakko 1994a), was used in the determination of NP, but only for the final six samples of this study (reactors 39-44). NP was determined by titrating a stirred mixture of 2 g sample (-100/+270 mesh) in 100 ml distilled water with 1.0N sulfuric acid. The titration was conducted using a Mettler DL21 automatic titrator equipped with a Ross combination pH electrode. The instrument was programmed for a pH stat titration with an endpoint of pH 6.00 and the minimum increment of acid addition was 0.005 ml. A 2 g sample was placed in a 150 ml glass beaker with 100 ml of distilled deionized water. The beaker was placed in a Thermolyne model 7200 auto stirrer and a Teflon magnetic stirring bar provided constant mixing of the solution. The pH probe was suspended in the beaker at a depth of approximately 2 cm above the stirring bar. pH, incremental and cumulative acid additions were recorded every thirty minutes. The titration continued until pH 6.0 was reached and less than 0.1 ml of acid was added over a period of four hours.

4.3.2.3. Mineralogy

4.3.2.3.1. Mineral Content and Chemistry

The mineral content and mineral chemistry of leached and unleached samples were determined by microprobe analysis of 100 to 125 mineral grains from each sample. Every attempt was made to pick the grains in a random manner, so that each mineral would be analyzed in proportion to their occurrence in the sample. Grains were either loose mounted on carbon tape or mounted in epoxy. Mineral chemistry analyses were conducted using a JEOL 8600 electron microprobe. Mineral standards were used for all calibrations. See Appendix 1, Attachment A1.2 for detailed methods.

In addition to microprobe determination, sulfide mineral contents were determined through a calculation based on the bulk chemistry of each sample for pyrrhotite (Po), chalcopyrite (Cp), and pentlandite (Pn). Solid-phase sulfur within each Duluth Complex sample was attributed to chalcopyrite (approximately 20% of copper associated with cubanite), pentlandite and pyrrhotite based on the presence of copper, nickel and iron along with solid-phase sulfur. This is a more accurate method of assessing sulfide speciation. This method assumes the lithology formed under equilibrium conditions, and the results are vulnerable to error if this assumption is incorrect.

Additionally, eight of the unleached samples analyzed above (0.40-1.44%S) had mineral and chemical composition determined by an independent lab (Midland Research Center, Nashwauk, MN). The McSwiggen data are presented in the text, while the Midland data are presented in Appendix 1, Attachment A1.3.

4.3.2.3.2. Mineral Evidence of Dissolution

Microprobe analysis (back scatter imaging of polished epoxy mounts) was used to assess visual evidence of dissolution in unleached and leached mineral grains. Evidence of leaching occurred in the form of pitting of grains, as well as the formation of coatings indicating oxidation. The thickness of coatings on mineral grains was assessed by examination of polished the epoxy-mounted samples.

4.3.3. Aqueous

4.3.3.1. pH, Conductivity and Alkalinity

The rinse water from each reactor was analyzed for specific conductance, pH, alkalinity and acidity at the Minnesota Department of Natural Resources (MDNR) laboratory in Hibbing, MN (see Table 6 for sampling frequency). Specific conductance was analyzed using a Myron L conductivity meter, while either a Radiometer 29 or an Orion SA720 meter was used for pH analyses. Alkalinity (for pH≥6.3) and acidity were determined using standard techniques for endpoints of 4.5 and 8.3, respectively (APHA et al. 1992).

4.3.3.2. Sulfate, Calcium, Magnesium and Metals

The volume of filtered effluent was determined by weighing the drainage. The rinse water was analyzed for SO_4, Ca, Mg, Na, K, Co, Cu, Ni, Zn, Fe, Al and Si. The timing of measurements for all reactors is listed in Table 6. Samples taken for metal analyses were acidified with 0.2 ml ultra-pure nitric acid per 50 ml sample.

Sulfate and metal concentrations were determined at the MNDNR lab in Hibbing, MN until 17 May 1994 (representing weeks 273 and 192 for the first two sets of samples). SO_4 was analyzed using an HF Scientific DRT-100 nephelometer for the barium sulfate turbidimetric method (APHA et al., 1992). Ca and Mg were analyzed with a Perkin Elmer 603 atomic absorption spectrophotometer (AAS). Subsequent metal and SO_4 determinations were conducted at the Minnesota Department of Agriculture (MDA) laboratory. From 17 May 1994 to 23 August 1999, metals were determined by AAS (Varian 400 SPECTRAA) with a Zeeman GFAA furnace was attached for low concentrations. Ca, Mg, sodium (Na), and potassium (K) were analyzed by AAS throughout the experiment. Subsequent analyses for metals other than Ca, Mg, Na, and K were conducted using inductively coupled plasma mass spectrometry (ICP-MS, Hewlett Packard HP4500 Series, model #G1820A). For $[SO_4] > 5$ mgL^{-1}, SO_4 was determined using a Technicon AA2 automated colorimeter. Lower concentrations were determined using a Dionex ion chromatograph and, after 10 November 1998, a Lachat QuickChem 8000.

4.4. Calculations

4.4.1. Problems with Ca and Mg Determinations Prior to Week 150

Ca and Mg were the predominant cations in drainage samples and SO_4 was the predominant anion. Calculation of the molar ratio of the sum of Ca and Mg concentrations to the SO_4 concentration for the initial 150 weeks indicated an excess of cations. The mean, median, and standard deviation for the ratios were 1.79, 1.39, and 1.41, respectively. It was recognized that this charge imbalance was unrealistic and it was suspected that the Ca and Mg analyses were in error. The secondary cations for these reactions are K and Na. The data for these cations also showed several similar inconsistencies and remains suspect throughout the dataset.

Unfortunately, only four to six values from the last 13 to 24 weeks were available for most of the reactors and no values were available for the reactors containing 2.06 and 3.12 percent sulfur (reactors 21 to 24). Initially the samples were analyzed using a 1:20 dilution factor. This may have been the source of the problem, allowing for erroneous calculation of the concentration of the cations present. The remaining available samples were re-analyzed using a 1:5 dilution to provide more accurate calculations of the cation concentrations. Lanthanum chloride was added to the blank used for the standardization, a procedure that was omitted in the initial analysis.

Reanalyzed Ca and Mg values yielded more reasonable charge balances based on molar ratios of the sum of Ca plus Mg concentrations to SO_4 concentration. The mean, median, and standard deviation of the ratios for the reanalyzed samples were 0.72, 0.65, and 0.29, much lower than the previously calculated results, as would be expected with decreasing pH. Average ratios for the three solids with drainage pH above 6.0 ranged from 0.92 to 1.27. For lower drainage pH, ratios ranged from 0.49 to 0.81. Lower ratios (indicating a cation deficit) at lower pH were assumed to result from significant concentrations of cations other than Ca and Mg in the more acidic drainages.

Regression analysis was used to define a relationship between the initial (1:20 dilution) analyses and the secondary (1:5 dilution) analyses. The initial analyses for Ca and Mg were then adjusted by linear transformation using the relationship defined. The molar ratios of the sum of the transformed Ca and Mg concentration to SO_4 concentration were then determined. The mean, median, and standard deviation of the molar ratios using the transformed concentrations were 1.51, 0.79, and 3.29. The large mean and standard deviation were the result of ratios that were unusually high for 41 of the 593 values transformed. These ratios ranged from 2.5 to 29, averaging 10.6. Of the 41 elevated values, 38 occurred between weeks 12 and 60, suggesting that the initial analyses during these weeks were particularly prone to error.

The more reasonable charge balance data indicates that transformed Ca and Mg concentrations are more accurate than the original analyses. Nonetheless, these values were determined by an unorthodox approach and, consequently, conclusions based on these data must be drawn with caution. Additional detail on the Ca and Mg data is presented by Lapakko (1993b). The problem was corrected after week 150 for the original reactors.

4.4.2. Chemical Mass Release

Cumulative released masses of sulfate, major cations, and trace metals were calculated as the product of observed concentration in the drainage and drainage volume. Missing concentrations were estimated as the average of previous and subsequent analyzed values. Initial values were averaged between the final pre-experiment rinse and the first observed value taken, except for samples started in 1997, which did not have pre-experiment rinses analyzed. It was assumed that experimental values after the last observed value (and prior to observed values for 1997 samples) were identical to the nearest observed value. Values reported as less than the detection limit were recorded as equal to one-half the detection limit.

4.4.3. Empirical Neutralization Potential for Drainage

Empirical neutralization potentials (ENP) were calculated to estimate the amount of acid neutralized by silicate dissolution prior to drainage pH decreasing and remaining below pH values of 7, 6, 5, 4.5, 4 and 3.5. The acid neutralized was calculated as the cumulative SO_4 release (in mg $CaCO_3$/g rock, see Table 21 for exact formula) prior to the point at which drainage pH decreased and remained below the specified pH value. If drainage pH from a given solid never decreased permanently below a specified value, the ENP was reported as "greater than" the total SO_4 release for the period of record. If drainage pH was continuously below the specified pH, ENP for that pH was reported as zero.

4.4.4. Rates of Release

Solute release rates of SO_4, Ca, Mg, Na, K, Co, Cu, Ni and Zn were determined for each sample from observed concentrations of each respective ion within the leachate. Iron, Al and Si release rates were calculated separately for Duluth Complex and Virginia Formation samples, and determined as the average of all samples in each group. Release was calculated as the product of observed concentration (mol) and volume of drainage (l), divided by number of seconds in a week. Rates of solute release were determined based on weekly concentration measurements.

SO_4 release (log transformed) and pH were plotted as a function of sulfur content (log transformed) using linear regression. This was done for the four sample periods detailed in section 4.4.5.1. Calcium, Mg, and Ca+Mg release (all log transformed) were plotted as a function of SO_4 release (log transformed) using linear regression during the four time periods.

During a three week period (July 1 to July 21, 2011) the ongoing samples to date (0.18, 0.22, 0.67 (39, 40), 0.72, 0.82, 0.92%S) where not rinsed due the State of Minnesota shutdown. Because of this change to the rinsing frequency, adjustments were made to the associated rate calculations. Observed sulfate, calcium, and magnesium release after the shutdown (week 728 for R39-R43, week 1171 for R1-R3) where divided by four in order to account for accumulated mass in the sample. For cumulative mass release calculations, zero mass release was entered for the weeks during the shutdown and the higher observed release measured after the shutdown was retained. For concentration vs. time figures (Appendix 3, Figures A3.1-A3.44) no adjustment was made. It should be noted that this change in rinsing frequency only affected 0.3-0.5% of the measured values during the entire period of record and had minimal effect on the overall release rate calculations.

4.4.5. Mineral Dissolution Rates

Five models were developed to determine ion release rates from major silicate and sulfide minerals in each sample. Silicate mineral dissolution and sulfide mineral oxidation rates were based on observed solute release rates, assumed mineral sources of solutes, determined mineral chemistry, and mineral surface areas. For each sample, mineral-specific surface areas were based on mineral content determined, calculated geometric surface areas, and surface roughness factors reported in the literature (Appendix 5, Table A5.1). Additionally, maximal gibbsite production was determined based on stoichiometric calculations.

4.4.5.1. Silicate Mineral Dissolution Rates

Four modeling approaches were used, all of which assumed stoichiometric release of major cations (Ca, Mg, Na, K) from the most common minerals in these samples (plagioclase, augite, hypersthene, olivine, biotite). That is, the ratio of major cations released to solution during the dissolution of each mineral was equal to that which existed prior to dissolution in each sample. The models are presented in order of most to least appropriate for these data. The first model was chosen as most appropriate because it is based on plagioclase, by far the most common mineral in these samples, and because the model is primarily based on Ca, which was thoroughly sampled throughout the experiment for all samples. Sodium, the basis for model 3, would normally be the preferred element to model for these samples because it is almost entirely exclusive to plagioclase, as well as not having any dramatic changes in solubility over the pH range found in this experiment. The reason it is not the basis for the preferred model in this experiment is the lack of Na analysis during the first eight years for the majority of samples. Magnesium was used in model 2 to determine augite dissolution, which was the basis for that model. Potassium was used as the basis for model 4, with plagioclase dissolution based on sodium as in model 3. Aluminum was not used in any models due to its infrequent sampling and low solubility until pH was lower than 5.

These models were applied to four periods of drainage conditions: (A) the initial period of highly variable ion release, (B) a more stable period prior to pH consistently falling below 4.4, (C) a period with pH consistently below 4.4 and concurrent increases of Ca and Mg release, and (D) a period when pH rises above 4.4 until the end of the experiment. The concurrent release of Ca and Mg in period C was crucial to model 1, because it indicated dissolution of augite, which was the only common sample mineral with approximately equal proportions of Ca and Mg.

In addition to the models mentioned above, maximal release of plagioclase and olivine were determined for the entire period of record. This was done for plagioclase by dividing cumulative Ca release (mmol, Table 25) by the average molar Ca content of each sample (Table 11). Olivine was computed similarly with cumulative Mg release (Table 25) and Mg content in olivine (Table 11).

4.4.5.1.1. Model 1

This model calculated a neutral-pH mechanism plagioclase dissolution rate for periods during which Ca release from a given sample was fairly constant, accompanied by augite dissolution during acidic periods (period C).

Calcium release was attributed solely to plagioclase dissolution. The periods used for plagioclase calculation excludes periods during which concurrent increases in rates of Ca and Mg release were observed. These periods of concurrent Ca and Mg release were likely due to augite dissolution, which was the only common mineral present in our samples with approximately equal amounts of the two elements. This presumed increase in augite dissolution typically began at pH 4.1-4.4. Relatively constant Ca release, both prior to reaching this pH and subsequent to rising above this pH, was attributed solely to plagioclase dissolution. The plagioclase dissolution rate was calculated as follows.

$$dplag/dt = (dCa/dt)_{obs}/[(A_{plag})_{geom}(SR_{plag})(m_{Ca/plag})]$$

where, $dplag/dt$ = rate of plagioclase dissolution (mol m^{-2} s^{-1}),
$(dCa/dt)_{obs}$ = observed rate of Ca release (mol s^{-1}),
$(A_{plag})_{geom}$ = geometrically calculated plagioclase surface area (m^2),
SR_{plag} = surface roughness factor for plagioclase (dimensionless), and

$m_{Ca/plag}$ = moles of Ca per mole plagioclase (dimensionless).

Surface roughness factor is a value accounting for the deviation of actual surface area from the smooth surface assumed in the geometric calculation assuming smooth spheres (see Table 48 for specific factors for each silicate mineral).

Geometric mineral surface area for all models was determined by the equation (see Table 48 for citations of mineral-specific information and Table 49 for specific silicate mineral values):

$$(A_m)_{geom} = (6*M_m)/(\rho*d)$$

where, $(A_m)_{geom}$ = surface area of mineral m,
M_m = mass of mineral m (g),
ρ = density (g/cm^3), and
d = diameter (cm).

All samples in the experiment were sieved to $0.0053 \text{ cm} < d < 0.0149 \text{ cm}$. Mean particle diameter was determined using a log-normal particle size distribution (Brantley and Mellott, 2000).

$$d_{geo\ mean} = (0.0053 \times 0.0149)^{0.5} = 0.0089 \text{ cm}$$

This model overestimated plagioclase dissolution rates. It assigned all observed Ca release to plagioclase dissolution. Furthermore, it provided a higher plagioclase dissolution rate than if Ca were preferentially leached.

During periods of concurrent increases in Ca and Mg (Period C), which typically began with pH<4.4, Ca release above the average rate of plagioclase dissolution from the prior period (Period B) was attributed to augite. This assumption could overestimate augite dissolution because the rate of plagioclase dissolution might have increased during these periods of decreasing pH.

$$daug/dt = (dCa/dt)_{obs}/[(A_{aug})_{geom}(SR_{aug})(m_{Ca/aug})]$$

This equation was used to calculate the rate of Mg release from augite by assuming stoichiometric release of Ca and Mg. Residual Mg (that not attributed to augite dissolution) was calculated by subtracting this value from the observed rate of Mg release. The residual Mg release could occur from olivine, hypersthene or biotite, and data analysis could not distribute the release among these minerals. Consequently, maximum dissolution rates were determined for each mineral, assuming all residual Mg release was from a single mineral. As mentioned above, it was assumed that minerals dissolved stoichiometrically.

$$dol/dt = (dMg/dt)_{res}/[(A_{ol})_{geom}(SR_{ol})(m_{Mg/ol})]$$

$$dhyp/dt = (dMg/dt)_{res}/[(A_{hyp})_{geom}(SR_{hyp})(m_{Mg/hyp})]$$

$$dbio/dt = (dMg/dt)_{res}/[(A_{bio})_{geom}(SR_{bio})(m_{Mg/bio})]$$

If calculated Mg release from augite dissolution exceeded observed Mg release, the calculated rate was rejected and observed Mg release was used to calculate augite dissolution.

$$daug/dt = (dMg/dt)_{obs}/[(A_{aug})_{geom}(SR_{aug})(m_{Mg/aug})]$$

In these cases, all Mg was attributed to augite dissolution, with no residual to attribute to other Mg-bearing minerals. These cases also resulted in orphan Ca, which was not attributed to the dissolution of any mineral.

The allotment of all available Ca to plagioclase dissolution during neutral periods (pH > ~4.4) prevents consideration of augite dissolution as a possible source of Ca and Mg release. Therefore, any Mg observed in the neutral period was attributed to dissolution of other ferromagnesian minerals. Maximum dissolution rates for each mineral were determined by assuming all Mg came from one mineral, and applying the previous dissolution equations.

4.4.5.1.2. Model 2

This model assumed all Mg release was due to stoichiometric augite dissolution. Because some Mg release might have come from other minerals, this assumption overestimated augite dissolution.

$$\mathrm{daug/dt} = (\mathrm{dMg/dt})_{\mathrm{obs}}/[(A_{\mathrm{aug}})_{\mathrm{geom}}(\mathrm{SR}_{\mathrm{aug}})(m_{\mathrm{Mg/aug}})]$$

The Ca release from augite was calculated using the augite dissolution rate above and assuming it dissolved stoichiometrically, releasing Ca and Mg proportionally. Therefore, Ca release from augite with respect to Mg content can be calculated using the following equation

$$(\mathrm{dCa/dt})_{\mathrm{aug}} = (m_{\mathrm{Ca/aug}}/m_{\mathrm{Mg/aug}})(\mathrm{dMg/dt})_{\mathrm{obs}}$$

If the observed Ca release rate exceeded that associated with augite dissolution, residual Ca was attributed to plagioclase dissolution. If observed Mg exceeded stoichiometric amounts of Ca, then Ca was used for determination of augite dissolution and there was no plagioclase dissolution. In this case, excess Mg was attributed to dissolution of hypersthene, olivine and biotite, by determining a maximum possible dissolution rate for each of these minerals based on excess Mg.

4.4.5.1.3. Model 3

In this model, plagioclase dissolution was calculated based on observed Na release rates for both neutral and acid conditions. It was assumed that Na was released stoichiometrically from plagioclase. Substantial Na release is only possible from plagioclase, as it comprises >86% of the Na present in the reactor. Potassium feldspar is the next most abundant source of Na, but comprises <13% of total Na. Cation speciation and mineral surface area information used in the previous calculations and results are presented in Table 48. Because Na data were not available for the entire period of record in most samples, this model was applied to samples begun in 1989 and 1990 beginning in weeks 402-422, the period after Na analysis began. For samples begun in 1997, the model was applied from week 12, when Na was first sampled.

$$\mathrm{dplag/dt} = (\mathrm{dNa/dt})_{\mathrm{obs}}/[(A_{\mathrm{plag}})_{\mathrm{geom}}(\mathrm{SR}_{\mathrm{plag}})(m_{\mathrm{Na/plag}})]$$

The rate of augite dissolution was then calculated based on the assumption that Na and Ca release from plagioclase was stoichiometric. Differences between observed rates of Ca release and calculated rates from plagioclase dissolution were attributed to augite dissolution. Calcium release from augite was assumed to be stoichiometric. In the event that observed Ca was less than the calculated Ca from plagioclase, there was assumed to be no augite dissolution.

$$\mathrm{daug/dt} = [(\mathrm{dCa/dt})_{\mathrm{obs}} - (m_{\mathrm{Ca/plag}}/\ m_{\mathrm{Na/plag}})(\mathrm{dNa/dt})]/\ [(A_{\mathrm{aug}})_{\mathrm{geom}}(\mathrm{SR}_{\mathrm{aug}})(m_{\mathrm{Ca/aug}})]$$

However, observed rates of Mg release must also be taken into account based on assumptions that Ca and Mg release from augite dissolution was stoichiometric. If observed Mg concentrations were less than the stoichiometric amount indicated by the difference between the observed rate of Ca release and that attributed to dissolution of plagioclase, then the rate calculated from residual Ca release was rejected and observed Mg release was used to calculate augite dissolution. In these cases, there was no residual Mg to attribute to dissolution of other ferromagnesian minerals. These cases also created orphan Ca, which was not attributed to the dissolution of any mineral.

Residual Mg was calculated as follows.

$$dMg_{res}/dt = (dMg/dt)_{obs} - (daug/dt \times [(A_{aug})_{geom} (SR_{aug})(m_{Mg/aug})])$$

The source of residual Mg release could not be determined by data analysis. To address this, it was assumed that the residual Mg was from olivine, hypersthene, or biotite. A maximal stoichiometric rate of dissolution using all residual Mg was determined for each mineral.

4.4.5.1.4. Model 4

This model began with the initial step in Model 3 (section 4.4.5.1.3), where plagioclase dissolution was calculated based on observed Na release rates for both neutral and acid conditions. Potassium release was measured over the same times as Na, and collection days for both elements were generally identical. The same limitations on interpretation of model 3 at early stages of sample dissolution also apply to this model.

$$dplag/dt = (dNa/dt)_{obs} / [(A_{plag})_{geom}(SR_{plag})(m_{Na/plag})]$$

The rates of biotite and potassium feldspar dissolution were then calculated based on the assumption that Na and K release from plagioclase was stoichiometric. Differences between observed rates of K release and calculated rates from plagioclase dissolution were attributed to each mineral individually to give a maximum dissolution rate for these conditions. The equation for the dissolution rate calculation, with biotite as an example, was:

$$dbio/dt = [(dK/dt)_{obs} - (m_{K/plag}/ m_{Na/plag})(dNa/dt)] / [(A_{bio})_{geom}(SR_{bio})(m_{K/bio})]$$

The rate of augite dissolution was calculated in the same manner as in Model 3. Residual Mg was then determined by subtracting Mg release attributed to biotite and augite dissolution from observed Mg release.

$$dMg_{res}/dt = (dMg/dt)_{obs} - (daug/dt \times [(A_{aug})_{geom} (SR_{aug})(m_{Mg/aug})]) - (dbio/dt \times [(A_{bio})_{geom}(SR_{bio})(m_{K/bio})])$$

Maximum stoichiometric rates of hypersthene and olivine were then determined based on residual Mg after biotite and augite dissolution. In the event that observed Mg was less than that attributed to biotite, than there was assumed to be no dissolution of other ferromagnesian minerals. In the event that there was no biotite in a sample, all Mg release was assumed to come from dissolution of augite, hypersthene and olivine. A maximal stoichiometric rate of dissolution using all residual Mg was determined for each mineral.

4.4.5.2. Comparison of Predicted and Observed Plagioclase Dissolution Stoichiometry

Observed Ca and Na release was plotted over the entire period of record for each sample (Appendix 7, Figures A7.1-A7.21). The ratio of observed Ca: Na release was also plotted and compared to the solid phase Ca: Na in plagioclase as determined by McSwiggen and Associates (Table 11, Appendix 1, Attachment A1.1).

4.4.5.3. Gibbsite Production

In order to determine whether gibbsite dissolution could be responsible for the high percentage of samples whose minimum pH was approximately 4.0, maximal gibbsite production was compared to acidity production. Maximal gibbsite production was determined by assuming that all Al released during plagioclase dissolution was used in gibbsite formation at the rate of two moles Al per mole gibbsite. To determine plagioclase dissolution, all Ca was assumed to come from plagioclase. Each mole of plagioclase was assumed to release 0.5 moles Ca and 1.5 moles Al. The amount of gibbsite was compared to the amount of acidity produced ((cumulative sulfate*2) – (cumulative Ca*2)) by the first time a sample's pH declined below 4.0.

4.4.5.4. Sulfide Mineral Oxidation Rate Determination

Pyrrhotite mass was calculated by estimating the amounts of sulfur associated with copper and nickel sulfides and assuming the remaining sulfur was present as pyrrhotite. The sulfur mass in grams associated with copper sulfides was calculated by multiplying the percent copper of a sample by 1.26 x 75/100. The first factor is a mass ratio of Cu to S, assuming all copper was equally divided between chalcopyrite ($CuFeS_2$) and cubanite ($CuFe_2S_3$), and the second factor determined S mass for the 75 g sample. It should be noted that this calculation differs from the method used to determine chalcopyrite content in the bulk samples, which attributed all Cu to chalcopyrite. Although the assumption of a chalcopyrite:cubanite ratio equal to one does not appear justified by grain analyses showing a 3:1 ratio in unleached samples, the low number of grains analyzed makes this ratio prone to error. Sulfur associated with nickel sulfide was determined by multiplying sample nickel content by 0.97 x 75/100. This formula is similar to the previous one and assumed all nickel was present as pentlandite ($Ni_{4.5}Fe_{4.5}S_8$). Sulfur associated with pyrrhotite was then determined by subtracting the sulfur associated with copper and nickel from the total sulfur content of a sample. Total mass of all sulfide minerals was determined as the sum of copper and nickel sulfides plus pyrrhotite. See Table 50 for specific sulfide mineral values. It should be noted that nickel associated with olivine was not accounted for in these calculations, however this would have a negligible effect on the calculated sulfide oxidation rates since 75% of the nickel, on average, was associated with pentlandite and pyrrhotite (Table 42).

Rates of sulfide mineral oxidation were calculated by dividing observed rates of SO_4 release by the surface area of sulfide minerals present (determined as in section 4.4.5.1.1). The rate of SO_4 release was determined based on observed SO_4 concentrations and the volume of drainage (Appendix 5, Table A5.0). Two calculations were made for sulfide mineral surface area, the first using a calculated pyrrhotite surface area and the second using a calculated surface area for all sulfide minerals present.

Sample sulfur depletion was determined using two methods. First, the amount of sulfur released as sulfate was subtracted from the amount of sulfur determined to be in the solids initially. Second, the amount of sulfur in leached solids from the replicate samples was subtracted from the amount of sulfur in unleached solids to determine sulfur depletion. The second method is likely to underestimate sulfur loss, as the replicate samples were removed from the experiment long before the other samples.

Sulfur present in each unreacted sample was determined using the equation $M_S = (S_0 / 100) * M_R$, where M_S = mass of sulfur present, S_0 = % of sample present as sulfur, and M_R = mass of sample. The mass of released sulfur was subtracted from the total initial sulfur values to determine sulfur depletion.

Five distinct stages during the period of record were selected to determine when S release occurred relative to other changes in sample measurements. These stages were bounded by the point pH drops below six, the point at which a major pH drop or increased SO_4 release begins, the point of minimum pH or maximum SO_4 release, the point pH begins to increase from the minimum, and termination of the experiment (Table 71).

4.4.6. Mineral Sources of Metals

Of the four metals of concern (Co, Cu, Ni, Zn), only Co and Ni had multiple potential mineral sources whose relative importance was not clear. For Co, these were cobaltite and pentlandite. For Ni, these were olivine, pyrrhotite, maucherite and pentlandite. This section describes the methods used to determine the relative importance of the sources.

To determine the maximum percent of cobalt present as cobaltite, (Co, Fe)AsS, in these samples, As:Co ratios were determined. A similar approach was used for maucherite ($Ni_{11}As_8$). Arsenic, Co and Ni values from unleached solid samples (Table 3) were used in this comparison. Due to the small amount of Zn and Co, a quantitative partitioning of mineral sources was not attempted for these metals. Any such analysis would have a high degree of uncertainty due to lack of reasonable surface roughness coefficients and oxidation rates for many potential mineral sources.

Calculation of maximum olivine dissolution rates assumed that all Mg in leachate resulted from olivine dissolution and that Ni was released stoichiometrically. As can be seen in Table 23, most samples have large fractions of Mg present in minerals other than olivine. Thus, the assumption of all Mg coming from olivine is likely to overestimate olivine dissolution.

To calculate the rate of Ni release from sulfide minerals, it was assumed that Ni associated with pyrrhotite and pentlandite (presented in Table 42) was present in the ratio $Ni_{sulfides}:(S_{total}-S_{cp,cb})$. Sulfur associated with copper sulfides (chalcopyrite and cubanite) was calculated by multiplying the percent copper of a sample by 1.26/100 × 75. The first factor is a mass ratio of Cu to S, assuming all copper was equally divided between chalcopyrite ($CuFeS_2$) and cubanite ($CuFe_2S_3$), and the second factor determined S mass for the 75 g sample.

5. RESULTS

This analysis of results begins with analysis of unleached solid samples, including particle size, chemical composition, neutralization potential and, finally, mineral abundance and chemistry. The second results section discusses methodological and environmental analyses, including humidity and temperature data, analysis of replicate samples, sample water retention and evaporation rates, and effects of volume of leachate on pH. The third section discusses ways to group samples based on leachate analyses that include characteristic time periods, sample groups with similar behavior, and correlations between sample chemistry and leachate characteristics among different time periods. The fourth section discusses results of silicate dissolution models, gibbsite production calculations, and sulfide mineral oxidation models. It should be noted that for the results section, reactors 39-44 are included with the Dunka blast hole samples as a single collection. These samples were stored for 8 to 20+ years prior to dissolution testing and therefore produced higher drainage pH and lower sulfate and metal release rates. These differences in drainage pH and release rates will be neglected for the following results section.

5.1. Unleached Solid-Phase Analyses

5.1.1. Particle Size

Samples were sieved to obtain the 0.053-0.149 mm fraction desired for the experiment. To determine the success of the particle size selection, Duluth Complex samples were examined to determine the extent to which finer grains were present. Perimeter:area ratios were used as an indicator of particle size for twelve samples. Most unleached samples had perimeter:1000 micron area ratios from 72-111 (Table 17). The 1.63%S sample had a much higher ratio of 255.6. Unleached samples had a mean perimeter:area ratio for all samples of 104. Mean particle diameter, determined assuming spherical particles, was a mean of 42.9 μm.

To assess the extent of very fine particles adsorbed to the surface of other grains, cleaned and uncleaned samples from the 0.22 and 0.40%S were compared. This revealed many small particles on the grain surface of two uncleaned-unleached samples (Figure 57).

5.1.2. Chemistry

5.1.2.1. Whole-Rock Chemical Composition

For Duluth Complex samples, total sulfur content of unleached samples ranged from 0.18-1.71%, with virtually all sulfur present as sulfide. Evolved CO_2 exceeded 0.15% in only the 0.40%S sample (0.64%). Loss on ignition for samples analyzed ranged from 1.1-4.5% (LOI2, adjusted for difference in O between FeO and Fe_2O_3). The major whole rock chemical components were SiO_2 (43.2-50.5%), Al_2O_3 (14.1-21.0%), FeO (8.6-14.4%), MgO (5.7-8.6%) and CaO (6.6-9.8%). Contents of K_2O (0.3-1.7%), Na_2O (0.3-3.0%), TiO_2 (0.5-3.6%), MnO (0.1-0.2%), Fe_2O_3 (0.64-4.85%) and P_2O_5 (0.04-0.3%) were low (Table 2).

In Virginia Formation samples, S and Fe_2O_3 contents differed from Duluth Complex samples. Virginia Formation samples had higher sulfur content (2.06-5.44%S) and lower Fe_2O_3 (below detection-0.51%). Evolved CO_2 was high relative to other samples in the 5.44%S sample, with a measurement of 0.32%. Loss on ignition for samples analyzed ranged from 1.7-3.8% (LOI2, adjusted for difference in O between FeO and Fe_2O_3). The major whole rock chemical components were SiO_2 (42.5-57.8%), Al_2O_3 (11.5-20.5%), FeO (9.9-17.1%), MgO (4.6-10.8%) and CaO (2.2-10.0%). Contents of K_2O (0.4-1.9%), Na_2O (1.3-3.0%), TiO_2 (0.8-1.8%), MnO (0.08-0.2%), Fe_2O_3 (0.64-4.85%) and P_2O_5 (0.1-0.3%) were low (Table 2).

Trace metal contents were generally low for all samples (Table 3). Metals that were the focus of environmental concern in these samples were fairly uniform, with content decreasing in the order Cu > Ni > Zn > Co. Metals (and their associated maximum values in mg kg^{-1}) present at higher concentrations were Ce (64.1), Rb (69), Bi (90.54), Co (120), Zr (234), V (304), Zn (305), Sr (348), Ba (508), Cr (653), Ni (718), and Cu (2220). The maximum reported concentration for most metals were less than 33 mg kg^{-1} (Ag, As, Cs, Dy, Er, Eu, Ga, Gd, Ge, Hf, Ho, In, La, Lu, Mo, Nb, Nd, Pb, Pr, Sb, Sm, Sn, Ta, Tb, Th, Tl, Tm, U, W, Y, Yb).

When comparing Duluth Complex and Virginia Formation samples, metal contents were similar. However, in light of the large differences in S%, Virginia Formation samples are relatively low in metals compared to Duluth Complex samples.

5.1.2.2. Neutralization Potential

Neutralization potentials for 19 unleached Duluth Complex samples (excluding 0.67(R40) and 0.82%S) were determined using the method of Sobek et al. (1978) and values ranged from 8-21 kg $CaCO_3$/ton of rock (Table 22). NP values determined using the NP_{pH6} test for all 1997 samples (reactors 39-44) ranged from 2.0-5.4 kg $CaCO_3$/MT rock. The neutralization potential as Ca and Mg carbonate for all Duluth Complex samples was <0.7-3.2 g $CaCO_3$ eq (kg rock)$^{-1}$, with the exception of the 0.4%S sample, which had 14.5 g $CaCO_3$ eq (kg rock)$^{-1}$ (Table 22). For comparison, acid potentials calculated for the solids ranged from 6-53 g $CaCO_3$ eq (kg rock)$^{-1}$ (Table 22, Figure 61).

Virginia Formation neutralization potentials determined using the method of Sobek et al. (1978) ranged from 0.5-14 kg $CaCO_3$/ton of rock (Table 22). Neutralization potential as Ca and Mg carbonate was <0.7-7.3 g $CaCO_3$ eq (kg rock)$^{-1}$ (Table 22). For comparison, acid potentials calculated for the solids ranged from 64-170 g $CaCO_3$ eq (kg rock)$^{-1}$ (Table 22).

5.1.3. Mineral Analysis

5.1.3.1. Mineral Abundance and Composition

Scanning electron microscope electron probing and visual point counts of silicate minerals identified plagioclase in all 25 samples, as well as hypersthene and augite in all samples except the 5.44%S. Ilmenite was present in 22 samples, olivine in 20 samples, and 19 samples contained biotite and potassium feldspar. Quartz and potassium feldspar were more abundant in Virginia Formation samples than Duluth Complex (Table 7). Plagioclase, olivine and augite were less common in Virginia Formation samples than Duluth Complex rock.

Abundance of sulfide minerals pyrrhotite, pentlandite, chalcopyrite, pyrite, and cubanite was determined by a point count modal analysis. Pyrrhotite was most common, as it was observed in 18 of 25 total samples, ranging from 0.8-13.9%. Pentlandite, cubanite, chalcopyrite, and pyrite were observed at least once (Table 10). Pyrrhotite, chalcopyrite and pentlandite were more accurately determined using chemical calculations. Using these calculations, pyrrhotite was still the most common sulfide mineral (0.02-13.7%), but all three minerals were found in every sample (Table 10).

Plagioclase (36-65%), augite (3-17%), hypersthene (3-28%), and olivine (0-39%) contributed 65-97% of mineral content in Duluth Complex samples. Fifteen samples contained the plagioclase species labradorite, while six samples contain the more sodium-rich species andesine (0.18, 0.22, 0.57, 1.44, 1.63 and 1.64%S). Unleached Duluth Complex silicate minerals had the following range of stoichiometric coefficients: plagioclase $(Ca_{0.40-0.63}Na_{0.32-0.55})Al_{1.44-1.66}Si_{2.35-2.57}O_8$, augite $((Ca_{0.76-0.95}Na_{0.01-0.03})(Mg_{0.36-0.84}Fe_{0.27-0.63}Ti_{0.01-0.02})(Si_{1.95-2.00}Al_{0.03-0.1})O_6)$, hypersthene $((Mg_{0.91-1.30}Fe_{0.63-1.66})_2Si_{1.97-2.00}O_6)$, and olivine $((Mg_{0.72-1.23}Fe_{0.75-1.25})Si_{0.99-1.01}O_4)$ (Table 11).

Unleached Duluth Complex sulfide minerals had the following range of stoichiometric coefficients: pyrrhotite $Fe_{6.91-7.93}S_8$, pyrite $Fe_{4.06-4.44}S_8$, chalcopyrite $(Cu_{4.16-4.66}Fe_{4.32-4.99})\ S_8$, cubanite $(Cu_{2.71-2.86}Fe_{5.49-5.59})\ S_8$ and pentlandite $(Ni_{4.61-5.16}Fe_{4.39-5.37})\ S_8$ (Table 8).

In unleached Virginia Formation samples, plagioclase (12-35%), augite (0-3%), hypersthene (0-12%), and olivine (0-1%) contribute 12-42% of mineral content. One sample contained the plagioclase species labradorite (3.12%S), two samples contained the more sodium-rich species andesine (2.06 and 3.71%S), and one contained neither (5.44%S). Unleached Virginia Formation silicate minerals had the following range of stoichiometric coefficients: plagioclase $(Ca_{0.32-0.56}Na_{0.38-0.66})Al_{1.34-1.60}Si_{2.41-2.67}O_8$, augite $((Ca_{0.81-0.97}Na_{0.002-0.02})(Mg_{0.34-0.74}Fe_{0.28-0.63}Ti_{0.005-0.01})(Si_{1.97-1.99}Al_{0.04-0.1})O_6)$, hypersthene $((Mg_{0.95-1.11}Fe_{0.78-0.96})_2Si_{1.96-1.98}O_6)$, and olivine $((Mg_{0.89}Fe_{1.06})Si_{1.01}O_4)$ (Table 10).

Unleached Virginia Formation sulfide minerals present in these samples had the following range of stoichiometric coefficients: pyrrhotite $Fe_{7.10-7.53}S_8$, pyrite $Fe_{4.07-4.55}S_8$ and chalcopyrite $(Cu_{4.17}Fe_{4.37})\ S_8$.

5.1.3.2. Mineral Grain Coatings

There were no coatings or dissolution features observed on unleached grains during analysis (Table 14), indicating no situ alteration or weathering of the samples prior to initiation of the experiment.

5.2. Reaction Conditions and Methodological Variables

5.2.1. Temperature and Relative Humidity

Average weekly temperatures ranged from 21-28°C, with the exception of seven weeks below 21°C and eight weeks above 28°C (mean 24.4°C, SD 1.6, 0.09 95% CI). Average weekly relative humidity ranged from 37-86% (mean 57.6%, SD 4.8, 0.3 95% CI) (Appendix 2, Table A2.2). The humidity weekly average only exceeded 75% four times, and only fell below 45% eleven times during the 24 year period of record.

5.2.2. Replication

Two replicate reactors from nineteen samples were compared based on average weekly drainage pH and SO_4, Ca and Mg concentrations for data sets ranging from 78-328 weeks, depending on replicate pair (Appendix 3, Figures A3.45-A3.63). Paired t-tests found no difference for any factor between replicate groups, so replicate samples (even-numbered reactors 2-38) were removed from the experiment to save time and resources. The t-test p-values, which describe the chance that any difference between replicate groups was coincidence, ranged from 0.371-0.822. A p-value ≤ 0.05, typical for these types of tests, was required to reject the null hypothesis. The null hypothesis for these t-tests was that there was no difference in means between groups of replicates. Thus there was a 37-82% chance that differences between replicates were due to random chance, indicating there were no differences between replicate groups. Although there were differences between replicates (Table 19), there were no systematic differences between the two groups when one set of samples was compared to a replicate set of samples.

When minimum drainage pH was compared between replicates, the p-value was 0.371, with a mean pH of 4.30 and the mean difference between replicates 0.04. The t-test for SO_4 had a p-value of 0.822, with a mean concentration of 25.7 mg/L and a mean difference of 0.5 mg/L. Ca ($p = 0.757$) had a mean of 3.06 mg/L and a mean difference of 0.02 mg/L. Mg ($p = 0.757$) had a mean of 1.92 mg/L and a mean difference of 0.02 mg/L.

5.2.3. Analysis of Water Retention and Evaporation of Samples

In a six-week trial, eight 75-g samples retained 11.8-21.1 ml water (mean 16.2 ml, SD 2.4) the day after each weekly 200 ml water addition. This was 15.7-28.1% moisture content (by weight). Approximately 75% of retained water evaporated within three days of rinsing (Table 18), with approximately equal amounts lost each day. Reactors were completely dry before the next weekly water addition and, at the rate of drying from the first two days, would have completely dried less than four days after water was added.

5.2.4. Analysis of Effect of Rinse Volume on Drainage pH

Difference in drainage volume had a significant, though small, effect on drainage pH (Table 20). Mean pH in the 10 ml sample was 0.11 (SD=0.096) lower than the drainage for the entire 200 ml rinse (paired t-test, $p<0.001$). Differences of this magnitude would not effect management recommendations of this research. Total drainage pH measurements of most samples (ten of sixteen) were within the eight-week range prior to the experiment. Of the six that were outside this range, all were lower, but only with a mean -0.0333, making any effect of the sampling method on total drainage pH measurements unlikely.

5.3. Drainage Quality and Geochemical Evolution of Solid Phase

Leachate from the samples had predictable changes that occurred based on sample characteristics and duration of experiment. Changes in Ca and Mg release from samples were used to define time periods A-D. Minimum pH during the experiment was the primary determinant when dividing samples into Groups I-III. Time periods and sample groups were used to organize results and predict water quality effects based on sample characteristics. To increase mechanistic understanding of experimental leaching on samples, particle size, sample chemistry, as well as mineral composition and coatings was analyzed for leached samples.

5.3.1. Sample Classification, Drainage Quality and Mass Release

In general, pH decreased and sulfate release rates increased as solid-phase sulfur content increased. Maximum SO_4, Ca, and Mg release rates for samples containing less than 1.12%S typically occurred during the first 100 weeks, while higher sulfur samples had peak rates after this period. pH gradually decreased to a minimum value in 270-425 weeks for most samples, before gradually increasing. Higher sulfur content produced sharper initial declines in pH, as well as lower pH minima. Coinciding with the pH minima were marked increases in SO_4 release rates. Ca and Mg release rates also rose sharply near the pH minimum, but these increases were less than that observed for SO_4. These trends in drainage quality were typical enough to classify the samples into characteristic time periods and groups.

There were four periods of pH change accompanied by Ca and Mg release changes. Drainage pH declined from period A through period C, before rising in period D. Sample release rates were highest in period A, declined in period B, rose in period C and declined again in period D. pH generally declined in the first three periods and rose in the fourth. Not all samples went through later periods. For example, samples with S content $\leq 0.22\%$ only exhibited periods A and B.

Samples were classified into three groups based on typical minimum drainage pH (Table 25). The drainage pH criterion was selected based on its importance in predicting the amount of treatment for wastewater. Group I (circumneutral) generally had $0.18 \leq S\% \leq 0.22$ and a minimum pH that was generally no lower than 6. Group II (acidic) generally had $0.40 \leq \%S \leq 0.70$ and a minimum pH from 4-6. Group III (strongly acidic) generally had greater than $0.71 \leq \%S \leq 1.64$ and a minimum pH well below 4. Samples comprising each group, as well as representative data for each group, are listed in Table 25. The terms describing groups (circumneutral to strongly acidic) were used to simplify data presentation relative to this experiment, and are not intended to apply to mine waste generally. Similarities in chemical characteristics and drainage quality effects of the sample groups are discussed below. It should be noted that reactors 39-44 have been included in these groupings for the results section. These samples were stored for 8 to 20+ years prior to dissolution testing and therefore produced higher drainage pH and lower sulfate and metal release rates.

5.3.1.1. Drainage Quality Changes over Time

Drainage pH, as well as Ca and Mg release were measured throughout the experiment and exhibited similar patterns among samples. These patterns were used to define four sequential sample periods (see definitions below). Some samples did not exhibit behavior typical of all periods. Calcium and magnesium concentrations were relatively high and variable at the onset of the experiment, with Ca concentrations exceeding Mg concentrations. Release decreased and stabilized for both at lower levels after periods of 35-138 weeks. Mg concentrations during the latter stages of dissolution decreased to a greater extent than Ca concentrations. Ca concentrations generally increased in response to pH declines, and decreased as pH rose. Na and K concentrations were determined starting in 1997 (after week 400 for most reactors), and were typically lower and more variable than calcium or magnesium concentrations (Appendix 3, Figures A3.1-A3.44). For a summary of exact lengths of periods for each sample see Table 24.

Samples were assigned to periods based on similarity of changes in pH and ion release. These periods were labeled Periods A-D, and are described as follows:

1.) Period A

Period A started at week 1 for each sample, and ended as Ca and Mg release rates stabilized. Sample pH gradually decreased throughout this period for all samples. pH was relatively variable among samples, ranging from 4.6-8.7. Group I samples stabilized from approximately 6-7, while sample groups II and III stabilized between 4.5-5.5 by the end of Period A. Initially, each sample had relatively high Ca and Mg release, with Ca concentrations typically exceeding Mg concentrations. Release gradually declined with time. This period lasted from 34-140 weeks, and was present in all samples.

2.) Period B

Period B began when Mg and Ca release rates stabilized at levels typically 20-60 percent of those in Period A. Sample pH typically decreased gradually throughout this period. Magnesium release exceeded Ca release in 11 of 21 samples (0.51, 0.57, 0.58, 0.67(R39), 0.71, 1.16, 1.40, 1.44, 1.63, 1.64, 1.71%S).

3.) Period C

Period C occurred in most group II samples (all but 0.82, 0.92, 1.71%S) and all group III Duluth Complex samples. No group I samples entered period C. It began with a relatively rapid pH decline (below ~4.4) and concurrent increases in SO_4, Ca, and Mg release, with SO_4 release increases typically occurring 10-50 weeks prior to Ca and Mg release increases. During this period it was common to have Mg spikes exceeding Ca release at the pH minimum. This increase in Ca release was particularly common in group III samples. Calcium, Mg and SO_4 release decreased as Period C ended.

4.) Period D

Period D occurred in most group II (all but 0.4, 0.82, 0.92, 1.71%S) and group III Duluth Complex samples (all but 1.40%S). No group I samples entered period D. The beginning of this period is marked by decreases in ion release rates and increasing pH (above ~4.2-4.4). When it occurred, this period continued to the experiment's termination. This period was characterized by gradually increasing pH (above ~4.2-4.4), and decreasing Ca, Mg, and SO_4 concentrations. Calcium release rates remained relatively stable during Period D, at levels similar to Period B, while Mg release rates gradually decreased to levels less than or equal to rates observed in Period B.

Sodium and K concentrations were typically more variable than Ca and Mg concentrations, and were not determined for the entire period of record for the 19 samples started in 1989 and 1990. In all aspects of drainage quality, the six samples started in 1997 generally had fewer of the fluctuations that characterized the earlier samples.

Iron, Al and Si were sampled similarly to Na and K. Iron and Al release rates were very low until pH reached 4 (Table 35, Figures 52, 53). Below pH 4, Fe release rates were 12.4 times faster than above pH 4. Aluminum rates were 21.5 times faster. Si release was less responsive to pH declines (Table 35, Figures 54). Although average Si release rates were 2.3 times faster below pH 4, this was based on only seven points, making an accurate determination of pH effects on Si release difficult. It should be noted that no metal analyses were performed from weeks 78-360. This should be kept in mind when reviewing the results.

5.3.1.2. Sample Groups

5.3.1.2.1. Group I

Group I samples had typical drainage pH values above 6.0 throughout the period of record (Table 27). This group consisted of three samples with 0.18, 0.22 and 0.72%S. Drainage pH tended to decrease and stabilize from 6.0–6.5. Drainage pH ranged from 7.5–8.0 initially, decreased to roughly 6.5 after 100 weeks, and stabilized between 6.0–6.5 by week 150 (Table 27, Figure 5).

SO_4 release generally decreased with time. Average release rates were initially 8.8×10^{-12} to 1.2×10^{-11} mol/s, with maxima from $1.3\text{-}3.0 \times 10^{-11}$ mol/s (Table 28). Rates decreased after 100-150 weeks to levels an average of 30% of initial rates (Figure 6). Average rates ranged from $2.5\text{-}5.0 \times 10^{-12}$ mol/s until week 350, and continued to decrease until the end of the period of record, when average rates ranged from 1.2×10^{-12} to 1.7×10^{-12} mol/s. Total release for the entire experiment was 1.1-2.3 mmol, with an average of 1.9 mmol (Table 25).

Ca release rates tended to decrease with time as well (Table 29). Average release rates during the initial 150 weeks were $1.1\text{-}1.8 \times 10^{-11}$ mol/s, with maximum release rates from $2.6\text{-}4.2 \times 10^{-11}$ mol/s. Rates decreased and stabilized after week 150, with average rates of $2.4\text{-}3.5 \times 10^{-12}$ mol/s and maximum release rates of 8.7×10^{-12} to 1.2×10^{-11} mol/s for the remainder of the experiment. Rates for each sample remained relatively constant during this final period (Figure 8). Total release for the entire experiment was 1.3-3.9 mmol, with an average of 2.9 mmol (Table 25).

At the beginning of the experiment, average Mg release was 3.5×10^{-12} to 1.6×10^{-11} mol/s and maxima were 7.7×10^{-12} to 5.5×10^{-11} mol/s (Table 30). Following week 150, release rates decreased, with values as high as 1.4×10^{-11} mol/s until week 350 for the 0.18 and 0.22%S samples and week 200 for the 0.72%S sample (Figure 9). After this period Mg release began to decrease relative to Ca, with average values 20 to 60% lower than Ca release. Total release for the entire experiment was 0.8-3.3 mmol, with an average of 2.0 mmol (Table 25).

Na and K release were determined following week 420 for the 0.18 and 0.22%S samples and for the entire period of record for the 0.72%S sample (Figures 10, 11). Potassium release rates gradually decreased during the experiment, while Na stayed in a range for all samples between 6.1×10^{-13} to 3.3×10^{-12} mol/s (Table 32, Figure 10). Average potassium release for all samples decreased from $8.2 \times 10\text{-}^{13}$ to 4.3×10^{-12} initially, to minima rates of $3.6 - 7.2 \times 10^{-13}$ mol/s by the end of the period of record (Table 33, Figure 11).

Sample metal release (Co, Cu, Ni, Zn) was slower than rates of other elements already discussed (Tables 36-39). Average release rates for periods A and B ranged from 4.9×10^{-15} to 5.1×10^{-14} mol/s for Co, 8.8×10^{-15} to 4.3×10^{-14} mol/s for Cu, 7.5×10^{-15} to 9.2×10^{-14} mol/s for Ni, and $2.8\text{-}6.6 \times 10^{-14}$ mol/s for Zn. Co generally varied little over time for each sample (Figure 12), although maximum release rates among samples ranged from 5.4×10^{-15} to 1.5×10^{-13} mol/s. Cu, Ni and Zn had a similar maximum range among samples (1.3×10^{-14} to 1.4×10^{-13}, 1.0×10^{-14} to 3.0×10^{-13}, 6.7×10^{-14} to 2.3×10^{-13} mol/s for Cu, Ni and Zn respectively), but individual samples were more variable over time. There were several spikes of 300-400% increases from preceding release rates (Figures 13-15). These spikes were quite rapid and tended to occur approximately concurrently with increased SO_4 release. Average release rates generally declined from period A to period B. Variation in pH was small over time among group I samples and there was no observed relationship between pH and metal release. Metal release from the 0.72%S sample displayed much less temporal variability than the other two samples in this group.

The empirical neutralization potential above pH 7 (ENP_{pH7}) for Group I samples was 0.3-0.6 mg $CaCO_3$/g rock (Table 21). ENP_{pH6} ranged from >1.5 to >3.1 mg $CaCO_3$/g rock. These ENP values were considerably lower than those determined by the method of Sobek et al. (1978) (16-17 mg $CaCO_3$/g, Table 22). The neutralization potential for the 0.72%S sample (determined by autotitrator method) was 3.4 mg $CaCO_3$/g rock.

5.3.1.2.2. Group II

Group II consisted of eleven samples with sulfur contents from 0.40-0.92% (excluding 0.71 and 0.72%) and 1.71%. Three samples (0.72, 0.92 and 1.17%S) were AMAX samples and had been stored for at least twenty years prior to experimental leaching. The long period of storage likely caused decreased release rates for sulfate, Ca and Mg, as well as slowing the pH decline.

This group includes samples for which drainage pH was below 6, but not below 4 for any sustained period. Drainage pH tended to decrease quickly during the initial weeks and plateau slightly. Gradual decreases were usually observed until weeks 250-300, when short but sharp drops to minimum values occurred at about pH 4.3. Gradual increases were observed shortly thereafter and continued to the end of the experiment. Initial pH values ranged from 6.8-7.9, while minimum pH ranged from 3.8-5.1. Minimum pH was reached during weeks 332-395 for eight of ten reactors, with 0.40 and 0.67%S samples reaching minimum pH at weeks 810 and 151, respectively. The 1.71%S sample was terminated after 144 weeks with a drainage pH value of 5.1. Drainage pH values near the end of the experiment ranged from 4-5 for all reactors (Table 27, Figure 5).

Sulfate release tended to decrease with time initially, only to increase after 200-250 weeks of dissolution, followed by decreases near the end of the experiment (Figure 6). These trends were moderated in samples having less rapid pH declines. SO_4 release rates during the initial period averaged 1.2-3.8 x 10^{-11} mol/s with a range from 1.6 x 10^{-12} to 1.0 x 10^{-10} mol/s (Table 28). Sulfate release began to increase as pH decreased below five, with most samples' maximum release coinciding with minimum pH. Maximum rates in the later years (Period C) ranged from 3.2 x 10^{-11} to 1.1 x 10^{-10} mol/s. These release rates then gradually declined for the remainder of the experiment. Rates ranged from 1.8 x 10^{-13} to 4.5 x 10^{-11} mol/s throughout this interval (Table 28). Total release for the entire experiment was 1.9-10 mmol, with an average of 6.4 mmol (Table 25).

Several reactors displayed periods of decreased SO_4 release either longer or shorter than those previously discussed (Figure 7). Several others did not experience subsequent release rate increases before the end of the experiment. Decreased release was observed for 234 weeks for the 0.67%S (R40) reactor before increases were noted, 80 weeks longer than the other reactors in this group. The 0.40%S reactor also behaved abnormally, undergoing 745 weeks of decreased release before pH dropped below 5, and rates began to increase. No release rate increases were observed for the 0.82 and 0.92%S reactors, both of which had a 750-week period of decreased release prior to the end of the experiment. In contrast to this prolonged release, the 0.58%S reactor experienced a very short period of decreased release only 30 weeks in length before increased release was observed. However, it should be noted that the 0.82 and 0.92%S samples were stored for 8 to 20+ years prior to dissolution testing and therefore produced higher drainage pH and lower sulfate and metal release rates.

For most samples in this group, Ca release rates tended to decrease from the highest average releases initially, increase after a period of relatively stable release, and decrease again near the end of the experiment (Figure 8). At the onset of the experiment (Period A), average Ca release rates ranged from 1.2-3.7 x 10^{-11} mol/s, with a range from 2.2 x 10^{-12} to 1.0 x 10^{-10} mol/s (Table 29). Release rates decreased and stabilized after 150 weeks to rates averaging 30% of those in period A (Table 29). Very little change was noted in release rates until pH levels reached ~4.4, which typically occurred during weeks 220-350. As pH declined below 4.4, release began to increase, with average rates ranging from 3.5 x 10^{-12} to 1.2 x 10^{-11} mol/s. Despite the increase, average rates were only 35% of those in the initial period. Release rates declined as pH rose, and generally stabilized after week 445 at average rates of 2.0-6.5 x 10^{-12} mol/s until the end of the experiment (Table 29). Total release for the entire experiment was 1.2-8.7 mmol, with an average of 3.3 mmol (Table 25).

Magnesium release behaved similarly to Ca release for most of the period of record. Release rates tended to decrease with time, with rates decreasing after an initial, highly variable period to lower, more stable levels, only to increase for a short time before steadily decreasing to the end of the experiment (Figure 9). Initial average rates were 4.3 x 10^{-12} to 1.6 x 10^{-11} and maxima from 8.5 x 10^{-12} to 7.3 x 10^{-11} mol/s (Table 30). Release rates decreased and stabilized after 39-140 weeks of dissolution to levels 20-60% below initial levels in 8 of 11 samples (Table 30). The rise in Mg in response to declining pH typically produced smaller release rates than Ca, although they were, on average, 70% higher than the reduced rates in period B. After this increase, rates stabilized similarly to Ca. However, unlike Ca release, Mg rates began another period of decline. Seven of eight longer-running samples (those started in 1989-90) had concentrations at the Mg detection limit near the end of this study. This equated to a release rate of approximately 6.0 x 10^{-13} mol/s. Total release for the entire experiment was 0.45-2.6 mmol, with an average of 1.4 mmol (Table 25).

For seven samples from group II (0.40, 0.41, 0.51, 0.57, 0.58 and both 0.67%S) Mg release rates increased after pH dropped below 4.5. For most of these samples (all except both 0.67%S), concurrent increases in Ca release were observed. During the concurrent increase, both Ca and Mg rates were, on average 60 and 80% higher than those in the previous stable release period, respectively (Tables 29, 30). pH stayed relatively constant for the 0.40%S sample much longer than other samples, not starting a noticeable decline until week 715. This was followed by Ca release rate increases at week 775, followed by slightly elevated Mg release rates at week 800 (Figures 8, 9).

The remaining group II samples (0.54, 0.82, 0.92, and 1.71%S) had no major changes in Mg or Ca release following the initial decrease (Tables 29, 30). In these cases, pH gradually decreased with time, reached minimum values of pH 4-5, and remained fairly constant until termination of the experiment. The 0.54%S sample did not display any increases even though pH dropped to 4.2 at week 270 and remained below 4.4 for 130 weeks (Appendix 3, Figure A3.11). As with other Group II reactors, release rates decreased to levels 10-35% of initial rates before termination (Tables 29, 30). Both Ca and Mg release rates tended to decrease with time, with Mg typically decreasing near detection limits.

Group II Na release rates generally remained stable throughout the period of record, with values from 6.3 x 10^{-13} (below detection limit) to 1.0 x 10^{-11} mol/s, and a mean for all samples of 2.0 x 10^{-12} mol/s (Table 32). Potassium release rates were less consistent, as exhibited by the wider range from 3.6 x 10^{-13} to 6.5 x 10^{-11} mol/s, with a mean value for all samples of 8.1 x 10^{-12} mol/s (Table 33). Rates seemed to decrease with time, although this is difficult to conclusively state because of early gaps in the record for many samples.

Trace metal concentrations varied with pH for the Group II reactors. Average release rates for periods A through D ranged from 4.9 x 10^{-15} to 4.0 x 10^{-13} mol/s for Co, 2.3 x 10^{-14} to 3.4 x 10^{-12} mol/s for Cu, 6.0 x 10^{-14} to 3.0 x 10^{-12} mol/s for Ni, and 2.4 x 10^{-14} to 3.3 x 10^{-13} mol/s for Zn (Tables 36-39). Peak release rates among samples during periods A through D ranged from 4.9 x 10^{-15} to 4.1 x 10^{-13} mol/s for Co, 6.7 x 10^{-14} to 4.5 x 10^{-12} mol/s for Cu, 9.7 x 10^{-14} to 5.9 x 10^{-12} mol/s for Ni, and 3.7 x 10^{-14} to 6.3 x 10^{-13} mol/s for Zn. During period A, when pH remained above 6, average Ni, Co, and Zn release rates ranged from 6.1 x 10^{-14} to 4.2 x 10^{-13} mol/s. As drainage pH decreased below six, Co, Ni, and Zn release rates increased by 3, 34, and 15%, respectively (Figures 16, 18, 19). Release of these three metals typically increased quickly, followed by a gradual decrease to previous levels (Figures 12, 14, 15). Copper release behaved differently, remaining below 1.2 x 10^{-12} mol/s until pH approached five (Figure 17). The Cu increase lagged other metals and formed more of a plateau, with peak values ranging from 2.7 x 10^{-13} to 4.5 x 10^{-12} mol/s (Table 37, Figure 13). The 0.54%S reactor differed from the others in that the Cu release never rose above 4.1 x 10^{-13} mol/s, even though drainage pH decreased to 4.2.

ENP_{pH7} for Group II samples was 0.1-1.2 mg $CaCO_3$/g rock, while ENP_{pH6} was 0.4-8.0 mg $CaCO_3$/g rock (Table 21). All but two samples had drainage pH persistently below 5, with an ENP_{pH5} range of 0.9-8.5 mg $CaCO_3$/g rock. ENP_{pH4} was only calculated for the 0.40 and 0.57%S samples (9.9 and 6.8 mg $CaCO_3$/g rock respectively). For the nine samples with NP determined by the method of Sobek et al. (1978) (12-19 mg $CaCO_3$/g rock except 0.92%S with NP=4 determined by the method of Sobek et al. 1978), ENP values were lower (Table 22). The NP values for the five samples determined by the autotitrator method were in closer agreement at 2.0-5.4 mg $CaCO_3$/g rock.

5.3.1.2.3. Group III

Group III consisted of seven Duluth Complex samples (0.71 and 1.12-1.64%S) and four Virginia Formation samples (2.06-5.44%S). Although Virginia Formation samples are included in this group, discussion focuses on Duluth Complex samples with more complete periods of record.

This group contains samples for which minimum pH values were less than 4. Sample pH initially ranged from 5.5-7.5, and was below 5 by week 75 in six of seven Duluth Complex samples. Drainage pH dropped steadily until reaching approximately 4.3, and subsequently declined rapidly to minimum values of 3.0-4.2 between weeks 274-304 (Table 27). The 0.71% sample exhibited this same behavior with slightly different timing, as pH fell below 5 at week 190, and minimum pH was observed at week 362. Rapid increases were observed shortly after minimum pH was reached until ~pH 5, with pH rising more gradually to the end of the experiment (Figure 5). Virginia Formation samples declined rapidly to pH minima of 2.9-4.2 (Table 41), and did not rise due to the short period of record (78 weeks). For ease of use and to conserve space, only tables containing the calculated dissolution rates of minerals present are included in this report. Tables displaying the release rates from individual reactors are located in Appendix 5.

SO_4 release was highest in group III among Duluth Complex samples. Rates tended to decrease, only to experience marked increases after a short period of fairly constant release, and conclude with gradual decreases toward the end of the period of record (Figure 6). Initial release rates ranged from 3.1×10^{-12} to 3.6×10^{-10} mol/s (Table 28) over a period lasting 38-127 weeks (Table 24). Release rates subsequently decreased and stabilized at 50-75% of initial release rates for 87-174 weeks. Release rates for this period ranged from 1.4×10^{-11} to 1.3×10^{-10} mol/s and remained relatively stable until pH reached ~4.6. As pH declined below 4.6, release rates began to increase dramatically, rising for 46-139 weeks before reaching peak values. Maximum release rates from $2.5\text{-}3.6 \times 10^{-10}$ mol/s typically occurred within 14 weeks of each sample's minimum pH (the 1.40%S sample took 39 weeks from the time of maximum sulfate release to reach minimum pH of 3.1). Peak rates were 3-9 times higher than the preceding stable period. Release rates began to decline shortly following maximum release, and continued to decrease through the end of the experiment. As pH rose, sulfate release rates decreased to levels at or below those observed prior to the period of increased release, and typically took 35-80 weeks to reach rates that occurred prior to the peaks. The only exception was the 1.40%S reactor, which was terminated 78 weeks after peak release, and did not completely return to pre-elevated values before the end of the experiment. Total release for Duluth Complex samples was 11.3-28.9 mmol, with an average of 21.7 mmol (Table 25).

Due to the Virginia Formation samples' much shorter period of record, total release was smaller at 5.5-14.5 mmol, with an average of 10.5 mmol (Table 25). Virginia Formation sulfate release behaved similarly to Duluth Complex samples in the inverse response to pH, and ranged from 1.5×10^{-11} to 3.0×10^{-9} mol/s, with a mean of 2.2×10^{-10} mol/s (Table 41).

For Duluth Complex samples, Ca release behaved similarly in group III as in groups I and II. Release tended to decrease with time initially, stabilize for a short period, then increase, and finally decrease and stabilize near the end of the experimental period. The initial period of increased Ca release lasted for 39-120 weeks. Rates ranged from 3.6×10^{-12} to 1.6×10^{-10} mol/s during this initial period (Table 29). Subsequently, a period of relatively stable release had rates from 7.3×10^{-13} to 2.3×10^{-11} mol/s, or 14-20% of initial rates. This period began between weeks 39-128 for all reactors, and lasted 87-174 weeks. As pH decreased below ~4.3, Ca release rates increased 2-3 times higher than the previous period rates, but still only 25-60% of the initial rates, on average. Release rates ranged from 3.6×10^{-13} to 3.2×10^{-11} mol/s during this period, and averaged 1.4×10^{-11} mol/s. Rates decreased quickly as pH began to rise, typically 80-150 weeks after increases were initially observed. As pH rose above ~4.4, Ca release rates decreased and quickly stabilized at rates similar to pre-elevated values, ranging from 2.2×10^{-12} to 1.4×10^{-11} mol/s and remained fairly constant for the remainder of the experiment. Total release for the experiment was 3.0-6.1 mmol, with an average of 4.1 mmol (Table 25).

Ca release from the Virginia Formation samples appeared to be similar to the initial erratic period of Duluth Complex samples. Release ranged from 8.4 x 10^{-12} to 8.0 x 10^{-10} mol/s during this period, and averaged 5.2 x 10^{-11} mol/s. Total release for the experiment was 1.6-3.7 mmol, with an average of 2.8 mmol (Table 25).

Group III Duluth Complex samples displayed Mg release patterns similar to those observed in groups I and II. Release rates decreased initially before stabilizing at lower levels. This preceded elevated release during low pH periods, which decreased again near the end of the experiment (Table 30). Initial release rates were 1.2 x 10^{-12} to 8.9 x 10^{-11} mol/s, for a period of 38-127 weeks. Mg release rates then began to decrease, stabilizing at levels 67% of initial rates, on average. These rates ranged from 1.2 x 10^{-12} to 2.5 x 10^{-11} mol/s, and the period of stable release lasted 87-174 weeks. As pH dropped to ~4.4, Mg release rates began to climb, eventually reaching rates as much as 4 times higher than initial rates (Figure 9). The elevated rates ranged from 3.5 x 10^{-12} to 8.2 x 10^{-11} mol/s, and typically took less than 25 weeks after pH decline to reach maximum release rate. Shortly after maximum release values were observed, pH began to rise, and release rates began to decrease. Rates quickly dropped below pre-elevated rates and continued to decline until termination of the experiment, with all reactors displaying release rates below pre-elevated rates (Table 30). This is contrary to Ca release rates, which stabilize following elevated release. This late decline in Mg release relative to Ca is similar to that observed in other samples. Total release for the entire experiment was 2.6-6.9 mmol, with an average of 5.0 mmol (Table 25).

Mg release from the Virginia Formation samples also appeared to be similar to the initial erratic period of Duluth Complex samples. Release ranged from 1.3 x 10^{-11} to 7.5 x 10^{-10} mol/s during this period, and averaged 6.7 x 10^{-11} mol/s. Total release for the experiment was 2.4-4.7 mmol, with an average of 3.5 mmol (Table 25).

Marked concurrent Mg and Ca release rate increases were once again observed in all reactors during low pH periods, with Mg release greatly exceeding Ca release in 6 of the 7 Duluth Complex samples (Table 25). As pH decreased below approximately 4.3, concurrent Ca and Mg release increases were noted. In the Virginia Formation samples, concurrent releases were hard to detect because of the short period and rapid pH decline.

Group III Na release was similar to the group I and II samples, with average values remaining relatively constant below 6.4 x 10^{-12} mol/s (Table 32). Potassium release was more variable, with rates similar to Group II samples (7.6 x 10^{-13} to 2.2 x 10^{-11} mol/s) (Table 33). Potassium release rates seemed to decrease, but the presence of a large number of anomalous values and irregularly collected data made determination of a distinct trend difficult. These results must be viewed with caution, as K and Na data were sparse for most samples when compared to Ca and Mg data. There was no Na or K data collected for Virginia Formation samples.

Group III had higher trace metal release than other group I and II samples (Tables 36-39). Average Duluth Complex release rates for periods A through D ranged from 6.8 x 10^{-15} to 2.1 x 10^{-12} mol/s for Co, 4.8 x 10^{-14} to 7.2 x 10^{-12} mol/s for Cu, 3.7 x 10^{-14} to 2.2 x 10^{-11} mol/s for Ni, and 4.0 x 10^{-14} to 7.2 x 10^{-13} mol/s for Zn. Peak Duluth Complex release rates among samples during periods A through D ranged from 1.8 x 10^{-14} to 2.9 x 10^{-12} mol/s for Co, 9.5 x 10^{-14} to 8.8 x 10^{-12} mol/s for Cu, 1.1 x 10^{-13} to 3.6 x 10^{-11} mol/s for Ni, and 4.7 x 10^{-14} to 9.8 x 10^{-13} mol/s for Zn. Ni release generally had an early peak as pH approached 6.0, and then declined until a similar peak later. This later peak coincided with a dramatic pH decline below 4.0 and a spike in sulfate release. Cu generally did not share the initial peak with Ni, but increased to its highest release rates concurrent with the second Ni peak. Co and Zn had similar patterns as Ni, although at lower release rates.

Virginia Formation and Duluth Complex samples had similar trace metal release behavior over the period of record shared by both. Average Virginia Formation release rates for the entire period of record ranged from 5.5 x 10^{-13} to 2.0 x 10^{-12} mol/s for Co, 5.1 x 10^{-14} to 2.0 x 10^{-12} mol/s for Cu, 2.6 x 10^{-12} to 1.9 x 10^{-11} mol/s for Ni, and 5.8 x 10^{-13} to 2.0 x 10^{-12} mol/s for Zn (Table 40). Peak Virginia Formation release rates during the entire period of record ranged from 1.0-6.7 x 10^{-12} mol/s for Co, 9.2 x 10^{-14} to 4.6 x 10^{-12} mol/s for Cu, 5.2 x 10^{-12} to 6.4 x 10^{-11} mol/s for Ni, and 1.1-7.1 x 10^{-12} mol/s for Zn.

ENP for Duluth Complex samples in Group III followed a similar pattern. The 1.40%S sample, for instance, had drainage below pH 7.0 very early and dropped below 3.5 before the end of the experiment. The ENPs calculated for this reactor at pH 6, 5, 4.5, 4, and 3.5 were 1.5, 3.8, 6.3, 10.4, and 13.1 mg $CaCO_3$/g rock, respectively (Table 21). In contrast to the results of Groups I and II, the NPs determined by the method of Sobek et al. (1978) (12-21 mg $CaCO_3$/g rock), were similar to the ENPs (Table 22). Virginia Formation samples had similar calculated ENPs to Duluth Complex samples (Table 21), despite being run for a much shorter period, but Virginia Formation NPs were generally lower.

5.3.1.3. Regressions Between pH, SO_4, Ca, Mg Release Rates and Solid Phase Composition

Sulfur depletion averaged 54.8% when determined as unleached solid %S minus sulfate release in leachate (Table 71). Sulfur depletion averaged 54.3% when determined as unleached solid %S minus leached solid %S (Table 71). There were large differences between methods for some samples, such as 103.7% for the sulfate method and 12.8% for the solids method with the 0.40%S sample. However, most samples had similar values between the two methods. Fifteen samples that had sulfur depletion determined using both methods. Of those, twelve had both values within 20% of the mean. A potential source of error for the leached solids analysis was that this was done on the replicate samples which were removed from the experiment long before the other samples. This would underestimate the loss of sulfur.

Sulfate release and pH were both correlated to the sample's sulfur content. Sulfate release increased with higher sulfur content (Figures 24-27, Table 34), with the greatest increases in periods B and C (slopes of average release = 1.03-1.35, r^2 = 0.52-0.78). Drainage pH decreased with higher sulfur content (Figures 20-23), with the steepest declines in periods A and B (slopes of average release = -1.69 to -1.37, r^2 = 0.34-0.45). Drainage pH was negatively correlated to average sulfate release (log transformed) for minimum, maximum, and average pH during all periods (Figures 28-31, Table 34). The greatest decreases in average releases occurred in periods A and B. Regression slopes of average release were from -1.65 to –1.17, and r^2 = 0.63-0.78.

Calcium and magnesium release was positively correlated to sulfate release (Figures 32-39, Table 34). The greatest increases were in periods C and D for both Ca (slopes of average releases = 0.59-0.60, r^2 = 0.68-0.94) and Mg (slopes of average releases = 0.94-1.42, r^2 = 0.60-0.88). When Ca and Mg release were added (Figures 40-43), the greatest increases were still in periods C and D (slopes of average releases = 0.71-0.92, r^2 = 0.94-0.97). Despite the rapid increase in Ca and Mg release, sulfate release rates were generally greater than the summation of Ca and Mg release in periods C and D, whereas they were more equal in periods A and B.

Metal content of unleached solids was not correlated to sulfur content for Co, Cu, Ni or Zn (Figures 44-47, r^2=0.03-0.08). However, metal release in leachate increased significantly with lower leachate pH for all four metals (Figures 16-19). Regressions of log metal release (mg/L) versus pH yielded slopes of -0.52 to -0.23, and r^2 of 0.25-0.54. Cobalt had a slope of –0.32, y-intercept of -0.54 and r^2 of 0.25 (Figure 48). Copper had a slope of –0.42, y-intercept of 0.37 and r^2 of 0.54 (Figure 49). Nickel had a slope of –0.52, y-intercept of 1.0 and r^2 of 0.41 (Figure 50). Zinc had a slope of –0.23, y-intercept of -0.63 and r^2 of 0.40 (Figure 51).

5.3.2. Leaching Effects

5.3.2.1. Particle Size

Leaching decreased the mean perimeter:area ratio of all samples 17% from 104 to 87 (Table 17). Mean particle diameter, determined assuming spherical particles, increased in leached samples. Leached particle diameter (46.6 μm) was 9% higher than unleached (42.9 μm). However, the effect differed among samples, with half showing a decreased ratio and half displaying an increase. Overall, there appeared to be no consistent effect of leaching on grain size and the decreasing ratio of perimeter to area is consistent with decreasing surface roughness.

Samples that had decreased ratios from leaching had higher initial ratios (127.1) than samples with increased ratios (81.3). The decreasing samples had a much larger mean change (-49.3%) than increasing samples (+8.8%). Of these six decreasing samples, three (0.58 (R15 & 16), 1.63 and 1.71%S) were the only photomicrographs which showed a much larger number of small particles in the unleached than leached samples (Figures 55, 56 for 0.58%S as example; Appendix 1, Attachment A1.2 for all samples). There was no obvious difference in drainage quality from these three samples when compared to others without an abundance of finer particles. Because these samples were mounted in epoxy whose surface was then polished (see Appendix 1, Attachment A1.2 for more detail on these methods), these smaller particles are not expected to be of the type examined in the particle cleaning analysis discussed in the next paragraph.

On uncleaned-leached, cleaned-leached and cleaned-unleached samples, adsorbed particulates were rare compared to uncleaned samples. These results were inferred from eight photos comparing washed and unwashed (Figure 57). The absence of detectable particles on the uncleaned-leached particles examined suggests that most surface particle were dissolved or washed off in the first 328 weeks. The samples that were compared likely overestimate the amount of adsorbed fines in the experiment as a whole, since they were both dry-sieved. Eleven of the twenty-five samples were wet-sieved and this would likely remove some of the adsorbed particles.

5.3.2.2. Chemistry

Total sulfur content of leached samples from the Duluth Complex declined to a range of 0.11-1.08%S (Table 4), which was 15-93% of original S, with a mean of 46%. This compares well with S depletion calculations based on measured sulfate in drainage, which had a range of 0-95% original S and a mean of 47% (Table 71). Evolved CO_2 did not exceed 0.11% in any sample and declined for all samples greater than 0.22%S. Loss on ignition (LOI2, adjusted for the difference in O between FeO and Fe_2CO_3) ranged from 1.3-3.4%. The major whole rock chemical constituents for all samples were SiO_2 (44.0-53.3%), Al_2O_3 (13.6-17.2%), CaO (0.6-8.8%), FeO (1.6-15.2%), and MgO (2.7-9.0%). Contents of K_2O (0.6-3.6%), Na_2O (1.2-2.7%), and TiO_2 (0.4-3.9%) were low (Table 4).

Total sulfur content of leached samples from the Virginia Formation declined to a range of 1.77-4.35%S, or 64-86% of original S, with a mean of 76%. Evolved CO_2 increased to greater than 0.62% for three of the four samples. Loss on ignition (LOI2, adjusted for difference in O between FeO and Fe_2CO_3) ranged from 2.8-12.5%. Virginia Formation samples continued to have higher percent Fe_2O_3, when compared to Duluth Complex samples.

Trace metal concentrations in leached samples remained similar to unleached quantities. Once again, the maximum reported value for most metals was less than 30 mg kg^{-1} (Ag, As, Bi, Cs, Dy, Er, Eu, Ga, Gd, Ge, Hf, Ho, In, La, Lu, Mo, Nb, Nd, Pb, Pr, Rb, Sb, Sm, Sn, Ta, Tb, Tl, Tm, Th, U, W, Yb). Metals (and their maximum concentration in mg kg^{-1}) present at higher concentrations were Y (217), Ce (46.8), Co (86), Zr (217), V (306), Zn (261), Sr (321), Ba (405), Cr (455), Ni (483), and Cu (>10000). The trace metal content of the leached samples displayed greater range than that of the unleached samples, especially copper. Cu concentrations for most of the samples ranged from 500 to 2000 ppm, with only one sample exceeding 2500 ppm. This sample (0.71% S) displayed Cu concentrations greater than 10000 ppm, and is therefore suspect due to the extreme nature of the value (Table 5). The only major differences between Duluth Complex and Virginia Formation samples were that Virginia Formation samples had lower Cu and higher Zn.

5.3.2.3. Mineralogy

5.3.2.3.1. Leaching Effects on Mineral Content

Of the 25 samples that underwent unleached chemical analyses, ten (two from 0.58%S) were analyzed using point count to determine the effects of leaching on mineralogy of all minerals. These samples leached for 144-328 weeks prior to termination. Chemical analysis of pyrrhotite, chalcopyrite and pentlandite showed the losses of sulfide mineral when compared to unleached samples, with the exception of the 0.71%S which showed a significant increase in copper content in the leached sample possibly due lack of a representative sample. Average sulfide mineral percent depletion decreased in the order Po>Pn>Cp with values of 64, 40, and 10% depletion, respectively (Table 9). Pyrrhotite grains were generally found in highly altered states, if at all, whereas chalcopyrite remained less altered in all samples (Tables 14, 15). This indicates that pyrrhotite underwent dissolution at a significantly higher rate than chalcopyrite. Microprobe analysis of pentlandite, pyrite and cubanite failed to detect grains in both unleached and leached analyses of any sample, so there was no way to determine oxidation of these minerals using point count.

Samples' silicate minerals displayed similar content to corresponding unleached samples, with plagioclase, augite, hypersthene, and olivine comprising 74-94% weight of samples. The percentage is slightly higher in the leached specimens than in the unleached materials. Other minerals, including amphibole, biotite, muscovite, chlorite, and cordierite were observed in approximately the same quantities as in unleached materials (Tables 7, 8).

5.3.2.3.2. Leaching Effect on Mineral Chemistry

Leached Duluth Complex sulfide minerals had the following range of stoichiometric coefficients: pyrrhotite $Fe_{7.48-7.60}S_8$, pyrite $Fe_{4.59}S_8$, chalcopyrite $(Cu_{4.22-4.38}Fe_{4.43-4.57})S_8$, and cubanite $(Cu_{2.75-2.99}Fe_{5.57-6.13})S_8$ (Table 12).

Leached Duluth Complex silicate minerals had the following range of stoichiometric coefficients: plagioclase $(Ca_{0.43-0.55}Na_{0.37-0.49})Al_{1.47-1.62}Si_{2.42-2.53}O_8$, augite $((Ca_{0.76-0.95}Na_{0.01-0.02})(Mg_{0.45-0.78}Fe_{0.35-0.54}Ti_{0.01-0.02})(Si_{1.95-2.00}Al_{0.06-0.09})O_6)$, hypersthene $((Mg_{0.92-1.11}Fe_{0.72-1.00})_2Si_{1.96-2.00}O_6)$, and olivine $((Mg_{0.70-1.14}Fe_{0.83-1.27})Si_{1.00-1.01}O_4)$ (Table 13).

5.3.2.3.3. Leaching Effects on Mineral Grain Coatings

Evidence for alteration of sulfide minerals during leaching was obtained in microprobe analysis of leached samples, with almost all sulfide minerals displaying oxide coatings and only limited coatings on some silicate minerals.

When pyrrhotite was observed, Fe-oxy-hydroxide coatings were generally present both on mineral surfaces and along parting planes within the minerals (Figure 58 for example). The latter observation is apparently the "veined" occurrence referred to by Jambor (2003). When measured, coating thicknesses ranged from 2-14 microns. Chalcopyrite coatings were also observed (Figure 59 for example), but these coatings were typically thinner than pyrrhotite at 0-6 microns, although some were observed at 10 microns. Consistent with section 5.3.2.3.1, this indicates that the extent of pyrrhotite leaching was greater than that of chalcopyrite leaching.

The 0.58%S unleached samples contained pyrrhotite and chalcopyrite in a 3:1 ratio, but slightly altered chalcopyrite grains were the dominant sulfides present in the leached solid. In the two leached 0.58%S samples, one sample (R16) had only one pyrrhotite grain, which was nearly completely altered and replaced by oxide minerals. The other sample (R15) had a 2:1 pyrrhotite: chalcopyrite ratio, but the pyrrhotite had oxide coatings 2-14 μm thick. Seven of the remaining ten leached samples (0.41, 0.51, 0.71, 1.16, 1.40, 1.44, and 1.63%S) had similar results, with many slightly- to moderately-altered chalcopyrite grains and few, highly altered pyrrhotite grains. In the 0.22, 0.40 and 1.71%S samples, more pyrrhotite grains were observed, but were once again more highly altered than nearby chalcopyrite grains, with the exception of the 1.71%S sample which had little sulfide alteration. In samples that leached for a short period of time, such as the 1.71%S sample, or a sample with relatively low solid-phase sulfur content (<0.40%S), pyrrhotite grains had a thin Fe-oxy-hydroxide coating, whereas chalcopyrite grains remained completely unreacted. In samples leached for longer periods of time or with higher sulfur content (>0.40% S), pyrrhotite grains showed evidence of advanced dissolution or were completely reacted away, whereas most chalcopyrite grains had a marginal coating, indicating a lesser degree (or slower rate) of dissolution (Table 16).

Coatings on sulfide grains provided information about the nature of leaching, as well as supplying a means of quantifying the extent of leaching within the sample. Coatings were typically a SiO_2-Fe-oxide-hydroxide phase. These coatings varied from just a few microns thick on non-reactive grains to complete replacement of sulfide mineral grains (Figure 58). It was found that sulfide minerals leached at different rates. Iron-bearing sulfides like pyrrhotite reacted much faster than Cu-bearing sulfides, such as chalcopyrite (Table 16).

Silicate minerals showed limited signs of dissolution. The lower sulfur samples (0.22 and 0.40%S) displayed no evidence of mineral dissolution, either from coatings or alteration features. As sulfur content increased, dissolution or alteration features increased in prevalence (Figure 59). The 0.58%S sample included several hypersthene grains with oxide coatings. More alteration was seen in the 1.16 and 1.40%S samples, where dissolution pits and grooves are found in plagioclase, amphibole, hypersthene, and olivine grains. Oxide coatings of 0-3 μm were observed on both olivine and hypersthene grains, and several greenalite-coated olivine grains were also observed. The 1.63%S sample contained several olivine and hypersthene grains with andesine coatings (Appendix 1, Attachment A1.2). Coatings were thicker on olivine grains in this sample, ranging from four to six microns. In general, as solid-phase sulfur content increased dissolution of silicate minerals also increased, in response to increased acid production. This resulted in increased thickness of coatings and extent of alteration features on silicate minerals in high sulfur solids (Table 15).

During microscopic analysis, several hypersthene and olivine grains were found with alteration structures. These alterations are unlike the oxide coatings found on other leached mineral grains, but it is not clear whether the alteration products are pre- or post-leaching. The dominant alteration phases observed are greenalite and serpentine. Pre-leaching weathering of the sample or some form of in situ alteration (serpentinization) could have produced these phases before any leaching from the experiment occurred. These phases may not have been observed in any unleached samples due to the small overall number of points counted, a possibility discussed earlier in this report (Table 15).

5.4. Mineral Dissolution

Mineral dissolution was examined through the use of several models. Models 1-4 determined silicate mineral dissolution rates based on an initial assumption of specific mineral contributing the observed release of a given solute. From this foundation, rates of dissolution of five to six other minerals were calculated using both logical inference and necessary assumptions. Model 1 was based on Ca, model 2 on Mg, model 3 on Na, and model 4 on K. Results of these models were compared in four different periods (A-D). Models 1-4 were also compared among sample groups and among three pairs of samples with different mineral and chemical composition.

Models 1-4 are numbered from what are considered strongest to weakest. Calcium and Mg-based models are preferred because all samples have analyses of these elements throughout the experimental period (144-1252 weeks). Sodium and potassium analyses were run much later in the experiment than other parameters and for many of the samples measurements were not collected for the first 300-400 weeks of dissolution, making models 3 and 4 less preferred. All sample periods mentioned match those described in earlier sections. Again, it should be noted that reactors 39-44 were stored for 8 to 20+ years prior to dissolution testing and therefore produced higher drainage pH and lower sulfate and metal release rates. These reactors are included in the following results section and the differences in drainage pH and release rates will be neglected.

Potential gibbsite production was also calculated to determine whether this mineral's neutralizing capacity could explain the common sample pH minimum of approximately 4.0. Oxidation of pyrrhotite alone, as well as all sulfide minerals combined was determined and compared among sample groups.

Likely mineral sources of Co and Ni were determined using calculations based on solid and leachate chemistry, as well as mineral abundance. These metals had multiple potential mineral sources, unlike Cu and Zn. Copper was likely from chalcopyrite and cubanite, while Zn was likely from sphalerite (McSwiggen 1999).

5.4.1. Silicate Dissolution Models

5.4.1.1. Plagioclase

Calculated plagioclase rates among the first three silicate dissolution models had similar patterns. Dissolution was usually greatest during period A, declined to its lowest rates in period B, increased in period C, and declined again in period D. Model 1 generally had the highest single and average rates.

Initially, potassium was used to determine plagioclase dissolution for model 4. However, in three samples with no biotite or potassium feldspar detected (0.72, 0.92 and 1.16%S), predicted plagioclase dissolution rates were approximately 20-120 times higher than comparable rates predicted by models 1-3, as well as generally higher than literature dissolution rates at comparable pH (e.g., Oxburgh et al. 1994). Because of this disparity, model 4 plagioclase dissolution was computed in the same manner as model 3.

During period A, average plagioclase dissolution ranged from 6.2×10^{-13} to 5.7×10^{-12} mol m^{-2} s^{-1}, with the highest rate in model 1 and the lowest in model 3 (Tables 52-54). Because of the lack of Na data for early samples, model 3 had only six samples during period A. The rates for model 3 samples were generally lower than results for the same samples using different models. The highest sample rate was 4.1 x 10^{-11} mol m^{-2} s^{-1} in model 1 and the lowest rate was zero in model 2.

During period B, average plagioclase dissolution ranged from 3.4 x 10^{-13} to 1.5 x 10^{-12} mol m^{-2} s^{-1} in the three models, with the highest rate in model 1 and the lowest in model 2 (Tables 52-54). The lack of Na data for samples initiated in 1989-1990 continued to limit data available for modeling, but there was an increase to nine samples with available Na data for modeling during period B. The highest sample rate was 9.3 x 10^{-12} mol m^{-2} s^{-1} in model 1 the lowest rate was zero in model 2.

During period C, average plagioclase dissolution ranged from 3.3 x 10^{-13} mol m^{-2} s^{-1} for model 2 to 9.2 x 10^{-13} mol m^{-2} s^{-1} for model 3 (Tables 52-54). Model 1 rates, which were the same as the average rates from period B because of model design, were higher than the other two models. Between models 2 and 3, the highest sample rate was 4.1 x 10^{-12} mol m^{-2} s^{-1} in model 2 and the lowest rate was zero in model 2.

During period D, average plagioclase dissolution ranged from 4.1 x 10^{-13} mol m^{-2} s^{-1} for model 2 to 1.3 x 10^{-12} mol m^{-2} s^{-1} for model 1 (Tables 52-54). The highest sample rate was 4.6 x 10^{-12} mol m^{-2} s^{-1} in model 1 and the lowest rate was zero in model 2.

Maximum plagioclase dissolution rates were determined based on sample stoichiometry and cumulative Ca release. Rates increased from group I, with an average of 1.0 x 10^{-9} mol m^{-2} s^{-1}, to group III, with an average of 1.9 x 10^{-9} mol m^{-2} s^{-1} (Table 51).

Observed Ca and Na release was compared to the solid phase Ca: Na ratio in plagioclase (section 4.4.5.2). In general, the Ca:Na ratio was higher in the observed drainage quality than was expected compared to the solid-phase stoichiometric Ca:Na ratio in plagioclase (Appendix 7, Figures A7.1-A7.21). The solid-phase average ratio ranged from 0.7 – 2.0, with an overall average value of 1.2. Whereas the average Ca:Na ratio in the drainage quality ranged from 1.9-23, with an overall average value of 4.7. This may indicate that there was preferential dissolution of calcium. The observed Ca:Na ratio may also be higher due to other sources of Ca release (i.e. augite), which are not accounted for in this analysis. A number of reactors (0.41, 0.51, 0.71, 1.16, 1.40, 1.44%S) displayed stoichiometric release of plagioclase early in the experiment (weeks 100-235). However the observed Ca:Na release ratio increased considerably as drainage pH decreased below 4.4, which could be associated with augite dissolution under acidic conditions. Future reporting should examine this in more detail.

5.4.1.2. Augite

Calculated augite dissolution rates in models 2, 3, and 4 were usually greatest during period A, declined in period B, increased in period C, and declined in period D to levels similar to period B. Model 1 calculated augite dissolution only during acidic conditions (period C). These values were the lowest calculated for all four models. Augite dissolution was calculated in model 4 in the same manner as model 3.

During period A, average augite dissolution ranged from 8.8 x 10^{-12} mol m^{-2} s^{-1} in model 3 to 9.5 x 10^{-12} mol m^{-2} s^{-1} in model 2 (Tables 53-56), with no augite dissolution determined in model 1. Because of the lack of Na and K data for early samples, period A of models 3 and 4 had only six samples. Augite dissolution rates for all samples in model 3 were lower than those in model 2. The highest sample rate was 5.0 x 10^{-11} mol m^{-2} s^{-1} in model 2 and the lowest rate was 1.1 x 10^{-12} in model 3.

During period B, average augite dissolution ranged from 1.9 x 10^{-12} mol m^{-2} s^{-1} in model 3 to 3.5 x 10^{-12}

mol m^{-2} s^{-1} in model 2 (Tables 53-56), with no augite dissolution determined in model 1. Because of the lack of Na and K data for early samples, models 3 and 4 had only nine samples during period B. The highest sample rate was 2.2 x 10^{-11} mol m^{-2} s^{-1} (model 2) and the lowest rate was zero (model 3).

During period C, average augite dissolution ranged from 3.3 x 10^{-12} mol m^{-2} s^{-1} in model 1 to 6.7 x 10^{-12} mol m^{-2} s^{-1} in model 2 (Tables 53-56). The highest rate among samples was 5.9 x 10^{-11} mol m^{-2} s^{-1} in model 2 and the lowest rate was zero in models 1 and 3.

During period D, average augite dissolution ranged from 1.3-2.3 x 10^{-12} mol m^{-2} s^{-1} with the highest rate in model 2 and the lowest in model 4 (Tables 53-56), and no augite dissolution determined in model 1. The highest sample rate was 1.4 x 10^{-11} mol m^{-2} s^{-1} in model 2 and the lowest rate was zero in model 3.

5.4.1.3. Hypersthene, Olivine and Biotite Dissolution

In models 1-3, calculated dissolution rates for ferromagnesian metals increased from periods A-C, and then declined to their lowest levels in period D. Model 4 rates behaved differently between the three minerals. Model 4 hypersthene and olivine rates decreased from period A to B, increased to the highest rates in period C and decreased in period D. Model 4 biotite rates decreased from periods A to C and then increased in period D. Model 1 had the highest average rates for all ferromagnesian metals in all periods.

During period A, average hypersthene dissolution ranged from 6.7 x 10^{-13} mol m^{-2} s^{-1} in model 2 to 5.5 x 10^{-12} mol m^{-2} s^{-1} in model 1 (Tables 52-56). Average olivine dissolution ranged from 4.3 x 10^{-13} mol m^{-2} s^{-1} in model 4 to 1.7 x 10^{-11} mol m^{-2} s^{-1} in model 1. Average biotite dissolution ranged from 1.3 x 10^{-13} mol m^{-2} s^{-1} in model 3 to 1.5 x 10^{-11} mol m^{-2} s^{-1} in model 4. For all samples, the highest rates for hypersthene, olivine, and biotite were 4.0 x 10^{-11}, 2.0 x 10^{-10}, and 6.2 x 10^{-11} mol m^{-2} s^{-1}, respectively, and they all occurred in model 1. All three minerals had a minimum sample rate of zero in models 2 and 3.

During period B, average hypersthene dissolution ranged from 6.9 x 10^{-13} mol m^{-2} s^{-1} to 3.4 x 10^{-12} mol m^{-2} s^{-1} in models 4 and 1, respectively (Tables 52-56). Average olivine dissolution ranged from 3.1 x 10^{-13} mol m^{-2} s^{-1} to 9.1 x 10^{-12} mol m^{-2} s^{-1} in models 4 and 1, respectively. Average biotite dissolution ranged from 2.8 x 10^{-12} to 1.0 x 10^{-11} mol m^{-2} s^{-1} in models 2 and 4, respectively. Hypersthene's highest sample rate was 2.9 x 10^{-11} mol m^{-2} s^{-1} in model 1, olivine's was 5.4 x 10^{-11} mol m^{-2} s^{-1} in model 1, and biotite's was 5.3 x 10^{-11} mol m^{-2} s^{-1} in model 4. All three minerals had a minimum sample rate of zero in models 2 and 3.

During period C, average hypersthene dissolution ranged from 2.7-4.4 x 10^{-12} mol m^{-2} s^{-1} in models 4 and 1, respectively (Tables 52-56). Average olivine dissolution ranged from 7.0 x 10^{-12} mol m^{-2} s^{-1} in model 4 to 1.6 x 10^{-11} mol m^{-2} s^{-1} in model 1. Average biotite dissolution ranged from 3.4-6.0 x 10^{-12} mol m^{-2} s^{-1} in models 2 and 1, respectively. For all samples, the highest rates for hypersthene, olivine, and biotite were 3.1 x 10^{-11}, 6.8 x 10^{-11}, and 3.3 x 10^{-11} mol m^{-2} s^{-1}, respectively, and they all occurred in model 1. All three minerals had a minimum value of zero in models 1, 2 and 3.

During period D, average hypersthene dissolution ranged from 1.3 x 10^{-13} mol m^{-2} s^{-1} in model 2 to 1.1 x 10^{-12} mol m^{-2} s^{-1} in model 1 (Tables 52-56). Average olivine dissolution ranged from 2.4 x 10^{-13} mol m^{-2} s^{-1} in model 4 to 5.0 x 10^{-12} mol m^{-2} s^{-1} in model 1. Average biotite dissolution ranged from 2.6 x 10^{-13} mol m^{-2} s^{-1} in model 2 to 4.4 x 10^{-12} mol m^{-2} s^{-1} in model 4. Hypersthene's highest sample rate was 7.0 x 10^{-12} mol m^{-2} s^{-1} in model 1, olivine's was 3.2 x 10^{-11} mol m^{-2} s^{-1} in model 1, and biotite's was 4.1 x 10^{-11} mol m^{-2} s^{-1} in model 4. All minerals had a minimum sample rate of zero in models 2 and 3.

Maximum olivine dissolution rates were determined based on sample stoichiometry and cumulative Mg release. Group I had an average of 4.1 x 10^{-9} mol m^{-2} s^{-1}, group II had an average of 3.0 x 10^{-9} mol m^{-2} s^{-1}, and group III had an average of 1.0 x 10^{-8} mol m^{-2} s^{-1} (Table 51).

5.4.1.4. Orphan Calcium

The potential for Ca release not attributed to any specific mineral occurred in period C of Model 1 and all periods of model 3. In model 3, average orphan Ca release declined throughout the experiment from 3.7 x 10^{-12} mol m^{-2} s^{-1} in period A to 3.6 x 10^{-13} mol m^{-2} s^{-1} in period D (Table 55). During period C, average orphan Ca in model 1 was 25% of that in model 3 (Table 52).

5.4.1.5. Potassium Feldspar

Potassium feldspar dissolution rates were only determined in model 4 because of its limited importance in modeled elements other than potassium. Average dissolution rates declined every period from 2.5 x 10^{-10} mol m^{-2} s^{-1} in period A to 1.8 x 10^{-11} mol m^{-2} s^{-1} in period D. The maximum dissolution rate of 4.7 x 10^{-10} mol m^{-2} s^{-1} occurred in period A, while the minimum rate of 6.3 x 10^{-13} occurred in period D (Table 56).

5.4.1.6. Comparison of Sample Groups and Specific Samples with Varying Mineralogies

Group III samples usually had the highest release rates regardless of mineral, model or period (Tables 60-63). In periods A and B of models 3 and 4, when there were no data for group III samples, group II generally had the fastest rates.

To compare model consistency among samples with different mineral contents, three pairs of individual samples were chosen. Dissolution rates of plagioclase, augite, hypersthene, olivine, and biotite were compared among models within pairs to determine consistency of model results for similar samples. Dissolution rates among sample pairs for each model were also compared to determine how mineral content differences affected model results (Tables 64-67, Figures 73-77).

The first pair of samples (0.72 and 1.16%S) had the most Ca, Na and K (>76%) contained in plagioclase, while most Mg (51-85%) was in olivine. The second pair of samples (0.67 (R40) and 0.82%S) had Na distribution similar to the first pair (99-100% in plagioclase), but differed in the distribution of Ca (67-68% in plagioclase), Mg (26-29% in augite) and K (67-69% as biotite). The third pair (1.40 and 1.64%S) had Ca (61% in plagioclase), Mg (35-36% in augite) and Na (97-98% in plagioclase) distribution similar to the second pair, but had most K (61-68%) as potassium feldspar.

Plagioclase typically had the best agreement between models 1-4, where in 8 of the 11 cases, the range in calculated plagioclase dissolution was less than a factor of 4. The best agreement in calculated plagioclase dissolution occurred in model 3. Biotite typically had the worst agreement between models 1-4, where in only 1 out of 11 cases, the range in calculated biotite dissolution was less than a factor of 3. It should be noted that the samples in set 1 (0.72 and 1.16%S) did not contain biotite.

Model 3 typically had the best agreement for each sample set where in 10 of the 18 cases, the range in calculated dissolution rates was less than a factor of 5. Agreement in model 3 was the best during period B. Model 2 typically has the worst agreement for each sample set where in only 4 out of 19 cases, the range in calculated dissolution rates were less than a factor of 4.

Rate period A typically had the best agreement for each sample set, where in 8 of the 16 cases, the range in calculated dissolution rates was less than a factor of 5. Agreement during period A was the best for calculated plagioclase dissolution rates. Rate period C typically had the worst agreement for each sample set, where in only 4 out of 18 cases, the range in calculated dissolution rates were less than a factor of 3.

5.4.2. Gibbsite Production

Potential gibbsite production was determined at the point pH dropped below 4.0, or at minimum pH where samples never had pH less than 4.0. Dissolution of maximal amounts of gibbsite was well in excess of acidity production for all samples except 1.44%S (Table 68).

5.4.3. Pyrrhotite and Combined Sulfide Minerals Oxidation Models

Oxidation of pyrrhotite and all sulfide minerals declined from period A to B, rose in period C, then declined in period D. Both pyrrhotite and all sulfide rates were highest in period C with average rates of 4.2×10^{-10} mol m^{-2} s^{-1} and 3.8×10^{-10} mol m^{-2} s^{-1}, respectively (Tables 69, 70). Average oxidation rates were approximately 10-20% higher for pyrrhotite than the combined sulfide minerals in periods B, C, and D.

When comparing results among sample groups, the pyrrhotite model had varied results with the fastest rates in period A for group I and period C for groups II and III. When modeling all sulfide minerals, group III had the fastest oxidation rates in period C, followed by group II in period C. Both the dependence of rate on period and group reflect the correlation of sulfide oxidation and pH.

5.4.4. Mineral Sources of Co and Ni

Cobaltite, (Co, Fe)AsS, is a common mineral source of Co. However, As in unleached solids is quite low for Duluth Complex samples (Table 3). To determine the maximum percent of cobalt present as cobaltite in these samples, As:Co ratios were determined. Thirteen of twenty-one samples had nondetectable As, while the remaining samples had As:Co ratios of 5.4-19.2% (mean 11.2%, 5.0% SD). Virginia Formation samples had ratios of 9.2-31.8% (mean 20.6%, 9.9% SD).

Maucherite ($Ni_{11}As_8$) is not a potentially important source of Ni for reasons similar to cobaltite. Duluth Complex samples had maximum Ni contributions of 1.6-7.9% (mean 3.6%, 2.1% SD) from maucherite. Virginia Formation samples had maximum contributions of 2.0-5.9% (mean 4.1%, 1.6% SD).

The major potential sources of Ni in these samples were pentlandite ($(Ni, Fe)_9S_8$), pyrrhotite ($Fe_{1-x}S$), and olivine ($(Mg,Fe)_2SiO_4$). In order to determine the possible sources, Ni content was analyzed in olivine, pyrrhotite, and pentlandite (only two grains identified in all samples) in the solid-phase samples. Expected Ni release was then determined from samples based on magnesium (olivine originated) and sulfate (sulfide mineral originated) release rates. Because only two grains of pentlandite were located in the Duluth Complex samples, it was necessary to estimate the nickel present in sulfides based on sample composition to estimate nickel release from sulfide minerals. These predicted values were compared to actual Ni release to ascertain likely sources of Ni in leachate. Finally, maximum olivine Ni release rates from the samples were estimated.

Most of the Ni in the solids was calculated to be present in sulfides, ranging from 66 to 100 percent in 18 of 21 samples (Table 42). The two samples in which all Ni was calculated to be present in sulfides contained no olivine. The fraction of Ni present in sulfides for the remaining three samples ranged from

–25% (0.92%S, see methods for possible sources of error), to 28 percent. Solid-phase analysis indicated Ni was a stoichiometrically low proportion of olivine (0.002 mol Ni/ mol ol, Table 42) and pyrrhotite (0.031 mol Ni/ mol po, Table 10). Pentlandite had the highest concentration of Ni at 4.88 mol Ni/ mol pent (Table 10).

The average aqueous release Ni/Mg ratio for all samples was approximately 29 – 87 times higher than the ratio found in olivine (Table 43). The three group I samples (0.18, 0.22, 0.72%S) had average release Ni/Mg ratios more similar to olivine (aqueous average 3-4 times ol ratio). Group I samples were the only samples to never decline below pH 6 for an extended period (Table 27).

When maximum olivine Ni release was calculated based on Mg release in leachate, calculated Ni release from olivine averaged <15% of actual Ni release (Table 44). Linear regression showed a significant positive correlation between sample sulfur content and calculated:observed Ni release in periods C and D (Table 45, Figure 62). In periods C and D, lower sulfur samples were absent. The increase in calculated release from olivine is due to increased Mg release. The increased Mg release likely resulted from increasing Mg-bearing mineral dissolution due to lower pH.

To determine the maximum possible rate of Ni release from olivine, the rate of observed Ni release was divided by the number moles of olivine present. This assumed that all Ni was the result of olivine dissolution. The rate range of group I samples (0.18, 0.22, 0.72 %S) was 4.9×10^{-8} to 2.3×10^{-6} mol Ni · $(\text{mol ol})^{-1}$ · week^{-1} (Table 46). The rate range of the two high-olivine (0.57, 0.92%S) samples with lower pH minima was 7.9×10^{-7} to 7.7×10^{-6} mol Ni · $(\text{mol ol})^{-1}$ · week^{-1}. Linear regression of all rates in Table 46 showed significant positive relationships between (mol Ni) · $(\text{mol ol})^{-1}$ · week^{-1} and %S (Table 47, Figure 63). The slopes of time periods B and C, which occurred after the initial rapid release of period A, were very similar.

Predicted Ni release from sulfide minerals was also determined using observed sulfate release multiplied by the Ni/S ratio in the sulfides. As can be seen in Figure 64, the predicted values are often higher than observed Ni release. For all samples, the median ratio of predicted to observed nickel release was 2.9. This data was broken into the rate periods A through D and cumulative probability distribution graphs were generated to determine the relationship between the ratio of predicted to observed Ni release as a function of pH (Figure 65). Looking at the cumulative probability of predicted vs observed Ni release for each rate period, periods A and B are fairly similar, with median values of 2.6 and 1.8, respectively. As pH decreased in period C, nickel release increased significantly, resulting in predicted values much closer to observed, with a 75th percentile predicted vs. observed nickel release ratio less than 5. As pH increased in period D, nickel release decreased much faster than sulfate release, resulting in higher predicted vs. observed nickel release ratios (median value of 9).

When comparing spikes in Ni release for individual samples in time series data to Mg and sulfate spikes (Appendix 3, Figures A3.1-A3.44), sulfate spikes generally matched the Ni spikes best. Of the twenty samples examined, sulfate spikes were the most similar to Ni spikes in eight samples (0.18, 0.22, 0.40, 0.41, 0.51, 0.54, 0.67 (R39), 0.82%S), while both Mg and sulfate were equally matched with Ni in four samples (0.67 (R40), 1.16, 1.40, 1.44%S). Six samples had Mg spikes more closely matching Ni (0.57, 0.58, 0.71, 1.12, 1.63, 1.71%S). Two samples had neither sulfate nor Mg dynamics that matched Ni (0.92 and 1.64%S). For group II and III samples, when drainage pH declined into acidic conditions, there was generally a corresponding spike in Mg release.

6. DISCUSSION

6.1. Introduction

The general objective of these experiments was to correlate rock composition and drainage water quality to aid in predicting management concerns for mining operations in the Duluth Complex of Northeastern Minnesota. The Duluth Complex is a large copper and nickel resource (Kingston et al. 1970), and contains elevated levels of platinum group elements (Anonymous 1992). Growing interest in mining of these resources highlights the importance of long-term studies, like this one, that will aid in determining drainage quality from mine wastes over time scales of decades to centuries.

Twenty-one samples with sulfur contents from 0.18-1.71% were ground to a well-defined size to maximize liberation of sulfide minerals and characterized with respect to chemistry, mineral content, and mineral chemistry. Weekly water additions over 144-1252 weeks allowed samples to fully dry each week in a sample chamber that was temperature and humidity-controlled. Leachate samples were analyzed to determine pH, sulfate, Ca, Mg, Na, and K (frequency varied among samples and analytes, Table 6). Cobalt, Cu, Ni, Zn, Fe, Al and Si were analyzed less frequently. Photomicrographs of unleached and leached samples were used to assess solid surfaces for evidence of mineral oxidation and dissolution. The results of this study allowed categorization of sample water quality based on duration of leaching and rock chemistry. These categories will aid in predicting treatment needs of mining wastes in the Duluth Complex.

The Duluth Complex samples came from three locations (Table 1). All seventeen Dunka blast hole samples were from the South Kawishiwi intrusion near Babbitt, Minnesota, and the only ARIMETCO and the three AMAX samples came from the Babbitt/Mesaba deposit of the Partridge River intrusion. The four Virginia Formation samples (2.06 ≤ %S ≤ 5.44, all Dunka blast hole) were terminated after 78 weeks of dissolution. During the short period of record, sulfate and pH behaved similarly to the higher %S Duluth Complex samples, though the changes proceeded more rapidly due to the higher S content. The data indicated that waste rock with sulfur content in this range would produce drainage in need of rigorous environmental controls. It was concluded that testing of rock with lower sulfur contents would provide information more beneficial to environmental mine waste management planning than continuation of the higher sulfur samples already known to produce strongly acidic drainage. Because of the differences in chemistry and experimental duration, this discussion is limited to Duluth Complex samples. Section 5.0 briefly addresses the drainage quality from these samples and all drainage quality data is presented in Appendix 3.

It should also be noted that reactors 39-44 have been omitted from the discussion section (with the exception of section 6.7.4). These samples were stored for 8 to 20+ years before dissolution testing, resulting in higher drainage pH and lower release rates compared to other Dunka blast hole samples. In addition, since these were initiated 7 to 8 years after reactors 1-38, these samples represent different analytical periods. Elimination of reactors 39-44 focuses this discussion section specifically on South Kawishiwi intrusion (SKI) samples. It should be noted that two of these reactors contained Dunka blast hole samples. These weathered samples displayed higher drainage pH and lower release compared to "fresh" samples (Appendix 7, Attachment A7.2). For drainage quality results on the Partridge River intrusion (PRI) and South Kawishiwi intrusion (SKI) samples, see results section 5.0.

Although the dissolution tests remain in progress for a subset of samples, the following discussion presents the first 24 years of data. The dissolution tests were conducted to determine the variation of drainage pH with sulfur content, categorize the samples based on this examination, and determine the variation of sulfate and major cation release rates with sulfur content. This data was also used to determine the variation of metal release with drainage pH and examine possible mineral sources of metals. In addition, these data were used to determine rates of sulfide oxidation and silicate dissolution as a function of time and drainage pH and provide a comparison with reported literature rates.

6.2. Sample Classification

Duluth Complex samples were divided into three groups based on the observation that drainage pH decreased as the solid-phase S content of samples increased.

Group I: $0.18 \leq \%S \leq 0.22$
Group II: $0.40 \leq \%S \leq 0.70$
Group III: $0.70 < \%S \leq 1.64$

Although there were some exceptions to the %S ranges stated above, these were all from samples with prolonged storage periods (0.72%S in group I; 0.82, 0.92, 1.71%S in group II). When sulfate release rates from the three AMAX samples from the present project (0.72, 0.92, 1.71%S), were compared to freshly ground samples of the same rock (0.59, 0.80, 1.87%, respectively) (Lapakko 1993a), rates of the stored samples were only 25-80% of the fresh samples (Appendix 7, Table A7.1). The prolonged storage might have resulted in formation of sulfide mineral coatings, which would cause slowing rates of acid production from sulfide oxidation. Janzen et al. (2000) has reported this phenomenon for pyrrhotite. Janzen stored two samples for 15 months in a desiccator and found the pyrrhotite surface areas had decreased by 85-90 percent.

Sulfate release and attendant acid production increased with sample group %S, while other release rates followed this trend due to decreasing pH. Minimum pH decreased as group solid-phase sulfur content increased. Metal release rates (Co, Cu, Ni, Zn) also increased with group sulfur content. Sodium and potassium had more limited sampling, but were much more similar among groups than other ions.

Group I had sulfur contents ranging from 0.18 to 0.22 % and typically produced drainage pH values of at least 6. Minimum pH ranged from 5.7-5.9 (mean 5.8, Table 80), but pH was generally between pH 6-6.5 by week 150. Average sulfate release rates were from 2.3×10^{-12} to 1.2×10^{-11} mol/s (Table 81). Average Ca release was 3.1×10^{-12} to 1.8×10^{-11} mol/s (Table 82). Average Mg release was 2.3×10^{-12} to 1.6×10^{-11} mol/s (Table 83). The range of average Na release was $1.3\text{-}1.4 \times 10^{-12}$ mol/s (Table 85). Average potassium release ranged from $3.3\text{-}5.7 \times 10^{-12}$ mol/s (Table 86). Average metal release rates ranged from 6.6×10^{-15} to 5.1×10^{-14} mol/s for Co, $2.1\text{-}4.3 \times 10^{-14}$ mol/s for Cu, $1.7\text{-}9.2 \times 10^{-14}$ mol/s for Ni, and $4.6\text{-}6.6 \times 10^{-14}$ mol/s for Zn (Tables 89-92). The circumneutral pH resulted in relatively low trace metal release, due to low metal solubility.

Group II had sustained minimum pH of 4-5 and $0.40 \leq \%S \leq 0.70$. Minimum pH ranged from 3.8-4.1 (mean 4.3, Table 80), and occurred between weeks 115-770. Average sulfate release rates were from 8.3×10^{-12} to 5.1×10^{-11} mol/s (Table 81). Average Ca release was 3.1×10^{-12} to 3.7×10^{-11} mol/s (Table 82). Average Mg release was 5.9×10^{-13} to 1.6×10^{-11} mol/s (Table 83). Na release rates ranged from 8.0×10^{-13} to 3.7×10^{-12} mol/s (mean 2.3×10^{-12} mol/s) (Table 85). Potassium release rates were from 3.7×10^{-13} to 7.6×10^{-12} mol/s (mean 3.9×10^{-12} mol/s) (Table 86). Average metal release rates ranged from 4.9×10^{-15} to 2.5×10^{-13} mol/s for Co, 5.2×10^{-14} to 3.4×10^{-12} mol/s for Cu, 7.3×10^{-14} to 1.6×10^{-12} mol/s for Ni, and 2.4×10^{-14} to 2.7×10^{-13} mol/s for Zn (Tables 89-92).

Group III had sustained minimum pH < 4 and $0.70 < \%S \leq 1.71$. Minimum pH ranged from 3.0-3.5 (mean 3.3, Table 80), and occurred between weeks 274-362. Average sulfate release rates were from 1.1×10^{-11} to 1.9×10^{-10} mol/s (Table 81). Average Ca release was 3.1×10^{-12} to 5.8×10^{-11} mol/s (Table

82). Average Mg release was 2.2×10^{-12} to 4.4×10^{-11} mol/s (Table 83). Sodium release was similar to that of samples from groups I and II, with average values remaining relatively constant below 6.4×10^{-12} mol/s (Table 85). Potassium release rates were similar to Group II samples (1.5×10^{-12} to 1.6×10^{-11} mol/s) (Table 86). Average metal release rates ranged from 6.8×10^{-15} to 2.1×10^{-12} mol/s for Co, 4.8×10^{-14} to 7.2×10^{-12} mol/s for Cu, 3.7×10^{-14} to 2.2×10^{-11} mol/s for Ni, and 4.0×10^{-14} to 7.2×10^{-13} mol/s for Zn (Tables 89-92).

6.3. Temporal Variation

There were typical changes in water quality that occurred sequentially within sample groups. These changes were driven by the balance between rates of acid production associated with sulfate release and neutralization from cation release. Water quality changes were characterized using four sequential periods (A-D). These periods were defined by typical changes in pH, SO_4, Ca and Mg (section 5.3.1.1). Drainage pH generally declined throughout the first three periods and rose in the fourth. Periods A and B were shorter for samples with greater %S (i.e., pH declined more rapidly), and some samples did not enter periods C and D. Calcium and Mg release rates were highest in period A, declined in period B, rose in period C and declined again in period D. Sulfate release followed a similar pattern of increases and declines, but the highest release rates were in period C. Because the periods of record for Duluth Complex samples ranged from 144-1252 weeks, use of experimental periods also assists comparison among samples and groups with different periods of record.

Period A started at week 1 for each sample, and ended as Ca and Mg release rates stabilized. SO_4 release tended to fluctuate during this period of cation stabilization. Drainage pH gradually decreased throughout this period, and varied among samples, ranging from 4.5-8.7 (Table 80). Group I samples stabilized at pH 6-7, while sample groups II and III stabilized between pH 4.5-5.5 by the end of Period A. Initially, each sample had relatively high and variable Ca and Mg release. Ca concentrations typically exceeded Mg concentrations, and both gradually declined with time. This period lasted from 34-140 weeks and occurred in all samples.

Period B began when Mg and Ca release rates stabilized at levels 20-30 percent of those in Period A. Average Mg release rates exceeded those of Ca in 11 of 21 samples. Similarly, average SO_4 release rates decreased 22-77 percent of those rates in Period A (Table 81). Drainage pH typically decreased gradually throughout this period (average pH= 6.5 group I, 5.2 group II, 4.6 group III). Period B lasted from 66-1118 weeks and occurred in all samples.

Period C began with a relatively rapid pH decline (below ~4.4) and concurrent increases in Ca, Mg and SO_4 release, with SO_4 release increases typically occurring 15-55 weeks prior to Ca and Mg release increases. During this period it was common to have Mg spikes exceeding Ca release at the pH minimum. This increase in Mg release was particularly common in group III samples. Ca, Mg and SO_4 release decreased as Period C ended. Period C occurred in all group II and III Dunka blast hole samples. No group I samples entered period C.

Period D was characterized by gradually increasing pH (above ~4.2-4.4), and Ca, Mg, and SO_4 release rates lower than period C. Calcium release rates remained relatively stable during Period D, at levels similar to Period B, while Mg release rates gradually decreased to levels less than or equal to rates observed in Period B. Period D occurred in most group II (all but 0.54%S) and group III Duluth Complex samples (all but 1.40%S). No group I samples entered period D.

6.3.1. Initial Flush

The flush of Ca, Mg SO_4 at the beginning of period A might be due to 1) the rapid dissolution of fine particles adhered to the mineral grains, 2) rapid dissolution and depletion of more reactive minerals present in small amounts, 3) rapid ion exchange, 4) exposure of new surfaces to oxidation and dissolution as a result of grinding, or 5) release of solutes generated by dissolution during sample storage. There was physical evidence that these samples might have had higher initial release rates due to adhered particles on mineral grain surfaces. Photomicrographs clearly show that some grains had numerous particles on grain surfaces that were removed by washing (Figure 57). Also, leached grains from the same sample were missing most of these particles, suggesting that these particles dissolved with time. Another indication that smaller particles dissolved was the decrease in the perimeter:area ratio after samples were leached (Table 17).

Smaller particles are likely to be from softer minerals, such as sulfides (Lapakko et al. 2004a), so this factor may contribute more to sulfate release than to release of other ions. On the other hand, fine particles would be more susceptible to loss from the bed by physical transport with the leachate. Crushing may result in less size reduction than expected of some softer minerals, such as biotite, which tend to resist the equally distributed force applied by most crushing methods (i.e. are "tougher", Chodos and Engel 1961). This limited size reduction would likely lower dissolution rates. Finally, there may be error in the perimeter:area measurements due to the how the grains were mounted having increased the likelihood of underestimating the area of larger particles (Appendix 1, Attachment A1.6).

The initial flush of ions is also typical in studies that have wet-sieved and sonicated grains prior to the start of the experiment (e.g., White and Brantley 2003), implying that adhered particles are not the only contributing factor in initial elevated release. Samples in this experiment that were wet-sieved showed a similar initial flush as dry sieved samples, further indicating the relative unimportance of adhered particles. Thus, the flush probably has more to do with other factors.

White and Brantley (2003) attributed an initial Ca flush from granite to dissolution of trace calcite. Further support for this interpretation was provided when they found the Ca flush in unweathered rock, but not weathered rock from the same core. Although point count data from Dunka blast hole samples detected calcite rarely and at low amounts, calcite might be more abundant than these data indicate. Discrepancies in point count data are likely due to error inherent in the point count method. With the number of grains measured (~100), the visual point count method has a 2-σ error level (86.5% confidence) that makes it possible that true values of mineral abundance under 10% could be 60-100% different from estimates. Samples with no grains of a certain mineral detected could have as much as 2% of the sample present as the undetected mineral grains. Evolved CO_2 from unleached samples was almost always more than in leached samples, showing loss of calcite. The calcite depletion may have been more than indicated by the CO_2 data because of either new calcite formation in mineral microsites or CO_2 absorbed into the lattice of minerals. Adsorption of CO_2 has been reported in olivine (Oberheuser et al. 1983, Schott and Berner 1983). Berg and Banwart (2000) have proposed a mechanism for CO_2 adsorption on anorthite where inorganic carbon is rapidly adsorbed, forming a reactive bi-dentate surface Al–carbonate complex that is released to solution in a much slower, irreversible step.

Initial flushes of cations due to rapid ion exchange have been known for a long time (e.g., Garrels and Howard 1959). These initial flushes are very rapid (~ one minute) and are due to reversible exchange of alkali ions on the feldspar surface with hydrogen ions in solution. This and other early research reported parabolic dissolution kinetics, which was thought to be due to armoring of surface layers that limited transport of reactants or products (Phillips et al. 2001). More recent laboratory experiments appear to favor the silicate dissolution model of Furrer and Stumm (1986), which was developed for simple oxide dissolution (Brantley and Chen 1995). This dissolution rate is a form of ligand-exchange reaction that is proportional to the concentration of surface complexes and valence of the metal ion. This model emphasized the control of silicate dissolution by surface reaction, rather than diffusion through a surface layer of reaction products (Blum and Stillings 1995).

Initial flushes of sulfate and Mg are most likely due to exposure of fresh mineral surfaces and fractures during grinding. Janzen et al. (1997) reported that surface area of pyrrhotite appears to be the most influential variable affecting oxidation rates, and differences in crushing methods were found to affect surface area of mineral grains smaller than 212 µm (the starting size used in this experiment) (Janzen et al. 1997). These differences may be due to differing strains on the mineral grains causing differing amounts of mineral grain fractures (Janzen et al. 1997). Fracture sites are particularly vulnerable to oxidation (Janzen et al. 1997, 2000). Eggleston et al. (1989) found dissolution rates of diopside (end member of the solution series containing augite) decreased with time, showing the importance of fresh surfaces in silicate mineral dissolution.

6.3.2. Biological Mediation

As time passes, sulfide oxidation increases, coincident with declining pH. The rates of sulfate release exceed the combined release of Ca and Mg, resulting in net increases in acidity. The accelerated rate of sulfate release below pH 4 was probably due to increased biologically mediated ferric-iron oxidation of the sulfide minerals. Chemical oxidation may have also increased, although the extent of increase was most likely slight relative to the increase in biological oxidation (Nordstrom 1982). Thus, group III sulfide mineral oxidation creates a positive feedback in which the decreased pH conditions from sulfide oxidation create conditions favorable to increased oxidation by bacteria.

6.3.3. Development of Coating (Shrinking Core)

As sulfide minerals oxidize, the outer layer becomes sulfur-depleted and an Fe^{III}-O layer forms that is resistant to oxidation of the underlying sulfide (Pratt et al. 1994a, b, Figure 66). This coating development, combined with depletion of sulfide minerals and continued dissolution of silicate minerals, results in the increasing pH characteristic of period D. Sulfide mineral abundance measured with point count and chemical analyses revealed a >50% decrease in pyrrhotite, while showing no significant decrease in chalcopyrite. Pyrrhotite oxidizes much faster than chalcopyrite (Jambor et al. 2005), and the relative increase in slower-oxidizing sulfide minerals may partially explain the decreased sulfate release, and consequent pH increase, in period D.

6.3.4. Calcium versus Magnesium

The instances of Mg release exceeding Ca release around the pH minima can be explained by the greater sensitivity of ferromagnesian minerals to decreasing pH. Augite dissolution was the major source of accelerated Mg release at lower pH (<4.5). Plagioclase, which contained the majority of Ca, was less sensitive to pH. This is shown by the consistently steeper regression slopes of Mg versus sulfate when compared to Ca versus sulfate (Table 87). However, average total Ca release was generally 1.4 to 2.5 times higher than total Mg release in the Group I and Group II samples, respectively (Table 79). Average Mg release only exceeded average Ca release for an entire period in group III during periods B and C. This was most likely due to the prolonged period at lower pH which resulted in increased olivine and hypersthene dissolution. Group III samples still had increased Ca release in period C, as did group II. However this increase was not enough to equal the greater increase in Mg release. Group III samples had the lowest pH, and olivine, the source of 28% of Mg in Duluth Complex samples (Table

23), displayed dissolution rates that are more sensitive to decreasing pH than labradorite (Liu et al. 2006, Rosso and Rimstidt 2000, Palandri and Kharaka 2004). Hypersthene, the source of 36% of Mg in Duluth Complex samples (Table 23), did not have rate equation information for comparison. Bronzite, which is similar to hypersthene, is more sensitive to pH than labradorite and has a faster dissolution rate than labradorite at pH 4 (Palandri and Kharaka 2004). The pH dependence of biotite dissolution rates under acidic conditions is roughly the same as that for labradorite and andesine (Tables 73, 77). Labradorite was the main source of Ca for these samples.

6.3.5. Silicate Coatings

Silicate mineral surface layers are modified or coated more slowly than sulfides (Tables 14, 15). This contributes to an increase in Ca and Mg release relative to sulfate release in the latter part of period C and period D. This increase in relative release contributes to the rise in pH starting in the latter part of period C, and the dominant factor influencing the increase is the decline in iron sulfide oxidation rate. White and Brantley (2003) reported slow development of depleted layers in plagioclase, based on lower Na release in weathered granite than unweathered indicating slowdown in plagioclase dissolution. The authors estimated that it would take 22,000 years for a rate decrease of about two orders of magnitude. Substantial Si-rich leached layers have often been found in laboratory dissolution experiments, which are often conducted in acidic solutions without Na, K, Mg, Ca or Al. Nesbitt et al. (1991) reported that in conditions in which cations exceeded the amount of H_3O^+ in solution, as they did in this experiment, labradorite dissolution was congruent and leached layers were small. In samples like the ones in this report, which had greater amounts of Fe from sulfide minerals than the granite samples of White and Brantley (2003), silicate coatings may form faster due to the presence of Fe^{3+} on mineral surfaces (Brantley 2003).

There was evidence of ferromagnesian mineral coating development based on Mg release. The greater decline in release of Mg relative to Ca indicated that olivine or hypersthene was developing coatings. If augite, which had roughly equal amounts of Ca and Mg, were coated, then a drop in Ca would also be expected. However, Ca release remained similar in periods B and D. The importance of olivine as a source of Mg is shown by the fact that the only samples with declining Mg release from period B to period C were the two with no olivine (0.40 and 0.54%S). The increased reaction rate as pH declined in period C could cause formation of coatings on olivine. Rates of fayalite dissolution have been reported to decrease with time, possibly due to formation of iron oxyhydroxide phases (Siever and Woodford 1979, Wogelius and Walther 1992). Welch and Banfield (2002) suggested that adsorption of ferric iron and formation of a thin "laihunite-like surface structure" might be responsible for the observed rate inhibition. Laihunite structures were reported present in field-altered olivine (Banfield et al. 1990, 1992). The presence of iron in olivine or the presence of other iron-bearing minerals might have contributed to slower rates of olivine (Fo_{57}) dissolution from a mixture of minerals (65% olivine (Fo_{57}), 20% plagioclase (An_{50}), 8% magnetite, 4% pyroxene, 3% serpentine) reported by Duro et. al (2005).

6.4. Variation with Sulfur Content

6.4.1. Acid Generation

A major concern associated with mining of the Duluth Complex is acidification of surrounding ground and surface water. The main source of acid from mine wastes is sulfide oxidation (Younger et al. 2002), and virtually all S in these unleached samples was present as sulfide. Solids with sulfur contents ≥ 0.4% produced drainage pH values below 6.0, and those with sulfur contents less than 0.22% produced typical drainage pH above 6.0. These values indicate an empirically demonstrated "acidification cutoff" of 0.22% S. The "critical sulfur content" is actually somewhere between 0.22 and 0.40 percent S but more refined definition of the value is limited by the absence of tested solids with sulfur contents in this range. Given the uncertainty in quantifying the critical sulfur cutoff more precisely, the empirically demonstrated value (0.22 %S) would be applied as a conservative value for mine waste management decisions.

Furthermore, while the 0.4%S sample generally maintained drainage pH above 6.0 for ~750 weeks, the rate of acid neutralization (reflected by the sum of calcium and magnesium release rates) by this sample was anomalously high relative to its sulfur content (Table 84). The high neutralization was due to the presence of 0.64% calcite (Table 2), which is rare in Duluth Complex rock. Thus, without elevated acid neutralization values, the sample would have acidified earlier than week 750. To illustrate this point, drainage pH from the 0.41%S sample fell below 6.0 after 75 weeks and generated a minimum drainage pH of 4.05 despite rates of sulfate release which were lower than those from the 0.40% S sample. Again, it should be noted that no samples were tested with sulfur content 0.22<%S<0.40. Samples in this range of sulfur content have been observed in other Duluth Complex laboratory experiments (Lapakko 2013b) to approach acidic conditions (pH<6). These data could affect the mine waste management sulfur groupings discussed in this report. Additional testing of samples with sulfur contents in the range of 0.2 to 0.4% could be conducted to refine this critical value.

Sulfide mineral oxidation was the source of acidity in these samples, as confirmed by the significant positive regressions between sulfate release (average and maximum) and %S in periods A-C (Table 34, Figures 24-27), as well as the negative regression relationship between pH and sulfate release in all periods (Table 34, Figures 28-31). This increase in sulfide oxidation drove the significant negative regressions of pH (minimum and average) versus %S in periods A-C (Table 87). The slopes of these regressions were essentially zero during period D (Figure 23). The decline of sulfate release for higher %S samples during period D (Figure 27) is likely due to coating development on sulfide minerals rather than sulfide mineral depletion. This is because the average sulfur depletion, calculated based on (1) sulfate release and (2) %S difference between leached and unleached, ranged from 54-68%. This leaves a large portion of sulfide minerals still potentially available for oxidation (Table 109).

Total sulfate release during the entire experiment differed among groups (Table 79). Total sulfate release for group I was 2.30-2.34 mmol (mean 2.32 mmol). Total sulfate release for Group II was 5.9-10 mmol (mean 8.2 mmol). Total sulfate release for group III was 11.3-28.9 mmol (mean 21.7 mmol). The large increases in sulfate release reflected the differences in pH minima among groups.

The type of sulfide minerals also affected sulfate release rate. Pyrrhotite and pentlandite are more rapid oxidizers than chalcopyrite (Kwong and Ferguson 1990, Ahonen and Tuovinen 1992), the other common sulfide mineral in these samples (Figures 58, 59). Pyrrhotite was by far the most common sulfide mineral in the samples (Table 7). This is supported by 1) the change in mineral content between unleached and leached samples (Table 9), 2) development of coatings, 3) higher sulfate release in solution compared to copper, and 4) fewer pyrrhotite grains were found in the leached samples (Table 15).

6.4.2. Acid Neutralization

6.4.2.1. Major Cation Release

Ultimately, pH is a reflection of the balance between acidity production from sulfide mineral oxidation and neutralization potential from dissolution of Ca and Mg-bearing silicate minerals. There is also a smaller amount of neutralization from Na and K cations. Higher sulfur content samples produced sharper initial declines in pH, as well as lower pH minima (Figure 5). Coinciding with the pH minima were marked increases in SO_4 release rates. Ca and Mg release rates also rose sharply near the pH minimum, which could be attributed to augite dissolution, but these increases were generally less than that observed for SO_4. Average Ca and Mg release rates doubled going from period B to period C, compared to the 3-fold increase in SO_4 release during this minimum pH period (Tables 81, 84).

Cumulative group release of SO_4 and Ca increased as solid-phase sulfur content increased (Table 79). Average cumulative Mg release was slightly less from group II than group I, but Ca+Mg release increased with increasing group sulfur content. In Group I, total Ca release was 3.4-3.9 mmol (mean 3.7 mmol) and total Mg release was 2.0-3.3 mmol (mean 2.7 mmol). The total of Ca and Mg release exceeded total sulfate release, explaining the circumneutral behavior of group I samples. Groups II and III generally had combined Ca and Mg release that did not exceed sulfate release, explaining the samples' pH decline. The only exception was the 0.40%S sample, which had exceptional neutralization capacity relative to its sulfur content (discussed later in section). The small difference between total Ca+Mg release and total sulfate release could be explained by measurement error or errors associated with interpolation to account for missing sample points. In group II, total Ca release was 2.7-8.7 mmol (mean 4.4 mmol), and total Mg release was 0.9-2.6 mmol (mean 1.8 mmol). In group III, total Ca release was 3.0-6.1 mmol (mean 4.1 mmol) and total Mg release was 2.6-6.9 mmol (mean 5.0 mmol).

Calcite is often present in igneous rock (White et al. 1999), but was not an important long-term source of neutralization in these samples. It was detected by point count in only one sample (0.58%S sample). Using carbon dioxide as a surrogate for calcite, the mineral was below detection limits in eight of twenty-one samples. The rapid dissolution of the calcite that was present likely contributed to the high initial Ca release. The potential importance of calcite is shown by the 0.40%S sample, which had the highest calcite (measured as CO_2, Table 2) and took 750 weeks before a sustained period below pH 6. It is possible that additional calcite formed during the experiment, as implied by the increase in CO_2 for two leached samples. However, this could also be explained by absorption of CO_2 into mineral lattices (Oberheuser et al. 1983) or by errors in sample analysis.

Because of the small amount of calcite, silicate mineral dissolution must have generated the majority of neutralization potential in most samples. However, despite the large percentage of samples occurring as silicate minerals, the ability of silicates to maintain a circumneutral pH is limited by a slow dissolution rate. The small percentage change in silicate mineral point counts after leaching, as well as model dissolution rates that were consistently slower than sulfide mineral oxidation rates, are consistent with the slow rate of silicate mineral dissolution.

Another limit on silicate minerals preventing acidification is that pyrrhotite, the most common mineral, oxidizes much faster at low pH when ferric iron is the oxidant (Janzen 1996), while most silicate minerals are less responsive to pH (Phillips et al. 2001). Rates of plagioclase dissolution in this experiment showed this insensitivity to pH, as indicated by the similarity in Ca release rates from period B through period D (Table 82). As with modeled sulfide mineral oxidation rates, silicate dissolution computed in this experiment was slower than most rates reported elsewhere. Some possible reasons for slower rates include, saturated fluids that became trapped in micro-pits that develop on the grain surface over time, formation of preferential flow paths through the sample, and wet-dry cycles causing intermittent periods of no dissolution (White and Brantley 2003). Additionally, the formation of leached layer or coatings, as discussed earlier, could slow silicate dissolution.

Silicate dissolution can be important in maintaining neutral conditions of low sulfur samples, as shown by an examination of cumulative mass release (Table 79). Each mole of Ca and Mg released by silicate dissolution can neutralize two moles of acidity, and each mole of sulfate released by sulfide oxidation produces two moles of acidity. Table 79 shows group I samples, which stayed above pH 6, had greater neutralization, indicated by Ca and Mg release, than acidity, indicated by sulfate release. Groups II and III had greater acidity than potential neutralization, explaining their decline in pH.

At the end of the period of record for all samples, there is still a large amount of untapped neutralization potential in silicate minerals. Using Ca release to determine maximal dissolution of plagioclase revealed that the highest potential dissolution of any sample was 16.3 mmol (Table 99), while the average abundance of plagioclase in each sample was 140 mmol, assuming 50% labradorite. Similarly, using Mg release to determine maximal dissolution of olivine revealed that the highest potential dissolution of any sample was 9.6 mmol (Table 99), while the average abundance of olivine in each sample was 49.7 mmol, assuming 11% olivine. It should be noted that olivine is not the only source of Mg release (i.e. augite, hypersthene) therefore the rate of maximum olivine dissolution calculated is probably an overestimation. When compared to the over-50% sulfide mineral depletion (Table 109), it is clear that sulfide mineral depletion occurred much faster than silicate mineral depletion.

In addition to neutralization by dissolution of the silicate minerals initially present, neutralization by some of their solid-phase reaction products must also be considered. Plagioclase dissolves to kaolinite, which dissolves to gibbsite. Gibbsite dissolution neutralizes six moles of acidity, and its dissolution rate increases at pH 4 due to increased solubility of Al. After determining maximal rates of gibbsite formation at pH ≥ 4 (Table 68), the potential amount of gibbsite was more than enough to offset all acidity production in the sample. There is a marked increase in Al release rates beginning near pH 4 for the Dunka blast hole samples (Table 88, Figure 53). It has been reported that kaolinite dissolution rates are fast enough to avoid affecting plagioclase dissolution rates at 22ºC and pH 4 (Yang and Steefel 2008). This relationship will likely be unchanged by pH in the acidic range, as the slope of log kaolinite dissolution rate versus pH is –0.09 from pH 1-6 at 25ºC (Nagy 1995). Reported kaolinite dissolution rates of approximately 3 x 10^{-12} mol m^{-2} s^{-1} (Nagy 1995) are similar to the rates for plagioclase dissolution found in this experiment.

Sodium and K release was not analyzed as frequently as other ions, but it indicates the potential neutralization from silicate mineral dissolution. For the six samples that had Na and K release rates for the entire period, K was higher initially and declined through time, while Na remained essentially constant. This indicates that K ion exchange dissolution may be a more important source of acid neutralization initially. Similar results have been found for Archean Greenstone in Minnesota (Lapakko et al. 2004b).

6.4.2.2. Neutralization Potentials

Offsetting the acidity generation, neutralization can come from dissolution of the calcium and magnesium fractions of carbonate minerals and silicate minerals. Calcite ($CaCO_3$) content of the rock samples tested, as indicated by CO_2 generated from unleached samples, was generally low. In all Duluth Complex samples except 0.4%S, the amount of Ca released in leachate prior to rapid pH decline was in excess of the sample's $CaCO_3$ content, indicating that calcite was likely depleted early in these experiments.

Of the methods used in this report to measure neutralization potential, the empirical neutralization potential (ENP) gives the most accurate measurement of sample neutralization potential. The ENP measures the amount of acid a sample can neutralize before drainage decreases below a certain pH. The ENP_{pH6} for all but one sample did not exceed 2 mg $CaCO_3$/g rock (Table 21). This is in good agreement with the calcium plus magnesium carbonate content implied by the CO_2 content of the rock samples [$NP(CO_2)$]. All but two of these values were less than 2.5 mg $CaCO_3$/g rock (Table 2). The extent of neutralization observed during the dissolution tests reflects a very low capacity for acid neutralization, which is consistent with the lack of carbonate minerals present and the low values of all NP measurements except those using the Sobek (1978) method (Tables 21, 22). The exception was the 0.4%S sample which had an ENP of 8 mg $CaCO_3$/g rock and an NP(CO_2) of 14 mg $CaCO_3$/g rock.

The pH of drainage from the group I samples (0.18, 0.22%S) rarely dropped below 6.0. The neutralization potentials above pH 6 for these solids were approximately 3 mg $CaCO_3$/g rock. The neutralization above pH 6 by these solids was at the upper end of the range observed for most samples. This was most likely due to the slow rate of acid generation by these low-sulfur solids, and the consequent low rate of silicate mineral dissolution required to neutralize the acid produced. That is, silicate mineral dissolution can neutralize acid to maintain circumneutral pH if and only if the rate of acid production is very slow.

Older methods of determining neutralization potential (NP), such as Sobek et al. (1978), overestimate the amount of NP present as calcium and magnesium carbonate (Lapakko 1994a). At circumneutral pH, carbonates dissolve faster than silicates and are more important in maintaining pH above 6 when the rate of acid production (iron sulfide mineral oxidation) is rapid. Although the rate of silicate mineral dissolution increases at lower pH, it is still very slow relative to rates of calcium and magnesium carbonate dissolution. More realistic estimations of the ability to maintain pH above 6 are given by the autotitrator NP and the NP calculated from CO_2 content (Figure 61).

6.5. Metal Release

Another concern associated with mining is metal contamination through leaching from mine wastes. The main metals of concern in the Duluth Complex are Co, Cu, Ni and Zn. Acidity from sulfide mineral oxidation was the controlling factor in metal concentrations of sample leachate, and all metal release rates increased with declining pH. Although metal release increased with lower pH, there were differences in temporal variation among metals. These differences may be due to differences in mineral sources of each metal and differences in mineral abundance among groups.

6.5.1. Mineral Sources of Metals

Likely mineral sources of Co and Ni were determined using calculations based on solid and leachate chemistry, as well as mineral abundance. These metals had multiple potential mineral sources, unlike Cu and Zn. Copper was likely from chalcopyrite and cubanite, while Zn was likely from sphalerite (McSwiggen 1999). Cobaltite, (Co, Fe)AsS, is a common mineral source of Co. However, As in unleached solids is quite low for Duluth Complex samples (Table 3), making it impossible for the majority of Co to be accounted for by cobaltite. A similar situation exists for Ni in maucherite ($Ni_{11}As_8$). Pentlandite was inferred to be the major mineral source for both of these metals.

Although cobaltite and maucherite could not account for the majority of Co and Ni present in these samples, dissolution of these minerals could have detrimental effects on the environment through arsenic release. No As was detected in these experiments, but waste rock piles or tailings basins with small amounts of cobaltite or maucherite could release significant amounts of As due to their large amounts of rock. Arsenic release at this scale could be potentially problematic.

6.5.1.1. Cobalt

Less than 20% of Co could be present as cobaltite, due to the amount of As present in solid samples. Pentlandite in these samples was common, and has been reported to have 1-1.4% Co by weight in the Duluth Complex (McSwiggen 1999). Other researchers have found pentlandite to occur commonly in the Duluth Complex, whereas cobaltite has not been found to be widespread in large amounts (Severson and Barnes 1991, Theriault et al. 2000).

6.5.1.2. Copper

Chalcopyrite and cubanite are the dominant sources of Cu in these samples. This is typical of Duluth Complex samples and these minerals are commonly found and widespread in the Duluth Complex (Stevenson et al. 1979).

6.5.1.3. Nickel

Pentlandite is common in the Duluth Complex (Severson and Barnes 1991, Theriault et al. 2000), and it has been reported to be the primary Ni ore mineral in the Duluth Complex (Severson and Barnes 1991). Furthermore, they indicate that most Ni in sulfides is held in pentlandite. Olivine is a relatively minor contributor of Ni (between 5-27%), except in samples with low sulfur content. Analysis of a subset of samples with low sulfur content allowed estimation of a maximal rate of Ni release from olivine. Maucherite was determined to be of minor potential importance due to the low amounts of As in the samples.

6.5.1.4. Zinc

Zinc was likely to have come primarily from sphalerite ((Zn, Fe)S). This mineral has been reported in minor amounts in the Duluth Complex (Stevenson et al. 1979, Theriault et al. 2000) and has been reported to be locally common (Severson and Barnes 1991). There could also be trace amounts of Zn contained in pyrrhotite.

6.5.2. Drainage Quality

6.5.2.1. Changes in Release with pH

Release of Co, Ni and Zn increased concurrently with sulfate release, and both metal and sulfate releases occurred during declines in pH. Copper release also increased as pH declined, but its increase lagged behind that of Co, Ni and Zn and had a more prolonged peak. Increased metal release was mainly due to greater sulfide oxidation and increased solubility of metals at lower pH, typically in the order Cu>Ni>Zn>Co. There was no strong relationship between metal content and S content of the rock samples (Table 3, Section 5.1.2.1), but there was a significant correlation between metal release and leachate pH (Figures 48-51). The trend was reflected by increasing metal release from low-sulfur samples in group I to higher-sulfur samples in groups II and III. That is, metal release from the higher-sulfur samples was a result of their lower pH rather than higher metal content.

6.5.2.2. Changes in Release over Time

Group I samples had similar temporal patterns for all metals (Tables 89-92). Release was highest in period A and declined in period B. Declines in group I average rates decreased in the order Zn<Cu<Ni<Co by 17, 44, 79, 85%, respectively. Drainage pH for these samples stabilized near 6.0 and, therefore, there was no increased metal release under acidic conditions. The decline in metal concentrations over time is consistent with the observed decline in sulfate concentrations. Both trends are assumed to be the result of decreasing amounts of sulfide minerals (and associated metals) available for leaching and coating of sulfide mineral surfaces (Appendix 1, Attachment A1.2).

Within the Group II samples the temporal release patterns for Cu were different from Co, Ni, and Zn (Tables 89-92). Cobalt, Ni, and Zn release rates declined in period B, whereas Cu releases increased steadily from period A through period C. The similarity in Co and Ni release are likely because both are largely released from pentlandite. Although cobalt was not reported in the mineralogical analysis, McSwiggen (1999) found pentlandite to have 1-1.5% Co by weight, making it a major source of Co in the Minnamax Cu-Ni sulfide deposit of the Duluth Complex. Copper is present in chalcopyrite, which oxidizes slower than pentlandite (Shaw et al. 1998, Jambor et al. 2005), perhaps contributing to the lag relative to Co and Ni.

Group III samples had the highest average release for all trace metals during period C, which corresponds to when minimum pH values were observed. These samples also had a similar temporal release pattern for Co, Ni, and Zn which differed from that of Cu (Tables 89-92). Average cobalt and nickel release rates decreased through all periods. Copper release increased through period C, then decreased, while Zn release peaked in period C and decreased.

Iron and Al had increased release rates below pH 4 (Table 88, Figures 52, 53). This was particularly evident with Al, which had an average release rate 18 times faster below pH 4 than at higher pH. The increased solubility of Al may indicate gibbsite dissolution. Although increased Al release from aluminosilicate minerals generally would be expected at lower pH, White and Brantley (2003) attributed increased Al release from plagioclase at lower pH to dissolution of secondary clays.

Cu and Zn release was entirely the result of sulfide oxidation. Nickel, and to a lesser extent cobalt, release could result from both sulfide mineral oxidation and olivine dissolution. The first evidence that sulfide minerals are the major source of nickel is the calculation that olivine only contains an average of 16% of Ni in the Dunka blast hole samples. Eliminating samples with an elevated fraction of Ni present as olivine (i.e. 0.57%S), this average decreases to 12% (Table 93). Second, peaks in Ni release coincided more often with sulfate than Mg release. Third, when Ni/Mg release ratios were analyzed, they were, on average, 60-times higher than the ratio found in olivine (Table 94). It should be noted, however, that samples with lower sulfate release rates, and consequently lower nickel release from sulfide minerals (0.18, 0.22%S) exhibited Ni/Mg release ratios more similar to Ni/Mg ratios in olivine (aqueous average 4 times higher than ol ratio). Fourth, Ni/Mg release ratios were generally similar between samples with olivine and those without (0.40 and 0.54%S), indicating limited importance of olivine as a Ni source in these samples.

Regression of calculated Ni release from olivine versus %S (Table 96, Figure 62) gives a positive correlation with higher sulfur samples at lower pH ranges. The increase in calculated release from olivine is based on increased Mg release. The increased Mg release likely resulted from increasing Mg-bearing mineral dissolution due to lower pH resulting from increased sulfide mineral oxidation rates. Despite the overestimation of olivine dissolution (Section 4.4.6), calculated Ni release from olivine dissolution was far lower than actual Ni release. This discrepancy between the calculation of maximal olivine dissolution and observed Ni release further emphasizes the importance of sulfide minerals as a Ni source. Both Ni and Mg release rates decrease from period A to period C, but Mg release declines faster than Ni. In period D, Mg release increases relative to Ni (Table 95), indicating a likely combination of sulfide mineral depletion and coatings on sulfide grains inhibiting oxidation.

The molar ratios of nickel to sulfur in the solids averaged 0.05 with a standard deviation of 0.03 (omitting the Group I samples). In contrast, the molar ratios of observed nickel to sulfur release averaged 0.09 with a standard deviation of 0.13. This comparison indicates that sulfur was released preferentially to nickel. That is, the ratio of sulfur release to the amount of sulfur in the solid exceeded the corresponding ratio for nickel. One factor contributing to this differential was the presence of some nickel in olivine (5-27%). A second factor is that pyrrhotite, the dominant sulfide mineral present in the samples, oxidizes more rapidly than pentlandite (Shaw et al. 1998).

Analysis of a subset of samples gave an estimate of maximal Ni release resulting from olivine dissolution. It was determined that low contribution of Ni from sulfide minerals was the main factor that increased agreement between calculated Ni from olivine and observed Ni release. The 0.57 %S sample had a very high percentage of total Ni (>72%) and Mg (>55%) in olivine. The predicted maximum Ni release in the Mg-based model was only 8 percent of the actual Ni release during period B (Table 95). The group I samples (0.18, 0.22%S) had calculated maximum Ni release rates that were 40% of actual release during period B (Table 95), despite variations in percent Ni and Mg from olivine (5-19% Ni, 14-21% Mg from olivine). Limited contribution of Ni from sulfide minerals, indicated by circumneutral pH in these samples, is most likely the controlling factor to the larger relative contributions of Ni from olivine.

Calculated maximum rates of olivine dissolution for group I samples during time period B approximated maximum olivine contribution to Ni release best for these samples. Average observed Ni release rates for group I samples was 1.1×10^{-8} mol Ni · week^{-1}(Table 95) or 3.9×10^{-7} mol Ni ·mol ol^{-1} · week^{-1} (Table 97). During period B, these samples were at steady state with neutral pH, and thus had minimal contributions of Ni from sulfide mineral oxidation. However, these calculations still disregard the likelihood that some Mg came from other sources, such as augite dissolution. Even with these overestimations, calculations still underestimated Ni release by a factor of three, indicating that there are significant sources of Ni from other minerals. Other data, including much higher Ni:Mg in the aqueous phase than in olivine, as well as increasing relative amounts of Ni with higher %S samples, reinforce the importance of sulfide minerals as the major source of Ni release. Thus, it was concluded that most Ni is released from sulfides, specifically pentlandite.

6.6. Sulfide Oxidation Rates

6.6.1. Data Summary

Calculated average pyrrhotite oxidation rates typically ranged from 1×10^{-10} to 3×10^{-10} mol m^{-2} s^{-1} during periods A and B, (Table 107), when drainage pH was typically above 4.5 and almost always above 4.0 (Figures 20, 21). Groups II and III had the highest sulfide oxidation rates in period C, with average rates typically ranging from 3.5×10^{-10} to 6×10^{-10} mol m^{-2} s^{-1}, and were coincident with pH minima typically in the threes (Figure 22). Rates from these two groups declined in period D due to both sulfide mineral depletion and coating of sulfide mineral surfaces. Bulk sulfide oxidation rates were slightly lower, a result of the larger surface area contributing to sulfate release for this calculation (Table 108).

Some systematic variation of rates among the samples was observed. The pyrrhotite oxidation rates reported for the 0.22%S sample were about an order of magnitude higher than the other samples (Table 107), and this is attributed to the low amount of pyrrhotite calculated for this sample. The assumptions that 1) copper was equally divided between chalcopyrite and cubanite (as opposed to entirely present in chalcopyrite) and 2) all nickel was present as pentlandite (ignoring Ni in olivine), would lend to underestimation of pyrrhotite content. Such error would be more pronounced for samples of low sulfur content. Consistent with this concept, the 0.18%S sample was calculated to have a pyrrhotite content less than zero.

The accelerated rates observed for some samples may be due to greater available sulfide surface areas and/or chemical or mineralogical differences for these samples. Some accelerated samples, such as 0.51

and 1.40%S, may have higher sulfide surface area due to subtle differences in sulfide grain size and/or "roughness" of the mineral surfaces. Other accelerated samples, such as 0.40 and 1.12%S, may oxidize faster due to lower copper content than other samples (Table 3). This difference, and/or its implication of a difference in chalcopyrite content, may influence the sulfide oxidation rate for these samples.

It is possible that under certain conditions copper has an inhibitive effect on iron sulfide oxidation. For example, Koch (1975) reported that the presence of copper in a sulfide such as chalcopyrite stabilizes the ferric iron present. It is also possible that copper released from chalcopyrite may have participated in an exchange reaction with iron present in pyrrhotite and, consequently, inhibited its oxidation. Similar reactions have been reported in which metals in solution exchange with sulfide-bound metals of higher solubility (Gaudin et al., 1959). If galvanic interactions of chalcopyrite and pyrrhotite contributed significantly to pyrrhotite oxidation (Ahonen et al., 1986; Natarajan et al., 1982), lower than normal oxidation rates might be expected for these samples.

These rates were generally within or at the lower range of reported rates for pyrrhotite oxidation (Figure 67), and direct comparisons of rates must consider experimental variables such as pH, temperature, and presence of bacteria (Table 72). Janzen et al. (2000) reported rates for oxidation of 12 pyrrhotite samples by oxygen at pH 2.75 and 22^{o}C. The rates determined based on sulfate release varied by about a factor of 70, ranging from 8.15 x 10^{-12} to 5.86 x 10^{-10} mol m^{-2} s^{-1} and averaging 2.0 x 10^{-10}. Kwong (1995) reported a rate above this range, 8.5 x 10^{-10} mol m^{-2} s^{-1}, under the same pH and temperature conditions. Within this range Steger (1982) reported a rate of 6.5 x 10^{-10} mol m^{-2} s^{-1}, for air oxidation of pyrrhotite at 62% relative humidity and 28^{o}C. Rates determined by Janzen et al. (2000) based on iron release were one to two orders of magnitude higher that those based on sulfate release. The associated ratio for rates determined by Kwong (1995) and Steger (1982) was almost always less than 10.

It should be noted that the 8 x 10^{-10} mol m^{-2} s^{-1} rate reported for Lapakko and Antonson (1994) in Table 72 was based on the first 150 weeks of this experiment. The rate was calculated for the 0.71%S sample and used different assumptions for calculating the amount of pyrrhotite present (yielding a value of 0.9 g rather than 0.79 g by methods in the present report) and a pyrrhotite roughness factor of 2.6 rather than 10. Using assumptions from the present report reduces the rate reported by Lapakko and Antonson (1994) to 2 x 10^{-10} mol m^{-2} s^{-1}, within the range for periods A and B in the present report (Table 107).

6.6.2. Factors Contributing to Lower Rates

Reaction rates for individual sulfide minerals were determined under ideal conditions for oxidation in the laboratory. The design of this experiment, in which samples were dry for approximately half of each week, may have reduced rates of oxidation directly, or indirectly, through evaporation creating saturated films at the mineral grain surface that inhibited dissolution. This evaporative process might also favor formation of coatings on the mineral grain that would resist dissolution. Effects of wetting and drying cycles are poorly understood, but Blum and Stillings (1995) state that it might make grain surfaces less reactive. The proposed mechanism for lower reactivity is initiated by dehydration of the surface, which destabilizes surface species. This leads to condensation reactions between surface groups, making the surface less reactive.

The length of the experiment might have reduced rates relative to the typically short experimental periods of most experiments by giving more time for leached layers to form on the mineral grains, thus slowing rates. This mechanism was clearly reflected by the low rates observed in period D (Table 107). Oxygen bonds with Fe^{III} at vacant sites on the pyrrhotite surface, creating an Fe^{III}-O rich layer above a S-depleted layer. As the Fe^{III}-O layer grows, electron transfer will be inhibited and oxidation will slow (Leopold and Lapakko 2001).

Coatings can also inhibit oxidation over time. Newly ground sulfide minerals have many fracture sites that are preferentially oxidized (Janzen et al. 1997). As time since grinding increases, iron oxyhydroxides form on these grains, reducing surface area dramatically and, thus, reducing reaction rates (Janzen et al. 2000). Janzen reported an 85-90% reduction in surface area (section 6.2).

Mineral oxidation, which increases surface area, is often assumed to speed up dissolution. However, microscopic features may trap water that is saturated with reaction products, rendering less of the surface area available to oxidation (Drever and Clow 1995, White and Brantley 2003). Over time, the formation of preferential flow paths through a sample may occur, leaving some mineral grains dry during the weekly water additions. Preferential flow paths are also thought to occur in soils, potentially isolating some mineral grains from oxidation (Blum and Stillings 1995).

High trace metal contents may also slow oxidation (Plumlee 1999), although others have found no effect (Janzen 1996). Finally, the fact that these were mixed mineral samples, as opposed to the relatively pure samples found in most experiments, presents the possibility of interactions with ions released from other minerals affecting oxidation rates.

6.6.3. Rates for Different Sulfide Minerals

Rates of sulfide oxidation for these samples were expected to be relatively rapid due to the generally high percentage of sulfide minerals occurring as pyrrhotite. Pyrrhotite is reported to be more reactive than other sulfide minerals present in these samples (Jambor 1994, Jambor et al. 2005). Pyrrhotite reacted more rapidly in these samples also, as shown by SEM photomicrographs. Images of individual samples showed that pyrrhotite grains were more abundant in unleached samples and far less abundant in leached samples (Appendix 1, Attachment A1.2). Additionally, pyrrhotite was approximately two-thirds of sulfide minerals in unleached samples and less than 10% of leached samples (Tables 7, 10). The few pyrrhotite grains that were found in leached samples were generally highly oxidized. Other sulfide mineral grains, such as chalcopyrite, found in the samples showed a generally small amount of oxidation, indicating a much slower reaction rate (Table 15).

Kwong and Ferguson (1990) supported this difference in oxidation rate, reporting that pyrrhotite in an abandoned Vancouver mine oxidized faster than chalcopyrite, which oxidized faster than pyrite. Pyrrhotite has also been found to oxidize faster than pentlandite (Ahonen and Tuovinen 1992). Jambor et al. (2005) ranked sulfide oxidation rates as pyrrhotite > pentlandite > pyrite > chalcopyrite. Data from this experiment support this ranking, with average sulfide mineral percent depletion decreasing in the order Po>Pn>Cp with values of 64, 40, and 10% depletion, respectively (Table 9).

It should be noted that pyrite was ignored as a potential source of sulfate release even thought it might have been present in small amounts. Pyrite was measured by visual point counts and, with the number of grains measured (~100), the 2-σ error level (86.5% confidence) of this method makes it possible that the pyrite (found in only one leached sample) could have over 100% error (Figure 60). Additionally, pyrite may have been present in other samples but not detected. Low percentage mineral abundances determined by point count are susceptible to large percentage differences between what was counted and what was actually present.

6.7. Silicate Mineral Dissolution Rates

6.7.1. Literature Review

The methods typically used by researchers to determine mineral dissolution rates are likely to find rates on the high end of a sample's potential range. Most experimentally determined dissolution rates used a homogenous mineral sample housed in a flow-through reactor that did not allow for buildup of dissolved elements or drying of grains. Also, samples were typically analyzed for a far shorter period of time than this experiment, reducing the likelihood of coatings forming on mineral grains and slowing dissolution.

6.7.1.1. Plagioclase

Labradorite and andesine are the most common forms of plagioclase in Duluth Complex rock, and the following discussion focuses on these minerals. Labradorite had experimental equations that gave rates ranging from 1.2 x 10^{-11} to 1.9 x 10^{-10} mol m^{-2} s^{-1} at pH 4 (Table 73). At pH 6, rates were from 1.2 x 10^{-12} to 1.9 x 10^{-11} mol m^{-2} s^{-1}. Andesine had experimental equations that gave rates ranging from 7.9 x 10^{-12} to 1.0 x 10^{-11} mol m^{-2} s^{-1} at pH 4. At pH 6, rates were about an order of magnitude slower (Table 73).

Labradorite rate equations presented by Sjöberg (1989), Sverdrup (1990), and Blum and Stillings (1995), yielded rates near 1 x 10^{-11} mol m^{-2} s^{-1} and 1.0 x 10^{-12} mol m^{-2} s^{-1} at pH 4 and 6, respectively (Table 73). Rates calculated from data presented by Welch and Ullman (1993) were about an order of magnitude higher at both pH values. In comparison, rates derived from the acid rate equation of Palandri and Kharaka (2004) were roughly three times higher than Blum and Stillings' rate at pH 4 and slightly higher at pH 6. The rate derived from the neutral rate equation of Palandri and Kharaka (2004) was six times higher at pH 6 than the rate using their acid rate equation. Palandri and Kharaka's (2004) acid and neutral equations were calculated to be equal at pH 4.83 for labradorite and pH 4.80 for andesine. Rate equations reported for andesine yielded rates that were roughly 20 to 80 percent of those for labradorite (Table 73).

Plagioclase dissolution rates are dependent on pH and rates can be inhibited by the presence of certain ions in solution. Al^{3+} has been found to be particularly effective in retarding dissolution of plagioclase. Chou and Wollast (1985) found that Al inhibited dissolution of albite at pH 3 with concentrations below 10^{-5} mol/l, while Na and Si had little effect. This inhibition may increase with increased temperature (Chen and Brantley 1997), but Oelkers (2001) disputes this. Nesbitt et al. (1991) believe that Al is more effective than other cations at inhibiting dissolution of labradorite. At typical environmental temperatures, significant Al inhibition is limited to low pH conditions. Chen and Brantley (1997) did not find important Al inhibition at pH 4.5 until temperatures reached 70ºC.

Although coatings can develop on mineral grains, McSwiggen's studies indicate that these develop slowly on plagioclase feldspars (Appendix 1, Attachment A1.2). The literature rates are generally faster than the calculated modeled dissolution rates during experimental leaching of Duluth Complex rock after pH declines below 6. Studies have been conducted to examine the potential of surface precipitates or "leached layers" to develop as plagioclase dissolution progresses and inhibit rates of dissolution. Nugent et al. (1998) observed thin (0.005-1 μm), discontinuous coatings of amorphous and crystalline aluminosilicate forming on the surface of albite during early stages of weathering in acidic soils. They suggested formation of such coatings might inhibit dissolution in the field relative to that in the laboratory.

Schweda et al. (1997) used SIMS to examine the near-surface composition of labradorite leached for 500 to 1200 hours in HCl solutions acidified to pH 1-3. They reported Na, Ca, and Al in the outer 100 nm were completely depleted after 1200 hours of leaching at pH 3. The depth of depletion increased with increasing reaction time and decreasing pH. However, no substantial decrease in dissolution rate resulted from the development of the leached layer.

Hellmann et al. (2003) further examined samples generated by Schweda et al. (1997). The authors concluded the leached layer, or altered zone, at the mineral surface was formed by dissolution and subsequent precipitation. They speculated the precipitate was probably a very permeable silica gel that should not serve to inhibit the dissolution rate.

The aforementioned studies were conducted on isolated plagioclase phases. It is possible that precipitates resulting from dissolution of other minerals present in rocks might inhibit plagioclase dissolution. Hodson (2003) reported that an amorphous iron-rich layer formed on anorthite dissolved in a 0.001 molar $FeCl_3$ solution at pH 2.6 for 250 days, and that the coating did not inhibit the anorthite dissolution rate.

Ganor et al. (2005) conducted flow-through reactor experiments at pH 1 on a bulk granite sample and plagioclase, alkali feldspar, and biotite/chlorite fractions separated from the granite. After about 50 days the experiment on the bulk granite was stopped, the solids were dried at $50^{o}C$ for approximately 50 days, and replaced into the reactor for additional dissolution. They reported that the rate of plagioclase dissolution decreased by roughly 85 percent as the iron coating increased from 0 to 1.5×10^{-5} moles per gram mineral. They noted that such coatings were more likely to develop under conditions in nature as opposed to those typically used in mineral dissolution experiments.

In summary, the rates of plagioclase do not appear to be inhibited by surface precipitates or leached layers formed during plagioclase dissolution. Iron precipitates have been observed to form on the surface of plagioclase minerals at low pH. The iron source in these experiments was either the leachate or other minerals present in the solid phase. Plagioclase dissolution was inhibited in one of the two cases.

6.7.1.2. Olivine

Most studies on olivine dissolution (Table 74) were conducted on forsterite, the Mg-rich end member of the solution series. Only one study examined fayalite, the Fe-rich end member, and one study examined a crushed rock sample of 65% olivine (Fo_{57}). Rates for this mixed sample were based on surface area for the entire sample, including non-olivine minerals, therefore literature results should be interpreted with caution.

Forsterite had experimental equations from seven papers at near 25 ºC, which gave rates ranging from 3.0×10^{-10} mol m^{-2} s^{-1} to 3.0×10^{-7} mol m^{-2} s^{-1} at pH 4 (Table 74). At pH 6, rates were from 3.0×10^{-11} mol m^{-2} s^{-1} to 9.8×10^{-8} mol m^{-2} s^{-1}. Palandri and Kharaka (2004) used the acid rate equation to derive rates of 1.9×10^{-9} and 2.1×10^{-10} mol m^{-2} s^{-1} for pH 4 and 6, respectively, at 25 ^{o}C. The rate derived from the neutral rate equation of Palandri and Kharaka (2004) at pH 6 was one-tenth the rate using their acid rate equation. Palandri and Kharaka's (2004) acid and neutral equations were calculated to be equal at pH 8.06 for forsterite.

The only acid rate equation for fayalite (Sverdrup 1990, also used by Palandri and Kharaka 2004) gives rates of 1.6×10^{-9} mol m^{-2} s^{-1} at pH 4 and 1.6×10^{-11} mol m^{-2} s^{-1} at pH 6. The rate derived from the neutral rate equation of Palandri and Kharaka (2004) was two orders of magnitude slower at pH 6 than the rate using their acid rate equation. Palandri and Kharaka's (2004) acid and neutral equations were calculated to be equal at pH 8.0 for fayalite.

In addition to the effects of pH on olivine dissolution, solute ion concentrations can also affect dissolution. Oelkers (2001) found that forsterite dissolution was independent of dissolved Mg and Si concentrations at pH 2 from 25-65 ºC. Addition of aqueous Al did not affect dissolution rates at pH 3 and 65 ºC (Chen and Brantley 2000). Dissolution of fayalite was found to be incongruous for all major cations at 25 ºC and pH 4.5 (Siever and Woodford 1979).

There have been several papers on olivine dissolution since 1998 (Khisina et al. 1998; Awad et al. 2000; Chen and Brantley 2000; Pokrovsky and Schott 2000a, b; Rosso and Rimstidt 2000; Oelkers 2001; Zakaznova-Herzog et al. 2008). Forsterite dissolution initially proceeds with a relatively rapid preferential release of Mg^{2+} followed by congruent dissolution (e.g. Luce et al. 1972, Siever and Woodford 1979, Zakaznova-Herzog et al. 2008). The initial magnesium release results from reaction with H^+ that yields a magnesium deficient (silica enriched) surface layer (Pokrovsky and Schott 2000b). The magnesium is released as a result of H^+ attack on an oxygen atom bonded with two magnesium atoms and one silicon atom (e.g. Liu et al. 2006). This reaction occurs more readily on the (111) surface than the (223, line above second 2 and 3) surface (Awad et al. 2000). The rate of subsequent dissolution is controlled by a ligand exchange reaction that releases silica to solution (Liu et al. 2006). This reaction is controlled by the breaking of the Mg-OH bond that holds silica, a reaction in which a proton is present in the activated complex (Liu et al. 2006).

Olivine rates of dissolution in nature are complicated by the presence of iron in the olivine and by the presence of other minerals. Rates of fayalite dissolution have been reported to decrease with time, possibly due to the formation of iron oxyhydroxide phases (Siever and Woodford 1979, Wogelius and Walther 1992). Iishi et al. (1997) reported oxidative dissolution of iron-rich olivines (Fa_{100}-$Fa_{70}Fo_{30}$) at 300°C and 100 bar formed laihunite and hematite precipitate layers in alkaline environments and hematite and amorphous silica in acidic environments. Santelli et al. (2001) found that fayalite dissolution in the presence of *acidithiobacillus ferrooxidans* in the pH range of 2 to 4 was 2 to 50 percent of that under abiotic conditions. They concluded that the rate of acid neutralization by silicate hydrolysis reactions could be significantly reduced in the presence of microorganisms. Welch and Banfield (2002) suggested that adsorption of ferric iron and formation of a thin “laihunite-like surface structure” might be responsible for the observed rate inhibition. The laihunite structures were reported present in field-altered olivine (Banfield et al. 1990, 1992). More refined work indicated that, rather than laihunite-like layers, crystal structure itself demonstrated a high degree of oxidation and ordering in a distorted olivine structure (Janney and Banfield 1998). The presence of iron in the olivine or the presence of other iron-bearing minerals might have contributed to the slower rates of olivine (Fo_{57}) dissolution from a mixture of minerals (65% olivine (Fo_{57}), 20% plagioclase (An_{50}), 8% magnetite, 4% pyroxene, 3% serpentine) reported by Duro et. al (2005).

6.7.1.3. Pyroxene Group Silicates

6.7.1.3.1. Hypersthene (Bronzite)

Hypersthene is the orthopyroxene reported to be present in Dunka blast hole samples used for dissolution experiments. However, no references were found that specifically report hypersthene dissolution data. Both hypersthene and bronzite are members of the orthopyroxene solid solution series that extends from enstatite ($MgSiO_3$) to ferrosilite ($FeSiO_3$). Hypersthene is 50-70% Mg, while bronzite is 70-88% Mg (Klein and Hurlburt 1985). Consequently, bronzite is considered an adequate representation of hypersthene.

Bronzite had experimental equations from two papers, which gave rates ranging from 4.6×10^{-12} mol m^{-2} s^{-1} to 3.2×10^{-9} mol m^{-2} s^{-1} at pH 4. At pH 6, rates were from 1.4×10^{-12} mol m^{-2} s^{-1} to 3.2×10^{-10} mol m^-

^{2} s^{-1} (Table 75). Palandri and Kharaka's (2004) acid rate equation yields rates of 1.3 x 10^{-11} mol m^{-2} s^{-1} at pH 4 and 6.3 x 10^{-13} mol m^{-2} s^{-1} at pH 6. The neutral rate equation of Palandri and Kharaka (2004) yields a rate three times faster at pH 6 than the rate using their acid rate equation. Palandri and Kharaka's (2004) acid and neutral equations were calculated to be equal at pH 5.23.

At pH 4.5 and 5.5, dissolution of hypersthene was found to be incongruent at all times for all major cations in the solid, although the sample was noted to not be a pure phase (Siever and Woodford 1979). Incongruent dissolution of bronzite was found at pH 1, with Mg being released more slowly than Si (Schott and Berner 1985).

6.7.1.3.2. Augite

Augite ($(Ca,Na)(Mg,Fe,Al)(Si,Al)_2O_6$) is a clinopyroxene that is closely related to the diopside-hedenbergite series but with some substitution of Na for Ca, Al for Mg (or Fe^{2+}), and Al for Si. Sverdrup (1990) reported rates ranging from 3.2 x 10^{-11} mol m^{-2} s^{-1} at pH 4 to 1.3 x 10^{-12} mol m^{-2} s^{-1} at pH 6 (Table 76). Palandri and Kharaka's (2004) acid rate equation gave rates of 2.4 x 10^{-10} mol m^{-2} s^{-1} at pH 4 and 9.5 x 10^{-12} mol m^{-2} s^{-1} at pH 6. The neutral rate equation of Palandri and Kharaka (2004) yields a rate nine times slower at pH 6 than the rate using their acid rate equation. Palandri and Kharaka's (2004) acid and neutral equations were calculated to be equal at pH 7.36.

During dissolution, the mineral surface had increasingly lower Fe:Si as pH declined (White and Yee 1985). Calcium depletion relative to Si was reported for diopside (Schott et al. 1981). Dissolution has also been reported to increase diopside surface area from 860 cm^2 g^{-1} to 1300-1940 cm^2 g^{-1} after 3400 hours (25 ºC, inlet pH 1-3.5) (Chen and Brantley 1998).

6.7.1.4. Biotite

Biotite ($K(Mg,Fe)_3(AlSiO_3O_{10})(OH)_2$) is a phyllosilicate. Kalinowski and Schweda (1996) reported rates ranging from 1.1 x 10^{-12} mol m^{-2} s^{-1} at pH 4 (based on initial mineral surface area) to 1.6 x 10^{-13} mol m^{-2} s^{-1} at pH 6 (based on final mineral surface area) (Table 77). Palandri and Kharaka's (2004) acid rate equation gave rates of 1.1 x 10^{-12} mol m^{-2} s^{-1} at pH 4 and 9.5 x 10^{-14} mol m^{-2} s^{-1} at pH 6. The neutral rate equation of Palandri and Kharaka (2004) yields a rate three times faster at pH 6 than the rate using their acid rate equation. Palandri and Kharaka's (2004) acid and neutral equations were calculated to be equal at pH 5.11.

Biotite does not typically dissolve stoichiometrically in aqueous acidic solutions (Wilson 2004). In the pH range of 5-5.5, Mg is the only detectable cation released (Acker and Bricker 1992). At pH 3, increased Si and Al concentrations indicate significant decomposition of the tetrahedral sheet, while higher Mg and Fe concentrations show continued dissolution of the octahedral sheet (Wilson 2004). At pH 3, initial rates of cation release are highly nonstoichiometric, but Mg/Fe and Mg/Si ratios approached stoichiometric concentrations after an initial period of high release (Taylor et al. 2000). Edge surfaces dissolved more quickly than basal surfaces (Turpault and Trotignon 1994). Biotite is very susceptible to weathering and may progress rapidly to vermiculite and then to kaolinite. Associated with this progression is an increase in mineral surface area (Kalinowski and Schweda 1996).

6.7.2. Silicate Dissolution Modeling Methods

Four modeling approaches were used to determine silicate mineral dissolution rates, all of which assumed stoichiometric release of major cations (Ca, Mg, Na, K) from the most common silicate minerals in Dunka blast hole samples (plagioclase, augite, hypersthene, olivine, biotite) (see section

4.4.5.1 for methods). Model 1 assigned all observed calcium release to plagioclase dissolution and, therefore, yields a plagioclase dissolution rate that is typically higher than those determined by other models. Calcium concentrations were determined frequently throughout the experiment for all samples. Plagioclase was by far the most common mineral in these samples and contained about three fourths of calcium present (Table 23). Augite contained virtually all of the remaining calcium but its dissolution rate was determined only under acidic conditions when calcium and magnesium concentrations increased concurrently. Model 1 calculated dissolution rates of olivine, hypersthene, and biotite in separate calculations that assigned all magnesium release to dissolution of each individual mineral. Thus, Model 1 calculations tend to favor high dissolution rates for all minerals except augite.

Model 2 assigned all observed magnesium release to augite dissolution. Similar to calcium, magnesium concentrations were also determined frequently for all samples. Plagioclase dissolution rates were determined only when the ratio of calcium release to magnesium release exceeded their corresponding ratio in augite. That is, plagioclase dissolution was only detected by this model if calcium release exceeded that which could be attributed to augite dissolution quantified by magnesium release. Dissolution rates of olivine, hypersthene and biotite were calculated only when calcium release limited the rate of augite dissolution. Under this condition the magnesium release was greater than that possible based on observed calcium release and the assumption that augite dissolution was stoichiometric. When the augite rate calculation yielded excess magnesium, separate calculations assigned the excess to each individual mineral. Model 2 calculations tend to favor high augite dissolution rates but limit rates of dissolution for other minerals due to the assignment of large amounts of magnesium and calcium release to augite.

Model 3 assigned all observed sodium release to plagioclase dissolution which, assuming stoichiometric dissolution, inferred calcium release from plagioclase. The observed rate of calcium release almost always exceeded that attributed to plagioclase dissolution (Table 26, Appendix 7, Figures A7.1-A7.21), and the excess was assigned to augite dissolution. The calculated rate of augite dissolution inferred a consequent magnesium release rate. The difference between the rate of magnesium release observed and that inferred by the augite rate calculation was assigned in total to olivine, hypersthene and biotite in separate calculations.

Model 4 calculated plagioclase dissolution rates based on the rate of sodium release and the assumption that all sodium was released due to stoichiometric dissolution of plagioclase. Calcium release from plagioclase was determined based on the plagioclase dissolution rate and the difference between this release and that observed was attributed to augite dissolution. The difference between observed potassium release and that calculated assuming stoichiometric release of K and Na from plagioclase was attributed to biotite dissolution. Magnesium release not attributed to dissolution of augite or biotite was assigned in total to dissolution of olivine and hypersthene dissolution in separate calculations. Thus this model provided well-defined solute-based dissolution rates for plagioclase, augite, and biotite, with rates for olivine and hypersthene both based on the residual magnesium. Sodium and potassium concentrations were determined much later in the experiment than other parameters and for many of the samples measurements were not collected for the first 300-400 weeks of dissolution.

Due to the assumptions used in each model, certain silicate mineral dissolution rates were overestimated and in some cases (i.e. olivine and hypersthene), maximum possible dissolution rates were determined. Sources of error common to all elements and models include: assumptions about the mineral source of elements, surface roughness factors assigned to specific minerals, time of dissolution (reactors were dry for roughly half the week), as well as sampling error associated with determining mineral chemistry, content and mass. The models often overestimated mineral dissolution by assuming the entirety of the element examined comes from one mineral. The models also assume that all minerals are dissolving stoichiometrically, which is not always the case. In addition, the rate of dissolution for each sample is based on an average mineral content, which was determined by microprobe analysis of 100 to 125 mineral grains. Errors resulting from the number of mineral grains examined in each sample (as explained in section 6.6) could have also lead to errors in determining mineral chemistry and mineral content of each sample, resulting in under or over estimates. These factors should be kept in mind when reviewing the following discussion section.

6.7.3. Comparison among Silicate Dissolution Models

Modeled silicate mineral dissolution rate statistics reported in Tables 100-104 were plotted for each mineral for comparative purposes amongst each model through periods A through D (Figures 68-72). Average model dissolution rates were plotted for each period, with the range representing the minimum and maximum values calculated. Average modeled rates in periods B-D ± a factor of 3 were graphed to show the central tendency. Cases where an absence of dissolution (zero) was calculated are designated with a red arrow. Average modeled rates were compared to the average period rates (top of figure) to show the range in dissolution rates between periods. At the bottom of each figure, the maximum to minimum rate ratios were reported to show the range in rates for each model. Also displayed at the bottom of the figures are the total number of rates (n) used in the statistics, as well as the percent of these values that are equal to zero (Percent of n=0), which represents an absence of dissolution. It should be noted that there were a number cases during periods B-D where more than 50% of the calculated rates used for the statistics were equal to zero, typically resulting in artificially low average dissolution rates. These data have been omitted from Figures 68-72 to improve resolution, but are reported in Table 105 for each silicate mineral.

Model 1 typically resulted in the highest plagioclase dissolution rates (Figure 68). This was due to the model assumption that all Ca was associated with plagioclase. For nonacidic periods (A, B, and D) the model assumed all Mg was available for olivine, hypersthene, and biotite dissolution, resulting in maximum possible dissolution rates of these three minerals. Because of this modeling assumption, olivine and hypersthene dissolution rates were typically the highest during model 1 as well (Figures 70, 71). Exceptions to this occurred during acidic period C where Mg and Ca (beyond that attributed to plagioclase dissolution, assuming a plagioclase dissolution rate equal to that in period B) were assumed to be released stoichiometrically from augite (Figure 69) and any residual Mg was then associated with olivine, hypersthene, and biotite (Figure 70-72). Another exception to this was biotite dissolution rates under non-acidic conditions from model 4 were higher than those from model 1 (discussed below).

Model 2 resulted in the highest augite dissolution rates (Figure 69). This was due to the fact that the model assumed all Mg release was associated with augite. Model 2 typically resulted in intermediate plagioclase dissolution rates, which were calculated based on residual Ca after augite dissolution (Figure 68). Similarly, dissolution rates of hypersthene and olivine, which were calculated based on residual Mg after augite dissolution, were also intermediate compared to models 1 and 4 (Figures 70, 71). Biotite dissolution rates for model 2 were also calculated based on the residual magnesium release rate after augite dissolution (Figure 72). These rates were typically the lowest calculated amongst the four models.

Model 3 typically resulted in intermediate dissolution rates for plagioclase that were higher than model 2, but lower than model 1 (Figure 68). This was due to the fact that the model assigned all Na release to plagioclase. It should be noted that plagioclase dissolution rates between models 1 and 3 where not equal. This indicates that the ratio of calcium to sodium release to solution differed from the stoichiometric ratio for the average plagioclase chemistry. Note that the plagioclase composition of a given sample was variable with respect to Ca/Na ratio. Thus it is conceivable, if not likely, that anorthitic fractions of the plagioclase dissolved more rapidly. This would yield a Ca/Na release to solution higher than that indicated by the average plagioclase stoichiometry (Table 26, Appendix 7, Figures A7.1-A7.21). Augite dissolution rates, which were based on the difference between Ca release observed and stoichiometric release of Ca and Na from plagioclase, were typically lowest in model 3, although not markedly lower (Figure 69). Hypersthene, olivine, and biotite dissolution rates, which were based on residual Mg after augite dissolution, where typically higher than model 2, but lower than model 1 (Figures 70-72). In a few instances, model 3 results produced the lowest dissolution rates amongst the four models. These included lower plagioclase, olivine, and biotite dissolution rates during period A, and lower biotite dissolution rates during period B. These exceptions may be due to the limited amount of Na drainage quality measurements during the beginning of the experiment.

Model 4 generally resulted in the highest biotite dissolution rates (Figure 72). The model calculated the rate of biotite dissolution based on the difference between K release observed and stoichiometric release of K and Na from plagioclase. Biotite dissolution rates were generally higher in model 4 than model 1 due to K release typically being higher than Mg release during non-acidic periods A, B, and D (Table 59). Mg release during acidic period C was typically higher than K release, resulting in slightly higher calculated biotite dissolution rates in model 1 (Figure 72). Rates of biotite dissolution in model 4 could be higher due to Mg release from other sources (i.e. augite, olivine). Biotite dissolution may also be overestimated in model 4 due to the fact that some of the potassium would be attributed to K-feldspar, but is not partitioned in the model. Potassium feldspar dissolution rates were calculated in model 4 using the same method that was used to determine biotite dissolution rates. That is, all potassium release was attributed to potassium feldspar. Similarly to biotite, K-feldspar dissolution rates where fairly similar throughout the period of record, with a slight increase in dissolution rates during acidic period C (Table 104). Hypersthene and olivine dissolution rates were the lowest in model 4 (Figures 70, 71). This was due to the fact that residual Mg used for the dissolution rate calculations was significantly lower after factoring in Mg release resulting from biotite and augite dissolution. It should be noted that plagioclase and augite dissolution rates were the same as in model 3.

The degree of agreement among models was dependent on the specific mineral rates calculated. For this analysis a factor of 3 from the average rates in periods B, C, and D (period A values omitted from average due to higher initial release rates) was used to develop a threshold of similar dissolution rates. In general, calculated plagioclase and augite dissolution rates were the closest among the four models over time. Calculated plagioclase dissolution rates fell within a factor of 3 from the overall average for periods B, C, and D approximately 80% of the time (Figure 68). Augite dissolution rates also showed good agreement among the four models, where 60% of all values fell within a factor of 3 from the overall average (Figure 69). The range in olivine, hypersthene, and biotite dissolution rates was larger between the four models. In general, the calculated dissolution rates were within a factor of 3 from the overall average approximately 45-55% of the time (Figures 70-72). These ranges in modeled dissolution rates are consistent with literature which reported variations in laboratory results differing by a factor of 2-5 (Blum and Stillings 1995, Lapakko et al. 2012). Future reporting should include additional analysis to further address these ranges in modeled silicate dissolution rates.

The range in calculated silicate mineral dissolution rates between some models during specified periods could be due to a number of factors. These may include, but are not limited to, differences in mineral content between samples, number of drainage quality measurements per sample, and calculated dissolution rates equal to zero which indicate an absence of dissolution. The calculated absence of dissolution may have had the most significant effect on the calculated statistics for each mineral dissolution model. For example, olivine dissolution rates calculated during period C for models 1-4 used at total of 840 values, 79 of those were zero values representing an absence of dissolution (Table 106). Because 90% of the values used in the calculations were greater than zero, the range in olivine dissolution rates between models is fairly consistent (+/-40%) (Figure 71). In contrast, olivine dissolution rates calculated during period B for models 1-4 used at total of 1,615 values, 376 of those were zero values. Because 25% of the values used in the calculations were equal to zero, the range in olivine dissolution rates between models is significant (1–250%) (Figure 71). Future analysis should examine these calculations in more detail.

In general, silicate mineral dissolution rates were slower than sulfide oxidation rates. Average sulfide oxidation rates were approximately 50 times faster than silicate dissolution rates, ranging from 20 – 400 times faster depending on the silicate mineral. Coatings formed far more slowly on silicate minerals than sulfides (Appendix 1, Attachment A1.2), indicating their reduced reactivity relative to sulfide minerals, particularly pyrrhotite.

6.7.4. Comparison of Modeled Dissolution Rates with Literature Values

In addition to individual experimental rates from the literature, modeled silicate dissolution rates were compared to acid and neutral rate equations from Palandri and Kharaka (2004) (see Figures 78, 79 for plagioclase example). These equations were developed by synthesizing all appropriate literature rates for each mineral, often including rates listed previously in the tables (Tables 73-77). The neutral rate equation indicates independence of pH in the circumneutral pH range. Palandri and Kharaka also list rates for basic pH ranges, although this is of lesser concern to dissolution of Duluth Complex rock associated with mining wastes. In this section, modeled silicate dissolution rates were compared to the summation of acid and neutral rate equations from Palandri and Kharaka (Table 78). Due to the lack of Na and K data during periods A and B for reactors 1-38, the samples stored for 8 years prior to kinetic test work (reactors 39-44) are included in this comparison in order to utilize available Na and K data. It should be noted that SO_4, Ca, and Mg release rates during these earlier periods were reasonably similar to reactors 1-38, with average release rates within 85, 75, and 40% of the overall average, respectively (Tables 28-30).

Additional comparisons with other literature rates are in Tables 73-77. These differences between modeled dissolution rates for each silicate mineral and reported literature rates could be due to a number of model assumptions (i.e. stoichiometric release, surface roughness factor) as well as the mineral purity of the samples analyzed in the literature.

6.7.4.1. Plagioclase

Modeled plagioclase dissolution rates during periods B-D were fairly consistent over time. Calculated rates were within a factor of three from the overall average (9.3×10^{-13} mol m^{-2} s^{-1}) in all four models (Figure 68). Plagioclase dissolution rates displayed little pH dependence, although there appeared to be a subtle dependence in models 3 and 4 when pH dropped below 4.5 (Figure 80). The range in plagioclase dissolution rates was fairly tight in models 1, 3, and 4 (within an order of magnitude) as pH dropped from 7 to 4. However, this range was much larger in model 2 (three orders of magnitude), which is most likely attributed to augite dissolution.

Calcium concentrations reflect the fairly constant modeled plagioclase rates with respect to pH and time. Increases in calcium release rates were often observed as pH decreased near and below 4. These increases were typically paralleled by increases in magnesium concentration. A total of 26 samples displayed drainage pH below 4.4. Out of those, 15 samples displayed increasing Ca and Mg, 5 samples displayed increasing Ca with no associated Mg increase, 2 samples displayed increasing Mg with no associated Ca increase, and 4 samples displayed no increase in Ca or Mg release. This parallel increase in Ca and Mg when pH < 4.4 is most likely attributed to augite dissolution, although plagioclase rates also might have increased in this pH range. The lack of rate dependence on dissolution time is consistent with conclusions from White and Brantley (2003). They reported very slow decreases in plagioclase dissolution rates, estimating that it would take over 22,000 years for a rate decrease of about two orders of magnitude.

Although modeled plagioclase dissolution rates were slower than reported rates for labradorite, model 1 likely overestimated the plagioclase dissolution rate. Initially, plagioclase dissolution overestimates could have been from rapid dissolution of Ca-rich minerals such as calcite. Later overestimation could have resulted from nonstoichiometric dissolution of intermediate feldspars (%An<75) at pH<5. Nonstoichiometric plagioclase dissolution has been reported in both field and laboratory (Blum and Stillings 1995), resulting in a Si-rich leached layer. This means that Ca could be preferentially released, although some claims of this have been attributed to dissolution of Ca-rich exsolution lamellae (Inskeep et al. 1991). There also could have been error resulting from the formula used to determine density of plagioclase (Table 48). This equation, which depended on percent anorthite, was subject to the error associated with the number of grains examined and could result in either higher or lower rate determinations.

More recent work has reported stoichiometric dissolution of plagioclase (e.g., White and Brantley 2003). Some results from this experiment indicate nonstoichiometric dissolution. Observed Ca:Na was generally higher than predicted by average stoichiometry of the sample (Table 26, Appendix 7, Attachment A7.1, Figures A7.1-A7.21), possibly indicating preferential release of Ca. Observed ratios were typically lower than values predicted from individual grain stoichiometry when pH>4.4, while the relationship was reversed when pH<4.4. Although some of these differences could be based on sampling error brought on by analysis of too few grains, the differences at pH<4.4 are quite large. These large differences between observed and predicted at lower pH could be due to the formation of Ca-poor depleted layers, or the dissolution of augite.

Most experimentally determined rates were conducted under conditions likely to give higher rates than this experiment, as noted earlier in Section 6.7.1. However, modeled plagioclase dissolution rates were approximately an order of magnitude faster than rates in fresh granite with 26% plagioclase, approximately 1.0 x 10-13 mol m^{-2} s^{-1} (White and Brantley 2003). White and Brantley's study is a good comparison to this experiment because it was conducted in a column reactor, ran for an extended period (6.2 years), and was conducted with ground rock rather than a homogeneous sample of a pure mineral.

Palandri and Kharaka (2004) labradorite and andesine dissolution rates were used for comparison with modeled plagioclase dissolution rates. Labradorite rates were 40-160 times higher at pH 4 and 3-20 times higher at pH 6 than modeled plagioclase dissolution rates. Andesine rates were 10-40 times higher at pH 4 and 0.7-7 times higher at pH 6 (Table 78). Model 1 rates were typically the closest to literature rates due to the assumption that all Ca was attributed to plagioclase. In contrast, differences between modeled and literature rates at pH 6 were the greatest in models 3 and 4, because plagioclase dissolution was calculated based on sodium release which was typically lower than calcium release.

6.7.4.2. Olivine

Modeled olivine dissolution rates during periods B-D were less consistent over time. Calculated rates were within a factor of three from the overall average (9.3×10^{-12} mol m^{-2} s^{-1}) in 7 out of 9 model runs (Figure 71). It should be noted that in a number of the model runs, a significant portion of the calculated rates were zero (≈3 to 50%), indicating a calculated absence of olivine dissolution. Olivine dissolution rates displayed a slight pH dependence, increasing by about a factor of three as pH dropped below 4.5

(Figure 82). This dependence was more apparent in models 3 and 4. The range in olivine dissolution rates was within approximately two orders of magnitude as pH dropped from 7 to 4 in all four models.

Although literature dissolution rates reported for olivine are much faster than those for plagioclase, the modeled maximum dissolution rates for olivine (generally assuming all Mg release from olivine) are only slightly faster than the modeled plagioclase dissolution rates. Reported rates of olivine dissolution are approximately two orders of magnitude faster than plagioclase, whereas average modeled rates were 1-3 times faster in period A (the first 34-144 weeks of dissolution) and 2-30 times faster in periods B through D (Table 57). Although this is, in part, potentially an artifact of the modeling assumptions, this might be due to inhibition of dissolution by alteration of the olivine surface, a phenomenon reported by several researchers.

The relative rates of plagioclase and olivine dissolution determined by these models must be considered based on the composition of the samples. Rates of calcium release were often greater than those of magnesium release. However, the plagioclase content of the samples was considerably higher than the olivine content. Plagioclase contents were typically near 50 percent. In contrast, olivine contents ranged from 5-20 percent, excluding two samples with no olivine (0.40, 0.54%S) and one sample with 39% olivine (0.92%S). Thus, the plagioclase contents were considerably higher than those of olivine. Consequently, calcium release rates exceeding magnesium release rates did not indicate plagioclase dissolution rates exceeding olivine dissolution rates.

Palandri and Kharaka (2004) forsterite and fayalite dissolution rates were used for comparison with modeled olivine dissolution rates. Forsterite rates were 120-270 times higher at pH 4 and 10-280 times higher at pH 6 than modeled olivine dissolution rates. Fayalite rates were 100-230 times higher at pH 4 and 0.9-20 times higher at pH 6 than modeled olivine dissolution rates (Table 78). Agreement with literature values typically was best in model 1, which assumed that all Mg release was associated with olivine, resulting in the maximum dissolution rates.

6.7.4.3. Pyroxene Group Silicates

6.7.4.3.1. Hypersthene (Bronzite)

Modeled hypersthene dissolution rates during periods B-D were less consistent over time. Calculated rates were within a factor of three from the overall average (2.4×10^{-12} mol m^{-2} s^{-1}) in 5 out of 7 model runs (Figure 70). It should be noted that in a number of the model runs, a significant portion of the calculated rates were zero (≈5 to 50%), indicating a calculated absence of hypersthene dissolution. Hypersthene dissolution rates displayed little pH dependence, increasing slightly (approximately 40%) as pH dropped below 4.5 (Figure 83). The range in hypersthene dissolution rates was within approximately two orders of magnitude as pH dropped from 7 to 4 in models 1 and 3 and approximately three orders of magnitude in models 2 and 4.

Palandri and Kharaka (2004) bronzite dissolution rates were used for comparison with modeled hypersthene dissolution rates. Bronzite rates were 3-5 times higher at pH 4 than modeled hypersthene dissolution rates. Bronzite rates at pH 6 were typically in good agreement with modeled hypersthene dissolution rates, within a factor of 4 (Table 78). Similar to olivine, model 1 hypersthene dissolution rates were the closest to literature values due to the assumption that all Mg was associated with hypersthene, resulting in the maximum dissolution rates.

6.7.4.3.2. Augite

Modeled augite dissolution rates during periods B-D were fairly consistent over time. Calculated rates were within a factor of three from the overall average (3.6×10^{-12} mol m^{-2} s^{-1}) in all four models (Figure 69). Augite dissolution rates displayed a strong pH dependence in model 1, but no significant pH dependence in models 2-4 was observed (Figure 81). The range in augite dissolution rates was typically within 1-2 orders of magnitude as pH dropped from 7 to 4 in all four models.

The concurrent release of Ca and Mg in period C was crucial to model 1, because it indicated dissolution of augite, which was the only common sample mineral with approximately equal proportions of Ca and Mg. This assumption was validated by reported labradorite and augite rates from four studies. Results from these four studies were graphically analyzed to determine that augite rates were faster than labradorite rates at pH<4 (McAdam et al. 2007). This difference in rates, combined with the stoichiometry of augite in these samples (Table 11), gave good justification for the concurrent release assumption.

Palandri and Kharaka (2004) augite dissolution rates were 40-70 times higher than modeled rates at pH 4. Modeled dissolution rates at pH 6 were in very good agreement with literature values, within 80% (Table 78). Model 2 rates were typically the closest to literature rates due to the assumption that all Mg release was associated with augite dissolution.

6.7.4.4. Biotite

Modeled biotite dissolution rates during periods B-D were less consistent over time. Calculated rates were within a factor of three from the overall average (3.8×10^{-12} mol m^{-2} s^{-1}) in 8 out of 10 model runs (Figure 72). It should be noted that in a number of the model runs, a significant portion of the calculated rates were zero (≈6 to 50%), indicating a calculated absence of biotite dissolution. Biotite dissolution rates displayed no significant pH dependence in all four models (Figure 84). The range in biotite dissolution rates was within approximately one order of magnitude as pH dropped from 7 to 4 in models 1 and 4 and approximately 2-3 orders of magnitude in models 2 and 3.

Modeled biotite dissolution rates were 2-5 times higher at pH 4 and 0.3-40 times higher at pH 6 than Palandri and Kharaka (2004) biotite dissolution rates (Table 78). These higher modeled rates were most likely due to the assumption in models 1-3 that all residual Mg could be associated with biotite. However, based on mineralogical analysis, biotite on average contributed approximately 14% of Mg present in the samples (Table 23). Modeled biotite dissolution rates may have also been higher due to an underestimation of surface roughness.

7. CONCLUSIONS

Fifteen 75-gram samples of Duluth Complex rock ($0.053 < d < 0.149$ mm) containing 0.18 to 1.71 percent sulfur were characterized (chemistry, mineral content, mineral chemistry), subjected to laboratory dissolution tests, and examined for dissolution features following these tests. The major elements present as oxides in the samples, in descending order were silicon, aluminum, iron, calcium, magnesium, sodium, and titanium. Heavy metals of greatest concern decreased in the order (with typical percent concentration ranges in parentheses) copper (0.05 – 0.14), nickel (typically 0.03 – 0.05), zinc (0.01 – 0.02), and cobalt (0.005 – 0.01) (Table 3). Plagioclase was the dominant host-rock mineral, comprising 40 to 60 volume percent. Olivine, hypersthene, and augite contents typically ranged from 5 to 20 percent, and ilmenite contents were typically reported as 3 to 8 percent. Lesser amounts of potassium feldspar, biotite, prehnite, and amphibole were also reported in some samples (Table 7). Based on chemical and mineralogical analyses, pyrrhotite was the major sulfide mineral, followed by chalcopyrite, cubanite, pentlandite, and lesser amounts of cobalt and zinc sulfides were present.

The samples were subjected to laboratory dissolution tests in which they were rinsed weekly with 200-mL volumes of distilled-deionized water for a period of 144 -1252 weeks. The volume of drainage was determined and drainage samples were analyzed at varying frequencies for pH, specific conductance, sulfate, silicon, calcium, magnesium, sodium, potassium, iron, aluminum, copper, nickel, cobalt, and zinc.

The objectives of the study were as follows.

1) Determine the variation of laboratory drainage pH with solid-phase sulfur content of Duluth Complex samples.
2) Based on the aforementioned relationship, categorize solids based on sulfur content and associated drainage pH.
3) Determine the variation of major ion release rates with solid-phase sulfur content and dissolution time.
4) Determine the empirical neutralization potentials of solids producing acidic drainage and compare these values to those determined by solid-phase analysis.
5) Determine rates of sulfide and silicate mineral dissolution as a function of dissolution time and drainage pH.

In general, drainage pH tended to decrease and release rates of heavy metals (copper, nickel, cobalt, zinc) and major cations (calcium, magnesium, sodium, potassium) tended to increase with increasing sulfur content (Section 6.4). Samples were divided into three groups based on sulfur content: Group I, 0.18, 0.22 %S; Group II, $0.40 \leq \%S \leq 0.70$; and Group III, $0.70 < \%S \leq 1.64$ (Section 6.2). As sulfur content increased, minimum pH decreased, and sulfate, major cation, and trace metal release increased. Drainage pH for the Group I samples was generally above 6.0. Based on drainage pH alone, disposal of waste rock in Group I would probably require no rigorous reclamation. Potential impacts of sulfate, copper, nickel, cobalt and zinc release from rock in this range of sulfur content would require consideration. The minimum drainage pH values for Groups II and III were 3.8 and 3.0, respectively. Minimum pH values and corresponding maximum sulfate release values were typically attained after 300 to 400 weeks (6 to 8 years) of dissolution. The maximum time to minimum pH was roughly 800 weeks, emphasizing the fact that short term drainage quality results do not necessarily reflect long-term trends. The decreasing sulfate release following attainment of maximum values was attributed to development of coatings on the sulfide mineral surface, and this was supported by photographs of leached sulfide grains. Diminishing sulfide mineral content over time contributed, to a lesser extent, to the decrease.

Neutralization potential (NP) is a measure of the capacity of a sample to neutralize acid, and this capacity was determined empirically based on the drainage quality observed in dissolution tests (Section 6.4.2). This empirical neutralization potential (ENP) was used for comparison with results from three methods used to determine NP based on solid-phase analysis. ENP values typically fell between 0.5 and 2 kg $CaCO_3$/t rock. NP calculated using carbon dioxide analysis to estimate total calcium plus magnesium carbonate content were closest to the ENP values (<0.7 to 2.5 kg $CaCO_3$/t rock), therefore the best estimate of the capacity of these samples to neutralize acid. Values determined on a subset of samples by a direct titration technique (Lapakko 1994a) yielded values roughly 1 to 3 kg $CaCO_3$/t rock higher than the observed values. Values determined by one common NP method (Sobek et al. 1978) almost always fell between 12 and 21 kg $CaCO_3$/t rock, substantially higher than the observed values (Table 22, Figure 61). These results indicate that caution must be exercised when selecting solid-phase methods for determining NP and interpreting the results generated.

These rock samples exhibited four typical periods of behavior characterized by declining pH in periods A and B, minimum pH in period C and increasing pH in period D (Section 6.3). All samples exhibited periods A and B, while only samples from groups II and III exhibited the more acidic pH and subsequent pH rise characteristic of periods C and D, respectively. The declining pH was due to increased acid production with increasing sulfide mineral surface area available for oxidation. The rise in pH after period C was caused by decreasing rates of sulfide mineral oxidation that was due to coating of the sulfide minerals and, to a lesser extent, diminishing amounts of sulfide minerals present. At the end of the experiment, there was typically 50% of sulfide minerals left unoxidized.

Two models were developed to determine rates of sulfide oxidation and four were developed for silicate dissolution. These rates were based on observed solute release, potential mineral sources of solutes, mineral chemistry, and mineral content. For each sample, mineral-specific surface areas were determined based on mineral content, geometric surface area, and surface roughness. Pyrrhotite oxidation rates were based on sulfate release and were highest during period C, coincident with minimum pH values (Section 6.6). Calculated rates of pyrrhotite oxidation during periods A and B were generally in reasonable agreement with rates reported for laboratory tests on pyrrhotite alone (i.e. in the absence of other minerals) (Janzen et al. 2000).

Silicate dissolution rates were generally in fair agreement among the four silicate dissolution models (Section 6.7). There did not appear to be strong dependence of rates on pH, with the exception of augite dissolution rates. Calculated silicate mineral dissolution rates were compared to rates published by Palandri and Kharaka (2004) (Table 78, Figures 80-84). Calcium-based rates of plagioclase dissolution for pH above about 5.5 were lower than published rates but within an order of magnitude. Calcium-based plagioclase rates at lower pH were much lower than published rates, as were plagioclase rates based on sodium dissolution. Similarly, calculated augite dissolution rates for pH above 5.5 tended to be lower than published rates but within an order of magnitude. Under more acidic conditions the calculated augite rates were generally more than an order of magnitude lower than published rates. The upper range of calculated hypersthene dissolution rates tended to be bounded by the published rates. For all pH values calculated olivine dissolution rates were generally far lower than published rates, and calculated biotite dissolution rates, whether based on magnesium or potassium release, tended to be one to two orders of magnitude higher than published rates.

Six Duluth Complex samples ($0.67 \leq \%\ S \leq 1.71$) that had been stored for eight to twenty years were also subjected to testing, typically for 809 weeks. These samples exhibited slower rates of sulfate release and higher drainage pH values than the aforementioned samples. Based on information presented by Janzen et al. (2000), this was attributed to the development of coatings on sulfide minerals during storage. It should be noted that during operation rock is exposed to elements immediately after blasting. Therefore, the storage time of drill core used to predict drainage quality in the field will affect the laboratory dissolution test results generated. That is, storage time for laboratory predictive test samples should be minimized, especially if the drill core samples have been crushed. Results from the tests on stored Duluth Complex samples were not included in modeling of pyrrhotite oxidation rates but were used in modeling silicate mineral dissolution rates (Section 6.7.4).

Four Virginia formation samples ($1.71 \leq \%\ S \leq 5.44$) were subjected to testing for 78 weeks. Due to their high sulfur contents, these samples generated acidic drainage relatively quickly. Drainage quality of these tests is briefly addressed in the results section, but is not included in the overall discussion. All drainage quality data are included in Appendix 3.

Practical implications of these results for environmentally sound management of waste rock generated by mining in Minnesota include the potential for managing waste rock based on sulfur content, a relatively simple analytical assessment. Based on drainage pH alone, disposal of waste rock in Group I ($\%S \leq 0.22\ \%$) would probably require no rigorous reclamation. Potential impacts of sulfate, copper, nickel, cobalt, and zinc release from rock in this range of sulfur content would require consideration. In order to meet water quality standards, waste rock producing drainage pH values similar to Group III samples ($0.70 < \%S \leq 1.64$) would require the most rigorous control measures of the samples tested. Elevated release of sulfate and heavy metals from these groups would likely require mitigation as well. The results have implications of substance to mine waste drainage quality prediction. First, caution that must be exercised when assessing the capacity of rock to neutralize acid based on solid-phase analyses designed to quantify NP. Second, results generated from short-term dissolution tests do not necessarily simulate long-term drainage quality. Emphasizing this point, drainage pH from one sample was circumneutral for 800 weeks and then acidified, reaching a minimum pH of 3.8. Third, tests conducted on samples that had been stored for 8 to 20 years yielded lower rates of sulfate release and higher drainage than samples within about one year of excavation. Therefore, samples used for mine waste drainage quality prediction should be tested as close to the time of their excavation as possible.

Additional work should be conducted to further the benefits generated to date. This includes continued dissolution testing to confidently define long-term trends, analysis of leached solids to increase understanding of chemical reactions controlling solute release (e.g. chemical precipitation and adsorption), and more detailed analysis of the present data and modeled mineral dissolution rates. Furthermore, the methods for calculating mineral dissolution rates and approaches for other aspects of data analysis developed for this project should be applied to experiments examining dissolution of Partridge River Intrusion rocks.

8. ACKNOWLEDGEMENTS

Funding for this report and laboratory work since July 2011 was provided by Minerals Cooperative Environmental Research and Iron Ore Cooperative Research State funding plus industry match. Funding for laboratory work prior to July 2011 was provided by State general fund. Bill Conger of LTV Steel Mining Company was responsible for particle size reduction, sample sieving, and neutralization potential analysis. Pat Geiselman conducted laboratory dissolution experiments. Debra Mayerich was responsible for data entry, and Mike Olson performed calculations and produced tables and graphs for the report text and appendices. Sulfide oxidation and silicate dissolution modeling was performed by Ethan Jenzen, Chev Kellogg, and Mike Olson.

9. REFERENCES

Acker, J.G., Bricker, O.P. 1992. The influence of pH on biotite dissolution and alteration kinetics at low temperature. Geochim. Cosmochim. Acta, 56, p. 3073-3092.

Ahonen, L., Hiltunen, P., Tuovinen, O. H. 1986. The role of pyrrhotite and pyrite in the bacterial leaching of chalcopyrite ores. In Fundamental and Applied Biohydrometallurgy. Lawrence, R. W., Branion, R. M. R., Ebner, H. G. (eds.). Elsevier, Amsterdam. p. 13-22.

Ahonen, L., Tuovinen, O. H. 1992. Bacterial oxidation of sulfide minerals in column leaching experiments at suboptimal temperatures. Applied and Environmental Microbiology, 58, pp. 600-606.

Alpers, C.N. 2000. Email communication from Charles Alpers, USGS, 12 May 2000.

Alpers, C. N., Blowes, D. W., Nordstrom, D. K., Jambor, J. L. 1994. Secondary minerals and acid-mine water chemistry. In Short Course Handbook on Environmental Geochemistry of Sulfide Mine Wastes, Waterloo, Ontario, May 1994. Mineralogical Association of Canada. p. 247-270.

American Public Health Association (APHA), American Water Works Association, Water Environment Federation. 1992. Standard Methods for the Examination of Water and Wastewater, 18th edition. American Public Health Association , Washington DC.

Anonymous. 1992. Skillings Mining Review, 81. p. 5.

ASTM. 2000. Annual Book of ASTM Standards, 11.04. American Society for Testing and Materials, West Conschohocken, PA.

Awad, A., Koster van Groos, K., Guggenheim, S. 2000. Forsteritic olivine: Effect of crystallographic direction on dissolution kinetics. Geochim. Cosmochim. Acta, 64(10), p. 1765-1772.

Banfield, J.F., Dyar, M.D., McGuire, A.V. 1992. The defect microstructure of oxidized mantle olivine from Dish Hill, California. American Mineralogist 77, p. 977-986.

Banfield, J.F., Veblen, D.R., Jones, B.F. 1990. Transmission electron microscopy of subsolidus oxidation and weathering of olivine. Contributions to Mineralogy and Petrology 106, p. 110-123.

Belzile, N., Chen, Y., Cai, M., Li, Y. 2004. A review on pyrrhotite oxidation. Journal of Geochemical Exploration, vol. 84, pp. 65-76.

Berg, A., Banwart, S.A. 2000. Carbon dioxide mediated dissolution of Ca-feldspar: implications for silicate weathering. Chemical Geology 163:25-42.

Biggs, F.R. 1989. Telephone conversation with Fred Biggs, Mining Engineer, Spokane Research Center, U.S. Bureau of Mines.

Blum, A. E. 1994. In Feldspars and their Reactions, I. Parson, ed., Kluwer Academic Publishers, p. 595-630.

Blum, A.E., Stillings, L.L. 1995. Feldspar dissolution kinetics. In: Chemical Weathering Rates of

Silicate Minerals, Mineral. Soc. Am. Short Course Vol 31 (ed. A.F. White and S.L. Brantley), Mineral. Soc. Am., p. 291-352.

Brantley, S.L. 2003. Reaction kinetics of primary rock-forming minerals under ambient conditions *in* Fresh water geochemistry, weathering and soils, J.I Drever (ed.), v. 5 of Treatise on geochemistry, K.K.Turekian and H.D. Holland (eds.), Pergamon Press, Oxford, pp. 73-117.

Brantley, S.L., Chen, Y. 1995. Chemical weathering rates of pyroxenes and amphiboles. In: Chemical Weathering Rates of Silicate Minerals, Mineral. Soc. Am. Short Course Vol 31 (ed. A.F. White and S.L. Brantley), Mineral. Soc. Am., p. 119-172.

Brantley, S.L., Mellott, N.P. 2000. Surface area and porosity of primary silicate minerals. American Mineralogist 85(11-12), p. 1767-1783.

Brown, R. 1989. Water management at Brenda Mines. In Proc. of the Thirteenth Annual British Columbia Mine Reclamation Symposium. June 7-9, 1989, Vernon, British Columbia. p. 8-17.

Busenberg, E., Clemency, C. 1976. The dissolution kinetics of feldspars at 25^o C and 1 atmosphere CO_2 partial pressure. Geochim. Cosmochim. Acta 40: 41-49.

Busenberg, E., Plummer, L.N. 1986. A comparative study of the dissolution and crystal growth kinetics of calcite and aragonite. F.A. Mumpton, ed., Studies in Diagenesis, U.S. Geological Survey Bulletin 1578. p. 139-168.

Busenberg, E., Plummer, L.N. 1982. The kinetics of dissolution of dolomite in CO_2-H_2O systems at 1.5^o to 65^o C and 0 to 1 atm P_{CO2}. American Journal of Science, v. 282. p. 45-78.

Chen, Y., Brantley, S.L. 1997. Temperature- and pH-dependence of albite dissolution rate at acid pH. Chemical Geology 135, p. 275-290.

Chen, Y., Brantley, S.L. 1998. Diopside and anthophyllite dissolution at 25 and 90^{0}C and acid pH. Chemical Geology 147(3-4), p. 233-248.

Chen, Y., Brantley, S.L. 2000. Dissolution of forsteritic olivine at 65^{0}C and $2<pH<5$. Chemical Geology 165, p. 267-281.

Chodos, A.A., Engel C.G. 1961. Fluorescent X-ray spectrographic analyses of amphibolite rocks. American Mineralogist 46, pp. 120-133.

Chou, L., Garrels, R.M., Wollast, R. (1989) Comparative study of the kinetics and mechanisms of dissolution of carbonate minerals. Chemical Geology, v. 78, no.3-4. p. 269-282

Chou, L., Wollast, R. 1985. Steady state kinetics and dissolution mechanisms of albite. American Journal of Science, 285. p. 963-993.

Ciccarelli, J.M., Weber, P.A., Stewart, W.S., Li, J., Schumann, R., Miller, S.D., Smart, R. St. C. 2009. Estimation of long-term silicate neutralization of acid rock drainage. In Proc. Securing the Future and 8th ICARD, June 22-26, 2009, Skellefteå, Sweden (CD ROM). 11 p.

Cravotta, C. A. 1994. Secondary iron-sulfate minerals as sources of sulfate and acidity: Geochemical evolution of acidic ground water at a reclaimed surface coal mine in Pennsylvania. In Environmental Geochemistry of Sulfide Oxidation; ACS Symposium Series 550; American Chemical Society: Washington, DC, 1993. pp. 343-364.

Crock, J.G., Lichte, F.E., Briggs, P.H. 1983. Determination of elements in National Bureau of Standards' geological reference materials SRM 278 obsidian and SRM 688 basalt by inductively coupled argon plasma-atomic emission spectrometry: Geostandards Newsletter, 7. p. 335-340.

Drever, J.I. 1988. The geochemistry of natural waters: Prentice Hall, Englewood Cliffs, New Jersey, 437 p.

Drever, J.I., Clow, D.W. 1995. Weathering rates in catchments. In: White, A.F. and Brantley, S.L. (Eds.), Chemical Weathering Rates of Silicate Minerals, Mineralogical Society of America, vol. 31, pp. 463-481.

Duro, L., El Aamrani, F., Rovira, M., Gimenez, J., Casas, I., de Pablo, J., Bruno, J. 2005. The dissolution of high-FeO olivine rock from the Lovasjarvi intrusion (SE-Finland) at 25^0C as a function of pH. Applied Geochemistry 20, p. 1284—1291.

Eggleston, C.M., Hochella, M.F., Parks, G.A. 1989. Sample preparation and aging effects on the dissolution rate and surface composition of diopside. Geochim. Cosmochim. Acta 53, p. 797-804.

Furrer, G, Stumm, W. 1986. The coordination chemistry of weathering, I: Dissolution kinetics of delta-Al_2O_3 and BeO. Geochim. Cosmochim. Acta 50:1847-1860.

Ganor, J., Roueff, E., Erel, Y., Blum, J. 2005. The dissolution kinetics of a granite and its minerals - Implications for comparison between laboratory and field dissolution rates. Geochim. Cosmochim. Acta 69: 607-621.

Garrels, R.M., Howard, P. 1959. Reactions of feldspar and mica with water at low temperature and pressure. Clays and Clay Minerals 6: 68-88.

Gaudin, A. M., Fuerstenau, D. W., Mao, G. W. 1959. Activation and deactivation studies with copper on sphalerite. Trans. AIME 214: 430–432.

Greenberg, J., Tomson, M. 1992. Precipitation and dissolution kinetics and equilibria of aqueous ferrous carbonate vs temperature. Applied Geochemistry, 7 (2), p. 185-190.

Hem, J.D. 1970. Study and interpretation of the chemical characteristics of natural water. Geological Survey Water-Supply Paper 1473, Washington, D.C. 363 p.

Hellmann, R., Penisson, J.M., Hervig, R.L., Thomassin, J.H., Abrioux, M.F. 2003. An EFTEM/HRTEM high-resolution study of the near surface of labradorite feldspar altered at acid pH: evidence for interfacial dissolution-reprecipitation. Phys Chem Minerals 30: 192-197.

Hodson, M.E. 2003. The influence of Fe-rich coatings on the dissolution of anorthite at pH 2.6. Geochimica et Cosmochimica Acta, 67(18), p. 3355-3363.

Hoffman, E.L. 1992. Instrumental neutron activation in geoanalysis. Jour. Geochem. Explor., 44. p. 297-319.

Iishi, K., Torigoe, K., Han, X. J. 1997. Oriented precipitate complexes in iron-rich olivines produced experimentally in aqueous oxidizing environment. Physics and Chemistry of Minerals 25, p. 8-14.

Inskeep, W.P., Nater, E.A., Bloom, P.R., Vandervoort, D.S., Erich, S.M. 1991. Characterization of laboratory weathered labradorite surfaces using X-ray photoelectron spectroscopy and transmission electron microscopy. Geochim. Cosmochim. Acta 55:787-800.

Iversen, I.R., Johannessen, M. 1987. Water pollution from abandoned mines in Norway. Report to the Norwegian State Pollution Control Authority and The Ministry of Industry by the Norwegian Institute for Water Research. 60 p.

Jambor, J.L. 1994. Mineralogy of sulfide-rich tailings and their oxidation products. In Environmental Geochemistry of Sulfide Mine-Wastes. Mineralogical Association of Canada, Short Course Handbook, Volume 22: 59-102.

Jambor, J.L. 2003. Mine-waste mineralogy and mineralogical perspectives of acid-base accounting. In Environmental Aspects of Mine Wastes (J.L. Jambor, D.W. Blowes, A.I.M. Ritchie, eds.). Mineralogical Association of Canada Short Course Volume 31. p. 117-145.

Jambor, J.L., Ptacek, C.J., Blowes, D.W., Moncur, M.C. 2005. Acid drainage from the oxidation of iron sulfides and sphalerite in mine wastes. Proceedings from: Lead and Zinc ’05, vol. 1.Fujisawa (Ed.). The Mining and Materials Processing Institute of Japan, pp. 715-737.

Janney, D.E., Banfield, J.F. 1998. Distribution of cations and vacancies and the structure of defects in oxidized intermediate olivine by atomic-resolution TEM and image simulation. American Mineralogist 83, p. 799-810.

Janzen, M.P. 1996. Role of ferric iron, trace metal content, and crystal structure on pyrrhotite oxidation. Master thesis, University of Waterloo, Waterloo, Ontario. 175 pp.

Janzen, M.P., Nicholson, R.V., Scharer, J.M. 1997. The role of enhanced particle surface area, crystal structure and trace metal content on pyrrhotite oxidation rates in tailings. In Proceeding of the Fourth International Conference on Acid Rock Drainage. Vol. 1. Vancouver, British Columbia, May 31 - June 6, 1997.

Janzen, M.P., Nicholson, R.V., Scharer, J.M. 2000. Pyrrhotite reaction kinetics: reaction rates for oxidation by oxygen, ferric iron, and for nonoxidative dissolution. Geochimica et Cosmochimica Acta, 64, 9, pp. 511-1522.

Jerz, J.K., Rimstidt, D.J. 2000. A reactor to measure pyrite oxidation in air. In Proceedings of the Fifth International Conference on Acid Rock Drainage. SME, Littleton, CO. p. 55-60.

Kalinowski, B.E., Schweda, P. 1996. Kinetics of muscovite, phlogopite, and biotite dissolution and alteration at pH 1-4, room temperature. Geochimica et Cosmochimica Acta , 60, 3. p. 367-385.

Khisina, N.R., Khramov, D.A., Kleschev, A.A., Langer, K. 1998. Laihunization as a mechanism of olivine oxidation. European Journal of Mineralogy 10, p. 229-238.

Kingston, G.A., Carillo, F.V., Gray, J.J., Mallory, P. 1970. U.S. Bureau of Mines IC 8469. 57 pp.

Klein, C,. Hurlbut, C.S. Jr. 1985. Manual of Mineralogy, 20th ed. John Wiley & Sons, New York. 596 pp.

Klein, C,. Hurlbut, C.S. Jr. 1999. Manual of Mineralogy, 21st ed. John Wiley & Sons, New York. 681 pp.

Kleinmann, R.L.P., Crerar, D.A., Pacelli, R.R. 1981. Biogeochemistry of acid mine drainage and a method to control acid formation. Mining Eng., v. 33. p. 300-306.

Koch, D. F. 1975. Electrochemistry of sulfide minerals. In Modern Aspects of Electrochemistry 10, J. O. Bockris, B. E. Conway (eds.): 211-237.

Kwong, E.C.M. 1995. Abiotic and biotic pyrrhotite dissolution. M.A.Sc. Thesis, Univ. Waterloo, Waterloo, Ontario.

Kwong, Y.T.J., Ferguson, K.D. 1990. Water chemistry and mineralogy at Mt. Washington: Implications to acid generation and metal leaching. In Acid Mine Drainage: Designing for Closure. (J.W. Gadsby, J.A. Malick & S.J. Day, eds). Bitech Publishers, Vancouver, British Columbia, 217-230.

Lapakko, K. A. 1988. Prediction of acid mine drainage from Duluth Complex mining wastes in northeastern Minnesota. In Mine Drainage and Surface Mine Reclamation. v. 1. Mine Water and Mine Waste. Proceedings of the 1988 Mine Drainage and Surface Mine Reclamation Conference. BuMines IC 9183. p. 180-190.

Lapakko, K.A. 1990. Regulatory mine waste characterization: A parallel to economic resource evaluation. In Mining and Mineral Processing Wastes, Proceedings of the Western Regional Symposium on Mining and Mineral Processing Wastes. Fiona Doyle, ed. Berkeley, California, May 30 - June 1, 1990. p. 31-39.

Lapakko, K.A. 1993a. Laboratory dissolution of drill core samples of Duluth Complex rock. Report to the US Bureau of Mines, Salt Lake City Research Center, Cooperative Agreement No. C0219003. MN Dep. Nat. Resour., Div. Of Minerals. St. Paul, MN. 28 p. plus appendices.

Lapakko, K.A. 1993b. Laboratory dissolution of blast hole samples of Duluth Complex rock. Report to the US Bureau of Mines, Salt Lake City Research Center, Cooperative Agreement No. C0219003. MN Dep. Nat. Resour., Div. Of Minerals. St. Paul, MN. 44 p. plus appendices.

Lapakko, K.A. 1993c. Field dissolution of test piles of Duluth Complex rock. Report to the US Bureau of Mines, Salt Lake City Research Center, Cooperative Agreement No. C0219003. MN Dep. Nat. Resour., Div. Of Minerals. St. Paul, MN. 41 p. plus appendices.

Lapakko, K.A. 1994a. Evaluation of neutralization potential determinations for metal mine waste and a proposed alternative. In Proc. Third International Conference on the Abatement of Acidic Drainage, April 25-29, 1994, Pittsburgh, PA. Vol. 1. p. 129-137.

Lapakko, K.A. 1994b. Comparison of Duluth Complex rock dissolution in the laboratory and field. In Proc. Third International Conference on the Abatement of Acidic Drainage, April 25-29, Pittsburgh, PA. Vol. 1. P. 270-278.

Lapakko, K. A., Antonson, D. A. 1993. Oxidation of sulfide minerals present in Duluth Complex rock: A laboratory study. In Environmental Geochemistry of Sulfide Oxidation; ACS Symposium Series 550; American Chemical Society: Washington, DC, 1993. p. 593-607.

Lapakko, K.A., Antonson, D.A. 1994. Oxidation of sulfide minerals present in Duluth Complex rock: A laboratory study. In: Environmental geochemistry of sulfide oxidation, ACS symposium series No. 550, American Chemical Society, Washington DC, pp. 593-607.

Lapakko, K.A., Antonson, D.A. 2002. Drainage pH, acid production, and acid neutralization for Archean greenstone rock. Preprint 02-73 In Proc. 2002 SME Annual Meeting, February 25-27, Phoenix, AZ (CD-ROM). Soc. For Mining, Metallurgy, and Exploration, Inc. Littleton, CO.

Lapakko, K.A., Antonson, D.A., Engstrom, J. 2004a. Analytical screening of abandoned waste rock piles. Report contract/order No. DACW45-02-P-212 to the U.S. Bureau of Land Management, Salt Lake City Office, June 2004. 91 pp. plus appendices.

Lapakko, K.A., Antonson, D.A., Folman, J.T., Engstrom, J. 2004b. Archean greenstone laboratory dissolution experiment. Final report contract JSP012018 to the U.S. Bureau of Land Management, Salt Lake City Office, 30 September 2004. 93 pp. plus appendices.

Lapakko, K.A., Antonson, D.A., Wagner, J.R. 1997. Mixing of limestone with finely-crushed acid-producing rock In Proc. Fourth Intl. Conf. On Acid Rock Drainage. Vol. 3, Vancouver, British Columbia, Canada, May 31 - June 6, 1997. p. 1345-1360.

Lapakko, K.A., Berndt, M. 2003. Comparison of acid production from pyrite and jarosite. In Proc. of the Sixth International Conference on Acid Rock Drainage. Australasian Institute of Mining and Metallurgy, Publication Series No 3-2003 (CD ROM). p. 461-467.

Lapakko, K.A., Olson, M.C., Antonson, D.A. 2013a. Duluth Complex Tailings Dissolution Experiment: Ten-year laboratory experiment. MN Dept. Nat. Resour. Div. Lands and Minerals, St. Paul, MN. 54 p. plus appendices.

Lapakko, K.A., Olson, M.C., Antonson, D.A. 2013b. Dissolution of Duluth Complex Rock from the Babbitt and Dunka Road Prospects: Eight-year laboratory experiment. MN Dept. Nat. Resour. Div. Lands and Minerals, St. Paul, MN. 88 p. plus appendices.

Lawrence, R.W. 1990. Prediction of the behaviour of mining and processing wastes in the environment. In Proc. Western Regional Symposium on Mining and Mineral Processing Wastes, F. Doyle (ed.), Soc. for Mining, Metallurgy, and Exploration, Inc., Littleton, CO. P. 115-121.

Leopold, E., Lapakko, K.L. 2001 Pyrrhotite oxidative dissolution: Reaction rates and mechanisms. Minnesota Department of Natural Resources. 12 p. plus appendices.

Liu, Y., Olsen, A.A., Rimstidt, D.J. 2006. Mechanism for the dissolution of olivine series mineral in acidic solutions. American Mineralogist, 91. pp. 455-458.

Luce, R.W., Bartlett, R.W., Parks, G.A. 1972. Dissolution kinetics of magnesium silicates. Geochimica et Cosmochimica Acta, 36. p. 35-50.

McAdam, A.C., Zolotov, M.Yu., Mironenko, M.V., Sharp, T.G. 2007. Preferential low-pH dissolution of pyroxene in plagioclase-pyroxene mixtures and implications for Martian low-albedo regions. Lunar and Planetary Science 38, abstract 1871.

McSwiggen, P.L. 1999. Platinum-palladium group minerals, gold, silver, and cobalt in the Minnamax copper-nickel sulfide deposit, Duluth Complex, northeastern Minnesota. Report of Investigation 54. Minnesota Geological Survey. University of Minnesota. Saint Paul, MN. 29 pp.

Miller, J.D., Jr., Green, J.C., Severson, M.J., Chandler, V.W., Peterson, D.E. 2001. Geologic map of the Duluth Complex and related rocks, northeastern Minnesota. Miscellaneous Map Series, M-119, scale 1:200,000, 2 sheets.

Miller, J.D., Jr., Severson, M.J., Foose, M.P. 2005. Bedrock geology of the Babbitt Northeast quadrangle, St. Louis and Lake Counties, Minnesota. Minnesota Geological Survey Miscellaneous Map M-160, scale 1:24,000.

Nagy, K.L. 1995. Dissolution and precipitation kinetics of sheet silicates. Mineralogical Society of America 31, p. 173-233.

Natarjan, K. A., Reid, K. J., Iwasaki, I. 1982. Microbial aspects of hydrometallurgical processing and environmental control of copper/nickel-bearing Duluth gabbro. In Proc. 55th Annual Meeting of the Minnesota Section, AIME and 43rd Annual Mining Symposium, January 13-15, 1982, Duluth, MN. 21 p.

Natural Resources Research Institute. 2013. http://www.nrri.umn.edu/egg/pubs_nonferrous.html. Site accessed December 2013.

Nesbitt, H.W., Jambor, J.L. 1998. Role of mafic minerals in neutralizing ARD, demonstrated using a chemical weathering methodology. In Cabri, L.J. and Vaughan, D.J. (eds.), Modern Approaches to Ore and Environmental Mineralogy. Mineralogical Association of Canada Short Course Series, v. 27. pp. 403-421.

Nesbitt, H.W., MaCrae, N.D., Shotyk, W. 1991. Congruent and incongruent dissolution of labradorite in dilute, acidic, salt solutions. Journal of Geology 99. pp. 429-442.

Nordstrom, D. K. 1982. Aqueous pyrite oxidation and the consequent formation of secondary iron minerals. In Acid Sulfate Weathering. K.A. Cedric, D.S. Fanning, and I.R. Hossner (eds.), Soil Sci. Soc. America Spec. Pub. 10. p. 37-56.

Nordstrom, D.K. 1999. Some fundamentals of aqueous geochemistry. In The Environmental Geochemistry of Mineral Deposits. Part A: Processes, Techniques, and Health Issues. Vol. 6A, Chapter 4. Reviews in Economic Geology. Society of Economic Geologists, Inc., Chelsea, MI. p. 117-123.

Nordstrom, D.K., Alpers, C.N. 1999. Geochemistry of acid mine waters. In The Environmental Geochemistry of Mineral Deposits. Part A: Processes, Techniques, and Health Issues. Vol. 6A, Ch. 4. Reviews in Economic Geology. Society of Economic Geologists, Inc., Chelsea, MI. p. 133-160.

Nugent, M. A., Maurice, P., Brantley, S. L. 1998. The field dissolution rate of feldspar in a Pennsylvania (USA) spodsol as measured by atomic force microscopy. Water Rock Interaction, AA Balkema, Rotterdam. P. 387-390.

Oberheuser, G., Kathrein, H., Demortier, G., Gonska, H., Freund, F. 1983. Carbon in olivine single crystals analyzed by the $^{12}C(d, p)^{13}C$ method and by photoelectron spectroscopy. Geochim. Cosmochim. Acta, 47(6), p. 1117-1129.

Oelkers, E.H. 2001. An experimental study of forsterite dissolution rates as a function of temperature and aqueous Mg and Si concentrations. Chemical Geology 175, p. 485-494.

Oxburgh, R., Drever, J.I., Sun, Y. 1994. Mechanism of plagioclase dissolution in acid solution at 25^0C. Geochim. Cosmochim. Acta 58, p. 661-669.

Palandri, J.L., Kharaka, Y.K. 2004. A compilation of rate parameters of water-mineral interaction kinetics for application to geochemical modeling. U.S. Geological Survey Open File Report 2004-1068. U.S. Geological Survey in cooperation with the National Energy Technology Laboratory - United States Department of Energy. 70 p.

Phillips, E., Doctor, D., Leopold, E., Lapakko, K. 2001. Dissolution of silicate minerals present in the Duluth Complex and Archean Greenstone formations. Minnesota Department of Natural Resources. 35 p.

Plumlee, G. 1999. The environmental geology of mineral deposits. In The Environmental Geochemistry of Mineral Deposits. Part A: Processes, Techniques, and Health Issues. Vol. 6A, Chapter 3. Reviews in Economic Geology. Society of Economic Geologists, Inc., Chelsea, MI. p. 71-116.

Pokrovsky, O.S., Schott S. 2000a. Forsterite surface composition in aqueous solutions: A combined potentiometric, electrokinetic, and spectroscopic approach. Geochim. Cosmochim. Acta, 64, p. 3299-3312.

Pokrovsky, O.S., Schott S. 2000b. Kinetics and mechanism of forsterite dissolution at 25^0C and pH from 1 to 12. Geochim. Cosmochim. Acta, 64, p. 3313-3325.

Pugh, C.E., Hossner, L.R., Dixon, J.B. 1984. Oxidation rate of iron sulfides as affected by surface area, morphology, oxygen concentration, and autotrophic bacteria. Soil Science, v. 137, no. 5. p. 309-314.

Pratt, AR; Muir, IL; Nesbitt, HW. 1994a. X-ray photoelectron and Auger electron spectroscopic studies of pyrrhotite and mechanism of air oxidation. Geochim. Cosmochim. Acta 58(2), 827-841.

Pratt, AR; Nesbitt, HW; Muir, IJ. 1994b. Generation of acids from mine waste: Oxidative leaching of pyrrhotite in dilute H_2SO_4 solutions at pH 3.0. Geochim. Cosmochim. Acta 58, 5147-5159.

Rosso, J.J., Rimstidt, J.D. 2000. A high resolution study of forsterite dissolution rates. Geochim. Cosmochim. Acta 64, p. 797-811.

Santelli, C.M., Banfield, J.F., Welch, S.A., Westrich, H.R. 2001. The effect of Fe-oxidizing bacteria on Fe-silicate mineral dissolution. Chemical Geology 180(1-4), p. 99-115.

Schott, J., Berner, R.A. 1983. X-ray photoelectron studies of the mechanism of iron silicate dissolution during weathering. Geochim. Cosmochim. Acta 47(12), p. 2233-2240.

Schott, J., Berner, R.A. 1985. Dissolution mechanisms of pyroxenes and olivines during weathering. The Chemistry of Weathering, D. Reidel Publishing Company, Dordrecht, Netherlands. P. 35-53.

Schott, J., Berner, R.A., Sjöberg, E.L. 1981. Mechanism of pyroxene and amphibole weathering - I. Experimental studies of iron-free minerals. Geochim. Cosmochim. Acta 45, p. 2123-2135.

Schweda, P., Sjöberg, L., Sodervall, U. 1997. Near-surface composition of acid-leached labradorite investigated by SIMS. Geochim. Cosmochim. Acta 60(10), 1985-1994.

Severson, M.J. 1994. Igneous stratigraphy of the South Kawishiwi Intrusion, Duluth Complex, Northeastern, Minnesota. Natural Resources Research Institute, Technical report NRRI/TR-93-34. 210 pages.

Severson, M.J., Barnes, R.A. 1991. Geology, mineralization, and geostatistics of the Minnamax/Babbitt Cu-Ni deposit (Local Boy Area), Minnesota. Part II: Mineralization and geostatistics. Natural Resources Research Institute, Technical report NRRI/TR-91/13b.

Singer, P.C., Stumm, W. 1970. Acid mine drainage: The rate determining step. Science, 167. p. 1121-1123.

Shaw, S.C., Groat, L.A., Jambor, J.L., Blowes, D.W., Hanton-Fong, C.J., Stuparyk, R. 1998. Mineralogical study of base metal tailings with various sulfide contents in laboratory columns and field lysimeters. Environmental Geology 33, p. 209-217.

Siever, R., Woodford, N. 1979. Dissolution kinetics and the weathering of mafic minerals. Geochim. Cosmochim. Acta 43. p. 717-724.

Sjöberg, L. 1989. Kinetics and non-stoichiometry of labradorite dissolution. Water-rock interaction WRI-6: Proceedings of the 6th international symposium, Malvern, UK. p. 639-642.

Smith, K.S. 1999. Metal sorption on mineral surfaces: An overview with examples relating to mineral deposits. In The Environmental Geochemistry of Mineral Deposits. Part B: Case Studies and Research Topics. Vol. 6B, Chapter 7. Filipek, L., Plumlee, G. (Volume Eds). Reviews in Economic Geology. Society of Economic Geologists, Inc., Chelsea, MI. p. 161-182.

Smith, K.S., Huyck, H.L.O. 1999. An overview of the abundance, relative mobility, bioavailability, and human toxicity of metals. In The Environmental Geochemistry of Mineral Deposits. Part A:Vol. 6A, Chapter 2. Plumlee, G., Logsdon, M. (Volume eds.). Reviews in Economic Geology. Society of Economic Geologists, Inc., Chelsea, MI. p. 29-70.

Sobek, A.A., Schuller, W.A., Freeman, J.R., Smith, R.M. 1978. Field and laboratory methods applicable to overburden and minesoils. EPA 600/2-78-054. 203 p.

Steger, H.F. 1982. Oxidation of sulfide minerals—VII: Effect of temperature and relative humidity on the oxidation of pyrrhotite. Chemical Geology 35. p. 281-295.

Stevenson, R.J., Kreisman, P.J., Sather, N.P. 1979. In Minnesota regional copper-nickel study; Chapter 1. MN Environmental Quality Board, Saint Paul MN . Vol. 3, 70 pp.

Stumm, W., Morgan, J.J. 1981. Aquatic chemistry - An introduction emphasizing chemical equilibria in natural waters. John Wiley & Sons, Inc. 470 pp.

Sverdrup, H.U. 1990. The kinetics of base cation release due to chemical weathering. Lund University Press. Lund, Sweden. 246 pp.

Taylor, A.S., Blum, J.D., Lasaga, A.C., Macinnis, I.N. 2000. Kinetics of dissolution and Sr release during biotite and phlogopite weathering. Geochim. Cosmochim. Acta, 64. p. 1191-1208.

Theriault, R.D., Barnes, S.J., Severson, M.J. 2000. Origin of Cu-Ni-PGE sulfide mineralization in the Partridge River Intrusion, Duluth Complex Minnesota. Economic Geology, Vol. 95, No. 5. pp. 929-943.

Turpault, M.P., Trotignon, L. 1994. The dissolution of biotite single crystals in dilute HNO_3 at 24°C: Evidence of an anisotropic corrosion process of micas in acidic solutions. Geochim. Cosmochim. Acta, 58(13). p. 2761-2775.

Weiblen, P.W., Morey, G.B. 1980. A summary of the stratigraphy, petrology, and structure of the Duluth Complex. American Journal of Science, Vol. 280-A, p. 88-133.

Welch, S.A., Banfield, J.F. 2002. Modification of olivine surface morphology and reactivity by microbial activity during chemical weathering. Geochim. Cosmochim. Acta, 66(2). p. 213-221.

Welch, S.A., Ullman, W.J. 1993. The effect of organic acids on plagioclase dissolution rates and stoichiometry. Chemical Geology 57, p. 2725-2736.

White, A.F., Brantley, S.F. 2003. The effect of time on the weathering of silicate minerals: why do weathering rates differ in the laboratory and field? Chemical Geology 202, p. 479-506.

White, A.F., Bullen, T.D., Davison, V.V., Schulz, M.S., Clow, D.W. 1999. The role of disseminated calcite in the chemical weathering rate of grainitoid rocks. Geochim. Cosmochim. Acta, Vol. 63, No. 13/14. p. 1939-1953.

White, A.F., Yee, A. 1985. Aqueous oxidation-reduction kinetics associated with coupled electron-cation transfer from iron-containing silicates at 25^0C. Geochim. Cosmochim. Acta, 49. p. 1263-1725.

White III, W W, 2000. Personal communication with William White III of the US Bureau of Land Management. Salt Lake Field Office, Salt Lake City, UT.

White, W. W. III, Jeffers, T. H. 1994. Chemical predictive modeling of acid mine drainage from metallic sulfide-bearing rock. In Environmental Geochemistry of Sulfide Oxidation; ACS Symposium Series 550; American Chemical Society: Washington, DC, 1993. p. 608-630.

Williamson, M.A., Rimstidt, J.D. 1994. The kinetics and electrochemical rate-determining step of aqueous pyrite oxidation. Geochim. Cosmochim. Acta, 58. p. 5443-5454.

Wilson, M.J. 2004. Weathering of the primary rock-forming minerals: processes, products and rates. Clay Minerals 39, p. 233-266.

Wogelius, R.A., Walther, J.V. 1992. Olivine dissolution kinetics at near-surface conditions. Chemical Geology 97(1-2), p. 101-112.

Yang, L., Steefel, C.I. 2008. Kaolinite dissolution and precipitation kinetics at 22C and pH 4.

Geochim. Cosmochim. Acta, 72. p. 99-116

Younger, P.L., Banwart, S.A., Hedin, R.S. 2002. Mine water: Hydrology, pollution, remediation. Kluwer Academic Publishers, Dordrecht. 442 pp.

Zakaznova-Herzog, V.P., Nesbitt, H.W., Bancroft, G.M., Tse, J.S. 2008. Characterization of leached layers on olivine and pyroxenes using high-resolution XPS and density functional calculations. Geochim. Cosmochim. Acta, 72. p. 69-86.

Table 1. High Sulfur experiment reactors and description of samples. DC = Duluth Complex and VF = Virginia Formation.

% Sulfur	Reactor	Sample Source	Rock Suite	Period of Record (weeks)
0.18[1]	1	Dunka BH	DC	1252[4]
	2	Dunka BH	DC	328
0.22[1]	3	Dunka BH	DC	1252[4]
	4	Dunka BH	DC	328
0.40[1]	5	Dunka BH	DC	909[5]
	6	Dunka BH	DC	328
0.41[1]	7	Dunka BH	DC	724
	8	Dunka BH	DC	328
0.51[1]	9	Dunka BH	DC	724
	10	Dunka BH	DC	328
0.54[1]	11	Dunka BH	DC	441
	12	Dunka BH	DC	328
0.57[1]	13	Dunka BH	DC	441
	14	Dunka BH	DC	328
0.58[1]	15	Dunka BH	DC	724
	16	Dunka BH	DC	328
0.67[3]	39	ARIMETCO	DC	809[4]
0.67[3]	40	Dunka BH	DC	809[4]
0.71[1]	17	Dunka BH	DC	724
	18	Dunka BH	DC	328
0.72[3]	42	AMAX	DC	809[4]
0.82[3]	43	Dunka BH	DC	809[4]
0.92[3]	41	AMAX	DC	809[4]
1.12[2]	35	Dunka BH	DC	360
	36	Dunka BH	DC	247
1.16[2]	29	Dunka BH	DC	643
	30	Dunka BH	DC	247
1.40[2]	37	Dunka BH	DC	360
	38	Dunka BH	DC	247
1.44[2]	33	Dunka BH	DC	643
	34	Dunka BH	DC	247
1.63[1]	19	Dunka BH	DC	724
	20	Dunka BH	DC	289
1.64[2]	31	Dunka BH	DC	360
	32	Dunka BH	DC	247
1.71[3]	44	AMAX	DC	144
2.06[1]	21	Dunka BH	VF	78
	22	Dunka BH	VF	78
3.12[1]	23	Dunka BH	VF	78
	24	Dunka BH	VF	78
3.72[1]	25	Dunka BH	VF	78
	26	Dunka BH	VF	78
5.44[1]	27	Dunka BH	VF	78
	28	Dunka BH	VF	78

[1] Reactor initiated week of February 14, 1989.
[2] Reactor initiated week of September 4, 1990.
[3] Reactor initiated week of August 12, 1997.
[4] Reactor was still active at time of report.
[5] Reactor was terminated after 909 weeks.

Table 2. Chemical composition (%) of unleached rock samples. Analyses by Actlabs, Inc.

%S	0.18	0.22	0.40	0.41	0.51	0.54	0.57	0.58	0.67	0.67	0.71	0.72	0.82
Reactor	1,2	3,4	5,6	7,8	9,10	11,12	13,14	15,16	39	40	17,18	42	43
CO_2	<0.03	<0.03	0.64	0.06	0.07	0.11	0.10	0.07	<0.03	<0.03	0.05	0.06	<0.03
Al_2O_3	18.92	19.82	17.68	16.20	14.89	16.27	14.75	17.64	18.32	16.26	18.17	20.98	16.76
CaO	8.75	9.18	7.6	8.71	7.76	8.35	7.79	7.77	8.69	8.35	7.60	9.77	8.37
Fe_2O_3	1.56	1.23	1.84	2.51	2.04	2.08	4.03	4.81	3.75	3.28	4.65	0.64	3.52
FeO	10.71	10.63	10.19	11.83	13.3	9.37	11.59	10.06	9.22	10.75	10.27	8.64	9.38
K_2O	0.33	0.50	0.72	0.71	0.89	1.13	0.92	0.99	0.60	0.72	0.78	0.30	0.74
MgO	7.85	6.27	5.81	6.91	6.66	8.61	7.98	5.84	7.53	6.88	6.96	7.24	6.75
MnO	0.139	0.124	0.181	0.177	0.188	0.156	0.185	0.150	0.16	0.21	0.133	0.1	0.15
Na_2O	2.59	3.03	2.45	2.78	2.60	1.80	2.54	2.78	0.33	0.28	2.55	2.78	2.33
P_2O_5	0.11	0.14	0.15	0.19	0.27	0.22	0.33	0.16	0.13	0.13	0.09	0.04	0.12
SiO_2	46.54	46.82	50.49	46.24	46.75	48.49	45.76	43.19	47.7	49.89	44.16	47.58	50.32
TiO_2	1.382	1.102	1.312	2.869	2.650	1.196	2.640	1.891	1.88	2.45	0.964	0.54	1.67
LOI[1]	0.25	0.31	0.66	-0.21	-0.23	1.41	0.26	3.39			2.87		
LOI2[2]	1.45	1.50	1.80	1.11	1.26	2.46	1.56	4.52			4.02		

%S	0.92	1.12	1.16	1.40	1.44	1.63	1.64	1.71	2.06	3.12	3.72	5.44
Reactor	41	35,36	29,30	37,38	33,34	19,20	31,32	44	21,22	23,24	25,26	28
CO_2	<0.03	<0.03	0.08	0.10	<0.03	0.11	0.14	0.06	0.12	<0.03	0.06	0.32
Al_2O_3	19.19	14.14	15.94	15.41	15.22	14.35	14.61	18.66	16.11	16.50	20.47	11.49
CaO	9	7.38	8.25	8.51	7.40	6.60	8.23	7.75	2.22	5.14	9.29	9.98
Fe_2O_3	1.02	2.45	2.15	4.85	3.33	1.73	3.85	4.13	0.40	0.51	nd	0.42
FeO	10.82	12.63	12.84	11.4	12.42	14.38	12.35	9.49	10.23	9.91	10.81	17.06
K_2O	0.41	1.74	0.75	0.67	0.96	1.25	0.86	0.65	1.88	1.09	0.42	0.55
MgO	7.5	5.65	6.73	6.41	7.00	6.60	6.33	8.28	4.56	5.71	6.60	10.79
MnO	0.15	0.184	0.175	0.176	0.163	0.175	0.191	0.14	0.082	0.106	0.113	0.205
Na_2O	0.33	2.44	2.70	2.58	2.58	2.55	2.49	2.3	2.03	2.27	2.99	1.27
P_2O_5	0.06	0.17	0.15	0.20	0.14	0.19	0.19	0.12	0.30	0.13	0.11	0.10
SiO_2	47.07	47.98	46.21	44.25	46.86	46.81	45.35	45.68	57.79	54.68	47.14	42.51
TiO_2	1.39	2.961	2.435	2.946	2.274	3.587	2.728	1.67	1.310	1.438	0.793	1.779
LOI[1]		0.93	0.33	1.08	0.40	1.28	1.48		2.10	1.51	0.44	1.92
LOI2[2]		2.34	1.77	2.36	1.79	2.89	2.86		3.25	2.62	1.65	3.83

[1] Loss on Ignition. LOI<0.01 represent a gain on ignition.

[2] Loss on Ignition adjusted for the difference in oxygen between FeO and Fe_2O_3.

Note: nd = not detected.

Table 3. Trace metal composition (ppm) of unleached rock samples. The four metals of greatest environmental concern (Co, Cu, Ni, Zn) are listed first. Analyses by Actlabs, Inc. Page 1 of 4.

%S	0.18	0.22	0.40	0.41	0.51	0.54	0.57	0.58	0.67	0.67	0.71	0.72	0.82
Reactor	1,2	3,4	5,6	7,8	9,10	11,12	13,14	15,16	39	40	17,18	42	43
Co	84	79	43	70	71	52	81	81	73	56	120	nd	45
Cu	1360	1350	512	788	1430	211	1290	1300	617	490	1160	517	601
Ni	525	484	231	511	473	174	398	396	523	261	388	254	204
Zn	102	103	123	160	103	171	187	183	119	187	126	59.2	148
Ag	nd	nd	nd	nd	nd	nd	nd	nd	nd	nd	nd	nd	nd
As	nd	nd	7	nd	nd	10	nd	nd	nd	3	10	nd	3
Ba	141	166	275	221	259	380	288	290	100	102	256	100	260
Bi	0.5	nd	nd	0.5	0.8	nd	1.8	1.7	49.78	90.54	1.7	12.67	44.06
Cr	167	152	296	266	232	484	185	187	92	166	170	45	190
Cs	0.6	0.5	1.5	1.1	1.4	2.3	1.5	1.5	0.6	0.8	1.9	nd	1.6
Hf	1.7	1.9	2.3	4.2	5.2	2.1	5.3	5.1	2.3	4.3	2.1	0.9	2.7
Mo	2	2	3	nd	3	3	nd	nd	2.13	1.85	3	2.71	2.20
Pb	5	nd	6	7	5	nd	10	10	12.9	19.2	12	15.1	14.8
Rb	7	11	17	22	28	39	30	30	nd	nd	26	nd	27
Sb	0.9	0.5	1.5	nd	0.7	1.0	0.5	0.5	0.2	0.3	0.5	nd	0.2
Sn	1	2	2	2	2	nd	3	3			2		
Sr	299	311	318	268	275	276	260	339	185	256	348	338	283
Ta	0.5	0.5	0.8	1.1	1.2	0.5	1.3	1.2	nd	nd	0.4	nd	nd
V	155	105	237	239	223	304	212	182	16.8	25.1	127	45.6	232
W	nd	nd	2	1	1	nd	2	2	nd	nd	nd	nd	nd
Y	11	13	21	25	30	18	31	16	nd	nd	11	5.17	20.7
Zr	55	64	78	138	166	68	172	92	15.3	28.3	71	21	151
Ce	17.9	23.1	45.1	32.6	43.8	30.1	47.3	47.1	16	28	18.3	8	30

Table 3. Trace metal composition (ppm) of unleached rock samples. The four metals of greatest environmental concern (Co, Cu, Ni, Zn) are listed first. Analyses by Actlabs, Inc. Page 2 of 4.

%S	0.92	1.12	1.16	1.40	1.44	1.63	1.64	1.71	2.06	3.12	3.72	5.44
Reactor	41	35,36	29,30	37,38	33,34	19,20	31,32	44	21,22	23,24	25,26	28
Co	67	70	83	91	87	81	95	82	44	52	87	117
Cu	752	800	1090	1560	1210	1180	2220	660	1300	1540	1280	1290
Ni	324	329	422	503	386	492	718	354	327	436	540	589
Zn	100	305	171	181	191	93	191	86.6	223	123	80	120
Ag	nd	nd	nd	nd	nd	6	8	nd	nd	nd	nd	nd
As	nd	9	nd	nd	nd	6	nd	11	14	13	8	19
Ba	100	405	210	201	251	288	249	135	508	274	142	155
Bi	37.5	0.6	0.8	0.7	0.6	nd	1.2	22.30	0.8	0.6	0.7	0.8
Cr	98	211	209	177	204	227	210	210	277	265	150	653
Cs	nd	2.0	1.5	1.5	1.7	2.2	1.7	1.8	6.5	4.5	0.5	1.4
Hf	1.2	5.7	4.7	6.8	4.1	4.7	5.6	0.5	4.3	3.1	1.8	2.3
Mo	1.21	3	2	2	nd	4	2	2.19	5	4	2	2
Pb	13.4	11	10	16	8	nd	7	22.7	21	13	5	5
Rb	nd	49	23	22	30	37	28	nd	69	45	11	21
Sb	nd	0.8	0.6	nd	nd	0.8	1.6	0.2	1.1	1.2	1.0	1.7
Sn		2	2	4	2	1	3		1	2	2	2
Sr	142	232	270	246	246	209	245	335	239	259	336	148
Ta	nd	1.4	1.2	1.5	1.2	1.4	1.4	nd	1.1	0.7	0.3	0.5
V	10.6	291	201	221	205	293	224	149	225	192	78	301
W	nd	4	nd	nd	nd	nd	4	nd	1	2	6	nd
Y	nd	29	25	28	24	28	31	4.48	32	18	10	20
Zr	11.8	195	152	234	129	157	182	25.5	143	101	64	72
Ce	15	40.7	33.0	35.9	34.1	39.4	39.8	6	64.1	39.2	17.7	24.6

Table 3. Trace metal composition (ppm) of unleached rock samples. Analyses by Actlabs, Inc. Page 3 of 4.

%S	0.18	0.22	0.40	0.41	0.51	0.54	0.57	0.58	0.67	0.67	0.71	0.72	0.82
Reactor	1,2	3,4	5,6	7,8	9,10	11,12	13,14	15,16	39	40	17,18	42	43
La	8.7	11.1	24.8	15.1	20.2	15.7	21.2	21.3	9	14.4	8.8	4.4	6.4
Lu	0.17	0.19	0.39	0.39	0.43	0.29	0.42	0.43	0.25	0.38	0.15	0.08	0.28
Nd	9.5	12.4	20.5	18.4	24.7	15.3	26.6	27.0	8		9.8	nd	14
Tb	0.3	0.4	0.6	0.8	0.9	0.5	1.0	1.0	nd	0.6	0.3	nd	nd
Th	0.8	10	1.5	1.6	2.1	0.9	2.2	2.2	0.8	1.3	1.1	nd	1.1
U	0.3	0.3	0.6	0.5	0.8	0.5	0.7	0.7	0.7	0.7	0.5	nd	nd
Yb	1.1	1.2	2.3	2.4	2.8	1.9	2.7	2.8	1.4	2.5	1.0	0.5	1.8
Ga	20	22	24	22	21	20	22	22			20		
Ge	1	nd	2	1	2	1	1	2			nd		
Nb	5	5	10	15	16	7	17	17			5		
In	nd	nd	nd	nd	nd	nd	nd	nd			nd		
Pr	2.03	2.62	4.79	3.87	5.19	3.41	5.56	5.62			2.09		
Sm	2.2	2.6	3.9	4.3	5.8	3.3	6.0	6.1	2.3	3.2	2.2	0.8	2.9
Gd	2.2	2.6	3.6	4.3	5.6	3.1	5.9	5.9			2.0		
Dy	2.0	2.4	3.5	4.4	5.5	3.2	5.6	5.6			1.8		
Ho	0.4	0.4	0.7	0.8	1.0	0.6	1.0	1.0			0.3		
Er	1.1	1.3	2.1	2.4	2.9	1.8	2.9	3.0			1.0		
Tm	0.16	0.18	0.32	0.36	0.43	0.27	0.44	0.43			0.14		
Tl	nd	nd	nd	0.1	0.1	0.2	0.2	0.2			0.3		
Eu	1.54	1.78	2.49	1.76	2.06	1.67	2.02	2.00	1.3	1.5	1.73	1	1.6

Table 3. Trace metal composition (ppm) of unleached rock samples. Analyses by Actlabs, Inc. Page 4 of 4.

%S	0.92	1.12	1.16	1.40	1.44	1.63	1.64	1.71	2.06	3.12	3.72	5.44
Reactor	41	35,36	29,30	37,38	33,34	19,20	31,32	44	21,22	23,24	25,26	28
La	8	20.5	15.7	16.5	16.7	19.1	18.5	4.5	31.6	19.7	8.5	11.3
Lu	0.15	0.46	0.40	0.47	0.40	0.45	0.47	0.08	0.49	0.29	0.15	0.28
Nd	6	21.8	18.8	20.2	17.9	21.3	22.3	nd	32.6	19.0	9.4	14.3
Tb	nd	0.8	0.8	0.9	0.7	0.8	1.0	nd	1.0	0.6	0.3	0.6
Th	0.5	2.8	1.8	2.0	2.6	2.2	2.5	nd	6.4	4.0	0.9	1.5
U	nd	1.4	0.6	0.7	1.1	1.4	0.6	nd	2.8	2.2	0.3	0.8
Yb	0.9	2.9	2.4	3.0	2.5	2.8	3.0	0.5	3.1	1.8	0.9	1.7
Ga		22	21	21	20	20	22		24	21	22	15
Ge		2	1	1	1	1	2		2	1	1	2
Nb		19	16	19	15	17	18		14	8	4	6
In		nd	nd	nd	nd	nd	nd		nd	nd	nd	nd
Pr		4.73	3.86	4.22	3.89	4.59	4.72		7.22	4.33	2.00	3.03
Sm	1.6	4.8	4.4	4.8	4.1	5.0	5.4	0.7	6.8	3.7	2.0	3.4
Gd		4.8	4.4	4.8	4.0	4.8	5.4		5.9	3.4	1.9	3.5
Dy		4.8	4.4	5.0	4.3	5.0	5.5		5.8	3.1	1.9	3.3
Ho		0.9	0.8	1.0	0.8	0.9	1.0		1.1	0.6	0.3	0.6
Er		2.8	2.5	2.8	2.5	2.8	3.0		3.2	1.8	1.0	1.8
Tm		0.43	0.38	0.42	0.37	0.42	0.46		0.49	0.26	0.14	0.27
Tl		0.3	0.1	0.2	0.2	0.3	0.2		1.9	1.2	nd	0.2
Eu	1.4	2.09	1.85	1.97	1.77	1.98	2.01	1.2	1.65	1.50	1.59	1.34

Note: nd = not detected.

Table 4. Chemical composition (%) of leached rock samples. Analyses by Actlabs, Inc. Page 1 of 2.

Original %S	0.18	0.22	0.40	0.41	0.51	0.54	0.54	0.57	0.57	0.58	0.71	1.12	1.12
Reactor	2	4	6	8	10	11	12	13	14	16	18	35	36
S	0.106	0.152	0.349	0.214	0.233	0.151	0.211	0.192	0.298	0.219	0.317	0.173	0.498
SO_4^{2-} as S	nd	nd	nd	nd	0.12	nd	0.06	nd	nd	nd	0.15	0.12	0.15
CO_2	0.077	0.037	0.059	0.037	0.040	0.106	0.051	0.040	0.033	0.051	nd	0.037	0.026
Al_2O_3	15.17	14.29	17.19	15.69	14.65	16.02	16.06	14.14	14.36	14.88	13.64	13.71	13.96
CaO	8.30	7.26	7.18	8.43	7.60	8.04	8.02	7.52	7.52	7.41	7.33	6.91	7.02
Fe_2O_3	7.57	3.53	1.43	1.00	1.86	0.98	1.37	2.62	2.63	1.25	1.45	2.76	2.50
FeO	6.77	12.27	11.41	13.99	14.22	10.77	10.64	13.74	13.79	12.96	15.22	12.81	12.91
K_2O	0.70	1.04	0.59	0.61	0.78	1.03	1.06	0.76	0.82	0.94	0.70	1.65	1.66
MgO	6.73	6.66	5.98	6.78	6.67	8.59	8.48	7.93	7.83	6.07	9.01	5.65	5.68
MnO	0.184	0.182	0.187	0.182	0.192	0.158	0.157	0.185	0.187	0.185	0.199	0.184	0.186
Na_2O	2.63	2.47	2.33	2.69	2.51	1.76	1.75	2.43	2.44	2.54	2.39	2.38	2.42
P_2O_5	0.25	0.22	0.16	0.18	0.27	0.11	0.12	0.34	0.32	0.20	0.18	0.17	0.16
SiO_2	47.51	44.56	50.58	45.82	47.10	48.49	48.71	44.88	45.46	47.40	46.05	47.89	48.16
TiO_2	2.454	3.900	1.430	2.972	2.751	1.167	1.176	2.851	2.813	3.238	1.993	3.037	3.006
LOI[1]	0.68	1.19	0.56	-0.18	0.18	1.52	1.59	0.67	0.50	0.69	0.28	1.20	1.13
LOI2[2]	1.44	2.56	1.84	1.39	1.77	2.73	2.78	2.21	2.04	2.14	1.98	2.63	2.58

Table 4. Chemical composition (%) of leached rock samples. Analyses by Actlabs, Inc. Page 2 of 2.

Original %S	1.16	1.16	1.40	1.40	1.44	1.63	1.64	1.64	2.06	3.12	3.72	5.44
Reactor	29	30	37	38	34	20	31	32	22	24	26	28
S	1.08	0.592	0.292	0.821	0.663	0.458	0.408	0.662	1.77	1.99	2.83	4.35
SO_4^{2-} as S	nd	0.27	0.09	0.15	0.33	0.24	0.15	0.18	0.05	1.08	1.23	1.86
CO_2	nd	0.011	0.055	0.040	nd	0.110	0.059	0.051	0.070	1.48	1.03	0.62
Al_2O_3	15.83	15.72	14.96	15.25	15.02	14.22	14.09	14.27	14.57	15.51	15.95	13.80
CaO	8.75	8.16	8.14	8.27	7.26	6.53	8.04	8.04	7.73	3.45	1.99	0.64
Fe_2O_3	2.06	1.62	6.24	4.50	3.09	3.63	5.37	5.05	5.64	5.84	8.14	10.51
FeO	13.17	14.03	10.69	12.41	12.80	12.60	11.32	11.51	11.98	5.10	3.43	1.56
K_2O	0.77	0.67	1.65	0.59	0.96	1.14	0.74	0.81	0.70	2.58	2.67	3.63
MgO	6.80	6.65	5.65	6.23	6.95	5.59	6.18	6.17	8.09	5.25	4.34	2.71
MnO	0.174	0.175	0.166	0.176	0.166	0.169	0.176	0.180	0.174	0.079	0.055	0.020
Na_2O	2.68	2.66	2.52	2.54	2.57	2.55	2.38	2.39	2.38	1.52	1.42	1.18
P_2O_5	0.15	0.14	0.19	0.16	0.14	0.17	0.18	0.18	0.18	0.10	0.12	0.09
SiO_2	45.93	45.95	44.15	44.08	46.80	46.82	44.63	44.69	43.97	52.72	52.55	53.32
TiO_2	2.434	2.441	3.074	3.052	2.306	3.572	2.792	2.777	2.169	0.709	0.655	0.408
LOI[1]	1.30	0.57	2.12	1.51	0.83	1.90	2.17	2.12	1.42	6.70	8.61	12.31
LOI2[2]	1.77	2.14	3.32	2.90	2.26	3.31	3.44	3.41	2.76	7.27	8.99	12.48

[1] Loss on Ignition. LOI<0.01 represent a gain on ignition.

[2] Loss on Ignition adjusted for the difference in oxygen between FeO and Fe_2O_3.

Note: nd = not detected.

Table 5. Trace metal composition (ppm) of leached rock samples. The four metals of greatest environmental concern (Co, Cu, Ni, Zn) are listed first. Analyses by Actlabs, Inc. Page 1 of 4.

Original %S	0.18	0.22	0.40	0.41	0.51	0.54	0.54	0.57	0.57	0.58	0.71	1.12	1.12
Reactor	2	4	6	8	10	11	12	13	14	16	18	35	36
Co	59	67	42	62	57	38	42	65	69	44	70	42	47
Cu	560	1140	624	777	1200	159	175	1210	1360	624	>10000	745	877
Ni	220	277	206	304	183	91	116	251	323	125	246	93	174
Zn	145	120	258	106	104	209	289	216	84	109	200	261	233
Ag	nd	nd	nd	nd	nd	nd	nd	nd	nd	nd	nd	nd	nd
As	nd	nd	7	nd	nd	8	8	nd	nd	nd	7	9	10
Ba	278	330	266	199	241	362	367	262	265	282	229	405	400
Bi	1.2	1.6	1.0	0.4	0.9	nd	nd	1.5	0.6	0.8	2.8	0.5	0.8
Cr	162	190	257	207	139	428	455	159	166	159	196	177	172
Cs	1.1	1.3	1.7	0.9	1.3	2.1	3.1	1.4	1.3	1.4	1.1	2.0	2.0
Hf	5.1	5.0	2.6	4.1	5.1	2.1	2.1	6.3	5.2	4.4	4.2	6.1	5.8
Mo	nd	2	3	nd	2	3	3	2	2	2	nd	3	4
Pb	7	6	10	nd	6	nd	6	14	nd	6	11	10	7
Rb	20	34	18	18	26	35	38	25	27	28	21	49	45
Sb	2.7	0.7	nd	nd	0.8	0.9	1.0	0.5	0.7	0.5	nd	0.8	0.9
Sn	2	2	2	2	3	1	1	3	3	2	2	3	2
Sr	290	273	321	259	271	262	267	249	246	271	263	232	228
Ta	1.2	1.5	0.9	1.2	1.2	0.5	0.5	1.4	1.3	1.3	1.0	1.5	1.5
V	209	296	253	236	222	283	296	220	216	259	182	306	293
W	1	1	1	nd	1	nd	nd	1	2	1	1	1.5	1.5
Y	30	29	23	24	31	68	17	217	31	29	135	29	29
Zr	173	158	86	129	162	68	71	217	168	132	135	212	192
Ce	42.3	39.9	44.7	31.7	42.2	28.0	29.1	46.8	46.5	38.3	34.0	40.8	41.0

Table 5. Trace metal composition (ppm) of leached rock samples. The four metals of greatest environmental concern (Co, Cu, Ni, Zn) are listed first. Analyses by Actlabs, Inc. Page 2 of 4.

Original %S	1.16	1.16	1.40	1.40	1.44	1.63	1.64	1.64	2.06	3.12	3.72	5.44
Reactor	29	30	37	38	34	20	31	32	22	24	26	28
Co	86	71	51	73	68	49	45	52	86	25	22	13
Cu	1110	1160	1750	1920	1270	1060	1770	1970	2310	129	102	129
Ni	454	369	210	483	277	275	159	252	403	77	298	44
Zn	181	184	185	42	213	158	66	124	170	187	349	296
Ag	nd	nd	nd	nd	nd	nd	nd	nd	nd	nd	nd	nd
As	nd	nd	nd	nd	9	7	6	6	5	8	20	13
Ba	214	207	194	192	250	300	233	250	228	372	422	465
Bi	1.2	1.6	2.4	0.6	0.8	0.9	1.0	1.8	1.5	0.5	0.6	0.4
Cr	227	184	223	149	172	254	162	163	167	327	754	178
Cs	1.6	1.5	1.3	1.2	1.7	2.6	1.5	1.7	1.7	6.2	7.7	9.0
Hf	4.8	4.8	5.9	4.9	4.5	5.2	5.5	5.8	4.0	2.6	2.9	3.1
Mo	nd	2	3	2	2	5	2	3	2	14	20	22
Pb	11	13	20	nd	12	7	nd	6	12	7	18	12
Rb	25	22	18	19	29	39	27	26	28	97	117	149
Sb	nd	0.5	0.6	0.9	0.7	0.7	0.6	0.7	nd	1.3	1.2	1.8
Sn	3	3	4	3	3	2	3	3	3	1	1	nd
Sr	271	270	242	236	244	229	238	246	237	171	146	136
Ta	1.2	1.2	1.5	1.5	1.2	1.4	1.4	1.4	1.1	0.5	0.6	0.5
V	206	200	229	219	206	316	227	229	194	279	231	248
W	nd	nd	nd	nd	nd	1	2	1	nd	2	3	3
Y	25	25	27	27	25	29	30	31	26	25	22	25
Zr	160	156	199	152	152	166	172	185	133	84	93	95
Ce	32.4	31.9	34.0	34.6	32.6	40.4	39.6	39.8	35.7	43.1	46.3	55.4

Table 5. Trace metal composition (ppm) of leached rock samples. Analyses by Actlabs, Inc. Page 3 of 4.

Original %S	0.18	0.22	0.40	0.41	0.51	0.54	0.54	0.57	0.57	0.58	0.71	1.12	1.12
Reactor	2	4	6	8	10	11	12	13	14	16	18	35	36
La	19.3	18.3	24.5	14.9	19.3	14.6	15.1	21.3	21.4	17.8	15.8	20.6	16.0
Lu	0.42	0.40	0.44	0.38	0.42	0.28	0.30	0.44	0.44	0.45	0.38	0.49	0.48
Nd	24.5	22.6	20.8	18.6	24.5	14.5	14.8	26.4	26.4	22.5	19.4	21.7	17.5
Tb	0.9	0.9	0.6	0.7	0.9	0.5	0.5	1.0	1.0	0.9	0.8	0.8	0.8
Th	1.8	2.6	1.5	1.7	2.3	2.9	1.8	2.5	2.2	1.7	1.7	3.0	3.0
U	0.6	0.7	0.6	0.5	0.8	0.4	0.4	0.7	0.7	0.6	0.5	1.0	1.2
Yb	2.7	2.6	2.6	2.3	2.9	1.8	1.8	2.9	2.9	2.9	2.4	3.0	3.1
Ga	21	21	26	21	21	19	20	21	21	20	21	22	21
Ge	2	2	2	2	2	2	2	2	2	2	3	2	2
Nb	17	18	12	15	16	7	7	18	18	17	13	20	19
In	nd	nd	nd	nd	nd	nd	nd	nd	nd	nd	nd	nd	nd
Pr	5.02	4.66	4.78	3.77	5.00	3.18	3.27	5.59	5.53	4.59	4.06	4.75	4.75
Sm	5.6	5.3	4.0	4.3	5.6	3.0	3.1	6.1	6.0	5.3	4.6	4.9	5.1
Gd	5.6	5.1	3.8	4.3	5.4	3.1	3.1	6.0	5.9	5.2	4.6	4.7	4.8
Dy	5.5	5.1	3.6	4.4	5.4	2.9	3.1	5.8	5.6	5.2	4..6	5.0	4.9
Ho	1.0	1.0	0.7	0.8	1.0	0.6	0.6	1.1	1.0	1.0	0.8	0.9	0.9
Er	2.9	2.7	2.2	2.4	2.9	1.8	1.8	3.0	3.0	2.8	2.4	2.8	2.9
Tm	0.42	0.40	0.35	0.36	0.44	0.25	0.26	0.44	0.44	0.44	0.38	0.44	0.44
Tl	0.2	0.2	0.2	0.1	0.1	0.1	0.2	0.2	0.1	0.1	0.2	0.3	0.3
Eu	2.04	1.99	2.42	1.78	2.01	1.55	1.62	2.00	1.98	2.07	1.77	2.10	2.11

Table 5. Trace metal composition (ppm) of leached rock samples. Analyses by Actlabs, Inc. Page 4 of 4.

Original %S	1.16	1.16	1.40	1.40	1.44	1.63	1.64	1.64	2.06	3.12	3.72	5.44
Reactor	29	30	37	38	34	20	31	32	22	24	26	28
La	15.2	18.3	15.8	16.0	16.0	19.4	18.3	18.4	16.8	23.6	24.0	28.4
Lu	0.41	0.41	0.43	0.44	0.41	0.47	0.47	0.49	0.38	0.46	0.38	0.42
Nd	18.3	18.1	19.6	19.2	17.5	22.6	22.2	22.6	20.2	21.1	21.6	27.2
Tb	0.7	0.7	0.8	0.8	0.7	0.9	0.9	0.9	0.8	0.6	0.6	0.7
Th	1.9	2.4	2.2	1.8	2.3	2.5	2.6	2.7	2.1	5.1	5.6	8.0
U	0.6	0.6	0.6	1.2	0.9	1.4	0.7	0.8	0.6	6.9	7.8	11.1
Yb	2.6	2.6	2.7	2.8	2.5	3.0	3.0	3.1	2.5	2.7	2.3	2.4
Ga	22	21	21	20	20	22	21	21	21	21	22	19
Ge	1	2	2	2	2	2	2	2	1	nd	1	nd
Nb	16	16	21	19	16	19	19	19	15	7	7	6
In	nd	nd	nd	nd	nd	nd	nd	nd	nd	nd	nd	nd
Pr	3.81	3.79	4.03	4.08	3.75	4.72	4.72	4.70	4.21	4.79	5.06	6.30
Sm	4.3	4.3	4.6	4.6	4.0	5.3	5.3	5.4	4.6	4.1	4.2	5.1
Gd	4.4	4.4	4.5	4.7	4.0	5.1	5.3	5.3	4.9	4.0	3.8	4.7
Dy	4.4	4.6	4.8	4.9	4.2	5.3	5.5	5.6	4.6	3.9	3.5	4.0
Ho	0.9	0.8	0.9	0.9	0.8	1.0	1.0	1.1	0.9	0.8	0.7	0.8
Er	2.5	2.5	2.7	2.7	2.4	3.0	3.0	3.0	2.5	2.5	2.0	2.2
Tm	0.40	0.37	0.40	0.42	0.36	0.46	0.45	0.45	0.38	0.40	0.34	0.37
Tl	0.2	0.2	0.2	nd	0.2	0.5	nd	0.1	0.3	1.8	2.9	3.3
Eu	1.91	1.89	1.87	1.88	1.71	2.08	1.98	1.98	1.88	1.48	1.48	1.35

Note: nd = not detected.

Table 6. Leachate sampling frequency for reactors. Column entries indicate sampling frequency and number of weeks sampled at that frequency for each analysis.

Reactor	Alkalinity/Acidity	pH/Specific Conductance	Sulfate	Calcium/Magnesium	Trace Metals	Sodium, Potassium, Iron, Aluminum, Silicon
1-20	Bi-monthly: 0-84 Monthly: 85-577 Bi-monthly: 578-1252	Weekly: 0-523 Monthly: 524-577 Bi-monthly: 578-1252	Weekly: 0-112 Monthly: 113-585 Bi-monthly: 586-1252	Bi-monthly: 0-20 Monthly: 21-625 Bi-monthly: 626-1252	Every three months: 12-60 Every 16-20 weeks: 403-553, 633-1252 Other: approximately 17 times irregularly in other weeks	Similar to Trace Metals starting in week 335
21-28	Monthly: 0-12 Every two months: 13-76	Weekly: 0-78	Bi-monthly: 0-68, 72-78	Bi-monthly: 4-34, 40-62 Other weeks: 0, 70	Bi-monthly: 4-62 Other: weeks 0, 70	None
29-38	Monthly: 0-609 Bi-monthly: 610-866	Weekly: 0-444 Monthly: 445-609 Bi-monthly: 610-866	Monthly: 0-609 Bi-monthly: 610-866	Monthly: 0-609 Bi-monthly: 610-866	Bi-monthly: 9-17 Other: 46 samples irregularly spread through period of record	Similar to Trace Metals starting in week 254
39-44	Monthly: 0-246 Bi-monthly: 247-809	Weekly: 0-81 Monthly: 82-246 Bi-monthly: 247-809	Monthly: 0-246 Bi-monthly: 247-809	Monthly: 0-246 Bi-monthly: 247-809	23 samples taken 8-36 weeks apart	Similar to Trace Metals

Table 7. Reactor mineral composition (%) before leaching. All determined by point count, with the exception of pyrrhotite, chalcopyrite and pentlandite, which were chemically determined by assuming that all Cu was present as chalcopyrite and all Ni as pentlandite. Numbers in parentheses following chalcopyrite are Cu ppm and following pentlandite are Ni ppm. Page 1 of 2.

	%S	0.18	0.22	0.4	0.41	0.51	0.54	0.57	0.58	0.67[1]	0.67[2]	0.71	0.72	0.82
Silicate														
Plagioclase		49.5	64.9	47.4	57.4	46.6	62.2	42.6	45.8	56.3	47.7	54.8	61.2	47.8
Hypersthene		17.4	5.4	27.6	8.7	17.8	19.8	5	15	4.2	14.4	12.2	3.3	15.7
Olivine		10.1	4.5	0	13	5.9	0	20.8	2.5	16.8	4.5	14.8	21.5	3.5
Augite		10.1	8.1	4.3	8.7	7.6	8.1	16.8	14.2	14.3	11.7	7.8	2.5	13
Biotite		1.8	2.7	1.7	2.6	2.5	2.7	0	0.8	0	6.3	1.7	0	3.5
Prehnite		1.8	0.9	1.7	0	0	0.9	0	0	0	0	0	4.1	0
Amphibole		0	0.9	0.9	0.9	1.7	0.9	0	0	0	0	0	0	0
K-Spar		0	3.6	3.4	0.9	5.1	0	4	5	1.7	0.9	0.9	0	0
Ilmenite		6.4	6.3	3.4	7.8	9.3	0	5.9	7.5	3.4	4.5	2.6	1.7	2.6
Quartz		0.9	0.9	2.6	0	0.8	1.8	1	0.8	0	1.8	0	0.8	0
Cordierite		0	0	3.4	0	0	0.9	0	0.8	0	7.2	0	0	5.2
Chlorite		0.9	0.8	0	0	0	0	0	0	0	0	0	4.1	2.6
Apatite		0	0	0	0	0	0	3	1.7	0	0	0.9	0	1.7
Stilpnomelane		0	0	0	0	0	0	0	0	0	0	0	0	0
Muscovite		0	0	0	0	0	0	0	0	0	0.9	0	0	0
Magnetite		0	0	0	0	0	0	1.0	0	0.8	0	0	0	0
Calcite		0	0	0	0	0	0	0	0.8	0	0	0	0	0
Garnet		0	0	0.9	0	0	0	0	0	0	0	0	0	0
Sillimanite		0	0	0	0	0	0	0	0	0	0	0	0	0
Scapolite		0	0	0	0	0	0	0	0.8	0	0	0	0	0
Sulfide														
Pyrrhotite		0.02	0.13	0.83	0.72	0.84	1.26	1.04	1.06	1.41	1.5	1.42	1.62	1.86
Chalcopyrite		0.39 (1360)	0.39 (1350)	0.15 (512)	0.23 (788)	0.41 (1430)	0.06 (211)	0.37 (1290)	0.37 (1300)	0.18 (617)	0.14 (490)	0.33 (1160)	0.15 (517)	0.17 (601)
Pentlandite		0.15 (525)	0.14 (484)	0.07 (231)	0.15 (511)	0.14 (473)	0.05 (174)	0.11 (398)	0.11 (396)	0.15 (523)	0.07 (261)	0.11 (388)	0.07 (254)	0.06 (204)
Pyrite		0	0	0.9	0	0	0	0	1.7	0	0	0	0	0
Cubanite		0	0	0	0	0	0	0	0	0	0	0	0	0
Unknown		0	0	0	0	0	0	0	0	0	0	0	0	0

Table 7. Reactor mineral composition (%) before leaching. All determined by point count, with the exception of pyrrhotite, chalcopyrite and pentlandite, which were chemically determined by assuming that all Cu was present as chalcopyrite and all Ni as pentlandite. Numbers in parentheses following chalcopyrite are Cu ppm and following pentlandite are Ni ppm. Page 2 of 2.

	%S	**0.92**	**1.12**	**1.16**	**1.40**	**1.44**	**1.63**	**1.64**	**1.71**	**2.06**	**3.12**	**3.72**	**5.44**
Silicate													
Plagioclase		44.6	39.7	58.4	46.2	52.9	36.4	45.8	45.5	27.7	34.8	18	11.5
Hypersthene		3.3	19.8	12.4	8.4	24.4	17.8	10.8	2.5	10.9	11.6	9.6	0
Olivine		38.8	4.1	16.8	5.9	5.9	5.6	3.3	19.8	0.8	0	0	0
Augite		4.1	5.8	9.7	11.8	2.5	5.6	13.3	2.5	2.5	0.9	2.6	0
Biotite		0	1.7	0	0	1.7	1.9	2.5	0.8	0.8	2.7	2.6	0.9
Prehnite		0	0.8	0	2.5	0	0	0.8	0.8	0	0	0.9	0
Amphibole		3.3	0.8	0	0.8	0	0.9	0	0	0	0	0	0
K-Spar		0	11.6	0	2.5	4.2	5.6	4.2	0.8	12.6	8	15	20.4
Ilmenite		2.5	7.4	1.8	8.4	3.4	8.4	8.3	5	4.2	0.9	0	0
Quartz		0	0	0	0	1.7	5.6	0	0	14.3	20.5	24	34.5
Cordierite		0	0.8	0	0	0	0.9	0.8	3.3	20.2	0	4.3	0
Chlorite		0.8	0	0	0	0	0	1.7	8.3	0	0	0.9	0
Apatite		0	0	0	0.8	0	4.7	0.8	0	0	0	0	0
Stilpnomelane		0	0	0	0	0	0	0	0	0	4.5	6.1	0
Muscovite		0	0.8	0	0	0	0	0.8	0	0	2.7	1.7	1.8
Magnetite		0	0	0	1.7	0.8	0	2.5	0	0	0	0	0
Calcite		0	0	0	0	0	0	0	0	0	1.8	0	0
Garnet		0	0	0	0	0	0	0.8	0	0	0	0	0
Sillimanite		0	0	0	0	0	0	0	0	0	0	0	0.9
Scapolite		0	0	0	0	0	0	0	0	0	0	0	0
Sulfide													
Pyrrhotite		2.05	2.54	2.55	3.02	3.23	3.69	3.42	4.04	4.78	7.35	8.9	13.2
Chalcopyrite		0.21 (752)	0.23 (800)	0.31 (1090)	0.45 (1560)	0.35 (1210)	0.34 (1180)	0.63 (2220)	0.19 (660)	0.37 (1300)	0.44 (1540)	0.4 (1280)	0.37 (1290)
Pentlandite		0.09 (324)	0.09 (329)	0.12 (422)	0.14 (503)	0.11 (386)	0.14 (4.92)	0.21 (718)	0.1 (354)	0.09 (327)	0.12 (436)	0.2 (540)	0.17 (589)
Pyrite		0	0.8	0	0	0	0	1.7	0	0	4.5	0.9	1.8
Cubanite		0.8	0	0.9	0	0	1.9	0	0.8	0	0	0	0
Unknown		0	0	0	0	0	0	0	0	0	0	0	15

[1] Reactor 39

[2] Reactor 40

Table 8. Reactor mineral composition (%) after leaching. All determined by point count, with the exception of pyrrhotite, chalcopyrite and pentlandite, which were chemically determined by assuming that all Cu was present as chalcopyrite and all Ni as pentlandite. Numbers in parentheses following chalcopyrite are Cu ppm and following pentlandite are Ni ppm. Only minerals detected are listed.

	%S	**0.40**	**0.41**	**0.51**	**0.58[1]**	**0.58[2]**	**0.71**	**1.40**	**1.44**	**1.63**	**1.71**
Silicate											
Plagioclase		46.7	52.1	44	42.5	54.1	48.6	55.6	45.9	52.3	47.4
Hypersthene		27	8.5	17.4	14.2	6.6	14.4	8.3	16.2	5.6	12.3
Olivine		0	12	10.1	1.8	8.2	20.7	6.5	9.9	1.9	21.9
Augite		5.8	12	11	15	13.1	10.8	17.6	12.6	13.1	0
Biotite		0	0	0	3.5	4.9	0.9	0.9	0.9	0.9	0
Prehnite		0	0	0	0	0	0	0.9	0	0	0
Amphibole		0	2.6	0.9	0	0	0	0	0	0	0
K-Spar		2.2	0.9	1.8	2.7	6.6	0	0.9	6.3	10.3	2.6
Ilmenite		6.6	6.8	11.9	11.5	3.3	1.8	9	5.4	8.4	4.4
Apatite		0	1.7	14.8	1.8	1.6	0	7.4	0	0	0
Cordierite		6.6	0	0	3.5	0	0	0	0	0	2.6
Quartz		0.7	0	0	1.8	0	0	0	0	7.5	0
Magnetite		0.7	0.9	0	0.9	0	0.9	1	0.9	0	0
Chlorite		0	0	0	0	0	0	0	0	0	4.4
Scapolite		0	1.7	0	0	0	0	0	0	0	0
Muscovite		0.7	0	0.9	0	0	0	0	0	0	0
Sulfide											
Pyrrhotite		0.68	0.29	0.27	0.36	0.38	0.05	0.28	1.3	0.84	4.4[4]
Chalcopyrite		0.18 (624)	0.22 (777)	0.34 (1200)	0.39 (624)[3]	0.18 (624)	0.86 (>10000)	0.5 (1920)	0.36 (1270)	0.3 (1060)	0[4]
Pentlandite		0.06 (206)	0.09 (304)	0.05 (183)	0.09 (125)[3]	0.04 (125)	0.07 (246)	0.06 (483)	0.08 (277)	0.08 (275)	0[4]
Pyrite		1.5	0	0	0	0	0	0	0	0	0
Cubanite		0	0.9	0	0.9	0	0.9	0	0	0	0

[1] Reactor 15, Cu and Ni analyses from Reactor 16

[2] Reactor 16

[3] Cu and Ni analyses from Reactor 16

[4] The 1.71%S sample had all values determined by point count.

Table 9. Mineral content calculated based on S, Cu, and Ni content from Actlabs (see calculation methods below). These samples leached for 144-328 weeks prior to termination.

Reactor	5	7	9	15[1]	16[1]	17	37	33	19	31[2]	Average[3]
Before leaching											
S	0.40	0.41	0.51	0.58	0.58	0.71	1.40	1.44	1.63	1.71	0.94
Cu	512	788	1430	1300	1300	1160	1560	1210	1180	660	1110
Ni	231	511	473	396	396	388	503	386	492	354	413
After leaching											
S	0.35	0.21	0.23	0.22	0.22	0.32	0.29	0.66	0.46	N/A	0.33
Cu	624	777	1200	624	624	>10000[4]	1920	1270	1060	N/A	1012
Ni	206	304	183	125	125	246	483	277	275	N/A	247

Reactor	5	7	9	15[1]	16[1]	17	37	33	19	31[2]	Average[3]
Before leaching											
Pyrrhotite	0.84	0.72	0.82	1.05	1.05	1.43	3.06	3.29	3.76	4.13	2.01
Chalcopyrite	0.15	0.23	0.41	0.38	0.38	0.34	0.45	0.35	0.34	0.19	0.32
Pentlandite	0.07	0.15	0.14	0.12	0.12	0.11	0.15	0.11	0.14	0.10	0.12
After leaching											
Pyrrhotite	0.68	0.27	0.24	0.37	0.37	-1.84[4]	0.13	1.30	0.83	N/A	0.53
Chalcopyrite	0.18	0.22	0.35	0.18	0.18	2.89[4]	0.55	0.37	0.31	N/A	0.29
Pentlandite	0.06	0.09	0.05	0.04	0.04	0.07	0.14	0.08	0.08	N/A	0.07
Final/Initial Ratio											
Pyrrhotite	0.82	0.38	0.29	0.35	0.35	-1.29	0.04	0.40	0.22	N/A	0.36
Chalcopyrite	1.22	0.99	0.84	0.48	0.48	8.62[4]	1.23	1.05	0.90	N/A	0.90
Pentlandite	0.89	0.59	0.39	0.32	0.32	0.63	0.96	0.72	0.56	N/A	0.60

[1] Both 0.58%S samples analyzed for solids

[2] No S, Cu, Ni content for leached 1.71%S sample. Sample omitted from average calculations.

[3] Average does not include 0.71%S sample

[4] Anomalous Cu content omitted Po and Cp average calculations

Pyrrhotite: S with no Cu and Ni is $Fe_{0.9}S$. Then {S - [Cu(2x32.06)/63.5 + Ni(8x32.06)/(4.5 x 58.7]} x (0.9 x 55.8 + 32.06)/32.06

Chalcopyrite: Assume all Cu with $CuFeS_2$. Then $CuFeS_2$ = [(2 x 32.06 + 63.5 + 55.8)/63.5] x % Cu = 2.89 x %Cu

Pentlandite: Assume all Ni with $(Ni, Fe)_9S_8$. Then $(Ni,Fe)_9S_8$ = [(4.5 x 58.7 + 4.5 x 55.8 + 8 x 32.06)/(4.5 x 58.7] x % Ni = 2.92 x %Ni

Table 10. Unleached sulfide mineral chemistry determined by microprobe analysis. Only minerals likely to be affected by leaching are displayed. Only samples where a grain was identified by point count had analyses to determine stoichiometric ratios. Chemical percent abundance was chemically determined by assuming that all Cu was present as chalcopyrite and all Ni as pentlandite. Stoichiometric formulas at top of table are based on the mean ratios of major elements for Duluth Complex samples. To determine the composition of the minerals in this study, substitute the mean sample values for each element into the stoichiometric formula. Page 1 of 4.

Pyrrhotite – $Fe_{7.18}S_8$

Sulfur %	Reactor	%, chemical	%, point count	N	Fe atoms	Ni atoms	Cu atoms
Duluth Complex							
0.18	1,2	0.02	0.9	1	7.007	0.031	0.033
0.221	3,4	0.13					
0.4	5,6	0.83	1.7	3	7.27	0.035	0.028
0.41	7,8	0.72					
0.51	9,10	0.84	2.5	2	7.041	0.062	0.011
0.54	11,12	1.26	1.8	2	7.017	0.016	0.019
0.57	13,14	1.04					
0.58	15,16	1.06	2.5	3	7.933	0.036	0.039
0.67	39	1.5	0.8	1	6.952	0.007	0.05
0.671	40	1.5					
0.71	17,18	1.42	4.3	5	7.222	0.019	0.008
0.72	42	1.62					
0.82	43	1.86	0.9	1	6.911	0.028	0.054
0.92	41	2.05	0.8	1	6.985	0.018	0.037
1.12	35,36	2.54	5	6	7.093	0.026	0.038
1.16	29,30	2.55					
1.4	37,38	3.02	7.6	9	7.669	0.038	0.013
1.44	33,34	3.23	1.7	2	7.096	0.047	0.007
1.63	19,20	3.69	4.7	6	7.222	0.052	0.026
1.64	31,32	3.42	1.7	2	7.04	0.02	0.075
1.71	44	4.04	9.1	11	7.27	0.037	0.007
	Mean				7.182	0.031	0.03
	Max				7.933	0.062	0.075
	Min				6.911	0.007	0.007
	St. Dev.				0.28	0.015	0.02
Virginia Formation							
2.06	21,22	4.78	5	6	7.144	0.029	0.029
3.12	23,24	7.35	7.1	8	7.095	0.02	0.052
3.72	25,26	8.88	13.9	16	7.526	0.012	0.031
5.44	27,28	13.17	13.3	15	7.489	0.01	0.029
	Mean				7.314	0.018	0.035
	Max				7.526	0.029	0.052
	Min				7.095	0.01	0.029
	St. Dev.				0.225	0.009	0.011

Table 10. Unleached sulfide mineral chemistry determined by microprobe analysis. Only minerals likely to be affected by leaching are displayed. Only samples where a grain was identified by point count had analyses to determine stoichiometric ratios. Chemical percent abundance was chemically determined by assuming that all Cu was present as chalcopyrite and all Ni as pentlandite. Stoichiometric formulas at top of table are based on the mean ratios of major elements for Duluth Complex samples. To determine the composition of the minerals in this study, substitute the mean sample values for each element into the stoichiometric formula. Page 2 of 4.

Chalcopyrite - $(Cu_{4.29}Fe_{4.47})S_8$

Sulfur %	Reactor	%, chemical	%, point count	N	Fe atoms	Ni atoms	Cu atoms
Duluth Complex							
0.181	1,2	0.39					
0.221	3,4	0.39					
0.4	5,6	0.15					
0.41	7,8	0.23					
0.51	9,10	0.41					
0.54	11,12	0.06	0.9	1	4.41	0.002	4.204
0.57	13,14	0.37					
0.58	15,16	0.37					
0.671	39	0.18	1.7	2	4.315	0.007	4.163
0.67	40	0.14					
0.71	17,18	0.33					
0.72	42	0.15	0.8	1	4.363	0.012	4.249
0.822	43	0.17	3.5	4	4.79	0.021	1.733
0.92	41	0.21					
1.12	35,36	0.23	0.8	1	4.298	0	4.281
1.16	29,30	0.31					
1.4	37,38	0.45	2.5	3	4.986	0.005	4.659
1.44	33,34	0.35	0.8	1	4.471	0	4.24
1.63	19,20	0.34					
1.64	31,32	0.63					
1.71	44	0.19	0.8	1	4.439	0	4.213
	Mean				4.469	0.004	4.287
	Max				4.986	0.021	4.659
	Min				4.315	0	4.163
	St. Dev.				0.237	0.005	0.168
Virginia Formation							
2.06	21,22	0.37	0.8	1	4.366	0	4.174
3.12	23,24	0.44					
3.72	25,26	0.37					
5.44	27,28	0.37					

Table 10. Unleached sulfide mineral chemistry determined by microprobe analysis. Only minerals likely to be affected by leaching are displayed. Only samples where a grain was identified by point count had analyses to determine stoichiometric ratios. Chemical percent abundance was chemically determined by assuming that all Cu was present as chalcopyrite and all Ni as pentlandite. Stoichiometric formulas at top of table are based on the mean ratios of major elements for Duluth Complex samples. To determine the composition of the minerals in this study, substitute the mean sample values for each element into the stoichiometric formula. Page 3 of 4.

Pentlandite - $(Ni_{4.89}Fe_{4.88})S_8$

Sulfur %	Reactor	%, chemical	%, point count	N	Fe atoms	Ni atoms	Cu atoms
Duluth Complex							
0.181	1,2	0.15					
0.221	3,4	0.14					
0.4	5,6	0.07					
0.41	7,8	0.15					
0.51	9,10	0.14					
0.541	11,12	0.05					
0.57	13,14	0.11					
0.58	15,16	0.11					
0.67	39	0.15					
0.671	40	0.07					
0.71	17,18	0.11					
0.72	42	0.07					
0.82	43	0.06					
0.92	41	0.09	0.8	1	4.385	4.609	0.016
1.12	35,36	0.09					
1.16	29,30	0.12					
1.4	37,38	0.14	0.8	1	5.366	5.162	0.043
1.44	33,34	0.11					
1.63	19,20	0.14					
1.64	31,32	0.21					
1.71	44	0.1					
	Mean				4.876	4.886	0.03
	Max				5.366	5.162	0.043
	Min				4.385	4.609	0.016
	St. Dev.				0.694	0.391	0.019
Virginia Formation							
2.06	21,22	0.09					
3.12	23,24	0.12					
3.72	25,26	0.15					
5.44	27,28	0.17					

Table 10. Unleached sulfide mineral chemistry determined by microprobe analysis. Only minerals likely to be affected by leaching are displayed. Only samples containing each mineral are displayed. Stoichiometric formulas at top of table are based on the mean ratios of major elements for Duluth Complex samples. To determine the composition of the minerals in this study, substitute the mean sample values for each element into the stoichiometric formula. Page 4 of 4.

Pyrite - $Fe_{4.28}S_8$

Sulfur %	Reactor	%, point count	N	Fe atoms	Ni atoms	Cu atoms
Duluth Complex						
0.4	5,6	1.5	1	4.296	0.023	0.001
0.58	15,16	1.7	2	4.443	0.027	0.026
1.12	35,36	0.8	1	4.061	0.02	0
1.64	31,32	1.7	2	4.299	0.073	0.231
	Mean			4.275	0.036	0.065
	Max			4.443	0.073	0.231
	Min			4.061	0.001	0
	St. Dev.			0.158	0.025	0.112
Virginia Formation						
3.12	23,24	4.5	5	4.072	0.012	0.007
3.72	25,26	0.9	1	4.356	0.001	0
5.44	27,28	1.8	2	4.546	0.014	0.02
	Mean			4.325	0.009	0.009
	Max			4.546	0.014	0.02
	Min			4.072	0.001	0
	St. Dev.			0.134	0.009	0.014

Cubanite - $Cu_{2.77}Fe_{5.59}S_8$

Sulfur %	Reactor	%, point count	N	Fe atoms	Ni atoms	Cu atoms
Duluth Complex						
0.92	41	0.8	1	5.487	0	2.705
1.16	29,30	0.9	1	5.599	0	2.862
1.63	19,20	1.9	1	5.675	0.019	2.729
1.71	44	0.8	1	5.607	0	2.79
	Mean			5.592	0.005	2.772
	Max			5.675	0.019	2.862
	Min			5.487	0	2.705
	St. Dev.			0.078	0.01	0.07

Note: N = number of samples analyzed for each Sulfur %

Note: Pyrrhotite, chalcopyrite and pentlandite percentages were determined using calculations from bulk chemistry. All other mineral percentages were determined using point counts.

[1] No chemical analysis performed

[2] These samples were listed as chalcopyrite in the McSwiggen analysis. However, due to the large deviation in expected Cu stoichiometry, they were not included in the calculation.

Table 11. Unleached silicate mineral chemistry, as determined through microprobe analysis. Only minerals likely to be affected by leaching are displayed. Only samples containing each mineral are displayed. Stoichiometric formulas at top of table are based on the mean ratios of major elements for Duluth Complex samples. To determine sample stoichiometry, substitute mean sample values for each element into the stoichiometric formula. Page 1 of 8.

Plagioclase - $(Ca_{0.51}Na_{0.45})Al_{1.54}Si_{2.46}O_8$

Sulfur %	**Reactor**	**%, point count**	**N**	**Ca**	**Mg**	**K**	**Na**	**Si**	**Al**	**Fe**	**Ti**
Duluth Complex											
0.18	1,2	49.5	54	0.471	0.002	0.032	0.468	2.505	1.501	0.012	0.001
0.22	3,4	64.9	72	0.446	0.002	0.033	0.521	2.532	1.46	0.017	0.002
0.4	5,6	47.4	55	0.537	0.001	0.026	0.422	2.441	1.563	0.009	0
0.41	7,8	57.4	65	0.525	0.002	0.019	0.43	2.45	1.554	0.008	0.001
0.51	9,10	46.6	55	0.51	0.003	0.02	0.459	2.472	1.524	0.012	0.001
0.54	11,12	62.2	59	0.628	0.012	0.017	0.318	2.347	1.655	0.014	0
0.57	13,14	42.6	43	0.473	0.004	0.022	0.462	2.497	1.51	0.02	0.001
0.58	15,16	45.8	55	0.492	0.002	0.022	0.453	2.483	1.522	0.016	0.002
0.67	39	56.3	67	0.53	0.003	0.021	0.472	2.417	1.578	0.016	0.001
0.67	40	47.7	53	0.514	0.001	0.015	0.48	2.495	1.49	0.01	0.001
0.71	17,18	54.8	63	0.507	0.005	0.023	0.452	2.47	1.527	0.017	0.001
0.72	42	61.2	74	0.602	0.002	0.015	0.393	2.38	1.611	0.009	0.003
0.82	43	47.8	55	0.508	0.013	0.019	0.425	2.456	1.551	0.017	0.001
0.92	41	44.6	54	0.568	0.002	0.024	0.387	2.423	1.578	0.01	0.001
1.12	35,36	39.7	48	0.49	0.002	0.018	0.462	2.501	1.5	0.014	0.001
1.16	29,30	58.4	66	0.53	0.003	0.02	0.436	2.449	1.546	0.017	0.002
1.4	37,38	46.2	55	0.501	0.003	0.018	0.445	2.477	1.526	0.018	0.002
1.44	33,34	52.9	61	0.48	0.002	0.024	0.459	2.473	1.538	0.02	0.002
1.63	19,20	36.4	19	0.396	0.003	0.02	0.55	2.568	1.444	0.011	0.001
1.64	31,32	45.8	55	0.478	0.002	0.018	0.478	2.513	1.485	0.016	0.001
1.71	44	45.5	53	0.555	0.011	0.027	0.374	2.394	1.617	0.017	0.002
	Mean			0.514	0.004	0.022	0.445	2.464	1.537	0.014	0.001
	Max			0.628	0.013	0.033	0.55	2.568	1.655	0.02	0.003
	Min			0.396	0.001	0.015	0.318	2.347	1.444	0.008	0
	St. Dev.			0.052	0.004	0.005	0.05	0.052	0.052	0.004	0.001
Virginia Formation											
2.06	21,22	27.7	31	0.325	0.003	0.02	0.625	2.665	1.339	0.009	0.001
3.12	23,24	34.8	39	0.561	0.001	0.029	0.381	2.411	1.6	0.008	0.001
3.72	25,26	18.3	21	0.407	0.001	0.02	0.583	2.56	1.441	0.007	0
5.44	27,28	11.5	13	0.322	0.001	0.031	0.663	2.645	1.351	0.01	0.001
	Mean			0.404	0.002	0.025	0.563	2.57	1.433	0.009	0.001
	Max			0.561	0.003	0.029	0.663	2.665	1.6	0.01	0.001
	Min			0.322	0.001	0.02	0.381	2.411	1.339	0.007	0
	St. Dev.			0.112	0.001	0.006	0.126	0.116	0.12	0.001	0.001

Table 11. Unleached silicate mineral chemistry, as determined through microprobe analysis. Only minerals likely to be affected by leaching are displayed. Only samples containing each mineral are displayed. Stoichiometric formulas at top of table are based on the mean ratios of major elements for Duluth Complex samples. To determine sample stoichiometry, substitute mean sample values for each element into the stoichiometric formula. Page 2 of 8.

Hypersthene - $(Mg_{1.06}Fe_{0.89})_2Si_{1.99}O_6$

Sulfur %	**Reactor**	**%, point count**	**N**	**Ca**	**Mg**	**K**	**Na**	**Si**	**Al**	**Fe**	**Ti**
Duluth Complex											
0.18	1,2	17.4	19	0.048	1.018	0.001	0.001	1.991	0.027	0.874	0.007
0.22	3,4	5.4	6	0.06	1.03	0.001	0.002	1.979	0.027	0.876	0.007
0.4	5,6	27.6	32	0.022	0.98	0	0.002	1.967	0.057	0.943	0.007
0.41	7,8	8.7	10	0.066	1.074	0.001	0.001	1.988	0.032	0.806	0.005
0.51	9,10	17.8	21	0.08	0.978	0	0.002	1.985	0.029	0.896	0.005
0.54	11,12	19.8	22	0.031	1.123	0.001	0.001	1.997	0.027	0.783	0.006
0.57	13,14	5	5	0.04	1.106	0	0	1.985	0.029	0.812	0.005
0.58	15,16	15	16	0.045	0.936	0.001	0	1.98	0.026	0.985	0.007
0.67	39	4.2	5	0.029	1.233	0	0	1.987	0.026	0.703	0.003
0.67	40	14.4	16	0.042	0.947	0.001	0.001	1.979	0.049	0.946	0.006
0.71	17,18	12.2	14	0.049	1.118	0	0.002	1.985	0.031	0.785	0.007
0.72	42	3.3	4	0.035	1.304	0	0.001	1.977	0.029	0.63	0.006
0.82	43	15.7	18	0.031	1.161	0.001	0.001	1.987	0.043	0.836	0.006
0.92	41	3.3	4	0.045	1.187	0	0	1.998	0.021	0.709	0.004
1.12	35,36	19.8	24	0.043	0.907	0	0.001	1.998	0.023	0.987	0.005
1.16	29,30	12.4	14	0.048	1.044	0.001	0.001	1.985	0.027	0.866	0.006
1.4	37,38	8.4	10	0.043	1.029	0.001	0.001	1.98	0.027	0.897	0.004
1.44	33,34	24.4	29	0.04	1.064	0.001	0.056	1.98	0.025	1.661	0.006
1.63	19,20	17.8	19	0.037	0.94	0.001	0.001	1.982	0.03	0.983	0.005
1.64	31,32	10.8	13	0.046	0.979	0	0.001	1.994	0.024	0.916	0.006
1.71	44	2.5	3	0.051	1.177	0	0	1.965	0.034	0.744	0.015
	Mean			0.044	1.064	0.001	0.004	1.984	0.031	0.888	0.006
	Max			0.08	1.304	0.001	0.056	1.998	0.057	1.661	0.015
	Min			0.022	0.907	0	0	1.965	0.021	0.63	0.003
	St. Dev.			0.013	0.107	0.001	0.012	0.009	0.009	0.203	0.002
Virginia Formation											
2.06	21,22	10.9	13	0.014	0.949	0.001	0.001	1.973	0.062	0.961	0.009
3.12	23,24	11.6	13	0.024	1.112	0.002	0.001	1.982	0.057	0.777	0.006
3.72	25,26	9.6	11	0.019	1.033	0.001	0.001	1.964	0.064	0.896	0.005
	Mean			0.019	1.031	0.001	0.001	1.973	0.061	0.878	0.007
	Max			0.024	1.112	0.002	0.001	1.982	0.064	0.961	0.009
	Min			0.014	0.949	0.001	0.001	1.964	0.057	0.777	0.005
	St. Dev.			0.005	0.082	0.001	0	0.009	0.004	0.093	0.002

Table 11. Unleached silicate mineral chemistry, as determined through microprobe analysis. Only minerals likely to be affected by leaching are displayed. Only samples containing each mineral are displayed. Stoichiometric formulas at top of table are based on the mean ratios of major elements for Duluth Complex samples. To determine sample stoichiometry, substitute mean sample values for each element into the stoichiometric formula. Page 3 of 8.

Olivine - $(Mg_{0.93}Fe_{1.05})Si_{1.00}O_4$

Sulfur %	**Reactor**	**%Olivine**	**N**	**Ca**	**Mg**	**K**	**Na**	**Si**	**Al**	**Fe**	**Ti**
Duluth Complex											
0.18	1,2	10.1	10	0.003	0.763	0	0.001	1.01	0.002	1.194	0.001
0.22	3,4	4.5	5	0.002	0.857	0	0.001	0.987	0	1.147	0.001
0.41	7,8	13	15	0.002	0.897	0	0.001	1.003	0	1.074	0.001
0.51	9,10	5.9	7	0.001	0.812	0	0.001	1.001	0	1.168	0.001
0.57	13,14	20.8	21	0.001	1.003	0	0.001	1.008	0.001	0.96	0.001
0.58	15,16	2.5	3	0.002	0.851	0	0	0.997	0.001	1.135	0
0.67	39	16.8	20	0.001	1.09	0	0	1.004	0	0.881	0.002
0.67	40	4.5	5	0.002	0.785	0	0.001	1.009	0	1.178	0
0.71	17,18	14.8	17	0.002	0.958	0	0.001	1.005	0.001	1.01	0.001
0.72	42	21.5	26	0.002	1.233	0.001	0	0.996	0	0.751	0.002
0.82	43	3.5	4	0.001	0.8	0.001	0.001	1.009	0.001	1.156	0.001
0.92	41	38.8	47	0.003	1.035	0.001	0	1.009	0.008	0.914	0.001
1.12	35,36	4.1	5	0.002	0.953	0	0	1.007	0.001	1.013	0
1.16	29,30	16.8	19	0.002	0.948	0	0.001	1.004	0.001	1.023	0.001
1.4	37,38	5.9	7	0.002	0.954	0	0.001	0.992	0	1.038	0.001
1.44	33,34	5.9	7	0.002	0.953	0	0.002	0.999	0.003	1.023	0.001
1.63	19,20	5.6	6	0.002	0.722	0	0.002	1	0.001	1.248	0.002
1.64	31,32	3.3	4	0.002	0.828	0	0	1.008	0	1.128	0.001
1.71	44	19.8	24	0.002	1.139	0	0.001	0.997	0.001	0.849	0.001
	Mean			0.002	0.925	0	0.001	1.002	0.001	1.047	0.001
	Max			0.003	1.233	0.001	0.002	1.01	0.008	1.248	0.002
	Min			0.001	0.722	0	0	0.987	0	0.751	0
	St. Dev.			0.001	0.135	0	0.001	0.006	0.002	0.132	0.001
Virginia Formation											
2.06	21,22	0.8	1	0.002	0.894	0	0	1.014	0	1.058	0.001

Table 11. Unleached silicate mineral chemistry, as determined through microprobe analysis. Only minerals likely to be affected by leaching are displayed. Only samples containing each mineral are displayed. Stoichiometric formulas at top of table are based on the mean ratios of major elements for Duluth Complex samples. To determine sample stoichiometry, substitute mean sample values for each element into the stoichiometric formula. Page 4 of 8.

Augite - $(Ca_{0.80}Na_{0.02})(Mg_{0.71}Fe_{0.40}Ti_{0.01})(Si_{1.97}Al_{0.07})O_6$											
Sulfur %	**Reactor**	**%Augite**	**N**	**Ca**	**Mg**	**K**	**Na**	**Si**	**Al**	**Fe**	**Ti**
Duluth Complex											
0.18	1,2	10.1	11	0.789	0.73	0	0.014	1.979	0.058	0.398	0.009
0.22	3,4	8.1	9	0.816	0.717	0	0.023	1.962	0.068	0.393	0.012
0.4	5,6	4.3	6	0.945	0.362	0	0.008	1.971	0.043	0.626	0.009
0.41	7,8	8.7	10	0.787	0.715	0.011	0.024	1.952	0.09	0.393	0.018
0.51	9,10	7.6	9	0.814	0.709	0.001	0.014	1.968	0.056	0.415	0.01
0.54	11,12	8.1	9	0.861	0.789	0.003	0.01	2	0.031	0.273	0.007
0.57	13,14	16.8	17	0.792	0.706	0.001	0.016	1.971	0.075	0.398	0.013
0.58	15,16	14.2	17	0.756	0.694	0.001	0.019	1.967	0.072	0.461	0.012
0.67	39	14.3	19	0.755	0.697	0	0.022	1.982	0.06	0.444	0.012
0.67	40	11.7	13	0.823	0.665	0.002	0.017	1.968	0.063	0.428	0.014
0.71	17,18	7.8	9	0.795	0.78	0	0.02	1.963	0.07	0.349	0.011
0.72	42	2.5	3	0.76	0.839	0.002	0.015	1.949	0.083	0.313	0.021
0.82	43	13	15	0.789	0.712	0.004	0.029	1.953	0.094	0.387	0.018
0.92	41	4.1	5	0.822	0.766	0.001	0.018	1.958	0.083	0.317	0.016
1.12	35,36	5.8	7	0.814	0.613	0.001	0.011	1.989	0.043	0.49	0.009
1.16	29,30	9.7	11	0.822	0.745	0	0.02	1.957	0.075	0.358	0.013
1.4	37,38	11.8	14	0.793	0.737	0.001	0.022	1.951	0.079	0.397	0.015
1.44	33,34	2.5	3	0.761	0.773	0.001	0.024	1.949	0.095	0.362	0.019
1.63	19,20	5.6	6	0.822	0.653	0.001	0.012	1.985	0.046	0.45	0.008
1.64	31,32	13.3	16	0.811	0.686	0.001	0.019	1.962	0.071	0.422	0.013
1.71	44	2.5	3	0.767	0.741	0.001	0.019	1.97	0.066	0.397	0.015
	Mean			0.804	0.706	0.002	0.018	1.967	0.068	0.403	0.013
	Max			0.945	0.839	0.011	0.029	2	0.095	0.626	0.021
	Min			0.755	0.362	0	0.008	1.949	0.031	0.273	0.007
	St. Dev.			0.042	0.093	0.002	0.005	0.014	0.017	0.073	0.004
Virginia Formation											
2.06	21,22	2.5	3	0.808	0.589	0	0.009	1.981	0.051	0.526	0.009
3.12	23,24	0.6	1	0.966	0.343	0.002	0.002	1.987	0.044	0.616	0.005
3.72	25,26	2.6	3	0.821	0.742	0.026	0.016	1.974	0.104	0.284	0.007
	Mean			0.865	0.558	0.009	0.009	1.981	0.066	0.475	0.007
	Max			0.966	0.742	0.026	0.016	1.987	0.104	0.616	0.009
	Min			0.808	0.343	0	0.002	1.974	0.044	0.284	0.005
	St. Dev.			0.088	0.201	0.014	0.007	0.007	0.033	0.172	0.002

Table 11. Unleached silicate mineral chemistry, as determined through microprobe analysis. Only minerals likely to be affected by leaching are displayed. Only samples containing each mineral are displayed. Stoichiometric formulas at top of table are based on the mean ratios of major elements for Duluth Complex samples. To determine sample stoichiometry, substitute mean sample values for each element into the stoichiometric formula. Page 5 of 8.

Potassium-Feldspar - $K_{0.77}Al_{1.05}Si_{2.96}O_8$

Sulfur %	**Reactor**	**%K-Spar**	**N**	**Ca**	**Mg**	**K**	**Na**	**Si**	**Al**	**Fe**	**Ti**
Duluth Complex											
0.22	3,4	3.6	4	0.014	0.001	0.778	0.195	2.973	1.023	0.013	0.001
0.40	5,6	3.4	3	0.082	0.000	0.721	0.139	2.815	1.229	0.009	0.002
0.41	7,8	0.9	1	0.010	0.000	0.882	0.097	2.972	1.031	0.008	0.000
0.51	9,10	5.1	6	0.013	0.001	0.781	0.209	2.967	1.027	0.012	0.002
0.57	13,14	4.0	4	0.006	0.000	0.877	0.121	2.971	1.026	0.011	0.001
0.58	15,16	5.0	6	0.023	0.000	0.791	0.161	2.948	1.060	0.010	0.003
0.67	39	1.7	2	0.026	0.001	0.754	0.202	2.957	1.047	0.002	0.003
0.67	40	0.9	1	0.009	0.000	0.867	0.145	2.963	1.037	0.004	0.000
0.71	17,18	0.9	1	0.003	0.000	0.772	0.218	2.987	1.008	0.013	0.000
1.12	35,36	11.6	14	0.013	0.001	0.738	0.240	2.972	1.029	0.007	0.001
1.40	37,38	2.5	3	0.021	0.000	0.757	0.206	2.960	1.041	0.014	0.001
1.44	33,34	4.2	5	0.017	0.000	0.800	0.163	2.964	1.043	0.007	0.001
1.63	19,20	5.6	6	0.012	0.003	0.808	0.138	2.970	1.036	0.014	0.001
1.64	31,32	4.2	5	0.014	0.001	0.826	0.141	2.959	1.041	0.017	0.002
1.71	44	0.8	1	0.027	0.001	0.443	0.486	2.956	1.049	0.020	0.001
	Mean			0.019	0.001	0.773	0.191	2.956	1.048	0.011	0.001
	Max			0.082	0.003	0.882	0.486	2.987	1.229	0.020	0.003
	Min			0.003	0.000	0.443	0.097	2.815	1.008	0.002	0.000
	St. Dev.			0.019	0.001	0.104	0.091	0.040	0.051	0.005	0.001
Virginia Formation											
2.06	21,22	12.6	15	0.010	0.001	0.742	0.239	2.969	1.033	0.005	0.001
3.12	23,24	8.0	9	0.046	0.009	0.745	0.189	2.897	1.106	0.021	0.001
3.72	25,26	14.8	17	0.002	0.001	0.834	0.143	2.971	1.034	0.006	0.005
5.44	27,28	20.4	23	0.004	0.001	0.838	0.133	2.980	1.024	0.009	0.002
	Mean			0.016	0.003	0.790	0.176	2.954	1.049	0.010	0.002
	Max			0.046	0.009	0.838	0.239	2.980	1.106	0.021	0.005
	Min			0.002	0.001	0.742	0.133	2.897	1.024	0.005	0.001
	St. Dev.			0.021	0.004	0.053	0.049	0.038	0.038	0.007	0.002

Table 11. Unleached silicate mineral chemistry, as determined through microprobe analysis. Only minerals likely to be affected by leaching are displayed. Only samples containing each mineral are displayed. Stoichiometric formulas at top of table are based on the mean ratios of major elements for Duluth Complex samples. To determine sample stoichiometry, substitute mean sample values for each element into the stoichiometric formula. Page 6 of 8.

Biotite - $K_{1.78}(Mg_{3.07}Fe_{2.03})(Al_{2.53}Si_{5.54}O_{20})(OH)_2$											
Sulfur %	**Reactor**	**%Biotite**	**N**	**Ca**	**Mg**	**K**	**Na**	**Si**	**Al**	**Fe**	**Ti**
Duluth Complex											
0.18	1,2	1.8	2	0.006	2.652	1.851	0.047	5.532	2.544	2.288	0.611
0.22	3,4	2.7	3	0.005	3.294	1.829	0.049	5.527	2.509	1.907	0.516
0.4	5,6	1.7	2	0.009	2.834	1.672	0.058	5.52	2.747	2.239	0.442
0.41	7,8	2.6	3	0.006	3.188	1.824	0.05	5.532	2.589	1.816	0.551
0.51	9,10	2.5	3	0.006	3.215	1.807	0.056	5.576	2.5	1.879	0.526
0.54	11,12	2.7	3	0.004	3.02	1.804	0.035	5.548	2.574	1.886	0.605
0.58	15,16	0.8	1	0	2.163	1.837	0.024	5.499	2.421	2.804	0.731
0.67	40	6.3	7	0.023	2.929	1.782	0.081	5.497	2.554	2.159	0.563
0.71	17,18	1.7	2	0.016	3.405	1.691	0.082	5.497	2.497	1.712	0.616
0.82	43	3.5	4	0.01	2.74	1.753	0.057	5.55	2.553	2.295	0.553
1.12	35,36	1.7	2	0.007	3.279	1.849	0.048	5.648	2.44	1.786	0.511
1.44	33,34	1.7	2	0.001	3.688	1.839	0.056	5.491	2.584	1.661	0.421
1.63	19,20	1.9	2	0.002	3.145	1.645	0.059	5.498	2.609	2.292	0.395
1.64	31,32	2.5	3	0.015	3.265	1.767	0.029	5.549	2.502	1.95	0.503
1.71	44	0.8	1	0.014	3.212	1.739	0.085	5.608	2.353	1.723	0.696
	Mean			0.008	3.069	1.779	0.054	5.538	2.532	2.026	0.549
	Max			0.023	3.688	1.851	0.085	5.648	2.747	2.804	0.731
	Min			0	2.163	1.645	0.024	5.491	2.353	1.661	0.395
	St. Dev.			0.006	0.366	0.067	0.018	0.045	0.092	0.312	0.094
Virginia Formation											
2.06	21,22	0.8	1	0.016	2.585	1.609	0.028	5.585	2.947	1.902	0.545
3.12	23,24	2.7	3	0.005	2.849	1.779	0.031	5.515	2.789	2.098	0.459
3.72	25,26	2.6	3	0.004	4.515	1.816	0.019	5.744	2.514	0.79	0.254
5.44	27,28	0.9	1	0.009	2.623	1.76	0.023	5.478	2.799	2.346	0.485
	Mean			0.009	3.143	1.741	0.025	5.581	2.762	1.784	0.436
	Max			0.016	4.515	1.816	0.031	5.744	2.947	2.346	0.545
	Min			0.004	2.585	1.609	0.019	5.478	2.514	0.79	0.254
	St. Dev.			0.005	0.922	0.091	0.005	0.118	0.181	0.687	0.126

Table 11. Unleached silicate mineral chemistry, as determined through microprobe analysis. Only minerals likely to be affected by leaching are displayed. Only samples containing each mineral are displayed. Stoichiometric formulas at top of table are based on the mean ratios of major elements for Duluth Complex samples. To determine sample stoichiometry, substitute mean sample values for each element into the stoichiometric formula. Page 7 of 8.

Prehnite - $Ca_{1.92}Al_{1.96}(Si_{3.03}O_9)(OH)_2$											
Sulfur %	**Reactor**	**%Prehnite**	**N**	**Ca**	**Mg**	**K**	**Na**	**Si**	**Al**	**Fe**	**Ti**
Duluth Complex											
0.18	1,2	1.8	2	1.936	0.003	0.001	0	3.015	1.997	0.029	0.002
0.22	3,4	0.9	1	1.957	0.002	0.001	0.009	3.026	1.966	0.029	0.001
0.4	5,6	1.7	2	1.959	0.003	0.001	0.009	2.979	2.029	0.022	0.002
0.54	11,12	0.9	1	1.891	0	0.001	0.007	3.074	1.968	0.006	0
0.72	42	4.1	5	1.915	0.005	0.004	0.022	2.99	2.035	0.022	0.002
1.12	35,36	0.8	1	1.959	0.003	0	0.006	3.039	1.958	0.02	0
1.4	37,38	2.5	3	1.893	0.034	0.001	0	3.024	1.949	0.095	0.003
1.64	31,32	0.8	1	1.94	0.007	0.001	0.003	3.086	1.707	0.309	0.004
1.71	44	0.8	1	1.864	0	0	0.01	3.047	2.022	0.005	0
	Average			1.924	0.006	0.001	0.007	3.031	1.959	0.06	0.002
	Max			1.959	0.034	0.004	0.022	3.086	2.035	0.309	0.004
	Min			1.864	0	0	0	2.979	1.707	0.005	0
	St. Dev.			0.035	0.011	0.001	0.007	0.035	0.1	0.097	0.001
Virginia Formation											
3.72	25,26	0.9	1	1.855	0.029	0.003	0.003	3.058	1.968	0.041	0.001

Table 11. Unleached silicate mineral chemistry, as determined through microprobe analysis. Only minerals likely to be affected by leaching are displayed. Only samples containing each mineral are displayed. Stoichiometric formulas at top of table are based on the mean ratios of major elements for Duluth Complex samples. To determine sample stoichiometry, substitute mean sample values for each element into the stoichiometric formula. Page 8 of 8.

Amphibole - $(Ca_{1.78}Na_{0.25})(Mg_{2.96}Fe_{2.15})(Al_{0.99}Si_{7.12})_8O_{22}(OH)$											
Sulfur %	**Reactor**	**% Amphibole**	**N**	**Ca**	**Mg**	**K**	**Na**	**Si**	**Al**	**Fe**	**Ti**
Duluth Complex											
0.22	3,4	0.9	1	1.691	2.436	0.106	0.504	6.631	2.056	2.17	0.017
0.4	5,6	0.9	1	1.687	3.48	0.038	0.109	7.626	0.522	1.574	0.062
0.41	7,8	0.9	1	1.837	3.047	0.074	0.397	6.802	1.242	1.904	0.244
0.51	9,10	1.7	2	1.889	2.707	0.01	0.032	7.25	0.553	2.778	0.114
0.54	11,12	1	1	1.482	4.264	0.001	0.015	7.269	0.075	2.552	0.008
0.92	41	3.3	4	1.267	3.098	0.006	0.168	7.578	0.708	2.259	0.017
1.12	35,36	0.8	1	2.237	3.077	0	0.326	7.16	1.04	1.388	0.113
1.4	37,38	0.8	1	2.25	2.606	0.165	0.357	6.788	1.365	1.806	0.217
1.63	19,20	0.9	1	1.654	1.962	0.142	0.316	6.974	1.381	2.883	0.114
	Mean			1.777	2.964	0.06	0.247	7.12	0.994	2.146	0.101
	Max			2.25	4.264	0.165	0.504	7.626	2.056	2.883	0.244
	Min			1.267	1.962	0	0.015	6.631	0.075	1.388	0.008
	St. Dev.			0.322	0.659	0.064	0.172	0.35	0.594	0.524	0.086

Note: N = number of samples analyzed for each Sulfur %
All element units are moles.

Table 12. Leached sulfide mineral abundance determined by microprobe analysis and point count. Only minerals likely to be affected by leaching are displayed. Only samples where a grain was identified by point count had analyses to determine stoichiometric ratios. Chemical percent abundance was chemically determined by assuming that all Cu was present as chalcopyrite and all Ni as pentlandite. Stoichiometric formulas at top of table are based on the mean ratios of major elements for Duluth Complex samples. To determine the composition of the minerals in this study, substitute the mean sample values for each element into the stoichiometric formula. Page 1 of 4.

Pyrrhotite – $Fe_{7.18}S_8$

Sulfur %	Reactor	%, chemical	%, point count	N	Fe atoms	Ni atoms	Cu atoms
Duluth Complex							
0.18	2	0.09					
0.22	4	0.05					
0.4	6	0.68	0.7	1	7.6	0.036	0.031
0.41	8	0.29					
0.51	10	0.27					
0.54	11	0.32					
0.54	12	0.46					
0.57	13	0.14					
0.57	14	0.36					
0.58	16	0.38					
0.71	18	0.05					
1.12	35	0.24					
1.12	36	1					
1.16	29	2.34					
1.16	30	1.13					
1.4	37	0.28					
1.4	38	1.5					
1.44	34	1.3					
1.63	20	0.84					
1.64	31	1.22					
1.64	32	1.15					
1.71	44	4.4	4.4	5	7.48	0.035	0.022
	Mean				7.54	0.036	0.027
	Max				7.48	0.035	0.022
	Min				7.6	0.036	0.031
	St. Dev.				0.085	0.001	0.006
Virginia Formation							
2.06	22	3.8					
3.12	24	4.93					
3.72	26	6.98					
5.44	28	10.84					

Table 12. Leached sulfide mineral abundance determined by microprobe analysis and point count. Only minerals likely to be affected by leaching are displayed. Only samples where a grain was identified by point count had analyses to determine stoichiometric ratios. Chemical percent abundance was chemically determined by assuming that all Cu was present as chalcopyrite and all Ni as pentlandite. Stoichiometric formulas at top of table are based on the mean ratios of major elements for Duluth Complex samples. To determine the composition of the minerals in this study, substitute the mean sample values for each element into the stoichiometric formula. Page 2 of 4.

Chalcopyrite - $(Cu_{4.29}Fe_{4.47})S_8$

Sulfur %	Reactor	%, chemical	%, point count	N	Fe atoms	Ni atoms	Cu atoms
Duluth Complex							
0.18	2	0.16					
0.22	4	0.33					
0.4	6	0.18					
0.41	8	0.22					
0.51	10	0.34					
0.54	11	0.05					
0.54	12	0.05					
0.57	13	0.35					
0.57	14	0.39					
0.58	16	0.39	0.0 (R15), 0.9 (R16)	1	4.43	0	4.378
0.71	18	0.86	0.9	1	4.441	0	4.221
1.12	35	0.21					
1.12	36	0.25					
1.16	29	0.32					
1.16	30	0.33					
1.4	37	0.5					
1.4	38	0.55					
1.44	34	0.36	0.9	1	4.566	0	4.247
1.63	20	0.3					
1.64	31	0.87					
1.64	32	0.56					
	Mean				4.479	0	4.282
	Max				4.43	0	4.221
	Min				4.566	0	4.378
	St. Dev.				0.076	0	0.084
Virginia Formation							
2.06	22	0.66					
3.12	24	0.04					
3.72	26	0.03					
5.44	28	0.04					

Table 12. Leached sulfide mineral abundance determined by microprobe analysis. There were no instances of this mineral found during point count of leached samples. Only minerals likely to be affected by leaching are displayed. Only samples where a grain was identified by point count had analyses to determine stoichiometric ratios. Chemical percent abundance was chemically determined by assuming that all Cu was present as chalcopyrite and all Ni as pentlandite. Stoichiometric formula at top of table is the same as the unleached sample, since there was no leached stoichiometric analysis. Page 3 of 4.

Pentlandite - ($Ni_{4.89}Fe_{4.88})S_8$						
Sulfur %	**Reactor**	**%, chemical**	**N**	**Fe atoms**	**Ni atoms**	**Cu atoms**
Duluth Complex						
0.18	2	0.06				
0.22	4	0.08				
0.4	6	0.06				
0.41	8	0.09				
0.51	10	0.05				
0.54	11	0.03				
0.54	12	0.03				
0.57	13	0.07				
0.57	14	0.09				
0.58	16	0.04				
0.71	18	0.07				
1.12	35	0.03				
1.12	36	0.05				
1.16	29	0.13				
1.16	30	0.11				
1.4	37	0.06				
1.4	38	0.14				
1.44	34	0.08				
1.63	20	0.08				
1.64	31	0.22				
1.64	32	0.07				
Virginia Formation						
2.06	22	0.12				
3.12	24	0.02				
3.72	26	0.09				
5.44	28	0.01				

Table 12. Leached sulfide mineral data determined by microprobe analysis. Only minerals likely to be affected by leaching are displayed. Only samples where a grain was identified by point count had analyses to determine stoichiometric ratios. Chemical percent abundance was chemically determined by assuming that all Cu was present as chalcopyrite and all Ni as pentlandite. Stoichiometric formulas at top of table are based on the mean ratios of major elements for Duluth Complex samples. To determine the composition of the minerals in this study, substitute the mean sample values for each element into the stoichiometric formula. Page 4 of 4.

Pyrite - $Fe_{4.59}S_8$						
Sulfur %	Reactor	%Pyrite	N	Fe atoms	Ni atoms	Cu atoms
Duluth Complex						
0.4	6	1.5	2	4.592	0.078	2.113

Cubanite - $Cu_{2.88}Fe_{5.79}S_8$						
Sulfur %	Reactor	%Cubanite	N	Fe atoms	Ni atoms	Cu atoms
Duluth Complex						
0.41	8	0.9	1	5.657	0.003	2.908
0.58	16	0.9	1	6.134	0.002	2.989
0.71	18	0.9	1	5.565	0	2.752
	Mean			5.785	0.001	2.883
	Max			6.134	0.003	2.989
	Min			5.565	0.002	2.752
	St. Dev.			0.305	0.002	0.12

Note: N = number of samples analyzed for each Sulfur %

Note: Pyrrhotite and chalcopyrite percentages were determined using calculations from bulk chemistry except for pyrrhotite in the 1.71%S sample, which was determined by point count. All other mineral percentages were determined using point counts. There were no analyses of leached samples for five samples that were still being run at the time of analysis (0.67 (reactors 39, 40), 0.72, 0.82 and 0.92%S).

Table 13. Leached silicate mineral chemistry, as determined through microprobe analysis. Only minerals likely to be affected by leaching are displayed. Only samples containing each mineral are displayed. Stoichiometric formulas at top of table are based on the mean ratios of major elements for Duluth Complex samples. To determine sample stoichiometry, substitute mean sample values for each element into the stoichiometric formula. Page 1 of 8.

Plagioclase - $(Ca_{0.48}Na_{0.45})Al_{1.53}Si_{2.48}O_8$											
Sulfur %	**Reactor**	**%, point count**	**N**	**Ca**	**Mg**	**K**	**Na**	**Si**	**Al**	**Fe**	**Ti**
Duluth Complex											
0.4	6	46.7	64	0.546	0.001	0.021	0.416	2.439	1.561	0.011	0.001
0.41	7	52.1	61	0.522	0.002	0.023	0.437	2.463	1.534	0.017	0.001
0.51	9	44	48	0.503	0.002	0.021	0.466	2.482	1.512	0.017	0.001
0.58	15	42.5	48	0.465	0.001	0.031	0.470	2.513	1.493	0.014	0.002
0.58	16	54.1	59	0.432	0.004	0.032	0.467	2.525	1.494	0.019	0.001
0.71	17	48.6	54	0.471	0.001	0.025	0.469	2.493	1.515	0.017	0.001
1.4	37	55.6	60	0.460	0.001	0.021	0.481	2.516	1.493	0.014	0.001
1.44	33	45.9	51	0.499	0.001	0.013	0.451	2.459	1.552	0.018	0.001
1.63	19	52.3	56	0.439	0.002	0.030	0.493	2.534	1.474	0.015	0.002
1.71	44	47.4	54	0.504	0.005	0.041	0.366	2.419	1.617	0.016	0.002
	Mean			0.484	0.002	0.026	0.452	2.484	1.525	0.016	0.001
	Max			0.546	0.005	0.041	0.493	2.534	1.617	0.019	0.002
	Min			0.432	0.001	0.013	0.366	2.419	1.474	0.011	0.001
	St. Dev.			0.037	0.001	0.008	0.037	0.039	0.043	0.002	0.000

Table 13. Leached silicate mineral chemistry, as determined through microprobe analysis. Only minerals likely to be affected by leaching are displayed. Only samples containing each mineral are displayed. Stoichiometric formulas at top of table are based on the mean ratios of major elements for Duluth Complex samples. To determine sample stoichiometry, substitute mean sample values for each element into the stoichiometric formula. Page 2 of 8.

Hypersthene - $(Mg_{1.01}Fe_{0. 89})_2Si_{1.98}O_6$											
Sulfur %	**Reactor**	**%, point count**	**N**	**Ca**	**Mg**	**K**	**Na**	**Si**	**Al**	**Fe**	**Ti**
Duluth Complex											
0.4	6	27	37	0.018	0.984	0.000	0.001	1.957	0.065	0.952	0.008
0.41	7	8.5	10	0.045	1.051	0.001	0.002	1.991	0.032	0.841	0.006
0.51	9	17.4	19	0.055	1.000	0.000	0.002	1.974	0.035	0.901	0.012
0.58	15	14.2	16	0.047	0.922	0.000	0.001	1.974	0.038	0.991	0.007
0.58	16	6.6	20	0.039	0.926	0.001	0.001	1.992	0.037	0.960	0.007
0.71	17	14.4	16	0.086	1.112	0.001	0.001	1.979	0.034	0.761	0.006
1.4	37	8.3	9	0.046	1.021	0.001	0.001	1.985	0.025	0.896	0.005
1.44	33	16.2	18	0.036	1.024	0.001	0.001	1.974	0.028	0.916	0.009
1.63	19	5.6	6	0.048	0.929	0.001	0.001	1.983	0.024	0.984	0.007
1.71	44	12.3	14	0.077	1.105	0.000	0.002	1.958	0.098	0.717	0.009
	Mean			0.050	1.007	0.001	0.001	1.977	0.042	0.892	0.008
	Max			0.086	1.112	0.001	0.002	1.992	0.098	0.991	0.012
	Min			0.018	0.922	0.000	0.001	1.957	0.024	0.717	0.005
	St. Dev.			0.020	0.070	0.000	0.001	0.012	0.023	0.093	0.002

Table 13. Leached silicate mineral chemistry, as determined through microprobe analysis. Only minerals likely to be affected by leaching are displayed. Only samples containing each mineral are displayed. Stoichiometric formulas at top of table are based on the mean ratios of major elements for Duluth Complex samples. To determine sample stoichiometry, substitute mean sample values for each element into the stoichiometric formula. Page 3 of 8.

Olivine - $(Mg_{0.89}Fe_{1.08})Si_{1.00}O_4$											
Sulfur %	**Reactor**	**%, point count**	**N**	**Ca**	**Mg**	**K**	**Na**	**Si**	**Al**	**Fe**	**Ti**
Duluth Complex											
0.4	6	0									
0.41	7	12	14	0.002	0.904	0.000	0.001	1.006	0.001	1.062	0.001
0.51	9	10.1	11	0.002	0.822	0.000	0.001	1.007	0.003	1.140	0.001
0.58	15	1.8	2	0.002	0.806	0.000	0.001	1.001	0.000	1.176	0.001
0.58	16	8.2	5	0.002	0.698	0.000	0.000	1.007	0.000	1.268	0.001
0.71	17	20.7	23	0.002	1.029	0.000	0.001	1.005	0.001	0.941	0.001
1.4	37	6.5	7	0.002	0.923	0.000	0.001	0.998	0.001	1.056	0.001
1.44	33	9.9	11	0.001	0.969	0.000	0.001	0.997	0.001	1.015	0.001
1.63	19	1.9	2	0.001	0.731	0.001	0.001	0.995	0.000	1.260	0.000
1.71	44	21.9	25	0.002	1.137	0.000	0.000	1.007	0.000	0.828	0.002
	Mean			0.002	0.891	0.000	0.001	1.003	0.001	1.083	0.001
	Max			0.002	1.137	0.001	0.001	1.007	0.003	1.268	0.002
	Min			0.001	0.698	0.000	0.000	0.995	0.000	0.828	0.000
	St. Dev.			0.000	0.142	0.000	0.000	0.005	0.001	0.145	0.000

Table 13. Leached silicate mineral chemistry, as determined through microprobe analysis. Only minerals likely to be affected by leaching are displayed. Only samples containing each mineral are displayed. Stoichiometric formulas at top of table are based on the mean ratios of major elements for Duluth Complex samples. To determine sample stoichiometry, substitute mean sample values for each element into the stoichiometric formula. Page 4 of 8.

Augite - $(Ca_{0.80}Na_{0.02})(Mg_{0.69}Fe_{0.42}Ti_{0.01})(Si_{1.96}Al_{0.08})O_6$											
Sulfur %	**Reactor**	**%, point count**	**N**	**Ca**	**Mg**	**K**	**Na**	**Si**	**Al**	**Fe**	**Ti**
Duluth Complex											
0.4	6	5.8	8	0.945	0.451	0.001	0.003	1.963	0.063	0.538	0.007
0.41	7	12	14	0.845	0.726	0.001	0.021	1.955	0.076	0.355	0.014
0.51	9	11	12	0.772	0.706	0.009	0.013	1.953	0.089	0.439	0.012
0.58	15	15	17	0.759	0.708	0.000	0.015	1.956	0.074	0.459	0.014
0.58	16	13.1	7	0.759	0.676	0.001	0.017	1.995	0.063	0.434	0.011
0.71	17	10.8	12	0.767	0.784	0.000	0.021	1.963	0.076	0.355	0.014
1.4	37	17.6	19	0.780	0.723	0.003	0.024	1.949	0.085	0.411	0.017
1.44	33	12.6	14	0.756	0.766	0.000	0.021	1.962	0.083	0.381	0.014
1.63	19	13.1	14	0.786	0.695	0.002	0.017	1.963	0.070	0.438	0.012
1.71	44	0									
	Mean			0.797	0.693	0.002	0.017	1.962	0.075	0.423	0.013
	Max			0.945	0.784	0.009	0.024	1.995	0.089	0.538	0.017
	Min			0.756	0.451	0.000	0.003	1.949	0.063	0.355	0.007
	St. Dev.			0.062	0.097	0.003	0.006	0.013	0.009	0.057	0.003

Table 13. Leached silicate mineral chemistry, as determined through microprobe analysis. Only minerals likely to be affected by leaching are displayed. Only samples containing each mineral are displayed. Stoichiometric formulas at top of table are based on the mean ratios of major elements for Duluth Complex samples. To determine sample stoichiometry, substitute mean sample values for each element into the stoichiometric formula. Page 5 of 8.

Potassium-Feldspar - $K_{0.77}Al_{1.08}Si_{2.93}O_8$											
Sulfur %	**Reactor**	**%, point count**	**N**	**Ca**	**Mg**	**K**	**Na**	**Si**	**Al**	**Fe**	**Ti**
Duluth Complex											
0.4	6	2.2	3	0.006	0.001	0.877	0.104	2.978	1.019	0.016	0.001
0.41	7	0.9	1	0.006	0.010	0.878	0.116	2.973	1.011	0.025	0.000
0.51	9	1.8	2	0.008	0.001	0.850	0.129	2.979	1.018	0.012	0.002
0.58	15	2.7	3	0.019	0.056	0.687	0.168	2.888	1.122	0.036	0.001
0.58	16	6.6	2	0.077	0.009	0.683	0.125	2.747	1.320	0.023	0.005
0.71	17	0									
1.4	37	0.9	1	0.004	0.000	0.848	0.121	2.960	1.053	0.003	0.003
1.44	33	6.3	7	0.013	0.001	0.799	0.176	2.967	1.034	0.011	0.001
1.63	19	10.3	11	0.014	0.012	0.728	0.210	2.946	1.056	0.024	0.002
1.71	44	2.6	3	0.037	0.027	0.531	0.375	2.925	1.067	0.031	0.000
	Mean			0.021	0.013	0.765	0.169	2.929	1.078	0.020	0.002
	Max			0.077	0.056	0.878	0.375	2.979	1.320	0.036	0.005
	Min			0.004	0.000	0.531	0.104	2.747	1.011	0.003	0.000
	St. Dev.			0.024	0.018	0.117	0.084	0.074	0.097	0.011	0.002

Table 13. Leached silicate mineral chemistry, as determined through microprobe analysis. Only minerals likely to be affected by leaching are displayed. Only samples containing each mineral are displayed. Stoichiometric formulas at top of table are based on the mean ratios of major elements for Duluth Complex samples. To determine sample stoichiometry, substitute mean sample values for each element into the stoichiometric formula. Page 6 of 8.

Biotite - $K_{1.78}(Mg_{2.72}Fe_{2.25})(Al_{2.53}Si_{5.54}O_{20})(OH)_2$

Sulfur %	Reactor	%, point count	N	Ca	Mg	K	Na	Si	Al	Fe	Ti
Duluth Complex											
0.4	6	0									
0.41	7	0									
0.51	9	0									
0.58	15	3.5	4	0.010	2.477	1.816	0.059	5.544	2.487	2.485	0.633
0.58	16	4.9	1	0.006	3.303	1.875	0.065	5.598	2.554	1.718	0.484
0.71	17	0.9	1	0.009	2.854	1.791	0.034	5.489	2.503	2.064	0.708
1.4	37	0.9	1	0.014	3.142	1.690	0.068	5.557	2.586	1.852	0.559
1.44	33	0.9	1	0.000	2.815	1.811	0.006	5.524	2.558	2.160	0.615
1.63	19	0.9	1	0.011	1.744	1.695	0.077	5.524	2.513	3.236	0.640
1.71	44	0									
	Mean			0.008	2.723	1.780	0.051	5.539	2.534	2.253	0.607
	Max			0.014	3.303	1.875	0.077	5.598	2.586	3.236	0.708
	Min			0.000	1.744	1.690	0.006	5.489	2.487	1.718	0.484
	St. Dev.			0.005	0.558	0.073	0.027	0.037	0.038	0.550	0.077

Table 13. Leached silicate mineral chemistry, as determined through microprobe analysis. Only minerals likely to be affected by leaching are displayed. Only samples containing each mineral are displayed. Stoichiometric formulas at top of table are based on the mean ratios of major elements for Duluth Complex samples. To determine sample stoichiometry, substitute mean sample values for each element into the stoichiometric formula. Page 7 of 8.

Prehnite - $Ca_{1.90}Al_{1.99}(Si_{3.03}O_9)(OH)_2$

Sulfur %	**Reactor**	**%, point count**	**N**	**Ca**	**Mg**	**K**	**Na**	**Si**	**Al**	**Fe**	**Ti**
Duluth Complex											
0.4	6										
0.41	7										
0.51	9										
0.58	15										
0.58	16										
0.71	17										
1.4	37	0.9	1	1.901	0.005	0.002	0.019	3.027	1.99	0.042	0.001
1.44	33										
1.63	19										
1.71	44										
	Mean			1.901	0.005	0.002	0.019	3.027	1.99	0.042	0.001
	Max										
	Min										
	St. Dev.										

Table 13. Leached silicate mineral chemistry, as determined through microprobe analysis. Only minerals likely to be affected by leaching are displayed. Only samples containing each mineral are displayed. Stoichiometric formulas at top of table are based on the mean ratios of major elements for Duluth Complex samples. To determine sample stoichiometry, substitute mean sample values for each element into the stoichiometric formula. Page 8 of 8.

Amphibole - $(Ca_{1.61}Na_{0.31})(Mg_{1.66}Fe_{2.16})(Al_{1.64}Si_{7.08})_8O_{22}(OH)$											
Sulfur %	**Reactor**	**%, point count**	**N**	**Ca**	**Mg**	**K**	**Na**	**Si**	**Al**	**Fe**	**Ti**
Duluth Complex											
0.4	6	0									
0.41	7	2.6	3	1.453	1.536	0.383	0.582	7.417	1.781	1.443	0.278
0.51	9	0.9	1	1.762	1.778	0.228	0.488	6.747	1.506	2.880	0.209
0.58	15	0									
0.58	16	0									
0.71	17	0									
1.4	37	0									
1.44	33	0									
1.63	19	0									
1.71	44	0									
	Mean			1.608	1.657	0.305	0.535	7.082	1.643	2.161	0.244
	Max			1.762	1.778	0.383	0.582	7.417	1.781	2.880	0.278
	Min			1.453	1.536	0.228	0.488	6.747	1.506	1.443	0.209
	St. Dev.			0.218	0.171	0.110	0.067	0.474	0.194	1.016	0.049

Note: N = number of samples analyzed for each Sulfur %
All element units are moles.

Table 14. Particle surface area and coating analysis for unleached samples (Analysis by McSwiggen and Associates).

Sulfur %	Reactor	Perimeter / 1 mm area	Sulfides present	Ratio	Coating (microns)	Silicate Comments	Other Information
0.22	4	106	chalcopyrite pyrrhotite	4 cp:1 po		no alteration	
0.4	5,6	76.7	chalcopyrite pyrrhotite	1 cp:3 po		no alteration	
0.41	7,8	110.9	chalcopyrite pyrrhotite	1 cp:1 po		no alteration	Sulfides unaltered
0.51	9,10	99.9	chalcopyrite pyrrhotite	2 cp:3 po		no alteration	
0.58	15,16	103.9	chalcopyrite pyrrhotite	1 cp:3 po		no alteration	
0.58	16	85.4	chalcopyrite pyrrhotite pentlandite	1 cp:2 po		no alteration	
0.71	17,18	81.8	chalcopyrite pyrrhotite	1 cp:1 po		no alteration	
1.16	29,30	72	chalcopyrite pyrrhotite	1 cp: 3 po			
1.4	37,38	72	chalcopyrite pyrrhotite pentlandite	1 cp: 3 po		no alteration	
1.44	33,34	80.9	chalcopyrite pyrrhotite	1 cp:8 po		no alteration	
1.63	19,20	255.6	chalcopyrite pyrrhotite	1 cp:3 po		no alteration	
1.71	44	105.3	chalcopyrite pyrrhotite	1 cp:3 po		no alteration	

Table 15. Particle surface area and coating analysis for leached samples (Analysis by McSwiggen and Associates).

Sulfur %	**Reactor**	**Reaction time (wks)**	**Perimeter/ 1 mm area**	**Sulfides present**	**Ratio**	**Coating (microns)**	**Silicate Comments**	**Other Information**
0.22	4	328	94.1	chalcopyrite pyrrhotite pyrite	4 cp:1 po	0-2 7	no coatings	Po more reacted than cp; oxide coating compositions reported
0.4	6	328	92.9	pyrrhotite			no reaction evidence	Sulfides clean to half reacted to oxide; oxide coating compositions reported
0.41	7	724	83	chalcopyrite		thin - 2	hypersthene shows some alteration	One chalcopyrite grain had small serpentine inclusion
0.51	9	724	111.3	chalcopyrite		2-6	no alteration or coatings	Cp is very altered, and oxide coating compositions are reported
0.58	15	724	80.1	chalcopyrite pyrrhotite	Only 1 pyrrhotite grain found	0-3 2-14	few coatings; hyp alteration	po is much more reacted than cp; sulfide and silicate oxide coating compositions
0.58	16	328	87.1	chalcopyrite pyrrhotite	Only 1 pyrrhotite grain found			pyrrhotite coating composition; po much more reacted than cp
0.71	17	724	85.7	chalcopyrite		2-4.6		Oxide coating compositions reported
1.16	29	643	75.5	chalcopyrite		2.3-5	greenalite coatings on oli	Oxide coating compositions, cp is only sulfide found (variably altered), pyrrhotite is gone
1.4	37	360	78.3	chalcopyrite		0-1	coatings on hyp (0-3 microns)	Oxide coating compositions, hyp coatings are post-crush, po gone, cp variably altered
1.44	33	643	79.9	chalcopyrite		4-10	1-3 micron oli coatings, hyp, plag, amph dissolution pits	large degree of sulfide alteration; oxide coatings compositions; first indication of silicate dissolution (grooves and pits)
1.63	19	724	85.9	chalcopyrite		3-10	Andesine coating on hyp (4 microns), 4-6 micron coating on oli	Highly altered sulfides, dominated by chalcopyrite, very little pyrrhotite left
1.71	44	144	87	pyrrhotite			no reaction evidence	little or no sulfide alteration

Table 16. Leached silicate mineral chemistry, as determined through microprobe analysis. Only minerals likely to be affected by leaching are displayed. Only samples containing each mineral are displayed. Stoichiometric formulas at top of table are based on average ratio of major elements to a constant amount of oxygen. Page 1 of 4.

Plagioclase - $(Ca_{0.48}Na_{0.45})Al_{1.53}Si_{2.48}O_8$

Sulfur %	Reactor	% Plagioclase	N	Ca	Mg	K	Na	Si	Al	Fe	Ti
0.40	6	46.7	64	0.546	0.001	0.021	0.416	2.439	1.561	0.011	0.001
0.41	7	52.1	61	0.522	0.002	0.023	0.437	2.463	1.534	0.017	0.001
0.51	9	44.0	48	0.503	0.002	0.021	0.466	2.482	1.512	0.017	0.001
0.58	15	42.5	48	0.465	0.001	0.031	0.470	2.513	1.493	0.014	0.002
0.58	16	52.2	59	0.432	0.004	0.032	0.467	2.525	1.494	0.019	0.001
0.71	17	48.7	54	0.471	0.001	0.025	0.469	2.493	1.515	0.017	0.001
1.40	37	55.6	60	0.460	0.001	0.021	0.481	2.516	1.493	0.014	0.001
1.44	33	46.0	51	0.499	0.001	0.013	0.451	2.459	1.552	0.018	0.001
1.63	19	52.3	56	0.439	0.002	0.030	0.493	2.534	1.474	0.015	0.002
1.71	44	47.4	54	0.504	0.005	0.041	0.366	2.419	1.617	0.016	0.002
	Mean			0.484	0.002	0.026	0.452	2.484	1.525	0.016	0.001
	Max			0.546	0.005	0.041	0.493	2.534	1.617	0.019	0.002
	Min			0.432	0.001	0.013	0.366	2.419	1.474	0.011	0.001
	St Dev			0.037	0.001	0.008	0.037	0.039	0.043	0.002	0.000

Hypersthene - $(Mg_{1.01}Fe_{0.89})Si_{1.98}O_6$

Sulfur %	Reactor	%Hypersthene	N	Ca	Mg	K	Na	Si	Al	Fe	Ti
0.40	6	27.0	37	0.018	0.984	0.000	0.001	1.957	0.065	0.952	0.008
0.41	7	8.6	10	0.045	1.051	0.001	0.002	1.991	0.032	0.841	0.006
0.51	9	17.4	19	0.055	1.000	0.000	0.002	1.974	0.035	0.901	0.012
0.58	15	14.2	16	0.047	0.922	0.000	0.001	1.974	0.038	0.991	0.007
0.58	16	17.7	20	0.039	0.926	0.001	0.001	1.992	0.037	0.960	0.007
0.71	17	14.4	15	0.086	1.112	0.001	0.001	1.979	0.034	0.761	0.006
1.40	37	8.3	9	0.046	1.021	0.001	0.001	1.985	0.025	0.896	0.005
1.44	33	16.2	18	0.036	1.024	0.001	0.001	1.974	0.028	0.916	0.009
1.63	19	5.6	6	0.048	0.929	0.001	0.001	1.983	0.024	0.984	0.007
1.71	44	12.3	14	0.077	1.105	0.000	0.002	1.958	0.0.98	0.717	0.009
	Mean			0.050	1.007	0.001	0.001	1.977	0.035	0.892	0.008
	Max			0.086	1.112	0.001	0.002	1.992	0.0.98	0.991	0.012
	Min			0.018	0.922	0	0.001	1.957	0.024	0.717	0.005
	St Dev			0.020	0.070	0.001	0.000	0.012	0.012	0.093	0.002

Table 16. Leached silicate mineral chemistry, as determined through microprobe analysis. Only minerals likely to be affected by leaching are displayed. Only samples containing each mineral are displayed. Stoichiometric formulas at top of table are based on average ratio of major elements to a constant amount of oxygen. Page 2 of 4.

Augite - $(Ca_{0.80}Na_{0.02})(Mg_{0.69}Fe_{0.42}Ti_{0.01})(Si_{1.96}Al_{0.08})O_6$

Sulfur %	Reactor	%Augite	N	Ca	Mg	K	Na	Si	Al	Fe	Ti
0.40	6	5.8	8	0.945	0.451	0.001	0.003	1.963	0.063	0.538	0.007
0.41	7	12.0	14	0.845	0.726	0.001	0.021	1.955	0.076	0.355	0.014
0.51	9	11.0	12	0.772	0.706	0.009	0.013	1.953	0.089	0.439	0.012
0.58	15	15.0	17	0.759	0.708	0.000	0.015	1.956	0.074	0.459	0.014
0.58	16	6.2	7	0.759	0.676	0.001	0.017	1.995	0.063	0.434	0.011
0.71	17	10.8	11	0.767	0.784	0.000	0.021	1.963	0.076	0.355	0.014
1.40	37	17.6	19	0.780	0.723	0.003	0.024	1.949	0.085	0.411	0.017
1.44	33	12.6	14	0.756	0.766	0.000	0.021	1.962	0.083	0.381	0.014
1.63	19	13.1	14	0.786	0.695	0.002	0.017	1.963	0.070	0.438	0.012
	Mean			0.797	0.693	0.002	0.017	1.962	0.075	0.423	0.013
	Max			0.945	0.784	0.009	0.024	1.995	0.089	0.538	0.017
	Min			0.756	0.451	0	0.003	1.949	0.063	0.355	0.007
	St. Dev			0.062	0.097	0.003	0.006	0.013	0.009	0.057	0.003

Olivine - $(Mg_{0.89}Fe_{1.08})Si_{1.00}O_4$

Sulfur %	Reactor	%Olivine	N	Ca	Mg	K	Na	Si	Al	Fe	Ti
0.41	7	12.0	14	0.002	0.904	0.000	0.001	1.006	0.001	1.062	0.001
0.51	9	10.1	11	0.002	0.822	0.000	0.001	1.007	0.003	1.140	0.001
0.58	15	1.8	2	0.002	0.806	0.000	0.001	1.001	0.000	1.176	0.001
0.58	16	4.4	5	0.002	0.698	0.000	0.000	1.007	0.000	1.268	0.001
0.71	17	20.7	23	0.002	1.029	0.000	0.001	1.005	0.001	0.941	0.001
1.40	37	6.5	7	0.002	0.923	0.000	0.001	0.998	0.001	1.056	0.001
1.44	33	9.9	11	0.001	0.969	0.000	0.001	0.997	0.001	1.015	0.001
1.63	19	1.9	3	0.001	0.731	0.001	0.001	0.995	0.000	1.260	0.000
1.71	44	21.9	25	0.002	1.137	0.000	0.000	1.007	0.000	0.828	0.002
	Mean			0.002	0.891	0.000	0.001	1.003	0.001	1.083	0.001
	Max			0.002	1.137	0.001	0.001	1.007	0.003	1.268	0.002
	Min			0.001	0.698	0	0	0.995	0	0.828	0
	St Dev			0.000	0.142	0.000	0.000	0.005	0.001	0.145	0.001

Table 16. Leached silicate mineral chemistry, as determined through microprobe analysis. Only minerals likely to be affected by leaching are displayed. Only samples containing each mineral are displayed. Stoichiometric formulas at top of table are based on average ratio of major elements to a constant amount of oxygen. Page 3 of 4.

Potassium Feldspar - $K_{0.77}Al_{1.08}Si_{2.93}O_8$

Sulfur %	Reactor	%K-Spar	N	Ca	Mg	K	Na	Si	Al	Fe	Ti
0.40	6	2.2	3	0.006	0.001	0.877	0.104	2.978	1.019	0.016	0.001
0.41	7	0.9	1	0.006	0.010	0.878	0.116	2.973	1.011	0.025	0.000
0.51	9	1.8	2	0.008	0.001	0.850	0.129	2.979	1.018	0.012	0.002
0.58	15	2.7	3	0.019	0.056	0.687	0.168	2.888	1.122	0.036	0.001
0.58	16	1.8	2	0.077	0.009	0.683	0.125	2.747	1.320	0.023	0.005
1.40	37	0.9	1	0.004	0.000	0.848	0.121	2.960	1.053	0.003	0.003
1.44	33	6.3	7	0.013	0.001	0.799	0.176	2.967	1.034	0.011	0.001
1.63	19	10.3	11	0.014	0.012	0.728	0.210	2.946	1.056	0.024	0.002
1.71	44	2.6	3	0.037	0.027	0.531	0.375	2.925	1.067	0.031	0.000
	Mean			0.020	0.013	0.765	0.169	2.929	1.078	0.020	0.002
	Max			0.077	0.056	0.878	0.375	2.979	1.32	0.036	0.005
	Min			0.004	0	0.531	0.104	2.747	1.011	0.003	0
	St Dev			0.023	0.018	0.117	0.084	0.074	0.097	0.010	0.002

Biotite - $K_{1.78}(Mg_{2.72}Fe_{2.25})(Al_{2.53}Si_{5.53}O_{20})(OH)_2$

Sulfur %	Reactor	%Biotite	N	Ca	Mg	K	Na	Si	Al	Fe	Ti
0.58	15	3.5	4	0.010	2.477	1.816	0.059	5.544	2.487	2.485	0.633
0.58	16	0.9	1	0.006	3.303	1.875	0.065	5.598	2.554	1.718	0.484
0.71	17	0.9	1	0.009	2.854	1.791	0.034	5.489	2.503	2.064	0.708
1.40	37	0.9	1	0.014	3.142	1.690	0.068	5.557	2.586	1.852	0.559
1.44	33	0.9	1	0.000	2.815	1.811	0.006	5.524	2.558	2.160	0.615
1.63	19	0.9	1	0.011	1.744	1.695	0.077	5.524	2.513	3.236	0.640
	Mean			0.008	2.723	1.780	0.051	5.539	2.534	2.252	0.607
	Max			0.014	3.303	1.875	0.077	5.598	2.586	3.236	0.708
	Min			0.000	1.744	1.690	0.006	5.489	2.487	1.718	0.484
	St Dev			0.005	0.558	0.073	0.027	0.037	0.038	0.550	0.077

Table 16. Leached silicate mineral chemistry, as determined through microprobe analysis. Only minerals likely to be affected by leaching are displayed. Only samples containing each mineral are displayed. Stoichiometric formulas at top of table are based on average ratio of major elements to a constant amount of oxygen. Page 4 of 4.

Amphibole - $(Ca_{1.61}Na_{0.54})(Mg_{1.66}Fe_{2.16})(Al_{1.64}Si_{7.08})_8O_{22}(OH)$

Sulfur %	Reactor	%Amphibole	N	Ca	Mg	K	Na	Si	Al	Fe	Ti
0.41	7	2.6	3	1.453	1.536	0.383	0.582	7.417	1.781	1.443	0.278
0.51	9	0.9	1	1.762	1.778	0.228	0.488	6.747	1.506	2.880	0.209
	Mean			1.608	1.657	0.306	0.535	7.082	1.644	2.162	0.244
	Max			1.762	1.778	0.383	0.582	7.417	1.781	2.88	0.278
	Min			1.453	1.536	0.228	0.488	6.747	1.506	1.443	0.209
	St Dev			0.218	0.171	0.110	0.066	0.474	0.194	1.016	0.049

Prehnite - $Ca_{1.90}Al_{1.99}(Si_{3.03}O_9)(OH)_2$

Sulfur %	Reactor	%Prehnite	N	Ca	Mg	K	Na	Si	Al	Fe	Ti
1.40	37	0.9	1	1.901	0.005	0.002	0.019	3.027	1.990	0.042	0.001

Note: N = number of samples analyzed for each Sulfur %

Table 17. Perimeter/1000 micron area of mineral grains from different samples. Analysis done by McSwiggen and Associates.

	Sample 1	Sample 2	Sample 3	Sample 4	Mean P	Particle Diameter[1] (μm)
0.22 R4 unleached	99.1	112.1	106.8		106.0	37.7
0.22 R4 leach	96.7	91.5			94.1	42.5
unleached/leach					1.13	0.87
0.40 R5&6 unleached	73.4	79.9			76.7	52.2
0.40 R6 leach	96.3	93.3	89.2		92.9	43.1
unleached/leach					0.83	1.21
0.41 R7&8 unleached	115.3	115.8	101.7		110.9	36.1
0.41 R7 leached	88.1	79.8	81.1		83.0	48.2
unleached/leach					1.34	0.75
0.51 R9&10 unleached	103.0	102.6	94.2		99.9	40.0
0.51 R9 leached	120.1	113.3	100.6		111.3	35.9
unleached/leach					0.90	1.11
0.58 R15&16 unleached	122.0	78.8	111.0		103.9	38.5
0.58 R15 leached	79.2	80.9			80.1	49.9
unleached/leach					1.30	0.77
0.58 R16 unleached	84.1	78.6	93.4		85.4	46.8
0.58 R16 leached	90.1	78.1	93.0		87.1	45.9
unleached/leach					0.98	1.02
0.71 R17&18 unleached	80.8	82.0	82.5		81.8	48.9
0.71 R17 leached	81.5	86.0	89.6		85.7	46.7
unleached/leach					0.95	1.05
1.16 R29&30 unleached	72.1	73.2	70.8		72.0	55.6
1.16 R29 leached	76.3	77.0	77.7	70.8	75.5	53.0
unleached/leach					0.95	1.05
1.40 R37&38 unleached	73.9	74.1	68.1		72.0	55.6
1.40 R37 leached	80.9	77.0	77.0		78.3	51.1
unleached/leach					0.92	1.09
1.44 R33&34 unleached	80.7	78.3	83.6		80.9	49.4
1.44 R33 leached	74.7	85.1			79.9	50.1
unleached/leach					1.01	0.99
1.63 R19&20 unleached	225.4	339.6	201.7		255.6	15.6
1.63 R19 leached	79.5	86.3	92.0		85.9	46.6
unleached/leach					2.98	0.34
1.71 R44 unleached	142.1	90.9	83.0		105.3	38.0
1.71 R44 leached	96.6	79.1	85.2		87.0	46.0
unleached/leach					1.21	0.83
Average unleached					104.2	42.9
Average leached					86.7	46.6
Average unleached/leached					1.21	0.92

[1] Particle diameter, d, was determined by assuming particles are spherical and smooth.
$P/A = \pi dn/[(\pi d^2/4)n] = 4\pi dn/(\pi d^2 n) = 4/d$, and $d = 4A/P$. $A=1000\ \mu m^2$, therefore $d= 4000/P$.

Table 18. Water retention/drying time of Duluth Complex rock used in the experiment. Cells were rinsed on Tuesdays after weighing. Numbers are weights of rock and reactor cell (plus water) in grams.

Week start date	Reactor	Mon	Tue	Wed	Tue-Wed	Moisture content	Thu	Wed - Thur	Fri	Thu-Fri	Percent evap
10/28/2003	Cell 1		147.7	165.9	18.2	24.3%	159	6.9	153.4	5.6	68.7%
	Cell 3		144.9	160.7	15.8	21.1%	154.4	6.3	149.2	5.2	72.8%
	Cell 5		154.1	174.6	20.5	27.3%	168.3	6.3	163	5.3	56.6%
	Cell 39		157.5	178.6	21.1	28.1%	171.3	7.3	166	5.3	59.7%
	Cell 40		154	174.3	20.3	27.1%	167.5	6.8	162.2	5.3	59.6%
	Cell 41		155.5	172.6	17.1	22.8%	165.9	6.7	160.8	5.1	69.0%
	Cell 42		157.4	178.2	20.8	27.7%	171.9	6.3	167	4.9	53.8%
	Cell 43		157.7	177.9	20.2	26.9%	170	7.9	163.8	6.2	69.8%
11/3/2003	Cell 1	147.7	147.7	163.7	16	21.3%	156.9	6.8	150.2	6.7	84.4%
	Cell 3	144.9	144.8	160.6	15.8	21.1%	154.7	5.9	149.3	5.4	71.5%
	Cell 5	154.1	154	171.4	17.4	23.2%	165.9	5.5	159.7	6.2	67.2%
	Cell 39	157.6	157.5	171.3	13.8	18.4%	165.9	5.4	160.5	5.4	78.3%
	Cell 40	154	153.9	169.7	15.8	21.1%	164.8	4.9	159.7	5.1	63.3%
	Cell 41	155.7	155.5	167.9	12.4	16.5%	161.6	6.3	156.6	5	91.1%
	Cell 42	157.4	157.4	171.4	14	18.7%	164.9	6.5	159.1	5.8	87.9%
	Cell 43	157.7	157.7	174.6	16.9	22.5%	168.7	5.9	163.2	5.5	67.5%
11/10/2003	Cell 1	147.7	147.7	165.1	17.4	23.2%	157.8	7.3	150.7	7.1	82.8%
	Cell 3	144.9	144.9	159.3	14.4	19.2%	153.3	6	147.5	5.8	81.9%
	Cell 5	154.1	154.1	174	19.9	26.5%	167.7	6.3	161.5	6.2	62.8%
	Cell 39	157.6	157.5	173.1	15.6	20.8%	166.8	6.3	161.2	5.6	76.3%
	Cell 40	154	154	169.2	15.2	20.3%	162.9	6.3	156.6	6.3	82.9%
	Cell 41	155.5	155.5	170.6	15.1	20.1%	164.8	5.8	158.8	6	78.1%
	Cell 42	157.4	157.4	175	17.6	23.5%	169.4	5.6	163.1	6.3	67.6%
	Cell 43	157.7	157.7	174.8	17.1	22.8%	168.3	6.5	162.9	5.4	69.6%
11/18/2003	Cell 1		147.2	164.8	17.6	23.5%	158.3	6.5	152	6.3	72.7%
	Cell 3		144.9	157.7	12.8	17.1%	151.7	6	146.2	5.5	89.8%
	Cell 5		154.1	169.5	15.4	20.5%	163	6.5	156.8	6.2	82.5%
	Cell 39		157.5	170.5	13	17.3%	164.5	6	159.1	5.4	87.7%
	Cell 40		153.9	169.5	15.6	20.8%	162.6	6.9	156.6	6	82.7%
	Cell 41		155.5	168.6	13.1	17.5%	162.2	6.4	157.2	5	87.0%
	Cell 42		157.4	172.9	15.5	20.7%	166.7	6.2	160.9	5.8	77.4%
	Cell 43		157.7	173.4	15.7	20.9%	166.5	6.9	160.9	5.6	79.6%
11/24/2003	Cell 1	147.7	Cells (dry) not weighed before rinsing	163.7	16	21.3%					
	Cell 3	144.9		157.9	13	17.3%					
	Cell 5	154		172.1	18.1	24.1%					
	Cell 39	157.5		175.5	18	24.0%					
	Cell 40	153.9		173.7	19.8	26.4%					
	Cell 41	155.5		169.5	14	18.7%					
	Cell 42	157.4		173.8	16.4	21.9%					
	Cell 43	157.7		174.2	16.5	22.0%					
12/1/2003	Cell 1	147.7	147.7	162.9	15.2	20.3%	154.6	8.3	149.4	5.2	88.8%
	Cell 3	144.8	144.8	156.6	11.8	15.7%	149.2	7.4	145.3	3.9	95.8%
	Cell 5	154	154	169.4	15.4	20.5%	162	7.4	156.8	5.2	81.8%
	Cell 39	157.5	157.5	170.6	13.1	17.5%	163.1	7.5	158.9	4.2	89.3%
	Cell 40	153.9	153.9	169.4	15.5	20.7%	160.1	9.3	154.8	5.3	94.2%
	Cell 41	155.5	155.5	168.9	13.4	17.9%	161.1	7.8	156.8	4.3	90.3%
	Cell 42	157.4	157.4	173.5	16.1	21.5%	166.5	7	161.5	5	74.5%
	Cell 43	157.7	157.7	173.8	16.1	21.5%	166.5	7.3	161.3	5.2	77.6%
Average		153.60	153.57	169.73	16.16	21.5%	163.03	6.63	157.51	5.52	76.9%
Min		144.80	144.80	156.60	11.80	15.7%	149.20	4.90	145.30	3.90	53.8%
Max		157.70	157.70	178.60	21.10	28.1%	171.90	9.30	167.00	7.10	95.8%
St Dev		4.571	4.569	5.552	2.359	3.1%	5.582	0.839	5.559	0.647	10.8%

Table 19. Differences between replicates for analyzed data. Minimum pH and average drainage concentrations (mg/L) for SO_4, Ca and Mg.

%S	Reactor pair	# weeks run	min pH mean	pH % diff	SO_4 mean	SO_4 % diff	Ca mean	Ca % diff	Mg mean	Mg % diff
0.18	1,2	328	6.07	0.33	3.03	6.50	0.95	0.38	0.45	5.34
0.22	3,4	328	6.16	0.08	2.88	2.21	1.01	0.14	0.63	3.63
0.4	5,6	328	5.96	0.42	7.79	7.28	2.61	3.76	0.26	0.07
0.41	7,8	328	4.79	2.61	3.58	0.89	0.84	0.91	0.30	1.86
0.51	9,10	328	4.08	0.74	7.03	12.38	1.32	5.01	0.49	8.97
0.54	11,12	328	4.14	0.48	9.70	6.14	3.03	0.38	0.76	7.38
0.57	13,14	328	4.24	2.01	8.10	6.28	1.28	0.86	0.84	2.24
0.58	15,16	328	4.06	0.74	9.89	4.14	1.30	0.39	0.90	3.36
0.71	17,18	328	4.12	1.21	7.76	11.56	0.92	7.09	0.96	15.71
1.12	35,36	247	3.64	3.99	25.86	14.59	4.64	3.19	0.83	11.75
1.16	29,30	247	4.00	0.63	13.52	16.06	1.46	5.43	0.98	12.85
1.4	37,38	247	4.02	0.25	15.02	4.17	2.15	0.05	1.20	0.59
1.44	33,34	247	3.82	0.39	21.01	0.81	1.69	0.13	1.08	1.19
1.63	19,20	289	3.62	7.73	26.39	11.80	2.33	7.74	2.34	2.23
1.64	31,32	247	3.83	1.96	30.04	13.98	3.67	10.89	2.10	5.30
2.06	21,22	78	4.25	1.18	35.89	3.10	4.45	2.78	4.37	1.76
3.12	23,24	78	3.60	2.78	114.48	14.62	9.79	3.61	5.25	8.55
3.72	25,26	78	3.73	0.67	57.64	10.49	7.10	1.01	5.48	1.34
5.44	27,28	78	3.13	7.20	93.90	6.44	7.39	2.66	7.38	1.75

Note: All % diff columns are % difference of each reactor from the mean of the replicates

Table 20. Effect of drainage volume on pH of effluent.

%S	Reactor	Mean pH (and range) for 8 weeks before test	pH, 10 ml drainage	pH, total drainage	pH difference (10 ml-total)
0.41	8	5.20 (5.12-5.39)	5.23	5.28	-0.05
0.51	10	4.65 (4.58-4.73)	4.61	4.58	0.03
0.54	11	4.7 (4.68-4.79)	4.58	4.69	-0.11
0.54	12	4.85 (4.87-4.98)	4.88	4.95	-0.07
0.57	13	5.05 (5.05-5.21)	4.92	5.04	-0.12
0.58	16	4.22 (4.14-4.22)	4.31	4.17	0.14
0.71	17	4.90 (4.86-4.96)	4.82	4.87	-0.05
0.71	18	4.45 (4.48-4.73)	4.27	4.42	-0.15
1.12	35	4.20 (4.16-4.21)	3.96	4.16	-0.13
1.16	29	4.35 (4.33-4.40)	4.15	4.30	-0.11
1.16	30	4.50 4.47-4.54)	4.24	4.43	-0.15
1.4	37	4.75 (4.7-4.79)	4.47	4.72	-0.19
1.63	19	4.08 (4.03-4.11)	3.90	4.03	-0.17
1.63	20	4.15 (4.12-4.18)	4.05	4.16	-0.18
1.64	31	4.30 (4.26-4.33)	4.06	4.23	-0.20
1.64	32	4.33 (4.31-4.37)	4.10	4.28	-0.25
Average		4.54	4.41	4.52	-0.11

Table 21. Empirical neutralization potentials[1] mg $CaCO_3$/g rock of drainage from samples.

Sulfur %	Reactor	pH 7	Week	pH 6	Week	pH 5	Week	pH 4.5	Week	pH 4	Week	pH 3.5	Week
Group I													
0.18	1	0.56	55	>3.07	1252[2]	>3.07	1252[2]	>3.07	1252[2]	>3.07	1252[2]	>3.07	1252[2]
0.22	3	0.46	55	>3.12	1252[2]	>3.12	1252[2]	>3.12	1252[2]	>3.12	1252[2]	>3.12	1252[2]
0.72[3]	42	0.31	51	>1.48	809[2]	>1.48	809[2]	>1.48	809[2]	>1.48	809[2]	>1.48	809[2]
Group II													
0.40	5	0.71	18	7.98	669	8.53	746	9.03	780	9.85	804	>12.93	909[2]
0.41	7	0.26	55	0.77	80	2.16	278	3.10	353	>7.83	724[2]	>7.83	724[2]
0.51	9	0.61	53	1.02	67	2.77	229	3.22	279	>11.42	724[2]	>11.42	724[2]
0.54	11	0.89	31	1.84	68	4.98	221	5.85	265	>10.60	441[2]	>10.60	441[2]
0.57	13	0.93	31	2.01	80	4.43	259	4.93	282	6.81	331	>9.81	441[2]
0.58	15	0.42	4	1.45	54	2.93	146	3.58	181	>13.37	724[2]	>13.37	724[2]
0.67[3]	39	0	0	0.41	12	0.94	31	2.02	100	>6.37	809[2]	>6.37	809[2]
0.67[4]	40	0.29	11	1.00	39	4.28	307	5.07	343	>10.44	809[2]	>10.44	809[2]
0.82[4]	43	0.23	12	0.56	23	2.48	277	>4.40	809[2]	>4.40	809[2]	>4.40	809[2]
0.92[3]	41	0.14	12	0.49	39	>2.50	809[2]	>2.50	809[2]	>2.50	809[2]	>2.50	809[2]
1.71[3]	44	1.17	33	2.00	58	4.25	144[2]	>4.25	144[2]	>4.25	144[2]	>4.25	144[2]
Group III													
0.71	17	0.27	16	0.79	54	3.17	229	3.81	280	6.41	341	>15.04	724[2]
1.12	35	0	0	0	0	4.60	57	7.45	131	11.52	200	16.26	249
1.16	29	0	0	1.54	32	2.48	59	3.92	131	10.15	255	13.48	276
1.40	37	0.62	4	1.49	34	3.78	95	6.29	194	10.39	259	13.11	276
1.44	33	0.55	2	1.01	8	2.20	51	3.88	104	13.40	252	14.27	259
1.63	19	0.57	4	1.66	22	4.32	102	6.61	164	18.16	275	19.29	283
1.64	31	0	0	0	0	3.02	10	9.14	131	15.24	235	17.68	259
Virginia Formation													
2.06	21	0	0	0.51	4	1.65	12	5.38	65	7.30	78[2]	>7.30	78[2]
3.12	23	0	0	2.11	3	3.56	15	4.30	17	17.34	75	>19.34	78[2]
3.72	25	0	0	0	0	0	0	2.65	13	10.63	75	>11.71	78[2]
5.44	27	0	0	0	0	0	0	0	0	6.13	13	>17.68	78[2]

[1] Empirical neutralization potentials (ENP) were calculated using cumulative sulfate release at the point after which the pH was consistently below the given threshold value. ENP = [(cum. mg SO_4)(100 mg $CaCO_3$/96.1 mg SO_4)]/(75 g rock).

[2] Full period of record. Samples did not consistently fall below threshold value.

[3] AMAX and ARIMETCO samples originated from core drilled between 1974 and 1977 and were stored for at least 20 years prior to initiation.

[4] Dunka blast hole samples originated from a blast on August 30, 1989 at the Dunka Mine and were stored for 8 years prior to initiation.

Table 22. Neutralization Potential (NP) of rock samples.

S%	Reactor	CO_2(%)	kg $CaCO_3$/t[1] rock				
			Acid Production	NP (Sobek 1978)	NP(pH6)[2]	NP[3] [(Ca/Mg)CO_3]	ENP(pH 6)
Group I, Duluth Complex							
0.18	1	<0.03	6	17		<0.7	>3.07
0.22	3	<0.03	7	16		<0.7	>3.12
0.72[4]	42	0.06	22	17	3.4	1.4	>1.48
Group II, Duluth Complex							
0.40	5	0.64	12	14		14.5	7.98
0.41	7	0.06	13	13		1.4	0.77
0.51	9	0.07	16	16		1.6	1.02
0.54	11	0.11	17	12		2.5	1.84
0.57	13	0.01	18	19		2.3	2.01
0.58	15	0.07	18	14		1.6	1.45
0.67[4]	39	<0.03	21	14	3.2	<0.7	0.41
0.67[5]	40	<0.03	21		2	<0.7	1.00
0.82[5]	43	<0.03	26		2.2	<0.7	0.56
0.92[4]	41	<0.03	29	4	2.1	<0.7	0.49
1.71[4]	44	0.06	53	21	5.4	1.4	2.00
Group III, Duluth Complex							
0.71	17	0.05	22	21		1.1	0.79
1.12	35	<0.03	35	15		<0.7	1.54
1.16	29	0.08	36	16		1.8	1.49
1.4	37	0.1	44	18		2.3	1.01
1.44	33	<0.03	45	16		<0.7	1.66
1.63	19	0.11	51	12		2.5	0
1.64	31	0.14	51	12		3.2	1.54
Virginia Formation							
2.06	21	0.12	64	14		2.7	0.51
3.12	23	<0.03	97	8		<0.7	2.11
3.72	25	0.06	116	5		1.4	0
5.44	27	0.32	170	0.5		7.3	0

[1] Metric ton = 1000 kg

[2] Autotitrator test slightly modified from (Lapakko 1994a). NP after 4 hours of less than or equal to 0.1 ml addition.

[3] Calculated from CO_2 content. NP [(Ca/Mg)CO_3] = 22.7 x percent CO_2

[4] AMAX and ARIMETCO samples originated from core drilled between 1974 and 1977 and were stored for at least 20 years prior to initiation.

[5] Dunka blast hole samples originated from a blast on August 30, 1989 at the Dunka Mine and were stored for 8 years prior to initiation.

Table 23. Mineralogical breakdown of cations present in samples (%). Blank entries indicate no mineral present in sample.

%S	**Reactor**	**Calcium**				**Magnesium**					**Sodium**		**Potassium**			
		Plag	Augite	Prehnite	Amphibole	Augite	Hyper	Olivine	Biotite	Amphibole	Plag	K-Spar	Plag	Biotite	K-Spar	Amphibole
Group I, Duluth Complex																
0.18	1	67.06	22.92	10.02		19.63	47.15	20.51	12.71		100		32.22	67.78		
0.22	3	74.53	17.02	4.53	3.92	22.07	21.14	14.66	33.80	8.33	97.97	2.03	21.47	49.50	28.07	0.96
0.72[1]	42	79.07	4.08	16.85		6.37	13.08	80.55			100		100			
Group II, Duluth Complex																
0.4	5	74.07	11.82	9.69	4.42	4.26	73.99		13.18	8.57	97.69	2.31	18.79	43.33	37.37	0.52
0.41	7	78.00	17.72		4.28	16.26	24.42	30.48	21.67	7.17	99.65	0.35	16.29	70.85	11.86	1.00
0.51	9	71.66	18.65		9.68	13.39	43.28	11.91	19.98	11.44	95.25	4.75	9.86	47.81	42.15	0.18
0.54	11	79.36	14.17	3.46	3.01	15.57	54.17		19.87	10.39	100		17.83	82.15		0.02
0.57	13	60.23	39.77			31.01	14.46	54.54			97.60	2.40	21.08		78.92	
0.58	15	67.73	32.27			35.51	50.59	7.67	6.24		96.26	3.74	15.66	22.85	61.49	
0.67[1]	39	73.43	26.57			29.79	15.48	54.73			98.72	1.28	47.98		52.02	
0.67[2]	40	71.80	28.20			17.93	31.42	8.14	42.52		99.43	0.57	5.62	88.24	6.13	
0.82[2]	43	70.30	29.70			23.21	45.71	7.02	24.05		100		12.89	87.11		
0.92[1]	41	77.04	10.25		12.71	5.47	6.82	69.91		17.80	100		98.18			1.82
1.71[1]	44	88.11	6.69	5.20		6.19	9.84	75.38	8.59		97.77	2.23	41.31	46.78	11.92	
Group III, Duluth Complex																
0.71	17	81.75	18.25			15.33	34.36	35.72	14.58		99.21	0.79	26.10	59.52	14.39	
1.12	35	70.66	17.15	5.69	6.50	10.63	53.68	11.68	16.66	7.36	86.82	13.18	5.75	25.31	68.93	
1.16	29	79.52	20.48			20.02	35.86	44.12			100		100			
1.4	37	59.29	23.97	12.12	4.61	34.71	34.50	22.47		8.32	97.56	2.44	29.12		66.26	4.62
1.44	33	93.03	6.97			4.86	65.25	14.13	15.76		97.26	2.74	16.37	40.31	43.32	
1.63	19	70.29	22.45		7.26	11.37	52.01	12.57	18.57	5.49	96.28	3.72	8.56	36.74	53.19	1.50
1.64	31	63.96	31.51	4.53		29.82	34.56	8.93	26.68		97.37	2.63	9.46	50.71	39.83	
Virginia Formation																
2.06	21	81.67	18.33			10.09	70.85	4.90	14.16		85.18	14.82	4.95	11.50	83.55	
3.12	23	97.12	2.88			0.99	62.02		36.99		89.76	10.24	8.57	40.80	50.63	
3.72	25	77.72	22.28			8.18	42.05		49.77		83.45	16.55	2.10	27.09	70.81	
5.44	27	100							100		73.75	26.25	1.87	8.32	89.81	
Min (Duluth Complex)		59.29	4.08	0.00	0.00	4.26	6.82	0.00	0.00	0.00	86.82	0.00	5.62	0.00	0.00	0.00
Max (Duluth Complex)		93.03	39.77	16.85	12.71	35.51	73.99	80.55	42.52	17.80	100.00	13.18	100.00	88.24	78.92	4.62
Avg (Duluth Complex)		73.85	20.03	3.43	2.69	17.78	36.27	27.86	14.04	4.04	97.85	2.15	31.17	39.00	29.33	0.51
Avg (Virginia Formation)		89.13	10.87	0.00	0.00	4.81	43.73	1.22	50.23	0.00	83.04	16.96	4.37	21.93	73.70	0.00
Average for all samples		76.30	18.56	2.88	2.26	15.71	37.47	23.60	19.83	3.39	95.48	4.52	26.88	36.27	36.43	0.42

[1] AMAX and ARIMETCO samples originated from core drilled between 1974 and 1977 and were stored for at least 20 years prior to initiation.

[2] Dunka blast hole samples originated from a blast on August 30, 1989 at the Dunka Mine and were stored for 8 years prior to initiation.

Table 24. Sample time periods beginning and duration for each sample. See section 5.3.1.1 for definition of periods.

		Weeks comprising each period				Length of Period			
		A	B	C	D	A	B	C	D
%S	**Reactor**								
Group I									
0.18	1	1-137	138-1252			137	1115		
0.22	3	1-134	135-1252			134	1118		
0.72[1]	42	1-34	35-809			34	775		
Group II									
0.40	5	1-140	141-769	770-867	868-909	140	629	98	42
0.41	7	1-129	130-351	352-439	440-724	129	222	88	285
0.51	9	1-140	141-277	278-383	384-724	140	137	106	341
0.54	11	1-137	138-278	279-441		137	141	163	
0.57	13	1-103	104-294	295-351	352-441	103	191	57	90
0.58	15	1-101	102-217	218-335	336-724	101	116	118	389
0.67[1]	39	1-39	40-111	112-195	196-809	39	72	84	614
0.67[2]	40	1-58	59-345	346-431	432-809	58	287	86	378
0.82[2]	43	1-54	55-809			54	755		
0.92[1]	41	1-54	55-809			54	755		
1.71[1]	44	1-78	79-144			78	66		
Group III									
0.71	17	1-100	101-274	275-426	427-724	100	174	152	298
1.12	35	1-127	128-214	215-348	349-360	127	87	134	12
1.16	29	1-38	39-189	190-382	383-643	38	151	193	261
1.40	37	1-74	75-209	210-360		74	135	151	
1.44	33	1-76	77-212	213-444	445-643	76	136	232	199
1.63	19	1-66	67-155	156-410	411-724	66	89	255	314
1.64	31	1-64	65-228	229-340	341-360	64	164	112	20

[1] AMAX and ARIMETCO samples originated from core drilled between 1974 and 1977 and were stored for at least 20 years prior to initiation.

[2] Dunka blast hole samples originated from a blast on August 30, 1989 at the Dunka Mine and were stored for 8 years prior to initiation.

Table 25. Minimum drainage pH, sulfate and major cation cumulative mass release (mmol) over the entire period of record.

%S	**Reactor**	**Period of Record (weeks)**	**Minimum pH**	**SO_4**	**Ca**	**Mg**	**Na**	**K**
Group I, 3 samples								
0.18	**1**	1252	5.67	2.30	3.37	2.02	1.60	5.69
0.22	**3**	1252	5.91	2.34	3.94	3.28	1.22	3.45
0.72[1]	**42**	809	5.60	1.11	1.26	0.80	0.65	1.70
Average			5.73	1.92	2.86	2.03	1.16	3.61
Group II, 11 samples								
0.4	**5**	909	3.78	9.70	8.74	0.93	0.48	2.99
0.41	**7**	724	4.05	5.87	2.71	1.48	0.93	2.00
0.51	**9**	724	3.95	8.56	3.80	1.71	1.13	1.38
0.54	**11**	441	4.08	7.95	5.12	1.56	0.48	0.84
0.57	**13**	441	3.86	7.36	2.88	2.60	0.72	1.35
0.58	**15**	724	3.98	10.0	3.13	2.45	1.06	2.69
0.67[1]	**39**	809	4.22	4.78	1.27	1.12	0.69	2.45
0.67[2]	**40**	809	4.04	7.83	3.80	1.52	0.96	1.93
0.82[2]	**43**	809	4.49	3.30	1.68	0.55	0.42	1.08
0.92[1]	**41**	809	4.89	1.88	1.16	0.45	0.67	1.37
1.71[1]	**44**	144	5.06	3.19	1.60	1.45	0.18	1.54
Average			4.22	6.40	3.26	1.44	0.70	1.78
Group III, Duluth Complex, 7 samples								
0.71	**17**	724	3.53	11.3	3.02	4.06	1.16	2.73
1.12	**35**	360	3.23	20.6	6.06	2.55	0.86	1.61
1.16	**29**	643	3.24	19.4	3.47	4.75	1.58	2.76
1.40	**37**	360	3.06	22.7	3.59	5.85	1.30	4.62
1.44	**33**	643	3.04	28.3	3.62	6.00	1.95	5.16
1.63	**19**	724	3.32	28.9	4.75	6.94	1.35	3.02
1.64	**31**	360	3.38	20.6	4.43	4.69	0.93	0.96
Average			3.26	21.7	4.13	4.98	1.30	2.98
Virginia Formation, 4 samples								
2.06	21	78	4.20	5.47	1.63	2.42	N/A	N/A
3.12	23	78	3.70	14.5	3.69	3.68	N/A	N/A
3.72	25	78	3.70	8.78	2.85	3.23	N/A	N/A
5.44	27	78	3.35	13.3	3.10	4.74	N/A	N/A
Average			3.74	10.5	2.82	3.52	N/A	N/A

[1] AMAX and ARIMETCO samples originated from core drilled between 1974 and 1977 and were stored for at least 20 years prior to initiation.

[2] Dunka blast hole samples originated from a blast on August 30, 1989 at the Dunka Mine and were stored for 8 years prior to initiation.

Table 26. Ca/Na drainage quality vs plagioclase stoichiometry

Reactor	%S	Ca:Na (obs)[1]	Ca:Na (stoic)[2]	Obs/stoic
1	0.18	2.06	1.01	2.05
3	0.22	3.05	0.86	3.55
5	0.4	23.11	1.27	18.16
7	0.41	2.89	1.22	2.37
9	0.51	3.47	1.11	3.12
11	0.54	10.76	1.97	5.45
13	0.57	4.07	1.02	3.97
15	0.58	3.05	1.09	2.81
39	0.67	1.87	1.12	1.66
40	0.67	4.03	1.07	3.75
17	0.71	2.53	1.12	2.26
42	0.72	1.98	1.53	1.29
43	0.82	3.60	1.20	3.00
41	0.92	1.86	1.47	1.26
35	1.12	7.36	1.06	6.94
29	1.16	2.15	1.22	1.77
37	1.4	2.74	1.13	2.43
33	1.44	1.90	1.05	1.81
19	1.63	3.28	0.72	4.55
44	1.71	8.82	1.48	5.95
Average		4.73	1.19	3.91
Min		1.86	0.72	1.26
Max		23.11	1.97	18.16

[1] Cumulative mass release ratio for Ca to Na for entire period of record

[2] Stoichiometric ratio of Ca to Na in plagioclase for each sample

Table 27. Sample pH by groups and time periods for all Duluth Complex samples (%S≤1.71).

%S	Reactor	Period A				Period B				Period C				Period D			
		Ave	Max	Min	n	Ave	Max	Min	n	Ave	Max	Min	n	Ave	Max	Min	n
Group I																	
0.18	**1**	6.90	7.90	6.20	134	6.42	7.18	5.67	565								
0.22	**3**	6.91	7.75	6.40	132	6.51	7.05	5.91	560								
0.72[1]	**42**	7.30	8.09	6.95	34	6.37	7.34	5.60	243								
Average		7.04	7.91	6.52	100	6.43	7.19	5.73	456								
Group II																	
0.40	**5**	6.60	7.40	6.16	139	6.13	6.69	4.58	453	4.21	4.53	3.78	45	4.67	4.98	4.50	21
0.41	**7**	6.51	8.35	5.34	128	5.13	6.13	4.47	222	4.22	4.56	4.05	87	4.75	5.82	4.26	127
0.51	**9**	6.30	8.70	5.08	139	5.07	5.45	4.61	137	4.18	4.51	3.95	105	4.64	6.04	4.07	182
0.54	**11**	6.13	8.05	5.13	136	4.98	5.55	4.24	141	4.39	4.77	4.08	162				
0.57	**13**	6.44	7.75	5.50	101	5.21	5.72	4.32	190	4.29	4.50	3.86	57	4.40	4.81	4.21	89
0.58	**15**	5.89	7.55	5.20	100	4.82	5.49	4.20	116	4.22	4.38	3.98	118	4.61	5.73	4.11	229
0.67[1]	**39**	5.59	6.81	4.82	39	4.67	4.81	4.32	56	4.36	4.60	4.22	27	5.34	6.17	4.37	148
0.67[2]	**40**	6.27	7.19	5.52	58	5.62	6.20	4.46	98	4.22	4.40	4.04	22	5.41	6.35	4.46	100
0.82[2]	**43**	6.09	7.52	5.31	54	5.28	6.12	4.49	217								
0.92[1]	**41**	6.43	8.13	5.62	53	5.55	6.25	4.89	219								
1.71[1]	**44**	6.62	7.60	5.66	76	5.42	6.12	5.06	32								
Average		6.26	7.73	5.39	93	5.26	5.87	4.51	171	4.26	4.53	4.00	78	4.83	5.70	4.28	128
Group III																	
0.71	**17**	6.15	7.65	5.11	100	5.08	5.45	4.41	173	4.22	4.95	3.53	151	4.90	5.43	4.52	140
1.12	**35**	4.87	5.85	4.48	125	4.13	4.52	3.81	87	3.61	4.17	3.23	133	4.09	4.18	3.98	12
1.16	**29**	6.38	6.95	5.69	37	4.62	5.70	4.14	150	3.93	4.78	3.24	192	4.95	5.64	4.50	106
1.40	**37**	5.92	7.30	4.78	73	4.81	5.18	4.01	134	3.66	4.49	3.06	150				
1.44	**33**	5.23	7.20	4.59	74	4.42	4.83	4.19	135	3.89	4.90	3.04	229	4.75	5.09	4.52	46
1.63	**19**	5.73	7.50	4.95	66	4.90	5.35	4.37	88	3.89	4.72	3.32	254	4.77	5.71	4.35	156
1.64	**31**	4.80	5.45	4.51	63	4.39	4.80	4.02	163	3.72	4.19	3.38	111	4.03	4.14	3.85	20
Average		5.58	6.84	4.87	77	4.62	5.12	4.14	133	3.84	4.60	3.26	174	4.58	5.03	4.29	80

[1] AMAX and ARIMETCO samples originated from core drilled between 1974 and 1977 and were stored for at least 20 years prior to initiation.

[2] Dunka blast hole samples originated from a blast on August 30, 1989 at the Dunka Mine and were stored for 8 years prior to initiation.

Table 28. Sample weekly sulfate release (mol/second) by groups and time periods for all Duluth Complex samples (%S≤1.71).

%S	Reactor	Period A				Period B				Period C				Period D			
		Ave	Max	Min	n	Ave	Max	Min	n	Ave	Max	Min	n	Ave	Max	Min	n
Group I																	
0.18	**1**	1.2E-11	3.0E-11	2.9E-12	59	2.3E-12	1.0E-11	1.9E-13	185								
0.22	**3**	1.0E-11	2.9E-11	3.0E-12	57	2.6E-12	9.3E-12	1.9E-13	187								
0.72[1]	**42**	8.8E-12	1.3E-11	3.9E-12	12	2.2E-12	7.9E-12	1.9E-13	120								
Average		1.0E-11	2.4E-11	3.3E-12	43	2.4E-12	9.2E-12	1.9E-13	164								
Group II																	
0.40	**5**	3.3E-11	7.4E-11	1.3E-11	61	9.9E-12	3.1E-11	3.0E-12	132	5.0E-11	1.1E-10	1.8E-11	21	1.2E-11	1.9E-11	7.9E-12	10
0.41	**7**	1.2E-11	3.8E-11	1.6E-12	58	9.5E-12	2.2E-11	3.0E-12	52	3.7E-11	5.0E-11	2.5E-11	21	1.1E-11	4.3E-11	2.3E-12	54
0.51	**9**	1.8E-11	4.7E-11	3.1E-12	61	8.3E-12	1.5E-11	3.0E-12	34	5.1E-11	7.7E-11	3.8E-11	25	1.6E-11	4.5E-11	3.4E-12	67
0.54	**11**	3.3E-11	7.0E-11	1.2E-11	60	2.3E-11	5.6E-11	6.0E-12	36	3.1E-11	5.9E-11	1.5E-11	38				
0.57	**13**	2.8E-11	4.2E-11	1.4E-11	50	1.8E-11	5.3E-11	3.0E-12	48	4.6E-11	7.4E-11	3.3E-11	13	3.1E-11	3.8E-11	2.3E-11	22
0.58	**15**	2.5E-11	1.0E-10	3.0E-12	49	2.6E-11	6.0E-11	1.3E-11	31	4.5E-11	7.1E-11	3.2E-11	27	1.5E-11	3.8E-11	3.4E-12	78
0.67[1]	**39**	3.2E-11	4.1E-11	1.4E-11	13	2.0E-11	2.6E-11	1.4E-11	16	2.6E-11	3.2E-11	2.0E-11	20	5.5E-12	2.2E-11	1.9E-13	79
0.67[2]	**40**	2.9E-11	6.0E-11	1.3E-11	18	1.5E-11	4.2E-11	9.3E-12	57	4.7E-11	6.3E-11	2.5E-11	10	6.2E-12	2.3E-11	1.8E-13	45
0.82[2]	**43**	2.2E-11	4.6E-11	1.0E-11	17	6.0E-12	1.8E-11	1.9E-13	113								
0.92[1]	**41**	1.3E-11	2.3E-11	7.4E-12	17	3.7E-12	1.2E-11	1.9E-13	112								
1.71[1]	**44**	3.8E-11	5.8E-11	2.8E-11	23	3.0E-11	4.0E-11	1.9E-11	17								
Average		2.6E-11	5.4E-11	1.1E-11	39	1.5E-11	3.4E-11	6.8E-12	59	4.2E-11	6.7E-11	2.6E-11	22	1.4E-11	3.3E-11	5.7E-12	51
Group III																	
0.71	**17**	2.0E-11	3.8E-11	3.1E-12	48	1.4E-11	2.9E-11	3.0E-12	45	7.4E-11	2.5E-10	1.4E-11	35	1.2E-11	3.3E-11	4.2E-12	58
1.12	**35**	7.3E-11	2.4E-10	2.6E-11	39	7.2E-11	9.0E-11	3.1E-11	20	1.4E-10	2.5E-10	3.9E-11	33	4.9E-11	5.2E-11	4.4E-11	3
1.16	**29**	4.2E-11	1.1E-10	2.0E-11	19	3.1E-11	5.8E-11	1.4E-11	37	1.2E-10	3.0E-10	1.8E-11	46	1.1E-11	2.8E-11	4.7E-12	47
1.40	**37**	4.5E-11	8.2E-11	2.7E-11	27	3.6E-11	8.9E-11	1.7E-11	32	1.9E-10	3.6E-10	6.2E-11	37				
1.44	**33**	4.9E-11	1.4E-10	2.3E-11	27	6.1E-11	1.3E-10	3.1E-11	32	1.4E-10	3.4E-10	1.8E-11	57	1.5E-11	2.6E-11	8.9E-12	32
1.63	**19**	5.4E-11	1.4E-10	1.8E-11	33	3.8E-11	5.8E-11	2.2E-11	29	1.4E-10	3.3E-10	3.5E-11	57	1.7E-11	4.7E-11	3.9E-12	61
1.64	**31**	1.2E-10	3.6E-10	6.0E-11	24	6.1E-11	9.0E-11	3.6E-11	38	1.3E-10	2.6E-10	5.2E-11	28	5.9E-11	6.7E-11	5.2E-11	5
Average		5.8E-11	1.6E-10	2.5E-11	31	4.5E-11	7.7E-11	2.2E-11	33	1.3E-10	3.0E-10	3.4E-11	42	2.7E-11	4.2E-11	2.0E-11	34

Note: The end of Period 1 for the 0.72%S sample was defined early relative to other samples. This means that Period 2 sulfate releases may be higher than expected.

[1] AMAX and ARIMETCO samples originated from core drilled between 1974 and 1977 and were stored for at least 20 years prior to initiation.

[2] Dunka blast hole samples originated from a blast on August 30, 1989 at the Dunka Mine and were stored for 8 years prior to initiation.

Table 29. Sample weekly calcium release (mol/second) by groups and time periods for all Duluth Complex samples (%S≤1.71).

%S	Reactor	Period A				Period B				Period C				Period D			
		Ave	Max	Min	n	Ave	Max	Min	n	Ave	Max	Min	n	Ave	Max	Min	n
Group I																	
0.18	**1**	1.6E-11	2.6E-11	1.0E-11	8	3.1E-12	1.2E-11	3.5E-13	189								
0.22	**3**	1.8E-11	3.1E-11	8.7E-12	7	3.5E-12	1.0E-11	3.6E-13	191								
0.72[1]	**42**	1.1E-11	4.2E-11	7.3E-12	12	2.4E-12	8.7E-12	3.5E-13	115								
Average		1.5E-11	3.3E-11	8.7E-12	9	3.0E-12	1.0E-11	3.6E-13	165								
Group II																	
0.40	**5**	3.7E-11	6.1E-11	2.7E-11	8	1.2E-11	2.8E-11	5.5E-12	133	1.2E-11	2.4E-11	4.8E-12	21	4.6E-12	6.8E-12	2.8E-12	9
0.41	**7**	1.7E-11	3.3E-11	3.6E-12	10	3.1E-12	1.2E-11	7.8E-13	52	5.7E-12	1.0E-11	3.5E-12	22	3.4E-12	7.2E-12	1.9E-12	54
0.51	**9**	1.9E-11	5.6E-11	2.2E-12	11	3.1E-12	5.2E-12	1.4E-12	33	8.8E-12	1.5E-11	5.8E-12	29	4.7E-12	1.6E-11	2.3E-12	66
0.54	**11**	3.4E-11	1.0E-10	1.1E-11	32	1.3E-11	2.2E-11	2.2E-12	37	9.0E-12	1.5E-11	5.2E-12	40				
0.57	**13**	2.5E-11	5.6E-11	8.5E-12	7	5.2E-12	1.2E-11	7.3E-13	45	8.6E-12	1.4E-11	5.7E-12	14	6.5E-12	8.6E-12	4.2E-12	21
0.58	**15**	2.0E-11	5.0E-11	5.2E-12	7	5.4E-12	1.0E-11	7.3E-13	24	6.8E-12	1.3E-11	3.6E-12	30	4.6E-12	1.1E-11	2.5E-12	80
0.67[1]	**39**	1.4E-11	3.1E-11	3.0E-12	13	2.8E-12	3.7E-12	1.5E-12	16	3.5E-12	4.3E-12	2.9E-12	21	2.0E-12	4.3E-12	3.4E-13	80
0.67[2]	**40**	1.8E-11	3.2E-11	3.6E-12	18	1.0E-11	1.4E-11	7.2E-12	56	9.3E-12	1.2E-11	7.9E-12	10	3.5E-12	7.9E-12	7.9E-13	44
0.82[2]	**43**	1.6E-11	3.1E-11	5.1E-12	17	3.0E-12	9.8E-12	3.3E-13	114								
0.92[1]	**41**	1.2E-11	2.2E-11	4.4E-12	17	1.9E-12	5.9E-12	9.0E-14	114								
1.71[1]	**44**	2.7E-11	5.0E-11	1.2E-11	23	6.2E-12	1.0E-11	3.6E-12	17								
Average		2.2E-11	4.8E-11	7.8E-12	15	5.9E-12	1.2E-11	2.2E-12	58	8.0E-12	1.3E-11	4.9E-12	23	4.2E-12	8.7E-12	2.1E-12	51
Group III																	
0.71	**17**	1.9E-11	2.7E-11	8.7E-12	6	3.1E-12	1.2E-11	7.3E-13	39	8.1E-12	2.8E-11	3.6E-13	38	4.3E-12	7.4E-12	2.2E-12	58
1.12	**35**	4.3E-11	8.2E-11	3.6E-12	27	1.3E-11	1.8E-11	8.0E-12	23	1.9E-11	3.2E-11	7.1E-12	33	8.7E-12	9.5E-12	7.8E-12	3
1.16	**29**	2.2E-11	3.4E-11	1.2E-11	10	5.7E-12	2.2E-11	2.3E-12	37	1.3E-11	2.8E-11	5.6E-12	48	4.6E-12	8.0E-12	2.9E-12	47
1.40	**37**	2.8E-11	5.6E-11	1.2E-11	18	8.3E-12	1.9E-11	4.4E-12	35	1.6E-11	2.7E-11	6.6E-12	38				
1.44	**33**	2.4E-11	6.1E-11	5.1E-12	16	5.0E-12	1.2E-11	2.2E-12	34	1.3E-11	2.7E-11	4.2E-12	57	3.8E-12	6.3E-12	2.5E-12	32
1.63	**19**	2.2E-11	5.0E-11	8.7E-12	22	7.6E-12	2.3E-11	3.6E-12	8	1.3E-11	2.7E-11	5.3E-12	64	4.9E-12	1.1E-11	2.5E-12	62
1.64	**31**	5.8E-11	1.6E-10	1.2E-11	12	9.9E-12	1.6E-11	6.4E-12	40	1.6E-11	2.4E-11	1.1E-11	28	1.1E-11	1.4E-11	9.9E-12	5
Average		3.1E-11	6.7E-11	8.8E-12	16	7.4E-12	1.7E-11	4.0E-12	31	1.4E-11	2.8E-11	5.7E-12	44	6.2E-12	9.4E-12	4.6E-12	35

Note: The end of Period 1 for the 0.72%S sample was defined early relative to other samples. This means that Period 2 Ca releases may be higher than expected.

[1] AMAX and ARIMETCO samples originated from core drilled between 1974 and 1977 and were stored for at least 20 years prior to initiation.

[2] Dunka blast hole samples originated from a blast on August 30, 1989 at the Dunka Mine and were stored for 8 years prior to initiation.

Table 30. Sample weekly magnesium release (mol/second) by groups and time periods for all Duluth Complex samples (%S≤1.71).

%S	Reactor	Period A				Period B				Period C				Period D			
		Ave	Max	Min	n	Ave	Max	Min	n	Ave	Max	Min	n	Ave	Max	Min	n
Group I																	
0.18	**1**	8.2E-12	1.2E-11	1.2E-12	9	2.3E-12	8.9E-12	5.5E-13	187								
0.22	**3**	1.6E-11	5.5E-11	3.5E-12	8	3.5E-12	1.4E-11	5.6E-13	191								
0.72[1]	**42**	3.5E-12	7.7E-12	6.0E-13	12	1.6E-12	6.1E-12	5.8E-13	118								
Average		9.1E-12	2.5E-11	1.8E-12	10	2.5E-12	9.8E-12	5.6E-13	165								
Group II																	
0.40	**5**	5.0E-12	9.8E-12	1.2E-12	7	1.3E-12	9.5E-12	5.7E-13	129	1.1E-12	2.7E-12	5.8E-13	21	5.9E-13	6.0E-13	5.8E-13	9
0.41	**7**	5.4E-12	9.5E-12	1.2E-12	8	2.9E-12	9.8E-12	5.9E-13	51	7.2E-12	1.8E-11	5.9E-13	22	1.3E-12	5.9E-12	5.5E-13	54
0.51	**9**	6.1E-12	1.2E-11	1.2E-12	10	3.5E-12	1.0E-11	1.2E-12	33	7.1E-12	1.7E-11	6.1E-13	29	1.5E-12	7.1E-12	5.6E-13	66
0.54	**11**	1.5E-11	7.3E-11	1.2E-12	30	4.5E-12	1.1E-11	1.2E-12	36	1.7E-12	7.5E-12	5.9E-13	41				
0.57	**13**	1.4E-11	2.1E-11	7.0E-12	8	7.8E-12	1.9E-11	1.2E-12	45	1.4E-11	3.5E-11	4.7E-12	14	4.6E-12	9.4E-12	5.9E-13	22
0.58	**15**	1.6E-11	3.1E-11	3.7E-12	8	8.5E-12	1.4E-11	1.2E-12	24	8.5E-12	1.3E-11	3.5E-12	29	1.3E-12	5.9E-12	5.6E-13	79
0.67[1]	**39**	1.1E-11	1.7E-11	4.8E-12	13	4.9E-12	9.6E-12	1.2E-12	16	6.2E-12	8.1E-12	3.3E-12	21	9.3E-13	3.6E-12	1.5E-13	79
0.67[2]	**40**	1.0E-11	1.7E-11	3.6E-12	18	3.0E-12	5.6E-12	6.0E-13	57	7.0E-12	9.3E-12	2.8E-12	10	9.4E-13	3.9E-12	4.1E-13	44
0.82[2]	**43**	6.4E-12	9.6E-12	2.4E-12	17	7.1E-13	2.5E-12	1.5E-13	114								
0.92[1]	**41**	4.3E-12	8.5E-12	6.1E-13	18	6.5E-13	2.4E-12	1.5E-13	112								
1.71[1]	**44**	1.4E-11	2.8E-11	2.4E-12	23	1.7E-11	2.1E-11	1.2E-11	17								
Average		9.8E-12	2.1E-11	2.7E-12	15	5.0E-12	1.0E-11	1.8E-12	58	6.6E-12	1.4E-11	2.1E-12	23	1.6E-12	5.2E-12	4.8E-13	50
Group III																	
0.71	**17**	1.6E-11	2.8E-11	9.6E-12	7	6.9E-12	2.2E-11	1.2E-12	39	2.1E-11	6.5E-11	5.9E-12	38	2.2E-12	9.4E-12	5.9E-13	58
1.12	**35**	7.5E-12	1.9E-11	1.2E-12	25	9.6E-12	1.4E-11	4.7E-12	24	1.4E-11	2.5E-11	7.0E-12	33	8.3E-12	9.5E-12	7.0E-12	3
1.16	**29**	1.2E-11	2.3E-11	1.2E-12	9	1.0E-11	2.5E-11	6.1E-12	36	2.7E-11	5.5E-11	5.8E-12	48	2.4E-12	1.1E-11	5.8E-13	47
1.40	**37**	1.0E-11	2.2E-11	1.2E-12	16	1.5E-11	1.9E-11	6.1E-12	33	4.4E-11	8.2E-11	7.2E-12	38				
1.44	**33**	1.3E-11	2.1E-11	7.3E-12	12	1.1E-11	1.7E-11	6.0E-12	35	2.9E-11	6.5E-11	3.5E-12	57	3.2E-12	7.0E-12	5.8E-13	32
1.63	**19**	3.3E-11	8.1E-11	1.4E-11	26	1.9E-11	2.2E-11	1.4E-11	7	2.4E-11	4.1E-11	8.3E-12	65	4.3E-12	1.4E-11	5.3E-13	62
1.64	**31**	3.9E-11	8.9E-11	7.1E-12	12	1.5E-11	2.4E-11	7.2E-12	41	2.4E-11	3.9E-11	1.3E-11	28	1.1E-11	1.4E-11	8.1E-12	5
Average		1.8E-11	4.0E-11	6.0E-12	15	1.2E-11	2.0E-11	6.5E-12	31	2.6E-11	5.3E-11	7.2E-12	44	5.2E-12	1.1E-11	2.9E-12	35

Note: The end of Period 1 for the 0.72%S sample was defined early relative to other samples. This means that Period 2 Mg releases may be higher than expected.

[1] AMAX and ARIMETCO samples originated from core drilled between 1974 and 1977 and were stored for at least 20 years prior to initiation.

[2] Dunka blast hole samples originated from a blast on August 30, 1989 at the Dunka Mine and were stored for 8 years prior to initiation.

Table 31. Sample weekly calcium+magnesium release (mol/second) by groups and time periods for all Duluth Complex samples (%S≤1.71).

%S	Reactor	Period A				Period B				Period C				Period D			
		Ave	Max	Min	n	Ave	Max	Min	n	Ave	Max	Min	n	Ave	Max	Min	n
Group I																	
0.18	**1**	2.4E-11	3.8E-11	1.4E-11	8	5.3E-12	1.7E-11	6.4E-13	187								
0.22	**3**	3.4E-11	8.0E-11	1.5E-11	7	7.0E-12	2.2E-11	9.7E-13	190								
0.72[1]	**42**	1.5E-11	4.7E-11	7.9E-12	12	3.9E-12	1.3E-11	4.1E-13	115								
Average		2.4E-11	5.5E-11	1.2E-11	9	5.4E-12	1.7E-11	6.7E-13	164								
Group II																	
0.40	**5**	4.3E-11	6.3E-11	3.1E-11	6	1.3E-11	3.0E-11	6.1E-12	128	1.3E-11	2.6E-11	5.4E-12	21	5.2E-12	7.4E-12	3.4E-12	9
0.41	**7**	2.5E-11	4.2E-11	7.2E-12	7	6.2E-12	1.9E-11	2.7E-12	48	1.3E-11	2.4E-11	6.3E-12	22	4.7E-12	1.1E-11	2.5E-12	54
0.51	**9**	2.6E-11	6.6E-11	3.4E-12	9	6.6E-12	1.2E-11	3.5E-12	32	1.6E-11	3.2E-11	8.7E-12	29	6.2E-12	2.3E-11	2.9E-12	66
0.54	**11**	5.0E-11	1.4E-10	2.0E-11	28	1.7E-11	2.9E-11	5.7E-12	36	1.1E-11	2.1E-11	5.8E-12	40				
0.57	**13**	3.8E-11	7.8E-11	1.8E-11	7	1.3E-11	2.7E-11	1.9E-12	45	2.3E-11	4.9E-11	1.0E-11	14	1.1E-11	1.7E-11	5.5E-12	21
0.58	**15**	3.5E-11	8.1E-11	8.8E-12	7	1.4E-11	2.4E-11	1.9E-12	24	1.5E-11	2.6E-11	1.0E-11	29	5.8E-12	1.4E-11	3.1E-12	79
0.67[1]	**39**	2.5E-11	4.8E-11	9.6E-12	12	7.7E-12	1.2E-11	4.2E-12	16	9.8E-12	1.2E-11	6.8E-12	21	2.9E-12	7.2E-12	1.5E-13	79
0.67[2]	**40**	2.8E-11	4.9E-11	7.3E-12	18	1.3E-11	1.9E-11	8.7E-12	56	1.6E-11	2.0E-11	1.1E-11	10	4.4E-12	1.0E-11	4.9E-13	44
0.82[2]	**43**	2.2E-11	4.0E-11	1.2E-11	17	3.7E-12	1.1E-11	1.3E-13	114								
0.92[1]	**41**	1.6E-11	2.7E-11	9.6E-12	17	2.5E-12	6.9E-12	6.0E-14	112								
1.71[1]	**44**	4.1E-11	7.2E-11	2.7E-11	23	2.4E-11	3.1E-11	1.5E-11	17								
Average		3.2E-11	6.4E-11	1.4E-11	14	1.1E-11	2.0E-11	4.6E-12	57	1.5E-11	2.6E-11	8.0E-12	23	5.8E-12	1.3E-11	2.6E-12	50
Group III																	
0.71	**17**	3.2E-11	4.3E-11	1.8E-11	6	1.0E-11	3.4E-11	1.9E-12	39	2.9E-11	8.9E-11	7.5E-12	37	6.6E-12	1.5E-11	2.7E-12	58
1.12	**35**	5.0E-11	1.0E-10	1.3E-11	25	2.2E-11	3.0E-11	1.5E-11	23	3.4E-11	5.5E-11	1.4E-11	33	1.7E-11	1.8E-11	1.5E-11	3
1.16	**29**	3.5E-11	4.8E-11	1.3E-11	9	1.6E-11	4.6E-11	9.7E-12	36	4.0E-11	7.7E-11	1.1E-11	48	7.0E-12	1.9E-11	3.5E-12	47
1.40	**37**	3.9E-11	6.4E-11	2.3E-11	16	2.3E-11	3.1E-11	1.6E-11	33	6.0E-11	1.1E-10	1.5E-11	38				
1.44	**33**	4.2E-11	7.6E-11	1.8E-11	12	1.7E-11	2.2E-11	1.0E-11	34	4.2E-11	8.9E-11	7.7E-12	57	7.0E-12	1.3E-11	3.1E-12	32
1.63	**19**	5.3E-11	9.3E-11	2.6E-11	22	2.6E-11	4.2E-11	1.8E-11	7	3.7E-11	5.9E-11	2.0E-11	64	9.2E-12	2.6E-11	3.1E-12	62
1.64	**31**	9.6E-11	2.4E-10	2.3E-11	12	2.5E-11	3.8E-11	1.8E-11	40	4.0E-11	6.3E-11	2.6E-11	28	2.1E-11	2.8E-11	1.8E-11	5
Average		5.0E-11	9.6E-11	1.9E-11	15	2.0E-11	3.5E-11	1.3E-11	30	4.0E-11	7.7E-11	1.4E-11	44	1.1E-11	2.0E-11	7.5E-12	35

Note: The end of Period 1 for the 0.72%S sample was defined early relative to other samples. This means that Period 2 Mg and Ca releases may be higher than expected.

[1] AMAX and ARIMETCO samples originated from core drilled between 1974 and 1977 and were stored for at least 20 years prior to initiation.

[2] Dunka blast hole samples originated from a blast on August 30, 1989 at the Dunka Mine and were stored for 8 years prior to initiation.

Table 32. Sample weekly sodium release (mol/second) by groups and time periods for all Duluth Complex samples (%S≤1.71).

%S	Reactor	Period A				Period B				Period C				Period D			
		Ave	Max	Min	n	Ave	Max	Min	n	Ave	Max	Min	n	Ave	Max	Min	n
Group I																	
0.18	**1**					1.4E-12	3.2E-12	6.1E-13	32								
0.22	**3**					1.3E-12	2.3E-12	6.2E-13	34								
0.72[1]	**42**	3.1E-12	3.3E-12	2.8E-12	2	1.2E-12	1.9E-12	6.2E-13	33								
Average		3.1E-12	3.3E-12	2.8E-12	2	1.3E-12	2.5E-12	6.2E-13	33								
Group II																	
0.40	**5**					8.0E-13	2.1E-12	6.2E-13	20	2.2E-12	3.4E-12	1.5E-12	7	8.7E-13	1.4E-12	6.2E-13	3
0.41	**7**									2.5E-12	2.8E-12	2.2E-12	2	2.0E-12	3.6E-12	1.4E-12	14
0.51	**9**													2.5E-12	5.1E-12	1.5E-12	17
0.54	**11**									2.1E-12	2.4E-12	1.8E-12	2				
0.57	**13**													3.7E-12	4.8E-12	2.6E-12	2
0.58	**15**													2.4E-12	1.0E-11	1.3E-12	18
0.67[1]	**39**	2.3E-12	2.7E-12	2.0E-12	2	2.6E-12	4.8E-12	1.7E-12	4	2.4E-12	2.8E-12	2.0E-12	7	1.2E-12	2.3E-12	6.2E-13	25
0.67[2]	**40**	1.9E-12	2.4E-12	1.7E-12	3	1.9E-12	3.6E-12	6.3E-13	18	2.7E-12	3.1E-12	2.4E-12	4	2.1E-12	3.7E-12	6.2E-13	10
0.82[2]	**43**	1.7E-12	2.4E-12	6.3E-13	3	7.9E-13	1.8E-12	6.2E-13	32								
0.92[1]	**41**	2.1E-12	2.2E-12	2.0E-12	3	1.2E-12	4.4E-12	6.3E-13	33								
1.71[1]	**44**	2.1E-12	2.8E-12	1.6E-12	4	1.8E-12	2.2E-12	1.4E-12	2								
Average		2.0E-12	2.5E-12	1.6E-12	3	1.5E-12	3.1E-12	9.2E-13	18	2.4E-12	2.9E-12	2.0E-12	4	2.1E-12	4.5E-12	1.2E-12	13
Group III																	
0.71	**17**									2.6E-12	3.0E-12	2.3E-12	2	2.3E-12	3.3E-12	1.6E-12	16
1.12	**35**									6.4E-12	9.2E-12	3.6E-12	2	3.0E-12	3.0E-12	3.0E-12	1
1.16	**29**									4.0E-12	5.5E-12	2.9E-12	3	2.4E-12	3.7E-12	1.5E-12	15
1.40	**37**									5.2E-12	5.9E-12	4.1E-12	3				
1.44	**33**									3.6E-12	7.1E-12	2.3E-12	7	2.2E-12	3.6E-12	1.5E-12	11
1.63	**19**									3.5E-12	3.5E-12	3.5E-12	1	2.4E-12	4.0E-12	1.6E-12	18
1.64	**31**									4.2E-12	4.2E-12	4.2E-12	1	4.1E-12	4.5E-12	3.8E-12	2
Average										4.2E-12	5.5E-12	3.3E-12	3	2.7E-12	3.7E-12	2.2E-12	11

[1] AMAX and ARIMETCO samples originated from core drilled between 1974 and 1977 and were stored for at least 20 years prior to initiation.

[2] Dunka blast hole samples originated from a blast on August 30, 1989 at the Dunka Mine and were stored for 8 years prior to initiation.

Table 33. Sample weekly potassium release (mol/second) by groups and time periods for all Duluth Complex samples (%S≤1.71).

%S	Reactor	Period A				Period B				Period C				Period D			
		Ave	Max	Min	n	Ave	Max	Min	n	Ave	Max	Min	n	Ave	Max	Min	n
Group I																	
0.18	**1**					5.7E-12	1.6E-11	7.2E-13	36								
0.22	**3**					3.3E-12	1.2E-11	3.6E-13	36								
0.72[1]	**42**	1.4E-11	1.8E-11	1.1E-11	2	2.9E-12	1.4E-11	3.6E-13	34								
Average		1.4E-11	1.8E-11	1.1E-11	2	4.0E-12	1.4E-11	4.8E-13	35								
Group II																	
0.40	**5**					4.6E-12	1.3E-11	1.3E-12	18	1.1E-12	2.2E-12	3.6E-13	7	3.7E-13	3.7E-13	3.7E-13	2
0.41	**7**									6.3E-12	8.0E-12	4.5E-12	2	3.7E-12	1.0E-11	1.2E-12	13
0.51	**9**													3.2E-12	9.2E-12	3.7E-13	17
0.54	**11**									3.6E-12	4.0E-12	3.2E-12	2				
0.57	**13**													7.6E-12	1.0E-11	4.9E-12	2
0.58	**15**													4.9E-12	1.7E-11	3.7E-13	17
0.67[1]	**39**	3.5E-11	6.5E-11	4.8E-12	2	1.4E-11	2.7E-11	2.6E-12	4	7.2E-12	1.3E-11	4.6E-12	7	1.4E-12	5.6E-12	3.6E-13	27
0.67[2]	**40**	1.3E-11	2.7E-11	5.8E-12	3	5.3E-12	1.8E-11	2.2E-12	19	3.5E-12	4.8E-12	1.5E-12	4	1.1E-12	2.4E-12	3.6E-13	12
0.82[2]	**43**	1.1E-11	1.8E-11	3.7E-12	3	1.1E-12	1.1E-11	3.6E-13	31								
0.92[1]	**41**	1.3E-11	2.5E-11	5.8E-12	3	1.5E-12	2.0E-11	3.7E-13	33								
1.71[1]	**44**	1.4E-11	1.9E-11	1.1E-11	4	1.8E-11	2.1E-11	1.5E-11	2								
Average		1.7E-11	3.1E-11	6.2E-12	3	7.4E-12	1.8E-11	3.7E-12	18	4.3E-12	6.4E-12	2.8E-12	4	3.2E-12	7.9E-12	1.1E-12	13
Group III																	
0.71	**17**									5.0E-12	6.1E-12	3.9E-12	2	6.0E-12	1.9E-11	9.0E-13	17
1.12	**35**									6.0E-12	7.4E-12	4.7E-12	2	6.2E-12	6.2E-12	6.2E-12	1
1.16	**29**									7.1E-12	9.8E-12	4.9E-12	3	3.4E-12	1.1E-11	1.0E-12	15
1.40	**37**									1.6E-11	2.1E-11	7.7E-12	3				
1.44	**33**									9.5E-12	2.2E-11	2.4E-12	7	1.5E-12	2.4E-12	7.6E-13	10
1.63	**19**									6.5E-12	6.5E-12	6.5E-12	1	6.2E-12	2.1E-11	1.5E-12	17
1.64	**31**									4.1E-12	4.1E-12	4.1E-12	1	6.0E-12	6.7E-12	5.3E-12	2
Average										7.7E-12	1.1E-11	4.9E-12	3	4.9E-12	1.1E-11	2.6E-12	10

[1] AMAX and ARIMETCO samples originated from core drilled between 1974 and 1977 and were stored for at least 20 years prior to initiation.

[2] Dunka blast hole samples originated from a blast on August 30, 1989 at the Dunka Mine and were stored for 8 years prior to initiation.

Table 34. Slopes, y-intercepts, and r^2 values from regression analysis of relationships among %S, sulfate, pH, Ca and Mg. See Figures 20-43 for data used.

independent	dependent	Period A			Period B			Period C			Period D		
		slope	y-int	r^2	slope	y-int	r^2	slope	y-int	r^2	slope	y-int	r^2
log %S	pH avg	-1.37	5.96	0.340	-1.69	4.98	0.452	-1.00	3.97	0.693	-0.46	4.62	0.070
log %S	pH max	-1.36	7.27	0.238	-1.84	5.55	0.387	-0.02	4.56	0.000	-1.63	5.23	0.254
log %S	pH min	-1.34	5.20	0.314	-1.21	4.39	0.339	-1.58	3.50	0.704	0.02	4.25	0.000
log %S	log SO_4 avg	0.82	1.28	0.525	1.35	1.09	0.521	1.03	1.68	0.779	0.76	1.00	0.140
log %S	log SO_4 max	0.71	1.67	0.317	0.85	1.43	0.413	1.37	2.03	0.671	0.33	1.35	0.163
log %S	log SO_4 min	1.19	0.93	0.563	1.93	0.64	0.399	0.37	1.25	0.172	1.49	0.62	0.147
log SO_4 avg	pH avg	-1.65	8.07	0.625	-1.17	6.27	0.757	-0.98	5.61	0.904	-1.06	5.69	0.961
log SO_4 avg	pH max	-1.97	9.76	0.638	-1.37	7.04	0.751	-0.13	4.76	0.019	-1.74	6.93	0.906
log SO_4 avg	pH min	-1.43	7.05	0.464	-0.94	5.41	0.718	-1.52	6.04	0.879	-0.45	4.71	0.512
log SO_4 avg	log Ca avg	0.43	0.55	0.533	0.38	0.10	0.473	0.60	-0.20	0.681	0.60	-0.13	0.937
log SO_4 avg	log Ca max	0.48	0.89	0.485	0.17	0.72	0.149	0.73	-0.12	0.608	0.28	0.43	0.541
log SO_4 avg	log Ca min	0.22	0.37	0.063	0.82	-0.82	0.610	0.38	-0.17	0.083	1.02	-0.78	0.917
log SO_4 avg	log Mg avg	0.56	0.08	0.379	0.75	-0.27	0.675	1.42	-1.49	0.604	0.94	-0.73	0.877
log SO_4 avg	log Mg max	0.56	0.45	0.284	0.36	0.52	0.391	1.24	-0.82	0.535	0.33	0.40	0.453
log SO_4 avg	log Mg min	0.54	-0.47	0.169	0.91	-0.87	0.636	1.28	-1.77	0.478	1.31	-1.57	0.811
log SO_4 avg	log Ca+Mg avg	0.50	0.68	0.696	0.55	0.28	0.764	0.92	-0.34	0.936	0.71	-0.03	0.971
log SO_4 avg	log Ca+Mg max	0.46	1.05	0.447	0.28	0.88	0.423	0.97	-0.14	0.718	0.33	0.67	0.538
log SO_4 avg	log Ca+Mg min	0.42	0.42	0.301	0.93	-0.48	0.716	0.61	-0.18	0.610	1.09	-0.70	0.954

Table 35. Iron, aluminum and silicon release rates for all Duluth Complex samples combined. Average, minimum and maximum rates are presented for entire period of record, as well as for pH>4 and pH≤4 (n = number of measurements).

Criteria	Stats	Fe (mol/s)	Al (mol/s)	Si (mol/s)
Entire period of record	Avg	5.00E-13	3.10E-12	1.21E-11
	Min	4.81E-15	1.03E-14	1.22E-13
	Max	3.67E-11	8.25E-11	1.73E-10
	n	441	445	425
pH > 4	Avg	2.73E-13	1.23E-12	1.18E-11
	Min	4.81E-15	1.03E-14	1.22E-13
	Max	3.67E-11	2.31E-11	1.73E-10
	n	410	414	418
pH ≤ 4	Avg	3.51E-12	2.81E-11	2.93E-11
	Min	1.20E-13	2.13E-14	4.51E-12
	Max	2.39E-11	8.25E-11	4.03E-11
	n	31	31	7

Table 36. Sample weekly cobalt release (mol/second) by groups and time periods for all Duluth Complex samples (%S≤1.71).

%S	Reactor	Period A				Period B				Period C				Period D			
		Ave	Max	Min	n	Ave	Max	Min	n	Ave	Max	Min	n	Ave	Max	Min	n
Group I																	
0.18	**1**	5.1E-14	1.5E-13	2.4E-14	9	6.6E-15	2.4E-14	4.8E-15	38								
0.22	**3**	4.0E-14	9.8E-14	2.4E-14	8	7.2E-15	2.0E-14	4.8E-15	39								
0.72[1]	**42**	5.0E-15	5.0E-15	5.0E-15	2	4.9E-15	5.4E-15	4.7E-15	33								
Average		3.2E-14	8.3E-14	1.8E-14	6	6.2E-15	1.7E-14	4.8E-15	37								
Group II																	
0.40	**5**	9.0E-14	2.0E-13	2.5E-14	8	1.1E-14	2.1E-14	4.9E-15	22	3.6E-14	7.3E-14	1.2E-14	6	4.9E-15	4.9E-15	4.8E-15	3
0.41	**7**	9.9E-14	2.0E-13	2.4E-14	11	7.4E-14	1.0E-13	5.1E-14	4	9.0E-14	1.2E-13	6.0E-14	4	1.1E-14	3.2E-14	4.6E-15	13
0.51	**9**	9.2E-14	2.1E-13	2.5E-14	11	3.7E-14	4.9E-14	2.6E-14	2	1.4E-13	2.4E-13	7.6E-14	4	1.1E-14	4.4E-14	4.8E-15	17
0.54	**11**	7.5E-14	2.0E-13	2.4E-14	33	5.0E-14	5.0E-14	5.0E-14	2	1.4E-14	2.3E-14	5.0E-15	6				
0.57	**13**	9.3E-14	2.4E-13	2.4E-14	8	1.4E-13	2.5E-13	4.9E-14	6	1.5E-13	2.1E-13	9.2E-14	2	3.7E-14	7.9E-14	1.5E-14	4
0.58	**15**	2.5E-13	3.4E-13	1.5E-13	8	1.1E-13	1.5E-13	9.8E-14	4	4.3E-14	4.3E-14	4.3E-14	1	8.7E-15	4.0E-14	4.7E-15	18
0.67[1]	**39**	4.0E-13	4.1E-13	3.9E-13	2	9.3E-14	1.5E-13	6.0E-14	4	4.8E-14	6.5E-14	3.8E-14	3	7.8E-15	3.1E-14	4.8E-15	27
0.67[2]	**40**	4.8E-14	8.9E-14	4.9E-15	3	5.8E-14	1.1E-13	3.7E-14	15	5.6E-14	8.7E-14	3.7E-14	4	6.3E-15	1.8E-14	4.7E-15	12
0.82[2]	**43**	1.0E-13	2.1E-13	5.0E-15	3	1.5E-14	8.7E-14	4.8E-15	31								
0.92[1]	**41**	2.5E-14	3.7E-14	5.0E-15	3	1.6E-14	5.0E-14	4.9E-15	31								
1.71[1]	**44**	5.0E-14	1.7E-13	4.9E-15	4	2.3E-13	2.3E-13	2.2E-13	2								
Average		1.2E-13	2.1E-13	6.2E-14	9	7.5E-14	1.1E-13	5.5E-14	11	7.2E-14	1.1E-13	4.5E-14	4	1.2E-14	3.6E-14	6.3E-15	13
Group III																	
0.71	**17**	1.8E-13	4.0E-13	2.5E-14	7	2.2E-13	3.0E-13	9.9E-14	5	1.2E-13	2.5E-13	1.2E-14	6	6.8E-15	1.8E-14	4.7E-15	15
1.12	**35**	1.0E-12	1.9E-12	9.9E-14	11	1.7E-13	2.4E-13	9.8E-14	2	1.1E-13	2.0E-13	2.8E-14	5	2.1E-14	2.1E-14	2.1E-14	1
1.16	**29**	3.6E-14	5.2E-14	2.6E-14	10	4.9E-13	5.7E-13	3.5E-13	4	1.8E-13	3.4E-13	6.2E-14	7	1.2E-14	3.5E-14	4.8E-15	13
1.40	**37**	1.6E-13	5.6E-13	2.5E-14	15	6.0E-13	6.0E-13	6.0E-13	1	4.4E-13	7.8E-13	2.0E-13	7				
1.44	**33**	2.7E-13	4.5E-13	2.6E-14	12	2.7E-13	3.0E-13	2.5E-13	2	1.9E-13	4.6E-13	3.3E-14	10	9.7E-15	2.1E-14	4.8E-15	10
1.63	**19**	6.6E-13	9.4E-13	2.0E-13	26	3.7E-13	5.5E-13	2.6E-13	3	1.2E-13	2.1E-13	3.3E-14	7	8.1E-15	2.1E-14	4.4E-15	16
1.64	**31**	2.1E-12	2.9E-12	4.9E-13	10	1.5E-13	1.5E-13	1.5E-13	1	1.3E-13	1.8E-13	5.8E-14	4	2.9E-14	3.0E-14	2.9E-14	2
Average		6.3E-13	1.0E-12	1.3E-13	13	3.3E-13	3.9E-13	2.6E-13	3	1.8E-13	3.4E-13	6.1E-14	7	1.5E-14	2.4E-14	1.1E-14	10

[1] AMAX and ARIMETCO samples originated from core drilled between 1974 and 1977 and were stored for at least 20 years prior to initiation.

[2] Dunka blast hole samples originated from a blast on August 30, 1989 at the Dunka Mine and were stored for 8 years prior to initiation.

Table 37. Sample weekly copper release (mol/second) by groups and time periods for all Duluth Complex samples (%S≤1.71).

%S	Reactor	Period A				Period B				Period C				Period D			
		Ave	Max	Min	n	Ave	Max	Min	n	Ave	Max	Min	n	Ave	Max	Min	n
Group I																	
0.18	**1**	4.3E-14	1.4E-13	2.2E-14	9	2.1E-14	5.6E-14	4.5E-15	37								
0.22	**3**	4.3E-14	1.4E-13	2.2E-14	8	2.6E-14	6.0E-14	1.4E-14	37								
0.72[1]	**42**	8.8E-15	1.3E-14	4.6E-15	2	2.2E-14	7.7E-14	4.5E-15	32								
Average		3.1E-14	9.5E-14	1.6E-14	6	2.3E-14	6.4E-14	7.5E-15	35								
Group II																	
0.40	**5**	5.4E-14	1.8E-13	2.3E-14	8	2.2E-13	9.0E-13	3.5E-14	22	8.4E-13	1.7E-12	2.9E-13	6	1.8E-13	2.1E-13	1.7E-13	3
0.41	**7**	1.5E-13	9.2E-13	2.3E-14	11	1.3E-12	1.8E-12	9.0E-13	4	1.5E-12	1.9E-12	9.7E-13	4	5.8E-13	1.2E-12	2.1E-13	13
0.51	**9**	7.9E-13	3.1E-12	2.2E-14	11	1.7E-12	2.1E-12	1.3E-12	2	3.4E-12	4.5E-12	2.8E-12	4	1.3E-12	3.3E-12	5.2E-14	17
0.54	**11**	5.2E-14	2.7E-13	2.2E-14	34	2.8E-13	2.8E-13	2.8E-13	2	2.2E-13	4.1E-13	7.6E-14	6				
0.57	**13**	1.3E-13	3.1E-13	2.2E-14	8	1.9E-12	4.1E-12	7.1E-13	6	2.4E-12	2.4E-12	2.4E-12	1	2.5E-12	3.0E-12	1.8E-12	4
0.58	**15**	2.0E-13	4.5E-13	2.3E-14	8	8.5E-13	1.1E-12	5.5E-13	4	1.1E-12	1.1E-12	1.1E-12	1	6.8E-13	1.3E-12	1.4E-13	18
0.67[1]	**39**	6.8E-13	1.3E-12	6.1E-14	2	1.4E-12	1.7E-12	1.1E-12	4	1.7E-12	2.2E-12	1.4E-12	3	6.4E-13	1.7E-12	1.9E-14	27
0.67[2]	**40**	2.7E-14	6.7E-14	4.5E-15	3	4.0E-13	1.3E-12	7.1E-14	15	1.3E-12	1.8E-12	8.3E-13	4	4.5E-13	1.0E-12	5.1E-14	12
0.82[2]	**43**	2.3E-13	3.6E-13	9.2E-15	3	4.9E-13	8.8E-13	1.9E-13	32								
0.92[1]	**41**	6.5E-14	1.6E-13	9.2E-15	3	7.7E-13	1.4E-12	3.3E-13	29								
1.71[1]	**44**	2.3E-14	7.3E-14	4.6E-15	4	2.0E-13	2.7E-13	1.4E-13	2								
Average		2.2E-13	6.6E-13	2.0E-14	9	8.6E-13	1.4E-12	5.1E-13	11	1.5E-12	2.0E-12	1.2E-12	4	9.1E-13	1.7E-12	3.5E-13	13
Group III																	
0.71	**17**	2.3E-13	6.9E-13	2.3E-14	7	2.0E-12	2.5E-12	1.3E-12	5	3.2E-12	5.4E-12	6.3E-13	6	1.9E-12	3.8E-12	8.3E-13	15
1.12	**35**	2.0E-13	7.8E-13	2.3E-14	11	1.3E-12	1.3E-12	1.2E-12	2	2.8E-12	4.7E-12	1.1E-12	5	9.1E-13	9.1E-13	9.1E-13	1
1.16	**29**	4.8E-14	9.5E-14	2.4E-14	10	1.2E-12	2.1E-12	3.2E-13	4	2.1E-12	4.5E-12	4.2E-13	7	1.2E-12	2.3E-12	9.0E-13	12
1.40	**37**	1.5E-13	9.8E-13	2.4E-14	15	1.7E-12	1.7E-12	1.7E-12	1	3.8E-12	6.7E-12	1.4E-12	7				
1.44	**33**	1.5E-13	6.0E-13	2.3E-14	12	7.4E-13	1.0E-12	4.6E-13	2	2.9E-12	5.4E-12	7.2E-13	10	3.7E-12	5.0E-12	1.2E-12	10
1.63	**19**	2.8E-13	7.5E-13	2.3E-14	26	9.9E-13	1.3E-12	4.2E-13	3	4.2E-12	7.6E-12	9.7E-13	8	1.8E-12	4.5E-12	3.6E-13	16
1.64	**31**	7.1E-13	1.3E-12	4.6E-14	10	3.2E-12	3.2E-12	3.2E-12	1	7.2E-12	8.8E-12	6.2E-12	4	3.4E-12	3.6E-12	3.3E-12	2
Average		2.5E-13	7.4E-13	2.6E-14	13	1.6E-12	1.9E-12	1.2E-12	3	3.7E-12	6.2E-12	1.6E-12	7	2.2E-12	3.4E-12	1.2E-12	9

[1] AMAX and ARIMETCO samples originated from core drilled between 1974 and 1977 and were stored for at least 20 years prior to initiation.

[2] Dunka blast hole samples originated from a blast on August 30, 1989 at the Dunka Mine and were stored for 8 years prior to initiation.

Table 38. Sample weekly nickel release (mol/second) by groups and time periods for all Duluth Complex samples (%S≤1.71).

%S	Reactor	Period A				Period B				Period C				Period D			
		Ave	Max	Min	n	Ave	Max	Min	n	Ave	Max	Min	n	Ave	Max	Min	n
Group I																	
0.18	**1**	9.2E-14	3.0E-13	2.4E-14	9	1.9E-14	5.5E-14	4.8E-15	37								
0.22	**3**	7.7E-14	2.0E-13	2.4E-14	8	1.7E-14	5.4E-14	4.8E-15	37								
0.72[1]	**42**	7.5E-15	1.0E-14	5.0E-15	2	1.0E-14	2.1E-14	4.7E-15	31								
Average		5.9E-14	1.7E-13	1.8E-14	6	1.5E-14	4.3E-14	4.8E-15	35								
Group II																	
0.40	**5**	4.5E-13	7.1E-13	1.0E-13	8	9.7E-14	2.9E-13	4.3E-14	22	6.1E-13	1.3E-12	1.9E-13	6	7.3E-14	9.7E-14	5.4E-14	3
0.41	**7**	1.2E-12	2.9E-12	2.4E-14	11	1.6E-12	2.7E-12	9.3E-13	4	1.6E-12	2.2E-12	1.1E-12	4	1.8E-13	5.9E-13	2.0E-14	13
0.51	**9**	9.1E-13	2.6E-12	2.6E-14	10	3.8E-13	4.1E-13	3.5E-13	2	1.6E-12	2.0E-12	1.1E-12	4	1.1E-13	6.0E-13	4.9E-15	17
0.54	**11**	3.7E-13	1.9E-12	2.5E-14	33	3.5E-13	3.5E-13	3.5E-13	2	1.2E-13	2.0E-13	4.6E-14	6				
0.57	**13**	8.3E-13	2.0E-12	2.4E-14	8	1.2E-12	1.9E-12	7.7E-13	6	1.3E-12	1.3E-12	1.3E-12	1	5.1E-13	1.1E-12	2.1E-13	4
0.58	**15**	1.5E-12	2.3E-12	1.0E-12	8	8.5E-13	1.1E-12	7.0E-13	4	4.7E-13	4.7E-13	4.7E-13	1	7.7E-14	4.6E-13	4.9E-15	18
0.67[1]	**39**	3.0E-12	5.9E-12	9.9E-15	2	1.6E-12	2.4E-12	1.2E-12	4	9.1E-13	1.2E-12	7.1E-13	3	9.4E-14	5.3E-13	4.8E-15	27
0.67[2]	**40**	4.3E-13	7.1E-13	6.8E-14	3	4.6E-13	7.9E-13	2.9E-13	15	6.7E-13	1.0E-12	4.4E-13	4	6.0E-14	2.2E-13	4.7E-15	12
0.82[2]	**43**	9.9E-13	2.0E-12	1.0E-13	3	1.7E-13	8.7E-13	2.7E-14	31								
0.92[1]	**41**	2.3E-13	3.7E-13	5.0E-15	3	2.2E-13	5.1E-13	5.1E-15	31								
1.71[1]	**44**	2.5E-13	8.8E-13	4.9E-15	4	1.1E-12	1.1E-12	1.1E-12	2								
Average		9.1E-13	2.0E-12	1.3E-13	8	7.3E-13	1.1E-12	5.3E-13	11	9.2E-13	1.2E-12	6.7E-13	4	1.6E-13	5.1E-13	4.4E-14	13
Group III																	
0.71	**17**	1.2E-12	3.2E-12	2.5E-14	7	2.3E-12	3.2E-12	8.0E-13	5	1.3E-12	2.2E-12	1.3E-13	6	4.9E-14	1.8E-13	4.7E-15	15
1.12	**35**	7.3E-12	1.3E-11	1.2E-12	11	1.4E-12	1.5E-12	1.4E-12	2	1.4E-12	2.6E-12	2.9E-13	5	2.1E-13	2.1E-13	2.1E-13	1
1.16	**29**	1.3E-13	2.6E-13	5.1E-14	10	5.6E-12	6.8E-12	3.6E-12	4	2.6E-12	4.9E-12	8.3E-13	7	1.4E-13	4.5E-13	3.5E-14	13
1.40	**37**	1.5E-12	6.4E-12	1.0E-13	15	6.6E-12	6.6E-12	6.6E-12	1	5.9E-12	1.1E-11	2.6E-12	6				
1.44	**33**	2.4E-12	3.7E-12	2.7E-13	12	2.5E-12	2.6E-12	2.5E-12	2	1.9E-12	4.6E-12	1.9E-13	10	7.2E-14	1.9E-13	3.4E-14	10
1.63	**19**	5.1E-12	7.1E-12	1.4E-12	26	3.0E-12	3.6E-12	2.7E-12	3	1.4E-12	2.8E-12	2.1E-13	8	3.7E-14	1.1E-13	4.7E-15	16
1.64	**31**	2.2E-11	3.6E-11	5.8E-12	10	2.2E-12	2.2E-12	2.2E-12	1	2.0E-12	2.9E-12	8.1E-13	4	3.9E-13	3.9E-13	3.8E-13	2
Average		5.7E-12	9.9E-12	1.3E-12	13	3.4E-12	3.8E-12	2.8E-12	3	2.3E-12	4.4E-12	7.2E-13	7	1.5E-13	2.6E-13	1.1E-13	10

[1] AMAX and ARIMETCO samples originated from core drilled between 1974 and 1977 and were stored for at least 20 years prior to initiation.

[2] Dunka blast hole samples originated from a blast on August 30, 1989 at the Dunka Mine and were stored for 8 years prior to initiation.

Table 39. Sample weekly zinc release (mol/second) by groups and time periods for all Duluth Complex samples (%S≤1.71).

%S	Reactor	Period A				Period B				Period C				Period D			
		Ave	Max	Min	n	Ave	Max	Min	n	Ave	Max	Min	n	Ave	Max	Min	n
Group I																	
0.18	**1**	6.6E-14	1.3E-13	2.2E-14	9	5.2E-14	2.2E-13	9.0E-15	38								
0.22	**3**	5.2E-14	8.8E-14	2.2E-14	8	4.6E-14	2.3E-13	1.3E-14	38								
0.72[1]	**42**	6.6E-14	6.7E-14	6.6E-14	2	2.8E-14	8.5E-14	4.4E-15	33								
Average		6.1E-14	9.5E-14	3.6E-14	6	4.2E-14	1.8E-13	8.9E-15	36								
Group II																	
0.40	**5**	1.0E-13	1.8E-13	4.5E-14	8	8.7E-14	2.6E-13	2.9E-14	22	1.0E-13	1.8E-13	4.8E-14	6	2.4E-14	3.7E-14	1.7E-14	3
0.41	**7**	1.4E-13	3.1E-13	2.2E-14	11	8.3E-14	1.8E-13	4.6E-14	4	1.8E-13	3.5E-13	7.0E-14	4	8.8E-14	1.8E-13	2.9E-14	13
0.51	**9**	1.8E-13	6.3E-13	2.3E-14	11	9.0E-14	9.2E-14	8.9E-14	2	1.6E-13	2.2E-13	1.2E-13	4	1.2E-13	3.5E-13	3.1E-14	17
0.54	**11**	1.4E-13	5.7E-13	2.2E-14	34	1.8E-13	1.8E-13	1.8E-13	2	1.4E-13	2.3E-13	6.2E-14	6				
0.57	**13**	1.7E-13	4.8E-13	2.2E-14	8	2.0E-13	2.2E-13	1.3E-13	6	2.3E-13	2.4E-13	2.2E-13	2	1.9E-13	2.5E-13	1.2E-13	4
0.58	**15**	2.7E-13	4.8E-13	2.2E-14	8	2.6E-13	4.0E-13	1.3E-13	4	8.8E-14	8.8E-14	8.8E-14	1	9.5E-14	2.0E-13	2.2E-14	18
0.67[1]	**39**	3.3E-13	4.1E-13	2.5E-13	2	2.0E-13	3.4E-13	9.0E-14	3	9.0E-14	1.1E-13	7.9E-14	3	3.9E-14	1.1E-13	1.1E-14	27
0.67[2]	**40**	1.4E-13	1.9E-13	8.5E-14	3	1.5E-13	3.1E-13	8.6E-14	15	1.1E-13	1.6E-13	8.4E-14	4	7.1E-14	1.8E-13	2.4E-14	12
0.82[2]	**43**	2.0E-13	3.4E-13	1.0E-13	3	5.4E-14	2.0E-13	4.5E-15	31								
0.92[1]	**41**	1.3E-13	1.5E-13	8.4E-14	3	3.7E-14	1.8E-13	4.4E-15	32								
1.71[1]	**44**	1.2E-13	2.5E-13	6.5E-14	4	1.2E-13	1.4E-13	9.0E-14	2								
Average		1.8E-13	3.6E-13	6.8E-14	9	1.3E-13	2.3E-13	8.0E-14	11	1.4E-13	2.0E-13	9.7E-14	4	8.9E-14	1.9E-13	3.6E-14	13
Group III																	
0.71	**17**	1.8E-13	4.0E-13	2.2E-14	7	1.8E-13	3.2E-13	9.0E-14	5	1.7E-13	2.5E-13	1.0E-13	6	8.9E-14	2.4E-13	4.6E-14	15
1.12	**35**	4.1E-13	8.0E-13	1.3E-13	11	3.1E-13	4.4E-13	1.8E-13	2	4.3E-13	5.9E-13	2.9E-13	5	2.4E-13	2.4E-13	2.4E-13	1
1.16	**29**	4.0E-14	4.7E-14	2.3E-14	10	3.7E-13	6.2E-13	1.8E-13	4	2.7E-13	5.0E-13	1.4E-13	7	1.4E-13	9.1E-13	3.5E-14	13
1.40	**37**	1.2E-13	5.0E-13	2.3E-14	15	2.7E-13	2.7E-13	2.7E-13	1	3.1E-13	5.0E-13	1.2E-13	7				
1.44	**33**	2.3E-13	3.6E-13	9.5E-14	12	1.8E-13	2.2E-13	1.4E-13	2	2.4E-13	5.0E-13	1.1E-13	10	7.5E-14	1.3E-13	3.7E-14	9
1.63	**19**	3.2E-13	6.3E-13	4.4E-14	26	4.3E-13	5.0E-13	3.3E-13	3	4.9E-13	8.5E-13	1.8E-13	8	1.7E-13	4.2E-13	4.0E-14	16
1.64	**31**	7.2E-13	9.8E-13	2.7E-13	10	2.2E-13	2.2E-13	2.2E-13	1	3.6E-13	4.0E-13	2.9E-13	4	2.2E-13	2.8E-13	1.6E-13	2
Average		2.9E-13	5.3E-13	8.7E-14	13	2.8E-13	3.7E-13	2.0E-13	3	3.2E-13	5.2E-13	1.8E-13	7	1.6E-13	3.7E-13	9.2E-14	9

[1] AMAX and ARIMETCO samples originated from core drilled between 1974 and 1977 and were stored for at least 20 years prior to initiation.

[2] Dunka blast hole samples originated from a blast on August 30, 1989 at the Dunka Mine and were stored for 8 years prior to initiation.

Table 40. Observed metal release from Virginia Formation samples. All samples had 28-32 measurements of metal release taken throughout the 78-week experimental period.

Reactor	%S	Co (mol/s)			Cu (mol/s)			Ni (mol/s)			Zn (mol/s)		
		Ave	Max	Min	Ave	Max	Min	Ave	Max	Min	Ave	Max	Min
21	2.06	1.79E-12	4.57E-12	8.86E-13	1.77E-12	4.56E-12	2.28E-14	1.65E-11	4.51E-11	7.12E-12	5.81E-13	1.11E-12	1.81E-13
22	2.06	2.02E-12	6.42E-12	9.06E-13	1.98E-12	4.45E-12	4.67E-14	1.87E-11	6.43E-11	8.19E-12	6.10E-13	1.16E-12	2.25E-13
23	3.12	5.48E-13	1.45E-12	9.97E-14	9.36E-14	2.71E-13	2.26E-14	2.60E-12	6.90E-12	2.55E-13	1.44E-12	4.13E-12	1.83E-13
24	3.12	5.86E-13	1.03E-12	2.42E-14	1.03E-13	3.08E-13	2.20E-14	2.87E-12	5.16E-12	2.42E-13	1.64E-12	2.70E-12	8.71E-14
25	3.72	7.16E-13	1.41E-12	4.80E-13	5.09E-14	9.37E-14	2.23E-14	2.90E-12	7.95E-12	1.47E-12	9.84E-13	2.41E-12	6.06E-13
26	3.72	7.40E-13	1.49E-12	3.78E-13	5.26E-14	9.23E-14	2.19E-14	2.99E-12	8.33E-12	1.61E-12	8.69E-13	2.29E-12	4.69E-13
27	5.44	8.84E-13	4.07E-12	3.45E-13	7.71E-14	4.00E-13	2.25E-14	4.59E-12	2.62E-11	1.52E-12	2.03E-12	7.12E-12	1.27E-12
28	5.44	1.09E-12	6.69E-12	4.20E-13	8.94E-14	4.39E-13	2.24E-14	4.81E-12	2.63E-11	1.20E-12	1.92E-12	7.00E-12	1.22E-12
Average		1.05E-12	3.39E-12	4.42E-13	5.28E-13	1.33E-12	2.54E-14	7.00E-12	2.38E-11	2.70E-12	1.26E-12	3.49E-12	5.30E-13

Table 41. Observed drainage pH, sulfate, calcium, and magnesium release from Virginia Formation samples.

Reactor	%S	pH			SO$_4$ (mol/s)			Ca (mol/s)			Mg (mol/s)		
		Ave	Max	Min	Ave	Max	Min	Ave	Max	Min	Ave	Max	Min
21	2.06	4.85	7.70	4.20	1.13E-10	3.10E-10	1.51E-11	3.18E-11	1.95E-10	1.02E-11	5.19E-11	1.29E-10	1.91E-11
22	2.06	4.85	7.80	4.30	1.06E-10	2.10E-10	4.85E-11	3.35E-11	2.15E-10	1.16E-11	5.37E-11	1.37E-10	2.16E-11
23	3.12	4.51	6.75	3.70	2.94E-10	1.42E-09	4.77E-11	6.87E-11	3.88E-10	2.65E-11	6.87E-11	5.28E-10	1.45E-11
24	3.12	4.38	6.50	3.50	3.86E-10	9.03E-10	7.11E-11	7.23E-11	4.03E-10	3.17E-11	5.63E-11	3.09E-10	1.41E-11
25	3.72	4.30	5.55	3.70	1.92E-10	1.30E-09	6.48E-11	5.21E-11	5.38E-10	1.84E-11	6.51E-11	4.28E-10	1.28E-11
26	3.72	4.31	5.55	3.75	1.53E-10	5.54E-10	7.25E-11	5.02E-11	5.46E-10	1.11E-11	6.55E-11	4.34E-10	1.37E-11
27	5.44	3.88	4.85	3.35	2.96E-10	3.03E-09	5.87E-11	5.12E-11	7.37E-10	8.35E-12	8.55E-11	7.50E-10	2.51E-11
28	5.44	3.84	5.00	2.90	2.53E-10	9.03E-10	8.00E-11	5.30E-11	8.03E-10	1.09E-11	8.64E-11	7.24E-10	2.68E-11
Average		4.37	6.21	3.68	2.24E-10	1.08E-09	5.73E-11	5.16E-11	4.78E-10	1.61E-11	6.66E-11	4.30E-10	1.85E-11

Table 42. Ni, Mg content and Ni-bearing mineral abundance in Duluth Complex solid samples.

%S	Ni ppm	Ni (g/sample)	Ni (mol/sample)	Olivine (mol/sample)	Ni ol (mols Ni/ mol ol)	Ni in ol (mol/sample)	fraction Ni as olivine	fraction Ni as pent/po	Mg (mols/mol ol)	ol Ni/Mg (molar)
Group I										
0.18	525	0.039	6.71E-04	0.043	0.003	1.28E-04	0.191	0.809	0.763	0.0039
0.22	484	0.036	6.18E-04	0.019	0.002	3.82E-05	0.062	0.938	0.857	0.0023
0.72[2]	254	0.019	3.25E-04	0.098	0.003	2.95E-04	0.910	0.090	1.233	0.0024
Group II										
0.40[1]	231	0.017	2.95E-04					1.000		
0.41	511	0.038	6.53E-04	0.056	0.003	1.68E-04	0.258	0.742	0.897	0.0033
0.51	473	0.035	6.04E-04	0.025	0.002	5.00E-05	0.083	0.917	0.812	0.0025
0.54[1]	174	0.013	2.22E-04					1.000		
0.57	398	0.030	5.09E-04	0.092	0.004	3.66E-04	0.721	0.279	1.003	0.0040
0.58	396	0.030	5.06E-04	0.011	0.001	1.07E-05	0.021	0.979	0.851	0.0012
0.67[2]	523	0.039	6.68E-04	0.075	0.003	2.25E-04	0.337	0.663	1.09	0.0028
0.67[3]	261	0.020	3.34E-04	0.019	0.001	1.52E-05	0.046	0.954	0.947	0.0008
0.82[3]	204	0.015	2.61E-04	0.015	0.001	1.49E-05	0.057	0.943	0.8	0.0013
0.92[2]	324	0.024	4.14E-04	0.173	0.003	5.18E-04	1.251	-0.251	1.035	0.0029
1.71[2]	354	0.027	4.52E-04	0.089	0.001	8.89E-05	0.196	0.804	1.139	0.0009
Group III										
0.71	388	0.029	4.96E-04	0.065	0.002	1.29E-04	0.260	0.740	0.958	0.0021
1.12	329	0.025	4.20E-04	0.018	0.002	3.58E-05	0.085	0.915	0.953	0.0021
1.16	422	0.032	5.39E-04	0.073	0.002	1.46E-04	0.271	0.729	0.958	0.0021
1.4	503	0.038	6.43E-04	0.026	0.003	7.67E-05	0.119	0.881	0.954	0.0031
1.44	386	0.029	4.93E-04	0.026	0.003	7.70E-05	0.156	0.844	0.953	0.0031
1.63	492	0.037	6.29E-04	0.023	0.002	4.68E-05	0.075	0.925	0.722	0.0028
1.64	718	0.054	9.17E-04	0.014	0.003	4.23E-05	0.046	0.954	0.828	0.0036
Average	398	0.030	5.08E-04	0.050	0.002	1.30E-04	0.245	0.755	0.934	0.0025

[1] Sample had no olivine detected by point count.

[2] AMAX and ARIMETCO samples originated from core drilled between 1974 and 1977 and were stored for at least 20 years prior to initiation.

[3] Dunka blast hole samples originated from a blast on August 30, 1989 at the Dunka Mine and were stored for 8 years prior to initiation.

Table 43. Average Ni/Mg ratio in Duluth Complex leachate during different sample periods. See appendix for details on period definition. Numbers in parentheses are the number of data points in each period. Blank cells indicate sample did not enter that time period.

%S	Reactor	Ni/Mg olivine	Average Ni/Mg ratio in leachate (molar)			
			Period A	Period B	Period C	Period D
Group I						
0.18	1	0.0038	0.015 (9)	0.011 (37)		
0.22	3	0.002	0.008 (8)	0.006 (37)		
0.72[2]	42	0.0024	0.002 (2)	0.009 (31)		
Group II						
0.40[1]	5	No ol	0.152 (7)	0.122 (21)	0.631 (6)	0.123 (3)
0.41	7	0.0033	0.493 (8)	0.461 (4)	0.166 (4)	0.134 (13)
0.51	9	0.0025	0.244 (8)	0.155 (2)	0.231 (4)	0.061 (17)
0.54[1]	11	No ol	0.042 (29)	0.064 (2)	0.086 (6)	
0.57	13	0.004	0.086 (8)	0.247 (6)	0.093 (1)	0.177 (4)
0.58	15	0.0012	0.124 (8)	0.204 (4)	0.079 (1)	0.073 (18)
0.67[3]	39	0.0028	0.208 (2)	0.483 (4)	0.147 (3)	0.102 (27)
0.67[3]	40	0.0008	0.039 (3)	0.186 (15)	0.086 (4)	0.040 (12)
0.82[2]	43	0.0013	0.124 (3)	0.270 (31)		
0.92[2]	41	0.0029	0.028 (3)	0.357 (30)		
1.71[2]	44	0.0009	0.014 (4)	0.063 (2)		
Group III						
0.71	17	0.0021	0.076 (7)	0.556 (5)	0.084 (6)	0.29 (15)
1.12	35	0.0021	0.989 (10)	0.215 (2)	0.075 (5)	0.030 (1)
1.16	29	0.0021	0.032 (9)	0.311 (3)	0.089 (7)	0.076 (13)
1.4	37	0.0031	0.184 (13)	no Ni:Mg measurements	0.135 (6)	
1.44	33	0.0031	0.214 (9)	0.295 (2)	0.055 (10)	0.041 (10)
1.63	19	0.0028	0.190 (26)	0.164 (2)	0.053 (8)	0.012 (16)
1.64	31	0.0036	0.603 (10)	0.159 (1)	0.075 (4)	0.037 (2)
Total Average		0.0025	0.184	0.217	0.139	0.072

[1] Sample had no olivine detected by point count.

[2] AMAX and ARIMETCO samples originated from core drilled between 1974 and 1977 and were stored for at least 20 years prior to initiation.

[3] Dunka blast hole samples originated from a blast on August 30, 1989 at the Dunka Mine and were stored for 8 years prior to initiation.

Table 44. Calculated and observed Ni release. Calculated based on Mg in leachate on days Ni was measured, multiplied by Ni:Mg in olivine. This method assumes all Mg comes from ol dissolution therefore it overestimates both Ni release and olivine dissolution. Blank cells indicate sample did not enter that time period.

%S	Calculated Ni release from ol (mol/week)				Observed Ni release rate in leachate (mol/week)				Calculated:Observed Ni from olivine			
	Period A	**Period B**	**Period C**	**Period D**	**Period A**	**Period B**	**Period C**	**Period D**	**Period A**	**Period B**	**Period C**	**Period D**
Group I												
0.18	1.96E-08	4.68E-09			5.58E-08	1.14E-08			35.1%	41.0%		
0.22	2.21E-08	4.26E-09			4.65E-08	1.03E-08			47.6%	41.5%		
0.72[2]	6.23E-09	2.29E-09			4.54E-09	6.08E-09			137.1%	37.6%		
Group II												
0.40[1]					2.73E-07	5.86E-08	3.69E-07	4.40E-08				
0.41	1.10E-08	8.59E-09	2.04E-08	2.74E-09	6.99E-07	9.81E-07	9.94E-07	1.07E-07	1.6%	0.9%	2.1%	2.6%
0.51	9.41E-09	3.62E-09	1.23E-08	2.67E-09	5.53E-07	2.28E-07	9.67E-07	6.94E-08	1.7%	1.6%	1.3%	3.9%
0.54[1]					2.25E-07	2.13E-07	7.03E-08					
0.57	3.32E-08	1.99E-08	3.40E-08	9.25E-09	5.00E-07	6.96E-07	7.93E-07	3.11E-07	6.6%	2.9%	4.3%	3.0%
0.58	1.14E-08	6.37E-09	4.18E-09	1.05E-09	8.90E-07	5.17E-07	2.82E-07	4.67E-08	1.3%	1.2%	1.5%	2.2%
0.67[2]	2.09E-08	9.01E-09	1.03E-08	1.45E-09	1.80E-06	9.86E-07	5.53E-07	5.66E-08	1.2%	0.9%	1.9%	2.6%
0.67[3]	5.28E-09	1.48E-09	3.94E-09		2.58E-07	2.79E-07	4.03E-07	6.05E-14	2.0%	0.5%	1.0%	
0.82[3]	5.44E-09	5.05E-10			5.96E-07	1.05E-07			0.9%	0.5%		
0.92[2]	1.20E-08	1.10E-09			1.41E-07	1.33E-07			8.5%	0.8%		
1.71[2]	6.98E-09	9.32E-09			1.50E-07	6.67E-07			4.7%	1.4%		
Group III												
0.71	1.98E-08	1.14E-08	2.56E-08	3.26E-09	7.03E-07	1.41E-06	8.01E-07	2.94E-08	2.8%	0.8%	3.2%	11.1%
1.12	1.26E-08	1.06E-08	2.11E-08	8.88E-09	4.39E-06	8.75E-07	8.28E-07	1.27E-07	0.3%	1.2%	2.5%	7.0%
1.16	1.47E-08	2.58E-08	3.67E-08	2.92E-09	7.83E-08	3.39E-06	1.60E-06	8.59E-08	18.8%	0.8%	2.3%	3.4%
1.4	1.61E-08		9.25E-08		9.26E-07	3.98E-06	3.55E-06		1.7%		2.6%	
1.44	2.40E-08	1.96E-08	6.07E-08	3.88E-09	1.46E-06	1.53E-06	1.13E-06	4.37E-08	1.6%	1.3%	5.4%	8.9%
1.63	5.48E-08	3.27E-08	4.18E-08	7.04E-09	3.07E-06	1.83E-06	8.49E-07	2.26E-08	1.8%	1.8%	4.9%	31.2%
1.64	9.07E-08	3.10E-08	5.59E-08	2.31E-08	1.34E-05	1.36E-06	1.19E-06	2.34E-07	0.7%	2.3%	4.7%	9.9%
Average	2.09E-08	1.12E-08	3.23E-08	6.02E-09	1.44E-06	9.17E-07	9.58E-07	9.06E-08	14.5%	7.7%	2.9%	7.8%

[1] Sample had no olivine by point count.

[2] AMAX and ARIMETCO samples originated from core drilled between 1974 and 1977 and were stored for at least 20 years prior to initiation.

[3] Dunka blast hole samples originated from a blast on August 30, 1989 at the Dunka Mine and were stored for 8 years prior to initiation.

Table 45. Regression results for calculated fraction of Ni from olivine versus percent sulfur in sample (data in Table 5). Periods A and B did not have a significant regression.

	slope	y-intercept	r^2
Period A			
Period B			
Period C	0.022	0.0074	0.463
Period D	0.120	-0.037	0.441

Table 46. Average sample weekly nickel release per mole olivine by time period. Blank cells indicate sample did not enter that time period.

%S	**Olivine (mol/sample)**	**mol Ni/mol olivine /week in leachate**			
		Period A	**Period B**	**Period C**	**Period D**
Group I					
0.18	0.044	1.27E-06	2.59E-07		
0.22	0.02	2.32E-06	5.13E-07		
0.72[1]	0.093	4.88E-08	6.54E-08		
Group II					
0.40	No ol				
0.41	0.056	1.25E-05	1.75E-05	1.77E-05	1.91E-06
0.51	0.026	2.13E-05	8.79E-06	3.72E-05	2.67E-06
0.54	No ol				
0.57	0.09	5.55E-06	7.74E-06	8.81E-06	3.46E-06
0.58	0.011	8.09E-05	4.70E-05	2.56E-05	4.25E-06
0.67[1]	0.073	2.47E-05	1.35E-05	7.58E-06	7.75E-07
0.67[2]	0.02	1.29E-05	1.40E-05	2.01E-05	
0.82[2]	0.015	3.97E-05	6.99E-06		
0.92[1]	0.168	8.37E-07	7.92E-07		
1.71[1]	0.086	1.74E-06	7.75E-06		
Group III					
0.71	0.064	1.10E-05	2.21E-05	1.25E-05	4.60E-07
1.12	0.018	2.44E-04	4.86E-05	4.60E-05	7.06E-06
1.16	0.073	1.07E-06	4.64E-05	2.19E-05	1.18E-06
1.4	0.026	3.56E-05	1.53E-04	1.37E-04	
1.44	0.026	5.62E-05	5.87E-05	4.34E-05	1.68E-06
1.63	0.024	1.28E-04	7.62E-05	3.54E-05	9.40E-07
1.64	0.014	9.54E-04	9.70E-05	8.49E-05	1.67E-05
Total Average		8.59E-05	3.30E-05	3.83E-05	3.73E-06

[1] AMAX and ARIMETCO samples originated from core drilled between 1974 and 1977 and were stored for at least 20 years prior to initiation.

[2] Dunka blast hole samples originated from a blast on August 30, 1989 at the Dunka Mine and were stored for 8 years prior to initiation.

Table 47. Regression results for average sample weekly nickel release per mole olivine (data in Table 7) by time period versus %S. Period D did not have a significant regression.

	slope	y-intercept	r^2
Period A	2.03E-4	-9.68E-5	0.200
Period B	5.39E-5	-1.54E-5	0.408
Period C	5.02E-5	-1.00E-5	0.393
Period D	4.20E-6	-2.50E-7	0.171

Table 48: Values used in the calculation of predicted mineral dissolution rates of mineral grains.

Mineral	Surface Roughness		Density	
	Coefficient	Source	ρ	Source
Labradorite	9.1	Brantley and Mellott, 2000	2.62+(%An * 0.0014)	Klein and Hurlbut, 1985
Andesine	11	Blum, A.E, 1994	2.62+(%An * 0.0014)	Klein and Hurlbut, 1985
Hypersthene	17	Sverdrup, 1990	3.25 + %$FeSiO_3$ * 0.006	Klein and Hurlbut, 1985
Olivine	12	Brantley and Mellott, 2000	3.27 + Fe_2SiO_4 * 0.012	Klein and Hurlbut, 1985
Augite	16	Average[3]	3.2 - 3.4 (3.3)[1]	Klein and Hurlbut, 1985
Biotite	17	Sverdrup, 1990	2.8 - 3.2 (3)[1]	Klein and Hurlbut, 1985
Amphibole	16	Brantley and Mellott, 2000	3.0 - 3.4[2] (3.2)[1]	Klein and Hurlbut, 1985
Orthoclase	5.8	Blum, A.E, 1994	2.57	Klein and Hurlbut, 1985
Prehnite	30	Rose, 1991	2.8 - 2.95 (2.88)[1]	Klein and Hurlbut, 1985

Note: Geometric Mean Grain Diameter (53 - 149um) = 89 microns

[1] Value in parentheses selected for calculation

[2] Range for Hornblende

[3] Average of values reported by Brantley and Mellott, 2000 (SR=14) and Brantley and Chen, 1995 (SR=18)

Table 49. Determination of mineral surface areas used for determining silicate mineral dissolution rates in models. Page 1 of 2.

%S	**Reactor**	**Plagioclase**				**K-Spar**				**Hypersthene**			
		SR = 9.1		**d = 0.0089 cm[1]**		**SR = 5.8**		**d = 0.0089 cm[1]**		**SR = 17.0**		**d = 0.0089 cm[1]**	
		Density	**Modal%**	**Mass**	**Area*SR (m^2)**	**Density**	**Modal%**	**Mass**	**Area*SR (m^2)**	**Density**	**Modal%**	**Mass**	**Area*SR (m^2)**
0.18	1	2.69	49.50	37.13	8.467	2.57				3.53	17.40	13.05	4.237
0.22	3	2.68	64.90	48.68	11.142	2.57	3.60	2.70	0.411	3.53	5.40	4.05	1.315
0.40	5	2.70	47.40	35.55	8.078	2.57	3.40	2.55	0.388	3.54	27.60	20.70	6.702
0.41	7	2.70	57.40	43.05	9.782	2.57	0.90	0.68	0.103	3.51	8.70	6.53	2.131
0.51	9	2.69	46.60	34.95	7.971	2.57	5.10	3.83	0.582	3.54	17.80	13.35	4.322
0.54	11	2.67	62.20	46.65	10.719	2.57				3.50	19.80	14.85	4.863
0.57	13	2.69	42.60	31.95	7.287	2.57	4.00	3.00	0.456	3.54	5.00	3.75	1.214
0.58	15	2.69	45.80	34.35	7.834	2.57	5.00	3.75	0.571	3.56	15.00	11.25	3.622
0.67	39	2.69	56.30	42.23	9.630	2.57	1.70	1.28	0.194	3.53	4.20	3.15	1.023
0.67	40	2.69	47.70	35.78	8.159	2.57	0.90	0.68	0.103	3.55	14.40	10.80	3.487
0.71	17	2.69	54.80	41.10	9.373	2.57	0.90	0.68	0.103	3.50	12.20	9.15	2.996
0.72	42	2.70	61.20	45.90	10.429	2.57				3.45	3.30	2.48	0.822
0.82	43	2.69	47.80	35.85	8.176	2.57				3.51	15.70	11.78	3.845
0.92	41	2.70	44.60	33.45	7.600	2.57				3.47	3.30	2.48	0.817
1.12	35	2.69	39.70	29.78	6.791	2.57	11.60	8.70	1.324	3.56	19.80	14.85	4.781
1.16	39	2.70	58.40	43.80	9.952	2.57				3.52	12.40	9.30	3.028
1.40	37	2.69	46.20	34.65	7.902	2.57	2.50	1.88	0.285	3.53	8.40	6.30	2.045
1.44	33	2.69	52.90	39.68	9.048	2.57	4.20	3.15	0.479	3.54	24.40	18.30	5.925
1.63	19	2.68	36.40	27.30	6.249	2.57	5.60	4.20	0.639	3.56	17.80	13.35	4.298
1.64	31	2.69	45.80	34.35	7.834	2.57	4.20	3.15	0.479	3.54	10.80	8.10	2.622
1.71	44	2.70	45.50	34.13	7.754	2.57	0.80	0.60	0.091	3.48	2.50	1.88	0.617
2.06	31	2.67	27.70	20.78	4.773	2.57	12.60	9.45	1.438	3.55	10.90	8.18	2.639
3.12	23	2.70	34.80	26.10	5.930	2.57	8.00	6.00	0.913	3.50	11.60	8.70	2.849
3.72	25	2.68	18.30	13.73	3.142	2.57	14.80	11.10	1.689	3.52	9.60	7.20	2.344
5.44	27	2.66	11.50	8.63	1.989	2.57	20.40	15.30	2.328	3.53			

[1] Geometric mean diameter

Table 49. Determination of mineral surface areas used for determining silicate mineral dissolution rates in models. Page 2 of 2.

%S	**Reactor**	**Augite**				**Olivine**				**Biotite**			
		SR = 16.0		**d = 0.0089 cm**[1]		**SR = 12.0**		**d = 0.0089 cm**[1]		**SR = 17.0**		**d = 0.0089 cm**[1]	
		Density	**Modal%**	**Mass**	**Area*SR (m^2)**	**Density**	**Modal%**	**Mass**	**Area*SR (m^2)**	**Density**	**Modal%**	**Mass**	**Area*SR (m^2)**
0.18	1	3.30	10.10	7.58	2.476	4.00	10.10	7.58	1.532	3.00	1.80	1.35	0.516
0.22	3	3.30	8.10	6.08	1.986	3.96	4.50	3.38	0.689	3.00	2.70	2.03	0.774
0.40	5	3.30	4.30	3.23	1.054					3.00	1.70	1.28	0.487
0.41	7	3.30	8.70	6.53	2.133	3.92	13.00	9.75	2.012				
0.51	9	3.30	7.60	5.70	1.863	3.98	5.90	4.43	0.899				
0.54	11	3.30	8.10	6.08	1.986					3.00	2.70	2.03	0.774
0.57	13	3.30	16.80	12.60	4.118	3.86	20.80	15.60	3.269				
0.58	15	3.30	14.20	10.65	3.481	4.00	2.50	1.88	0.379	3.00	0.80	0.60	0.229
0.67	39	3.30	14.30	10.73	3.506	3.89	16.80	12.60	2.620				
0.67	40	3.30	11.70	8.78	2.868	3.74	4.50	3.38	0.730	3.00	6.30	4.73	1.805
0.71	17	3.30	7.80	5.85	1.912	3.72	14.80	11.10	2.414	3.00	1.70	1.28	0.487
0.72	42	3.30	2.50	1.88	0.613	3.98	21.50	16.13	3.278				
0.82	43	3.30	13.00	9.75	3.187	3.83	3.50	2.63	0.554	3.00	3.50	2.63	1.003
0.92	41	3.30	4.10	3.08	1.005	3.89	38.80	29.10	6.052	3.00			
1.12	35	3.30	5.80	4.35	1.422	3.89	4.10	3.08	0.639	3.00	1.70	1.28	0.487
1.16	39	3.30	9.70	7.28	2.378	3.90	16.80	12.60	2.614				
1.40	37	3.30	11.80	8.85	2.893	3.56	5.90	4.43	1.006				
1.44	33	3.30	2.50	1.88	0.613	4.03	5.90	4.43	0.888	3.00	1.70	1.28	0.487
1.63	19	3.30	5.60	4.20	1.373	3.96	5.60	4.20	0.858	3.00	1.90	1.43	0.544
1.64	31	3.30	13.30	9.98	3.260	3.78	3.30	2.48	0.530	3.00	2.50	1.88	0.716
1.71	44	3.30	2.50	1.88	0.613	3.78	19.80	14.85	3.178	3.00	0.80	0.60	0.229
2.06	31	3.30	2.50	1.88	0.613	3.92	0.80	0.60	0.124	3.00	0.80	0.60	0.229
3.12	23	3.30	0.90	0.68	0.221					3.00	2.70	2.03	0.774
3.72	25	3.30	2.60	1.95	0.637					3.00	2.60	1.95	0.745
5.44	27									3.00	0.90	0.68	0.258

[1] Geometric mean diameter

Table 50. Determination of mineral surface areas used for determining sulfide mineral dissolution rates in models. Page 1 of 2.

Reactor	**Sulfide Mineral**			**Pentlandite** **d = 0.0089 cm^2, SR = 10[1]** **density = 4.8, ratio = 0.97[2]**			**Chalcopyrite** **d = 0.0089 cm^2, SR = 10[1]** **density = 4.19, ratio = 1.01[3]**		
	%S	**%Cu**	**%Ni**	**%**	**Mass (g)**	**SA (m^2)**	**%**	**Mass (g)**	**SA (m^2)**
1	0.18	0.136	0.0525	0.0509	0.0382	0.0054	0.1374	0.1030	0.0166
3	0.22	0.135	0.0484	0.0469	0.0352	0.0050	0.1364	0.1023	0.0165
5	0.4	0.0512	0.0231	0.0224	0.0168	0.0024	0.0517	0.0388	0.0062
7	0.41	0.0788	0.0511	0.0496	0.0372	0.0052	0.0796	0.0597	0.0096
9	0.51	0.143	0.0473	0.0459	0.0344	0.0048	0.1444	0.1083	0.0175
11	0.54	0.0211	0.0174	0.0169	0.0127	0.0018	0.0213	0.0160	0.0026
13	0.57	0.129	0.0398	0.0386	0.0290	0.0041	0.1303	0.0977	0.0157
15	0.58	0.13	0.0396	0.0384	0.0288	0.0041	0.1313	0.0985	0.0159
39	0.67	0.0617	0.0523	0.0507	0.0380	0.0054	0.0623	0.0467	0.0075
40	0.67	0.049	0.0523	0.0507	0.0380	0.0054	0.0495	0.0371	0.0060
17	0.71	0.116	0.0388	0.0376	0.0282	0.0040	0.1172	0.0879	0.0142
42	0.72	0.0517	0.0254	0.0246	0.0185	0.0026	0.0522	0.0392	0.0063
43	0.82	0.0601	0.0204	0.0198	0.0148	0.0021	0.0607	0.0455	0.0073
41	0.92	0.0752	0.0324	0.0314	0.0236	0.0033	0.0760	0.0570	0.0092
35	1.12	0.08	0.0324	0.0314	0.0236	0.0033	0.0808	0.0606	0.0098
29	1.16	0.109	0.0329	0.0319	0.0239	0.0034	0.1101	0.0826	0.0133
37	1.4	0.156	0.0503	0.0488	0.0366	0.0051	0.1576	0.1182	0.0190
33	1.44	0.121	0.0386	0.0374	0.0281	0.0040	0.1222	0.0917	0.0148
19	1.63	0.118	0.0492	0.0477	0.0358	0.0050	0.1192	0.0894	0.0144
20	1.63	0.118	0.0492	0.0477	0.0358	0.0050	0.1192	0.0894	0.0144
31	1.64	0.222	0.0718	0.0696	0.0522	0.0073	0.2242	0.1682	0.0271
44	1.71	0.066	0.0354	0.0343	0.0258	0.0036	0.0667	0.0500	0.0081

[1] Surface roughness factor of 10 in the lower range of those reported in Janzen 2000

[2] Pentlandite $(Fe, Ni)_9S_8$; Ni *4.5/S*8 = 264.11 / 256.56 = 0.97

[3] Chalcopyrite $(CuFe)S_2$; Cu/S*2 = 63.55 / 64.14 = 1.01

Table 50. Determination of mineral surface areas used for determining sulfide mineral dissolution rates in models. Page 2 of 2.

Reactor	**Sulfide Mineral**			**Cubanite** **d = 0.0089 cm2, SR = 10[1]** **density = 4.7, ratio = 1.51[2]**			**Pyrrhotite** **d = 0.0089 cm2, SR = 10[1]** **density = 4.61, ratio = 2.57[3]**			**Sulfide SA**
	%S	**%Cu**	**%Ni**	**%**	**Mass (g)**	**SA (m^2)**	**%**	**Mass (g)**	**SA (m^2)**	**m^2**
1	0.18	0.136	0.0525	0.2054	0.1540	0.0221	-0.0218	-0.0164	0.0000	0.0441
3	0.22	0.135	0.0484	0.2039	0.1529	0.0220	0.0941	0.0705	0.0103	0.0537
5	0.4	0.0512	0.0231	0.0773	0.0580	0.0083	0.8370	0.6278	0.0919	0.1089
7	0.41	0.0788	0.0511	0.1190	0.0892	0.0128	0.7199	0.5399	0.0791	0.1067
9	0.51	0.143	0.0473	0.2159	0.1619	0.0233	0.8216	0.6162	0.0903	0.1358
11	0.54	0.0211	0.0174	0.0319	0.0239	0.0034	1.2889	0.9666	0.1416	0.1494
13	0.57	0.129	0.0398	0.1948	0.1461	0.0210	1.0311	0.7733	0.1133	0.1541
15	0.58	0.13	0.0396	0.1963	0.1472	0.0211	1.0547	0.7910	0.1159	0.1569
39	0.67	0.0617	0.0523	0.0932	0.0699	0.0100	1.4289	1.0717	0.1570	0.1799
40	0.67	0.049	0.0523	0.0740	0.0555	0.0080	1.4616	1.0962	0.1605	0.1798
17	0.71	0.116	0.0388	0.1752	0.1314	0.0189	1.4269	1.0701	0.1567	0.1937
42	0.72	0.0517	0.0254	0.0781	0.0586	0.0084	1.6523	1.2392	0.1815	0.1988
43	0.82	0.0601	0.0204	0.0908	0.0681	0.0098	1.9005	1.4254	0.2088	0.2280
41	0.92	0.0752	0.0324	0.1136	0.0852	0.0122	2.0879	1.5659	0.2293	0.2541
35	1.12	0.08	0.0324	0.1208	0.0906	0.0130	2.5895	1.9421	0.2844	0.3105
29	1.16	0.109	0.0329	0.1646	0.1234	0.0177	2.6165	1.9624	0.2874	0.3218
37	1.4	0.156	0.0503	0.2356	0.1767	0.0254	3.0678	2.3009	0.3370	0.3866
33	1.44	0.121	0.0386	0.1827	0.1370	0.0197	3.2906	2.4680	0.3615	0.3999
19	1.63	0.118	0.0492	0.1782	0.1336	0.0192	3.7594	2.8195	0.4130	0.4516
20	1.63	0.118	0.0492	0.1782	0.1336	0.0192	3.7594	2.8195	0.4130	0.4516
31	1.64	0.222	0.0718	0.3352	0.2514	0.0361	3.4597	2.5948	0.3800	0.4506
44	1.71	0.066	0.0354	0.0997	0.0747	0.0107	4.1341	3.1006	0.4541	0.4765

[1] Surface roughness factor of 10 in the lower range of those reported in Janzen 2000

[2] Cubanite ($CuFe_2S_3$); Cu/S*3 = 63.55 / 96.21 = 1.51

[3] Pyrrhotite (Fe(0.9)S); ((0.9*Fe+S)/S) = (0.9*55.85+32.07)/32.07 = 2.57

Table 51. Maximum amount of plagioclase and olivine dissolution based on cumulative Ca and Mg release (Table 25) and sample stoichiometry (Table 11).

%S	**Reactor**	**Period of Record (weeks)**	**Minimum pH**	**Maximum plagioclase dissolution**		**Maximum olivine dissolution**	
				(mmol)	**(mol m^{-2} s^{-1})**	**(mmol)**	**(mol m^{-2} s^{-1})**
Group I, 3 samples							
0.18	**1**	1252	5.67	7.165	1.40E-09	2.649	2.85E-09
0.22	**3**	1252	5.91	8.833	1.31E-09	3.830	9.17E-09
0.72[1]	**42**	809	5.60	2.089	3.31E-10	0.646	3.26E-10
Average			5.73	6.029	1.01E-09	2.375	4.12E-09
Group II, 11 samples							
0.4	**5**	909	3.78	16.266	3.32E-09		
0.41	**7**	724	4.05	5.167	8.72E-10	1.652	1.36E-09
0.51	**9**	724	3.95	7.447	1.54E-09	2.110	3.87E-09
0.54	**11**	441	4.08	8.153	1.26E-09		
0.57	**13**	441	3.86	6.081	1.38E-09	2.593	1.31E-09
0.58	**15**	724	3.98	6.364	1.34E-09	2.873	1.25E-08
0.67[1]	**39**	809	4.22	2.403	4.12E-10	1.029	6.48E-10
0.67[2]	**40**	809	4.04	7.386	1.49E-09	1.934	4.37E-09
0.82[2]	**43**	809	4.49	3.312	6.69E-10	0.691	2.06E-09
0.92[1]	**41**	809	4.89	2.037	4.42E-10	0.439	1.20E-10
1.71[1]	**44**	144	5.06	2.881	6.13E-10	1.275	6.62E-10
Average			4.22	6.136	1.21E-09	1.622	2.99E-09
Group III, Duluth Complex, 7 samples							
0.71	**17**	724	3.53	5.954	1.05E-09	4.237	2.90E-09
1.12	**35**	360	3.23	12.361	3.01E-09	2.676	6.91E-09
1.16	**29**	643	3.24	6.556	1.09E-09	5.014	3.17E-09
1.4	**37**	360	4.03	7.168	1.50E-09	6.132	1.01E-08
1.44	**33**	643	3.04	7.532	1.37E-09	6.293	1.17E-08
1.63	**19**	724	3.32	11.983	3.17E-09	9.617	1.85E-08
1.64	**31**	360	3.38	9.263	1.95E-09	5.668	1.77E-08
Average			3.40	8.688	1.88E-09	5.663	1.01E-08
Virginia Formation, 4 samples							
2.06	21	78	4.20	5.014	1.73E-09	2.706	3.61E-08
3.12	23	78	3.70	6.574	1.83E-09		
3.72	25	78	3.70	7.004	3.68E-09		
5.44	27	78	3.35	9.639	8.00E-09		
Average			3.74	7.058	3.81E-09	2.706	3.61E-08

[1] AMAX and ARIMETCO samples originated from core drilled between 1974 and 1977 and were stored for at least 20 years prior to initiation.

[2] Dunka blast hole samples originated from a blast on August 30, 1989 at the Dunka Mine and were stored for 8 years prior to initiation.

Table 52. Model 1, Periods A-D Silicate Mineral Dissolution Rates. Page 1 of 4.

Model 1, Period A																		
R#	%S	N	Plag (mol $m^{-2}s^{-1}$)				Hyp (mol $m^{-2}s^{-1}$)				Ol (mol $m^{-2}s^{-1}$)				Bio (mol $m^{-2}s^{-1}$)			
			Ave	S.D.	Max	Min	Ave	S.D.	Max	Min	Ave	S.D.	Max	Min	Ave	S.D.	Max	Min
1	0.18	8	4.0E-12	1.4E-12	6.6E-12	2.5E-12	1.9E-12	7.4E-13	2.7E-12	2.7E-13	7.0E-12	2.7E-12	1.0E-11	9.9E-13	6.0E-12	2.3E-12	8.6E-12	8.5E-13
3	0.22	7	3.7E-12	1.7E-12	6.2E-12	1.7E-12	1.2E-11	1.2E-11	4.0E-11	2.6E-12	2.6E-11	2.8E-11	9.2E-11	5.9E-12	6.1E-12	6.5E-12	2.1E-11	1.4E-12
5	0.40	8	8.4E-12	2.6E-12	1.4E-11	6.2E-12	7.6E-13	5.1E-13	1.5E-12	1.8E-13					3.6E-12	2.4E-12	7.1E-12	8.4E-13
7	0.41	10	3.3E-12	2.0E-12	6.4E-12	7.0E-13	2.4E-12	1.2E-12	4.1E-12	5.2E-13	3.0E-12	1.5E-12	5.3E-12	6.6E-13	2.3E-12	1.2E-12	4.0E-12	5.0E-13
9	0.51	11	4.7E-12	4.1E-12	1.4E-11	5.4E-13	1.4E-12	9.6E-13	2.9E-12	2.8E-13	8.4E-12	5.6E-12	1.7E-11	1.6E-12	2.7E-12	1.8E-12	5.4E-12	5.1E-13
11	0.54	32	5.0E-12	2.5E-12	1.5E-11	1.7E-12	2.8E-12	2.6E-12	1.3E-11	2.2E-13					6.6E-12	6.0E-12	3.1E-11	5.0E-13
13	0.57	7	7.2E-12	4.5E-12	1.6E-11	2.4E-12	1.0E-11	3.4E-12	1.6E-11	5.2E-12	4.2E-12	1.4E-12	6.4E-12	2.1E-12				
15	0.58	7	5.3E-12	3.7E-12	1.3E-11	1.3E-12	4.7E-12	2.8E-12	9.1E-12	1.1E-12	5.0E-11	2.9E-11	9.5E-11	1.1E-11	3.2E-11	1.9E-11	6.2E-11	7.4E-12
39[1]	0.67	13	2.6E-12	1.8E-12	6.1E-12	5.8E-13	9.0E-12	2.8E-12	1.3E-11	3.8E-12	4.0E-12	1.2E-12	5.9E-12	1.7E-12				
40[2]	0.67	18	4.2E-12	1.4E-12	7.7E-12	8.7E-13	3.1E-12	1.1E-12	5.1E-12	1.1E-12	1.8E-11	6.3E-12	2.9E-11	6.3E-12	1.9E-12	6.9E-13	3.2E-12	6.8E-13
17	0.71	6	3.9E-12	1.6E-12	5.6E-12	1.8E-12	4.7E-12	2.0E-12	8.4E-12	2.9E-12	6.8E-12	2.9E-12	1.2E-11	4.1E-12	9.4E-12	4.0E-12	1.7E-11	5.8E-12
42[1]	0.72	12	1.8E-12	1.6E-12	6.7E-12	1.2E-12	3.3E-12	2.0E-12	7.2E-12	5.6E-13	8.6E-13	5.3E-13	1.9E-12	1.5E-13				
43[2]	0.82	17	3.8E-12	1.6E-12	7.5E-12	1.2E-12	1.4E-12	5.4E-13	2.1E-12	5.3E-13	1.4E-11	5.4E-12	2.2E-11	5.3E-12	2.3E-12	8.7E-13	3.5E-12	8.6E-13
41[1]	0.92	17	2.8E-12	1.0E-12	5.1E-12	1.0E-12	4.4E-12	2.3E-12	8.7E-12	6.3E-13	6.8E-13	3.5E-13	1.4E-12	9.7E-14				
35	1.12	27	1.3E-11	6.4E-12	2.5E-11	1.1E-12	1.7E-12	9.4E-13	4.4E-12	2.7E-13	1.2E-11	6.7E-12	3.2E-11	1.9E-12	4.7E-12	2.6E-12	1.2E-11	7.4E-13
29	1.16	10	4.2E-12	1.3E-12	6.5E-12	2.3E-12	3.7E-12	2.0E-12	7.1E-12	3.9E-13	4.7E-12	2.6E-12	9.1E-12	5.0E-13				
37	1.40	18	7.1E-12	2.9E-12	1.4E-11	2.9E-12	4.8E-12	2.7E-12	1.0E-11	5.8E-13	1.0E-11	5.9E-12	2.3E-11	1.3E-12				
33	1.44	16	5.4E-12	4.7E-12	1.4E-11	1.2E-12	2.1E-12	6.3E-13	3.3E-12	1.2E-12	1.6E-11	4.7E-12	2.4E-11	8.6E-12	7.3E-12	2.2E-12	1.1E-11	4.0E-12
19	1.63	22	8.7E-12	5.2E-12	2.0E-11	3.5E-12	8.1E-12	4.4E-12	2.0E-11	3.5E-12	5.3E-11	2.9E-11	1.3E-10	2.3E-11	1.9E-11	1.0E-11	4.7E-11	8.3E-12
31	1.64	12	1.5E-11	1.1E-11	4.1E-11	3.1E-12	1.5E-11	8.2E-12	3.4E-11	2.8E-12	8.8E-11	4.8E-11	2.0E-10	1.6E-11	1.6E-11	9.0E-12	3.8E-11	3.1E-12
44[1]	1.71	23	6.3E-12	2.0E-12	1.2E-11	2.9E-12	2.0E-11	9.0E-12	3.8E-11	3.3E-12	3.9E-12	1.8E-12	7.6E-12	6.6E-13	1.9E-11	8.9E-12	3.8E-11	3.3E-12
Summary			5.7E-12	3.1E-12	4.1E-11	5.4E-13	5.5E-12	3.0E-12	4.0E-11	1.8E-13	1.7E-11	9.6E-12	2.0E-10	9.7E-14	9.3E-12	5.2E-12	6.2E-11	5.0E-13

Note: N=number of experimental observations used to model dissolution rates.

Note: Zeroes indicate a calculated absence of dissolution. Blank cells indicate there was none of that mineral present in the sample.

[1] AMAX and ARIMETCO samples originated from core drilled between 1974 and 1977 and were stored for at least 20 years prior to initiation.

[2] Dunka blast hole samples originated from a blast on August 30, 1989 at the Dunka Mine and were stored for 8 years prior to initiation.

Table 52. Model 1, Periods A-D Silicate Mineral Dissolution Rates. Page 2 of 4.

Model 1, Period B																		
R#	%S	N	Plag (mol m^{-2}s^{-1})				Hyp (mol m^{-2}s^{-1})				Ol (mol m^{-2}s^{-1})				Bio (mol m^{-2}s^{-1})			
			Ave	S.D.	Max	Min	Ave	S.D.	Max	Min	Ave	S.D.	Max	Min	Ave	S.D.	Max	Min
1	0.18	189	7.7E-13	3.8E-13	3.0E-12	8.8E-14	5.3E-13	4.8E-13	2.1E-12	1.3E-13	2.0E-12	1.8E-12	7.6E-12	4.7E-13	1.7E-12	1.5E-12	6.5E-12	4.0E-13
3	0.22	191	7.0E-13	3.1E-13	2.1E-12	7.3E-14	2.6E-12	1.8E-12	1.1E-11	4.1E-13	6.0E-12	4.2E-12	2.4E-11	9.5E-13	1.4E-12	9.8E-13	5.7E-12	2.2E-13
5	0.40	133	2.7E-12	1.0E-12	6.4E-12	1.3E-12	1.9E-13	2.1E-13	1.5E-12	8.6E-14					9.1E-13	9.9E-13	6.9E-12	4.1E-13
7	0.41	52	6.1E-13	3.8E-13	2.4E-12	1.5E-13	1.3E-12	8.1E-13	4.3E-12	2.6E-13	1.6E-12	1.0E-12	5.4E-12	3.3E-13	1.2E-12	7.8E-13	4.1E-12	2.5E-13
9	0.51	33	7.5E-13	2.2E-13	1.3E-12	3.5E-13	8.2E-13	4.4E-13	2.4E-12	2.8E-13	4.7E-12	2.6E-12	1.4E-11	1.6E-12	1.5E-12	8.1E-13	4.4E-12	5.2E-13
11	0.54	37	1.9E-12	5.7E-13	3.2E-12	3.2E-13	8.1E-13	4.3E-13	2.0E-12	2.1E-13					1.9E-12	1.0E-12	4.7E-12	5.0E-13
13	0.57	45	1.5E-12	7.2E-13	3.5E-12	2.1E-13	5.8E-12	2.0E-12	1.4E-11	8.6E-13	2.4E-12	8.3E-13	5.7E-12	3.5E-13				
15	0.58	24	1.4E-12	4.8E-13	2.6E-12	1.9E-13	2.5E-12	8.0E-13	4.2E-12	3.5E-13	2.6E-11	8.4E-12	4.4E-11	3.7E-12	1.7E-11	5.5E-12	2.9E-11	2.4E-12
39[1]	0.67	16	5.4E-13	1.3E-13	7.3E-13	2.9E-13	3.9E-12	1.7E-12	7.6E-12	9.6E-13	1.7E-12	7.4E-13	3.4E-12	4.3E-13				
40[2]	0.67	56	2.4E-12	3.6E-13	3.4E-12	1.7E-12	9.1E-13	3.6E-13	1.7E-12	1.8E-13	5.2E-12	2.1E-12	9.7E-12	1.1E-12	5.7E-13	2.2E-13	1.0E-12	1.1E-13
17	0.71	39	6.4E-13	4.2E-13	2.5E-12	1.5E-13	2.1E-12	1.0E-12	6.6E-12	3.6E-13	3.0E-12	1.5E-12	9.5E-12	5.2E-13	4.1E-12	2.1E-12	1.3E-11	7.2E-13
42[1]	0.72	115	3.8E-13	2.1E-13	1.4E-12	5.6E-14	1.5E-12	1.0E-12	5.6E-12	5.4E-13	3.9E-13	2.7E-13	1.5E-12	1.4E-13				
43[2]	0.82	114	7.2E-13	5.4E-13	2.4E-12	8.0E-14	1.6E-13	8.1E-14	5.6E-13	3.3E-14	1.6E-12	8.2E-13	5.6E-12	3.3E-13	2.6E-13	1.3E-13	9.0E-13	5.4E-14
41[1]	0.92	114	4.3E-13	2.9E-13	1.4E-12	2.1E-14	6.7E-13	2.4E-13	2.5E-12	1.5E-13	1.0E-13	3.7E-14	3.9E-13	2.4E-14				
35	1.12	23	3.8E-12	7.9E-13	5.3E-12	2.4E-12	2.2E-12	5.8E-13	3.3E-12	1.1E-12	1.6E-11	4.1E-12	2.4E-11	7.7E-12	6.0E-12	1.6E-12	9.0E-12	2.9E-12
29	1.16	37	1.1E-12	7.7E-13	4.1E-12	4.3E-13	3.1E-12	1.2E-12	7.8E-12	1.9E-12	4.0E-12	1.6E-12	9.9E-12	2.4E-12				
37	1.40	35	2.1E-12	7.9E-13	4.8E-12	1.1E-12	7.1E-12	1.4E-12	9.2E-12	2.9E-12	1.5E-11	3.0E-12	2.0E-11	6.3E-12				
33	1.44	34	1.2E-12	3.9E-13	2.7E-12	5.1E-13	1.8E-12	4.7E-13	2.7E-12	9.4E-13	1.3E-11	3.5E-12	2.0E-11	7.0E-12	6.3E-12	1.7E-12	9.5E-12	3.3E-12
19	1.63	8	3.1E-12	2.6E-12	9.3E-12	1.5E-12	4.6E-12	5.8E-13	5.4E-12	3.6E-12	3.0E-11	3.8E-12	3.5E-11	2.3E-11	1.1E-11	1.4E-12	1.3E-11	8.4E-12
31	1.64	40	2.6E-12	6.5E-13	4.3E-12	1.7E-12	5.9E-12	1.5E-12	9.3E-12	2.8E-12	3.4E-11	8.5E-12	5.4E-11	1.6E-11	6.4E-12	1.6E-12	1.0E-11	3.1E-12
44[1]	1.71	17	1.4E-12	3.7E-13	2.4E-12	8.4E-13	2.4E-11	3.5E-12	2.9E-11	1.6E-11	4.8E-12	7.1E-13	5.8E-12	3.3E-12	2.4E-11	3.5E-12	2.9E-11	1.6E-11
Summary			1.5E-12	5.9E-13	9.3E-12	2.1E-14	3.4E-12	9.8E-13	2.9E-11	3.3E-14	9.1E-12	2.6E-12	5.4E-11	2.4E-14	5.6E-12	1.6E-12	2.9E-11	5.4E-14

Note: N=number of experimental observations used to model dissolution rates.

Note: Zeroes indicate a calculated absence of dissolution. Blank cells indicate there was none of that mineral present in the sample.

[1] AMAX and ARIMETCO samples originated from core drilled between 1974 and 1977 and were stored for at least 20 years prior to initiation.

[2] Dunka blast hole samples originated from a blast on August 30, 1989 at the Dunka Mine and were stored for 8 years prior to initiation.

Table 52. Model 1, Periods A-D Silicate Mineral Dissolution Rates. Page 3 of 4.

Model 1, Period C																						
R#	%S	N	Aug (mol m^{-2}s^{-1})				Hyp (mol m^{-2}s^{-1})				Ol (mol m^{-2}s^{-1})				Bio (mol m^{-2}s^{-1})				Orphan Ca (mol m^{-2}s^{-1})			
			Ave	S.D.	Max	Min	Ave	S.D.	Max	Min	Ave	S.D.	Max	Min	Ave	S.D.	Max	Min	Ave	S.D.	Max	Min
5	0.40	21	1.5E-12	2.4E-12	7.0E-12	0.0E+00	8.1E-14	6.3E-14	2.1E-13	0.0E+00					3.9E-13	3.0E-13	1.0E-12	0.0E+00	7.2E-13	1.8E-12	6.3E-12	0.0E+00
7	0.41	22	1.4E-12	7.6E-13	3.1E-12	2.3E-13	2.2E-12	1.8E-12	6.8E-12	0.0E+00	2.8E-12	2.2E-12	8.6E-12	0.0E+00	2.1E-12	1.7E-12	6.5E-12	0.0E+00	3.3E-13	8.4E-13	3.4E-12	0.0E+00
9	0.51	29	3.1E-12	1.4E-12	7.4E-12	4.6E-13	7.1E-13	5.8E-13	2.0E-12	0.0E+00	4.1E-12	3.4E-12	1.2E-11	0.0E+00	1.3E-12	1.1E-12	3.6E-12	0.0E+00	1.1E-12	2.2E-12	8.1E-12	0.0E+00
11	0.54	40	1.0E-13	3.0E-13	1.5E-12	0.0E+00	2.6E-13	2.6E-13	1.1E-12	0.0E+00					6.1E-13	6.1E-13	2.6E-12	0.0E+00	8.2E-14	2.8E-13	1.3E-12	0.0E+00
13	0.57	14	1.0E-12	6.9E-13	2.6E-12	1.6E-13	8.3E-12	4.8E-12	2.1E-11	3.1E-12	3.4E-12	2.0E-12	8.5E-12	1.3E-12					0.0E+00	0.0E+00	0.0E+00	0.0E+00
15	0.58	30	6.1E-13	7.6E-13	2.9E-12	0.0E+00	2.1E-12	9.2E-13	3.9E-12	6.5E-13	2.2E-11	9.7E-12	4.1E-11	6.8E-12	1.4E-11	6.3E-12	2.7E-11	4.4E-12	0.0E+00	0.0E+00	0.0E+00	0.0E+00
39[1]	0.67	21	2.8E-13	1.6E-13	5.7E-13	5.1E-14	4.4E-12	1.1E-12	6.1E-12	2.0E-12	1.9E-12	4.9E-13	2.7E-12	8.8E-13					0.0E+00	0.0E+00	0.0E+00	0.0E+00
40[2]	0.67	10	6.6E-14	2.0E-13	6.4E-13	0.0E+00	2.1E-12	6.5E-13	2.8E-12	8.5E-13	1.2E-11	3.7E-12	1.6E-11	4.9E-12	1.3E-12	4.1E-13	1.7E-12	5.3E-13	0.0E+00	0.0E+00	0.0E+00	0.0E+00
17	0.71	38	3.3E-12	3.1E-12	1.6E-11	0.0E+00	4.8E-12	4.1E-12	1.6E-11	1.4E-13	7.0E-12	6.0E-12	2.3E-11	2.0E-13	9.7E-12	8.3E-12	3.3E-11	2.8E-13	0.0E+00	0.0E+00	0.0E+00	0.0E+00
35	1.12	33	6.4E-12	6.1E-12	1.7E-11	0.0E+00	2.0E-12	7.6E-13	3.8E-12	7.8E-13	1.4E-11	5.4E-12	2.7E-11	5.5E-12	5.5E-12	2.1E-12	1.0E-11	2.1E-12	0.0E+00	0.0E+00	0.0E+00	0.0E+00
29	1.16	48	3.9E-12	3.1E-12	1.1E-11	0.0E+00	6.2E-12	3.1E-12	1.3E-11	0.0E+00	8.0E-12	4.0E-12	1.7E-11	0.0E+00					1.5E-14	1.0E-13	7.0E-13	0.0E+00
37	1.40	38	3.5E-12	2.6E-12	8.0E-12	0.0E+00	1.7E-11	7.5E-12	3.1E-11	3.4E-12	3.8E-11	1.6E-11	6.8E-11	7.5E-12					0.0E+00	0.0E+00	0.0E+00	0.0E+00
33	1.44	57	1.8E-11	1.6E-11	4.8E-11	0.0E+00	3.2E-12	1.8E-12	7.1E-12	5.5E-13	2.4E-11	1.3E-11	5.3E-11	4.1E-12	1.1E-11	6.2E-12	2.5E-11	1.9E-12	0.0E+00	0.0E+00	0.0E+00	0.0E+00
19	1.63	64	4.7E-12	4.4E-12	1.7E-11	0.0E+00	4.9E-12	1.5E-12	8.2E-12	3.1E-13	3.2E-11	1.0E-11	5.3E-11	2.0E-12	1.1E-11	3.6E-12	1.9E-11	7.3E-13	0.0E+00	0.0E+00	0.0E+00	0.0E+00
31	1.64	28	2.2E-12	1.5E-12	5.3E-12	2.6E-13	7.4E-12	1.9E-12	1.1E-11	4.0E-12	4.3E-11	1.1E-11	6.7E-11	2.4E-11	8.2E-12	2.1E-12	1.3E-11	4.4E-12	0.0E+00	0.0E+00	0.0E+00	0.0E+00
Summary			3.3E-12	2.9E-12	4.8E-11	0.0E+00	4.4E-12	2.1E-12	3.1E-11	0.0E+00	1.6E-11	6.7E-12	6.8E-11	0.0E+00	6.0E-12	3.0E-12	3.3E-11	0.0E+00	1.5E-13	3.5E-13	8.1E-12	0.0E+00

Note: For this period, model assumptions dictate plagioclase dissolution rates to be the same as Period B averages for each sample.

Note: N=number of experimental observations used to model dissolution rates.

Note: Zeroes indicate a calculated absence of dissolution. Blank cells indicate there was none of that mineral present in the sample.

[1] AMAX and ARIMETCO samples originated from core drilled between 1974 and 1977 and were stored for at least 20 years prior to initiation.

[2] Dunka blast hole samples originated from a blast on August 30, 1989 at the Dunka Mine and were stored for 8 years prior to initiation.

Table 52. Model 1, Periods A-D Silicate Mineral Dissolution Rates. Page 4 of 4.

Model 1, Period D																		
R#	%S	N	Plag (mol $m^{-2}s^{-1}$)				Hyp (mol $m^{-2}s^{-1}$)				Ol (mol $m^{-2}s^{-1}$)				Bio (mol $m^{-2}s^{-1}$)			
			Ave	S.D.	Max	Min	Ave	S.D.	Max	Min	Ave	S.D.	Max	Min	Ave	S.D.	Max	Min
5	0.40	9	1.1E-12	2.6E-13	1.6E-12	6.4E-13	8.9E-14	9.3E-16	9.1E-14	8.8E-14					4.2E-13	4.4E-15	4.3E-13	4.2E-13
7	0.41	54	6.7E-13	2.1E-13	1.4E-12	3.6E-13	5.6E-13	5.6E-13	2.6E-12	2.4E-13	7.1E-13	7.1E-13	3.3E-12	3.1E-13	5.4E-13	5.4E-13	2.5E-12	2.3E-13
9	0.51	66	1.2E-12	5.6E-13	3.9E-12	5.6E-13	3.5E-13	3.9E-13	1.7E-12	1.3E-13	2.0E-12	2.2E-12	9.7E-12	7.7E-13	6.4E-13	7.1E-13	3.1E-12	2.4E-13
13	0.57	21	1.9E-12	4.1E-13	2.5E-12	1.2E-12	3.4E-12	1.7E-12	7.0E-12	4.4E-13	1.4E-12	7.0E-13	2.9E-12	1.8E-13				
15	0.58	80	1.2E-12	4.3E-13	2.8E-12	6.5E-13	3.9E-13	3.8E-13	1.7E-12	1.6E-13	4.1E-12	4.0E-12	1.8E-11	1.7E-12	2.7E-12	2.6E-12	1.2E-11	1.1E-12
39[1]	0.67	80	3.9E-13	2.2E-13	8.5E-13	6.7E-14	7.4E-13	6.1E-13	2.9E-12	1.2E-13	3.3E-13	2.7E-13	1.3E-12	5.2E-14				
40[2]	0.67	44	8.4E-13	4.6E-13	1.9E-12	1.9E-13	2.8E-13	2.2E-13	1.2E-12	1.2E-13	1.6E-12	1.3E-12	6.8E-12	7.1E-13	1.8E-13	1.4E-13	7.4E-13	7.7E-14
17	0.71	58	9.1E-13	2.6E-13	1.6E-12	4.5E-13	6.7E-13	6.4E-13	2.8E-12	1.8E-13	9.7E-13	9.2E-13	4.1E-12	2.5E-13	1.3E-12	1.3E-12	5.7E-12	3.5E-13
35	1.12	3	2.6E-12	2.6E-13	2.8E-12	2.3E-12	1.9E-12	2.9E-13	2.2E-12	1.6E-12	1.4E-11	2.1E-12	1.6E-11	1.1E-11	5.2E-12	8.0E-13	6.0E-12	4.4E-12
29	1.16	47	8.8E-13	2.2E-13	1.5E-12	5.4E-13	7.5E-13	7.6E-13	3.4E-12	1.8E-13	9.5E-13	9.7E-13	4.3E-12	2.4E-13				
33	1.44	32	8.7E-13	1.5E-13	1.5E-12	5.8E-13	5.1E-13	2.3E-13	1.1E-12	9.2E-14	3.8E-12	1.7E-12	8.2E-12	6.9E-13	1.8E-12	7.9E-13	3.9E-12	3.2E-13
19	1.63	62	2.0E-12	8.7E-13	4.6E-12	9.9E-13	1.1E-12	8.6E-13	3.5E-12	1.3E-13	7.0E-12	5.6E-12	2.3E-11	8.5E-13	2.5E-12	2.0E-12	8.3E-12	3.1E-13
31	1.64	5	2.9E-12	4.2E-13	3.6E-12	2.6E-12	4.1E-12	8.6E-13	5.5E-12	3.2E-12	2.4E-11	5.0E-12	3.2E-11	1.8E-11	4.5E-12	9.5E-13	6.0E-12	3.5E-12
Summary			1.3E-12	3.6E-13	4.6E-12	6.7E-14	1.1E-12	5.8E-13	7.0E-12	8.8E-14	5.0E-12	2.1E-12	3.2E-11	5.2E-14	2.0E-12	9.9E-13	1.2E-11	7.7E-14

Note: N=number of experimental observations used to model dissolution rates.

Note: Zeroes indicate a calculated absence of dissolution. Blank cells indicate there was none of that mineral present in the sample.

[1] AMAX and ARIMETCO samples originated from core drilled between 1974 and 1977 and were stored for at least 20 years prior to initiation.

[2] Dunka blast hole samples originated from a blast on August 30, 1989 at the Dunka Mine and were stored for 8 years prior to initiation.

Table 53. Model 2, Periods A-D Silicate Mineral Dissolution Rates. Page 1 of 4.

Model 2, Period A																						
R#	%S	N	Aug (mol $m^{-2}s^{-1}$)				Plag (mol $m^{-2}s^{-1}$)				Hyp (mol $m^{-2}s^{-1}$)				Ol (mol $m^{-2}s^{-1}$)				Bio (mol $m^{-2}s^{-1}$)			
			Ave	S.D.	Max	Min	Ave	S.D.	Max	Min	Ave	S.D.	Max	Min	Ave	S.D.	Max	Min	Ave	S.D.	Max	Min
1	0.18	8	4.4E-12	1.8E-12	6.5E-12	6.4E-13	1.9E-12	1.2E-12	3.4E-12	0.0E+00	3.5E-14	9.8E-14	2.8E-13	0.0E+00	1.3E-13	3.6E-13	1.0E-12	0.0E+00	1.1E-13	3.1E-13	8.8E-13	0.0E+00
3	0.22	7	7.7E-12	4.9E-12	1.6E-11	2.5E-12	1.2E-12	1.2E-12	3.0E-12	0.0E+00	3.6E-12	9.0E-12	2.4E-11	0.0E+00	8.2E-12	2.1E-11	5.5E-11	0.0E+00	1.9E-12	4.8E-12	1.3E-11	0.0E+00
5	0.40	8	1.9E-11	1.3E-11	4.2E-11	3.0E-12	5.5E-12	4.1E-12	1.3E-11	2.1E-12	0.0E+00	0.0E+00	0.0E+00	0.0E+00					0.0E+00	0.0E+00	0.0E+00	0.0E+00
7	0.41	10	4.7E-12	2.4E-12	8.5E-12	7.8E-13	2.6E-12	1.9E-12	4.9E-12	0.0E+00	1.8E-14	4.8E-14	1.3E-13	0.0E+00	2.3E-14	6.1E-14	1.6E-13	0.0E+00	1.8E-14	4.6E-14	1.2E-13	0.0E+00
9	0.51	11	5.1E-12	5.0E-12	1.8E-11	8.9E-13	3.4E-12	3.7E-12	1.1E-11	1.2E-13	0.0E+00	0.0E+00	0.0E+00	0.0E+00	0.0E+00	0.0E+00	0.0E+00	0.0E+00	0.0E+00	0.0E+00	0.0E+00	0.0E+00
11	0.54	32	8.9E-12	5.6E-12	2.1E-11	7.5E-13	3.1E-12	2.1E-12	9.8E-12	0.0E+00	4.5E-13	1.7E-12	8.4E-12	0.0E+00					1.1E-12	3.9E-12	2.0E-11	0.0E+00
13	0.57	7	4.2E-12	1.7E-12	7.3E-12	2.4E-12	3.2E-12	3.3E-12	9.4E-12	0.0E+00	6.1E-13	1.1E-12	2.9E-12	0.0E+00	2.5E-13	4.6E-13	1.2E-12	0.0E+00				
15	0.58	7	5.6E-12	3.7E-12	1.3E-11	1.5E-12	1.4E-12	1.5E-12	4.2E-12	0.0E+00	2.5E-13	6.7E-13	1.8E-12	0.0E+00	2.7E-12	7.1E-12	1.9E-11	0.0E+00	1.7E-12	4.6E-12	1.2E-11	0.0E+00
39[1]	0.67	13	3.6E-12	1.8E-12	6.9E-12	1.1E-12	8.5E-13	1.1E-12	3.0E-12	0.0E+00	1.8E-12	2.6E-12	7.7E-12	0.0E+00	7.9E-13	1.1E-12	3.4E-12	0.0E+00				
40[2]	0.67	18	5.2E-12	2.0E-12	8.8E-12	1.5E-12	1.3E-12	8.0E-13	2.7E-12	0.0E+00	3.4E-14	1.0E-13	4.1E-13	0.0E+00	1.9E-13	6.0E-13	2.3E-12	0.0E+00	2.1E-14	6.5E-14	2.5E-13	0.0E+00
17	0.71	6	8.6E-12	2.2E-12	1.1E-11	5.7E-12	1.1E-12	1.2E-12	3.1E-12	0.0E+00	2.2E-13	4.2E-13	1.0E-12	0.0E+00	3.3E-13	6.1E-13	1.5E-12	0.0E+00	4.5E-13	8.4E-13	2.1E-12	0.0E+00
42[1]	0.72	12	6.8E-12	4.2E-12	1.5E-11	1.2E-12	1.3E-12	1.5E-12	6.0E-12	5.0E-13	0.0E+00	0.0E+00	0.0E+00	0.0E+00	0.0E+00	0.0E+00	0.0E+00	0.0E+00				
43[2]	0.82	17	2.7E-12	1.1E-12	4.2E-12	1.0E-12	2.1E-12	1.4E-12	5.3E-12	0.0E+00	3.4E-14	1.4E-13	5.8E-13	0.0E+00	3.4E-13	1.4E-12	5.9E-12	0.0E+00	5.6E-14	2.3E-13	9.4E-13	0.0E+00
41[1]	0.92	17	5.2E-12	2.6E-12	1.1E-11	7.9E-13	1.8E-12	1.1E-12	3.8E-12	0.0E+00	2.6E-13	1.1E-12	4.5E-12	0.0E+00	4.1E-14	1.7E-13	7.0E-13	0.0E+00				
35	1.12	27	1.0E-11	8.6E-12	3.9E-11	1.4E-12	1.0E-11	5.8E-12	2.3E-11	0.0E+00	1.4E-13	5.1E-13	2.0E-12	0.0E+00	1.0E-12	3.6E-12	1.5E-11	0.0E+00	3.9E-13	1.4E-12	5.6E-12	0.0E+00
29	1.16	10	6.7E-12	3.4E-12	1.3E-11	7.0E-13	2.0E-12	1.4E-12	4.4E-12	3.7E-14	0.0E+00	0.0E+00	0.0E+00	0.0E+00	0.0E+00	0.0E+00	0.0E+00	0.0E+00				
37	1.40	18	5.1E-12	2.8E-12	1.1E-11	5.8E-13	4.7E-12	3.5E-12	1.2E-11	0.0E+00	2.3E-13	6.2E-13	1.9E-12	0.0E+00	5.0E-13	1.4E-12	4.2E-12	0.0E+00				
33	1.44	16	2.2E-11	9.7E-12	4.3E-11	1.1E-11	4.1E-12	4.1E-12	1.2E-11	0.0E+00	3.6E-13	6.4E-13	1.5E-12	0.0E+00	2.6E-12	4.8E-12	1.1E-11	0.0E+00	1.2E-12	2.2E-12	5.2E-12	0.0E+00
19	1.63	22	1.8E-11	9.9E-12	4.1E-11	7.7E-12	3.9E-13	9.9E-13	4.2E-12	0.0E+00	3.6E-12	4.6E-12	1.8E-11	0.0E+00	2.4E-11	3.0E-11	1.2E-10	0.0E+00	8.5E-12	1.1E-11	4.2E-11	0.0E+00
31	1.64	12	1.6E-11	1.0E-11	4.0E-11	3.2E-12	4.2E-12	4.8E-12	1.3E-11	0.0E+00	1.2E-12	2.1E-12	6.0E-12	0.0E+00	6.9E-12	1.2E-11	3.5E-11	0.0E+00	1.3E-12	2.3E-12	6.6E-12	0.0E+00
44[1]	1.71	23	2.9E-11	1.3E-11	5.0E-11	5.3E-12	3.1E-12	2.1E-12	6.1E-12	0.0E+00	1.2E-12	3.0E-12	1.0E-11	0.0E+00	2.5E-13	6.1E-13	2.0E-12	0.0E+00	1.2E-12	3.0E-12	9.9E-12	0.0E+00
Summary			9.5E-12	5.2E-12	5.0E-11	5.8E-13	2.8E-12	2.3E-12	2.3E-11	0.0E+00	6.7E-13	1.4E-12	2.4E-11	0.0E+00	2.5E-12	4.5E-12	1.2E-10	0.0E+00	1.2E-12	2.3E-12	4.2E-11	0.0E+00

Note: N=number of experimental observations used to model dissolution rates.

Note: Zeroes indicate a calculated absence of dissolution. Blank cells indicate there was none of that mineral present in the sample.

[1] AMAX and ARIMETCO samples originated from core drilled between 1974 and 1977 and were stored for at least 20 years prior to initiation.

[2] Dunka blast hole samples originated from a blast on August 30, 1989 at the Dunka Mine and were stored for 8 years prior to initiation.

Table 53. Model 2, Periods A-D Silicate Mineral Dissolution Rates. Page 2 of 4.

Model 2, Period B																						
R#	%S	N	Aug (mol m^{-2}s^{-1})				Plag (mol m^{-2}s^{-1})				Hyp (mol m^{-2}s^{-1})				Ol (mol m^{-2}s^{-1})				Bio (mol m^{-2}s^{-1})			
			Ave	S.D.	Max	Min	Ave	S.D.	Max	Min	Ave	S.D.	Max	Min	Ave	S.D.	Max	Min	Ave	S.D.	Max	Min
1	0.18	189	1.0E-12	7.6E-13	3.9E-12	1.8E-13	2.7E-13	3.2E-13	2.7E-12	0.0E+00	1.0E-13	2.6E-13	1.3E-12	0.0E+00	3.9E-13	9.7E-13	4.9E-12	0.0E+00	3.3E-13	8.3E-13	4.2E-12	0.0E+00
3	0.22	191	1.8E-12	9.1E-13	6.1E-12	2.2E-13	1.2E-13	2.4E-13	1.9E-12	0.0E+00	7.2E-13	1.2E-12	8.3E-12	0.0E+00	1.7E-12	2.8E-12	1.9E-11	0.0E+00	3.9E-13	6.5E-13	4.4E-12	0.0E+00
5	0.40	133	3.4E-12	3.3E-12	1.5E-11	1.5E-12	2.0E-12	1.1E-12	6.1E-12	0.0E+00	1.3E-14	8.2E-14	8.6E-13	0.0E+00					6.0E-14	3.9E-13	4.1E-12	0.0E+00
7	0.41	52	1.4E-12	8.5E-13	5.3E-12	3.9E-13	1.7E-13	3.4E-13	1.9E-12	0.0E+00	3.6E-13	5.7E-13	2.3E-12	0.0E+00	4.6E-13	7.2E-13	2.9E-12	0.0E+00	3.5E-13	5.4E-13	2.2E-12	0.0E+00
9	0.51	33	1.8E-12	5.4E-13	2.8E-12	9.1E-13	9.2E-14	1.5E-13	5.9E-13	0.0E+00	2.7E-13	4.8E-13	2.1E-12	0.0E+00	1.5E-12	2.8E-12	1.2E-11	0.0E+00	4.9E-13	8.8E-13	3.8E-12	0.0E+00
11	0.54	37	2.9E-12	1.7E-12	8.4E-12	7.5E-13	1.2E-12	5.9E-13	2.6E-12	0.0E+00	1.2E-14	5.3E-14	2.9E-13	0.0E+00					2.8E-14	1.2E-13	6.7E-13	0.0E+00
13	0.57	45	1.6E-12	7.1E-13	3.7E-12	2.2E-13	3.4E-14	1.2E-13	6.3E-13	0.0E+00	2.4E-12	1.7E-12	8.3E-12	0.0E+00	9.8E-13	7.0E-13	3.4E-12	0.0E+00				
15	0.58	24	2.0E-12	7.8E-13	3.9E-12	2.8E-13	4.0E-14	2.0E-13	9.7E-13	0.0E+00	1.1E-12	5.4E-13	2.0E-12	0.0E+00	1.1E-11	5.6E-12	2.1E-11	0.0E+00	7.5E-12	3.7E-12	1.4E-11	0.0E+00
39[1]	0.67	16	1.0E-12	2.9E-13	1.4E-12	5.0E-13	2.0E-14	8.0E-14	3.2E-13	0.0E+00	2.0E-12	1.8E-12	6.6E-12	0.0E+00	8.7E-13	7.7E-13	2.9E-12	0.0E+00				
40[2]	0.67	56	1.6E-12	6.2E-13	2.9E-12	3.2E-13	1.5E-12	3.3E-13	2.2E-12	1.0E-12	0.0E+00	0.0E+00	0.0E+00	0.0E+00	0.0E+00	0.0E+00	0.0E+00	0.0E+00	0.0E+00	0.0E+00	0.0E+00	0.0E+00
17	0.71	39	2.0E-12	1.2E-12	7.8E-12	4.8E-13	1.7E-14	1.0E-13	6.4E-13	0.0E+00	1.2E-12	8.1E-13	3.4E-12	0.0E+00	1.7E-12	1.2E-12	5.0E-12	0.0E+00	2.4E-12	1.6E-12	6.9E-12	0.0E+00
42[1]	0.72	115	2.9E-12	1.8E-12	9.3E-12	7.6E-13	1.7E-13	1.6E-13	8.8E-13	0.0E+00	6.6E-14	3.1E-13	1.9E-12	0.0E+00	1.8E-14	8.1E-14	5.0E-13	0.0E+00				
43[2]	0.82	114	3.0E-13	1.7E-13	1.1E-12	6.5E-14	5.4E-13	4.9E-13	2.0E-12	0.0E+00	6.2E-15	1.8E-14	6.1E-14	0.0E+00	6.3E-14	1.8E-13	6.2E-13	0.0E+00	1.0E-14	3.0E-14	9.9E-14	0.0E+00
41[1]	0.92	114	8.1E-13	4.7E-13	3.5E-12	1.1E-13	2.8E-13	2.5E-13	1.2E-12	0.0E+00	6.2E-14	1.1E-13	2.7E-13	0.0E+00	9.7E-15	1.7E-14	4.2E-14	0.0E+00				
35	1.12	23	9.4E-12	2.0E-12	1.3E-11	5.4E-12	4.9E-13	6.5E-13	1.9E-12	0.0E+00	2.8E-13	3.5E-13	1.3E-12	0.0E+00	2.0E-12	2.5E-12	9.2E-12	0.0E+00	7.7E-13	9.6E-13	3.5E-12	0.0E+00
29	1.16	37	2.9E-12	2.1E-12	1.1E-11	1.2E-12	0.0E+00	0.0E+00	0.0E+00	0.0E+00	1.5E-12	6.5E-13	3.2E-12	2.2E-14	1.9E-12	8.3E-13	4.0E-12	2.8E-14				
37	1.40	35	3.4E-12	1.1E-12	5.5E-12	1.9E-12	9.6E-14	5.5E-13	3.2E-12	0.0E+00	3.6E-12	1.3E-12	6.8E-12	0.0E+00	8.0E-12	2.9E-12	1.5E-11	0.0E+00				
33	1.44	34	1.0E-11	2.6E-12	1.8E-11	4.7E-12	4.2E-14	2.2E-13	1.3E-12	0.0E+00	1.1E-12	4.9E-13	2.1E-12	0.0E+00	7.8E-12	3.7E-12	1.6E-11	0.0E+00	3.7E-12	1.7E-12	7.4E-12	0.0E+00
19	1.63	8	6.7E-12	5.8E-12	2.0E-11	3.2E-12	0.0E+00	0.0E+00	0.0E+00	0.0E+00	3.1E-12	1.3E-12	4.4E-12	3.2E-13	2.0E-11	8.7E-12	2.9E-11	2.1E-12	7.4E-12	3.2E-12	1.0E-11	7.6E-13
31	1.64	40	3.6E-12	8.1E-13	5.5E-12	2.4E-12	6.3E-14	2.3E-13	1.0E-12	0.0E+00	2.8E-12	1.4E-12	5.0E-12	0.0E+00	1.6E-11	8.1E-12	2.9E-11	0.0E+00	3.0E-12	1.5E-12	5.5E-12	0.0E+00
44[1]	1.71	17	1.3E-11	3.4E-12	2.2E-11	7.7E-12	0.0E+00	0.0E+00	0.0E+00	0.0E+00	1.6E-11	2.8E-12	2.1E-11	8.4E-12	3.1E-12	5.5E-13	4.1E-12	1.7E-12	1.5E-11	2.7E-12	2.0E-11	8.2E-12
Summary			3.5E-12	1.5E-12	2.2E-11	6.5E-14	3.4E-13	2.9E-13	6.1E-12	0.0E+00	1.7E-12	7.7E-13	2.1E-11	0.0E+00	4.1E-12	2.3E-12	2.9E-11	0.0E+00	2.8E-12	1.3E-12	2.0E-11	0.0E+00

Note: N=number of experimental observations used to model dissolution rates.

Note: Zeroes indicate a calculated absence of dissolution. Blank cells indicate there was none of that mineral present in the sample.

[1] AMAX and ARIMETCO samples originated from core drilled between 1974 and 1977 and were stored for at least 20 years prior to initiation.

[2] Dunka blast hole samples originated from a blast on August 30, 1989 at the Dunka Mine and were stored for 8 years prior to initiation.

Table 53. Model 2, Periods A-D Silicate Mineral Dissolution Rates. Page 3 of 4.

Model 2, Period C																						
R#	%S	N	Aug (mol $m^{-2}s^{-1}$)				Plag (mol $m^{-2}s^{-1}$)				Hyp (mol $m^{-2}s^{-1}$)				Ol (mol $m^{-2}s^{-1}$)				Bio (mol $m^{-2}s^{-1}$)			
			Ave	S.D.	Max	Min	Ave	S.D.	Max	Min	Ave	S.D.	Max	Min	Ave	S.D.	Max	Min	Ave	S.D.	Max	Min
5	0.40	21	2.9E-12	1.8E-12	7.0E-12	1.5E-12	2.1E-12	8.9E-13	4.1E-12	7.6E-13	0.0E+00	0.0E+00	0.0E+00	0.0E+00					0.0E+00	0.0E+00	0.0E+00	0.0E+00
7	0.41	22	2.8E-12	1.0E-12	4.3E-12	3.9E-13	1.9E-13	3.8E-13	1.3E-12	0.0E+00	1.2E-12	1.5E-12	5.6E-12	0.0E+00	1.6E-12	1.9E-12	7.0E-12	0.0E+00	1.2E-12	1.4E-12	5.4E-12	0.0E+00
9	0.51	29	4.5E-12	1.9E-12	9.4E-12	4.6E-13	5.0E-13	8.3E-13	2.7E-12	0.0E+00	2.9E-13	3.7E-13	1.4E-12	0.0E+00	1.7E-12	2.2E-12	7.8E-12	0.0E+00	5.3E-13	6.9E-13	2.5E-12	0.0E+00
11	0.54	40	1.0E-12	9.6E-13	3.9E-12	3.8E-13	1.1E-12	4.2E-13	2.1E-12	8.8E-14	0.0E+00	0.0E+00	0.0E+00	0.0E+00					0.0E+00	0.0E+00	0.0E+00	0.0E+00
13	0.57	14	2.6E-12	7.2E-13	4.1E-12	1.6E-12	3.1E-14	6.2E-14	1.6E-13	0.0E+00	5.0E-12	4.7E-12	1.7E-11	0.0E+00	2.0E-12	1.9E-12	7.1E-12	0.0E+00				
15	0.58	30	2.4E-12	7.2E-13	4.9E-12	1.4E-12	1.4E-13	2.6E-13	7.9E-13	0.0E+00	8.3E-13	8.0E-13	2.9E-12	0.0E+00	8.7E-12	8.4E-12	3.0E-11	0.0E+00	5.6E-12	5.4E-12	2.0E-11	0.0E+00
39[1]	0.67	21	1.3E-12	1.6E-13	1.6E-12	1.1E-12	5.3E-16	2.4E-15	1.1E-14	0.0E+00	2.3E-12	1.1E-12	4.1E-12	0.0E+00	1.0E-12	4.9E-13	1.8E-12	0.0E+00				
40[2]	0.67	10	3.4E-12	9.1E-13	4.3E-12	1.5E-12	3.1E-13	4.3E-13	1.1E-12	0.0E+00	1.7E-13	1.8E-13	5.4E-13	0.0E+00	9.9E-13	1.0E-12	3.1E-12	0.0E+00	1.1E-13	1.1E-13	3.4E-13	0.0E+00
17	0.71	38	5.2E-12	3.2E-12	1.8E-11	2.4E-13	2.8E-14	1.1E-13	5.4E-13	0.0E+00	4.0E-12	4.1E-12	1.5E-11	0.0E+00	5.8E-12	5.9E-12	2.2E-11	0.0E+00	8.1E-12	8.2E-12	3.1E-11	0.0E+00
35	1.12	33	1.5E-11	6.0E-12	2.6E-11	6.1E-12	5.5E-13	7.1E-13	2.4E-12	0.0E+00	3.0E-13	5.1E-13	1.6E-12	0.0E+00	2.1E-12	3.6E-12	1.1E-11	0.0E+00	8.1E-13	1.4E-12	4.3E-12	0.0E+00
29	1.16	48	6.7E-12	3.1E-12	1.4E-11	2.9E-12	2.5E-14	1.7E-13	1.2E-12	0.0E+00	4.7E-12	3.1E-12	1.2E-11	0.0E+00	5.9E-12	3.9E-12	1.5E-11	0.0E+00				
37	1.40	38	7.0E-12	2.7E-12	1.2E-11	2.9E-12	1.7E-15	1.1E-14	6.5E-14	0.0E+00	1.4E-11	7.4E-12	2.7E-11	0.0E+00	3.0E-11	1.6E-11	6.0E-11	0.0E+00				
33	1.44	57	2.8E-11	1.6E-11	5.9E-11	7.4E-12	7.8E-15	3.7E-14	2.1E-13	0.0E+00	2.4E-12	1.7E-12	6.3E-12	0.0E+00	1.8E-11	1.3E-11	4.7E-11	0.0E+00	8.6E-12	6.1E-12	2.2E-11	0.0E+00
19	1.63	64	1.1E-11	4.4E-12	2.4E-11	4.6E-12	4.5E-14	3.1E-13	2.4E-12	0.0E+00	3.4E-12	1.5E-12	6.7E-12	0.0E+00	2.2E-11	9.8E-12	4.3E-11	0.0E+00	8.1E-12	3.6E-12	1.6E-11	0.0E+00
31	1.64	28	5.9E-12	1.5E-12	9.0E-12	4.0E-12	0.0E+00	0.0E+00	0.0E+00	0.0E+00	4.2E-12	1.9E-12	8.2E-12	8.1E-13	2.4E-11	1.1E-11	4.8E-11	4.7E-12	4.6E-12	2.1E-12	9.0E-12	8.9E-13
Summary			6.7E-12	3.0E-12	5.9E-11	2.4E-13	3.3E-13	3.1E-13	4.1E-12	0.0E+00	2.8E-12	1.9E-12	2.7E-11	0.0E+00	9.6E-12	6.1E-12	6.0E-11	0.0E+00	3.4E-12	2.6E-12	3.1E-11	0.0E+00

Note: N=number of experimental observations used to model dissolution rates.

Note: Zeroes indicate a calculated absence of dissolution. Blank cells indicate there was none of that mineral present in the sample.

[1] AMAX and ARIMETCO samples originated from core drilled between 1974 and 1977 and were stored for at least 20 years prior to initiation.

[2] Dunka blast hole samples originated from a blast on August 30, 1989 at the Dunka Mine and were stored for 8 years prior to initiation.

Table 53. Model 2, Periods A-D Silicate Mineral Dissolution Rates. Page 4 of 4.

Model 2, Period D																						
R#	%S	N	Aug (mol m^{-2}s^{-1})				Plag (mol m^{-2}s^{-1})				Hyp (mol m^{-2}s^{-1})				Ol (mol m^{-2}s^{-1})				Bio (mol m^{-2}s^{-1})			
			Ave	S.D.	Max	Min	Ave	S.D.	Max	Min	Ave	S.D.	Max	Min	Ave	S.D.	Max	Min	Ave	S.D.	Max	Min
5	0.40	9	1.5E-12	1.6E-14	1.6E-12	1.5E-12	7.0E-13	2.6E-13	1.2E-12	2.9E-13	0.0E+00	0.0E+00	0.0E+00	0.0E+00					0.0E+00	0.0E+00	0.0E+00	0.0E+00
7	0.41	54	8.2E-13	7.7E-13	3.1E-12	3.6E-13	4.0E-13	2.0E-13	8.9E-13	0.0E+00	1.8E-14	9.3E-14	5.9E-13	0.0E+00	2.2E-14	1.2E-13	7.5E-13	0.0E+00	1.7E-14	9.0E-14	5.7E-13	0.0E+00
9	0.51	66	1.1E-12	1.1E-12	5.4E-12	4.2E-13	7.7E-13	4.3E-13	2.7E-12	0.0E+00	1.3E-14	8.6E-14	6.6E-13	0.0E+00	7.8E-14	5.0E-13	3.8E-12	0.0E+00	2.5E-14	1.6E-13	1.2E-12	0.0E+00
13	0.57	21	1.5E-12	6.7E-13	2.6E-12	2.0E-13	5.1E-13	5.8E-13	2.1E-12	0.0E+00	2.5E-13	7.2E-13	3.2E-12	0.0E+00	1.0E-13	3.0E-13	1.3E-12	0.0E+00				
15	0.58	80	5.8E-13	6.3E-13	3.8E-12	2.3E-13	7.9E-13	3.9E-13	2.4E-12	0.0E+00	8.7E-15	6.9E-14	6.1E-13	0.0E+00	9.1E-14	7.2E-13	6.4E-12	0.0E+00	5.9E-14	4.7E-13	4.2E-12	0.0E+00
39[1]	0.67	80	3.7E-13	3.3E-13	1.4E-12	6.1E-14	2.0E-13	1.9E-13	6.4E-13	0.0E+00	4.7E-14	1.1E-13	5.8E-13	0.0E+00	2.1E-14	4.8E-14	2.6E-13	0.0E+00				
40[2]	0.67	44	4.9E-13	3.8E-13	2.0E-12	2.1E-13	5.6E-13	3.4E-13	1.4E-12	1.4E-14	0.0E+00	0.0E+00	0.0E+00	0.0E+00	0.0E+00	0.0E+00	0.0E+00	0.0E+00	0.0E+00	0.0E+00	0.0E+00	0.0E+00
17	0.71	58	1.4E-12	1.3E-12	4.3E-12	3.9E-13	4.5E-13	2.1E-13	8.1E-13	0.0E+00	3.1E-14	1.6E-13	1.1E-12	0.0E+00	4.6E-14	2.3E-13	1.6E-12	0.0E+00	6.4E-14	3.1E-13	2.3E-12	0.0E+00
35	1.12	3	7.5E-12	7.3E-13	8.2E-12	6.7E-12	0.0E+00	0.0E+00	0.0E+00	0.0E+00	4.2E-13	2.4E-13	6.9E-13	2.6E-13	3.0E-12	1.7E-12	4.9E-12	1.9E-12	1.1E-12	6.5E-13	1.9E-12	7.1E-13
29	1.16	47	1.1E-12	9.2E-13	4.1E-12	3.3E-13	4.5E-13	2.5E-13	9.6E-13	0.0E+00	1.1E-13	3.2E-13	1.8E-12	0.0E+00	1.4E-13	4.1E-13	2.2E-12	0.0E+00				
33	1.44	32	6.4E-12	2.6E-12	1.4E-11	1.2E-12	1.8E-13	2.0E-13	7.1E-13	0.0E+00	3.1E-14	5.7E-14	2.4E-13	0.0E+00	2.3E-13	4.2E-13	1.8E-12	0.0E+00	1.1E-13	2.0E-13	8.6E-13	0.0E+00
19	1.63	62	3.7E-12	2.3E-12	1.0E-11	5.9E-13	2.6E-13	3.2E-13	1.2E-12	0.0E+00	2.4E-13	4.1E-13	1.4E-12	0.0E+00	1.6E-12	2.7E-12	9.0E-12	0.0E+00	5.7E-13	9.7E-13	3.2E-12	0.0E+00
31	1.64	5	4.1E-12	6.1E-13	5.1E-12	3.6E-12	1.3E-14	3.0E-14	6.7E-14	0.0E+00	5.6E-13	4.0E-13	1.0E-12	0.0E+00	3.3E-12	2.3E-12	6.0E-12	0.0E+00	6.2E-13	4.4E-13	1.1E-12	0.0E+00
Summary			2.3E-12	9.5E-13	1.4E-11	6.1E-14	4.1E-13	2.6E-13	2.7E-12	0.0E+00	1.3E-13	2.1E-13	3.2E-12	0.0E+00	7.1E-13	7.9E-13	9.0E-12	0.0E+00	2.6E-13	3.3E-13	4.2E-12	0.0E+00

Note: Zeroes indicate a calculated absence of dissolution. Blank cells indicate there was none of that mineral present in the sample.

Note: N=number of experimental observations used to model dissolution rates.

[1] AMAX and ARIMETCO samples originated from core drilled between 1974 and 1977 and were stored for at least 20 years prior to initiation.

[2] Dunka blast hole samples originated from a blast on August 30, 1989 at the Dunka Mine and were stored for 8 years prior to initiation.

Table 54. Model 3, Periods A-D Silicate Mineral Dissolution Rates. Page 1 of 4.

Model 3, Period A																						
R#	%S	N	Plag (mol $m^{-2}s^{-1}$)				Aug (mol $m^{-2}s^{-1}$)				Hyp (mol $m^{-2}s^{-1}$)				Ol (mol $m^{-2}s^{-1}$)				Bio (mol $m^{-2}s^{-1}$)			
			Ave	S.D.	Max	Min	Ave	S.D.	Max	Min	Ave	S.D.	Max	Min	Ave	S.D.	Max	Min	Ave	S.D.	Max	Min
39[1]	0.67	2	5.1E-13	9.9E-14	5.8E-13	4.4E-13	2.7E-12	2.3E-12	4.4E-12	1.1E-12	4.7E-12	6.5E-12	9.3E-12	9.8E-14	2.1E-12	2.9E-12	4.1E-12	4.3E-14				
40[2]	0.67	3	4.9E-13	9.8E-14	6.0E-13	4.2E-13	5.4E-12	9.8E-13	6.2E-12	4.3E-12	0.0E+00	0.0E+00	0.0E+00	0.0E+00	0.0E+00	0.0E+00	0.0E+00	0.0E+00	0.0E+00	0.0E+00	0.0E+00	0.0E+00
42[1]	0.72	2	7.5E-13	8.7E-14	8.1E-13	6.9E-13	7.2E-12	1.0E-12	7.9E-12	6.5E-12	4.8E-13	3.0E-13	6.9E-13	2.7E-13	1.3E-13	7.9E-14	1.8E-13	7.1E-14				
43[2]	0.82	3	4.9E-13	2.7E-13	6.9E-13	1.8E-13	2.7E-12	9.9E-13	3.7E-12	1.7E-12	2.4E-13	4.2E-13	7.3E-13	0.0E+00	2.5E-12	4.3E-12	7.4E-12	0.0E+00	4.0E-13	6.9E-13	1.2E-12	0.0E+00
41[1]	0.92	3	7.2E-13	2.6E-14	7.4E-13	6.9E-13	5.7E-12	4.8E-12	1.1E-11	1.5E-12	2.5E-12	4.4E-12	7.6E-12	0.0E+00	3.9E-13	6.8E-13	1.2E-12	0.0E+00				
44[1]	1.71	4	7.3E-13	1.7E-13	9.6E-13	5.6E-13	2.9E-11	8.8E-12	4.2E-11	2.4E-11	0.0E+00	0.0E+00	0.0E+00	0.0E+00	0.0E+00	0.0E+00	0.0E+00	0.0E+00	0.0E+00	0.0E+00	0.0E+00	0.0E+00
Summary			6.2E-13	1.2E-13	9.6E-13	1.8E-13	8.8E-12	3.2E-12	4.2E-11	1.1E-12	1.3E-12	1.9E-12	9.3E-12	0.0E+00	8.4E-13	1.3E-12	7.4E-12	0.0E+00	1.3E-13	2.3E-13	1.2E-12	0.0E+00

Note: Zeroes indicate a calculated absence of dissolution. Blank cells indicate there was none of that mineral present in the sample.

Note: N=number of experimental observations used to model dissolution rates.

[1] AMAX and ARIMETCO samples originated from core drilled between 1974 and 1977 and were stored for at least 20 years prior to initiation.

[2] Dunka blast hole samples originated from a blast on August 30, 1989 at the Dunka Mine and were stored for 8 years prior to initiation.

Table 54. Model 3, Periods A-D Silicate Mineral Dissolution Rates. Page 2 of 4.

Model 3, Period B																						
R#	%S	N	Plag (mol $m^{-2}s^{-1}$)				Aug (mol $m^{-2}s^{-1}$)				Hyp (mol $m^{-2}s^{-1}$)				Ol (mol $m^{-2}s^{-1}$)				Bio (mol $m^{-2}s^{-1}$)			
			Ave	S.D.	Max	Min	Ave	S.D.	Max	Min	Ave	S.D.	Max	Min	Ave	S.D.	Max	Min	Ave	S.D.	Max	Min
1	0.18	32	3.6E-13	1.6E-13	8.1E-13	1.5E-13	5.1E-13	3.8E-13	1.8E-12	0.0E+00	1.7E-13	3.4E-13	1.7E-12	0.0E+00	6.2E-13	1.3E-12	6.1E-12	0.0E+00	5.3E-13	1.1E-12	5.2E-12	0.0E+00
3	0.22	34	2.2E-13	8.9E-14	4.0E-13	1.1E-13	1.1E-12	4.7E-13	2.4E-12	2.1E-13	8.8E-13	1.2E-12	5.2E-12	0.0E+00	2.0E-12	2.7E-12	1.2E-11	0.0E+00	4.7E-13	6.2E-13	2.7E-12	0.0E+00
5	0.40	20	2.3E-13	1.2E-13	6.3E-13	1.8E-13	3.4E-12	3.2E-12	1.1E-11	1.5E-12	1.9E-14	6.4E-14	2.7E-13	0.0E+00					9.2E-14	3.0E-13	1.3E-12	0.0E+00
39[1]	0.67	4	5.7E-13	3.2E-13	1.0E-12	3.7E-13	1.6E-13	2.0E-13	4.1E-13	0.0E+00	4.4E-12	3.3E-12	8.1E-12	1.8E-13	2.0E-12	1.4E-12	3.6E-12	7.9E-14				
40[2]	0.67	18	4.8E-13	1.7E-13	9.2E-13	1.6E-13	1.5E-12	6.4E-13	2.8E-12	3.2E-13	0.0E+00	0.0E+00	0.0E+00	0.0E+00	0.0E+00	0.0E+00	0.0E+00	0.0E+00	0.0E+00	0.0E+00	0.0E+00	0.0E+00
42[1]	0.72	33	2.9E-13	1.3E-13	4.7E-13	1.5E-13	1.2E-12	1.3E-12	4.1E-12	0.0E+00	1.2E-12	1.1E-12	4.9E-12	0.0E+00	3.2E-13	2.9E-13	1.3E-12	0.0E+00				
43[2]	0.82	32	2.3E-13	9.8E-14	5.2E-13	1.8E-13	2.0E-13	1.3E-13	5.2E-13	0.0E+00	3.7E-14	5.8E-14	1.5E-13	0.0E+00	3.7E-13	5.8E-13	1.5E-12	0.0E+00	6.0E-14	9.4E-14	2.4E-13	0.0E+00
41[1]	0.92	33	4.0E-13	2.7E-13	1.5E-12	2.1E-13	2.8E-13	3.1E-13	8.0E-13	0.0E+00	6.3E-13	6.4E-13	3.1E-12	0.0E+00	9.8E-14	9.8E-14	4.9E-13	0.0E+00				
44[1]	1.71	2	6.1E-13	2.0E-13	7.5E-13	4.7E-13	8.9E-12	4.7E-12	1.2E-11	5.6E-12	1.9E-11	1.6E-12	2.0E-11	1.7E-11	3.7E-12	3.3E-13	4.0E-12	3.5E-12	1.8E-11	1.6E-12	1.9E-11	1.7E-11
Summary			3.8E-13	1.7E-13	1.5E-12	1.1E-13	1.9E-12	1.3E-12	1.2E-11	0.0E+00	2.9E-12	9.2E-13	2.0E-11	0.0E+00	1.1E-12	8.4E-13	1.2E-11	0.0E+00	3.2E-12	6.2E-13	1.9E-11	0.0E+00

Note: Zeroes indicate a calculated absence of dissolution. Blank cells indicate there was none of that mineral present in the sample.

Note: N=number of experimental observations used to model dissolution rates.

[1] AMAX and ARIMETCO samples originated from core drilled between 1974 and 1977 and were stored for at least 20 years prior to initiation.

[2] Dunka blast hole samples originated from a blast on August 30, 1989 at the Dunka Mine and were stored for 8 years prior to initiation.

Table 54. Model 3, Periods A-D Silicate Mineral Dissolution Rates. Page 3 of 4.

Model 3, Period C

R#	%S	N	Plag (mol $m^{-2}s^{-1}$)				Aug (mol $m^{-2}s^{-1}$)				Hyp (mol $m^{-2}s^{-1}$)				Ol (mol $m^{-2}s^{-1}$)				Bio (mol $m^{-2}s^{-1}$)			
			Ave	S.D.	Max	Min	Ave	S.D.	Max	Min	Ave	S.D.	Max	Min	Ave	S.D.	Max	Min	Ave	S.D.	Max	Min
5	0.40	7	6.4E-13	2.2E-13	9.9E-13	4.3E-13	2.8E-12	2.0E-12	7.0E-12	1.5E-12	0.0E+00	0.0E+00	0.0E+00	0.0E+00					0.0E+00	0.0E+00	0.0E+00	0.0E+00
7	0.41	2	5.9E-13	1.1E-13	6.7E-13	5.1E-13	1.5E-12	8.7E-15	1.5E-12	1.4E-12	2.7E-12	1.5E-12	3.7E-12	1.7E-12	3.4E-12	1.8E-12	4.7E-12	2.1E-12	2.6E-12	1.4E-12	3.6E-12	1.6E-12
11	0.54	2	6.2E-13	1.3E-13	7.2E-13	5.3E-13	8.8E-13	6.9E-13	1.4E-12	3.9E-13	2.5E-13	3.5E-13	5.0E-13	0.0E+00					5.8E-13	8.2E-13	1.2E-12	0.0E+00
39[1]	0.67	7	5.3E-13	5.5E-14	6.2E-13	4.4E-13	3.7E-13	1.8E-13	7.0E-13	1.6E-13	4.0E-12	7.6E-13	4.8E-12	2.6E-12	1.8E-12	3.3E-13	2.1E-12	1.2E-12				
40[2]	0.67	4	7.0E-13	7.8E-14	7.9E-13	6.1E-13	2.7E-12	3.7E-13	3.1E-12	2.2E-12	7.6E-13	5.1E-13	1.1E-12	0.0E+00	4.4E-12	2.9E-12	6.1E-12	0.0E+00	4.7E-13	3.2E-13	6.6E-13	0.0E+00
17	0.71	2	6.2E-13	1.2E-13	7.0E-13	5.3E-13	1.9E-12	3.9E-13	2.2E-12	1.7E-12	2.0E-12	9.0E-13	2.7E-12	1.4E-12	2.9E-12	1.3E-12	3.9E-12	2.0E-12	4.1E-12	1.8E-12	5.4E-12	2.8E-12
35	1.12	2	2.0E-12	1.3E-12	2.9E-12	1.2E-12	4.5E-12	6.4E-12	9.0E-12	0.0E+00	2.0E-12	3.8E-13	2.3E-12	1.7E-12	1.4E-11	2.7E-12	1.6E-11	1.2E-11	5.4E-12	1.0E-12	6.1E-12	4.7E-12
29	1.16	3	9.1E-13	3.0E-13	1.3E-12	6.8E-13	3.2E-12	2.0E-12	5.5E-12	1.9E-12	6.9E-12	5.8E-12	1.4E-11	2.7E-12	8.8E-12	7.5E-12	1.7E-11	3.4E-12				
37	1.40	3	1.5E-12	2.6E-13	1.7E-12	1.2E-12	5.3E-12	1.5E-12	6.2E-12	3.6E-12	1.8E-11	5.7E-12	2.5E-11	1.4E-11	4.0E-11	1.2E-11	5.4E-11	3.2E-11				
33	1.44	7	8.6E-13	4.0E-13	1.7E-12	5.6E-13	1.4E-11	6.5E-12	2.4E-11	6.7E-12	3.5E-12	1.8E-12	6.2E-12	9.6E-13	2.6E-11	1.3E-11	4.6E-11	7.2E-12	1.2E-11	6.4E-12	2.2E-11	3.4E-12
19	1.63	1	1.0E-12	N/A	N/A	N/A	7.8E-12	N/A	N/A	N/A	2.6E-12	N/A	N/A	N/A	1.7E-11	N/A	N/A	N/A	6.1E-12	N/A	N/A	N/A
31	1.64	1	1.1E-12	N/A	N/A	N/A	3.7E-12	N/A	N/A	N/A	4.9E-12	N/A	N/A	N/A	2.8E-11	N/A	N/A	N/A	5.3E-12	N/A	N/A	N/A
Summary			9.2E-13	2.9E-13	2.9E-12	4.3E-13	4.0E-12	2.0E-12	2.4E-11	0.0E+00	4.0E-12	1.8E-12	2.5E-11	0.0E+00	1.5E-11	5.3E-12	5.4E-11	0.0E+00	4.1E-12	1.7E-12	2.2E-11	0.0E+00

Note: Zeroes indicate a calculated absence of dissolution. Blank cells indicate there was none of that mineral present in the sample.

Note: N=number of experimental observations used to model dissolution rates.

[1] AMAX and ARIMETCO samples originated from core drilled between 1974 and 1977 and were stored for at least 20 years prior to initiation.

[2] Dunka blast hole samples originated from a blast on August 30, 1989 at the Dunka Mine and were stored for 8 years prior to initiation.

Table 54. Model 3, Periods A-D Silicate Mineral Dissolution Rates. Page 4 of 4.

Model 3, Period D																						
R#	%S	N	Plag (mol m^{-2}s^{-1})				Aug (mol m^{-2}s^{-1})				Hyp (mol m^{-2}s^{-1})				Ol (mol m^{-2}s^{-1})				Bio (mol m^{-2}s^{-1})			
			Ave	S.D.	Max	Min	Ave	S.D.	Max	Min	Ave	S.D.	Max	Min	Ave	S.D.	Max	Min	Ave	S.D.	Max	Min
5	0.40	3	2.6E-13	1.2E-13	4.0E-13	1.8E-13	1.5E-12	1.7E-14	1.6E-12	1.5E-12	0.0E+00	0.0E+00	0.0E+00	0.0E+00					0.0E+00	0.0E+00	0.0E+00	0.0E+00
7	0.41	14	4.8E-13	1.6E-13	8.5E-13	3.2E-13	3.6E-13	2.2E-13	8.3E-13	0.0E+00	3.3E-13	5.9E-13	1.6E-12	0.0E+00	4.2E-13	7.4E-13	2.0E-12	0.0E+00	3.2E-13	5.6E-13	1.5E-12	0.0E+00
9	0.51	17	6.9E-13	2.6E-13	1.4E-12	4.1E-13	6.0E-13	5.2E-13	2.1E-12	0.0E+00	2.0E-13	3.7E-13	1.2E-12	0.0E+00	1.2E-12	2.1E-12	7.2E-12	0.0E+00	3.7E-13	6.7E-13	2.3E-12	0.0E+00
13	0.57	2	1.1E-12	4.6E-13	1.4E-12	7.7E-13	6.0E-13	1.5E-13	7.1E-13	4.9E-13	2.2E-12	8.7E-13	2.8E-12	1.6E-12	9.0E-13	3.5E-13	1.2E-12	6.5E-13				
15	0.58	18	6.7E-13	5.6E-13	2.9E-12	3.6E-13	3.2E-13	2.0E-13	9.3E-13	0.0E+00	2.2E-13	5.6E-13	2.0E-12	0.0E+00	2.4E-12	5.9E-12	2.1E-11	0.0E+00	1.5E-12	3.8E-12	1.4E-11	0.0E+00
39[1]	0.67	25	2.6E-13	1.1E-13	5.0E-13	1.4E-13	2.0E-13	1.7E-13	7.4E-13	0.0E+00	3.5E-13	4.5E-13	1.6E-12	0.0E+00	1.5E-13	2.0E-13	7.0E-13	0.0E+00				
40[2]	0.67	10	5.4E-13	2.1E-13	9.5E-13	1.6E-13	4.7E-13	4.7E-13	1.5E-12	0.0E+00	6.3E-14	1.0E-13	3.1E-13	0.0E+00	3.6E-13	5.9E-13	1.8E-12	0.0E+00	3.9E-14	6.4E-14	1.9E-13	0.0E+00
17	0.71	16	5.5E-13	1.3E-13	7.9E-13	3.9E-13	9.9E-13	7.6E-13	2.7E-12	0.0E+00	3.2E-13	6.0E-13	2.1E-12	0.0E+00	4.6E-13	8.6E-13	3.1E-12	0.0E+00	6.4E-13	1.2E-12	4.3E-12	0.0E+00
35	1.12	1	9.4E-13	N/A	N/A	N/A	4.0E-12	N/A	N/A	N/A	8.1E-13	N/A	N/A	N/A	5.7E-12	N/A	N/A	N/A	2.2E-12	N/A	N/A	N/A
29	1.16	15	5.5E-13	1.3E-13	8.5E-13	3.5E-13	5.9E-13	2.9E-13	1.1E-12	3.3E-13	3.4E-13	5.8E-13	1.7E-12	0.0E+00	4.4E-13	7.4E-13	2.2E-12	0.0E+00				
33	1.44	11	5.2E-13	1.5E-13	8.7E-13	3.6E-13	2.6E-12	1.4E-12	4.3E-12	0.0E+00	1.8E-13	2.1E-13	6.8E-13	0.0E+00	1.3E-12	1.6E-12	5.1E-12	0.0E+00	6.3E-13	7.5E-13	2.4E-12	0.0E+00
19	1.63	18	6.9E-13	2.0E-13	1.2E-12	4.7E-13	2.5E-12	1.8E-12	6.4E-12	5.9E-13	4.3E-13	6.7E-13	1.8E-12	0.0E+00	2.8E-12	4.4E-12	1.2E-11	0.0E+00	1.0E-12	1.6E-12	4.3E-12	0.0E+00
31	1.64	2	1.1E-12	1.2E-13	1.2E-12	1.0E-12	2.3E-12	4.1E-14	2.4E-12	2.3E-12	2.1E-12	5.8E-15	2.1E-12	2.1E-12	1.2E-11	3.4E-14	1.2E-11	1.2E-11	2.3E-12	6.4E-15	2.3E-12	2.3E-12
Summary			6.4E-13	2.2E-13	2.9E-12	1.4E-13	1.3E-12	5.0E-13	6.4E-12	0.0E+00	5.8E-13	4.2E-13	2.8E-12	0.0E+00	2.4E-12	1.6E-12	2.1E-11	0.0E+00	9.0E-13	9.7E-13	1.4E-11	0.0E+00

Note: Zeroes indicate a calculated absence of dissolution. Blank cells indicate there was none of that mineral present in the sample.

Note: N=number of experimental observations used to model dissolution rates.

[1] AMAX and ARIMETCO samples originated from core drilled between 1974 and 1977 and were stored for at least 20 years prior to initiation.

[2] Dunka blast hole samples originated from a blast on August 30, 1989 at the Dunka Mine and were stored for 8 years prior to initiation.

Table 55. Model 3, Periods A-D Orphan Calcium Rates.

Model 3, Orphan Calcium (mol $m^{-2}s^{-1}$)																	
R#	%S	Period A				Period B				Period C				Period D			
		Ave	S.D.	Max	Min	Ave	S.D.	Max	Min	Ave	S.D.	Max	Min	Ave	S.D.	Max	Min
1	0.18					1.7E-13	3.1E-13	1.2E-12	0.0E+00								
3	0.22					3.1E-14	1.7E-13	9.7E-13	0.0E+00								
5	0.4					4.6E-12	2.4E-12	9.0E-12	0.0E+00	6.5E-12	3.2E-12	1.2E-11	2.7E-12	1.6E-12	1.3E-13	1.7E-12	1.5E-12
7	0.41									0.0E+00	0.0E+00	0.0E+00	0.0E+00	2.3E-13	3.6E-13	1.2E-12	0.0E+00
9	0.51													3.2E-13	4.2E-13	1.4E-12	0.0E+00
11	0.54									9.5E-13	1.3E-12	1.9E-12	0.0E+00				
13	0.57													0.0E+00	0.0E+00	0.0E+00	0.0E+00
15	0.58													8.0E-13	5.9E-13	1.6E-12	0.0E+00
39[1]	0.67	0.0E+00	0.0E+00	0.0E+00	0.0E+00	0.0E+00	0.0E+00	0.0E+00	0.0E+00	0.0E+00	0.0E+00	0.0E+00	0.0E+00	2.8E-13	5.3E-13	1.9E-12	0.0E+00
40[2]	0.67	2.2E-12	2.6E-12	5.1E-12	1.5E-13	5.2E-12	1.3E-12	6.8E-12	2.1E-12	2.8E-13	5.6E-13	1.1E-12	0.0E+00	4.9E-13	6.8E-13	1.9E-12	0.0E+00
17	0.71									0.0E+00	0.0E+00	0.0E+00	0.0E+00	2.7E-13	3.2E-13	1.0E-12	0.0E+00
42[1]	0.72	0.0E+00	0.0E+00	0.0E+00	0.0E+00	4.9E-14	2.3E-13	1.3E-12	0.0E+00								
43[2]	0.82	7.5E-12	1.0E-11	1.9E-11	0.0E+00	1.5E-12	1.8E-12	6.8E-12	0.0E+00								
41[1]	0.92	3.4E-12	5.5E-12	9.8E-12	0.0E+00	7.7E-14	2.1E-13	8.4E-13	0.0E+00								
35	1.12									0.0E+00	0.0E+00	0.0E+00	0.0E+00	0.0E+00		0.0E+00	0.0E+00
29	1.16									0.0E+00	0.0E+00	0.0E+00	0.0E+00	4.3E-13	5.0E-13	1.5E-12	0.0E+00
37	1.4									0.0E+00	0.0E+00	0.0E+00	0.0E+00				
33	1.44									0.0E+00	0.0E+00	0.0E+00	0.0E+00	1.3E-13	4.1E-13	1.4E-12	0.0E+00
19	1.63									0.0E+00		0.0E+00	0.0E+00	1.2E-13	3.0E-13	1.1E-12	0.0E+00
31	1.64									0.0E+00		0.0E+00	0.0E+00	0.0E+00	0.0E+00	0.0E+00	0.0E+00
44[1]	1.71	9.2E-12	5.7E-12	1.2E-11	5.9E-13	0.0E+00	0.0E+00	0.0E+00	0.0E+00								
Summary		3.7E-12	4.0E-12	1.9E-11	0.0E+00	1.3E-12	7.1E-13	9.0E-12	0.0E+00	6.4E-13	5.1E-13	1.2E-11	0.0E+00	3.6E-13	3.5E-13	1.9E-12	0.0E+00

Note: Zeroes indicate a calculated absence of dissolution. Blank cells indicate there was none of that mineral present in the sample.

[1] AMAX and ARIMETCO samples originated from core drilled between 1974 and 1977 and were stored for at least 20 years prior to initiation.

[2] Dunka blast hole samples originated from a blast on August 30, 1989 at the Dunka Mine and were stored for 8 years prior to initiation.

Table 56. Model 4, Periods A-D Silicate Mineral Dissolution Rates. Page 1 of 4.

Model 4, Period A																						
R#	%S	N	Bio (mol $m^{-2}s^{-1}$)				K-spar (mol $m^{-2}s^{-1}$)				Aug (mol $m^{-2}s^{-1}$)				Hyp (mol $m^{-2}s^{-1}$)				Ol (mol $m^{-2}s^{-1}$)			
			Ave	S.D.	Max	Min	Ave	S.D.	Max	Min	Ave	S.D.	Max	Min	Ave	S.D.	Max	Min	Ave	S.D.	Max	Min
39[1]	0.67	2					2.4E-10	2.9E-10	4.4E-10	3.2E-11	2.7E-12	2.3E-12	4.4E-12	1.1E-12	4.7E-12	6.5E-12	9.3E-12	9.8E-14	2.1E-12	2.9E-12	4.1E-12	4.3E-14
40[2]	0.67	3	4.1E-12	3.6E-12	8.2E-12	1.8E-12	1.5E-10	1.3E-10	3.0E-10	6.4E-11	5.4E-12	9.8E-13	6.2E-12	4.3E-12	0.0E+00	0.0E+00	0.0E+00	0.0E+00	0.0E+00	0.0E+00	0.0E+00	0.0E+00
42[1]	0.72	2									7.2E-12	1.0E-12	7.9E-12	6.5E-12	4.8E-13	3.0E-13	6.9E-13	2.7E-13	1.3E-13	7.9E-14	1.8E-13	7.1E-14
43[2]	0.82	3	6.4E-12	4.1E-12	1.0E-11	2.1E-12					2.7E-12	9.9E-13	3.7E-12	1.7E-12	0.0E+00	0.0E+00	0.0E+00	0.0E+00	0.0E+00	0.0E+00	0.0E+00	0.0E+00
41[1]	0.92	3									5.7E-12	4.8E-12	1.1E-11	1.5E-12	2.5E-12	4.4E-12	7.6E-12	0.0E+00	3.9E-13	6.8E-13	1.2E-12	0.0E+00
44[1]	1.71	4	3.6E-11	1.0E-11	4.7E-11	2.7E-11	3.5E-10	1.0E-10	4.7E-10	2.7E-10	2.9E-11	8.8E-12	4.2E-11	2.4E-11	0.0E+00	0.0E+00	0.0E+00	0.0E+00	0.0E+00	0.0E+00	0.0E+00	0.0E+00
Summary			1.5E-11	5.9E-12	4.7E-11	1.8E-12	2.5E-10	1.7E-10	4.7E-10	3.2E-11	8.8E-12	3.2E-12	4.2E-11	1.1E-12	1.3E-12	1.9E-12	9.3E-12	0.0E+00	4.3E-13	6.1E-13	4.1E-12	0.0E+00

Note: Zeroes indicate a calculated absence of dissolution. Blank cells indicate there was none of that mineral present in the sample.

Note: N=number of experimental observations used to model dissolution rates.

Note: Plagioclase dissolution calculations in Model 4 are the same as Model 3 (see Table AZ).

[1] AMAX and ARIMETCO samples originated from core drilled between 1974 and 1977 and were stored for at least 20 years prior to initiation.

[2] Dunka blast hole samples originated from a blast on August 30, 1989 at the Dunka Mine and were stored for 8 years prior to initiation.

Table 56. Model 4, Periods A-D Silicate Mineral Dissolution Rates. Page 2 of 4.

Model 4, Period B																						
R#	%S	N	Bio (mol $m^{-2}s^{-1}$)				K-spar (mol $m^{-2}s^{-1}$)				Aug (mol $m^{-2}s^{-1}$)				Hyp (mol $m^{-2}s^{-1}$)				Ol (mol $m^{-2}s^{-1}$)			
			Ave	S.D.	Max	Min	Ave	S.D.	Max	Min	Ave	S.D.	Max	Min	Ave	S.D.	Max	Min	Ave	S.D.	Max	Min
1	0.18	32	6.0E-12	5.3E-12	1.7E-11	7.0E-13					5.1E-13	3.8E-13	1.8E-12	0.0E+00	3.1E-15	1.8E-14	1.0E-13	0.0E+00	1.2E-14	6.5E-14	3.7E-13	0.0E+00
3	0.22	33	2.3E-12	2.4E-12	8.6E-12	2.0E-13	1.0E-11	1.1E-11	3.8E-11	8.9E-13	1.1E-12	4.7E-13	2.4E-12	2.1E-13	2.2E-14	1.3E-13	7.3E-13	0.0E+00	5.0E-14	2.9E-13	1.7E-12	0.0E+00
5	0.40	18	5.6E-12	4.2E-12	1.5E-11	1.5E-12	1.6E-11	1.2E-11	4.5E-11	4.3E-12	3.6E-12	3.3E-12	1.1E-11	1.5E-12	0.0E+00	0.0E+00	0.0E+00	0.0E+00				
39[1]	0.67	4					9.3E-11	7.1E-11	1.8E-10	1.7E-11	1.6E-13	2.0E-13	4.1E-13	0.0E+00	4.4E-12	3.3E-12	8.1E-12	1.8E-13	2.0E-12	1.4E-12	3.6E-12	7.9E-14
40[2]	0.67	18	1.6E-12	1.2E-12	5.6E-12	6.5E-13	5.8E-11	4.3E-11	2.0E-10	2.3E-11	1.5E-12	6.4E-13	2.8E-12	3.2E-13	0.0E+00	0.0E+00	0.0E+00	0.0E+00	0.0E+00	0.0E+00	0.0E+00	0.0E+00
42[1]	0.72	32									1.1E-12	1.2E-12	3.8E-12	0.0E+00	1.2E-12	1.1E-12	4.9E-12	0.0E+00	3.2E-13	2.9E-13	1.3E-12	0.0E+00
43[2]	0.82	28	6.2E-13	1.2E-12	6.3E-12	1.7E-13					1.8E-13	1.2E-13	2.7E-13	0.0E+00	2.8E-15	7.1E-15	2.8E-14	0.0E+00	2.8E-14	7.2E-14	2.8E-13	0.0E+00
41[1]	0.92	31									2.7E-13	3.1E-13	8.0E-13	0.0E+00	5.7E-13	4.4E-13	1.5E-12	0.0E+00	8.8E-14	6.9E-14	2.4E-13	0.0E+00
44[1]	1.71	2	4.5E-11	1.1E-11	5.3E-11	3.8E-11	4.5E-10	1.1E-10	5.2E-10	3.7E-10	8.9E-12	4.7E-12	1.2E-11	5.6E-12	0.0E+00	0.0E+00	0.0E+00	0.0E+00	0.0E+00	0.0E+00	0.0E+00	0.0E+00
Summary			1.0E-11	4.2E-12	5.3E-11	1.7E-13	1.3E-10	4.9E-11	5.2E-10	8.9E-13	1.9E-12	1.3E-12	1.2E-11	0.0E+00	6.9E-13	5.5E-13	8.1E-12	0.0E+00	3.1E-13	2.8E-13	3.6E-12	0.0E+00

Note: Zeroes indicate a calculated absence of dissolution. Blank cells indicate there was none of that mineral present in the sample.

Note: N=number of experimental observations used to model dissolution rates.

Note: Plagioclase dissolution calculations in Model 4 are the same as Model 3 (see Table AZ).

[1] AMAX and ARIMETCO samples originated from core drilled between 1974 and 1977 and were stored for at least 20 years prior to initiation.

[2] Dunka blast hole samples originated from a blast on August 30, 1989 at the Dunka Mine and were stored for 8 years prior to initiation.

Table 56. Model 4, Periods A-D Silicate Mineral Dissolution Rates. Page 3 of 4.

Model 4, Period C																						
R#	%S	N	Bio (mol m^{-2}s^{-1})				K-spar (mol m^{-2}s^{-1})				Aug (mol m^{-2}s^{-1})				Hyp (mol m^{-2}s^{-1})				Ol (mol m^{-2}s^{-1})			
			Ave	S.D.	Max	Min	Ave	S.D.	Max	Min	Ave	S.D.	Max	Min	Ave	S.D.	Max	Min	Ave	S.D.	Max	Min
5	0.40	7	1.2E-12	9.9E-13	2.5E-12	3.2E-13	3.5E-12	2.9E-12	7.2E-12	9.4E-13	2.8E-12	2.0E-12	7.0E-12	1.5E-12	0.0E+00	0.0E+00	0.0E+00	0.0E+00				
7	0.41	2	4.5E-12	1.8E-12	5.8E-12	3.2E-12	6.8E-11	2.8E-11	8.7E-11	4.8E-11	1.5E-12	8.7E-15	1.5E-12	1.4E-12	2.0E-13	2.8E-13	3.9E-13	0.0E+00	2.5E-13	3.5E-13	5.0E-13	0.0E+00
11	0.54	2	2.5E-12	4.1E-13	2.8E-12	2.2E-12					8.8E-13	6.9E-13	1.4E-12	3.9E-13	0.0E+00	0.0E+00	0.0E+00	0.0E+00				
39[1]	0.67	7					4.8E-11	1.9E-11	8.8E-11	3.1E-11	3.7E-13	1.8E-13	7.0E-13	1.6E-13	4.0E-12	7.6E-13	4.8E-12	2.6E-12	1.8E-12	3.3E-13	2.1E-12	1.2E-12
40[2]	0.67	4	1.1E-12	4.6E-13	1.5E-12	4.6E-13	3.9E-11	1.7E-11	5.3E-11	1.6E-11	2.7E-12	3.7E-13	3.1E-12	2.2E-12	0.0E+00	0.0E+00	0.0E+00	0.0E+00	0.0E+00	0.0E+00	0.0E+00	0.0E+00
17	0.71	2	5.9E-12	1.8E-12	7.2E-12	4.6E-12	6.1E-11	1.9E-11	7.5E-11	4.8E-11	1.9E-12	3.9E-13	2.2E-12	1.7E-12	0.0E+00	0.0E+00	0.0E+00	0.0E+00	0.0E+00	0.0E+00	0.0E+00	0.0E+00
35	1.12	2	6.4E-12	2.3E-12	8.0E-12	4.8E-12	5.9E-12	2.1E-12	7.4E-12	4.4E-12	4.5E-12	6.4E-12	9.0E-12	0.0E+00	0.0E+00	0.0E+00	0.0E+00	0.0E+00	0.0E+00	0.0E+00	0.0E+00	0.0E+00
29	1.16	3									3.2E-12	2.0E-12	5.5E-12	1.9E-12	6.9E-12	5.8E-12	1.4E-11	2.7E-12	8.8E-12	7.5E-12	1.7E-11	3.4E-12
37	1.40	3					7.2E-11	3.3E-11	9.7E-11	3.5E-11	5.3E-12	1.5E-12	6.2E-12	3.6E-12	1.8E-11	5.7E-12	2.5E-11	1.4E-11	4.0E-11	1.2E-11	5.4E-11	3.2E-11
33	1.44	7	1.0E-11	6.9E-12	2.4E-11	2.5E-12	2.4E-11	1.6E-11	5.5E-11	6.0E-12	1.4E-11	6.5E-12	2.4E-11	6.7E-12	9.0E-13	8.8E-13	2.0E-12	0.0E+00	6.7E-12	6.5E-12	1.5E-11	0.0E+00
19	1.63	1	7.1E-12	N/A	N/A	N/A	1.2E-11	N/A	N/A	N/A	7.8E-12	N/A	N/A	N/A	0.0E+00	N/A	N/A	N/A	0.0E+00	N/A	N/A	N/A
31	1.64	1	3.1E-12	N/A	N/A	N/A	1.0E-11	N/A	N/A	N/A	3.7E-12	N/A	N/A	N/A	2.0E-12	N/A	N/A	N/A	1.2E-11	N/A	N/A	N/A
Summary			4.7E-12	2.1E-12	2.4E-11	3.2E-13	3.4E-11	1.7E-11	9.7E-11	9.4E-13	4.0E-12	2.0E-12	2.4E-11	0.0E+00	2.7E-12	1.3E-12	2.5E-11	0.0E+00	7.0E-12	3.4E-12	5.4E-11	0.0E+00

Note: Zeroes indicate a calculated absence of dissolution. Blank cells indicate there was none of that mineral present in the sample.
Note: N=number of experimental observations used to model dissolution rates.
Note: Plagioclase dissolution calculations in Model 4 are the same as Model 3 (see Table AZ).

[1] AMAX and ARIMETCO samples originated from core drilled between 1974 and 1977 and were stored for at least 20 years prior to initiation.

[2] Dunka blast hole samples originated from a blast on August 30, 1989 at the Dunka Mine and were stored for 8 years prior to initiation.

Table 56. Model 4, Periods A-D Silicate Mineral Dissolution Rates. Page 4 of 4.

Model 4, Period D																						
R#	%S	N	Bio (mol m^{-2}s^{-1})				K-spar (mol m^{-2}s^{-1})				Aug (mol m^{-2}s^{-1})				Hyp (mol m^{-2}s^{-1})				Ol (mol m^{-2}s^{-1})			
			Ave	S.D.	Max	Min	Ave	S.D.	Max	Min	Ave	S.D.	Max	Min	Ave	S.D.	Max	Min	Ave	S.D.	Max	Min
5	0.40	2	4.0E-13	3.4E-15	4.1E-13	4.0E-13	1.2E-12	1.0E-14	1.2E-12	1.2E-12	1.6E-12	1.3E-14	1.6E-12	1.5E-12	0.0E+00	0.0E+00	0.0E+00	0.0E+00				
7	0.41	12	2.8E-12	2.0E-12	7.5E-12	8.1E-13	4.1E-11	3.0E-11	1.1E-10	1.2E-11	3.9E-13	2.1E-13	8.3E-13	0.0E+00	2.0E-14	7.0E-14	2.4E-13	0.0E+00	2.6E-14	8.8E-14	3.1E-13	0.0E+00
9	0.51	16	2.3E-12	1.8E-12	6.9E-12	2.2E-13	6.7E-12	5.2E-12	2.0E-11	6.3E-13	6.1E-13	5.4E-13	2.1E-12	0.0E+00	2.8E-14	1.1E-13	4.5E-13	0.0E+00	1.6E-13	6.5E-13	2.6E-12	0.0E+00
13	0.57	2					1.8E-11	9.4E-12	2.5E-11	1.2E-11	6.0E-13	1.5E-13	7.1E-13	4.9E-13	2.2E-12	8.7E-13	2.8E-12	1.6E-12	9.0E-13	3.5E-13	1.2E-12	6.5E-13
15	0.58	17	1.1E-11	1.3E-11	4.1E-11	6.9E-13	1.1E-11	1.2E-11	3.8E-11	6.4E-13	3.2E-13	2.1E-13	9.3E-13	0.0E+00	3.5E-14	1.4E-13	6.0E-13	0.0E+00	3.7E-13	1.5E-12	6.3E-12	0.0E+00
39[1]	0.67	25					9.3E-12	1.0E-11	3.8E-11	2.1E-12	2.0E-13	1.7E-13	7.4E-13	0.0E+00	3.5E-13	4.5E-13	1.6E-12	0.0E+00	1.5E-13	2.0E-13	7.0E-13	0.0E+00
40[2]	0.67	10	2.6E-13	1.1E-13	4.3E-13	8.8E-14	9.5E-12	3.8E-12	1.5E-11	3.2E-12	4.7E-13	4.7E-13	1.5E-12	0.0E+00	0.0E+00	0.0E+00	0.0E+00	0.0E+00	0.0E+00	0.0E+00	0.0E+00	0.0E+00
17	0.71	16	7.4E-12	7.8E-12	2.3E-11	9.9E-13	7.7E-11	8.1E-11	2.3E-10	1.0E-11	9.9E-13	7.6E-13	2.7E-12	0.0E+00	0.0E+00	0.0E+00	0.0E+00	0.0E+00	0.0E+00	0.0E+00	0.0E+00	0.0E+00
35	1.12	1	6.8E-12	N/A	N/A	N/A	6.3E-12	N/A	N/A	N/A	4.0E-12	N/A	N/A	N/A	0.0E+00	N/A	N/A	N/A	0.0E+00	N/A	N/A	N/A
29	1.16	15									5.9E-13	2.9E-13	1.1E-12	3.3E-13	3.4E-13	5.8E-13	1.7E-12	0.0E+00	4.4E-13	7.4E-13	2.2E-12	0.0E+00
33	1.44	9	1.4E-12	6.0E-13	2.5E-12	7.2E-13	3.3E-12	1.4E-12	5.9E-12	1.7E-12	2.7E-12	1.5E-12	4.3E-12	0.0E+00	5.6E-14	1.2E-13	3.2E-13	0.0E+00	4.2E-13	8.6E-13	2.4E-12	0.0E+00
19	1.63	17	6.9E-12	6.3E-12	2.4E-11	1.6E-12	1.2E-11	1.1E-11	4.1E-11	2.7E-12	2.3E-12	1.6E-12	6.4E-12	5.9E-13	6.0E-14	2.4E-13	1.0E-12	0.0E+00	3.9E-13	1.6E-12	6.6E-12	0.0E+00
31	1.64	2	4.6E-12	7.5E-13	5.1E-12	4.1E-12	1.5E-11	2.4E-12	1.6E-11	1.3E-11	2.3E-12	4.1E-14	2.4E-12	2.3E-12	0.0E+00	0.0E+00	0.0E+00	0.0E+00	0.0E+00	0.0E+00	0.0E+00	0.0E+00
Summary			4.4E-12	3.6E-12	4.1E-11	8.8E-14	1.8E-11	1.5E-11	2.3E-10	6.3E-13	1.3E-12	5.0E-13	6.4E-12	0.0E+00	2.4E-13	2.1E-13	2.8E-12	0.0E+00	2.4E-13	5.5E-13	6.6E-12	0.0E+00

Note: Zeroes indicate a calculated absence of dissolution. Blank cells indicate there was none of that mineral present in the sample.

Note: N=number of experimental observations used to model dissolution rates.

Note: Plagioclase dissolution calculations in Model 4 are the same as Model 3 (see Table AZ).

[1] AMAX and ARIMETCO samples originated from core drilled between 1974 and 1977 and were stored for at least 20 years prior to initiation.

[2] Dunka blast hole samples originated from a blast on August 30, 1989 at the Dunka Mine and were stored for 8 years prior to initiation.

Table 57. Comparison of silicate mineral dissolution model statistics (values reported in Tables 52-56)

Period	Model	Plagioclase (mol m^{-2}s^{-1})				Augite (mol m^{-2}s^{-1})				Hypersthene (mol m^{-2}s^{-1})				Olivine (mol m^{-2}s^{-1})				Biotite (mol m^{-2}s^{-1})			
		Ave	S.D.	Max	Min[1]	Ave	S.D.	Max	Min[1]	Ave	S.D.	Max	Min[1]	Ave	S.D.	Max	Min[1]	Ave	S.D.	Max	Min[1]
A	1	5.7E-12	3.1E-12	4.1E-11	5.4E-13					5.5E-12	3.0E-12	4.0E-11	1.8E-13	1.7E-11	9.6E-12	2.0E-10	9.7E-14	9.3E-12	5.2E-12	6.2E-11	5.0E-13
	2	2.8E-12	2.3E-12	2.3E-11	0.0E+00	9.5E-12	5.2E-12	5.0E-11	5.8E-13	6.7E-13	1.4E-12	2.4E-11	0.0E+00	2.5E-12	4.5E-12	1.2E-10	0.0E+00	1.2E-12	2.3E-12	4.2E-11	0.0E+00
	3	6.2E-13	1.2E-13	9.6E-13	1.8E-13	8.8E-12	3.2E-12	4.2E-11	1.1E-12	1.3E-12	1.9E-12	9.3E-12	0.0E+00	8.4E-13	1.3E-12	7.4E-12	0.0E+00	1.3E-13	2.3E-13	1.2E-12	0.0E+00
	4									1.3E-12	1.9E-12	9.3E-12	0.0E+00	4.3E-13	6.1E-13	4.1E-12	0.0E+00	1.5E-11	5.9E-12	4.7E-11	1.8E-12
	max /min	9.3	24.9	43.3	N/A	1.1	1.7	1.2	1.8	8.3	2.2	4.3	N/A	40.2	15.9	49.0	N/A	116.0	25.8	52.1	N/A
B	1	1.5E-12	5.9E-13	9.3E-12	2.1E-14					3.4E-12	9.8E-13	2.9E-11	3.3E-14	9.1E-12	2.6E-12	5.4E-11	2.4E-14	5.6E-12	1.6E-12	2.9E-11	5.4E-14
	2	3.4E-13	2.9E-13	6.1E-12	0.0E+00	3.5E-12	1.5E-12	2.2E-11	6.5E-14	1.7E-12	7.7E-13	2.1E-11	0.0E+00	4.1E-12	2.3E-12	2.9E-11	0.0E+00	2.8E-12	1.3E-12	2.0E-11	0.0E+00
	3	3.8E-13	1.7E-13	1.5E-12	1.1E-13	1.9E-12	1.3E-12	1.2E-11	0.0E+00	2.9E-12	9.2E-13	2.0E-11	0.0E+00	1.1E-12	8.4E-13	1.2E-11	0.0E+00	3.2E-12	6.2E-13	1.9E-11	0.0E+00
	4									6.9E-13	5.5E-13	8.1E-12	0.0E+00	3.1E-13	2.8E-13	3.6E-12	0.0E+00	1.0E-11	4.2E-12	5.3E-11	1.7E-13
	max /min	4.3	3.4	6.3	N/A	1.8	1.2	1.8	N/A	5.0	1.8	3.6	N/A	29.7	9.3	15.1	N/A	3.7	6.9	2.7	N/A
C	1	1.5E-12	5.9E-13	9.3E-12	2.1E-14	3.3E-12	2.9E-12	4.8E-11	0.0E+00	4.4E-12	2.1E-12	3.1E-11	0.0E+00	1.6E-11	6.7E-12	6.8E-11	0.0E+00	6.0E-12	3.0E-12	3.3E-11	0.0E+00
	2	3.3E-13	3.1E-13	4.1E-12	0.0E+00	6.7E-12	3.0E-12	5.9E-11	2.4E-13	2.8E-12	1.9E-12	2.7E-11	0.0E+00	9.6E-12	6.1E-12	6.0E-11	0.0E+00	3.4E-12	2.6E-12	3.1E-11	0.0E+00
	3	9.2E-13	2.9E-13	2.9E-12	4.3E-13	4.0E-12	2.0E-12	2.4E-11	0.0E+00	4.0E-12	1.8E-12	2.5E-11	0.0E+00	1.5E-11	5.3E-12	5.4E-11	0.0E+00	4.1E-12	1.7E-12	2.2E-11	0.0E+00
	4									2.7E-12	1.3E-12	2.5E-11	0.0E+00	7.0E-12	3.4E-12	5.4E-11	0.0E+00	4.7E-12	2.1E-12	2.4E-11	3.2E-13
	max /min	4.4	2.0	3.2	N/A	2.0	1.5	2.5	N/A	1.6	1.5	1.2	N/A	2.4	2.0	1.2	N/A	1.8	1.8	1.5	N/A
D	1	1.3E-12	3.6E-13	4.6E-12	6.7E-14					1.1E-12	5.8E-13	7.0E-12	8.8E-14	5.0E-12	2.1E-12	3.2E-11	5.2E-14	2.0E-12	9.9E-13	1.2E-11	7.7E-14
	2	4.1E-13	2.6E-13	2.7E-12	0.0E+00	2.3E-12	9.5E-13	1.4E-11	6.1E-14	1.3E-13	2.1E-13	3.2E-12	0.0E+00	7.1E-13	7.9E-13	9.0E-12	0.0E+00	2.6E-13	3.3E-13	4.2E-12	0.0E+00
	3	6.4E-13	2.2E-13	2.9E-12	1.4E-13	1.3E-12	5.0E-13	6.4E-12	0.0E+00	5.8E-13	4.2E-13	2.8E-12	0.0E+00	2.4E-12	1.6E-12	2.1E-11	0.0E+00	9.0E-13	9.7E-13	1.4E-11	0.0E+00
	4									2.4E-13	2.1E-13	2.8E-12	0.0E+00	2.4E-13	5.5E-13	6.6E-12	0.0E+00	4.4E-12	3.6E-12	4.1E-11	8.8E-14
	max /min	3.3	1.7	1.7	N/A	1.8	1.9	2.1	N/A	8.6	2.8	2.5	N/A	21.2	3.9	4.9	N/A	17.1	10.9	9.8	N/A

[1] No range in minimum values reported due to zero values calculated

Note: Plagioclase dissolution calculations in Model 1, Period C are the same as Period B.

Note: Plagioclase and augite dissolution calculations in Model 4 are the same as Model 3.

Table 58. Total number of calculated mineral dissolution rates for each model during the specified rate period and the total number of cases where the models calculated an absence of dissolution (zero value). Associated percentage is the comparison of zero values cases to total number of cases.

Sorted by model, than period

Model	Period	Plagioclase			Augite			Hypersthene			Olivine			Biotite		
		Total n	zero	%	Total n	zero	%	Total n	zero	%	Total n	zero	%	Total n	zero	%
1	A	301	0	0%				296	0	0%	259	0	0%	220	0	0%
	B	1352	0	0%				1345	0	0%	1180	0	0%	985	0	0%
	C				493	93	19%	491	22	4%	430	13	3%	370	21	6%
	D	561	0	0%				560	0	0%	551	0	0%	412	0	0%
2	A	280	56	20%	301	0	0%	280	224	80%	246	193	78%	207	162	78%
	B	1332	528	40%	1352	0	0%	1332	804	60%	1168	649	56%	975	607	62%
	C	491	368	75%	493	0	0%	491	123	25%	430	62	14%	370	117	32%
	D	559	91	16%	561	0	0%	559	468	84%	550	459	83%	412	351	85%
3	A	17	0	0%	17	0	0%	17	11	65%	17	11	65%	10	9	90%
	B	208	0	0%	208	34	16%	206	77	37%	187	60	32%	137	70	51%
	C	41	0	0%	41	1	2%	41	9	22%	32	1	3%	28	9	32%
	D	152	0	0%	152	11	7%	152	72	47%	149	69	46%	110	55	50%
4	A	17	0	0%	17	0	0%	17	12	71%	17	12	71%	10	0	0%
	B	208	0	0%	208	34	16%	196	129	66%	179	112	63%	131	0	0%
	C	41	0	0%	41	1	2%	41	22	54%	32	13	41%	28	0	0%
	D	152	0	0%	152	11	7%	144	112	78%	142	110	77%	102	0	0%

Sorted by period, than model

Period	Model	Plagioclase			Augite			Hypersthene			Olivine			Biotite		
		Total n	zero	%	Total n	zero	%	Total n	zero	%	Total n	zero	%	Total n	zero	%
A	1	301	0	0%				296	0	0%	259	0	0%	220	0	0%
	2	280	56	20%	301	0	0%	280	224	80%	246	193	78%	207	162	78%
	3	17	0	0%	17	0	0%	17	11	65%	17	11	65%	10	9	90%
	4	17	0	0%	17	0	0%	17	12	71%	17	12	71%	10	0	0%
B	1	1352	0	0%				1345	0	0%	1180	0	0%	985	0	0%
	2	1332	528	40%	1352	0	0%	1332	804	60%	1168	649	56%	975	607	62%
	3	208	0	0%	208	34	16%	206	77	37%	187	60	32%	137	70	51%
	4	208	0	0%	208	34	16%	196	129	66%	179	112	63%	131	0	0%
C	1				493	93	19%	491	22	4%	430	13	3%	370	21	6%
	2	491	368	75%	493	0	0%	491	123	25%	430	62	14%	370	117	32%
	3	41	0	0%	41	1	2%	41	9	22%	32	1	3%	28	9	32%
	4	41	0	0%	41	1	2%	41	22	54%	32	13	41%	28	0	0%
D	1	561	0	0%				560	0	0%	551	0	0%	412	0	0%
	2	559	91	16%	561	0	0%	559	468	84%	550	459	83%	412	351	85%
	3	152	0	0%	152	11	7%	152	72	47%	149	69	46%	110	55	50%
	4	152	0	0%	152	11	7%	144	112	78%	142	110	77%	102	0	0%

Table 59. Comparison of Model 1 and 4 biotite dissolution rates and ratio of K/Mg release rates. Instances where the calculated biotite dissolution rate was higher in model 1 than model 4 typically correspond to lower K/Mg release ratio (highlighted values).

R#	%S	Period A			Period B			Period C			Period D		
		Model 1	Model 4	M4/M1	Model 1	Model 4	M4/M1	Model 1	Model 4	M4/M1	Model 1	Model 4	M4/M1
1	0.18	6.0E-12			1.7E-12	6.0E-12	3.58						
3	0.22	6.1E-12			1.4E-12	2.3E-12	1.68						
5	0.40	3.6E-12			9.1E-13	5.6E-12	6.22	3.9E-13	1.2E-12	3.10	4.2E-13	4.0E-13	0.95
7	0.41	2.3E-12			1.2E-12			2.1E-12	4.5E-12	2.10	5.4E-13	2.8E-12	5.10
9	0.51	2.7E-12			1.5E-12			1.3E-12			6.4E-13	2.3E-12	3.69
15	0.58	3.2E-11			1.7E-11			1.4E-11			2.7E-12	1.1E-11	4.20
17	0.71	9.4E-12			4.1E-12			9.7E-12	5.9E-12	0.61	1.3E-12	7.4E-12	5.49
33	1.44	7.3E-12			6.3E-12			1.1E-11	1.0E-11	0.91	1.8E-12	1.4E-12	0.79
19	1.63	1.9E-11			1.1E-11			1.1E-11	7.1E-12	0.62	2.5E-12	6.9E-12	2.73

R#	%S	Period A			Period B			Period C			Period D		
		Mg	K	K/Mg	Mg	K	K/Mg	Mg	K	K/Mg	Mg	K	K/Mg
1	0.18	8.2E-12			2.3E-12	5.7E-12	2.52						
3	0.22	1.6E-11			3.5E-12	3.3E-12	0.92						
5	0.4	5.0E-12			1.3E-12	4.6E-12	3.71	1.1E-12	1.1E-12	0.98	5.9E-13	3.7E-13	0.63
7	0.41	5.4E-12			2.9E-12			7.2E-12	6.3E-12	0.87	1.3E-12	3.7E-12	2.86
9	0.51	6.1E-12			3.5E-12			7.1E-12			1.5E-12	3.2E-12	2.17
15	0.58	1.6E-11			8.5E-12			8.5E-12			1.3E-12	4.9E-12	3.65
17	0.71	1.6E-11			6.9E-12			2.1E-11	5.0E-12	0.24	2.2E-12	6.0E-12	2.70
33	1.44	1.3E-11			1.1E-11			2.9E-11	9.5E-12	0.33	3.2E-12	1.5E-12	0.46
19	1.63	3.3E-11			1.9E-11			2.4E-11	6.5E-12	0.27	4.3E-12	6.2E-12	1.45

Table 60. Model 1, Sample Group Average Silicate Mineral Dissolution Rates.

Model 1, Average rates by sample group																						
Period	Group	N	Plag (mol m^{-2}s^{-1})				Aug (mol m^{-2}s^{-1})				Hyp (mol m^{-2}s^{-1})				Ol (mol m^{-2}s^{-1})				Bio (mol m^{-2}s^{-1})			
			Ave	S.D.	Max	Min	Ave	S.D.	Max	Min	Ave	S.D.	Max	Min	Ave	S.D.	Max	Min	Ave	S.D.	Max	Min
A	I	9	3.2E-12	1.6E-12	6.5E-12	1.8E-12					5.6E-12	5.0E-12	1.7E-11	1.1E-12	1.1E-11	1.0E-11	3.5E-11	2.3E-12	6.1E-12	4.4E-12	1.5E-11	1.1E-12
	II	15	4.9E-12	2.5E-12	1.1E-11	1.8E-12					5.4E-12	2.5E-12	1.0E-11	1.5E-12	1.2E-11	5.8E-12	2.1E-11	3.3E-12	8.9E-12	5.1E-12	1.9E-11	1.8E-12
	III	16	8.2E-12	4.8E-12	1.8E-11	2.3E-12					5.7E-12	3.0E-12	1.3E-11	1.6E-12	2.7E-11	1.4E-11	6.2E-11	7.9E-12	1.1E-11	5.6E-12	2.5E-11	4.4E-12
B	I	165	6.2E-13	3.0E-13	2.2E-12	7.3E-14					1.5E-12	1.1E-12	6.1E-12	3.6E-13	2.8E-12	2.1E-12	1.1E-11	5.2E-13	1.5E-12	1.2E-12	6.1E-12	3.1E-13
	II	58	1.3E-12	4.6E-13	2.7E-12	4.9E-13					3.7E-12	9.7E-13	6.3E-12	1.8E-12	5.4E-12	1.9E-12	1.0E-11	1.2E-12	5.9E-12	1.6E-12	9.9E-12	2.5E-12
	III	31	2.1E-12	9.2E-13	4.7E-12	1.1E-12					3.8E-12	9.6E-13	6.3E-12	1.9E-12	1.7E-11	3.7E-12	2.5E-11	9.1E-12	6.7E-12	1.7E-12	1.1E-11	3.7E-12
C	I		6.2E-13	3.0E-13	2.2E-12	7.3E-14																
	II	23	1.3E-12	4.6E-13	2.7E-12	4.9E-13	1.0E-12	8.3E-13	3.2E-12	1.1E-13	2.5E-12	1.3E-12	5.5E-12	8.2E-13	7.7E-12	3.6E-12	1.5E-11	2.3E-12	3.3E-12	1.7E-12	7.1E-12	8.3E-13
	III	44	2.1E-12	9.2E-13	4.7E-12	1.1E-12	6.0E-12	5.3E-12	1.8E-11	3.8E-14	6.6E-12	3.0E-12	1.3E-11	1.3E-12	2.4E-11	9.5E-12	4.4E-11	6.1E-12	9.3E-12	4.5E-12	2.0E-11	1.9E-12
D	I																					
	II	51	1.0E-12	3.6E-13	2.1E-12	5.3E-13					8.4E-13	5.5E-13	2.4E-12	1.9E-13	1.7E-12	1.5E-12	7.0E-12	6.2E-13	9.0E-13	8.0E-13	3.7E-12	4.2E-13
	III	35	1.7E-12	3.6E-13	2.6E-12	1.3E-12					1.5E-12	6.1E-13	3.1E-12	8.9E-13	8.4E-12	2.7E-12	1.5E-11	5.3E-12	3.1E-12	1.2E-12	6.0E-12	1.8E-12

Table 61. Model 2, Sample Group Average Silicate Mineral Dissolution Rates.

Model 2, Average rates by sample group																						
Period	Group	N	Aug (mol m^{-2}s^{-1})				Plag (mol m^{-2}s^{-1})				Hyp (mol m^{-2}s^{-1})				Ol (mol m^{-2}s^{-1})				Bio (mol m^{-2}s^{-1})			
			Ave	S.D.	Max	Min	Ave	S.D.	Max	Min	Ave	S.D.	Max	Min	Ave	S.D.	Max	Min	Ave	S.D.	Max	Min
A	I	9	6.3E-12	3.6E-12	1.2E-11	1.4E-12	1.5E-12	1.3E-12	4.1E-12	1.7E-13	1.2E-12	3.0E-12	8.1E-12	0.0E+00	2.8E-12	7.0E-12	1.9E-11	0.0E+00	1.0E-12	2.5E-12	6.8E-12	0.0E+00
	II	15	8.5E-12	4.7E-12	1.7E-11	1.7E-12	2.6E-12	2.1E-12	6.7E-12	2.1E-13	4.3E-13	9.5E-13	3.3E-12	0.0E+00	5.1E-13	1.3E-12	3.8E-12	0.0E+00	5.1E-13	1.5E-12	5.4E-12	0.0E+00
	III	16	1.2E-11	6.7E-12	2.8E-11	4.3E-12	3.8E-12	3.1E-12	1.0E-11	5.3E-15	8.2E-13	1.3E-12	4.3E-12	0.0E+00	5.0E-12	7.5E-12	2.6E-11	0.0E+00	2.4E-12	3.5E-12	1.2E-11	0.0E+00
B	I	165	1.9E-12	1.2E-12	6.4E-12	3.9E-13	1.9E-13	2.4E-13	1.8E-12	0.0E+00	3.0E-13	6.0E-13	3.8E-12	0.0E+00	6.9E-13	1.3E-12	8.1E-12	0.0E+00	3.6E-13	7.4E-13	4.3E-12	0.0E+00
	II	58	2.7E-12	1.2E-12	6.3E-12	1.2E-12	5.3E-13	3.3E-13	1.7E-12	9.2E-14	2.0E-12	7.3E-13	3.9E-12	7.6E-13	2.1E-12	1.3E-12	5.2E-12	1.9E-13	3.0E-12	1.0E-12	5.6E-12	1.0E-12
	III	31	5.5E-12	2.2E-12	1.2E-11	2.8E-12	1.0E-13	2.5E-13	1.1E-12	0.0E+00	1.9E-12	9.1E-13	3.7E-12	4.9E-14	8.3E-12	4.0E-12	1.5E-11	3.0E-13	3.5E-12	1.8E-12	6.7E-12	1.5E-13
C	I																					
	II	23	2.6E-12	1.0E-12	5.0E-12	1.0E-12	5.4E-13	4.1E-13	1.5E-12	1.1E-13	1.2E-12	1.1E-12	4.0E-12	0.0E+00	2.7E-12	2.6E-12	9.5E-12	0.0E+00	1.2E-12	1.3E-12	4.6E-12	0.0E+00
	III	44	1.1E-11	5.3E-12	2.3E-11	4.0E-12	9.4E-14	1.9E-13	9.8E-13	0.0E+00	4.7E-12	2.9E-12	1.1E-11	1.2E-13	1.6E-11	9.1E-12	3.5E-11	6.8E-13	6.0E-12	4.3E-12	1.6E-11	1.8E-13
D	I																					
	II	51	9.0E-13	5.6E-13	2.8E-12	4.3E-13	5.6E-13	3.4E-13	1.6E-12	4.3E-14	4.8E-14	1.5E-13	8.1E-13	0.0E+00	5.2E-14	2.8E-13	2.1E-12	0.0E+00	2.0E-14	1.4E-13	1.2E-12	0.0E+00
	III	35	4.0E-12	1.4E-12	7.6E-12	2.1E-12	2.3E-13	1.7E-13	6.2E-13	0.0E+00	2.3E-13	2.6E-13	1.0E-12	4.4E-14	1.4E-12	1.3E-12	4.3E-12	3.1E-13	5.0E-13	5.1E-13	1.9E-12	1.4E-13

Table 62. Model 3, Sample Group Average Silicate Mineral Dissolution Rates.

Model 3, Average rates by sample group																						
Period	Group	N	Plag (mol m^{-2}s^{-1})				Aug (mol m^{-2}s^{-1})				Hyp (mol m^{-2}s^{-1})				Ol (mol m^{-2}s^{-1})				Bio (mol m^{-2}s^{-1})			
			Ave	S.D.	Max	Min	Ave	S.D.	Max	Min	Ave	S.D.	Max	Min	Ave	S.D.	Max	Min	Ave	S.D.	Max	Min
A	I	2	7.5E-13	8.7E-14	8.1E-13	6.9E-13	7.2E-12	1.0E-12	7.9E-12	6.5E-12	4.8E-13	3.0E-13	6.9E-13	2.7E-13	1.3E-13	7.9E-14	1.8E-13	7.1E-14				
	II	3	5.9E-13	1.3E-13	7.2E-13	4.6E-13	9.1E-12	3.6E-12	1.3E-11	6.4E-12	1.5E-12	2.3E-12	3.5E-12	2.0E-14	9.9E-13	1.6E-12	2.5E-12	8.6E-15	1.3E-13	2.3E-13	4.0E-13	0.0E+00
	III																					
B	I	33	2.9E-13	1.3E-13	5.6E-13	1.4E-13	9.4E-13	7.2E-13	2.8E-12	6.9E-14	7.5E-13	8.7E-13	3.9E-12	0.0E+00	9.8E-13	1.4E-12	6.4E-12	0.0E+00	5.0E-13	8.5E-13	4.0E-12	0.0E+00
	II	18	4.2E-13	2.0E-13	8.9E-13	2.6E-13	2.4E-12	1.5E-12	4.6E-12	1.2E-12	3.9E-12	9.4E-13	5.2E-12	2.9E-12	1.2E-12	4.9E-13	1.9E-12	7.1E-13	4.6E-12	5.0E-13	5.2E-12	4.3E-12
	III																					
C	I																					
	II	4	6.1E-13	1.2E-13	7.6E-13	5.0E-13	1.6E-12	6.5E-13	2.7E-12	1.1E-12	1.5E-12	6.1E-13	2.0E-12	8.6E-13	3.2E-12	1.7E-12	4.3E-12	1.1E-12	9.1E-13	6.3E-13	1.4E-12	4.0E-13
	III	3	1.1E-12	4.7E-13	1.5E-12	8.9E-13	5.8E-12	3.4E-12	8.3E-12	3.6E-12	5.7E-12	2.9E-12	8.1E-12	4.1E-12	2.0E-11	7.5E-12	2.6E-11	1.5E-11	6.6E-12	3.1E-12	9.0E-12	4.5E-12
D	I																					
	II	13	5.7E-13	2.7E-13	1.2E-12	3.3E-13	5.9E-13	2.5E-13	1.2E-12	2.9E-13	4.8E-13	4.2E-13	1.4E-12	2.3E-13	8.9E-13	1.7E-12	5.7E-12	1.1E-13	4.5E-13	1.0E-12	3.6E-12	0.0E+00
	III	11	7.3E-13	1.5E-13	9.7E-13	5.9E-13	2.2E-12	8.4E-13	3.5E-12	1.2E-12	6.9E-13	4.1E-13	1.5E-12	4.8E-13	3.8E-12	1.5E-12	6.7E-12	3.0E-12	1.3E-12	8.9E-13	3.1E-12	8.9E-13

Table 63. Model 4, Sample Group Average Silicate Mineral Dissolution Rates.

Model 4, Average rates by sample group																						
Period	Group	N	Bio (mol $m^{-2}s^{-1}$)				K-spar (mol $m^{-2}s^{-1}$)				Aug (mol $m^{-2}s^{-1}$)				Hyp (mol $m^{-2}s^{-1}$)				Ol (mol $m^{-2}s^{-1}$)			
			Ave	S.D.	Max	Min	Ave	S.D.	Max	Min	Ave	S.D.	Max	Min	Ave	S.D.	Max	Min	Ave	S.D.	Max	Min
A	I	2									7.2E-12	1.0E-12	7.9E-12	6.5E-12	4.8E-13	3.0E-13	6.9E-13	2.7E-13	1.3E-13	7.9E-14	1.8E-13	7.1E-14
	II	3	1.5E-11	5.9E-12	2.2E-11	1.0E-11	2.5E-10	1.7E-10	4.0E-10	1.2E-10	9.1E-12	3.6E-12	1.3E-11	6.4E-12	1.4E-12	2.2E-12	3.4E-12	2.0E-14	4.9E-13	7.1E-13	1.1E-12	8.6E-15
	III																					
B	I	32	4.1E-12	3.9E-12	1.3E-11	4.5E-13	1.0E-11	1.1E-11	3.8E-11	8.9E-13	9.1E-13	6.9E-13	2.7E-12	6.9E-14	4.1E-13	4.1E-13	1.9E-12	0.0E+00	1.3E-13	2.1E-13	1.1E-12	0.0E+00
	II	17	1.3E-11	4.4E-12	2.0E-11	9.9E-12	1.5E-10	5.9E-11	2.4E-10	1.0E-10	2.4E-12	1.6E-12	4.6E-12	1.2E-12	8.3E-13	6.2E-13	1.6E-12	3.0E-14	4.1E-13	3.2E-13	8.2E-13	1.6E-14
	III																					
C	I																					
	II	4	2.3E-12	9.3E-13	3.1E-12	1.5E-12	4.0E-11	1.7E-11	5.9E-11	2.4E-11	1.6E-12	6.5E-13	2.7E-12	1.1E-12	8.5E-13	2.1E-13	1.0E-12	5.2E-13	6.8E-13	2.3E-13	8.7E-13	3.8E-13
	III	3	6.6E-12	3.7E-12	9.8E-12	4.4E-12	3.1E-11	1.8E-11	4.3E-11	1.9E-11	5.8E-12	3.4E-12	8.3E-12	3.6E-12	4.0E-12	2.5E-12	6.1E-12	2.7E-12	9.6E-12	5.3E-12	1.4E-11	6.7E-12
D	I																					
	II	12	3.4E-12	3.4E-12	1.1E-11	4.4E-13	1.4E-11	1.0E-11	3.6E-11	4.5E-12	5.9E-13	2.5E-13	1.2E-12	2.9E-13	3.8E-13	2.3E-13	8.1E-13	2.3E-13	2.7E-13	4.7E-13	1.8E-12	1.1E-13
	III	10	5.4E-12	3.9E-12	1.2E-11	2.8E-12	2.3E-11	2.4E-11	6.1E-11	6.8E-12	2.1E-12	8.4E-13	3.5E-12	1.2E-12	7.7E-14	1.9E-13	5.0E-13	0.0E+00	2.1E-13	6.4E-13	1.9E-12	0.0E+00

Note: Plagioclase dissolution calculations in Model 4 are the same as Model 3 (see Table BE).

Table 64. Model 1, Comparison of Silicate Mineral Dissolution Rates from Samples with Differing Mineralogy.

Model 1, Comparison of rates from samples with differing mineralogy																					
Period	%S, Reactor	Plag (mol m^{-2}s^{-1})				Aug (mol m^{-2}s^{-1})				Hyp (mol m^{-2}s^{-1})				Ol (mol m^{-2}s^{-1})				Bio (mol m^{-2}s^{-1})			
		Ave	S.D.	Max	Min	Ave	S.D.	Max	Min	Ave	S.D.	Max	Min	Ave	S.D.	Max	Min	Ave	S.D.	Max	Min
A	0.72, 1.16	3.0E-12	1.4E-12	6.6E-12	1.7E-12					3.5E-12	2.0E-12	7.2E-12	4.8E-13	2.8E-12	1.6E-12	5.5E-12	3.2E-13				
	0.67 (R40), 0.82	4.0E-12	1.5E-12	7.6E-12	1.0E-12					2.2E-12	8.2E-13	3.6E-12	8.1E-13	1.6E-11	5.9E-12	2.5E-11	5.8E-12	2.1E-12	7.8E-13	3.3E-12	7.7E-13
	1.4, 1.64	1.1E-11	7.1E-12	2.8E-11	3.0E-12					9.9E-12	5.4E-12	2.2E-11	1.7E-12	4.9E-11	2.7E-11	1.1E-10	8.8E-12	1.6E-11	9.0E-12	3.8E-11	3.1E-12
B	0.72, 1.16	7.2E-13	4.9E-13	2.7E-12	2.4E-13					2.3E-12	1.1E-12	6.7E-12	1.2E-12	2.2E-12	9.2E-13	5.7E-12	1.3E-12				
	0.67 (R40), 0.82	1.6E-12	4.5E-13	2.9E-12	9.0E-13					5.3E-13	2.2E-13	1.1E-12	1.1E-13	3.4E-12	1.4E-12	7.6E-12	6.9E-13	4.1E-13	1.8E-13	9.8E-13	8.4E-14
	1.4, 1.64	2.4E-12	7.2E-13	4.6E-12	1.4E-12					6.5E-12	1.4E-12	9.2E-12	2.8E-12	2.5E-11	5.8E-12	3.7E-11	1.1E-11	6.4E-12	1.6E-12	1.0E-11	3.1E-12
C	0.72, 1.16	7.2E-13	4.9E-13	2.7E-12	2.4E-13	3.9E-12	3.1E-12	1.1E-11	0.0E+00	6.2E-12	3.1E-12	1.3E-11	0.0E+00	8.0E-12	4.0E-12	1.7E-11	0.0E+00				
	0.67 (R40), 0.82	1.6E-12	4.5E-13	2.9E-12	9.0E-13	6.6E-14	2.0E-13	6.4E-13	0.0E+00	2.1E-12	6.5E-13	2.8E-12	8.5E-13	1.2E-11	3.7E-12	1.6E-11	4.9E-12	1.3E-12	4.1E-13	1.7E-12	5.3E-13
	1.4, 1.64	2.4E-12	7.2E-13	4.6E-12	1.4E-12	2.8E-12	2.0E-12	6.7E-12	1.3E-13	1.2E-11	4.7E-12	2.1E-11	3.7E-12	4.1E-11	1.4E-11	6.7E-11	1.6E-11	8.2E-12	2.1E-12	1.3E-11	4.4E-12
D	0.72, 1.16	8.8E-13	2.2E-13	1.5E-12	5.4E-13					7.5E-13	7.6E-13	3.4E-12	1.8E-13	9.5E-13	9.7E-13	4.3E-12	2.4E-13				
	0.67 (R40), 0.82	8.4E-13	4.6E-13	1.9E-12	1.9E-13					2.8E-13	2.2E-13	1.2E-12	1.2E-13	1.6E-12	1.3E-12	6.8E-12	7.1E-13	1.8E-13	1.4E-13	7.4E-13	7.7E-14
	1.4, 1.64	2.9E-12	4.2E-13	3.6E-12	2.6E-12					4.1E-12	8.6E-13	5.5E-12	3.2E-12	2.4E-11	5.0E-12	3.2E-11	1.8E-11	4.5E-12	9.5E-13	6.0E-12	3.5E-12

Mineralogical breakdown of cations present (%) for specific samples and minerals (see Table U for full mineralogical breakdown)

%S	Reactor	Calcium				Magnesium					Sodium		Potassium			
		Plag	Augite	Prehnite	Amphibole	Augite	Hyper	Olivine	Biotite	Amphibole	Plag	K-Spar	Plag	Biotite	K-Spar	Amphibole
0.72	42	94.09	5.91			4.90	10.17	84.93			100.00		100.00			
1.16	29	76.36	23.64			17.72	31.30	50.98			100.00		100.00			
0.67	40	68.15	31.85			25.90	44.55	15.03	14.52		99.44	0.56	15.02	68.73	16.25	
0.82	43	66.52	33.48			29.18	52.09	11.23	7.50		100.00		33.24	66.76		
1.40	37	60.97	29.45	8.15	1.44	34.57	33.96	29.37		2.10	97.59	2.41	30.83		67.72	1.45
1.64	31	61.29	35.95	2.76		36.46	41.43	13.93	8.18		97.39	2.61	15.08	23.74	61.18	

Table 65. Model 2, Comparison of Silicate Mineral Dissolution Rates from Samples with Differing Mineralogy.

Model 2, Comparison of rates from samples with differing mineralogy

Period	%S, Reactor	Plag (mol m^{-2}s^{-1})				Aug (mol m^{-2}s^{-1})				Hyp (mol m^{-2}s^{-1})				Ol (mol m^{-2}s^{-1})				Bio (mol m^{-2}s^{-1})			
		Ave	S.D.	Max	Min	Ave	S.D.	Max	Min	Ave	S.D.	Max	Min	Ave	S.D.	Max	Min	Ave	S.D.	Max	Min
A	0.72, 1.16	1.6E-12	1.4E-12	5.2E-12	2.7E-13	6.7E-12	3.8E-12	1.4E-11	9.3E-13	0.0E+00	0.0E+00	0.0E+00	0.0E+00	0.0E+00	0.0E+00	0.0E+00	0.0E+00				
	0.67 (R40), 0.82	1.7E-12	1.1E-12	4.0E-12	0.0E+00	4.0E-12	1.5E-12	6.5E-12	1.3E-12	3.4E-14	1.2E-13	4.9E-13	0.0E+00	2.7E-13	1.0E-12	4.1E-12	0.0E+00	3.8E-14	1.5E-13	6.0E-13	0.0E+00
	1.4, 1.64	4.4E-12	4.1E-12	1.3E-11	0.0E+00	1.0E-11	6.6E-12	2.5E-11	1.9E-12	7.0E-13	1.3E-12	3.9E-12	0.0E+00	3.7E-12	6.8E-12	2.0E-11	0.0E+00	1.3E-12	2.3E-12	6.6E-12	0.0E+00
B	0.72, 1.16	8.3E-14	8.0E-14	4.4E-13	0.0E+00	2.9E-12	1.9E-12	1.0E-11	9.6E-13	7.9E-13	4.8E-13	2.5E-12	1.1E-14	9.8E-13	4.5E-13	2.3E-12	1.4E-14				
	0.67 (R40), 0.82	1.0E-12	4.1E-13	2.1E-12	5.1E-13	9.3E-13	4.0E-13	2.0E-12	1.9E-13	3.1E-15	9.1E-15	3.1E-14	0.0E+00	3.1E-14	9.2E-14	3.1E-13	0.0E+00	5.1E-15	1.5E-14	5.0E-14	0.0E+00
	1.4, 1.64	8.0E-14	3.9E-13	2.1E-12	0.0E+00	3.5E-12	9.6E-13	5.5E-12	2.2E-12	3.2E-12	1.4E-12	5.9E-12	0.0E+00	1.2E-11	5.5E-12	2.2E-11	0.0E+00	3.0E-12	1.5E-12	5.5E-12	0.0E+00
C	0.72, 1.16	2.5E-14	1.7E-13	1.2E-12	0.0E+00	6.7E-12	3.1E-12	1.4E-11	2.9E-12	4.7E-12	3.1E-12	1.2E-11	0.0E+00	5.9E-12	3.9E-12	1.5E-11	0.0E+00				
	0.67 (R40), 0.82	3.1E-13	4.3E-13	1.1E-12	0.0E+00	3.4E-12	9.1E-13	4.3E-12	1.5E-12	1.7E-13	1.8E-13	5.4E-13	0.0E+00	9.9E-13	1.0E-12	3.1E-12	0.0E+00	1.1E-13	1.1E-13	3.4E-13	0.0E+00
	1.4, 1.64	8.6E-16	5.3E-15	3.3E-14	0.0E+00	6.5E-12	2.1E-12	1.0E-11	3.4E-12	9.0E-12	4.7E-12	1.8E-11	4.0E-13	2.7E-11	1.4E-11	5.4E-11	2.4E-12	4.6E-12	2.1E-12	9.0E-12	8.9E-13
D	0.72, 1.16	4.5E-13	2.5E-13	9.6E-13	0.0E+00	1.1E-12	9.2E-13	4.1E-12	3.3E-13	1.1E-13	3.2E-13	1.8E-12	0.0E+00	1.4E-13	4.1E-13	2.2E-12	0.0E+00				
	0.67 (R40), 0.82	5.6E-13	3.4E-13	1.4E-12	1.4E-14	4.9E-13	3.8E-13	2.0E-12	2.1E-13	0.0E+00	0.0E+00	0.0E+00	0.0E+00	0.0E+00	0.0E+00	0.0E+00	0.0E+00	0.0E+00	0.0E+00	0.0E+00	0.0E+00
	1.4, 1.64	1.3E-14	3.0E-14	6.7E-14	0.0E+00	4.1E-12	6.1E-13	5.1E-12	3.6E-12	5.6E-13	4.0E-13	1.0E-12	0.0E+00	3.3E-12	2.3E-12	6.0E-12	0.0E+00	6.2E-13	4.4E-13	1.1E-12	0.0E+00

Mineralogical breakdown of cations present (%) for specific samples and minerals (see Table U for full mineralogical breakdown)

%S	Reactor	Calcium				Magnesium					Sodium		Potassium			
		Plag	Augite	Prehnite	Amphibole	Augite	Hyper	Olivine	Biotite	Amphibole	Plag	K-Spar	Plag	Biotite	K-Spar	Amphibole
0.72	42	94.09	5.91			4.90	10.17	84.93			100.00		100.00			
1.16	29	76.36	23.64			17.72	31.30	50.98			100.00		100.00			
0.67	40	68.15	31.85			25.90	44.55	15.03	14.52		99.44	0.56	15.02	68.73	16.25	
0.82	43	66.52	33.48			29.18	52.09	11.23	7.50		100.00		33.24	66.76		
1.40	37	60.97	29.45	8.15	1.44	34.57	33.96	29.37		2.10	97.59	2.41	30.83		67.72	1.45
1.64	31	61.29	35.95	2.76		36.46	41.43	13.93	8.18		97.39	2.61	15.08	23.74	61.18	

Table 66. Model 3, Comparison of Silicate Mineral Dissolution Rates from Samples with Differing Mineralogy.

Model 3, Comparison of rates from samples with differing mineralogy																					
Period	%S, Reactor	Plag (mol $m^{-2}s^{-1}$)				Aug (mol $m^{-2}s^{-1}$)				Hyp (mol $m^{-2}s^{-1}$)				Ol (mol $m^{-2}s^{-1}$)				Bio (mol $m^{-2}s^{-1}$)			
		Ave	S.D.	Max	Min	Ave	S.D.	Max	Min	Ave	S.D.	Max	Min	Ave	S.D.	Max	Min	Ave	S.D.	Max	Min
A	0.72, 1.16	7.5E-13	8.7E-14	8.1E-13	6.9E-13	7.2E-12	1.0E-12	7.9E-12	6.5E-12	4.8E-13	3.0E-13	6.9E-13	2.7E-13	1.3E-13	7.9E-14	1.8E-13	7.1E-14				
	0.67 (R40), 0.82	4.9E-13	1.8E-13	6.5E-13	3.0E-13	4.0E-12	9.9E-13	5.0E-12	3.0E-12	1.2E-13	2.1E-13	3.7E-13	0.0E+00	1.2E-12	2.1E-12	3.7E-12	0.0E+00	2.0E-13	3.4E-13	6.0E-13	0.0E+00
	1.4, 1.64																				
B	0.72, 1.16	2.9E-13	1.3E-13	4.7E-13	1.5E-13	1.2E-12	1.3E-12	4.1E-12	0.0E+00	1.2E-12	1.1E-12	4.9E-12	0.0E+00	3.2E-13	2.9E-13	1.3E-12	0.0E+00				
	0.67 (R40), 0.82	3.6E-13	1.4E-13	7.2E-13	1.7E-13	8.5E-13	3.9E-13	1.6E-12	1.6E-13	1.8E-14	2.9E-14	7.3E-14	0.0E+00	1.8E-13	2.9E-13	7.4E-13	0.0E+00	3.0E-14	4.7E-14	1.2E-13	0.0E+00
	1.4, 1.64																				
C	0.72, 1.16	9.1E-13	3.0E-13	1.3E-12	6.8E-13	3.2E-12	2.0E-12	5.5E-12	1.9E-12	6.9E-12	5.8E-12	1.4E-11	2.7E-12	8.8E-12	7.5E-12	1.7E-11	3.4E-12				
	0.67 (R40), 0.82	7.0E-13	7.8E-14	7.9E-13	6.1E-13	2.7E-12	3.7E-13	3.1E-12	2.2E-12	7.6E-13	5.1E-13	1.1E-12	0.0E+00	4.4E-12	2.9E-12	6.1E-12	0.0E+00	4.7E-13	3.2E-13	6.6E-13	0.0E+00
	1.4, 1.64	1.3E-12	2.6E-13	1.4E-12	1.1E-12	4.5E-12	1.5E-12	5.0E-12	3.7E-12	1.2E-11	5.7E-12	1.5E-11	9.6E-12	3.4E-11	1.2E-11	4.1E-11	3.0E-11	5.3E-12		5.3E-12	5.3E-12
D	0.72, 1.16	5.5E-13	1.3E-13	8.5E-13	3.5E-13	5.9E-13	2.9E-13	1.1E-12	3.3E-13	3.4E-13	5.8E-13	1.7E-12	0.0E+00	4.4E-13	7.4E-13	2.2E-12	0.0E+00				
	0.67 (R40), 0.82	5.4E-13	2.1E-13	9.5E-13	1.6E-13	4.7E-13	4.7E-13	1.5E-12	0.0E+00	6.3E-14	1.0E-13	3.1E-13	0.0E+00	3.6E-13	5.9E-13	1.8E-12	0.0E+00	3.9E-14	6.4E-14	1.9E-13	0.0E+00
	1.4, 1.64	1.1E-12	1.2E-13	1.2E-12	1.0E-12	2.3E-12	4.1E-14	2.4E-12	2.3E-12	2.1E-12	5.8E-15	2.1E-12	2.1E-12	1.2E-11	3.4E-14	1.2E-11	1.2E-11	2.3E-12	6.4E-15	2.3E-12	2.3E-12

Mineralogical breakdown of cations present (%) for specific samples and minerals (see Table U for full mineralogical breakdown)

%S	Reactor	Calcium				Magnesium					Sodium		Potassium			
		Plag	Augite	Prehnite	Amphibole	Augite	Hyper	Olivine	Biotite	Amphibole	Plag	K-Spar	Plag	Biotite	K-Spar	Amphibole
0.72	42	94.09	5.91			4.90	10.17	84.93			100.00		100.00			
1.16	29	76.36	23.64			17.72	31.30	50.98			100.00		100.00			
0.67	40	68.15	31.85			25.90	44.55	15.03	14.52		99.44	0.56	15.02	68.73	16.25	
0.82	43	66.52	33.48			29.18	52.09	11.23	7.50		100.00		33.24	66.76		
1.40	37	60.97	29.45	8.15	1.44	34.57	33.96	29.37		2.10	97.59	2.41	30.83		67.72	1.45
1.64	31	61.29	35.95	2.76		36.46	41.43	13.93	8.18		97.39	2.61	15.08	23.74	61.18	

Table 67. Model 4, Comparison of Silicate Mineral Dissolution Rates from Samples with Differing Mineralogy.

Model 4, Comparison of rates from samples with differing mineralogy																					
Period	%S, Reactor	Bio (mol m^{-2}s^{-1})				K-spar (mol m^{-2}s^{-1})				Aug (mol m^{-2}s^{-1})				Hyp (mol m^{-2}s^{-1})				Ol (mol m^{-2}s^{-1})			
		Ave	S.D.	Max	Min	Ave	S.D.	Max	Min	Ave	S.D.	Max	Min	Ave	S.D.	Max	Min	Ave	S.D.	Max	Min
A	0.72, 1.16									7.2E-12	1.0E-12	7.9E-12	6.5E-12	4.8E-13	3.0E-13	6.9E-13	2.7E-13	1.3E-13	7.9E-14	1.8E-13	7.1E-14
	0.67 (R40), 0.82	5.3E-12	3.8E-12	9.2E-12	1.9E-12	1.5E-10	1.3E-10	3.0E-10	6.4E-11	4.0E-12	9.9E-13	5.0E-12	3.0E-12	0.0E+00	0.0E+00	0.0E+00	0.0E+00	0.0E+00	0.0E+00	0.0E+00	0.0E+00
	1.4, 1.64																				
B	0.72, 1.16									1.1E-12	1.2E-12	3.8E-12	0.0E+00	1.2E-12	1.1E-12	4.9E-12	0.0E+00	3.2E-13	2.9E-13	1.3E-12	0.0E+00
	0.67 (R40), 0.82	1.1E-12	1.2E-12	5.9E-12	4.1E-13	5.8E-11	4.3E-11	2.0E-10	2.3E-11	8.4E-13	3.8E-13	1.5E-12	1.6E-13	1.4E-15	3.6E-15	1.4E-14	0.0E+00	1.4E-14	3.6E-14	1.4E-13	0.0E+00
	1.4, 1.64																				
C	0.72, 1.16									3.2E-12	2.0E-12	5.5E-12	1.9E-12	6.9E-12	5.8E-12	1.4E-11	2.7E-12	8.8E-12	7.5E-12	1.7E-11	3.4E-12
	0.67 (R40), 0.82	1.1E-12	4.6E-13	1.5E-12	4.6E-13	3.9E-11	1.7E-11	5.3E-11	1.6E-11	2.7E-12	3.7E-13	3.1E-12	2.2E-12	0.0E+00	0.0E+00	0.0E+00	0.0E+00	0.0E+00	0.0E+00	0.0E+00	0.0E+00
	1.4, 1.64	3.1E-12		3.1E-12	3.1E-12	4.1E-11	3.3E-11	5.4E-11	2.2E-11	4.5E-12	1.5E-12	5.0E-12	3.7E-12	1.0E-11	5.7E-12	1.3E-11	8.2E-12	2.6E-11	1.2E-11	3.3E-11	2.2E-11
D	0.72, 1.16									5.9E-13	2.9E-13	1.1E-12	3.3E-13	3.4E-13	5.8E-13	1.7E-12	0.0E+00	4.4E-13	7.4E-13	2.2E-12	0.0E+00
	0.67 (R40), 0.82	2.6E-13	1.1E-13	4.3E-13	8.8E-14	9.5E-12	3.8E-12	1.5E-11	3.2E-12	4.7E-13	4.7E-13	1.5E-12	0.0E+00	0.0E+00	0.0E+00	0.0E+00	0.0E+00	0.0E+00	0.0E+00	0.0E+00	0.0E+00
	1.4, 1.64	4.6E-12	7.5E-13	5.1E-12	4.1E-12	1.5E-11	2.4E-12	1.6E-11	1.3E-11	2.3E-12	4.1E-14	2.4E-12	2.3E-12	0.0E+00	0.0E+00	0.0E+00	0.0E+00	0.0E+00	0.0E+00	0.0E+00	0.0E+00

Mineralogical breakdown of cations present (%) for specific samples and minerals (see Table U for full mineralogical breakdown)

%S	Reactor	Calcium				Magnesium					Sodium		Potassium			
		Plag	Augite	Prehnite	Amphibole	Augite	Hyper	Olivine	Biotite	Amphibole	Plag	K-Spar	Plag	Biotite	K-Spar	Amphibole
0.72	42	94.09	5.91			4.90	10.17	84.93			100.00		100.00			
1.16	29	76.36	23.64			17.72	31.30	50.98			100.00		100.00			
0.67	40	68.15	31.85			25.90	44.55	15.03	14.52		99.44	0.56	15.02	68.73	16.25	
0.82	43	66.52	33.48			29.18	52.09	11.23	7.50		100.00		33.24	66.76		
1.40	37	60.97	29.45	8.15	1.44	34.57	33.96	29.37		2.10	97.59	2.41	30.83		67.72	1.45
1.64	31	61.29	35.95	2.76		36.46	41.43	13.93	8.18		97.39	2.61	15.08	23.74	61.18	

Note: Plagioclase dissolution calculations in Model 4 are the same as Model 3 (see Table BI).

Table 68. Potential gibbsite production and neutralization capacity (NC) for experiment until pH minima or initial decline of pH below 4.0.

%S	**Reactor**	week of P5 pH	5th percentile pH	first week below pH 4	Ca release (mmol)	SO4 release (mmol)	Acidity (mmol H+)	Gibbsite at pH 4 or pH min (mmol)	Gibbsite NC	Gibbsite NC-acidity
Group I, Duluth Complex										
0.18	**1**	754	6.12		2.72	2.06	-1.31	4.08	24.5	25.8
0.22	**3**	523	6.25		2.73	1.82	-1.82	4.09	24.6	26.4
0.72[1]	**42**	615	5.95		1.13	1.02	-0.22	1.70	10.2	10.4
Average			6.11		2.19	1.63	-1.12	3.29	19.7	20.9
Group II, Duluth Complex										
0.40	**5**	770	4.37	804	8.14	7.39	-1.50	12.2	73.3	74.8
0.41	**7**	374	4.17		1.93	2.73	1.60	2.90	17.4	15.8
0.51	**9**	287	4.1	357	2.75	4.88	4.25	4.13	24.8	20.5
0.54	**11**	276	4.24		4.21	4.66	0.92	6.31	37.9	36.9
0.57	**13**	369	4.27	331	2.40	5.11	5.42	3.60	21.6	16.2
0.58	**15**	293	4.15	330	2.06	6.68	9.24	3.09	18.6	9.33
0.67[1]	**39**	135	4.36		0.44	2.05	3.23	0.66	3.95	0.72
0.67[2]	**40**	411	4.26		2.84	5.99	6.29	4.26	25.6	19.3
0.82[2]	**43**	325	4.78		1.25	2.03	1.58	1.87	11.2	9.63
0.92[1]	**41**	291	5.21		0.80	1.25	0.91	1.20	7.21	6.30
1.71[1]	**44**	115	5.25		1.50	2.69	2.37	2.25	13.5	11.1
Average			4.47		2.57	4.13	3.12	3.86	23.2	20.1
Group III, Duluth Complex										
0.71	**17**	374	3.88	331	1.73	4.34	5.22	2.60	15.6	10.4
1.12	**35**	264	3.33	194	4.27	8.40	8.27	6.40	38.4	30.1
1.16	**29**	319	3.39	234	1.49	6.38	9.78	2.24	13.5	3.68
1.40	**37**	295	3.16	257	2.37	7.64	10.5	3.56	21.3	10.8
1.44	**33**	274	3.18	234	1.42	8.64	14.4	2.13	12.8	-1.68
1.63	**19**	289	3.43	257	2.40	12.4	19.9	3.59	21.6	1.63
1.64	**31**	268	3.48	235	3.28	11.4	16.3	4.92	29.5	13.3
Average			3.41		2.42	8.46	12.1	3.63	21.8	9.7
Virginia Formation										
2.06	21	66	4.3		1.47	4.10	5.25	2.21	13.3	8.01
3.12	23	45	3.85	43	2.70	5.82	6.24	4.05	24.3	18.0
3.72	25	63	3.9	60	2.40	5.74	6.69	3.60	21.6	14.9
5.44	27	36	3.65	3	2.03	3.40	2.74	3.05	18.3	15.5
Average			3.93		2.15	4.76	5.23	3.22	19.3	14.1

[1] AMAX and ARIMETCO samples originated from core drilled between 1974 and 1977 and were stored for at least 20 years prior to initiation.

[2] Dunka blast hole samples originated from a blast on August 30, 1989 at the Dunka Mine and were stored for 8 years prior to initiation.

Table 69. Calculated pyrrhotite oxidation rates for all Duluth Complex samples.

R#	%S	Period A				Period B				Period C				Period D			
		Ave	S.D.	Max	Min	Ave	S.D.	Max	Min	Ave	S.D.	Max	Min	Ave	S.D.	Max	Min
Group I																	
1	0.18[1]	N/A	N/A	N/A	N/A	N/A	N/A	N/A	N/A								
3	0.22	1.25E-08	6.55E-09	3.47E-08	3.55E-09	3.10E-09	2.55E-09	1.12E-08	2.25E-10								
42	0.72[2]	4.94E-11	1.49E-11	7.32E-11	2.21E-11	1.25E-11	8.01E-12	4.47E-11	1.05E-12								
Average		6.28E-09	3.28E-09	3.47E-08	2.21E-11	1.56E-09	1.28E-09	1.12E-08	1.05E-12								
Group II																	
5	0.4	3.78E-10	1.47E-10	8.34E-10	1.50E-10	1.12E-10	4.93E-11	3.51E-10	3.39E-11	5.62E-10	3.34E-10	1.23E-09	1.99E-10	1.30E-10	3.63E-11	2.09E-10	8.92E-11
7	0.41	1.62E-10	1.35E-10	5.12E-10	2.12E-11	1.29E-10	7.49E-11	3.03E-10	4.06E-11	5.08E-10	9.97E-11	6.83E-10	3.41E-10	1.52E-10	1.36E-10	5.90E-10	3.17E-11
9	0.51	2.28E-10	1.42E-10	5.81E-10	3.89E-11	1.04E-10	4.63E-11	1.86E-10	3.76E-11	6.37E-10	1.15E-10	9.56E-10	4.79E-10	2.04E-10	1.51E-10	5.65E-10	4.19E-11
11	0.54	2.37E-10	9.74E-11	4.97E-10	8.59E-11	1.61E-10	8.10E-11	4.02E-10	4.28E-11	2.23E-10	7.50E-11	4.25E-10	1.10E-10				
13	0.57	2.65E-10	7.20E-11	4.00E-10	1.35E-10	1.74E-10	9.00E-11	5.10E-10	2.87E-11	4.46E-10	1.10E-10	7.15E-10	3.17E-10	2.96E-10	4.97E-11	3.66E-10	2.17E-10
15	0.58	2.32E-10	1.89E-10	9.57E-10	2.86E-11	2.48E-10	9.54E-11	5.61E-10	1.27E-10	4.18E-10	8.96E-11	6.65E-10	3.01E-10	1.43E-10	9.46E-11	3.60E-10	3.15E-11
39	0.67[2]	2.10E-10	5.61E-11	2.71E-10	9.06E-11	1.33E-10	2.46E-11	1.73E-10	9.26E-11	1.73E-10	1.92E-11	2.10E-10	1.33E-10	3.58E-11	3.84E-11	1.43E-10	1.23E-12
40	0.67[3]	1.83E-10	6.77E-11	3.81E-10	8.52E-11	9.78E-11	3.35E-11	2.64E-10	5.94E-11	2.98E-10	8.50E-11	3.98E-10	1.57E-10	3.97E-11	3.79E-11	1.49E-10	1.17E-12
43	0.82[3]	1.08E-10	4.95E-11	2.24E-10	5.04E-11	2.91E-11	1.59E-11	8.61E-11	9.15E-13								
41	0.92[2]	5.59E-11	2.00E-11	1.02E-10	3.28E-11	1.64E-11	1.04E-11	5.21E-11	8.39E-13								
44	1.71[2]	8.52E-11	2.04E-11	1.28E-10	6.15E-11	6.58E-11	1.13E-11	8.81E-11	4.28E-11								
Average		1.95E-10	9.06E-11	9.57E-10	2.12E-11	1.15E-10	4.84E-11	5.61E-10	8.39E-13	4.08E-10	1.16E-10	1.23E-09	1.10E-10	1.43E-10	7.76E-11	5.90E-10	1.17E-12
Group III																	
17	0.71	1.36E-10	5.69E-11	2.54E-10	2.06E-11	9.32E-11	3.64E-11	1.94E-10	2.04E-11	5.01E-10	4.33E-10	1.67E-09	9.74E-11	8.17E-11	4.52E-11	2.19E-10	2.84E-11
35	1.12	2.61E-10	1.49E-11	8.73E-10	9.22E-11	2.57E-10	8.01E-12	3.22E-10	1.12E-10	4.86E-10	2.64E-10	9.05E-10	1.39E-10	1.75E-10	1.46E-11	1.86E-10	1.59E-10
29	1.16	1.52E-10	4.95E-11	4.03E-10	7.33E-11	1.12E-10	1.59E-11	2.07E-10	5.12E-11	4.23E-10	2.80E-10	1.07E-09	6.57E-11	4.00E-11	2.10E-11	1.00E-10	1.70E-11
37	1.4	1.40E-10	2.00E-11	2.53E-10	8.21E-11	1.09E-10	1.04E-11	2.74E-10	5.23E-11	5.88E-10	3.02E-10	1.11E-09	1.91E-10				
33	1.44	1.38E-10	1.36E-10	3.92E-10	6.57E-11	1.74E-10	5.57E-11	3.58E-10	8.69E-11	3.91E-10	2.64E-10	9.52E-10	5.15E-11	4.38E-11	1.46E-11	7.51E-11	2.52E-11
19	1.63	1.33E-10	8.07E-11	3.36E-10	4.51E-11	9.33E-11	3.84E-11	1.43E-10	5.32E-11	3.45E-10	2.80E-10	8.14E-10	8.77E-11	4.23E-11	2.10E-11	1.15E-10	9.54E-12
31	1.64	3.34E-10	5.65E-11	9.80E-10	1.65E-10	1.69E-10	4.02E-11	2.46E-10	9.86E-11	3.60E-10	3.02E-10	7.21E-10	1.44E-10	1.61E-10	1.61E-11	1.85E-10	1.43E-10
Average		1.85E-10	5.92E-11	9.80E-10	2.06E-11	1.44E-10	2.93E-11	3.58E-10	2.04E-11	4.42E-10	3.04E-10	1.67E-09	5.15E-11	9.07E-11	2.21E-11	2.19E-10	9.54E-12
Summary[4]		1.91E-10	7.84E-11	9.80E-10	2.06E-11	1.27E-10	4.10E-11	5.61E-10	8.39E-13	4.24E-10	2.04E-10	1.67E-09	5.15E-11	1.19E-10	5.20E-11	5.90E-10	1.17E-12

[1] Reactor 1 calculated to have pyrrhotite content less than zero

[2] AMAX and ARIMETCO samples originated from core drilled between 1974 and 1977 and were stored for at least 20 years prior to initiation.

[3] Dunka blast hole samples originated from a blast on August 30, 1989 at the Dunka Mine and were stored for 8 years prior to initiation.

[4] Overall calculations does not include group I due to the low amount of pyrrhotite calculated for reactor 3

Table 70. Calculated sulfide oxidation rates (all sulfide minerals combined) for all Duluth Complex samples.

R#	%S	Period A				Period B				Period C				Period D			
		Ave	S.D.	Max	Min	Ave	S.D.	Max	Min	Ave	S.D.	Max	Min	Ave	S.D.	Max	Min
Group I																	
1	0.18	4.81E-10	2.82E-10	1.21E-09	1.19E-10	9.48E-11	9.23E-11	4.20E-10	7.70E-12								
3	0.22	4.17E-10	2.18E-10	1.16E-09	1.18E-10	1.03E-10	8.51E-11	3.74E-10	7.51E-12								
42	0.72[1]	4.68E-11	1.32E-10	6.93E-11	2.09E-11	1.18E-11	4.44E-11	4.23E-11	9.99E-13								
Average		3.15E-10	2.11E-10	1.21E-09	2.09E-11	7.00E-11	7.39E-11	4.20E-10	9.99E-13								
Group II																	
5	0.4	3.41E-10	1.32E-10	7.52E-10	1.35E-10	1.01E-10	4.44E-11	3.17E-10	3.05E-11	5.07E-10	3.01E-10	1.11E-09	1.79E-10	1.17E-10	3.27E-11	1.89E-10	8.04E-11
7	0.41	1.32E-10	1.10E-10	4.18E-10	1.73E-11	1.06E-10	6.12E-11	2.47E-10	3.32E-11	4.15E-10	8.15E-11	5.58E-10	2.79E-10	1.24E-10	1.11E-10	4.82E-10	2.59E-11
9	0.51	1.74E-10	1.08E-10	4.42E-10	2.96E-11	7.89E-11	3.53E-11	1.41E-10	2.86E-11	4.85E-10	8.78E-11	7.27E-10	3.64E-10	1.55E-10	1.15E-10	4.30E-10	3.19E-11
11	0.54	2.29E-10	9.42E-11	4.81E-10	8.31E-11	1.56E-10	7.83E-11	3.89E-10	4.13E-11	2.16E-10	7.26E-11	4.11E-10	1.06E-10				
13	0.57	2.18E-10	5.93E-11	3.29E-10	1.11E-10	1.43E-10	7.41E-11	4.19E-10	2.36E-11	3.67E-10	9.06E-11	5.88E-10	2.61E-10	2.43E-10	4.09E-11	3.01E-10	1.79E-10
15	0.58	1.92E-10	1.56E-10	7.90E-10	2.36E-11	2.05E-10	7.87E-11	4.63E-10	1.05E-10	3.45E-10	7.39E-11	5.49E-10	2.49E-10	1.18E-10	7.81E-11	2.97E-10	2.60E-11
39	0.67[1]	1.92E-10	5.14E-11	2.48E-10	8.29E-11	1.21E-10	2.26E-11	1.59E-10	8.48E-11	1.58E-10	1.76E-11	1.92E-10	1.22E-10	3.28E-11	3.52E-11	1.31E-10	1.13E-12
40	0.67[2]	1.70E-10	6.27E-11	3.53E-10	7.90E-11	9.06E-11	3.10E-11	2.45E-10	5.51E-11	2.77E-10	7.88E-11	3.69E-10	1.46E-10	3.68E-11	3.51E-11	1.38E-10	1.08E-12
43	0.82[2]	1.02E-10	4.70E-11	2.13E-10	4.79E-11	2.77E-11	1.51E-11	8.18E-11	8.70E-13								
41	0.92[1]	5.26E-11	1.88E-11	9.58E-11	3.09E-11	1.54E-11	9.76E-12	4.90E-11	7.90E-13								
44	1.71[1]	8.28E-11	1.99E-11	1.25E-10	5.97E-11	6.40E-11	1.10E-11	8.57E-11	4.16E-11								
Average		1.71E-10	7.82E-11	7.90E-10	1.73E-11	1.01E-10	4.19E-11	4.63E-10	7.90E-13	3.46E-10	1.01E-10	1.11E-09	1.06E-10	1.18E-10	6.39E-11	4.82E-10	1.08E-12
Group III																	
17	0.71	1.19E-10	5.00E-11	2.23E-10	1.81E-11	8.19E-11	3.20E-11	1.71E-10	1.79E-11	4.41E-10	3.81E-10	1.47E-09	8.56E-11	7.18E-11	3.97E-11	1.93E-10	2.49E-11
35	1.12	2.48E-10	1.29E-10	8.29E-10	8.76E-11	2.45E-10	5.30E-11	3.06E-10	1.07E-10	4.62E-10	2.51E-10	8.60E-10	1.32E-10	1.67E-10	1.39E-11	1.77E-10	1.51E-10
29	1.16	1.42E-10	7.56E-11	3.77E-10	6.86E-11	1.05E-10	3.59E-11	1.93E-10	4.79E-11	3.96E-10	2.63E-10	1.00E-09	6.16E-11	3.75E-11	1.96E-11	9.40E-11	1.59E-11
37	1.4	1.29E-10	5.22E-11	2.33E-10	7.58E-11	1.01E-10	3.71E-11	2.53E-10	4.83E-11	5.42E-10	2.79E-10	1.02E-09	1.76E-10				
33	1.44	1.30E-10	8.35E-11	3.70E-10	6.20E-11	1.64E-10	6.23E-11	3.38E-10	8.20E-11	3.69E-10	2.66E-10	8.98E-10	4.86E-11	4.13E-11	9.70E-12	7.08E-11	2.38E-11
19	1.63	1.26E-10	6.34E-11	3.19E-10	4.28E-11	8.86E-11	2.51E-11	1.35E-10	5.05E-11	3.27E-10	1.47E-10	7.73E-10	8.32E-11	4.01E-11	2.80E-11	1.10E-10	9.06E-12
31	1.64	3.02E-10	1.83E-10	8.86E-10	1.49E-10	1.52E-10	3.90E-11	2.22E-10	8.91E-11	3.26E-10	1.46E-10	6.51E-10	1.30E-10	1.45E-10	1.46E-11	1.67E-10	1.29E-10
Average		1.71E-10	9.09E-11	8.86E-10	1.81E-11	1.34E-10	4.06E-11	3.38E-10	1.79E-11	4.09E-10	2.48E-10	1.47E-09	4.86E-11	8.38E-11	2.09E-11	1.93E-10	9.06E-12
Summary		1.92E-10	1.01E-10	1.21E-09	1.73E-11	1.07E-10	4.61E-11	4.63E-10	7.90E-13	3.76E-10	1.69E-10	1.47E-09	4.86E-11	1.02E-10	4.41E-11	4.82E-10	1.08E-12

[1] AMAX and ARIMETCO samples originated from core drilled between 1974 and 1977 and were stored for at least 20 years prior to initiation.

[2] Dunka blast hole samples originated from a blast on August 30, 1989 at the Dunka Mine and were stored for 8 years prior to initiation.

Table 71. Sulfur depletion statistics. The first method was based on initial %S minus S lost as determined by sulfate concentration in leachate. The cumulative S depletion for this sulfate-based method (%S depletion (sulfate)) is displayed next to the right-most column (%S Depletion (solids)), which determines S depletion as unleached sample %S minus leached sample %S. Leached solids ran for less time than full experimental period, so are likely to underestimate S loss.

Reactor	**%S**	**Start of experiment until pH<6**		**Major pH drop and/or major sulfate release starts**		**Minimum pH and/or max sulfate release**		**pH increase begins**		**End of experiment**		**%S Depletion (sulfate)**	**% S Depletion (solids)**	
		Week	**%S remaining**	**Week**	**%S remaining**	**Week**	**%S remaining**	**Week**	**%S remaining**	**Week**	**%S remaining**		**Week**	**% S depletion**
1	0.18	#								1252	45.3	54.7	328	41.1
3	0.22	#								1252	54.6	45.4	328	30.9
5	0.40	400	48.5	720	33.3	810	17.4	825	8.5	909	-3.7	103.7	328	12.8
7	0.41	80	94.0	265	83.9	395	65.9	480	48.5	724	38.8	61.2	328	47.8
9	0.51	70	93.0	250	81.8	355	59.8	404	48.6	724	28.2	71.8	328	54.3
11	0.54	57	90.9	215	71.0	290	59.3	385	42.7	441	37.0	63.0	441	72
13	0.57	75	89.4	257	75.2	340	59.4	390	51.1	441	44.8	55.2	441	66.3
15	0.58	55	91.9	140	84.3	280	60.3	335	49.9	724	26.1	73.9	328	62.2
39	0.67[1]	15	97.6	80	92.2	120	88.6	180	82.2	809	69.5	30.5		(a)
40	0.67[2]	140	88.8	250	83.3	380	67.8	420	60.6	809	50.0	50.0		(a)
17	0.71	50	96.7	275	83.4	350	67.3	375	50.4	724	32.1	67.9	328	55.4
42	0.72[1]	#								809	93.4	6.6		(a)
43	0.82[2]	25	97.6							809	82.8	17.2		(a)
41	0.92[1]	102	96.8							809	91.3	8.7		(a)
35	1.12	*		205	66.2	270	42.6	290	32.3	360	21.3	78.7	360	84.6
29	1.16	35	95.5	140	88.7	280	60.2	315	43.5	643	28.3	71.7	643	6.9
37	1.40	35	96.5	192	85.8	282	66.2	345	34.9	360	30.8	69.2	360	79.1
33	1.44	10	97.6	220	76.9	280	57.2	330	34.2	643	16.0	84.0	247	54
19	1.63	20	96.9	120	90.7	290	59.5	355	38.8	724	24.3	75.7	289	71.9
31	1.64	*		220	72.3	275	60.0	290	55.2	360	46.2	53.8	360	75.1
44	1.71[1]	70	95.4							144	92.0	8.0		(a)
Average			91.7		77.9		59.4		45.4		45.2	54.8		54.3
Std Dev			11.9		14.4		14.9		16.0		26.9	26.9		23.2

* Started at pH<6.0

\# pH never <6.0 for sustained period

(a) Leached solids not analyzed to date

1 AMAX and ARIMETCO samples originated from core drilled between 1974 and 1977 and were stored for at least 20 years prior to initiation.

2 Dunka blast hole samples originated from a blast on August 30, 1989 at the Dunka Mine and were stored for 8 years prior to initiation.

PAGE INTENTIONALLY LEFT BLANK

Table 72. Reported rates of pyrrhotite oxidation

Samples	Oxidant	Conditions	Rate (mol m^{-2} s^{-1}) Iron-based	Rate (mol m^{-2} s^{-1}) Sulfate-based	Reference
Monoclinic	Air	68% r.h.[1], 52 °C	1.5E-8	6.0E-10	Steger and Desjardins 1978[2]
Monoclinic	Air	62% r.h.[1], 28 °C	3.9E-9	6.5E-10	Steger 1982[2]
		62% r.h.[1], 35 °C	5.0E-9	7.1E-10	
		62% r.h.[1], 43 °C	6.3E-9	7.8E-10	
		62% r.h.[1], 50 °C	8.9E-9	8.4E-10	
		37% r.h.[1], 50 °C	3.2E-9	8.0E-10	
		50% r.h.[1], 50 °C	4.4E-9	9.1E-10	
		55% r.h.[1], 50 °C	5.2E-9	9.1E-10	
		75% r.h.[1], 50 °C	1.1E-8	9.0E-10	
Museum-grade	Air flow reactor	pH= 2-6			Nicholson and Sharer 1994[3]
		10 °C	3.1E-9		
		22 °C	8.5E-9		
		33 °C	3.3E-8		
Museum-grade samples from N. America	Air flow reactor	Abiotic			Kwong 1995
		22 °C, pH= 2	2.28E-9	8.51E-10	
		35 °C, pH= 2	2.87E-9		
		35 °C, pH= 3	3.86E-9		
		35 °C, pH= 4	2.51E-9		
Museum-grade samples from N. America	Air flow reactor	Biotic			Kwong 1995
		22 °C, pH= 2	6.74E-9	6.97E-9	
		35 °C, pH= 2	8.76E-9		
		35 °C, pH= 4	6.91E-9		
12 samples, various locations from N. America	Air flow reactor	22 °C, pH= 2	4.0E-9	2.0E-10	Janzen et al. 2000
Dunka blast holes, Duluth Complex	Air	pH=3.5-7.4 22.5-29 °C r.h.=38-88%		8E-10	Lapakko and Antonson 1994
12 samples, various locations from N. America	Fe^{3+}	25 °C			Janzen et al. 2000
		Fe^{3+}=0.2 mM, pH=2.75	3.5E-8		
		Fe^{3+}=0.2 mM, pH=2. 5	3.1E-8		
		Fe^{3+}=1.0 mM, pH=2. 5	6.8E-8		
Museum-grade samples from N. America	Fe^{3+}	pH= 2, 22 °C Fe^{3+} ~10^{-3} M	1.44E-8	2.05E-9	Kwong 1995
12 samples, various locations from N. America	Non-oxidative dissolution	25 °C, pH= 2.75	5E-10		Janzen et al. 2000
Monoclinic	log k= -8.04, n= -0.597				Palandri and Kharaka 2004[4]
Hexagonal	log k= -6.79, n= -0.090				Palandri and Kharaka 2004[4]

MNDNR average modeled pyrrhotite oxidation rates	
1.91E-10	Period A
1.27E-10	Period B
4.24E-10	Period C
1.19E-10	Period D

[1] relative humidity

[2] Mean estimated using and average particle specific surface area from Janzen et al. 2000

[3] Average value of oxidation rates

[4] Log(rate) = log k – n·pH

Table 73. Report rates of labradorite and andesine dissolution and dependences on pH.
Log(rate) = log k – n·pH

Element measured	Log k	n	pH[a]	rate at pH 4[b]	rate at pH 6[b]	Reference
Labradorite						
Si	-7.73	0.5	3.1-5.3	1.9E-10	1.9E-11	Welch and Ullman 1993; calculated using labradorite B sample
Si	-8.86	0.5	1-6	1.4E-11	1.4E-12	Sjöberg 1989
Ca, Mg, Na, K	-8.93	0.5		1.2E-11	1.2E-12	Sverdrup 1990 (rate from Blum and Stillings 1995), 25 C
	-9.33	0.4	2-5.1	1.2E-11	1.9E-12	From Blum and Stillings 1995 (listed as Oxburgh et al. 1994 which has no labradorite rates)
	-7.87	0.63	0.84-6	4.1E-11	2.2E-12	Palandri and Kharaka 2004
	-10.91[c]	0	NR		1.2E-11	Palandri and Kharaka 2004
Andesine						
Si	-9.10	0.5	3.1-5.1	7.9E-12	7.9E-13	Oxburgh et al. 1994
	-9.0	0.5	2-5	1.0E-11	1.0E-12	Blum and Stillings 1995, from figure, p. 307 (rates from Oxburgh et al. 1994 and Casey et al. 1991)
	-8.88	0.54	2-4.11	9.1E-12	7.6E-13	Palandri and Kharaka 2004
	-11.47[c]	0	5.1-7.7		3.4E-12	Palandri and Kharaka 2004

[a] pH range over which experiments were conducted

[b] Rate calculated at specified pH, mol m^{-2} s^{-1}

[c] Neutral mechanism rate

NR: Not reported

Table 74. Reported rates of forsteritic and fayalitic olivine dissolution. Log(rate) = log k – n·pH

Mineral	Element measured	Log k	n	pH [a]	rate at pH 4 [b]	Rate at pH 6 [b]	Reference
Olivine (Fo)		-7.0	0.56	1.8-4.6 (approx)	5.8E-10	4.4E-11	Blum and Lasaga 1988, calculated from data in Chen and Brantley 2000
Olivine (Fo_{91})	Mg	-7.00	0.53	2-5.7	7.6E-10	6.6E-11	Wogelius and Walther 1991, calculated from atmospheric CO_2 data (batch and flow-through)
Olivine (Fo_{91})	Si	-7.10	0.53	2-5.7	6.0E-10	5.2E-11	Wogelius and Walther 1991, calculated from atmospheric CO_2 data (batch and flow-through)
Olivine (Fo_{57})	Si	-7.52	0.50	acid	3.0E-10	3.0E-11	Duro et al. 2005, sample was 65% olivine
Olivine (Fo_{91})	Mg	-5.57	0.24	1.66-3.92	3.0E-07	9.8E-08	Luce et al. 1972 (batch)
Olivine (Fo_{91})	Si	-6.54	0.20	1.66-3.92	4.6E-08	1.8E-08	Luce et al. 1972 (batch)
Olivine (Fo_{100})	Mg	-7.72	0.16	1.98-5.25	4.4E-09	2.1E-09	Golubev et al. 2005, CO2 free
Olivine (Fo_{100})	Si	-7.59	0.19	1.98-5.25	4.5E-09	1.9E-09	Golubev et al. 2005, CO2 free
Olivine (Fo_{92})	Mg, Si	-6.86	0.53	1.8-3.8	1.0E-09	9.1E-11	Rosso and Rimstidt 2000, weighted averaged data at 25C
Olivine (Fo_{91})	Mg	-6.53	0.60	1.03-4.2	1.2E-09	7.4E-11	Pokrovsky and Schott 2000b, 25C, CO2 free
Olivine (Fo_{91})	Si	-6.60	0.51	1.03-4.95	2.3E-09	2.2E-10	Pokrovsky and Schott 2000b, 25C, CO2 free
Olivine (Fo_{6})	Si, Fe	10.0	0.69	2-3	2.3E-09	4.9E-10	Wogelius and Walther 1992, rate = $1.1 \times 10^{-10} a_{H+}^{0.69} + 3.2 \times 10^{-14} + 1.2 \times 10^{-16} a_{H+}^{-0.31}$
Olivine (Fo)		-6.85	0.47	1.03-8.71	1.9E-09	2.1E-10	Palandri and Kharaka 2004
Olivine (Fo)		-10.64		9.3-12.06		2.3E-11	Palandri and Kharaka 2004
Olivine (Fa)		-4.80	1	acid [c]	1.6E-09	1.6E-11	Palandri and Kharaka 2004, Sverdrup 1990 is only source
Olivine (Fa)		-12.80		neutral [c]		1.6E-13	Palandri and Kharaka 2004

[a] pH range over which experiments were conducted

[b] Rate calculated at specified pH, mol m^{-2} s^{-1}

[c] range not specified by Palandri and Kharaka

Table 75. Reported rates of bronzite dissolution. Log(rate) = log k – n·pH

Mineral	Element measured	Log k	n	pH [a]	rate at pH 4 [b]	rate at pH 6 [b]	Reference
Bronzite	Si	-10.3	0.26	1-6	4.6E-12	1.4E-12	Schott and Berner 1983
Bronzite	Si	-6.5	0.5	1-4.5	3.2E-9	3.2E-10	Grandstaff 1977
Bronzite	Mg	-5.8	0.5	1-4.5	1.6E-8	1.6E-9	Grandstaff 1977
Bronzite		-8.30	0.65	acid [c]	1.3E-11	6.3E-13	Palandri and Kharaka 2004, from Sverdrup 1990 using two papers above
Bronzite		-11.70		neutral [c]		2.0E-12	Palandri and Kharaka 2004, from Sverdrup 1990 using two papers above

[a] pH range over which experiments were conducted

[b] Rate calculated at specified pH, mol m^{-2} s^{-1}

[c] range not specified by Palandri and Kharaka

Table 76. Reported rates of augite dissolution. Log(rate) = log k – n·pH

Mineral	Element measured	Log k	n	pH[a]	rate at pH 4[b]	rate at pH 6[b]	Reference
Augite	Ca, Mg	-7.7	0.7	2.5-6	3.2E-11	1.3E-12	Sverdrup 1990
Augite		-6.82	0.7	acid[a]	2.4E-10	9.5E-12	Palandri and Kharaka 2004, includes Sverdrup 1990
Augite		-11.97		neutral[c]		1.1E-12	Palandri and Kharaka 2004, includes Sverdrup 1990

[a] pH range over which experiments were conducted

[b] Rate calculated at specified pH, mol m^{-2} s^{-1}

[c] range not specified by Palandri and Kharaka, but original papers had pH range of 1-7.5

Table 77. Reported rates of biotite dissolution. Log(rate) = log k – n·pH

Mineral	Element measured	Log k	n	pH [c]	rate at pH 4 [d]	rate at pH 6 [d]	Reference
Biotite	Weighted avg of several elements	-9.5[a] -10.7[b]	0.61[a] 0.35[b]	1-4	1.1E-12 7.9E-13	6.9E-14 1.6E-13	Kalinowski and Schweda 1996
Biotite		-9.84	0.53	acid [e]	1.1E-12	9.5E-14	Palandri and Kharaka 2004
Biotite		-12.55		neutral [e]		2.8E-13	Palandri and Kharaka 2004

[a] Normalized by initial surface area

[b] Normalized by final surface area

[c] pH range over which experiments were conducted

[d] Rate calculated at specified pH, mol m^{-2} s^{-1}

[e] range not specified by Palandri and Kharaka

Table 78. Comparison of modeled silicate dissolution rates and Palandri and Kharaka rates (mol m^{-2} s^{-1}).

MNDNR modeled dissolution rates							Palandri & Kharaka 2004 rates				P&K / MNDNR	
Mineral	Model	Periods	Avg pH	rate at pH 4	rate at pH 6	rates at pH 4 / pH6	Mineral	rate at pH 4	rate at pH 6	rates at pH 4 / pH6	pH 4	pH 6
Plagioclase	1	A, D	6.15, 4.72	1.3E-12	5.7E-12	0.23	Labradorite	5.3E-11	1.5E-11	3.6	41	2.6
	2	A, C	6.15, 4.07	3.3E-13	2.8E-12	0.12					161	5.2
	3, 4	A, C	6.32, 4.11	9.2E-13	6.2E-13	1.5					58	23
	1	A, D	6.15, 4.72	1.3E-12	5.7E-12	0.23	Andesine	1.3E-11	4.1E-12	3.0	9.6	0.73
	2	A, C	6.15, 4.07	3.3E-13	2.8E-12	0.12					38	1.5
	3, 4	A, C	6.32, 4.11	9.2E-13	6.2E-13	1.5					14	6.7
Augite	1	C	4.07	3.3E-12			Augite	2.4E-10	1.1E-11	23	73	
	2	A, C	6.15, 4.07	6.7E-12	9.5E-12	0.71					36	1.1
	3, 4	A, C	6.32, 4.11	4E-12	8.8E-12	0.45					60	1.2
Olivine	1	A, C	6.15, 4.07	1.6E-11	1.7E-11	0.94	Forsterite	1.9E-09	2.4E-10	8.0	118	14
	2	A, C	6.15, 4.07	9.6E-12	2.5E-12	3.8					196	95
	3	A, C	6.32, 4.11	1.5E-11	8.4E-13	17.86					126	282
	4	A, C	6.32, 4.11	7E-12	1.4E-12	5.0					269	169
	1	A, C	6.15, 4.07	1.6E-11	1.7E-11	0.94	Fayalite	1.6E-09	1.6E-11	99	99	0.94
	2	A, C	6.15, 4.07	9.6E-12	2.5E-12	3.8					165	6.4
	3	A, C	6.32, 4.11	1.5E-11	8.4E-13	17.86					106	19
	4	A, C	6.32, 4.11	7E-12	1.4E-12	5.0					226	11
Hypersthene	1	A, C	6.15, 4.07	4.4E-12	5.5E-12	0.80	Bronzite	1.5E-11	2.6E-12	5.6	3.3	0.48
	2	A, C	6.15, 4.07	2.8E-12	6.7E-13	4.2					5.2	3.9
	3	A, C	6.32, 4.11	4E-12	1.3E-12	3.1					3.6	2.0
	4	A, C	6.32, 4.11	2.7E-12	3.5E-12	0.77					5.4	0.75
Biotite	1	A, C	6.15, 4.07	6E-12	9.3E-12	0.65	Biotite	1.4E-12	3.8E-13	3.7	0.23	0.041
	2	A, C	6.15, 4.07	3.4E-12	1.2E-12	2.8					0.41	0.31
	3	A, C	6.32, 4.11	4.1E-12	1.3E-13	31.54					0.34	2.9
	4	A, C	6.32, 4.11	4.7E-12	1.5E-11	0.31					0.29	0.025
K-spar	4	A, C	6.32, 4.11	3.44E-11	2.45E-10	0.14	K-spar	1.3E-12	4.8E-13	2.6	0.037	0.0019

Table 79. Minimum drainage pH, sulfate and major cation cumulative mass release (mmol) over the entire period of record (excludes R39-44).

%S	Reactor	Period of Record (weeks)	Minimum pH	SO_4	Ca	Mg	Na	K
Group I, 2 samples								
0.18	**1**	1252	5.67	2.304	3.375	2.021	1.598	5.689
0.22	**3**	1252	5.91	2.337	3.940	3.282	1.223	3.450
Average			5.79	2.321	3.657	2.652	1.410	4.569
Group II, 6 samples								
0.4	**5**	909	3.78	9.701	8.735	0.930	0.477	2.987
0.41	**7**	724	4.05	5.872	2.713	1.482	0.930	2.003
0.51	**9**	724	3.95	8.562	3.798	1.713	1.126	1.383
0.54	**11**	441	4.08	7.953	5.120	1.564	0.480	0.845
0.57	**13**	441	3.86	7.359	2.877	2.601	0.717	1.353
0.58	**15**	724	3.98	10.030	3.131	2.445	1.055	2.694
Average			3.95	8.246	4.396	1.789	0.798	1.877
Group III, Duluth Complex, 7 samples								
0.71	**17**	724	3.53	11.282	3.019	4.059	1.163	2.735
1.12	**35**	360	3.23	20.618	6.057	2.550	0.861	1.609
1.16	**29**	643	3.24	19.443	3.475	4.754	1.577	2.760
1.4	**37**	360	3.06	22.652	3.591	5.850	1.305	4.624
1.44	**33**	643	3.04	28.302	3.615	5.998	1.946	5.162
1.63	**19**	724	3.32	28.860	4.745	6.943	1.349	3.022
1.64	**31**	360	3.38	20.624	4.427	4.694	0.932	0.957
Average			3.26	21.683	4.133	4.978	1.305	2.981
Virginia Formation, 4 samples								
2.06	21	78	4.20	5.471	1.629	2.419	N/A	N/A
3.12	23	78	3.70	14.506	3.688	3.679	N/A	N/A
3.72	25	78	3.70	8.779	2.851	3.234	N/A	N/A
5.44	27	78	3.35	13.262	3.104	4.742	N/A	N/A
Average			3.74	10.504	2.818	3.519	N/A	N/A

Table 80. Sample pH by groups and time periods for all Dunka blast hole samples (excludes R39-44).

%S	Reactor	Period A				Period B				Period C				Period D			
		Ave	Max	Min	n	Ave	Max	Min	n	Ave	Max	Min	n	Ave	Max	Min	n
Group I																	
0.18	**1**	6.90	7.90	6.20	134	6.42	7.18	5.67	565								
0.22	**3**	6.91	7.75	6.40	132	6.51	7.05	5.91	560								
Average		6.91	7.83	6.30	133	6.47	7.12	5.79	563								
Group II																	
0.4	**5**	6.60	7.40	6.16	139	6.13	6.69	4.58	453	4.21	4.53	3.78	45	4.67	4.98	4.50	21
0.41	**7**	6.51	8.35	5.34	128	5.13	6.13	4.47	222	4.22	4.56	4.05	87	4.75	5.82	4.26	127
0.51	**9**	6.30	8.70	5.08	139	5.07	5.45	4.61	137	4.18	4.51	3.95	105	4.64	6.04	4.07	182
0.54	**11**	6.13	8.05	5.13	136	4.98	5.55	4.24	141	4.39	4.77	4.08	162				
0.57	**13**	6.44	7.75	5.50	101	5.21	5.72	4.32	190	4.29	4.50	3.86	57	4.40	4.81	4.21	89
0.58	**15**	5.89	7.55	5.20	100	4.82	5.49	4.20	116	4.22	4.38	3.98	118	4.61	5.73	4.11	229
Average		6.31	7.97	5.40	124	5.22	5.84	4.40	210	4.25	4.54	3.95	96	4.61	5.48	4.23	130
Group III																	
0.71	**17**	6.15	7.65	5.11	100	5.08	5.45	4.41	173	4.22	4.95	3.53	151	4.90	5.43	4.52	140
1.12	**35**	4.87	5.85	4.48	125	4.13	4.52	3.81	87	3.61	4.17	3.23	133	4.09	4.18	3.98	12
1.16	**29**	6.38	6.95	5.69	37	4.62	5.70	4.14	150	3.93	4.78	3.24	192	4.95	5.64	4.50	106
1.4	**37**	5.92	7.30	4.78	73	4.81	5.18	4.01	134	3.66	4.49	3.06	150				
1.44	**33**	5.23	7.20	4.59	74	4.42	4.83	4.19	135	3.89	4.90	3.04	229	4.75	5.09	4.52	46
1.63	**19**	5.73	7.50	4.95	66	4.90	5.35	4.37	88	3.89	4.72	3.32	254	4.77	5.71	4.35	156
1.64	**31**	4.80	5.45	4.51	63	4.39	4.80	4.02	163	3.72	4.19	3.38	111	4.03	4.14	3.85	20
Average		5.58	6.84	4.87	77	4.62	5.12	4.14	133	3.84	4.60	3.26	174	4.58	5.03	4.29	80

Table 81. Sample weekly sulfate release (mol/second) by groups and time periods for all Dunka blast hole samples (excludes R39-44).

%S	Reactor	Period A				Period B				Period C				Period D			
		Ave	Max	Min	n	Ave	Max	Min	n	Ave	Max	Min	n	Ave	Max	Min	n
Group I																	
0.18	**1**	1.2E-11	3.0E-11	2.9E-12	59	2.3E-12	1.0E-11	1.9E-13	185								
0.22	**3**	1.0E-11	2.9E-11	3.0E-12	57	2.6E-12	9.3E-12	1.9E-13	187								
Average		1.1E-11	2.9E-11	2.9E-12	58	2.5E-12	9.9E-12	1.9E-13	186								
Group II																	
0.4	**5**	3.3E-11	7.4E-11	1.3E-11	61	9.9E-12	3.1E-11	3.0E-12	132	5.0E-11	1.1E-10	1.8E-11	21	1.2E-11	1.9E-11	7.9E-12	10
0.41	**7**	1.2E-11	3.8E-11	1.6E-12	58	9.5E-12	2.2E-11	3.0E-12	52	3.7E-11	5.0E-11	2.5E-11	21	1.1E-11	4.3E-11	2.3E-12	54
0.51	**9**	1.8E-11	4.7E-11	3.1E-12	61	8.3E-12	1.5E-11	3.0E-12	34	5.1E-11	7.7E-11	3.8E-11	25	1.6E-11	4.5E-11	3.4E-12	67
0.54	**11**	3.3E-11	7.0E-11	1.2E-11	60	2.3E-11	5.6E-11	6.0E-12	36	3.1E-11	5.9E-11	1.5E-11	38				
0.57	**13**	2.8E-11	4.2E-11	1.4E-11	50	1.8E-11	5.3E-11	3.0E-12	48	4.6E-11	7.4E-11	3.3E-11	13	3.1E-11	3.8E-11	2.3E-11	22
0.58	**15**	2.5E-11	1.0E-10	3.0E-12	49	2.6E-11	6.0E-11	1.3E-11	31	4.5E-11	7.1E-11	3.2E-11	27	1.5E-11	3.8E-11	3.4E-12	78
Average		2.5E-11	6.2E-11	7.8E-12	57	1.6E-11	4.0E-11	5.2E-12	56	4.3E-11	7.3E-11	2.7E-11	24	1.7E-11	3.7E-11	7.9E-12	46
Group III																	
0.71	**17**	2.0E-11	3.8E-11	3.1E-12	48	1.4E-11	2.9E-11	3.0E-12	45	7.4E-11	2.5E-10	1.4E-11	35	1.2E-11	3.3E-11	4.2E-12	58
1.12	**35**	7.3E-11	2.4E-10	2.6E-11	39	7.2E-11	9.0E-11	3.1E-11	20	1.4E-10	2.5E-10	3.9E-11	33	4.9E-11	5.2E-11	4.4E-11	3
1.16	**29**	4.2E-11	1.1E-10	2.0E-11	19	3.1E-11	5.8E-11	1.4E-11	37	1.2E-10	3.0E-10	1.8E-11	46	1.1E-11	2.8E-11	4.7E-12	47
1.4	**37**	4.5E-11	8.2E-11	2.7E-11	27	3.6E-11	8.9E-11	1.7E-11	32	1.9E-10	3.6E-10	6.2E-11	37				
1.44	**33**	4.9E-11	1.4E-10	2.3E-11	27	6.1E-11	1.3E-10	3.1E-11	32	1.4E-10	3.4E-10	1.8E-11	57	1.5E-11	2.6E-11	8.9E-12	32
1.63	**19**	5.4E-11	1.4E-10	1.8E-11	33	3.8E-11	5.8E-11	2.2E-11	29	1.4E-10	3.3E-10	3.5E-11	57	1.7E-11	4.7E-11	3.9E-12	61
1.64	**31**	1.2E-10	3.6E-10	6.0E-11	24	6.1E-11	9.0E-11	3.6E-11	38	1.3E-10	2.6E-10	5.2E-11	28	5.9E-11	6.7E-11	5.2E-11	5
Average		5.8E-11	1.6E-10	2.5E-11	31	4.5E-11	7.7E-11	2.2E-11	33	1.3E-10	3.0E-10	3.4E-11	42	2.7E-11	4.2E-11	2.0E-11	34

Table 82. Sample weekly calcium release (mol/second) by groups and time periods for all Dunka blast hole samples (excludes R39-44).

%S	Reactor	Period A				Period B				Period C				Period D			
		Ave	Max	Min	n	Ave	Max	Min	n	Ave	Max	Min	n	Ave	Max	Min	n
Group I																	
0.18	**1**	1.6E-11	2.6E-11	1.0E-11	8	3.1E-12	1.2E-11	3.5E-13	189								
0.22	**3**	1.8E-11	3.1E-11	8.7E-12	7	3.5E-12	1.0E-11	3.6E-13	191								
Average		1.7E-11	2.9E-11	9.4E-12	8	3.3E-12	1.1E-11	3.6E-13	190								
Group II																	
0.4	**5**	3.7E-11	6.1E-11	2.7E-11	8	1.2E-11	2.8E-11	5.5E-12	133	1.2E-11	2.4E-11	4.8E-12	21	4.6E-12	6.8E-12	2.8E-12	9
0.41	**7**	1.7E-11	3.3E-11	3.6E-12	10	3.1E-12	1.2E-11	7.8E-13	52	5.7E-12	1.0E-11	3.5E-12	22	3.4E-12	7.2E-12	1.9E-12	54
0.51	**9**	1.9E-11	5.6E-11	2.2E-12	11	3.1E-12	5.2E-12	1.4E-12	33	8.8E-12	1.5E-11	5.8E-12	29	4.7E-12	1.6E-11	2.3E-12	66
0.54	**11**	3.4E-11	1.0E-10	1.1E-11	32	1.3E-11	2.2E-11	2.2E-12	37	9.0E-12	1.5E-11	5.2E-12	40				
0.57	**13**	2.5E-11	5.6E-11	8.5E-12	7	5.2E-12	1.2E-11	7.3E-13	45	8.6E-12	1.4E-11	5.7E-12	14	6.5E-12	8.6E-12	4.2E-12	21
0.58	**15**	2.0E-11	5.0E-11	5.2E-12	7	5.4E-12	1.0E-11	7.3E-13	24	6.8E-12	1.3E-11	3.6E-12	30	4.6E-12	1.1E-11	2.5E-12	80
Average		2.5E-11	6.0E-11	9.6E-12	13	6.9E-12	1.5E-11	1.9E-12	54	8.5E-12	1.5E-11	4.8E-12	26	4.8E-12	9.8E-12	2.7E-12	46
Group III																	
0.71	**17**	1.9E-11	2.7E-11	8.7E-12	6	3.1E-12	1.2E-11	7.3E-13	39	8.1E-12	2.8E-11	3.6E-13	38	4.3E-12	7.4E-12	2.2E-12	58
1.12	**35**	4.3E-11	8.2E-11	3.6E-12	27	1.3E-11	1.8E-11	8.0E-12	23	1.9E-11	3.2E-11	7.1E-12	33	8.7E-12	9.5E-12	7.8E-12	3
1.16	**29**	2.2E-11	3.4E-11	1.2E-11	10	5.7E-12	2.2E-11	2.3E-12	37	1.3E-11	2.8E-11	5.6E-12	48	4.6E-12	8.0E-12	2.9E-12	47
1.4	**37**	2.8E-11	5.6E-11	1.2E-11	18	8.3E-12	1.9E-11	4.4E-12	35	1.6E-11	2.7E-11	6.6E-12	38				
1.44	**33**	2.4E-11	6.1E-11	5.1E-12	16	5.0E-12	1.2E-11	2.2E-12	34	1.3E-11	2.7E-11	4.2E-12	57	3.8E-12	6.3E-12	2.5E-12	32
1.63	**19**	2.2E-11	5.0E-11	8.7E-12	22	7.6E-12	2.3E-11	3.6E-12	8	1.3E-11	2.7E-11	5.3E-12	64	4.9E-12	1.1E-11	2.5E-12	62
1.64	**31**	5.8E-11	1.6E-10	1.2E-11	12	9.9E-12	1.6E-11	6.4E-12	40	1.6E-11	2.4E-11	1.1E-11	28	1.1E-11	1.4E-11	9.9E-12	5
Average		3.1E-11	6.7E-11	8.8E-12	16	7.4E-12	1.7E-11	4.0E-12	31	1.4E-11	2.8E-11	5.7E-12	44	6.2E-12	9.4E-12	4.6E-12	35

Table 83. Sample weekly magnesium release (mol/second) by groups and time periods for all Dunka blast hole samples (excludes R39-44).

%S	Reactor	Period A				Period B				Period C				Period D			
		Ave	Max	Min	n	Ave	Max	Min	n	Ave	Max	Min	n	Ave	Max	Min	n
Group I																	
0.18	**1**	8.2E-12	1.2E-11	1.2E-12	9	2.3E-12	8.9E-12	5.5E-13	187								
0.22	**3**	1.6E-11	5.5E-11	3.5E-12	8	3.5E-12	1.4E-11	5.6E-13	191								
Average		1.2E-11	3.3E-11	2.3E-12	9	2.9E-12	1.2E-11	5.6E-13	189								
Group II																	
0.4	**5**	5.0E-12	9.8E-12	1.2E-12	7	1.3E-12	9.5E-12	5.7E-13	129	1.1E-12	2.7E-12	5.8E-13	21	5.9E-13	6.0E-13	5.8E-13	9
0.41	**7**	5.4E-12	9.5E-12	1.2E-12	8	2.9E-12	9.8E-12	5.9E-13	51	7.2E-12	1.8E-11	5.9E-13	22	1.3E-12	5.9E-12	5.5E-13	54
0.51	**9**	6.1E-12	1.2E-11	1.2E-12	10	3.5E-12	1.0E-11	1.2E-12	33	7.1E-12	1.7E-11	6.1E-13	29	1.5E-12	7.1E-12	5.6E-13	66
0.54	**11**	1.5E-11	7.3E-11	1.2E-12	30	4.5E-12	1.1E-11	1.2E-12	36	1.7E-12	7.5E-12	5.9E-13	41				
0.57	**13**	1.4E-11	2.1E-11	7.0E-12	8	7.8E-12	1.9E-11	1.2E-12	45	1.4E-11	3.5E-11	4.7E-12	14	4.6E-12	9.4E-12	5.9E-13	22
0.58	**15**	1.6E-11	3.1E-11	3.7E-12	8	8.5E-12	1.4E-11	1.2E-12	24	8.5E-12	1.3E-11	3.5E-12	29	1.3E-12	5.9E-12	5.6E-13	79
Average		1.0E-11	2.6E-11	2.6E-12	12	4.7E-12	1.2E-11	9.8E-13	53	6.6E-12	1.6E-11	1.8E-12	26	1.9E-12	5.8E-12	5.7E-13	46
Group III																	
0.71	**17**	1.6E-11	2.8E-11	9.6E-12	7	6.9E-12	2.2E-11	1.2E-12	39	2.1E-11	6.5E-11	5.9E-12	38	2.2E-12	9.4E-12	5.9E-13	58
1.12	**35**	7.5E-12	1.9E-11	1.2E-12	25	9.6E-12	1.4E-11	4.7E-12	24	1.4E-11	2.5E-11	7.0E-12	33	8.3E-12	9.5E-12	7.0E-12	3
1.16	**29**	1.2E-11	2.3E-11	1.2E-12	9	1.0E-11	2.5E-11	6.1E-12	36	2.7E-11	5.5E-11	5.8E-12	48	2.4E-12	1.1E-11	5.8E-13	47
1.4	**37**	1.0E-11	2.2E-11	1.2E-12	16	1.5E-11	1.9E-11	6.1E-12	33	4.4E-11	8.2E-11	7.2E-12	38				
1.44	**33**	1.3E-11	2.1E-11	7.3E-12	12	1.1E-11	1.7E-11	6.0E-12	35	2.9E-11	6.5E-11	3.5E-12	57	3.2E-12	7.0E-12	5.8E-13	32
1.63	**19**	3.3E-11	8.1E-11	1.4E-11	26	1.9E-11	2.2E-11	1.4E-11	7	2.4E-11	4.1E-11	8.3E-12	65	4.3E-12	1.4E-11	5.3E-13	62
1.64	**31**	3.9E-11	8.9E-11	7.1E-12	12	1.5E-11	2.4E-11	7.2E-12	41	2.4E-11	3.9E-11	1.3E-11	28	1.1E-11	1.4E-11	8.1E-12	5
Average		1.8E-11	4.0E-11	6.0E-12	15	1.2E-11	2.0E-11	6.5E-12	31	2.6E-11	5.3E-11	7.2E-12	44	5.2E-12	1.1E-11	2.9E-12	35

Table 84. Sample weekly calcium+magnesium release (mol/second) by groups and time periods for all Dunka blast hole samples (excludes R39-44).

%S	Reactor	Period A				Period B				Period C				Period D			
		Ave	Max	Min	n	Ave	Max	Min	n	Ave	Max	Min	n	Ave	Max	Min	n
Group I																	
0.18	**1**	2.4E-11	3.8E-11	1.4E-11	8	5.3E-12	1.7E-11	6.4E-13	187								
0.22	**3**	3.4E-11	8.0E-11	1.5E-11	7	7.0E-12	2.2E-11	9.7E-13	190								
Average		2.9E-11	5.9E-11	1.4E-11	8	6.2E-12	1.9E-11	8.0E-13	189								
Group II																	
0.4	**5**	4.3E-11	6.3E-11	3.1E-11	6	1.3E-11	3.0E-11	6.1E-12	128	1.3E-11	2.6E-11	5.4E-12	21	5.2E-12	7.4E-12	3.4E-12	9
0.41	**7**	2.5E-11	4.2E-11	7.2E-12	7	6.2E-12	1.9E-11	2.7E-12	48	1.3E-11	2.4E-11	6.3E-12	22	4.7E-12	1.1E-11	2.5E-12	54
0.51	**9**	2.6E-11	6.6E-11	3.4E-12	9	6.6E-12	1.2E-11	3.5E-12	32	1.6E-11	3.2E-11	8.7E-12	29	6.2E-12	2.3E-11	2.9E-12	66
0.54	**11**	5.0E-11	1.4E-10	2.0E-11	28	1.7E-11	2.9E-11	5.7E-12	36	1.1E-11	2.1E-11	5.8E-12	40				
0.57	**13**	3.8E-11	7.8E-11	1.8E-11	7	1.3E-11	2.7E-11	1.9E-12	45	2.3E-11	4.9E-11	1.0E-11	14	1.1E-11	1.7E-11	5.5E-12	21
0.58	**15**	3.5E-11	8.1E-11	8.8E-12	7	1.4E-11	2.4E-11	1.9E-12	24	1.5E-11	2.6E-11	1.0E-11	29	5.8E-12	1.4E-11	3.1E-12	79
Average		3.6E-11	7.7E-11	1.5E-11	11	1.2E-11	2.4E-11	3.6E-12	52	1.5E-11	3.0E-11	7.8E-12	26	6.6E-12	1.4E-11	3.5E-12	46
Group III																	
0.71	**17**	3.2E-11	4.3E-11	1.8E-11	6	1.0E-11	3.4E-11	1.9E-12	39	2.9E-11	8.9E-11	7.5E-12	37	6.6E-12	1.5E-11	2.7E-12	58
1.12	**35**	5.0E-11	1.0E-10	1.3E-11	25	2.2E-11	3.0E-11	1.5E-11	23	3.4E-11	5.5E-11	1.4E-11	33	1.7E-11	1.8E-11	1.5E-11	3
1.16	**29**	3.5E-11	4.8E-11	1.3E-11	9	1.6E-11	4.6E-11	9.7E-12	36	4.0E-11	7.7E-11	1.1E-11	48	7.0E-12	1.9E-11	3.5E-12	47
1.4	**37**	3.9E-11	6.4E-11	2.3E-11	16	2.3E-11	3.1E-11	1.6E-11	33	6.0E-11	1.1E-10	1.5E-11	38				
1.44	**33**	4.2E-11	7.6E-11	1.8E-11	12	1.7E-11	2.2E-11	1.0E-11	34	4.2E-11	8.9E-11	7.7E-12	57	7.0E-12	1.3E-11	3.1E-12	32
1.63	**19**	5.3E-11	9.3E-11	2.6E-11	22	2.6E-11	4.2E-11	1.8E-11	7	3.7E-11	5.9E-11	2.0E-11	64	9.2E-12	2.6E-11	3.1E-12	62
1.64	**31**	9.6E-11	2.4E-10	2.3E-11	12	2.5E-11	3.8E-11	1.8E-11	40	4.0E-11	6.3E-11	2.6E-11	28	2.1E-11	2.8E-11	1.8E-11	5
Average		5.0E-11	9.6E-11	1.9E-11	15	2.0E-11	3.5E-11	1.3E-11	30	4.0E-11	7.7E-11	1.4E-11	44	1.1E-11	2.0E-11	7.5E-12	35

Table 85. Sample weekly sodium release (mol/second) by groups and time periods for all Dunka blast hole samples (excludes R39-44).

%S	Reactor	Period A				Period B				Period C				Period D			
		Ave	Max	Min	n	Ave	Max	Min	n	Ave	Max	Min	n	Ave	Max	Min	n
Group I																	
0.18	**1**					1.4E-12	3.2E-12	6.1E-13	32								
0.22	**3**					1.3E-12	2.3E-12	6.2E-13	34								
Average						1.4E-12	2.8E-12	6.1E-13	33								
Group II																	
0.4	**5**					8.0E-13	2.1E-12	6.2E-13	20	2.2E-12	3.4E-12	1.5E-12	7	8.7E-13	1.4E-12	6.2E-13	3
0.41	**7**									2.5E-12	2.8E-12	2.2E-12	2	2.0E-12	3.6E-12	1.4E-12	14
0.51	**9**													2.5E-12	5.1E-12	1.5E-12	17
0.54	**11**									2.1E-12	2.4E-12	1.8E-12	2				
0.57	**13**													3.7E-12	4.8E-12	2.6E-12	2
0.58	**15**													2.4E-12	1.0E-11	1.3E-12	18
Average						8.0E-13	2.1E-12	6.2E-13	20	2.3E-12	2.9E-12	1.8E-12	4	2.3E-12	5.0E-12	1.5E-12	11
Group III																	
0.71	**17**									2.6E-12	3.0E-12	2.3E-12	2	2.3E-12	3.3E-12	1.6E-12	16
1.12	**35**									6.4E-12	9.2E-12	3.6E-12	2	3.0E-12	3.0E-12	3.0E-12	1
1.16	**29**									4.0E-12	5.5E-12	2.9E-12	3	2.4E-12	3.7E-12	1.5E-12	15
1.4	**37**									5.2E-12	5.9E-12	4.1E-12	3				
1.44	**33**									3.6E-12	7.1E-12	2.3E-12	7	2.2E-12	3.6E-12	1.5E-12	11
1.63	**19**									3.5E-12	3.5E-12	3.5E-12	1	2.4E-12	4.0E-12	1.6E-12	18
1.64	**31**									4.2E-12	4.2E-12	4.2E-12	1	4.1E-12	4.5E-12	3.8E-12	2
Average										4.2E-12	5.5E-12	3.3E-12	3	2.7E-12	3.7E-12	2.2E-12	11

Table 86. Sample weekly potassium release (mol/second) by groups and time periods for all Dunka blast hole samples (excludes R39-44).

%S	Reactor	Period A				Period B				Period C				Period D			
		Ave	Max	Min	n	Ave	Max	Min	n	Ave	Max	Min	n	Ave	Max	Min	n
Group I																	
0.18	**1**					5.7E-12	1.6E-11	7.2E-13	36								
0.22	**3**					3.3E-12	1.2E-11	3.6E-13	36								
Average						4.5E-12	1.4E-11	5.4E-13	36								
Group II																	
0.4	**5**					4.6E-12	1.3E-11	1.3E-12	18	1.1E-12	2.2E-12	3.6E-13	7	3.7E-13	3.7E-13	3.7E-13	2
0.41	**7**									6.3E-12	8.0E-12	4.5E-12	2	3.7E-12	1.0E-11	1.2E-12	13
0.51	**9**													3.2E-12	9.2E-12	3.7E-13	17
0.54	**11**									3.6E-12	4.0E-12	3.2E-12	2				
0.57	**13**													7.6E-12	1.0E-11	4.9E-12	2
0.58	**15**													4.9E-12	1.7E-11	3.7E-13	17
Average						4.6E-12	1.3E-11	1.3E-12	18	3.7E-12	4.8E-12	2.7E-12	4	3.9E-12	9.5E-12	1.4E-12	10
Group III																	
0.71	**17**									5.0E-12	6.1E-12	3.9E-12	2	6.0E-12	1.9E-11	9.0E-13	17
1.12	**35**									6.0E-12	7.4E-12	4.7E-12	2	6.2E-12	6.2E-12	6.2E-12	1
1.16	**29**									7.1E-12	9.8E-12	4.9E-12	3	3.4E-12	1.1E-11	1.0E-12	15
1.4	**37**									1.6E-11	2.1E-11	7.7E-12	3				
1.44	**33**									9.5E-12	2.2E-11	2.4E-12	7	1.5E-12	2.4E-12	7.6E-13	10
1.63	**19**									6.5E-12	6.5E-12	6.5E-12	1	6.2E-12	2.1E-11	1.5E-12	17
1.64	**31**									4.1E-12	4.1E-12	4.1E-12	1	6.0E-12	6.7E-12	5.3E-12	2
Average										7.7E-12	1.1E-11	4.9E-12	3	4.9E-12	1.1E-11	2.6E-12	10

Table 87. Slopes, y-intercepts, and r^2 values from regression analysis of relationships among %S, sulfate, pH, Ca and Mg (excludes R39-44).

independent	dependent	Period A			Period B			Period C			Period D		
		slope	y-int	r^2	slope	y-int	r^2	slope	y-int	r^2	slope	y-int	r^2
log %S	pH avg	-1.75	5.76	0.656	-2.03	4.77	0.751	-0.96	3.95	0.722	-0.30	4.57	0.046
log %S	pH max	-1.66	7.14	0.359	-2.27	5.29	0.772	-0.03	4.57	0.001	-1.47	5.17	0.237
log %S	pH min	-1.65	5.00	0.672	-1.57	4.20	0.681	-1.48	3.45	0.793	0.05	4.24	0.003
log %S	log SO_4 avg	0.92	1.36	0.727	1.53	1.25	0.874	0.98	1.70	0.868	0.36	1.07	0.051
log %S	log SO_4 max	0.88	1.81	0.656	1.01	1.57	0.762	1.28	2.08	0.800	0.21	1.37	0.083
log %S	log SO_4 min	1.22	0.95	0.593	2.21	0.90	0.872	0.36	1.26	0.162	0.58	0.79	0.051
log SO_4 avg	pH avg	-1.65	8.03	0.672	-1.32	6.42	0.850	-1.02	5.67	0.897	-1.12	5.76	0.942
log SO_4 avg	pH max	-2.08	9.93	0.650	-1.45	7.11	0.842	-0.18	4.86	0.032	-2.05	7.29	0.919
log SO_4 avg	pH min	-1.24	6.76	0.437	-1.08	5.53	0.854	-1.47	5.95	0.861	-0.71	5.01	0.699
log SO_4 avg	log Ca avg	0.38	0.65	0.575	0.30	0.20	0.391	0.51	-0.03	0.652	0.52	-0.04	0.899
log SO_4 avg	log Ca max	0.51	0.89	0.582	0.14	0.80	0.147	0.51	0.27	0.580	0.17	0.56	0.230
log SO_4 avg	log Ca min	0.21	0.41	0.067	0.68	-0.67	0.578	0.43	-0.27	0.091	0.79	-0.50	0.926
log SO_4 avg	log Mg avg	0.40	0.30	0.241	0.62	-0.09	0.639	1.64	-1.86	0.652	1.08	-0.90	0.866
log SO_4 avg	log Mg max	0.43	0.67	0.191	0.19	0.78	0.360	1.20	-0.74	0.474	0.15	0.61	0.117
log SO_4 avg	log Mg min	0.33	-0.18	0.067	0.80	-0.72	0.670	1.63	-2.37	0.612	1.48	-1.77	0.768
log SO_4 avg	log Ca+Mg avg	0.42	0.81	0.771	0.44	0.43	0.812	0.92	-0.34	0.921	0.70	-0.01	0.947
log SO_4 avg	log Ca+Mg max	0.44	1.13	0.461	0.19	1.02	0.352	0.83	0.13	0.669	0.18	0.85	0.208
log SO_4 avg	log Ca+Mg min	0.39	0.48	0.278	0.77	-0.30	0.709	0.68	-0.30	0.636	1.02	-0.62	0.918

Table 88. Iron, aluminum and silicon release rates for all Dunka blast hole samples combined. Average, minimum and maximum rates are presented for entire period of record, as well as for pH>4 and pH≤4 (n = number of measurements) (excludes R39-44).

Criteria	Stats	Fe (mol/s)	Al (mol/s)	Si (mol/s)
Entire period of record	Avg	6.75E-13	4.58E-12	1.60E-11
	Min	4.81E-15	1.05E-14	1.26E-13
	Max	3.67E-11	8.25E-11	9.58E-11
	n	270	271	232
pH > 4	Avg	3.07E-13	1.54E-12	1.56E-11
	Min	4.81E-15	1.05E-14	1.26E-13
	Max	3.67E-11	2.31E-11	9.58E-11
	n	239	240	225
pH ≤ 4	Avg	3.51E-12	2.81E-11	2.93E-11
	Min	1.20E-13	2.13E-14	4.51E-12
	Max	2.39E-11	8.25E-11	4.03E-11
	n	31	31	7

Table 89. Sample weekly cobalt release (mol/second) by groups and time periods for all Dunka blast hole samples (excludes R39-44).

%S	Reactor	Period A				Period B				Period C				Period D			
		Ave	Max	Min	n	Ave	Max	Min	n	Ave	Max	Min	n	Ave	Max	Min	n
Group I																	
0.18	**1**	5.1E-14	1.5E-13	2.4E-14	9	6.6E-15	2.4E-14	4.8E-15	38								
0.22	**3**	4.0E-14	9.8E-14	2.4E-14	8	7.2E-15	2.0E-14	4.8E-15	39								
Average		4.5E-14	1.2E-13	2.4E-14	9	6.9E-15	2.2E-14	4.8E-15	39								
Group II																	
0.4	**5**	9.0E-14	2.0E-13	2.5E-14	8	1.1E-14	2.1E-14	4.9E-15	22	3.6E-14	7.3E-14	1.2E-14	6	4.9E-15	4.9E-15	4.8E-15	3
0.41	**7**	9.9E-14	2.0E-13	2.4E-14	11	7.4E-14	1.0E-13	5.1E-14	4	9.0E-14	1.2E-13	6.0E-14	4	1.1E-14	3.2E-14	4.6E-15	13
0.51	**9**	9.2E-14	2.1E-13	2.5E-14	11	3.7E-14	4.9E-14	2.6E-14	2	1.4E-13	2.4E-13	7.6E-14	4	1.1E-14	4.4E-14	4.8E-15	17
0.54	**11**	7.5E-14	2.0E-13	2.4E-14	33	5.0E-14	5.0E-14	5.0E-14	2	1.4E-14	2.3E-14	5.0E-15	6				
0.57	**13**	9.3E-14	2.4E-13	2.4E-14	8	1.4E-13	2.5E-13	4.9E-14	6	1.5E-13	2.1E-13	9.2E-14	2	3.7E-14	7.9E-14	1.5E-14	4
0.58	**15**	2.5E-13	3.4E-13	1.5E-13	8	1.1E-13	1.5E-13	9.8E-14	4	4.3E-14	4.3E-14	4.3E-14	1	8.7E-15	4.0E-14	4.7E-15	18
Average		1.2E-13	2.3E-13	4.6E-14	13	7.0E-14	1.0E-13	4.7E-14	7	7.9E-14	1.2E-13	4.8E-14	4	1.5E-14	4.0E-14	6.9E-15	11
Group III																	
0.71	**17**	1.8E-13	4.0E-13	2.5E-14	7	2.2E-13	3.0E-13	9.9E-14	5	1.2E-13	2.5E-13	1.2E-14	6	6.8E-15	1.8E-14	4.7E-15	15
1.12	**35**	1.0E-12	1.9E-12	9.9E-14	11	1.7E-13	2.4E-13	9.8E-14	2	1.1E-13	2.0E-13	2.8E-14	5	2.1E-14	2.1E-14	2.1E-14	1
1.16	**29**	3.6E-14	5.2E-14	2.6E-14	10	4.9E-13	5.7E-13	3.5E-13	4	1.8E-13	3.4E-13	6.2E-14	7	1.2E-14	3.5E-14	4.8E-15	13
1.4	**37**	1.6E-13	5.6E-13	2.5E-14	15	6.0E-13	6.0E-13	6.0E-13	1	4.4E-13	7.8E-13	2.0E-13	7				
1.44	**33**	2.7E-13	4.5E-13	2.6E-14	12	2.7E-13	3.0E-13	2.5E-13	2	1.9E-13	4.6E-13	3.3E-14	10	9.7E-15	2.1E-14	4.8E-15	10
1.63	**19**	6.6E-13	9.4E-13	2.0E-13	26	3.7E-13	5.5E-13	2.6E-13	3	1.2E-13	2.1E-13	3.3E-14	7	8.1E-15	2.1E-14	4.4E-15	16
1.64	**31**	2.1E-12	2.9E-12	4.9E-13	10	1.5E-13	1.5E-13	1.5E-13	1	1.3E-13	1.8E-13	5.8E-14	4	2.9E-14	3.0E-14	2.9E-14	2
Average		6.3E-13	1.0E-12	1.3E-13	13	3.3E-13	3.9E-13	2.6E-13	3	1.8E-13	3.4E-13	6.1E-14	7	1.5E-14	2.4E-14	1.1E-14	10

Table 90. Sample weekly copper release (mol/second) by groups and time periods for all Dunka blast hole samples (excludes R39-44).

%S	Reactor	Period A				Period B				Period C				Period D			
		Ave	Max	Min	n	Ave	Max	Min	n	Ave	Max	Min	n	Ave	Max	Min	n
Group I																	
0.18	**1**	4.3E-14	1.4E-13	2.2E-14	9	2.1E-14	5.6E-14	4.5E-15	37								
0.22	**3**	4.3E-14	1.4E-13	2.2E-14	8	2.6E-14	6.0E-14	1.4E-14	37								
Average		4.3E-14	1.4E-13	2.2E-14	9	2.4E-14	5.8E-14	9.0E-15	37								
Group II																	
0.4	**5**	5.4E-14	1.8E-13	2.3E-14	8	2.2E-13	9.0E-13	3.5E-14	22	8.4E-13	1.7E-12	2.9E-13	6	1.8E-13	2.1E-13	1.7E-13	3
0.41	**7**	1.5E-13	9.2E-13	2.3E-14	11	1.3E-12	1.8E-12	9.0E-13	4	1.5E-12	1.9E-12	9.7E-13	4	5.8E-13	1.2E-12	2.1E-13	13
0.51	**9**	7.9E-13	3.1E-12	2.2E-14	11	1.7E-12	2.1E-12	1.3E-12	2	3.4E-12	4.5E-12	2.8E-12	4	1.3E-12	3.3E-12	5.2E-14	17
0.54	**11**	5.2E-14	2.7E-13	2.2E-14	34	2.8E-13	2.8E-13	2.8E-13	2	2.2E-13	4.1E-13	7.6E-14	6				
0.57	**13**	1.3E-13	3.1E-13	2.2E-14	8	1.9E-12	4.1E-12	7.1E-13	6	2.4E-12	2.4E-12	2.4E-12	1	2.5E-12	3.0E-12	1.8E-12	4
0.58	**15**	2.0E-13	4.5E-13	2.3E-14	8	8.5E-13	1.1E-12	5.5E-13	4	1.1E-12	1.1E-12	1.1E-12	1	6.8E-13	1.3E-12	1.4E-13	18
Average		2.3E-13	8.8E-13	2.3E-14	13	1.0E-12	1.7E-12	6.2E-13	7	1.6E-12	2.0E-12	1.3E-12	4	1.1E-12	1.8E-12	4.8E-13	11
Group III																	
0.71	**17**	2.3E-13	6.9E-13	2.3E-14	7	2.0E-12	2.5E-12	1.3E-12	5	3.2E-12	5.4E-12	6.3E-13	6	1.9E-12	3.8E-12	8.3E-13	15
1.12	**35**	2.0E-13	7.8E-13	2.3E-14	11	1.3E-12	1.3E-12	1.2E-12	2	2.8E-12	4.7E-12	1.1E-12	5	9.1E-13	9.1E-13	9.1E-13	1
1.16	**29**	4.8E-14	9.5E-14	2.4E-14	10	1.2E-12	2.1E-12	3.2E-13	4	2.1E-12	4.5E-12	4.2E-13	7	1.2E-12	2.3E-12	9.0E-13	12
1.4	**37**	1.5E-13	9.8E-13	2.4E-14	15	1.7E-12	1.7E-12	1.7E-12	1	3.8E-12	6.7E-12	1.4E-12	7				
1.44	**33**	1.5E-13	6.0E-13	2.3E-14	12	7.4E-13	1.0E-12	4.6E-13	2	2.9E-12	5.4E-12	7.2E-13	10	3.7E-12	5.0E-12	1.2E-12	10
1.63	**19**	2.8E-13	7.5E-13	2.3E-14	26	9.9E-13	1.3E-12	4.2E-13	3	4.2E-12	7.6E-12	9.7E-13	8	1.8E-12	4.5E-12	3.6E-13	16
1.64	**31**	7.1E-13	1.3E-12	4.6E-14	10	3.2E-12	3.2E-12	3.2E-12	1	7.2E-12	8.8E-12	6.2E-12	4	3.4E-12	3.6E-12	3.3E-12	2
Average		2.5E-13	7.4E-13	2.6E-14	13	1.6E-12	1.9E-12	1.2E-12	3	3.7E-12	6.2E-12	1.6E-12	7	2.2E-12	3.4E-12	1.2E-12	9

Table 91. Sample weekly nickel release (mol/second) by groups and time periods for all Dunka blast hole samples (excludes R39-44).

%S	Reactor	Period A				Period B				Period C				Period D			
		Ave	Max	Min	n	Ave	Max	Min	n	Ave	Max	Min	n	Ave	Max	Min	n
Group I																	
0.18	**1**	9.2E-14	3.0E-13	2.4E-14	9	1.9E-14	5.5E-14	4.8E-15	37								
0.22	**3**	7.7E-14	2.0E-13	2.4E-14	8	1.7E-14	5.4E-14	4.8E-15	37								
Average		8.5E-14	2.5E-13	2.4E-14	9	1.8E-14	5.5E-14	4.8E-15	37								
Group II																	
0.4	**5**	4.5E-13	7.1E-13	1.0E-13	8	9.7E-14	2.9E-13	4.3E-14	22	6.1E-13	1.3E-12	1.9E-13	6	7.3E-14	9.7E-14	5.4E-14	3
0.41	**7**	1.2E-12	2.9E-12	2.4E-14	11	1.6E-12	2.7E-12	9.3E-13	4	1.6E-12	2.2E-12	1.1E-12	4	1.8E-13	5.9E-13	2.0E-14	13
0.51	**9**	9.1E-13	2.6E-12	2.6E-14	10	3.8E-13	4.1E-13	3.5E-13	2	1.6E-12	2.0E-12	1.1E-12	4	1.1E-13	6.0E-13	4.9E-15	17
0.54	**11**	3.7E-13	1.9E-12	2.5E-14	33	3.5E-13	3.5E-13	3.5E-13	2	1.2E-13	2.0E-13	4.6E-14	6				
0.57	**13**	8.3E-13	2.0E-12	2.4E-14	8	1.2E-12	1.9E-12	7.7E-13	6	1.3E-12	1.3E-12	1.3E-12	1	5.1E-13	1.1E-12	2.1E-13	4
0.58	**15**	1.5E-12	2.3E-12	1.0E-12	8	8.5E-13	1.1E-12	7.0E-13	4	4.7E-13	4.7E-13	4.7E-13	1	7.7E-14	4.6E-13	4.9E-15	18
Average		8.6E-13	2.1E-12	2.0E-13	13	7.4E-13	1.1E-12	5.2E-13	7	9.6E-13	1.2E-12	7.0E-13	4	1.9E-13	5.7E-13	5.9E-14	11
Group III																	
0.71	**17**	1.2E-12	3.2E-12	2.5E-14	7	2.3E-12	3.2E-12	8.0E-13	5	1.3E-12	2.2E-12	1.3E-13	6	4.9E-14	1.8E-13	4.7E-15	15
1.12	**35**	7.3E-12	1.3E-11	1.2E-12	11	1.4E-12	1.5E-12	1.4E-12	2	1.4E-12	2.6E-12	2.9E-13	5	2.1E-13	2.1E-13	2.1E-13	1
1.16	**29**	1.3E-13	2.6E-13	5.1E-14	10	5.6E-12	6.8E-12	3.6E-12	4	2.6E-12	4.9E-12	8.3E-13	7	1.4E-13	4.5E-13	3.5E-14	13
1.4	**37**	1.5E-12	6.4E-12	1.0E-13	15	6.6E-12	6.6E-12	6.6E-12	1	5.9E-12	1.1E-11	2.6E-12	6				
1.44	**33**	2.4E-12	3.7E-12	2.7E-13	12	2.5E-12	2.6E-12	2.5E-12	2	1.9E-12	4.6E-12	1.9E-13	10	7.2E-14	1.9E-13	3.4E-14	10
1.63	**19**	5.1E-12	7.1E-12	1.4E-12	26	3.0E-12	3.6E-12	2.7E-12	3	1.4E-12	2.8E-12	2.1E-13	8	3.7E-14	1.1E-13	4.7E-15	16
1.64	**31**	2.2E-11	3.6E-11	5.8E-12	10	2.2E-12	2.2E-12	2.2E-12	1	2.0E-12	2.9E-12	8.1E-13	4	3.9E-13	3.9E-13	3.8E-13	2
Average		5.7E-12	9.9E-12	1.3E-12	13	3.4E-12	3.8E-12	2.8E-12	3	2.3E-12	4.4E-12	7.2E-13	7	1.5E-13	2.6E-13	1.1E-13	10

Table 92. Sample weekly zinc release (mol/second) by groups and time periods for all Dunka blast hole samples (excludes R39-44).

%S	Reactor	Period A				Period B				Period C				Period D			
		Ave	Max	Min	n	Ave	Max	Min	n	Ave	Max	Min	n	Ave	Max	Min	n
Group I																	
0.18	**1**	6.6E-14	1.3E-13	2.2E-14	9	5.2E-14	2.2E-13	9.0E-15	38								
0.22	**3**	5.2E-14	8.8E-14	2.2E-14	8	4.6E-14	2.3E-13	1.3E-14	38								
Average		5.9E-14	1.1E-13	2.2E-14	9	4.9E-14	2.2E-13	1.1E-14	38								
Group II																	
0.4	**5**	1.0E-13	1.8E-13	4.5E-14	8	8.7E-14	2.6E-13	2.9E-14	22	1.0E-13	1.8E-13	4.8E-14	6	2.4E-14	3.7E-14	1.7E-14	3
0.41	**7**	1.4E-13	3.1E-13	2.2E-14	11	8.3E-14	1.8E-13	4.6E-14	4	1.8E-13	3.5E-13	7.0E-14	4	8.8E-14	1.8E-13	2.9E-14	13
0.51	**9**	1.8E-13	6.3E-13	2.3E-14	11	9.0E-14	9.2E-14	8.9E-14	2	1.6E-13	2.2E-13	1.2E-13	4	1.2E-13	3.5E-13	3.1E-14	17
0.54	**11**	1.4E-13	5.7E-13	2.2E-14	34	1.8E-13	1.8E-13	1.8E-13	2	1.4E-13	2.3E-13	6.2E-14	6				
0.57	**13**	1.7E-13	4.8E-13	2.2E-14	8	2.0E-13	2.2E-13	1.3E-13	6	2.3E-13	2.4E-13	2.2E-13	2	1.9E-13	2.5E-13	1.2E-13	4
0.58	**15**	2.7E-13	4.8E-13	2.2E-14	8	2.6E-13	4.0E-13	1.3E-13	4	8.8E-14	8.8E-14	8.8E-14	1	9.5E-14	2.0E-13	2.2E-14	18
Average		1.7E-13	4.4E-13	2.6E-14	13	1.5E-13	2.2E-13	1.0E-13	7	1.5E-13	2.2E-13	1.0E-13	4	1.0E-13	2.0E-13	4.3E-14	11
Group III																	
0.71	**17**	1.8E-13	4.0E-13	2.2E-14	7	1.8E-13	3.2E-13	9.0E-14	5	1.7E-13	2.5E-13	1.0E-13	6	8.9E-14	2.4E-13	4.6E-14	15
1.12	**35**	4.1E-13	8.0E-13	1.3E-13	11	3.1E-13	4.4E-13	1.8E-13	2	4.3E-13	5.9E-13	2.9E-13	5	2.4E-13	2.4E-13	2.4E-13	1
1.16	**29**	4.0E-14	4.7E-14	2.3E-14	10	3.7E-13	6.2E-13	1.8E-13	4	2.7E-13	5.0E-13	1.4E-13	7	1.4E-13	9.1E-13	3.5E-14	13
1.4	**37**	1.2E-13	5.0E-13	2.3E-14	15	2.7E-13	2.7E-13	2.7E-13	1	3.1E-13	5.0E-13	1.2E-13	7				
1.44	**33**	2.3E-13	3.6E-13	9.5E-14	12	1.8E-13	2.2E-13	1.4E-13	2	2.4E-13	5.0E-13	1.1E-13	10	7.5E-14	1.3E-13	3.7E-14	9
1.63	**19**	3.2E-13	6.3E-13	4.4E-14	26	4.3E-13	5.0E-13	3.3E-13	3	4.9E-13	8.5E-13	1.8E-13	8	1.7E-13	4.2E-13	4.0E-14	16
1.64	**31**	7.2E-13	9.8E-13	2.7E-13	10	2.2E-13	2.2E-13	2.2E-13	1	3.6E-13	4.0E-13	2.9E-13	4	2.2E-13	2.8E-13	1.6E-13	2
Average		2.9E-13	5.3E-13	8.7E-14	13	2.8E-13	3.7E-13	2.0E-13	3	3.2E-13	5.2E-13	1.8E-13	7	1.6E-13	3.7E-13	9.2E-14	9

Table 93. Ni, Mg content and Ni-bearing mineral abundance in Dunka blast hole samples (excludes R39-44).

%S	Ni ppm	Ni (g/sample)	Ni (mol/sample)	Olivine (mol/sample)	Ni ol (mols Ni/ mol ol)	Ni in ol (mol/sample)	fraction Ni as olivine	fraction Ni as pent/po	Mg (mols/mol ol)	ol Ni/Mg (molar)
Group I										
0.18	525	0.039	6.71E-04	0.043	0.003	1.28E-04	0.191	0.809	0.763	0.0039
0.22	484	0.036	6.18E-04	0.019	0.002	3.82E-05	0.062	0.938	0.857	0.0023
Group II										
0.40[1]	231	0.017	2.95E-04					1.000		
0.41	511	0.038	6.53E-04	0.056	0.003	1.68E-04	0.258	0.742	0.897	0.0033
0.51	473	0.035	6.04E-04	0.025	0.002	5.00E-05	0.083	0.917	0.812	0.0025
0.54[1]	174	0.013	2.22E-04					1.000		
0.57	398	0.030	5.09E-04	0.092	0.004	3.66E-04	0.721	0.279	1.003	0.0040
0.58	396	0.030	5.06E-04	0.011	0.001	1.07E-05	0.021	0.979	0.851	0.0012
Group III										
0.71	388	0.029	4.96E-04	0.065	0.002	1.29E-04	0.260	0.740	0.958	0.0021
1.12	329	0.025	4.20E-04	0.018	0.002	3.58E-05	0.085	0.915	0.953	0.0021
1.16	422	0.032	5.39E-04	0.073	0.002	1.46E-04	0.271	0.729	0.958	0.0021
1.4	503	0.038	6.43E-04	0.026	0.003	7.67E-05	0.119	0.881	0.954	0.0031
1.44	386	0.029	4.93E-04	0.026	0.003	7.70E-05	0.156	0.844	0.953	0.0031
1.63	492	0.037	6.29E-04	0.023	0.002	4.68E-05	0.075	0.925	0.722	0.0028
1.64	718	0.054	9.17E-04	0.014	0.003	4.23E-05	0.046	0.954	0.828	0.0036
Average	429	0.032	3.42E-04	0.038	0.002	1.01E-04	0.156	0.844	0.885	0.0028

[1] Sample had no olivine detected by point count.

Table 94. Average Ni/Mg ratio in Dunka blast hole sample leachate during different sample periods. See appendix for details on period definition. Numbers in parentheses are the number of data points in each period. Blank cells indicate sample did not enter that time period (excludes R39-44).

%S	**Reactor**	**Ni/Mg olivine**	**Average Ni/Mg ratio in leachate (molar)**			
			Period A	**Period B**	**Period C**	**Period D**
Group I						
0.18	1	0.0038	0.015 (9)	0.011 (37)		
0.22	3	0.002	0.008 (8)	0.006 (37)		
Group II						
0.40[1]	5	No ol	0.152 (7)	0.122 (21)	0.631 (6)	0.123 (3)
0.41	7	0.0033	0.493 (8)	0.461 (4)	0.166 (4)	0.134 (13)
0.51	9	0.0025	0.244 (8)	0.155 (2)	0.231 (4)	0.061 (17)
0.54[1]	11	No ol	0.042 (29)	0.064 (2)	0.086 (6)	
0.57	13	0.004	0.086 (8)	0.247 (6)	0.093 (1)	0.177 (4)
0.58	15	0.0012	0.124 (8)	0.204 (4)	0.079 (1)	0.073 (18)
Group III						
0.71	17	0.0021	0.076 (7)	0.556 (5)	0.084 (6)	0.29 (15)
1.12	35	0.0021	0.989 (10)	0.215 (2)	0.075 (5)	0.030 (1)
1.16	29	0.0021	0.032 (9)	0.311 (3)	0.089 (7)	0.076 (13)
1.4	37	0.0031	0.184 (13)	no Ni:Mg measurements	0.135 (6)	
1.44	33	0.0031	0.214 (9)	0.295 (2)	0.055 (10)	0.041 (10)
1.63	19	0.0028	0.190 (26)	0.164 (2)	0.053 (8)	0.012 (16)
1.64	31	0.0036	0.603 (10)	0.159 (1)	0.075 (4)	0.037 (2)
Total Average		0.0028	0.230	0.212	0.142	0.072

[1] Sample had no olivine detected by point count.

Table 95. Calculated and observed Ni release for Dunka blast hole samples. Calculated based on Mg in leachate on days Ni was measured, multiplied by Ni:Mg in olivine. This method assumes all Mg comes from ol dissolution therefore it overestimates both Ni release and olivine dissolution. Blank cells indicate sample did not enter that time period (excludes R39-44).

%S	**Calculated Ni release from ol (mol/week)**				**Observed Ni release rate in leachate (mol/week)**				**Calculated:Observed Ni from olivine**			
	Period A	**Period B**	**Period C**	**Period D**	**Period A**	**Period B**	**Period C**	**Period D**	**Period A**	**Period B**	**Period C**	**Period D**
Group I												
0.18	1.96E-08	4.68E-09			5.58E-08	1.14E-08			35.1%	41.0%		
0.22	2.21E-08	4.26E-09			4.65E-08	1.03E-08			47.6%	41.5%		
Group II												
0.40[1]					2.73E-07	5.86E-08	3.69E-07	4.40E-08				
0.41	1.10E-08	8.59E-09	2.04E-08	2.74E-09	6.99E-07	9.81E-07	9.94E-07	1.07E-07	1.6%	0.9%	2.1%	2.6%
0.51	9.41E-09	3.62E-09	1.23E-08	2.67E-09	5.53E-07	2.28E-07	9.67E-07	6.94E-08	1.7%	1.6%	1.3%	3.9%
0.54[1]					2.25E-07	2.13E-07	7.03E-08					
0.57	3.32E-08	1.99E-08	3.40E-08	9.25E-09	5.00E-07	6.96E-07	7.93E-07	3.11E-07	6.6%	2.9%	4.3%	3.0%
0.58	1.14E-08	6.37E-09	4.18E-09	1.05E-09	8.90E-07	5.17E-07	2.82E-07	4.67E-08	1.3%	1.2%	1.5%	2.2%
Group III												
0.71	1.98E-08	1.14E-08	2.56E-08	3.26E-09	7.03E-07	1.41E-06	8.01E-07	2.94E-08	2.8%	0.8%	3.2%	11.1%
1.12	1.26E-08	1.06E-08	2.11E-08	8.88E-09	4.39E-06	8.75E-07	8.28E-07	1.27E-07	0.3%	1.2%	2.5%	7.0%
1.16	1.47E-08	2.58E-08	3.67E-08	2.92E-09	7.83E-08	3.39E-06	1.60E-06	8.59E-08	18.8%	0.8%	2.3%	3.4%
1.4	1.61E-08		9.25E-08		9.26E-07	3.98E-06	3.55E-06		1.7%		2.6%	
1.44	2.40E-08	1.96E-08	6.07E-08	3.88E-09	1.46E-06	1.53E-06	1.13E-06	4.37E-08	1.6%	1.3%	5.4%	8.9%
1.63	5.48E-08	3.27E-08	4.18E-08	7.04E-09	3.07E-06	1.83E-06	8.49E-07	2.26E-08	1.8%	1.8%	4.9%	31.2%
1.64	9.07E-08	3.10E-08	5.59E-08	2.31E-08	1.34E-05	1.36E-06	1.19E-06	2.34E-07	0.7%	2.3%	4.7%	9.9%
Average	2.61E-08	1.49E-08	3.68E-08	6.48E-09	1.81E-06	1.14E-06	1.03E-06	1.02E-07	9.4%	8.1%	3.2%	8.3%

[1] Sample had no olivine by point count.

Table 96. Regression results for calculated fraction of Ni from olivine versus percent sulfur in sample (data in Table 5). Periods A and B did not have a significant regression (excludes R39-44).

	slope	y-intercept	r^2
Period A			
Period B			
Period C	0.020	0.012	0.423
Period D	0.120	-0.032	0.422

Table 97. Average sample weekly nickel release per mole olivine by time period for Dunka blast hole samples. Blank cells indicate sample did not enter that time period (excludes R39-44).

%S	Olivine (mol/sample)	mol Ni/mol olivine /week in leachate			
		Period A	**Period B**	**Period C**	**Period D**
Group I					
0.18	0.044	1.27E-06	2.59E-07		
0.22	0.02	2.32E-06	5.13E-07		
Group II					
0.40	No ol				
0.41	0.056	1.25E-05	1.75E-05	1.77E-05	1.91E-06
0.51	0.026	2.13E-05	8.79E-06	3.72E-05	2.67E-06
0.54	No ol				
0.57	0.09	5.55E-06	7.74E-06	8.81E-06	3.46E-06
0.58	0.011	8.09E-05	4.70E-05	2.56E-05	4.25E-06
Group III					
0.71	0.064	1.10E-05	2.21E-05	1.25E-05	4.60E-07
1.12	0.018	2.44E-04	4.86E-05	4.60E-05	7.06E-06
1.16	0.073	1.07E-06	4.64E-05	2.19E-05	1.18E-06
1.4	0.026	3.56E-05	1.53E-04	1.37E-04	
1.44	0.026	5.62E-05	5.87E-05	4.34E-05	1.68E-06
1.63	0.024	1.28E-04	7.62E-05	3.54E-05	9.40E-07
1.64	0.014	9.54E-04	9.70E-05	8.49E-05	1.67E-05
Total Average		1.19E-04	4.49E-05	4.27E-05	4.03E-06

Table 98. Regression results for average sample weekly nickel release per mole olivine (data in Table 7) by time period versus %S. Period D did not have a significant regression (excludes R39-44).

	slope	y-intercept	r^2
Period A	2.59E-4	-1.11E-4	0.278
Period B	6.85E-5	-1.60E-5	0.669
Period C	4.72E-5	-5.15E-6	0.352
Period D	3.93E-6	1.87E-7	0.151

Table 99. Maximum amount of plagioclase and olivine dissolution based on cumulative Ca and Mg release (Table 79) and sample stoichiometry (Table 11) (excludes R39-44).

%S	**Reactor**	**Period of Record (weeks)**	**Minimum pH**	**Maximum plagioclase dissolution**		**Maximum olivine dissolution**	
				(mmol)	**(mol m^{-2} s^{-1})**	**(mmol)**	**(mol m^{-2} s^{-1})**
Group I, 2 samples							
0.18	**1**	1252	5.67	7.165	1.40E-09	2.649	2.85E-09
0.22	**3**	1252	5.91	8.833	1.31E-09	3.830	9.17E-09
Average			5.79	7.999	1.35E-09	3.240	6.01E-09
Group II, 6 samples							
0.4	**5**	909	3.78	16.266	3.32E-09		
0.41	**7**	724	4.05	5.167	8.72E-10	1.652	1.36E-09
0.51	**9**	724	3.95	7.447	1.54E-09	2.110	3.87E-09
0.54	**11**	441	4.08	8.153	1.26E-09		
0.57	**13**	441	3.86	6.081	1.38E-09	2.593	1.31E-09
0.58	**15**	724	3.98	6.364	1.34E-09	2.873	1.25E-08
Average			3.95	8.247	1.62E-09	2.307	4.76E-09
Group III, Duluth Complex, 7 samples							
0.71	**17**	724	3.53	5.954	1.05E-09	4.237	2.90E-09
1.12	**35**	360	3.23	12.361	3.01E-09	2.676	6.91E-09
1.16	**29**	643	3.24	6.556	1.09E-09	5.014	3.17E-09
1.4	**37**	360	3.06	7.168	1.50E-09	6.132	1.01E-08
1.44	**33**	643	3.04	7.532	1.37E-09	6.293	1.17E-08
1.63	**19**	724	3.32	11.983	3.17E-09	9.617	1.85E-08
1.64	**31**	360	3.38	9.263	1.95E-09	5.668	1.77E-08
Average			3.26	8.688	1.88E-09	5.663	1.01E-08
Virginia Formation, 4 samples							
2.06	21	78	4.20	5.014	1.73E-09	2.706	3.61E-08
3.12	23	78	3.70	6.574	1.83E-09		
3.72	25	78	3.70	7.004	3.68E-09		
5.44	27	78	3.35	9.639	8.00E-09		
Average			3.74	7.058	3.81E-09	2.706	3.61E-08

Table 100. Model 1, Periods A-D Silicate Mineral Dissolution Rates for all Dunka blast hole samples (excludes R39-44). Page 1 of 4.

Model 1, Period A																		
R#	%S	N	Plag (mol m^{-2}s^{-1})				Hyp (mol m^{-2}s^{-1})				Ol (mol m^{-2}s^{-1})				Bio (mol m^{-2}s^{-1})			
			Ave	S.D.	Max	Min	Ave	S.D.	Max	Min	Ave	S.D.	Max	Min	Ave	S.D.	Max	Min
1	0.18	8	4.0E-12	1.4E-12	6.6E-12	2.5E-12	1.9E-12	7.4E-13	2.7E-12	2.7E-13	7.0E-12	2.7E-12	1.0E-11	9.9E-13	6.0E-12	2.3E-12	8.6E-12	8.5E-13
3	0.22	7	3.7E-12	1.7E-12	6.2E-12	1.7E-12	1.2E-11	1.2E-11	4.0E-11	2.6E-12	2.6E-11	2.8E-11	9.2E-11	5.9E-12	6.1E-12	6.5E-12	2.1E-11	1.4E-12
5	0.40	8	8.4E-12	2.6E-12	1.4E-11	6.2E-12	7.6E-13	5.1E-13	1.5E-12	1.8E-13					3.6E-12	2.4E-12	7.1E-12	8.4E-13
7	0.41	10	3.3E-12	2.0E-12	6.4E-12	7.0E-13	2.4E-12	1.2E-12	4.1E-12	5.2E-13	3.0E-12	1.5E-12	5.3E-12	6.6E-13	2.3E-12	1.2E-12	4.0E-12	5.0E-13
9	0.51	11	4.7E-12	4.1E-12	1.4E-11	5.4E-13	1.4E-12	9.6E-13	2.9E-12	2.8E-13	8.4E-12	5.6E-12	1.7E-11	1.6E-12	2.7E-12	1.8E-12	5.4E-12	5.1E-13
11	0.54	32	5.0E-12	2.5E-12	1.5E-11	1.7E-12	2.8E-12	2.6E-12	1.3E-11	2.2E-13					6.6E-12	6.0E-12	3.1E-11	5.0E-13
13	0.57	7	7.2E-12	4.5E-12	1.6E-11	2.4E-12	1.0E-11	3.4E-12	1.6E-11	5.2E-12	4.2E-12	1.4E-12	6.4E-12	2.1E-12				
15	0.58	7	5.3E-12	3.7E-12	1.3E-11	1.3E-12	4.7E-12	2.8E-12	9.1E-12	1.1E-12	5.0E-11	2.9E-11	9.5E-11	1.1E-11	3.2E-11	1.9E-11	6.2E-11	7.4E-12
17	0.71	6	3.9E-12	1.6E-12	5.6E-12	1.8E-12	4.7E-12	2.0E-12	8.4E-12	2.9E-12	6.8E-12	2.9E-12	1.2E-11	4.1E-12	9.4E-12	4.0E-12	1.7E-11	5.8E-12
35	1.12	27	1.3E-11	6.4E-12	2.5E-11	1.1E-12	1.7E-12	9.4E-13	4.4E-12	2.7E-13	1.2E-11	6.7E-12	3.2E-11	1.9E-12	4.7E-12	2.6E-12	1.2E-11	7.4E-13
29	1.16	10	4.2E-12	1.3E-12	6.5E-12	2.3E-12	3.7E-12	2.0E-12	7.1E-12	3.9E-13	4.7E-12	2.6E-12	9.1E-12	5.0E-13				
37	1.40	18	7.1E-12	2.9E-12	1.4E-11	2.9E-12	4.8E-12	2.7E-12	1.0E-11	5.8E-13	1.0E-11	5.9E-12	2.3E-11	1.3E-12				
33	1.44	16	5.4E-12	4.7E-12	1.4E-11	1.2E-12	2.1E-12	6.3E-13	3.3E-12	1.2E-12	1.6E-11	4.7E-12	2.4E-11	8.6E-12	7.3E-12	2.2E-12	1.1E-11	4.0E-12
19	1.63	22	8.7E-12	5.2E-12	2.0E-11	3.5E-12	8.1E-12	4.4E-12	2.0E-11	3.5E-12	5.3E-11	2.9E-11	1.3E-10	2.3E-11	1.9E-11	1.0E-11	4.7E-11	8.3E-12
31	1.64	12	1.5E-11	1.1E-11	4.1E-11	3.1E-12	1.5E-11	8.2E-12	3.4E-11	2.8E-12	8.8E-11	4.8E-11	2.0E-10	1.6E-11	1.6E-11	9.0E-12	3.8E-11	3.1E-12
Summary			6.6E-12	3.7E-12	4.1E-11	5.4E-13	5.1E-12	3.0E-12	4.0E-11	1.8E-13	2.2E-11	1.3E-11	2.0E-10	5.0E-13	9.7E-12	5.6E-12	6.2E-11	5.0E-13

Note: N=number of experimental observations used to model dissolution rates.
Note: Zeroes indicate a calculated absence of dissolution. Blank cells indicate there was none of that mineral present in the sample.

Table 100. Model 1, Periods A-D Silicate Mineral Dissolution Rates for all Dunka blast hole samples (excludes R39-44). Page 2 of 4.

Model 1, Period B																		
R#	%S	N	Plag (mol $m^{-2}s^{-1}$)				Hyp (mol $m^{-2}s^{-1}$)				Ol (mol $m^{-2}s^{-1}$)				Bio (mol $m^{-2}s^{-1}$)			
			Ave	S.D.	Max	Min	Ave	S.D.	Max	Min	Ave	S.D.	Max	Min	Ave	S.D.	Max	Min
1	0.18	189	7.7E-13	3.8E-13	3.0E-12	8.8E-14	5.3E-13	4.8E-13	2.1E-12	1.3E-13	2.0E-12	1.8E-12	7.6E-12	4.7E-13	1.7E-12	1.5E-12	6.5E-12	4.0E-13
3	0.22	191	7.0E-13	3.1E-13	2.1E-12	7.3E-14	2.6E-12	1.8E-12	1.1E-11	4.1E-13	6.0E-12	4.2E-12	2.4E-11	9.5E-13	1.4E-12	9.8E-13	5.7E-12	2.2E-13
5	0.40	133	2.7E-12	1.0E-12	6.4E-12	1.3E-12	1.9E-13	2.1E-13	1.5E-12	8.6E-14					9.1E-13	9.9E-13	6.9E-12	4.1E-13
7	0.41	52	6.1E-13	3.8E-13	2.4E-12	1.5E-13	1.3E-12	8.1E-13	4.3E-12	2.6E-13	1.6E-12	1.0E-12	5.4E-12	3.3E-13	1.2E-12	7.8E-13	4.1E-12	2.5E-13
9	0.51	33	7.5E-13	2.2E-13	1.3E-12	3.5E-13	8.2E-13	4.4E-13	2.4E-12	2.8E-13	4.7E-12	2.6E-12	1.4E-11	1.6E-12	1.5E-12	8.1E-13	4.4E-12	5.2E-13
11	0.54	37	1.9E-12	5.7E-13	3.2E-12	3.2E-13	8.1E-13	4.3E-13	2.0E-12	2.1E-13					1.9E-12	1.0E-12	4.7E-12	5.0E-13
13	0.57	45	1.5E-12	7.2E-13	3.5E-12	2.1E-13	5.8E-12	2.0E-12	1.4E-11	8.6E-13	2.4E-12	8.3E-13	5.7E-12	3.5E-13				
15	0.58	24	1.4E-12	4.8E-13	2.6E-12	1.9E-13	2.5E-12	8.0E-13	4.2E-12	3.5E-13	2.6E-11	8.4E-12	4.4E-11	3.7E-12	1.7E-11	5.5E-12	2.9E-11	2.4E-12
17	0.71	39	6.4E-13	4.2E-13	2.5E-12	1.5E-13	2.1E-12	1.0E-12	6.6E-12	3.6E-13	3.0E-12	1.5E-12	9.5E-12	5.2E-13	4.1E-12	2.1E-12	1.3E-11	7.2E-13
35	1.12	23	3.8E-12	7.9E-13	5.3E-12	2.4E-12	2.2E-12	5.8E-13	3.3E-12	1.1E-12	1.6E-11	4.1E-12	2.4E-11	7.7E-12	6.0E-12	1.6E-12	9.0E-12	2.9E-12
29	1.16	37	1.1E-12	7.7E-13	4.1E-12	4.3E-13	3.1E-12	1.2E-12	7.8E-12	1.9E-12	4.0E-12	1.6E-12	9.9E-12	2.4E-12				
37	1.40	35	2.1E-12	7.9E-13	4.8E-12	1.1E-12	7.1E-12	1.4E-12	9.2E-12	2.9E-12	1.5E-11	3.0E-12	2.0E-11	6.3E-12				
33	1.44	34	1.2E-12	3.9E-13	2.7E-12	5.1E-13	1.8E-12	4.7E-13	2.7E-12	9.4E-13	1.3E-11	3.5E-12	2.0E-11	7.0E-12	6.3E-12	1.7E-12	9.5E-12	3.3E-12
19	1.63	8	3.1E-12	2.6E-12	9.3E-12	1.5E-12	4.6E-12	5.8E-13	5.4E-12	3.6E-12	3.0E-11	3.8E-12	3.5E-11	2.3E-11	1.1E-11	1.4E-12	1.3E-11	8.4E-12
31	1.64	40	2.6E-12	6.5E-13	4.3E-12	1.7E-12	5.9E-12	1.5E-12	9.3E-12	2.8E-12	3.4E-11	8.5E-12	5.4E-11	1.6E-11	6.4E-12	1.6E-12	1.0E-11	3.1E-12
Summary			1.6E-12	7.0E-13	9.3E-12	7.3E-14	2.8E-12	9.2E-13	1.4E-11	8.6E-14	1.2E-11	3.5E-12	5.4E-11	3.3E-13	5.0E-12	1.7E-12	2.9E-11	2.2E-13

Note: N=number of experimental observations used to model dissolution rates.
Note: Zeroes indicate a calculated absence of dissolution. Blank cells indicate there was none of that mineral present in the sample.

Table 100. Model 1, Periods A-D Silicate Mineral Dissolution Rates for all Dunka blast hole samples (excludes R39-44). Page 3 of 4.

Model 1, Period C																						
R#	%S	N	Aug (mol m^{-2}s^{-1})				Hyp (mol m^{-2}s^{-1})				Ol (mol m^{-2}s^{-1})				Bio (mol m^{-2}s^{-1})				Orphan Ca (mol m^{-2}s^{-1})			
			Ave	S.D.	Max	Min	Ave	S.D.	Max	Min	Ave	S.D.	Max	Min	Ave	S.D.	Max	Min	Ave	S.D.	Max	Min
5	0.40	21	1.5E-12	2.4E-12	7.0E-12	0.0E+00	8.1E-14	6.3E-14	2.1E-13	0.0E+00					3.9E-13	3.0E-13	1.0E-12	0.0E+00	7.2E-13	1.8E-12	6.3E-12	0.0E+00
7	0.41	22	1.4E-12	7.6E-13	3.1E-12	2.3E-13	2.2E-12	1.8E-12	6.8E-12	0.0E+00	2.8E-12	2.2E-12	8.6E-12	0.0E+00	2.1E-12	1.7E-12	6.5E-12	0.0E+00	3.3E-13	8.4E-13	3.4E-12	0.0E+00
9	0.51	29	3.1E-12	1.4E-12	7.4E-12	4.6E-13	7.1E-13	5.8E-13	2.0E-12	0.0E+00	4.1E-12	3.4E-12	1.2E-11	0.0E+00	1.3E-12	1.1E-12	3.6E-12	0.0E+00	1.1E-12	2.2E-12	8.1E-12	0.0E+00
11	0.54	40	1.0E-13	3.0E-13	1.5E-12	0.0E+00	2.6E-13	2.6E-13	1.1E-12	0.0E+00					6.1E-13	6.1E-13	2.6E-12	0.0E+00	8.2E-14	2.8E-13	1.3E-12	0.0E+00
13	0.57	14	1.0E-12	6.9E-13	2.6E-12	1.6E-13	8.3E-12	4.8E-12	2.1E-11	3.1E-12	3.4E-12	2.0E-12	8.5E-12	1.3E-12					0.0E+00	0.0E+00	0.0E+00	0.0E+00
15	0.58	30	6.1E-13	7.6E-13	2.9E-12	0.0E+00	2.1E-12	9.2E-13	3.9E-12	6.5E-13	2.2E-11	9.7E-12	4.1E-11	6.8E-12	1.4E-11	6.3E-12	2.7E-11	4.4E-12	0.0E+00	0.0E+00	0.0E+00	0.0E+00
17	0.71	38	3.3E-12	3.1E-12	1.6E-11	0.0E+00	4.8E-12	4.1E-12	1.6E-11	1.4E-13	7.0E-12	6.0E-12	2.3E-11	2.0E-13	9.7E-12	8.3E-12	3.3E-11	2.8E-13	0.0E+00	0.0E+00	0.0E+00	0.0E+00
35	1.12	33	6.4E-12	6.1E-12	1.7E-11	0.0E+00	2.0E-12	7.6E-13	3.8E-12	7.8E-13	1.4E-11	5.4E-12	2.7E-11	5.5E-12	5.5E-12	2.1E-12	1.0E-11	2.1E-12	0.0E+00	0.0E+00	0.0E+00	0.0E+00
29	1.16	48	3.9E-12	3.1E-12	1.1E-11	0.0E+00	6.2E-12	3.1E-12	1.3E-11	0.0E+00	8.0E-12	4.0E-12	1.7E-11	0.0E+00					1.5E-14	1.0E-13	7.0E-13	0.0E+00
37	1.40	38	3.5E-12	2.6E-12	8.0E-12	0.0E+00	1.7E-11	7.5E-12	3.1E-11	3.4E-12	3.8E-11	1.6E-11	6.8E-11	7.5E-12					0.0E+00	0.0E+00	0.0E+00	0.0E+00
33	1.44	57	1.8E-11	1.6E-11	4.8E-11	0.0E+00	3.2E-12	1.8E-12	7.1E-12	5.5E-13	2.4E-11	1.3E-11	5.3E-11	4.1E-12	1.1E-11	6.2E-12	2.5E-11	1.9E-12	0.0E+00	0.0E+00	0.0E+00	0.0E+00
19	1.63	64	4.7E-12	4.4E-12	1.7E-11	0.0E+00	4.9E-12	1.5E-12	8.2E-12	3.1E-13	3.2E-11	1.0E-11	5.3E-11	2.0E-12	1.1E-11	3.6E-12	1.9E-11	7.3E-13	0.0E+00	0.0E+00	0.0E+00	0.0E+00
31	1.64	28	2.2E-12	1.5E-12	5.3E-12	2.6E-13	7.4E-12	1.9E-12	1.1E-11	4.0E-12	4.3E-11	1.1E-11	6.7E-11	2.4E-11	8.2E-12	2.1E-12	1.3E-11	4.4E-12	0.0E+00	0.0E+00	0.0E+00	0.0E+00
Summary			3.8E-12	3.3E-12	4.8E-11	0.0E+00	4.6E-12	2.2E-12	3.1E-11	0.0E+00	1.8E-11	7.6E-12	6.8E-11	0.0E+00	6.5E-12	3.2E-12	3.3E-11	0.0E+00	1.7E-13	4.0E-13	8.1E-12	0.0E+00

Note: For this period, model assumptions dictate plagioclase dissolution rates to be the same as Period B averages for each sample.
Note: N=number of experimental observations used to model dissolution rates.
Note: Zeroes indicate a calculated absence of dissolution. Blank cells indicate there was none of that mineral present in the sample.

Table 100. Model 1, Periods A-D Silicate Mineral Dissolution Rates for all Dunka blast hole samples (excludes R39-44). Page 4 of 4.

Model 1, Period D																		
R#	%S	N	Plag (mol $m^{-2}s^{-1}$)				Hyp (mol $m^{-2}s^{-1}$)				Ol (mol $m^{-2}s^{-1}$)				Bio (mol $m^{-2}s^{-1}$)			
			Ave	S.D.	Max	Min	Ave	S.D.	Max	Min	Ave	S.D.	Max	Min	Ave	S.D.	Max	Min
5	0.40	9	1.1E-12	2.6E-13	1.6E-12	6.4E-13	8.9E-14	9.3E-16	9.1E-14	8.8E-14					4.2E-13	4.4E-15	4.3E-13	4.2E-13
7	0.41	54	6.7E-13	2.1E-13	1.4E-12	3.6E-13	5.6E-13	5.6E-13	2.6E-12	2.4E-13	7.1E-13	7.1E-13	3.3E-12	3.1E-13	5.4E-13	5.4E-13	2.5E-12	2.3E-13
9	0.51	66	1.2E-12	5.6E-13	3.9E-12	5.6E-13	3.5E-13	3.9E-13	1.7E-12	1.3E-13	2.0E-12	2.2E-12	9.7E-12	7.7E-13	6.4E-13	7.1E-13	3.1E-12	2.4E-13
13	0.57	21	1.9E-12	4.1E-13	2.5E-12	1.2E-12	3.4E-12	1.7E-12	7.0E-12	4.4E-13	1.4E-12	7.0E-13	2.9E-12	1.8E-13				
15	0.58	80	1.2E-12	4.3E-13	2.8E-12	6.5E-13	3.9E-13	3.8E-13	1.7E-12	1.6E-13	4.1E-12	4.0E-12	1.8E-11	1.7E-12	2.7E-12	2.6E-12	1.2E-11	1.1E-12
17	0.71	58	9.1E-13	2.6E-13	1.6E-12	4.5E-13	6.7E-13	6.4E-13	2.8E-12	1.8E-13	9.7E-13	9.2E-13	4.1E-12	2.5E-13	1.3E-12	1.3E-12	5.7E-12	3.5E-13
35	1.12	3	2.6E-12	2.6E-13	2.8E-12	2.3E-12	1.9E-12	2.9E-13	2.2E-12	1.6E-12	1.4E-11	2.1E-12	1.6E-11	1.1E-11	5.2E-12	8.0E-13	6.0E-12	4.4E-12
29	1.16	47	8.8E-13	2.2E-13	1.5E-12	5.4E-13	7.5E-13	7.6E-13	3.4E-12	1.8E-13	9.5E-13	9.7E-13	4.3E-12	2.4E-13				
33	1.44	32	8.7E-13	1.5E-13	1.5E-12	5.8E-13	5.1E-13	2.3E-13	1.1E-12	9.2E-14	3.8E-12	1.7E-12	8.2E-12	6.9E-13	1.8E-12	7.9E-13	3.9E-12	3.2E-13
19	1.63	62	2.0E-12	8.7E-13	4.6E-12	9.9E-13	1.1E-12	8.6E-13	3.5E-12	1.3E-13	7.0E-12	5.6E-12	2.3E-11	8.5E-13	2.5E-12	2.0E-12	8.3E-12	3.1E-13
31	1.64	5	2.9E-12	4.2E-13	3.6E-12	2.6E-12	4.1E-12	8.6E-13	5.5E-12	3.2E-12	2.4E-11	5.0E-12	3.2E-11	1.8E-11	4.5E-12	9.5E-13	6.0E-12	3.5E-12
Summary			1.5E-12	3.7E-13	4.6E-12	3.6E-13	1.3E-12	6.1E-13	7.0E-12	8.8E-14	5.9E-12	2.4E-12	3.2E-11	1.8E-13	2.2E-12	1.1E-12	1.2E-11	2.3E-13

Note: N=number of experimental observations used to model dissolution rates.
Note: Zeroes indicate a calculated absence of dissolution. Blank cells indicate there was none of that mineral present in the sample.

Table 101. Model 2, Periods A-D Silicate Mineral Dissolution Rates for all Dunka blast hole samples (excludes R39-44). Page 1 of 4.

Model 2, Period A																						
R#	%S	N	Aug (mol $m^{-2}s^{-1}$)				Plag (mol $m^{-2}s^{-1}$)				Hyp (mol $m^{-2}s^{-1}$)				Ol (mol $m^{-2}s^{-1}$)				Bio (mol $m^{-2}s^{-1}$)			
			Ave	S.D.	Max	Min	Ave	S.D.	Max	Min	Ave	S.D.	Max	Min	Ave	S.D.	Max	Min	Ave	S.D.	Max	Min
1	0.18	8	4.4E-12	1.8E-12	6.5E-12	6.4E-13	1.9E-12	1.2E-12	3.4E-12	0.0E+00	3.5E-14	9.8E-14	2.8E-13	0.0E+00	1.3E-13	3.6E-13	1.0E-12	0.0E+00	1.1E-13	3.1E-13	8.8E-13	0.0E+00
3	0.22	7	7.7E-12	4.9E-12	1.6E-11	2.5E-12	1.2E-12	1.2E-12	3.0E-12	0.0E+00	3.6E-12	9.0E-12	2.4E-11	0.0E+00	8.2E-12	2.1E-11	5.5E-11	0.0E+00	1.9E-12	4.8E-12	1.3E-11	0.0E+00
5	0.40	8	1.9E-11	1.3E-11	4.2E-11	3.0E-12	5.5E-12	4.1E-12	1.3E-11	2.1E-12	0.0E+00	0.0E+00	0.0E+00	0.0E+00					0.0E+00	0.0E+00	0.0E+00	0.0E+00
7	0.41	10	4.7E-12	2.4E-12	8.5E-12	7.8E-13	2.6E-12	1.9E-12	4.9E-12	0.0E+00	1.8E-14	4.8E-14	1.3E-13	0.0E+00	2.3E-14	6.1E-14	1.6E-13	0.0E+00	1.8E-14	4.6E-14	1.2E-13	0.0E+00
9	0.51	11	5.1E-12	5.0E-12	1.8E-11	8.9E-13	3.4E-12	3.7E-12	1.1E-11	1.2E-13	0.0E+00	0.0E+00	0.0E+00	0.0E+00	0.0E+00	0.0E+00	0.0E+00	0.0E+00	0.0E+00	0.0E+00	0.0E+00	0.0E+00
11	0.54	32	8.9E-12	5.6E-12	2.1E-11	7.5E-13	3.1E-12	2.1E-12	9.8E-12	0.0E+00	4.5E-13	1.7E-12	8.4E-12	0.0E+00					1.1E-12	3.9E-12	2.0E-11	0.0E+00
13	0.57	7	4.2E-12	1.7E-12	7.3E-12	2.4E-12	3.2E-12	3.3E-12	9.4E-12	0.0E+00	6.1E-13	1.1E-12	2.9E-12	0.0E+00	2.5E-13	4.6E-13	1.2E-12	0.0E+00				
15	0.58	7	5.6E-12	3.7E-12	1.3E-11	1.5E-12	1.4E-12	1.5E-12	4.2E-12	0.0E+00	2.5E-13	6.7E-13	1.8E-12	0.0E+00	2.7E-12	7.1E-12	1.9E-11	0.0E+00	1.7E-12	4.6E-12	1.2E-11	0.0E+00
17	0.71	6	8.6E-12	2.2E-12	1.1E-11	5.7E-12	1.1E-12	1.2E-12	3.1E-12	0.0E+00	2.2E-13	4.2E-13	1.0E-12	0.0E+00	3.3E-13	6.1E-13	1.5E-12	0.0E+00	4.5E-13	8.4E-13	2.1E-12	0.0E+00
35	1.12	27	1.0E-11	8.6E-12	3.9E-11	1.4E-12	1.0E-11	5.8E-12	2.3E-11	0.0E+00	1.4E-13	5.1E-13	2.0E-12	0.0E+00	1.0E-12	3.6E-12	1.5E-11	0.0E+00	3.9E-13	1.4E-12	5.6E-12	0.0E+00
29	1.16	10	6.7E-12	3.4E-12	1.3E-11	7.0E-13	2.0E-12	1.4E-12	4.4E-12	3.7E-14	0.0E+00	0.0E+00	0.0E+00	0.0E+00	0.0E+00	0.0E+00	0.0E+00	0.0E+00				
37	1.40	18	5.1E-12	2.8E-12	1.1E-11	5.8E-13	4.7E-12	3.5E-12	1.2E-11	0.0E+00	2.3E-13	6.2E-13	1.9E-12	0.0E+00	5.0E-13	1.4E-12	4.2E-12	0.0E+00				
33	1.44	16	2.2E-11	9.7E-12	4.3E-11	1.1E-11	4.1E-12	4.1E-12	1.2E-11	0.0E+00	3.6E-13	6.4E-13	1.5E-12	0.0E+00	2.6E-12	4.8E-12	1.1E-11	0.0E+00	1.2E-12	2.2E-12	5.2E-12	0.0E+00
19	1.63	22	1.8E-11	9.9E-12	4.1E-11	7.7E-12	3.9E-13	9.9E-13	4.2E-12	0.0E+00	3.6E-12	4.6E-12	1.8E-11	0.0E+00	2.4E-11	3.0E-11	1.2E-10	0.0E+00	8.5E-12	1.1E-11	4.2E-11	0.0E+00
31	1.64	12	1.6E-11	1.0E-11	4.0E-11	3.2E-12	4.2E-12	4.8E-12	1.3E-11	0.0E+00	1.2E-12	2.1E-12	6.0E-12	0.0E+00	6.9E-12	1.2E-11	3.5E-11	0.0E+00	1.3E-12	2.3E-12	6.6E-12	0.0E+00
Summary			9.7E-12	5.7E-12	4.3E-11	5.8E-13	3.3E-12	2.7E-12	2.3E-11	0.0E+00	7.1E-13	1.4E-12	2.4E-11	0.0E+00	3.6E-12	6.2E-12	1.2E-10	0.0E+00	1.4E-12	2.6E-12	4.2E-11	0.0E+00

Note: N=number of experimental observations used to model dissolution rates.
Note: Zeroes indicate a calculated absence of dissolution. Blank cells indicate there was none of that mineral present in the sample.

Table 101. Model 2, Periods A-D Silicate Mineral Dissolution Rates for all Dunka blast hole samples (excludes R39-44). Page 2 of 4.

Model 2, Period B

R#	%S	N	Aug (mol $m^{-2}s^{-1}$)				Plag (mol $m^{-2}s^{-1}$)				Hyp (mol $m^{-2}s^{-1}$)				Ol (mol $m^{-2}s^{-1}$)				Bio (mol $m^{-2}s^{-1}$)			
			Ave	S.D.	Max	Min	Ave	S.D.	Max	Min	Ave	S.D.	Max	Min	Ave	S.D.	Max	Min	Ave	S.D.	Max	Min
1	0.18	189	1.0E-12	7.6E-13	3.9E-12	1.8E-13	2.7E-13	3.2E-13	2.7E-12	0.0E+00	1.0E-13	2.6E-13	1.3E-12	0.0E+00	3.9E-13	9.7E-13	4.9E-12	0.0E+00	3.3E-13	8.3E-13	4.2E-12	0.0E+00
3	0.22	191	1.8E-12	9.1E-13	6.1E-12	2.2E-13	1.2E-13	2.4E-13	1.9E-12	0.0E+00	7.2E-13	1.2E-12	8.3E-12	0.0E+00	1.7E-12	2.8E-12	1.9E-11	0.0E+00	3.9E-13	6.5E-13	4.4E-12	0.0E+00
5	0.40	133	3.4E-12	3.3E-12	1.5E-11	1.5E-12	2.0E-12	1.1E-12	6.1E-12	0.0E+00	1.3E-14	8.2E-14	8.6E-13	0.0E+00					6.0E-14	3.9E-13	4.1E-12	0.0E+00
7	0.41	52	1.4E-12	8.5E-13	5.3E-12	3.9E-13	1.7E-13	3.4E-13	1.9E-12	0.0E+00	3.6E-13	5.7E-13	2.3E-12	0.0E+00	4.6E-13	7.2E-13	2.9E-12	0.0E+00	3.5E-13	5.4E-13	2.2E-12	0.0E+00
9	0.51	33	1.8E-12	5.4E-13	2.8E-12	9.1E-13	9.2E-14	1.5E-13	5.9E-13	0.0E+00	2.7E-13	4.8E-13	2.1E-12	0.0E+00	1.5E-12	2.8E-12	1.2E-11	0.0E+00	4.9E-13	8.8E-13	3.8E-12	0.0E+00
11	0.54	37	2.9E-12	1.7E-12	8.4E-12	7.5E-13	1.2E-12	5.9E-13	2.6E-12	0.0E+00	1.2E-14	5.3E-14	2.9E-13	0.0E+00					2.8E-14	1.2E-13	6.7E-13	0.0E+00
13	0.57	45	1.6E-12	7.1E-13	3.7E-12	2.2E-13	3.4E-14	1.2E-13	6.3E-13	0.0E+00	2.4E-12	1.7E-12	8.3E-12	0.0E+00	9.8E-13	7.0E-13	3.4E-12	0.0E+00				
15	0.58	24	2.0E-12	7.8E-13	3.9E-12	2.8E-13	4.0E-14	2.0E-13	9.7E-13	0.0E+00	1.1E-12	5.4E-13	2.0E-12	0.0E+00	1.1E-11	5.6E-12	2.1E-11	0.0E+00	7.5E-12	3.7E-12	1.4E-11	0.0E+00
17	0.71	39	2.0E-12	1.2E-12	7.8E-12	4.8E-13	1.7E-14	1.0E-13	6.4E-13	0.0E+00	1.2E-12	8.1E-13	3.4E-12	0.0E+00	1.7E-12	1.2E-12	5.0E-12	0.0E+00	2.4E-12	1.6E-12	6.9E-12	0.0E+00
35	1.12	23	9.4E-12	2.0E-12	1.3E-11	5.4E-12	4.9E-13	6.5E-13	1.9E-12	0.0E+00	2.8E-13	3.5E-13	1.3E-12	0.0E+00	2.0E-12	2.5E-12	9.2E-12	0.0E+00	7.7E-13	9.6E-13	3.5E-12	0.0E+00
29	1.16	37	2.9E-12	2.1E-12	1.1E-11	1.2E-12	0.0E+00	0.0E+00	0.0E+00	0.0E+00	1.5E-12	6.5E-13	3.2E-12	2.2E-14	1.9E-12	8.3E-13	4.0E-12	2.8E-14				
37	1.40	35	3.4E-12	1.1E-12	5.5E-12	1.9E-12	9.6E-14	5.5E-13	3.2E-12	0.0E+00	3.6E-12	1.3E-12	6.8E-12	0.0E+00	8.0E-12	2.9E-12	1.5E-11	0.0E+00				
33	1.44	34	1.0E-11	2.6E-12	1.8E-11	4.7E-12	4.2E-14	2.2E-13	1.3E-12	0.0E+00	1.1E-12	4.9E-13	2.1E-12	0.0E+00	7.8E-12	3.7E-12	1.6E-11	0.0E+00	3.7E-12	1.7E-12	7.4E-12	0.0E+00
19	1.63	8	6.7E-12	5.8E-12	2.0E-11	3.2E-12	0.0E+00	0.0E+00	0.0E+00	0.0E+00	3.1E-12	1.3E-12	4.4E-12	3.2E-13	2.0E-11	8.7E-12	2.9E-11	2.1E-12	7.4E-12	3.2E-12	1.0E-11	7.6E-13
31	1.64	40	3.6E-12	8.1E-13	5.5E-12	2.4E-12	6.3E-14	2.3E-13	1.0E-12	0.0E+00	2.8E-12	1.4E-12	5.0E-12	0.0E+00	1.6E-11	8.1E-12	2.9E-11	0.0E+00	3.0E-12	1.5E-12	5.5E-12	0.0E+00
Summary			3.6E-12	1.7E-12	2.0E-11	1.8E-13	3.0E-13	3.2E-13	6.1E-12	0.0E+00	1.2E-12	7.5E-13	8.3E-12	0.0E+00	5.7E-12	3.2E-12	2.9E-11	0.0E+00	2.2E-12	1.3E-12	1.4E-11	0.0E+00

Note: N=number of experimental observations used to model dissolution rates.
Note: Zeroes indicate a calculated absence of dissolution. Blank cells indicate there was none of that mineral present in the sample.

Table 101. Model 2, Periods A-D Silicate Mineral Dissolution Rates for all Dunka blast hole samples (excludes R39-44). Page 3 of 4.

Model 2, Period C																						
R#	%S	N	Aug (mol m^{-2}s^{-1})				Plag (mol m^{-2}s^{-1})				Hyp (mol m^{-2}s^{-1})				Ol (mol m^{-2}s^{-1})				Bio (mol m^{-2}s^{-1})			
			Ave	S.D.	Max	Min	Ave	S.D.	Max	Min	Ave	S.D.	Max	Min	Ave	S.D.	Max	Min	Ave	S.D.	Max	Min
5	0.40	21	2.9E-12	1.8E-12	7.0E-12	1.5E-12	2.1E-12	8.9E-13	4.1E-12	7.6E-13	0.0E+00	0.0E+00	0.0E+00	0.0E+00					0.0E+00	0.0E+00	0.0E+00	0.0E+00
7	0.41	22	2.8E-12	1.0E-12	4.3E-12	3.9E-13	1.9E-13	3.8E-13	1.3E-12	0.0E+00	1.2E-12	1.5E-12	5.6E-12	0.0E+00	1.6E-12	1.9E-12	7.0E-12	0.0E+00	1.2E-12	1.4E-12	5.4E-12	0.0E+00
9	0.51	29	4.5E-12	1.9E-12	9.4E-12	4.6E-13	5.0E-13	8.3E-13	2.7E-12	0.0E+00	2.9E-13	3.7E-13	1.4E-12	0.0E+00	1.7E-12	2.2E-12	7.8E-12	0.0E+00	5.3E-13	6.9E-13	2.5E-12	0.0E+00
11	0.54	40	1.0E-12	9.6E-13	3.9E-12	3.8E-13	1.1E-12	4.2E-13	2.1E-12	8.8E-14	0.0E+00	0.0E+00	0.0E+00	0.0E+00					0.0E+00	0.0E+00	0.0E+00	0.0E+00
13	0.57	14	2.6E-12	7.2E-13	4.1E-12	1.6E-12	3.1E-14	6.2E-14	1.6E-13	0.0E+00	5.0E-12	4.7E-12	1.7E-11	0.0E+00	2.0E-12	1.9E-12	7.1E-12	0.0E+00				
15	0.58	30	2.4E-12	7.2E-13	4.9E-12	1.4E-12	1.4E-13	2.6E-13	7.9E-13	0.0E+00	8.3E-13	8.0E-13	2.9E-12	0.0E+00	8.7E-12	8.4E-12	3.0E-11	0.0E+00	5.6E-12	5.4E-12	2.0E-11	0.0E+00
17	0.71	38	5.2E-12	3.2E-12	1.8E-11	2.4E-13	2.8E-14	1.1E-13	5.4E-13	0.0E+00	4.0E-12	4.1E-12	1.5E-11	0.0E+00	5.8E-12	5.9E-12	2.2E-11	0.0E+00	8.1E-12	8.2E-12	3.1E-11	0.0E+00
35	1.12	33	1.5E-11	6.0E-12	2.6E-11	6.1E-12	5.5E-13	7.1E-13	2.4E-12	0.0E+00	3.0E-13	5.1E-13	1.6E-12	0.0E+00	2.1E-12	3.6E-12	1.1E-11	0.0E+00	8.1E-13	1.4E-12	4.3E-12	0.0E+00
29	1.16	48	6.7E-12	3.1E-12	1.4E-11	2.9E-12	2.5E-14	1.7E-13	1.2E-12	0.0E+00	4.7E-12	3.1E-12	1.2E-11	0.0E+00	5.9E-12	3.9E-12	1.5E-11	0.0E+00				
37	1.40	38	7.0E-12	2.7E-12	1.2E-11	2.9E-12	1.7E-15	1.1E-14	6.5E-14	0.0E+00	1.4E-11	7.4E-12	2.7E-11	0.0E+00	3.0E-11	1.6E-11	6.0E-11	0.0E+00				
33	1.44	57	2.8E-11	1.6E-11	5.9E-11	7.4E-12	7.8E-15	3.7E-14	2.1E-13	0.0E+00	2.4E-12	1.7E-12	6.3E-12	0.0E+00	1.8E-11	1.3E-11	4.7E-11	0.0E+00	8.6E-12	6.1E-12	2.2E-11	0.0E+00
19	1.63	64	1.1E-11	4.4E-12	2.4E-11	4.6E-12	4.5E-14	3.1E-13	2.4E-12	0.0E+00	3.4E-12	1.5E-12	6.7E-12	0.0E+00	2.2E-11	9.8E-12	4.3E-11	0.0E+00	8.1E-12	3.6E-12	1.6E-11	0.0E+00
31	1.64	28	5.9E-12	1.5E-12	9.0E-12	4.0E-12	0.0E+00	0.0E+00	0.0E+00	0.0E+00	4.2E-12	1.9E-12	8.2E-12	8.1E-13	2.4E-11	1.1E-11	4.8E-11	4.7E-12	4.6E-12	2.1E-12	9.0E-12	8.9E-13
Summary			7.4E-12	3.4E-12	5.9E-11	2.4E-13	3.6E-13	3.2E-13	4.1E-12	0.0E+00	3.1E-12	2.1E-12	2.7E-11	0.0E+00	1.1E-11	7.1E-12	6.0E-11	0.0E+00	3.7E-12	2.9E-12	3.1E-11	0.0E+00

Note: N=number of experimental observations used to model dissolution rates.
Note: Zeroes indicate a calculated absence of dissolution. Blank cells indicate there was none of that mineral present in the sample.

Table 101. Model 2, Periods A-D Silicate Mineral Dissolution Rates for all Dunka blast hole samples (excludes R39-44). Page 4 of 4.

Model 2, Period D																						
R#	%S	N	Aug (mol m^{-2}s^{-1})				Plag (mol m^{-2}s^{-1})				Hyp (mol m^{-2}s^{-1})				Ol (mol m^{-2}s^{-1})				Bio (mol m^{-2}s^{-1})			
			Ave	S.D.	Max	Min	Ave	S.D.	Max	Min	Ave	S.D.	Max	Min	Ave	S.D.	Max	Min	Ave	S.D.	Max	Min
5	0.40	9	1.5E-12	1.6E-14	1.6E-12	1.5E-12	7.0E-13	2.6E-13	1.2E-12	2.9E-13	0.0E+00	0.0E+00	0.0E+00	0.0E+00					0.0E+00	0.0E+00	0.0E+00	0.0E+00
7	0.41	54	8.2E-13	7.7E-13	3.1E-12	3.6E-13	4.0E-13	2.0E-13	8.9E-13	0.0E+00	1.8E-14	9.3E-14	5.9E-13	0.0E+00	2.2E-14	1.2E-13	7.5E-13	0.0E+00	1.7E-14	9.0E-14	5.7E-13	0.0E+00
9	0.51	66	1.1E-12	1.1E-12	5.4E-12	4.2E-13	7.7E-13	4.3E-13	2.7E-12	0.0E+00	1.3E-14	8.6E-14	6.6E-13	0.0E+00	7.8E-14	5.0E-13	3.8E-12	0.0E+00	2.5E-14	1.6E-13	1.2E-12	0.0E+00
13	0.57	21	1.5E-12	6.7E-13	2.6E-12	2.0E-13	5.1E-13	5.8E-13	2.1E-12	0.0E+00	2.5E-13	7.2E-13	3.2E-12	0.0E+00	1.0E-13	3.0E-13	1.3E-12	0.0E+00				
15	0.58	80	5.8E-13	6.3E-13	3.8E-12	2.3E-13	7.9E-13	3.9E-13	2.4E-12	0.0E+00	8.7E-15	6.9E-14	6.1E-13	0.0E+00	9.1E-14	7.2E-13	6.4E-12	0.0E+00	5.9E-14	4.7E-13	4.2E-12	0.0E+00
17	0.71	58	1.4E-12	1.3E-12	4.3E-12	3.9E-13	4.5E-13	2.1E-13	8.1E-13	0.0E+00	3.1E-14	1.6E-13	1.1E-12	0.0E+00	4.6E-14	2.3E-13	1.6E-12	0.0E+00	6.4E-14	3.1E-13	2.3E-12	0.0E+00
35	1.12	3	7.5E-12	7.3E-13	8.2E-12	6.7E-12	0.0E+00	0.0E+00	0.0E+00	0.0E+00	4.2E-13	2.4E-13	6.9E-13	2.6E-13	3.0E-12	1.7E-12	4.9E-12	1.9E-12	1.1E-12	6.5E-13	1.9E-12	7.1E-13
29	1.16	47	1.1E-12	9.2E-13	4.1E-12	3.3E-13	4.5E-13	2.5E-13	9.6E-13	0.0E+00	1.1E-13	3.2E-13	1.8E-12	0.0E+00	1.4E-13	4.1E-13	2.2E-12	0.0E+00				
33	1.44	32	6.4E-12	2.6E-12	1.4E-11	1.2E-12	1.8E-13	2.0E-13	7.1E-13	0.0E+00	3.1E-14	5.7E-14	2.4E-13	0.0E+00	2.3E-13	4.2E-13	1.8E-12	0.0E+00	1.1E-13	2.0E-13	8.6E-13	0.0E+00
19	1.63	62	3.7E-12	2.3E-12	1.0E-11	5.9E-13	2.6E-13	3.2E-13	1.2E-12	0.0E+00	2.4E-13	4.1E-13	1.4E-12	0.0E+00	1.6E-12	2.7E-12	9.0E-12	0.0E+00	5.7E-13	9.7E-13	3.2E-12	0.0E+00
31	1.64	5	4.1E-12	6.1E-13	5.1E-12	3.6E-12	1.3E-14	3.0E-14	6.7E-14	0.0E+00	5.6E-13	4.0E-13	1.0E-12	0.0E+00	3.3E-12	2.3E-12	6.0E-12	0.0E+00	6.2E-13	4.4E-13	1.1E-12	0.0E+00
Summary			2.7E-12	1.1E-12	1.4E-11	2.0E-13	4.1E-13	2.6E-13	2.7E-12	0.0E+00	1.5E-13	2.3E-13	3.2E-12	0.0E+00	8.5E-13	9.4E-13	9.0E-12	0.0E+00	2.9E-13	3.7E-13	4.2E-12	0.0E+00

Note: Zeroes indicate a calculated absence of dissolution. Blank cells indicate there was none of that mineral present in the sample.
Note: N=number of experimental observations used to model dissolution rates.

Table 102. Model 3, Periods A-D Silicate Mineral Dissolution Rates for all Dunka blast hole samples (excludes R39-44). Page 1 of 4.

Model 3, Period A																						
R#	%S	N	Plag (mol $m^{-2}s^{-1}$)				Aug (mol $m^{-2}s^{-1}$)				Hyp (mol $m^{-2}s^{-1}$)				Ol (mol $m^{-2}s^{-1}$)				Bio (mol $m^{-2}s^{-1}$)			
			Ave	S.D.	Max	Min	Ave	S.D.	Max	Min	Ave	S.D.	Max	Min	Ave	S.D.	Max	Min	Ave	S.D.	Max	Min
N/A			N/A				N/A				N/A				N/A				N/A			
Summary			N/A				N/A				N/A				N/A				N/A			

Note: Zeroes indicate a calculated absence of dissolution. Blank cells indicate there was none of that mineral present in the sample.
Note: N=number of experimental observations used to model dissolution rates.

Table 102. Model 3, Periods A-D Silicate Mineral Dissolution Rates for all Dunka blast hole samples (excludes R39-44). Page 2 of 4.

Model 3, Period B																						
R#	%S	N	Plag (mol $m^{-2}s^{-1}$)				Aug (mol $m^{-2}s^{-1}$)				Hyp (mol $m^{-2}s^{-1}$)				Ol (mol $m^{-2}s^{-1}$)				Bio (mol $m^{-2}s^{-1}$)			
			Ave	S.D.	Max	Min	Ave	S.D.	Max	Min	Ave	S.D.	Max	Min	Ave	S.D.	Max	Min	Ave	S.D.	Max	Min
1	0.18	32	3.6E-13	1.6E-13	8.1E-13	1.5E-13	5.1E-13	3.8E-13	1.8E-12	0.0E+00	1.7E-13	3.4E-13	1.7E-12	0.0E+00	6.2E-13	1.3E-12	6.1E-12	0.0E+00	5.3E-13	1.1E-12	5.2E-12	0.0E+00
3	0.22	34	2.2E-13	8.9E-14	4.0E-13	1.1E-13	1.1E-12	4.7E-13	2.4E-12	2.1E-13	8.8E-13	1.2E-12	5.2E-12	0.0E+00	2.0E-12	2.7E-12	1.2E-11	0.0E+00	4.7E-13	6.2E-13	2.7E-12	0.0E+00
5	0.40	20	2.3E-13	1.2E-13	6.3E-13	1.8E-13	3.4E-12	3.2E-12	1.1E-11	1.5E-12	1.9E-14	6.4E-14	2.7E-13	0.0E+00					9.2E-14	3.0E-13	1.3E-12	0.0E+00
Summary			2.7E-13	1.2E-13	8.1E-13	1.1E-13	1.7E-12	1.3E-12	1.1E-11	0.0E+00	3.6E-13	5.2E-13	5.2E-12	0.0E+00	1.3E-12	2.0E-12	1.2E-11	0.0E+00	3.6E-13	6.7E-13	5.2E-12	0.0E+00

Note: Zeroes indicate a calculated absence of dissolution. Blank cells indicate there was none of that mineral present in the sample.
Note: N=number of experimental observations used to model dissolution rates.

Table 102. Model 3, Periods A-D Silicate Mineral Dissolution Rates for all Dunka blast hole samples (excludes R39-44). Page 3 of 4.

Model 3, Period C																						
R#	%S	N	Plag (mol m^{-2}s^{-1})				Aug (mol m^{-2}s^{-1})				Hyp (mol m^{-2}s^{-1})				Ol (mol m^{-2}s^{-1})				Bio (mol m^{-2}s^{-1})			
			Ave	S.D.	Max	Min	Ave	S.D.	Max	Min	Ave	S.D.	Max	Min	Ave	S.D.	Max	Min	Ave	S.D.	Max	Min
5	0.40	7	6.4E-13	2.2E-13	9.9E-13	4.3E-13	2.8E-12	2.0E-12	7.0E-12	1.5E-12	0.0E+00	0.0E+00	0.0E+00	0.0E+00					0.0E+00	0.0E+00	0.0E+00	0.0E+00
7	0.41	2	5.9E-13	1.1E-13	6.7E-13	5.1E-13	1.5E-12	8.7E-15	1.5E-12	1.4E-12	2.7E-12	1.5E-12	3.7E-12	1.7E-12	3.4E-12	1.8E-12	4.7E-12	2.1E-12	2.6E-12	1.4E-12	3.6E-12	1.6E-12
11	0.54	2	6.2E-13	1.3E-13	7.2E-13	5.3E-13	8.8E-13	6.9E-13	1.4E-12	3.9E-13	2.5E-13	3.5E-13	5.0E-13	0.0E+00					5.8E-13	8.2E-13	1.2E-12	0.0E+00
17	0.71	2	6.2E-13	1.2E-13	7.0E-13	5.3E-13	1.9E-12	3.9E-13	2.2E-12	1.7E-12	2.0E-12	9.0E-13	2.7E-12	1.4E-12	2.9E-12	1.3E-12	3.9E-12	2.0E-12	4.1E-12	1.8E-12	5.4E-12	2.8E-12
35	1.12	2	2.0E-12	1.3E-12	2.9E-12	1.2E-12	4.5E-12	6.4E-12	9.0E-12	0.0E+00	2.0E-12	3.8E-13	2.3E-12	1.7E-12	1.4E-11	2.7E-12	1.6E-11	1.2E-11	5.4E-12	1.0E-12	6.1E-12	4.7E-12
29	1.16	3	9.1E-13	3.0E-13	1.3E-12	6.8E-13	3.2E-12	2.0E-12	5.5E-12	1.9E-12	6.9E-12	5.8E-12	1.4E-11	2.7E-12	8.8E-12	7.5E-12	1.7E-11	3.4E-12				
37	1.40	3	1.5E-12	2.6E-13	1.7E-12	1.2E-12	5.3E-12	1.5E-12	6.2E-12	3.6E-12	1.8E-11	5.7E-12	2.5E-11	1.4E-11	4.0E-11	1.2E-11	5.4E-11	3.2E-11				
33	1.44	7	8.6E-13	4.0E-13	1.7E-12	5.6E-13	1.4E-11	6.5E-12	2.4E-11	6.7E-12	3.5E-12	1.8E-12	6.2E-12	9.6E-13	2.6E-11	1.3E-11	4.6E-11	7.2E-12	1.2E-11	6.4E-12	2.2E-11	3.4E-12
19	1.63	1	1.0E-12	N/A	N/A	N/A	7.8E-12	N/A	N/A	N/A	2.6E-12	N/A	N/A	N/A	1.7E-11	N/A	N/A	N/A	6.1E-12	N/A	N/A	N/A
31	1.64	1	1.1E-12	N/A	N/A	N/A	3.7E-12	N/A	N/A	N/A	4.9E-12	N/A	N/A	N/A	2.8E-11	N/A	N/A	N/A	5.3E-12	N/A	N/A	N/A
Summary			9.9E-13	3.5E-13	2.9E-12	4.3E-13	4.5E-12	2.4E-12	2.4E-11	0.0E+00	4.3E-12	2.1E-12	2.5E-11	0.0E+00	1.8E-11	6.5E-12	5.4E-11	2.0E-12	4.5E-12	1.9E-12	2.2E-11	0.0E+00

Note: Zeroes indicate a calculated absence of dissolution. Blank cells indicate there was none of that mineral present in the sample.
Note: N=number of experimental observations used to model dissolution rates.

Table 102. Model 3, Periods A-D Silicate Mineral Dissolution Rates for all Dunka blast hole samples (excludes R39-44). Page 4 of 4.

Model 3, Period D																						
R#	%S	N	Plag (mol $m^{-2}s^{-1}$)				Aug (mol $m^{-2}s^{-1}$)				Hyp (mol $m^{-2}s^{-1}$)				Ol (mol $m^{-2}s^{-1}$)				Bio (mol $m^{-2}s^{-1}$)			
			Ave	S.D.	Max	Min	Ave	S.D.	Max	Min	Ave	S.D.	Max	Min	Ave	S.D.	Max	Min	Ave	S.D.	Max	Min
5	0.40	3	2.6E-13	1.2E-13	4.0E-13	1.8E-13	1.5E-12	1.7E-14	1.6E-12	1.5E-12	0.0E+00	0.0E+00	0.0E+00	0.0E+00					0.0E+00	0.0E+00	0.0E+00	0.0E+00
7	0.41	14	4.8E-13	1.6E-13	8.5E-13	3.2E-13	3.6E-13	2.2E-13	8.3E-13	0.0E+00	3.3E-13	5.9E-13	1.6E-12	0.0E+00	4.2E-13	7.4E-13	2.0E-12	0.0E+00	3.2E-13	5.6E-13	1.5E-12	0.0E+00
9	0.51	17	6.9E-13	2.6E-13	1.4E-12	4.1E-13	6.0E-13	5.2E-13	2.1E-12	0.0E+00	2.0E-13	3.7E-13	1.2E-12	0.0E+00	1.2E-12	2.1E-12	7.2E-12	0.0E+00	3.7E-13	6.7E-13	2.3E-12	0.0E+00
13	0.57	2	1.1E-12	4.6E-13	1.4E-12	7.7E-13	6.0E-13	1.5E-13	7.1E-13	4.9E-13	2.2E-12	8.7E-13	2.8E-12	1.6E-12	9.0E-13	3.5E-13	1.2E-12	6.5E-13				
15	0.58	18	6.7E-13	5.6E-13	2.9E-12	3.6E-13	3.2E-13	2.0E-13	9.3E-13	0.0E+00	2.2E-13	5.6E-13	2.0E-12	0.0E+00	2.4E-12	5.9E-12	2.1E-11	0.0E+00	1.5E-12	3.8E-12	1.4E-11	0.0E+00
17	0.71	16	5.5E-13	1.3E-13	7.9E-13	3.9E-13	9.9E-13	7.6E-13	2.7E-12	0.0E+00	3.2E-13	6.0E-13	2.1E-12	0.0E+00	4.6E-13	8.6E-13	3.1E-12	0.0E+00	6.4E-13	1.2E-12	4.3E-12	0.0E+00
35	1.12	1	9.4E-13	N/A	N/A	N/A	4.0E-12	N/A	N/A	N/A	8.1E-13	N/A	N/A	N/A	5.7E-12	N/A	N/A	N/A	2.2E-12	N/A	N/A	N/A
29	1.16	15	5.5E-13	1.3E-13	8.5E-13	3.5E-13	5.9E-13	2.9E-13	1.1E-12	3.3E-13	3.4E-13	5.8E-13	1.7E-12	0.0E+00	4.4E-13	7.4E-13	2.2E-12	0.0E+00				
33	1.44	11	5.2E-13	1.5E-13	8.7E-13	3.6E-13	2.6E-12	1.4E-12	4.3E-12	0.0E+00	1.8E-13	2.1E-13	6.8E-13	0.0E+00	1.3E-12	1.6E-12	5.1E-12	0.0E+00	6.3E-13	7.5E-13	2.4E-12	0.0E+00
19	1.63	18	6.9E-13	2.0E-13	1.2E-12	4.7E-13	2.5E-12	1.8E-12	6.4E-12	5.9E-13	4.3E-13	6.7E-13	1.8E-12	0.0E+00	2.8E-12	4.4E-12	1.2E-11	0.0E+00	1.0E-12	1.6E-12	4.3E-12	0.0E+00
31	1.64	2	1.1E-12	1.2E-13	1.2E-12	1.0E-12	2.3E-12	4.1E-14	2.4E-12	2.3E-12	2.1E-12	5.8E-15	2.1E-12	2.1E-12	1.2E-11	3.4E-14	1.2E-11	1.2E-11	2.3E-12	6.4E-15	2.3E-12	2.3E-12
Summary			6.9E-13	2.3E-13	2.9E-12	1.8E-13	1.5E-12	5.3E-13	6.4E-12	0.0E+00	6.5E-13	4.4E-13	2.8E-12	0.0E+00	2.8E-12	1.9E-12	2.1E-11	0.0E+00	1.0E-12	1.1E-12	1.4E-11	0.0E+00

Note: Zeroes indicate a calculated absence of dissolution. Blank cells indicate there was none of that mineral present in the sample.
Note: N=number of experimental observations used to model dissolution rates.

Table 103. Model 3, Periods A-D Orphan Calcium Rates for all Dunka blast hole samples (excludes R39-44).

Model 3, Orphan Calcium (mol $m^{-2}s^{-1}$)																	
R#	%S	Period A				Period B				Period C				Period D			
		Ave	S.D.	Max	Min	Ave	S.D.	Max	Min	Ave	S.D.	Max	Min	Ave	S.D.	Max	Min
1	0.18					1.7E-13	3.1E-13	1.2E-12	0.0E+00								
3	0.22					3.1E-14	1.7E-13	9.7E-13	0.0E+00								
5	0.4					4.6E-12	2.4E-12	9.0E-12	0.0E+00	6.5E-12	3.2E-12	1.2E-11	2.7E-12	1.6E-12	1.3E-13	1.7E-12	1.5E-12
7	0.41									0.0E+00	0.0E+00	0.0E+00	0.0E+00	2.3E-13	3.6E-13	1.2E-12	0.0E+00
9	0.51													3.2E-13	4.2E-13	1.4E-12	0.0E+00
11	0.54									9.5E-13	1.3E-12	1.9E-12	0.0E+00				
13	0.57													0.0E+00	0.0E+00	0.0E+00	0.0E+00
15	0.58													8.0E-13	5.9E-13	1.6E-12	0.0E+00
17	0.71									0.0E+00	0.0E+00	0.0E+00	0.0E+00	2.7E-13	3.2E-13	1.0E-12	0.0E+00
35	1.12									0.0E+00	0.0E+00	0.0E+00	0.0E+00	0.0E+00		0.0E+00	0.0E+00
29	1.16									0.0E+00	0.0E+00	0.0E+00	0.0E+00	4.3E-13	5.0E-13	1.5E-12	0.0E+00
37	1.4									0.0E+00	0.0E+00	0.0E+00	0.0E+00				
33	1.44									0.0E+00	0.0E+00	0.0E+00	0.0E+00	1.3E-13	4.1E-13	1.4E-12	0.0E+00
19	1.63									0.0E+00		0.0E+00	0.0E+00	1.2E-13	3.0E-13	1.1E-12	0.0E+00
31	1.64									0.0E+00		0.0E+00	0.0E+00	0.0E+00	0.0E+00	0.0E+00	0.0E+00
Summary		N/A	N/A	N/A	N/A	1.6E-12	9.6E-13	9.0E-12	0.0E+00	7.4E-13	5.7E-13	1.2E-11	0.0E+00	3.5E-13	3.0E-13	1.7E-12	0.0E+00

Note: Zeroes indicate a calculated absence of dissolution. Blank cells indicate there was none of that mineral present in the sample.

Table 104. Model 4, Periods A-D Silicate Mineral Dissolution Rates for all Dunka blast hole samples (excludes R39-44). Page 1 of 4.

Model 4, Period A																						
R#	%S	N	Bio (mol $m^{-2}s^{-1}$)				K-spar (mol $m^{-2}s^{-1}$)				Aug (mol $m^{-2}s^{-1}$)				Hyp (mol $m^{-2}s^{-1}$)				Ol (mol $m^{-2}s^{-1}$)			
			Ave	S.D.	Max	Min	Ave	S.D.	Max	Min	Ave	S.D.	Max	Min	Ave	S.D.	Max	Min	Ave	S.D.	Max	Min
N/A			N/A				N/A				N/A				N/A				N/A			
Summary			N/A				N/A				N/A				N/A				N/A			

Note: Zeroes indicate a calculated absence of dissolution. Blank cells indicate there was none of that mineral present in the sample.
Note: N=number of experimental observations used to model dissolution rates.
Note: Plagioclase dissolution calculations in Model 4 are the same as Model 3 (see Table AZ).

Table 104. Model 4, Periods A-D Silicate Mineral Dissolution Rates for all Dunka blast hole samples (excludes R39-44). Page 2 of 4.

Model 4, Period B																						
R#	%S	N	Bio (mol $m^{-2}s^{-1}$)				K-spar (mol $m^{-2}s^{-1}$)				Aug (mol $m^{-2}s^{-1}$)				Hyp (mol $m^{-2}s^{-1}$)				Ol (mol $m^{-2}s^{-1}$)			
			Ave	S.D.	Max	Min	Ave	S.D.	Max	Min	Ave	S.D.	Max	Min	Ave	S.D.	Max	Min	Ave	S.D.	Max	Min
1	0.18	32	6.0E-12	5.3E-12	1.7E-11	7.0E-13					5.1E-13	3.8E-13	1.8E-12	0.0E+00	3.1E-15	1.8E-14	1.0E-13	0.0E+00	1.2E-14	6.5E-14	3.7E-13	0.0E+00
3	0.22	33	2.3E-12	2.4E-12	8.6E-12	2.0E-13	1.0E-11	1.1E-11	3.8E-11	8.9E-13	1.1E-12	4.7E-13	2.4E-12	2.1E-13	2.2E-14	1.3E-13	7.3E-13	0.0E+00	5.0E-14	2.9E-13	1.7E-12	0.0E+00
5	0.40	18	5.6E-12	4.2E-12	1.5E-11	1.5E-12	1.6E-11	1.2E-11	4.5E-11	4.3E-12	3.6E-12	3.3E-12	1.1E-11	1.5E-12	0.0E+00	0.0E+00	0.0E+00	0.0E+00				
Summary			4.6E-12	4.0E-12	1.7E-11	2.0E-13	1.3E-11	1.1E-11	4.5E-11	8.9E-13	1.7E-12	1.3E-12	1.1E-11	0.0E+00	8.4E-15	4.8E-14	7.3E-13	0.0E+00	3.1E-14	1.8E-13	1.7E-12	0.0E+00

Note: Zeroes indicate a calculated absence of dissolution. Blank cells indicate there was none of that mineral present in the sample.
Note: N=number of experimental observations used to model dissolution rates.
Note: Plagioclase dissolution calculations in Model 4 are the same as Model 3 (see Table AZ).

Table 104. Model 4, Periods A-D Silicate Mineral Dissolution Rates for all Dunka blast hole samples (excludes R39-44). Page 3 of 4.

Model 4, Period C																						
R#	%S	N	Bio (mol $m^{-2}s^{-1}$)				K-spar (mol $m^{-2}s^{-1}$)				Aug (mol $m^{-2}s^{-1}$)				Hyp (mol $m^{-2}s^{-1}$)				Ol (mol $m^{-2}s^{-1}$)			
			Ave	S.D.	Max	Min	Ave	S.D.	Max	Min	Ave	S.D.	Max	Min	Ave	S.D.	Max	Min	Ave	S.D.	Max	Min
5	0.40	7	1.2E-12	9.9E-13	2.5E-12	3.2E-13	3.5E-12	2.9E-12	7.2E-12	9.4E-13	2.8E-12	2.0E-12	7.0E-12	1.5E-12	0.0E+00	0.0E+00	0.0E+00	0.0E+00				
7	0.41	2	4.5E-12	1.8E-12	5.8E-12	3.2E-12	6.8E-11	2.8E-11	8.7E-11	4.8E-11	1.5E-12	8.7E-15	1.5E-12	1.4E-12	2.0E-13	2.8E-13	3.9E-13	0.0E+00	2.5E-13	3.5E-13	5.0E-13	0.0E+00
11	0.54	2	2.5E-12	4.1E-13	2.8E-12	2.2E-12					8.8E-13	6.9E-13	1.4E-12	3.9E-13	0.0E+00	0.0E+00	0.0E+00	0.0E+00				
17	0.71	2	5.9E-12	1.8E-12	7.2E-12	4.6E-12	6.1E-11	1.9E-11	7.5E-11	4.8E-11	1.9E-12	3.9E-13	2.2E-12	1.7E-12	0.0E+00	0.0E+00	0.0E+00	0.0E+00	0.0E+00	0.0E+00	0.0E+00	0.0E+00
35	1.12	2	6.4E-12	2.3E-12	8.0E-12	4.8E-12	5.9E-12	2.1E-12	7.4E-12	4.4E-12	4.5E-12	6.4E-12	9.0E-12	0.0E+00	0.0E+00	0.0E+00	0.0E+00	0.0E+00	0.0E+00	0.0E+00	0.0E+00	0.0E+00
29	1.16	3									3.2E-12	2.0E-12	5.5E-12	1.9E-12	6.9E-12	5.8E-12	1.4E-11	2.7E-12	8.8E-12	7.5E-12	1.7E-11	3.4E-12
37	1.40	3					7.2E-11	3.3E-11	9.7E-11	3.5E-11	5.3E-12	1.5E-12	6.2E-12	3.6E-12	1.8E-11	5.7E-12	2.5E-11	1.4E-11	4.0E-11	1.2E-11	5.4E-11	3.2E-11
33	1.44	7	1.0E-11	6.9E-12	2.4E-11	2.5E-12	2.4E-11	1.6E-11	5.5E-11	6.0E-12	1.4E-11	6.5E-12	2.4E-11	6.7E-12	9.0E-13	8.8E-13	2.0E-12	0.0E+00	6.7E-12	6.5E-12	1.5E-11	0.0E+00
19	1.63	1	7.1E-12	N/A	N/A	N/A	1.2E-11	N/A	N/A	N/A	7.8E-12	N/A	N/A	N/A	0.0E+00	N/A	N/A	N/A	0.0E+00	N/A	N/A	N/A
31	1.64	1	3.1E-12	N/A	N/A	N/A	1.0E-11	N/A	N/A	N/A	3.7E-12	N/A	N/A	N/A	2.0E-12	N/A	N/A	N/A	1.2E-11	N/A	N/A	N/A
Summary			5.1E-12	2.4E-12	2.4E-11	3.2E-13	3.2E-11	1.7E-11	9.7E-11	9.4E-13	4.5E-12	2.4E-12	2.4E-11	0.0E+00	2.8E-12	1.6E-12	2.5E-11	0.0E+00	8.5E-12	4.5E-12	5.4E-11	0.0E+00

Note: Zeroes indicate a calculated absence of dissolution. Blank cells indicate there was none of that mineral present in the sample.
Note: N=number of experimental observations used to model dissolution rates.
Note: Plagioclase dissolution calculations in Model 4 are the same as Model 3 (see Table AZ).

Table 104. Model 4, Periods A-D Silicate Mineral Dissolution Rates for all Dunka blast hole samples (excludes R39-44). Page 4 of 4.

Model 4, Period D																						
R#	%S	N	Bio (mol m^{-2}s^{-1})				K-spar (mol m^{-2}s^{-1})				Aug (mol m^{-2}s^{-1})				Hyp (mol m^{-2}s^{-1})				Ol (mol m^{-2}s^{-1})			
			Ave	S.D.	Max	Min	Ave	S.D.	Max	Min	Ave	S.D.	Max	Min	Ave	S.D.	Max	Min	Ave	S.D.	Max	Min
5	0.40	2	4.0E-13	3.4E-15	4.1E-13	4.0E-13	1.2E-12	1.0E-14	1.2E-12	1.2E-12	1.6E-12	1.3E-14	1.6E-12	1.5E-12	0.0E+00	0.0E+00	0.0E+00	0.0E+00				
7	0.41	12	2.8E-12	2.0E-12	7.5E-12	8.1E-13	4.1E-11	3.0E-11	1.1E-10	1.2E-11	3.9E-13	2.1E-13	8.3E-13	0.0E+00	2.0E-14	7.0E-14	2.4E-13	0.0E+00	2.6E-14	8.8E-14	3.1E-13	0.0E+00
9	0.51	16	2.3E-12	1.8E-12	6.9E-12	2.2E-13	6.7E-12	5.2E-12	2.0E-11	6.3E-13	6.1E-13	5.4E-13	2.1E-12	0.0E+00	2.8E-14	1.1E-13	4.5E-13	0.0E+00	1.6E-13	6.5E-13	2.6E-12	0.0E+00
13	0.57	2					1.8E-11	9.4E-12	2.5E-11	1.2E-11	6.0E-13	1.5E-13	7.1E-13	4.9E-13	2.2E-12	8.7E-13	2.8E-12	1.6E-12	9.0E-13	3.5E-13	1.2E-12	6.5E-13
15	0.58	17	1.1E-11	1.3E-11	4.1E-11	6.9E-13	1.1E-11	1.2E-11	3.8E-11	6.4E-13	3.2E-13	2.1E-13	9.3E-13	0.0E+00	3.5E-14	1.4E-13	6.0E-13	0.0E+00	3.7E-13	1.5E-12	6.3E-12	0.0E+00
17	0.71	16	7.4E-12	7.8E-12	2.3E-11	9.9E-13	7.7E-11	8.1E-11	2.3E-10	1.0E-11	9.9E-13	7.6E-13	2.7E-12	0.0E+00	0.0E+00	0.0E+00	0.0E+00	0.0E+00	0.0E+00	0.0E+00	0.0E+00	0.0E+00
35	1.12	1	6.8E-12	N/A	N/A	N/A	6.3E-12	N/A	N/A	N/A	4.0E-12	N/A	N/A	N/A	0.0E+00	N/A	N/A	N/A	0.0E+00	N/A	N/A	N/A
29	1.16	15									5.9E-13	2.9E-13	1.1E-12	3.3E-13	3.4E-13	5.8E-13	1.7E-12	0.0E+00	4.4E-13	7.4E-13	2.2E-12	0.0E+00
33	1.44	9	1.4E-12	6.0E-13	2.5E-12	7.2E-13	3.3E-12	1.4E-12	5.9E-12	1.7E-12	2.7E-12	1.5E-12	4.3E-12	0.0E+00	5.6E-14	1.2E-13	3.2E-13	0.0E+00	4.2E-13	8.6E-13	2.4E-12	0.0E+00
19	1.63	17	6.9E-12	6.3E-12	2.4E-11	1.6E-12	1.2E-11	1.1E-11	4.1E-11	2.7E-12	2.3E-12	1.6E-12	6.4E-12	5.9E-13	6.0E-14	2.4E-13	1.0E-12	0.0E+00	3.9E-13	1.6E-12	6.6E-12	0.0E+00
31	1.64	2	4.6E-12	7.5E-13	5.1E-12	4.1E-12	1.5E-11	2.4E-12	1.6E-11	1.3E-11	2.3E-12	4.1E-14	2.4E-12	2.3E-12	0.0E+00	0.0E+00	0.0E+00	0.0E+00	0.0E+00	0.0E+00	0.0E+00	0.0E+00
Summary			4.9E-12	4.0E-12	4.1E-11	2.2E-13	1.9E-11	1.7E-11	2.3E-10	6.3E-13	1.5E-12	5.3E-13	6.4E-12	0.0E+00	2.5E-13	2.1E-13	2.8E-12	0.0E+00	2.7E-13	6.4E-13	6.6E-12	0.0E+00

Note: Zeroes indicate a calculated absence of dissolution. Blank cells indicate there was none of that mineral present in the sample.
Note: N=number of experimental observations used to model dissolution rates.
Note: Plagioclase dissolution calculations in Model 4 are the same as Model 3 (see Table AZ).

Table 105. Comparison of silicate mineral dissolution model statistics (values reported in Tables 100-104) (excludes R39-44).

Period	Model	Plagioclase (mol m^{-2}s^{-1})				Augite (mol m^{-2}s^{-1})				Hypersthene (mol m^{-2}s^{-1})				Olivine (mol m^{-2}s^{-1})				Biotite (mol m^{-2}s^{-1})			
		Ave	S.D.	Max	Min[1]	Ave	S.D.	Max	Min[1]	Ave	S.D.	Max	Min[1]	Ave	S.D.	Max	Min[1]	Ave	S.D.	Max	Min[1]
A	1	6.6E-12	3.7E-12	4.1E-11	5.4E-13					5.1E-12	3.0E-12	4.0E-11	1.8E-13	2.2E-11	1.3E-11	2.0E-10	5.0E-13	9.7E-12	5.6E-12	6.2E-11	5.0E-13
	2	3.3E-12	2.7E-12	2.3E-11	0.0E+00	9.7E-12	5.7E-12	4.3E-11	5.8E-13	7.1E-13	1.4E-12	2.4E-11	0.0E+00	3.6E-12	6.2E-12	1.2E-10	0.0E+00	1.4E-12	2.6E-12	4.2E-11	0.0E+00
	3	N/A	N/A	N/A	N/A	N/A`	N/A`	N/A	N/A	N/A	N/A	N/A	N/A	N/A	N/A	N/A	N/A	N/A	N/A	N/A	N/A
	4									N/A	N/A	N/A	N/A	N/A	N/A	N/A	N/A	N/A	N/A	N/A	N/A
	max /min	2.0	1.4	1.8	N/A	1.0	1.0	1.0	1.0	7.1	2.1	1.7	N/A	6.3	2.1	1.7	N/A	7.0	2.1	1.5	N/A
B	1	1.6E-12	7.0E-13	9.3E-12	7.3E-14					2.8E-12	9.2E-13	1.4E-11	8.6E-14	1.2E-11	3.5E-12	5.4E-11	3.3E-13	5.0E-12	1.7E-12	2.9E-11	2.2E-13
	2	3.0E-13	3.2E-13	6.1E-12	0.0E+00	3.6E-12	1.7E-12	2.0E-11	1.8E-13	1.2E-12	7.5E-13	8.3E-12	0.0E+00	5.7E-12	3.2E-12	2.9E-11	0.0E+00	2.2E-12	1.3E-12	1.4E-11	0.0E+00
	3	2.7E-13	1.2E-13	8.1E-13	1.1E-13	1.7E-12	1.3E-12	1.1E-11	0.0E+00	3.6E-13	5.2E-13	5.2E-12	0.0E+00	1.3E-12	2.0E-12	1.2E-11	0.0E+00	3.6E-13	6.7E-13	5.2E-12	0.0E+00
	4									8.4E-15	4.8E-14	7.3E-13	0.0E+00	3.1E-14	1.8E-13	1.7E-12	0.0E+00	4.6E-12	4.0E-12	1.7E-11	2.0E-13
	max /min	6.1	5.6	11.4	N/A	2.2	1.2	1.8	N/A	328.5	19.1	19.2	N/A	395.1	19.5	32.7	N/A	13.7	6.0	5.5	N/A
C	1					3.8E-12	3.3E-12	4.8E-11	0.0E+00	4.6E-12	2.2E-12	3.1E-11	0.0E+00	1.8E-11	7.6E-12	6.8E-11	0.0E+00	6.5E-12	3.2E-12	3.3E-11	0.0E+00
	2	3.6E-13	3.2E-13	4.1E-12	0.0E+00	7.4E-12	3.4E-12	5.9E-11	2.4E-13	3.1E-12	2.1E-12	2.7E-11	0.0E+00	1.1E-11	7.1E-12	6.0E-11	0.0E+00	3.7E-12	2.9E-12	3.1E-11	0.0E+00
	3	9.9E-13	3.5E-13	2.9E-12	4.3E-13	4.5E-12	2.4E-12	2.4E-11	0.0E+00	4.3E-12	2.1E-12	2.5E-11	0.0E+00	1.8E-11	6.5E-12	5.4E-11	2.0E-12	4.5E-12	1.9E-12	2.2E-11	0.0E+00
	4									2.8E-12	1.6E-12	2.5E-11	0.0E+00	8.5E-12	4.5E-12	5.4E-11	0.0E+00	5.1E-12	2.4E-12	2.4E-11	3.2E-13
	max /min	2.7	1.1	1.4	N/A	1.9	1.4	2.5	N/A	1.6	1.4	1.2	N/A	2.1	1.7	1.2	N/A	1.7	1.7	1.5	N/A
D	1	1.5E-12	3.7E-13	4.6E-12	3.6E-13					1.3E-12	6.1E-13	7.0E-12	8.8E-14	5.9E-12	2.4E-12	3.2E-11	1.8E-13	2.2E-12	1.1E-12	1.2E-11	2.3E-13
	2	4.1E-13	2.6E-13	2.7E-12	0.0E+00	2.7E-12	1.1E-12	1.4E-11	2.0E-13	1.5E-13	2.3E-13	3.2E-12	0.0E+00	8.5E-13	9.4E-13	9.0E-12	0.0E+00	2.9E-13	3.7E-13	4.2E-12	0.0E+00
	3	6.9E-13	2.3E-13	2.9E-12	1.8E-13	1.5E-12	5.3E-13	6.4E-12	0.0E+00	6.5E-13	4.4E-13	2.8E-12	0.0E+00	2.8E-12	1.9E-12	2.1E-11	0.0E+00	1.0E-12	1.1E-12	1.4E-11	0.0E+00
	4									2.5E-13	2.1E-13	2.8E-12	0.0E+00	2.7E-13	6.4E-13	6.6E-12	0.0E+00	4.9E-12	4.0E-12	4.1E-11	2.2E-13
	max /min	3.5	1.6	1.7	N/A	1.8	2.0	2.1	N/A	8.3	2.9	2.5	N/A	21.6	3.7	4.9	N/A	17.0	11.0	9.8	N/A

[1] No range in minimum values reported due to zero values calculated

Note: Plagioclase dissolution calculations in Model 1, Period C are the same as Period B.

Note: Plagioclase and augite dissolution calculations in Model 4 are the same as Model 3.

Table 106. Total number of calculated mineral dissolution rates for each model during the specified rate period and the total number of cases where the models calculated an absence of dissolution (zero value). Associated percentage is the comparison of zero values cases to total number of cases (excludes R39-44).

Sorted by model, than period

Model	Period	Plagioclase			Augite			Hypersthene			Olivine			Biotite		
		Total n	zero	%	Total n	zero	%	Total n	zero	%	Total n	zero	%	Total n	zero	%
1	A	201	0	0%				195	0	0%	158	0	0%	162	0	0%
	B	920	0	0%				911	0	0%	746	0	0%	797	0	0%
	C				462	85	18%	460	22	5%	399	13	3%	360	21	6%
	D	437	0	0%				437	0	0%	428	0	0%	368	0	0%
2	A	181	42	23%	201	0	0%	181	139	77%	147	108	73%	149	111	74%
	B	902	447	50%	920	0	0%	902	455	50%	738	300	41%	788	449	57%
	C	460	342	74%	462	0	0%	460	118	26%	399	57	14%	360	113	31%
	D	436	75	17%	437	0	0%	436	361	83%	427	352	82%	368	307	83%
3	A	0	0	N/A	0	0	N/A	0	0	N/A	0	0	N/A	0	0	N/A
	B	86	0	0%	86	1	1%	85	30	35%	66	13	20%	85	30	35%
	C	30	0	0%	30	1	3%	30	8	27%	21	0	0%	24	8	33%
	D	117	0	0%	117	6	5%	117	58	50%	114	55	48%	100	49	49%
4	A	0	0	N/A	0	0	N/A	0	0	N/A	0	0	N/A	0	0	N/A
	B	86	0	0%	86	1	1%	82	80	98%	65	63	97%	83	0	0%
	C	30	0	0%	30	1	3%	30	18	60%	21	9	43%	24	0	0%
	D	117	0	0%	117	6	5%	109	94	86%	107	92	86%	92	0	0%

Sorted by period, than model

Model	Period	Plagioclase			Augite			Hypersthene			Olivine			Biotite		
		Total n	zero	%	Total n	zero	%	Total n	zero	%	Total n	zero	%	Total n	zero	%
1	A	201	0	0%				195	0	0%	158	0	0%	162	0	0%
2		181	42	23%	201	0	0%	181	139	77%	147	108	73%	149	111	74%
3		0	0	N/A	0	0	N/A	0	0	N/A	0	0	N/A	0	0	N/A
4		0	0	N/A	0	0	N/A	0	0	N/A	0	0	N/A	0	0	N/A
1	B	920	0	0%				911	0	0%	746	0	0%	797	0	0%
2		902	447	50%	920	0	0%	902	455	50%	738	300	41%	788	449	57%
3		86	0	0%	86	1	1%	85	30	35%	66	13	20%	85	30	35%
4		86	0	0%	86	1	1%	82	80	98%	65	63	97%	83	0	0%
1	C				462	85	18%	460	22	5%	399	13	3%	360	21	6%
2		460	342	74%	462	0	0%	460	118	26%	399	57	14%	360	113	31%
3		30	0	0%	30	1	3%	30	8	27%	21	0	0%	24	8	33%
4		30	0	0%	30	1	3%	30	18	60%	21	9	43%	24	0	0%
1	D	437	0	0%				437	0	0%	428	0	0%	368	0	0%
2		436	75	17%	437	0	0%	436	361	83%	427	352	82%	368	307	83%
3		117	0	0%	117	6	5%	117	58	50%	114	55	48%	100	49	49%
4		117	0	0%	117	6	5%	109	94	86%	107	92	86%	92	0	0%

Table 107. Calculated pyrrhotite oxidation rates for all Dunka blast hole samples (excludes R39-44).

R#	%S	Period A				Period B				Period C				Period D			
		Ave	S.D.	Max	Min	Ave	S.D.	Max	Min	Ave	S.D.	Max	Min	Ave	S.D.	Max	Min
Group I																	
1	0.18	N/A	N/A	N/A	N/A	N/A	N/A	N/A	N/A								
3	0.22	1.25E-08	6.55E-09	3.47E-08	3.55E-09	3.10E-09	2.55E-09	1.12E-08	2.25E-10								
Average		1.25E-08	6.55E-09	3.47E-08	3.55E-09	3.10E-09	2.55E-09	1.12E-08	2.25E-10								
Group II																	
5	0.4	3.78E-10	1.47E-10	8.34E-10	1.50E-10	1.12E-10	4.93E-11	3.51E-10	3.39E-11	5.62E-10	3.34E-10	1.23E-09	1.99E-10	1.30E-10	3.63E-11	2.09E-10	8.92E-11
7	0.41	1.62E-10	1.35E-10	5.12E-10	2.12E-11	1.29E-10	7.49E-11	3.03E-10	4.06E-11	5.08E-10	9.97E-11	6.83E-10	3.41E-10	1.52E-10	1.36E-10	5.90E-10	3.17E-11
9	0.51	2.28E-10	1.42E-10	5.81E-10	3.89E-11	1.04E-10	4.63E-11	1.86E-10	3.76E-11	6.37E-10	1.15E-10	9.56E-10	4.79E-10	2.04E-10	1.51E-10	5.65E-10	4.19E-11
11	0.54	2.37E-10	9.74E-11	4.97E-10	8.59E-11	1.61E-10	8.10E-11	4.02E-10	4.28E-11	2.23E-10	7.50E-11	4.25E-10	1.10E-10				
13	0.57	2.65E-10	7.20E-11	4.00E-10	1.35E-10	1.74E-10	9.00E-11	5.10E-10	2.87E-11	4.46E-10	1.10E-10	7.15E-10	3.17E-10	2.96E-10	4.97E-11	3.66E-10	2.17E-10
15	0.58	2.32E-10	1.89E-10	9.57E-10	2.86E-11	2.48E-10	9.54E-11	5.61E-10	1.27E-10	4.18E-10	8.96E-11	6.65E-10	3.01E-10	1.43E-10	9.46E-11	3.60E-10	3.15E-11
Average		2.51E-10	1.30E-10	9.57E-10	2.12E-11	1.55E-10	7.28E-11	5.61E-10	2.87E-11	4.66E-10	1.37E-10	1.23E-09	1.10E-10	1.85E-10	9.34E-11	5.90E-10	3.15E-11
Group III																	
17	0.71	1.36E-10	5.69E-11	2.54E-10	2.06E-11	9.32E-11	3.64E-11	1.94E-10	2.04E-11	5.01E-10	4.33E-10	1.67E-09	9.74E-11	8.17E-11	4.52E-11	2.19E-10	2.84E-11
35	1.12	2.61E-10		8.73E-10	9.22E-11	2.57E-10		3.22E-10	1.12E-10	4.86E-10	2.64E-10	9.05E-10	1.39E-10	1.75E-10	1.46E-11	1.86E-10	1.59E-10
29	1.16	1.52E-10		4.03E-10	7.33E-11	1.12E-10		2.07E-10	5.12E-11	4.23E-10	2.80E-10	1.07E-09	6.57E-11	4.00E-11	2.10E-11	1.00E-10	1.70E-11
37	1.4	1.40E-10		2.53E-10	8.21E-11	1.09E-10		2.74E-10	5.23E-11	5.88E-10	3.02E-10	1.11E-09	1.91E-10				
33	1.44	1.38E-10	1.36E-10	3.92E-10	6.57E-11	1.74E-10	5.57E-11	3.58E-10	8.69E-11	3.91E-10	2.64E-10	9.52E-10	5.15E-11	4.38E-11	1.46E-11	7.51E-11	2.52E-11
19	1.63	1.33E-10	8.07E-11	3.36E-10	4.51E-11	9.33E-11	3.84E-11	1.43E-10	5.32E-11	3.45E-10	2.80E-10	8.14E-10	8.77E-11	4.23E-11	2.10E-11	1.15E-10	9.54E-12
31	1.64	3.34E-10	5.65E-11	9.80E-10	1.65E-10	1.69E-10	4.02E-11	2.46E-10	9.86E-11	3.60E-10	3.02E-10	7.21E-10	1.44E-10	1.61E-10	1.61E-11	1.85E-10	1.43E-10
Average		1.85E-10	8.25E-11	9.80E-10	2.06E-11	1.44E-10	4.27E-11	3.58E-10	2.04E-11	4.42E-10	3.04E-10	1.67E-09	5.15E-11	9.07E-11	2.21E-11	2.19E-10	9.54E-12
Summary[2]		2.15E-10	1.11E-10	9.80E-10	2.06E-11	1.49E-10	6.08E-11	5.61E-10	2.04E-11	4.53E-10	2.27E-10	1.67E-09	5.15E-11	1.34E-10	5.45E-11	5.90E-10	9.54E-12

[1] Reactor 1 calculated to have pyrrhotite content less than zero

[2] Overall calculations does not include group I due to the low amount of pyrrhotite calculated for reactor 3

Table 108. Calculated sulfide oxidation rates (all sulfide minerals combined) for all Dunka blast hole samples (excludes R39-44).

R#	%S	Period A				Period B				Period C				Period D			
		Ave	S.D.	Max	Min	Ave	S.D.	Max	Min	Ave	S.D.	Max	Min	Ave	S.D.	Max	Min
Group I																	
1	0.18	4.81E-10	2.82E-10	1.21E-09	1.19E-10	9.48E-11	9.23E-11	4.20E-10	7.70E-12								
3	0.22	4.17E-10	2.18E-10	1.16E-09	1.18E-10	1.03E-10	8.51E-11	3.74E-10	7.51E-12								
Average		4.49E-10	2.50E-10	1.21E-09	1.18E-10	9.91E-11	8.87E-11	4.20E-10	7.51E-12								
Group II																	
5	0.4	3.41E-10	1.32E-10	7.52E-10	1.35E-10	1.01E-10	4.44E-11	3.17E-10	3.05E-11	5.07E-10	3.01E-10	1.11E-09	1.79E-10	1.17E-10	3.27E-11	1.89E-10	8.04E-11
7	0.41	1.32E-10	1.10E-10	4.18E-10	1.73E-11	1.06E-10	6.12E-11	2.47E-10	3.32E-11	4.15E-10	8.15E-11	5.58E-10	2.79E-10	1.24E-10	1.11E-10	4.82E-10	2.59E-11
9	0.51	1.74E-10	1.08E-10	4.42E-10	2.96E-11	7.89E-11	3.53E-11	1.41E-10	2.86E-11	4.85E-10	8.78E-11	7.27E-10	3.64E-10	1.55E-10	1.15E-10	4.30E-10	3.19E-11
11	0.54	2.29E-10	9.42E-11	4.81E-10	8.31E-11	1.56E-10	7.83E-11	3.89E-10	4.13E-11	2.16E-10	7.26E-11	4.11E-10	1.06E-10				
13	0.57	2.18E-10	5.93E-11	3.29E-10	1.11E-10	1.43E-10	7.41E-11	4.19E-10	2.36E-11	3.67E-10	9.06E-11	5.88E-10	2.61E-10	2.43E-10	4.09E-11	3.01E-10	1.79E-10
15	0.58	1.92E-10	1.56E-10	7.90E-10	2.36E-11	2.05E-10	7.87E-11	4.63E-10	1.05E-10	3.45E-10	7.39E-11	5.49E-10	2.49E-10	1.18E-10	7.81E-11	2.97E-10	2.60E-11
Average		2.14E-10	1.10E-10	7.90E-10	1.73E-11	1.32E-10	6.20E-11	4.63E-10	2.36E-11	3.89E-10	1.18E-10	1.11E-09	1.06E-10	1.52E-10	7.55E-11	4.82E-10	2.59E-11
Group III																	
17	0.71	1.19E-10	5.00E-11	2.23E-10	1.81E-11	8.19E-11	3.20E-11	1.71E-10	1.79E-11	4.41E-10	3.81E-10	1.47E-09	8.56E-11	7.18E-11	3.97E-11	1.93E-10	2.49E-11
35	1.12	2.48E-10	1.29E-10	8.29E-10	8.76E-11	2.45E-10	5.30E-11	3.06E-10	1.07E-10	4.62E-10	2.51E-10	8.60E-10	1.32E-10	1.67E-10	1.39E-11	1.77E-10	1.51E-10
29	1.16	1.42E-10	7.56E-11	3.77E-10	6.86E-11	1.05E-10	3.59E-11	1.93E-10	4.79E-11	3.96E-10	2.63E-10	1.00E-09	6.16E-11	3.75E-11	1.96E-11	9.40E-11	1.59E-11
37	1.4	1.29E-10	5.22E-11	2.33E-10	7.58E-11	1.01E-10	3.71E-11	2.53E-10	4.83E-11	5.42E-10	2.79E-10	1.02E-09	1.76E-10				
33	1.44	1.30E-10	8.35E-11	3.70E-10	6.20E-11	1.64E-10	6.23E-11	3.38E-10	8.20E-11	3.69E-10	2.66E-10	8.98E-10	4.86E-11	4.13E-11	9.70E-12	7.08E-11	2.38E-11
19	1.63	1.26E-10	6.34E-11	3.19E-10	4.28E-11	8.86E-11	2.51E-11	1.35E-10	5.05E-11	3.27E-10	1.47E-10	7.73E-10	8.32E-11	4.01E-11	2.80E-11	1.10E-10	9.06E-12
31	1.64	3.02E-10	1.83E-10	8.86E-10	1.49E-10	1.52E-10	3.90E-11	2.22E-10	8.91E-11	3.26E-10	1.46E-10	6.51E-10	1.30E-10	1.45E-10	1.46E-11	1.67E-10	1.29E-10
Average		1.71E-10	9.09E-11	8.86E-10	1.81E-11	1.34E-10	4.06E-11	3.38E-10	1.79E-11	4.09E-10	2.48E-10	1.47E-09	4.86E-11	8.38E-11	2.09E-11	1.93E-10	9.06E-12
Summary		2.25E-10	1.20E-10	1.21E-09	1.73E-11	1.28E-10	5.56E-11	4.63E-10	7.51E-12	4.00E-10	1.88E-10	1.47E-09	4.86E-11	1.15E-10	4.57E-11	4.82E-10	9.06E-12

Table 109. Sulfur depletion statistics. The first method was based on initial %S minus S lost as determined by sulfate concentration in leachate. The cumulative S depletion for this sulfate-based method (%S depletion (sulfate)) is displayed next to the right-most column (%S Depletion (solids)), which determines S depletion as unleached sample %S minus leached sample %S. Leached solids ran for less time than full experimental period, so are likely to underestimate S loss (excludes R39-44).

Reactor	**%S**	**Start of experiment until pH<6**		**Major pH drop and/or major sulfate release starts**		**Minimum pH and/or max sulfate release**		**pH increase begins**		**End of experiment**		**%S Depletion (sulfate)**	**% S Depletion (solids)**	
		Week	**%S remaining**	**Week**	**%S remaining**	**Week**	**%S remaining**	**Week**	**%S remaining**	**Week**	**%S remaining**		**Week**	**% S depletion**
1	0.18	#								1252	45.3	54.7	328	41.1
3	0.22	#								1252	54.6	45.4	328	30.9
5	0.40	400	48.5	720	33.3	810	17.4	825	8.5	909	-3.7	103.7	328	12.8
7	0.41	80	94.0	265	83.9	395	65.9	480	48.5	724	38.8	61.2	328	47.8
9	0.51	70	93.0	250	81.8	355	59.8	404	48.6	724	28.2	71.8	328	54.3
11	0.54	57	90.9	215	71.0	290	59.3	385	42.7	441	37.0	63.0	441	72
13	0.57	75	89.4	257	75.2	340	59.4	390	51.1	441	44.8	55.2	441	66.3
15	0.58	55	91.9	140	84.3	280	60.3	335	49.9	724	26.1	73.9	328	62.2
17	0.71	50	96.7	275	83.4	350	67.3	375	50.4	724	32.1	67.9	328	55.4
35	1.12	*		205	66.2	270	42.6	290	32.3	360	21.3	78.7	360	84.6
29	1.16	35	95.5	140	88.7	280	60.2	315	43.5	643	28.3	71.7	643	6.9
37	1.40	35	96.5	192	85.8	282	66.2	345	34.9	360	30.8	69.2	360	79.1
33	1.44	10	97.6	220	76.9	280	57.2	330	34.2	643	16.0	84.0	247	54
19	1.63	20	96.9	120	90.7	290	59.5	355	38.8	724	24.3	75.7	289	71.9
31	1.64	*		220	72.3	275	60.0	290	55.2	360	46.2	53.8	360	75.1
Average			90.1		76.4		56.5		41.4		31.3	68.7		54.3
Std Dev			14.1		14.8		13.2		12.3		14.4	14.4		23.2

* Started at pH<6.0
# pH never <6.0 for sustained period

Figure 1. The Duluth Complex and associated intrusions in the area of the Dunka Mine and orientation of western footwall rock suites (Miller et al, 2001).

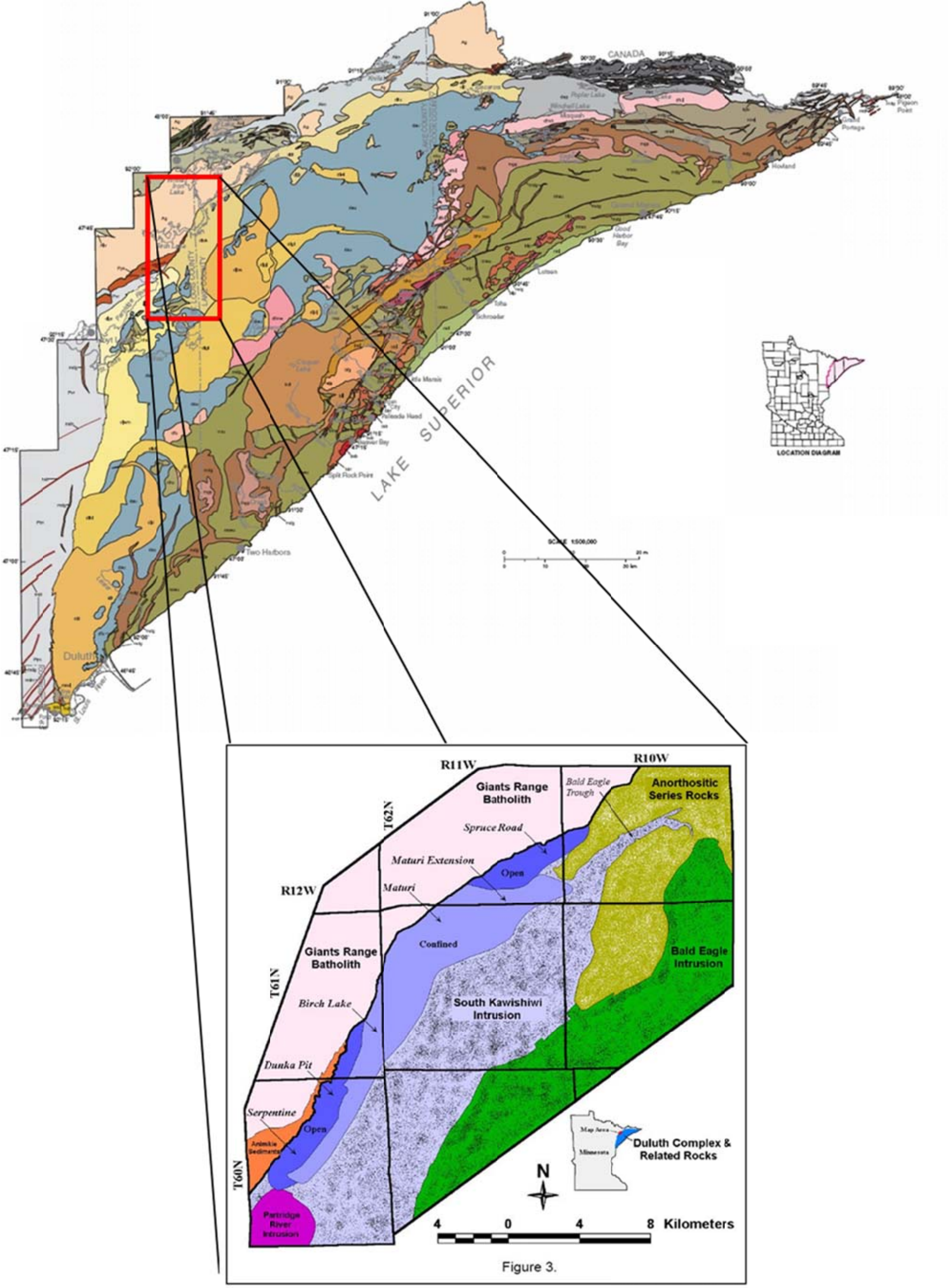

Figure 2. Cross Section from the northwest to the southeast across the Dunka Pit (Miller et al, 2005).

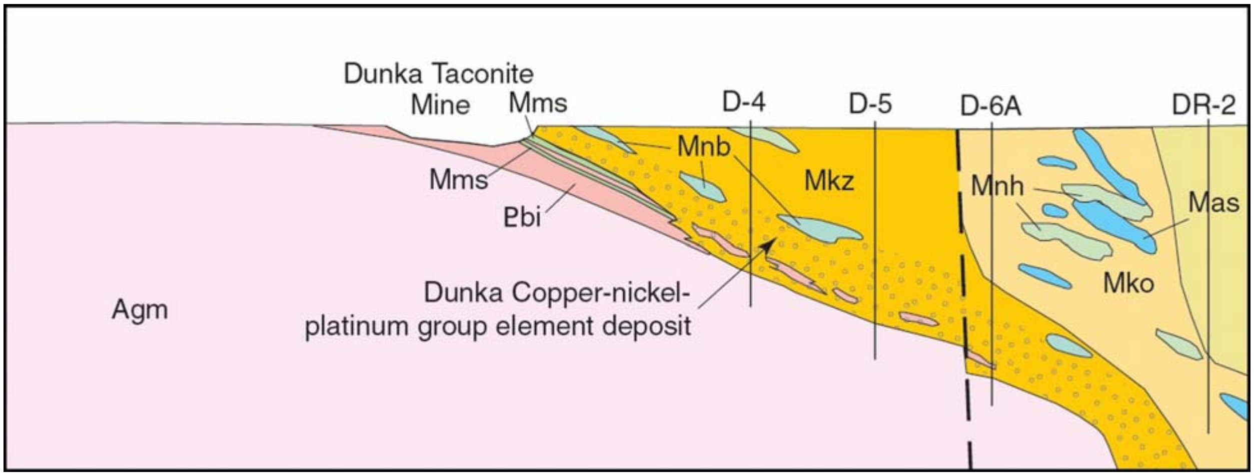

Relevant Geologic Map and Cross Section Symbols (After Miller et al, 2005):

Mesoproterozoic-- Duluth Complex, Layered Series--South Kawishiwi intrusion:

Mnb: Basaltic hornfels—Fine-grained, granoblastic to poikiloblastic basaltic hornfels; consists of variable amounts of plagioclase, augite, olivine, hypersthene, and inverted pigeonite.

Mkz: Contact zone—Varitextured olivine gabbro, augite troctolite, gabbronorite, norite, and footwall inclusions; commonly sulfide-bearing.

Mms: Mafic footwall sill—Mafic sills in the Paleoproterozoic footwall near the base of the Virginia Formation. Contains variable amounts of plagioclase, orthopyroxene, clinopyroxene, olivine, amphibole, and lesser amounts of biotite.

Paleoproterozoic--Animikie Group:

Pvf: Virginia Formation—A well bedded sequence of graywacke and slate, locally carbonaceous and sulfidic, that are strongly recrystallized and locally partially melted (metatexite and diatexite) by the Duluth Complex. Also occurs as hornfels inclusions in the contact zone of the South Kawishiwi intrusion.

Pbi: Biwabik Iron Formation—Well bedded, iron-bearing strata of alternating cherty intervals and slaty intervals.

Neoarchean--Giants Range batholith:

Agm: Quartz monzonite, granite, and monzodiorite—Pink to dark greenish-gray, hornblendebearing, coarse-grained and variably porphyritic, variably magnetic.

Figure 3. Map of the Duluth Complex basal contact and associated sulfide mineral deposits.

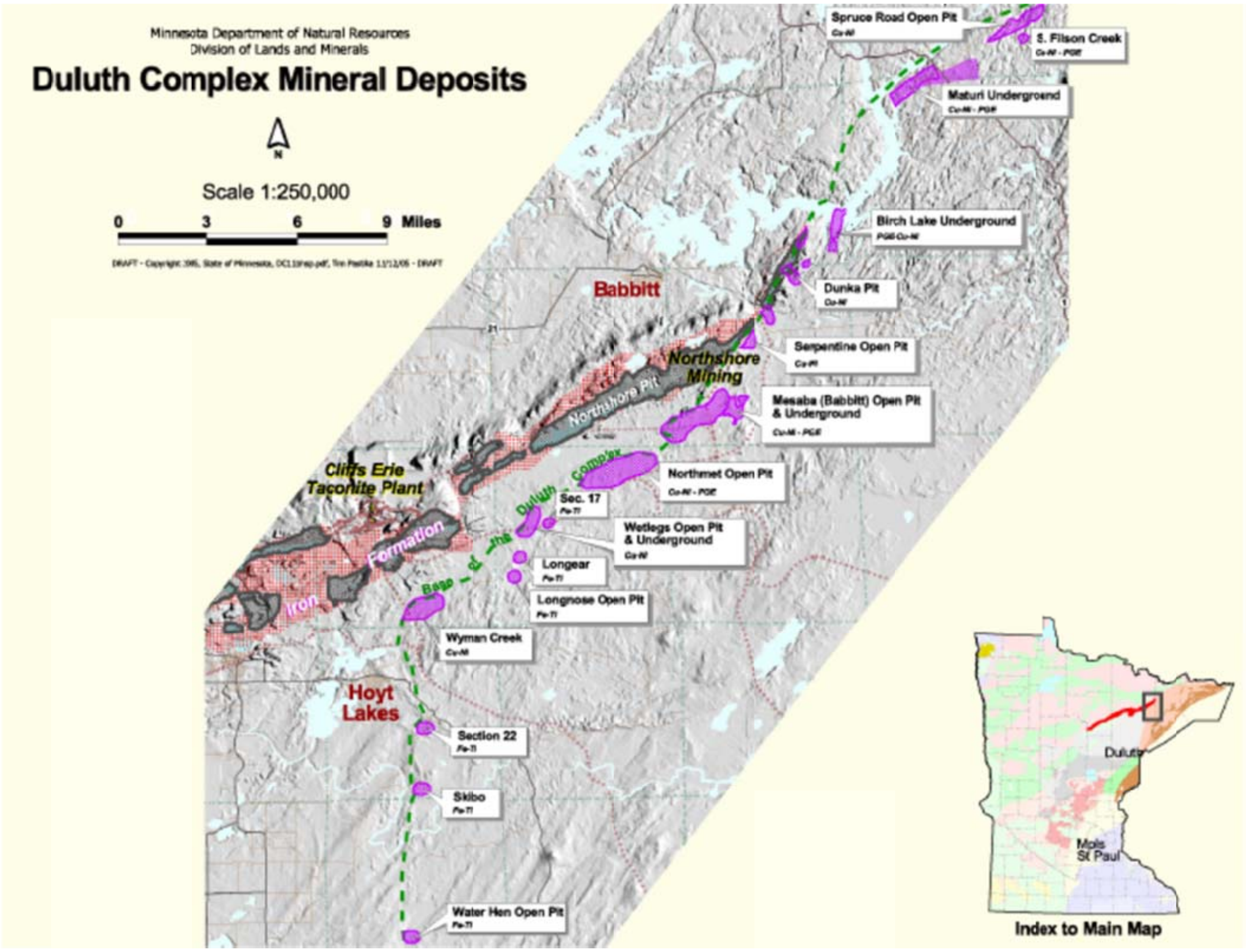

Figure 4. Experiment reactor diagram and picture

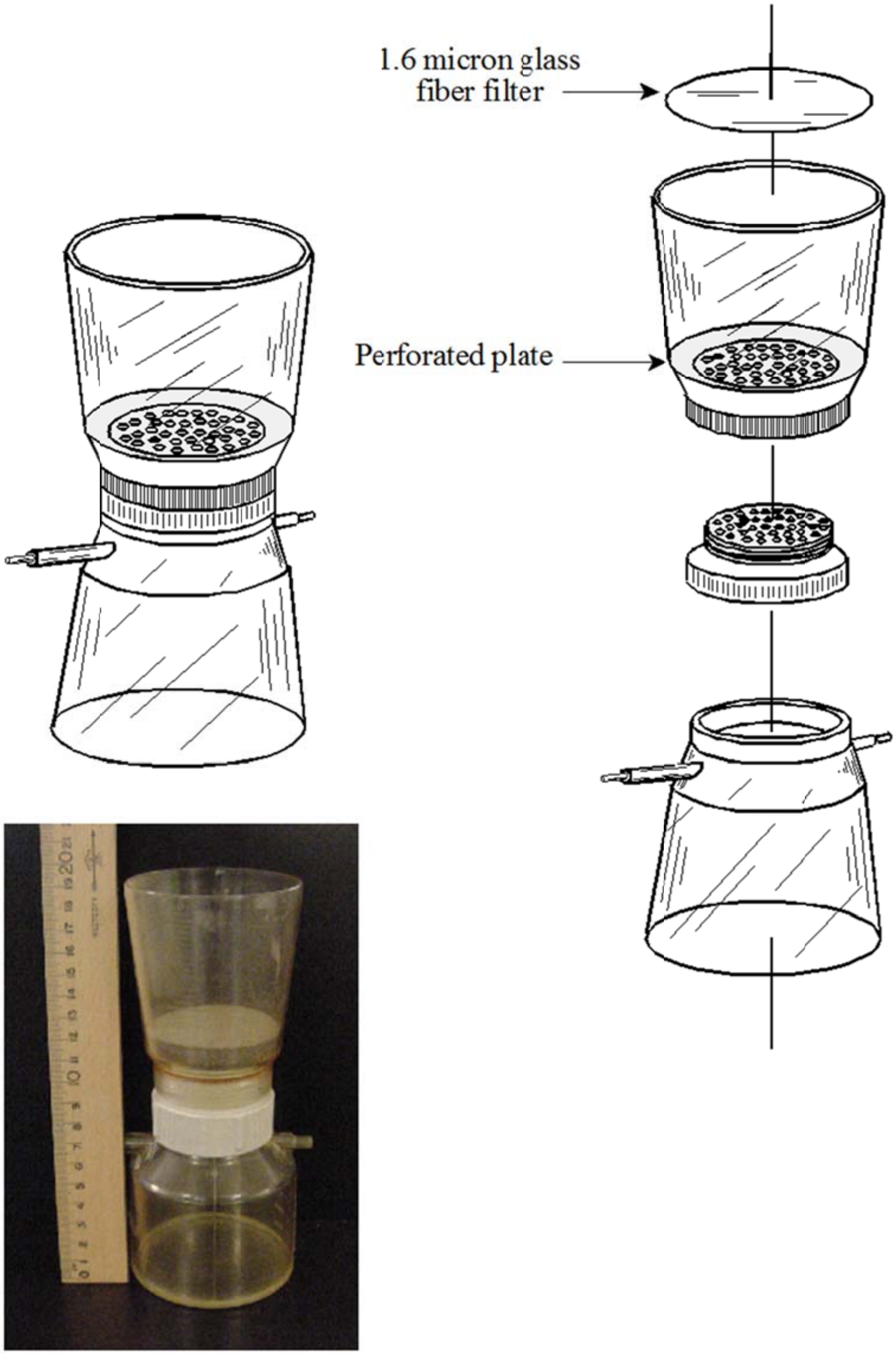

Figure 5. pH vs. time for each sample group with similar behavior. Weeks 0-5 were omitted to improve resolution.

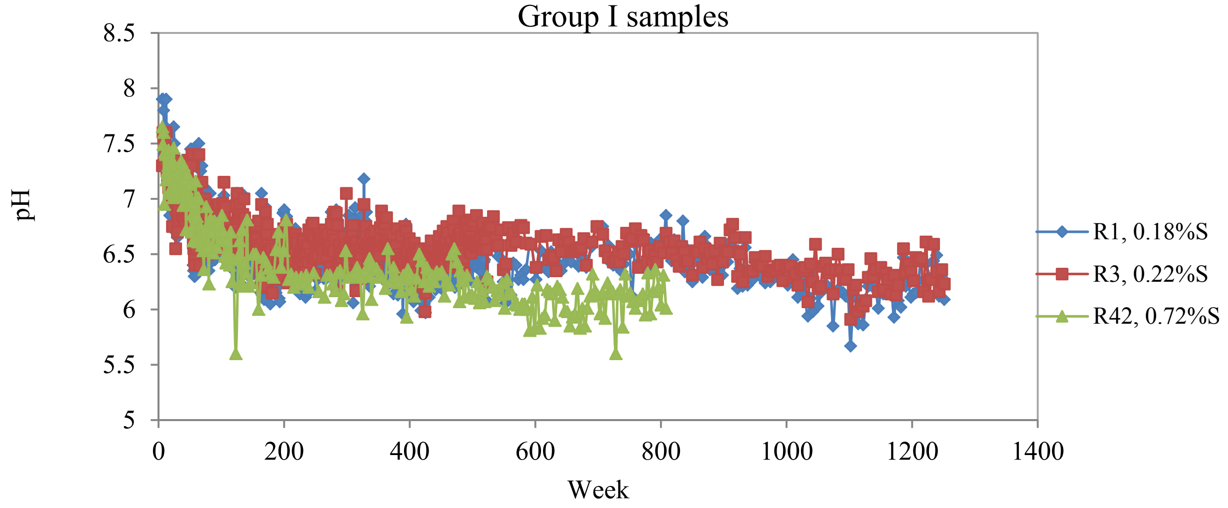
Group I samples

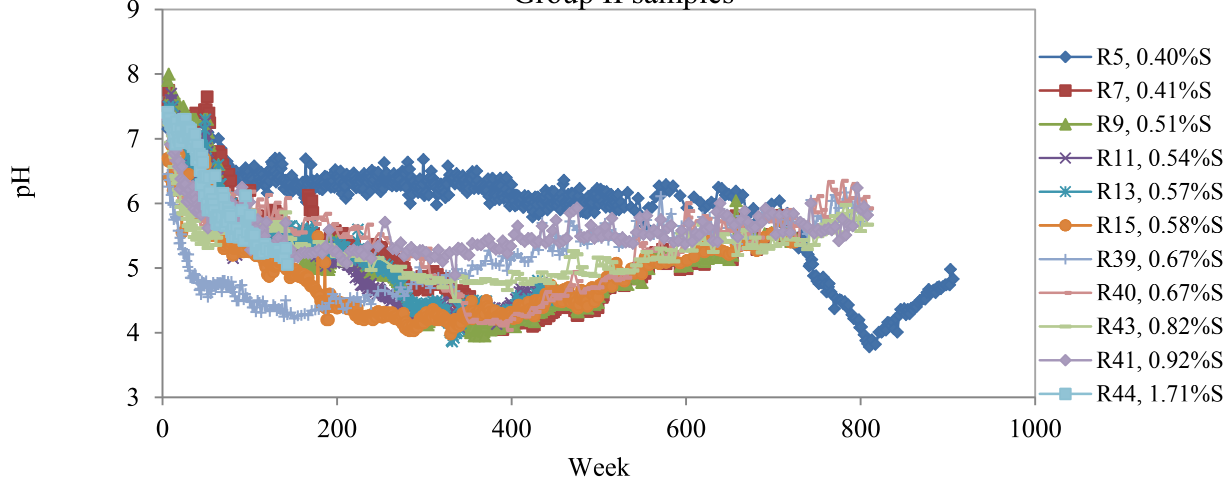
Group II samples

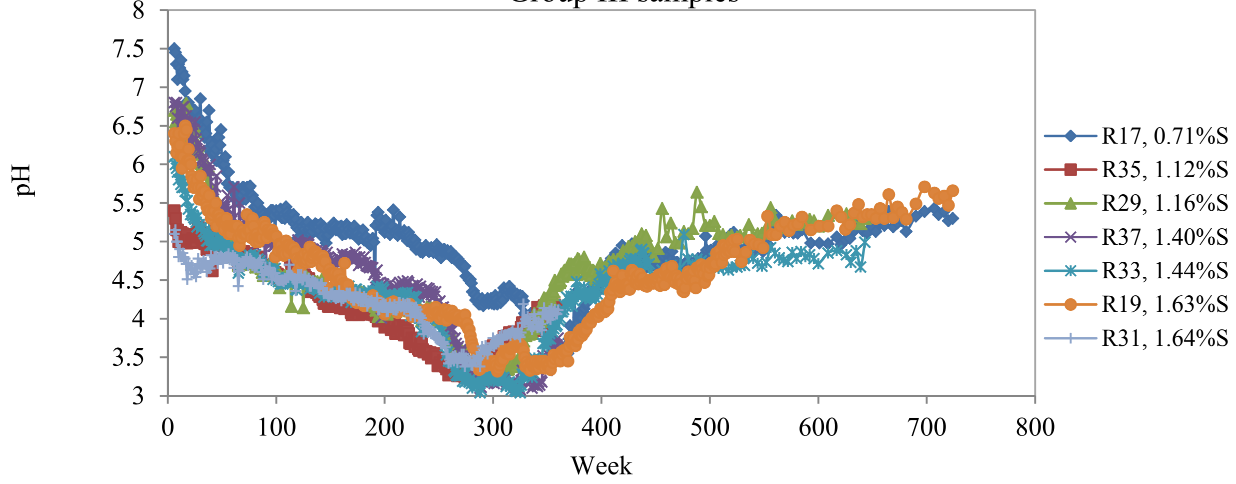
Group III samples

Figure 6. Sulfate release vs. time for each sample group with similar behavior. Weeks 0-5 were omitted to improve resolution.

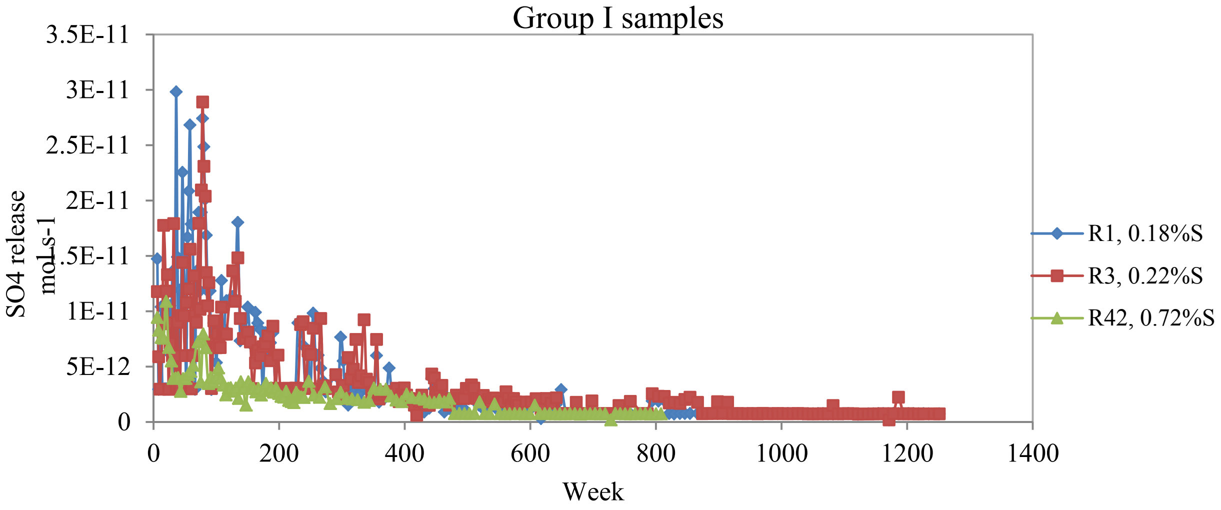

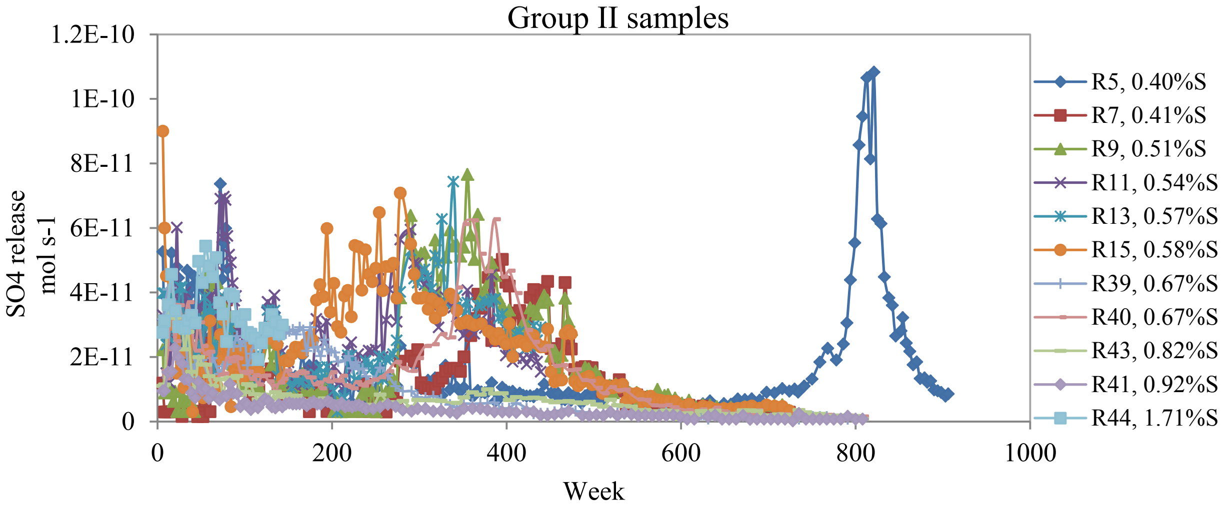

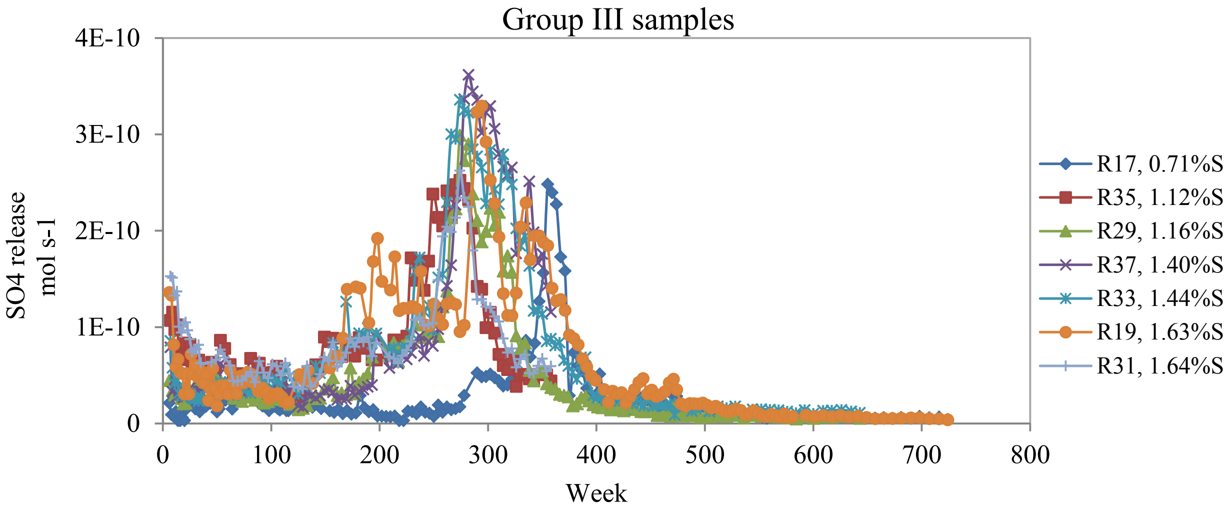

Figure 7. Sulfate release vs. time for Group II samples (0.40, 0.58, 0.67 (R40), 0.82, 0.92 %S). Weeks 0-5 were omitted to improve resolution.

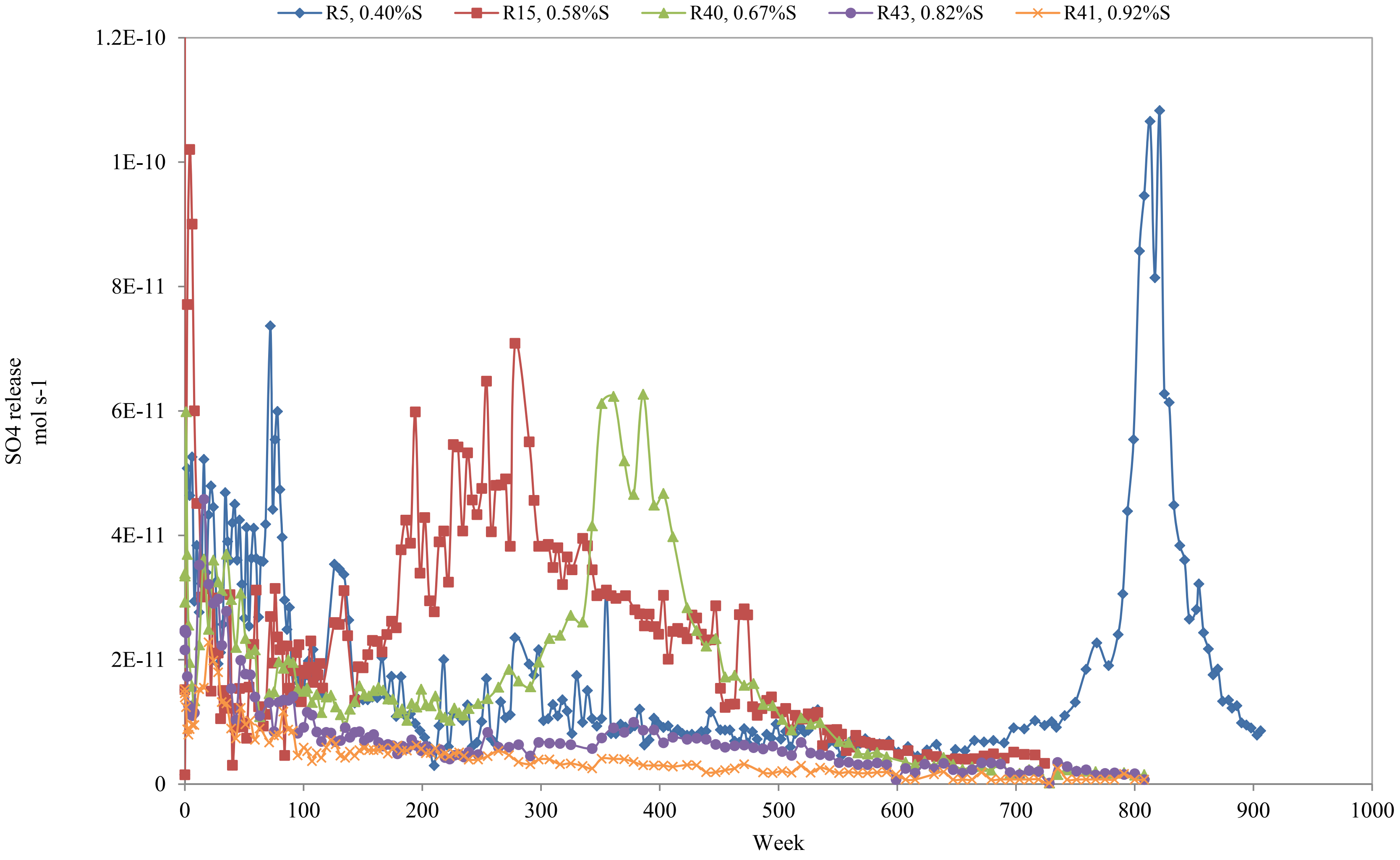

Figure 8. Calcium release vs. time for each sample group with similar behavior. Weeks 0-5 were omitted to improve resolution.

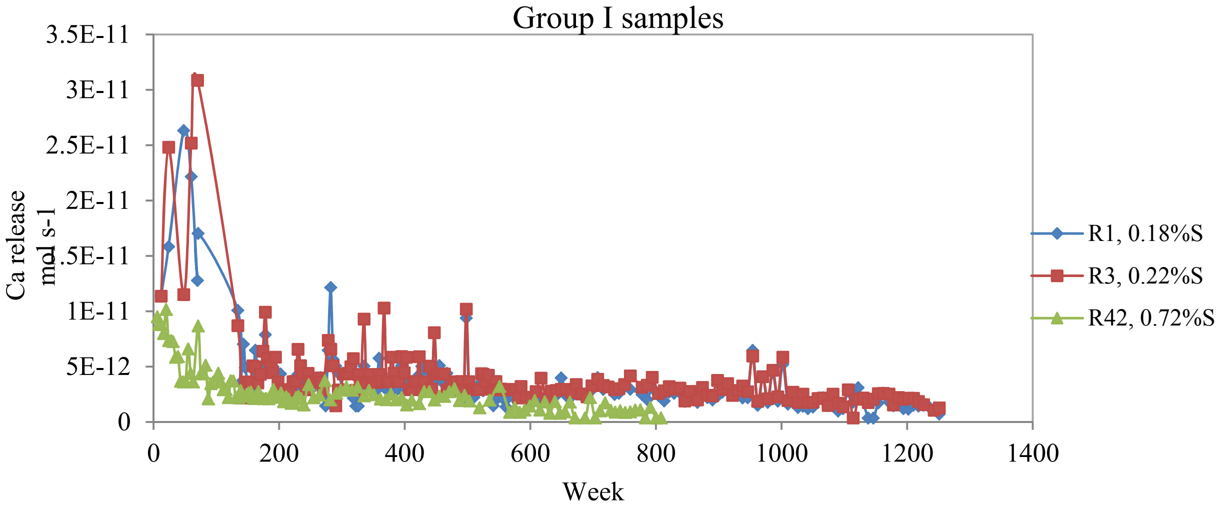

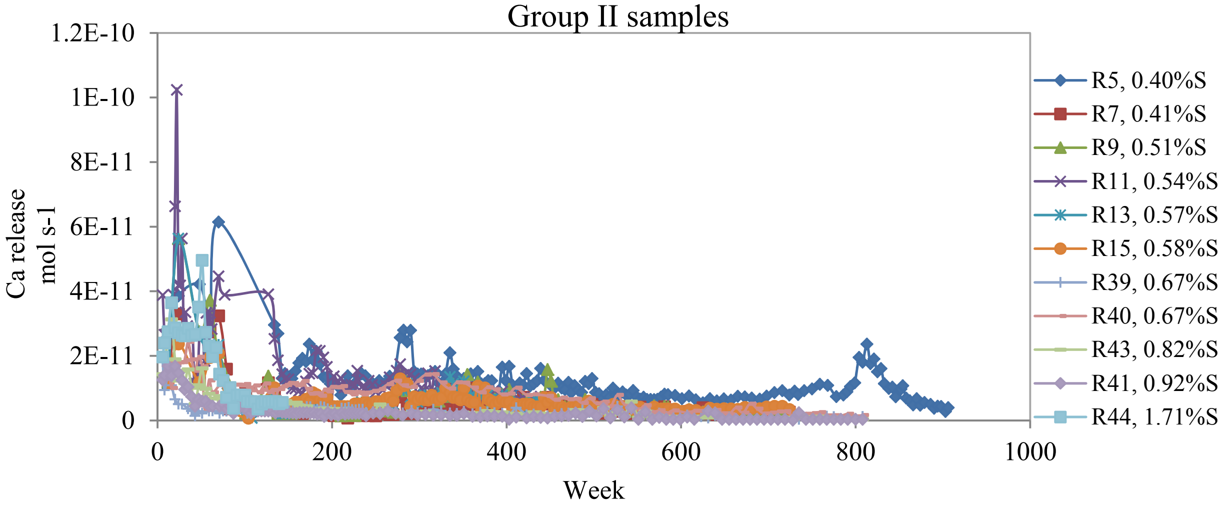

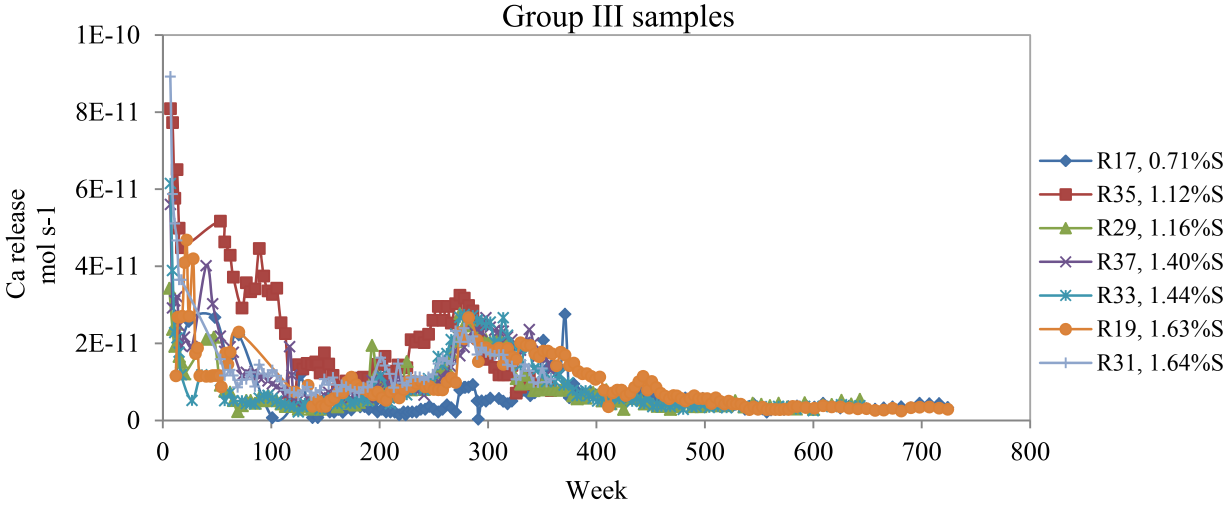

Figure 9. Magnesium release vs. time for each sample group with similar behavior. Weeks 0-5 were omitted to improve resolution.

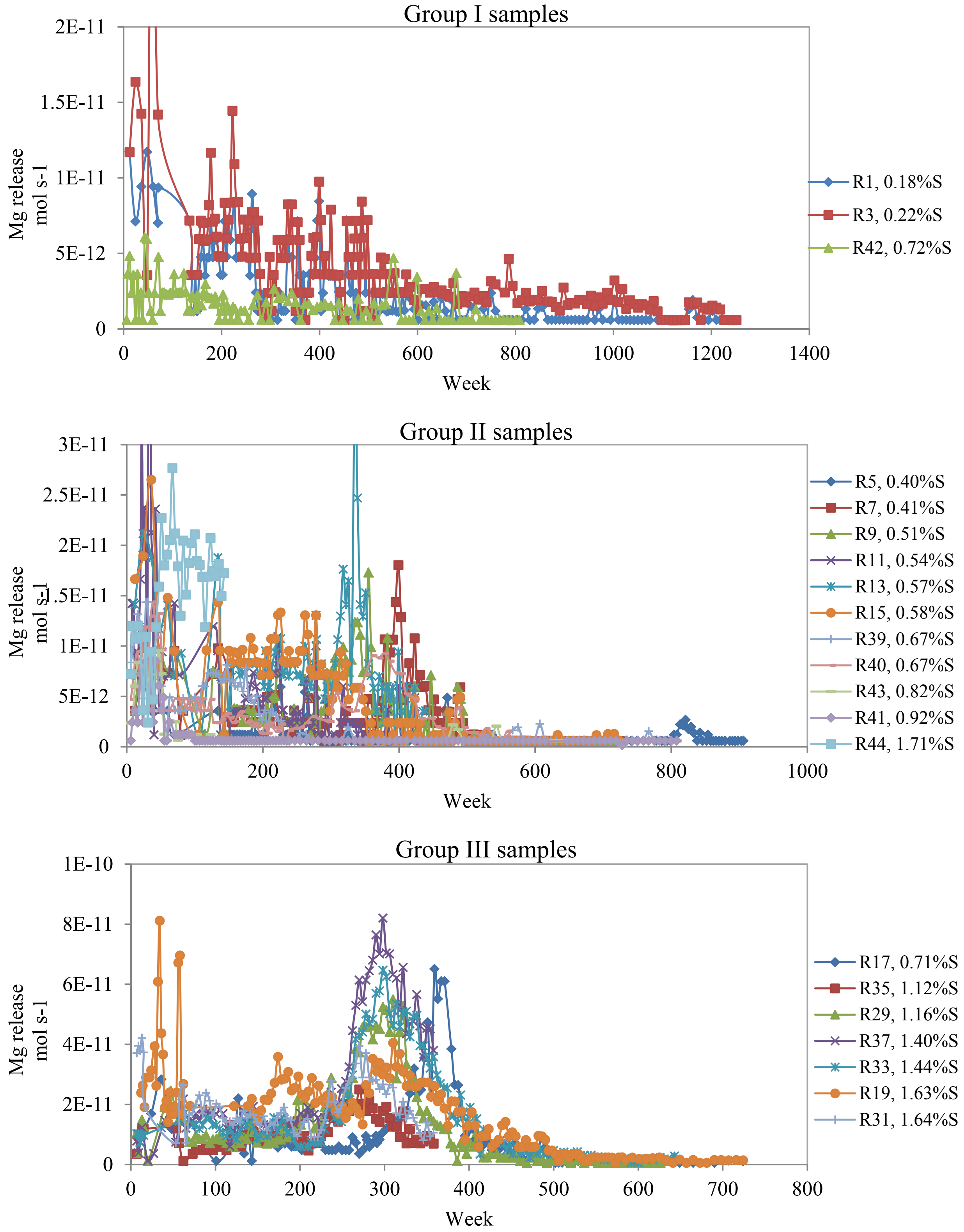

Figure 10. Sodium release vs. time for each sample group with similar behavior. Weeks 0-5 were omitted to improve resolution.

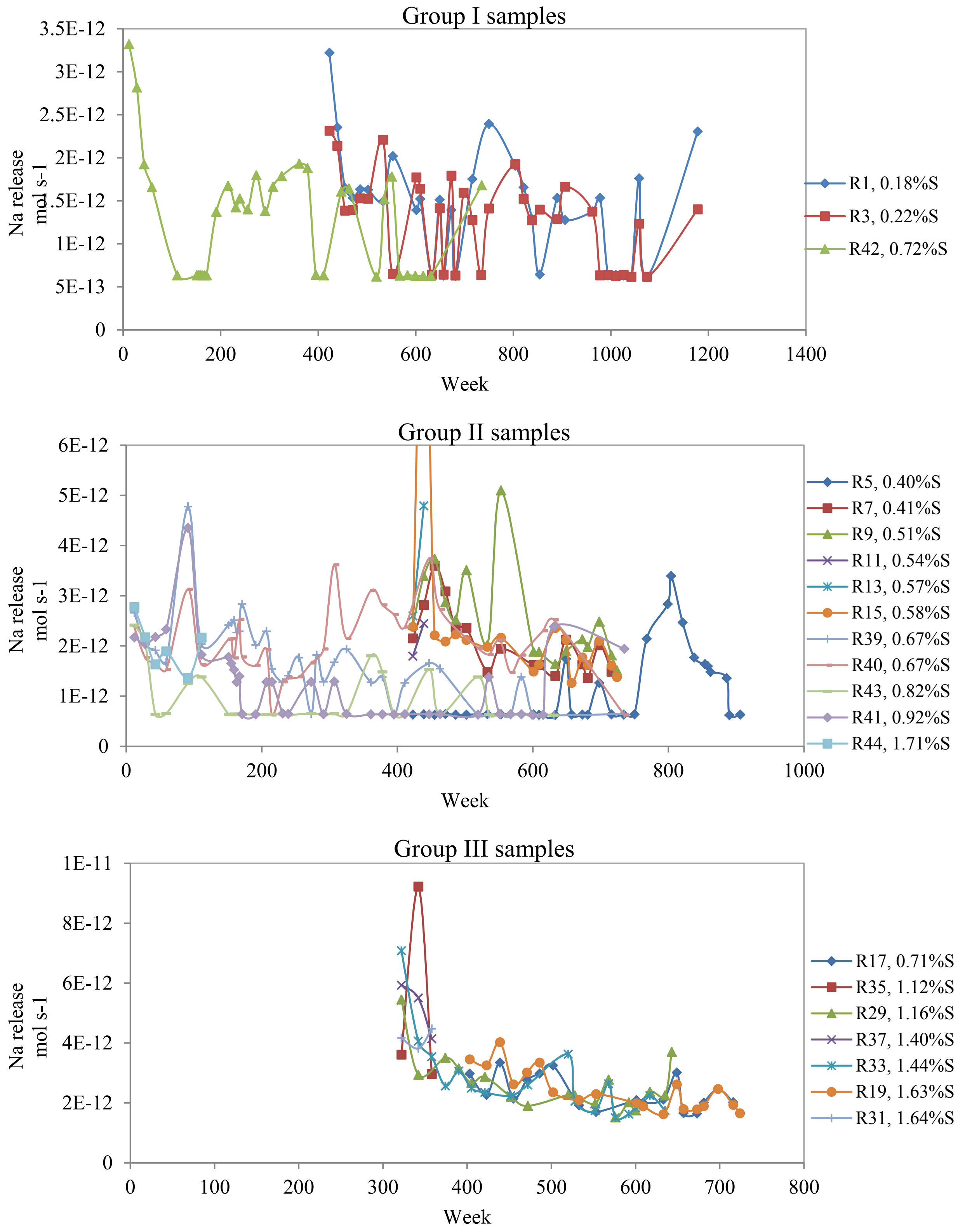

Figure 11. Potassium release vs. time for each sample group with similar behavior. Weeks 0-5 were omitted to improve resolution.

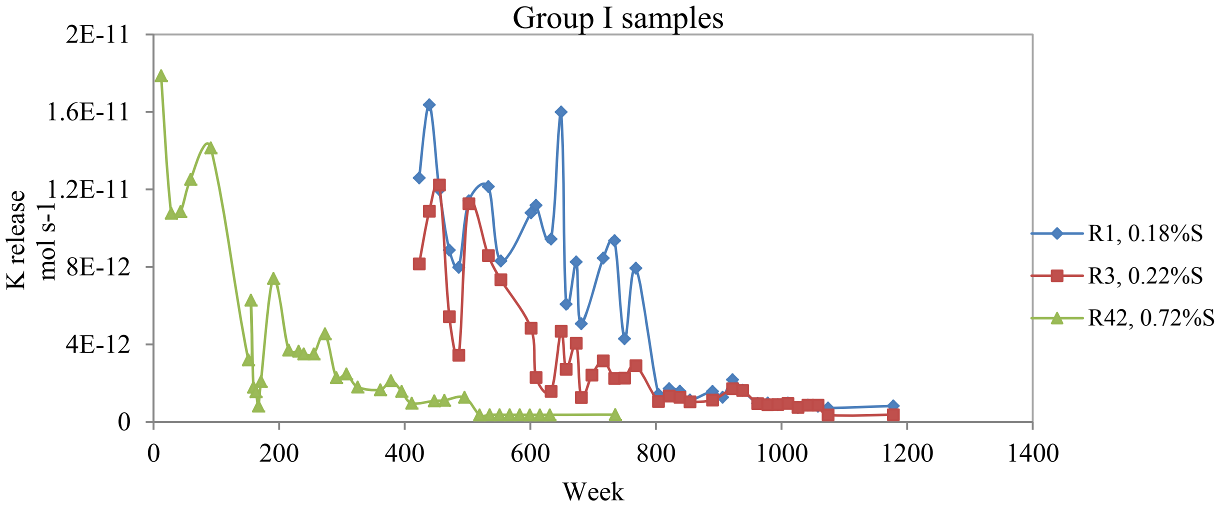

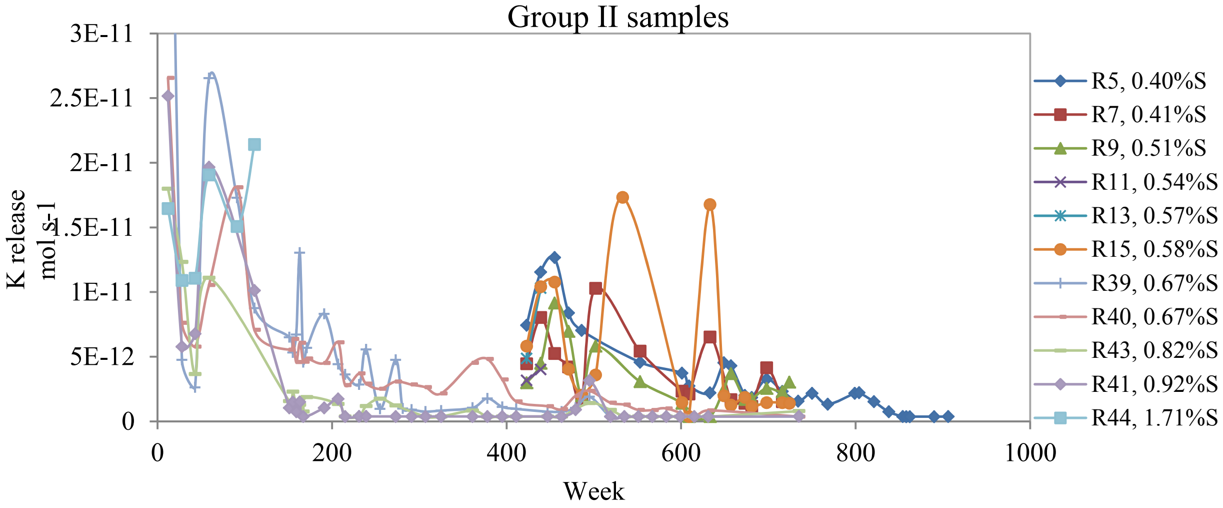

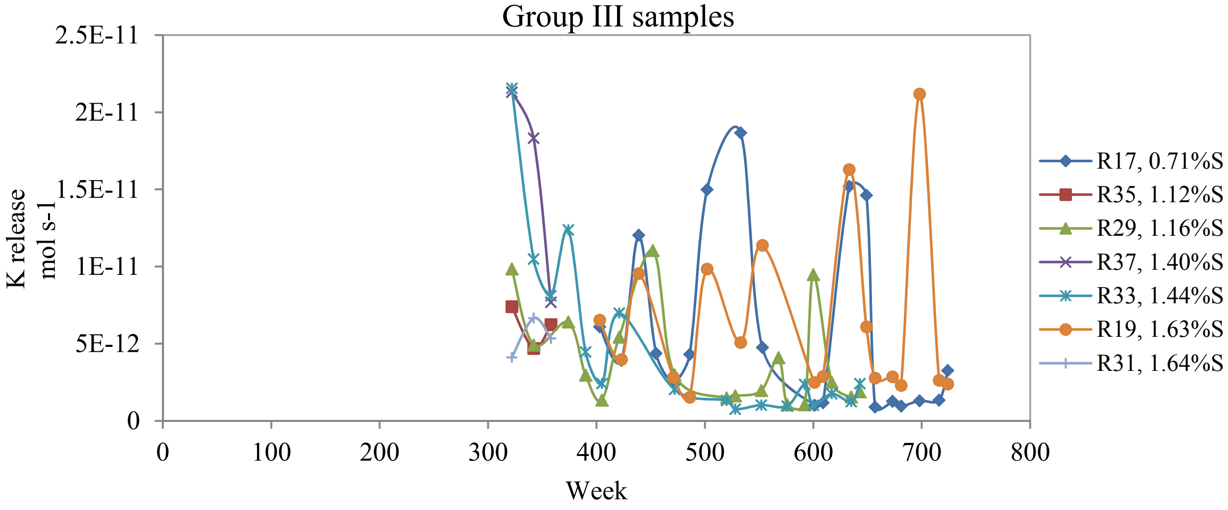

Figure 12. Cobalt release vs. time for each sample group with similar behavior. Weeks 0-5 were omitted to improve resolution.

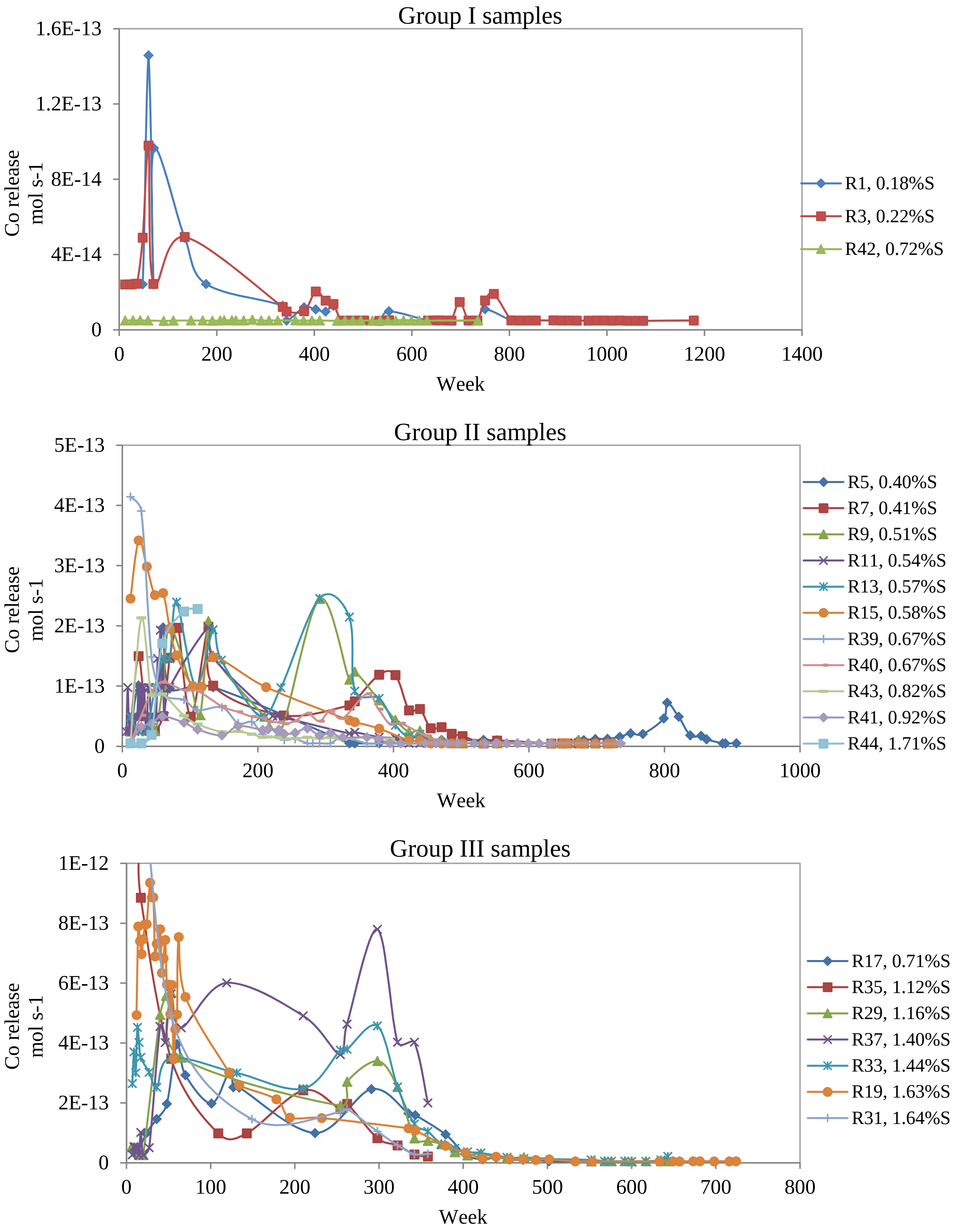

Figure 13. Copper release vs. time for each sample group with similar behavior. Weeks 0-5 were omitted to improve resolution.

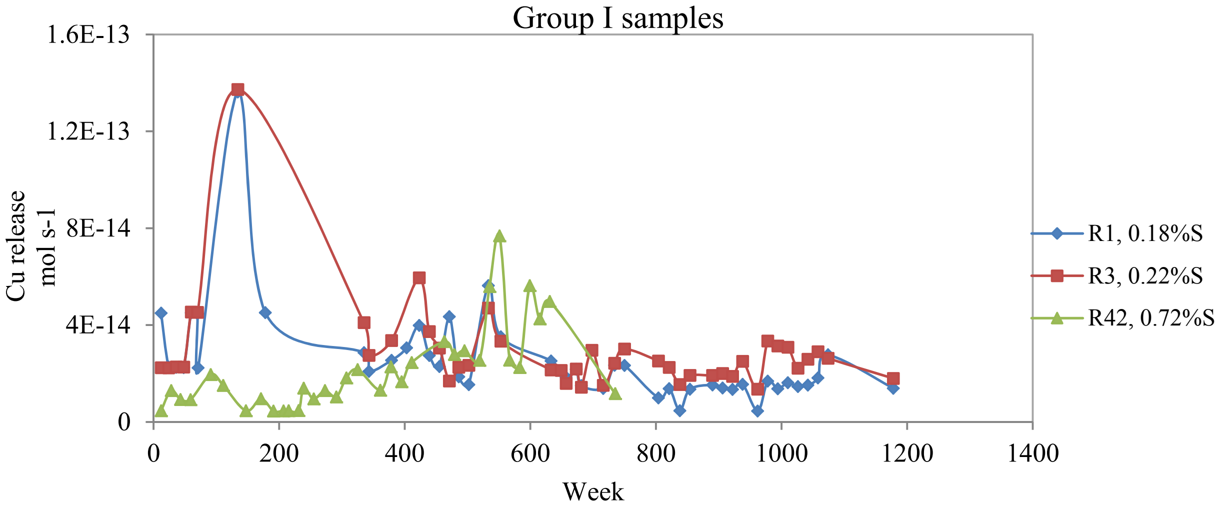
Group I samples

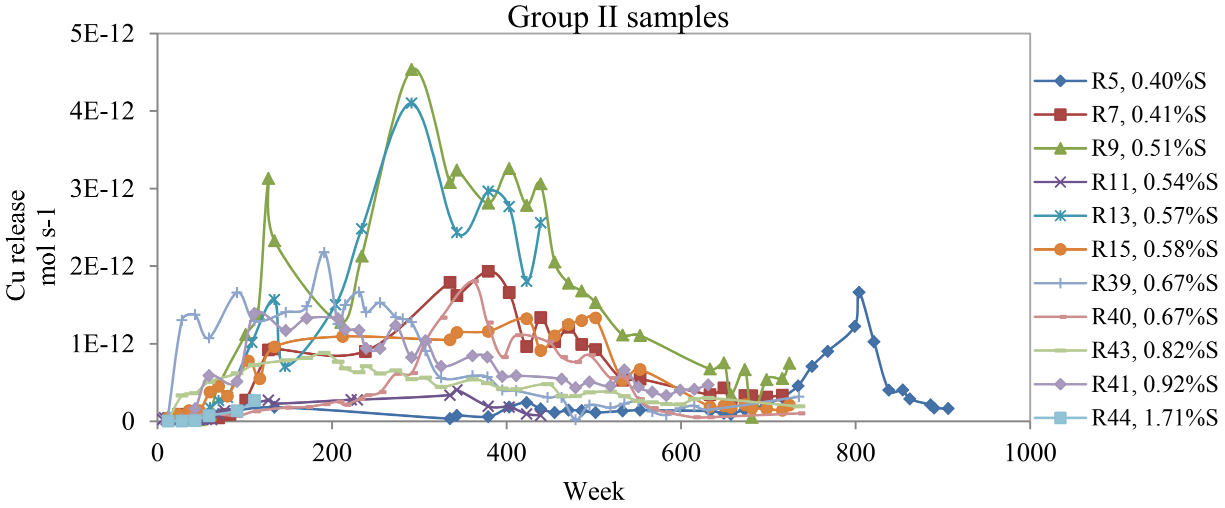
Group II samples

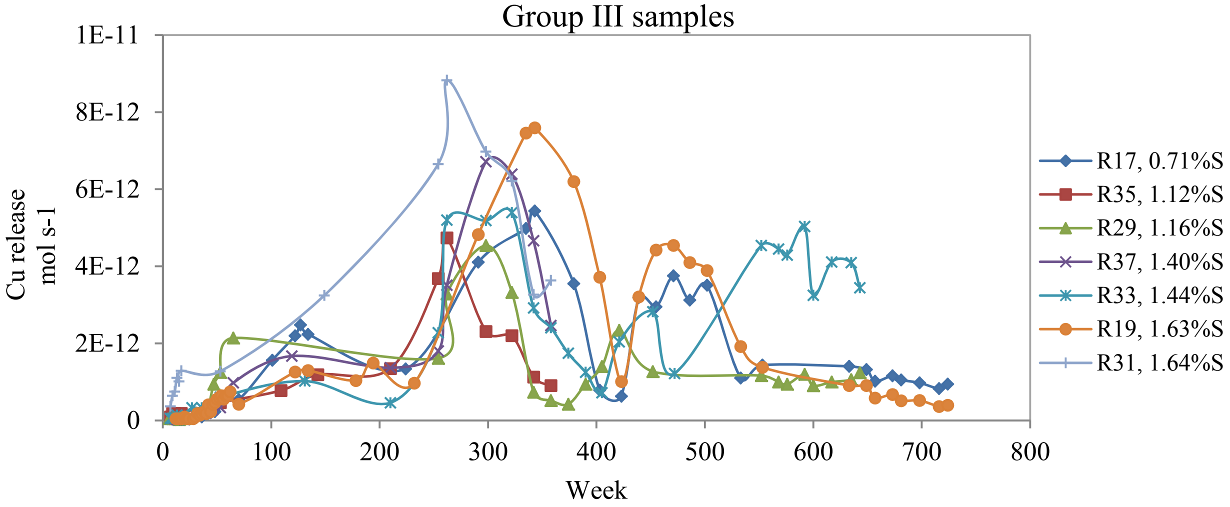
Group III samples

Figure 14. Nickel release vs. time for each sample group with similar behavior. Weeks 0-5 were omitted to improve resolution.

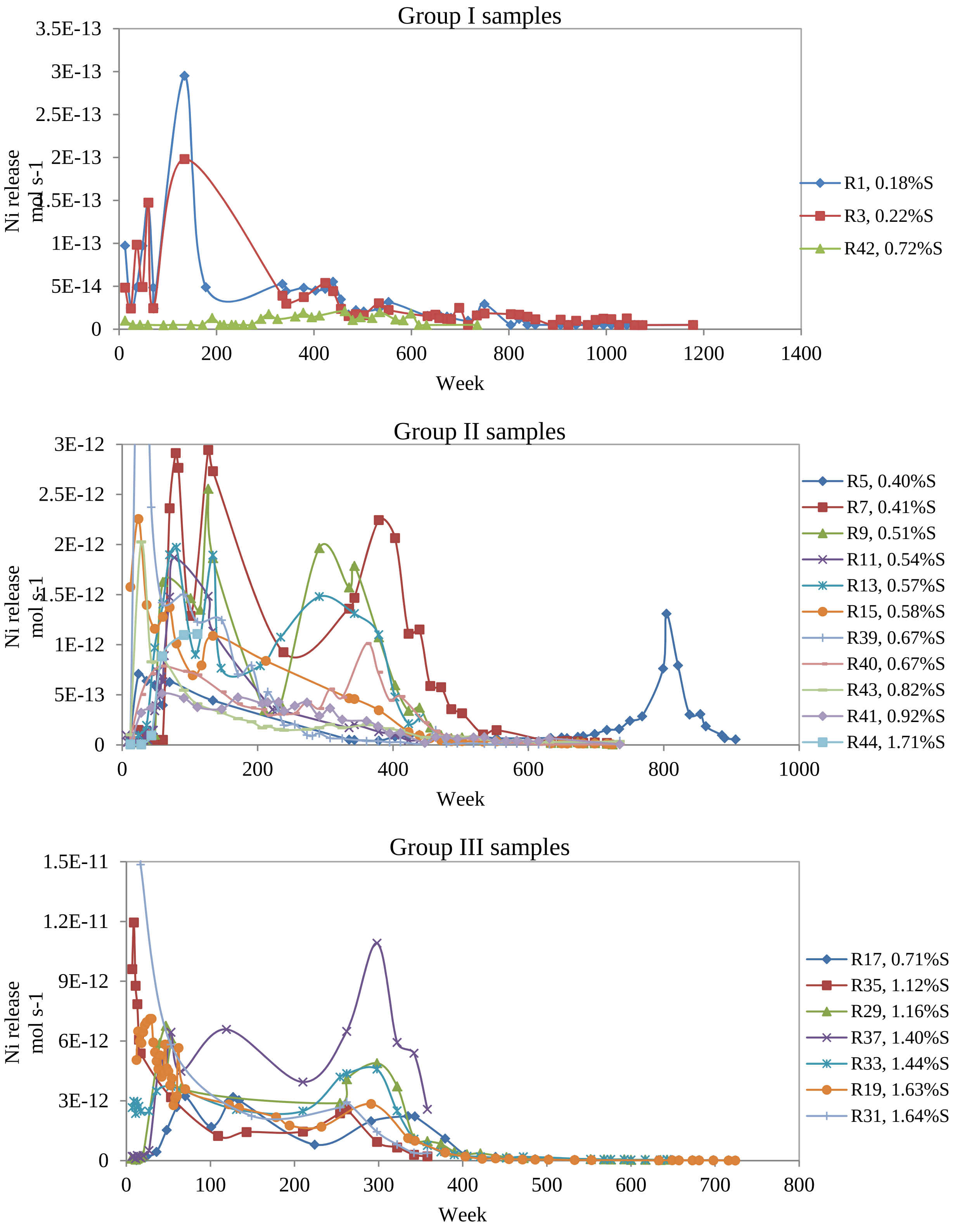

Figure 15. Zinc release vs. time for each sample group with similar behavior. Weeks 0-5 were omitted to improve resolution.

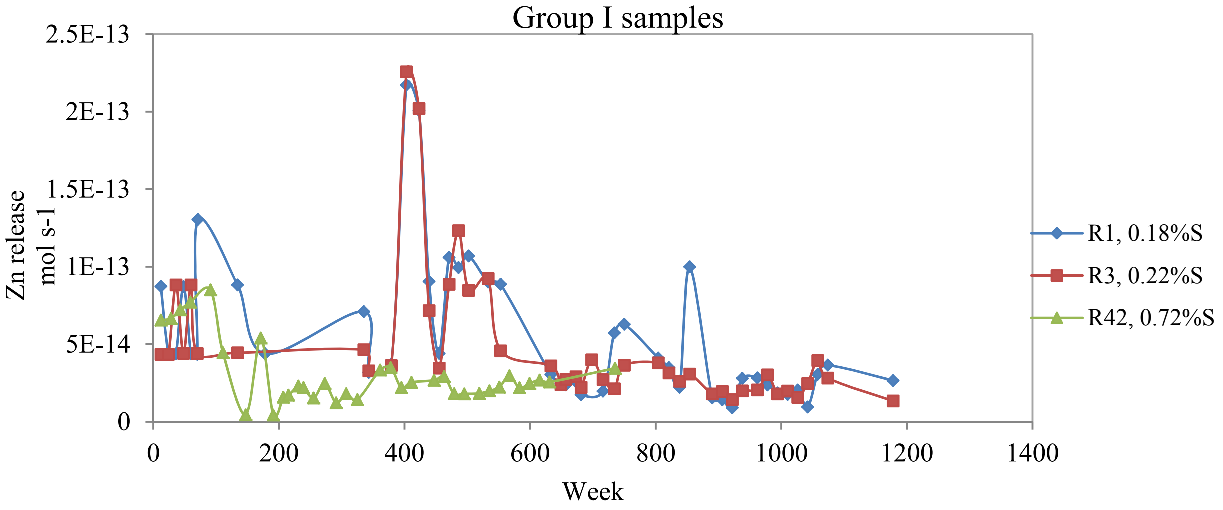

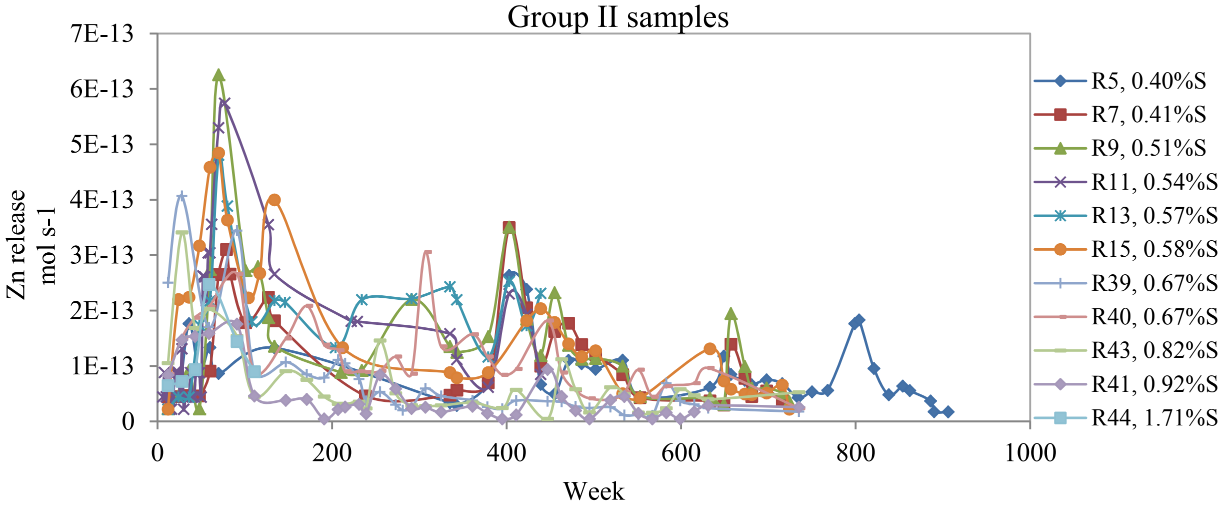

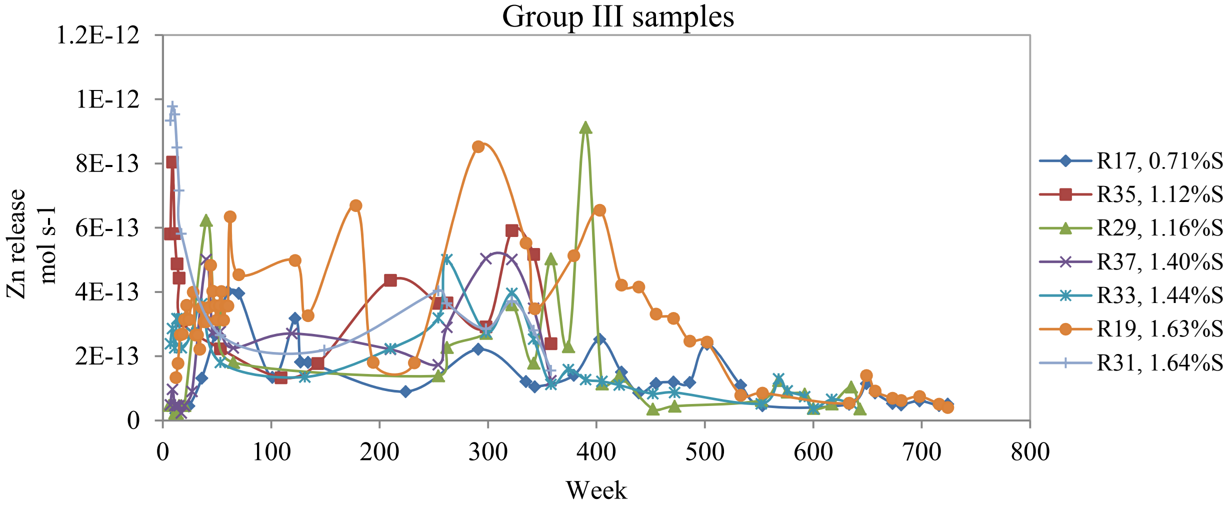

Figure 16. Cobalt release vs. pH for group II reactors

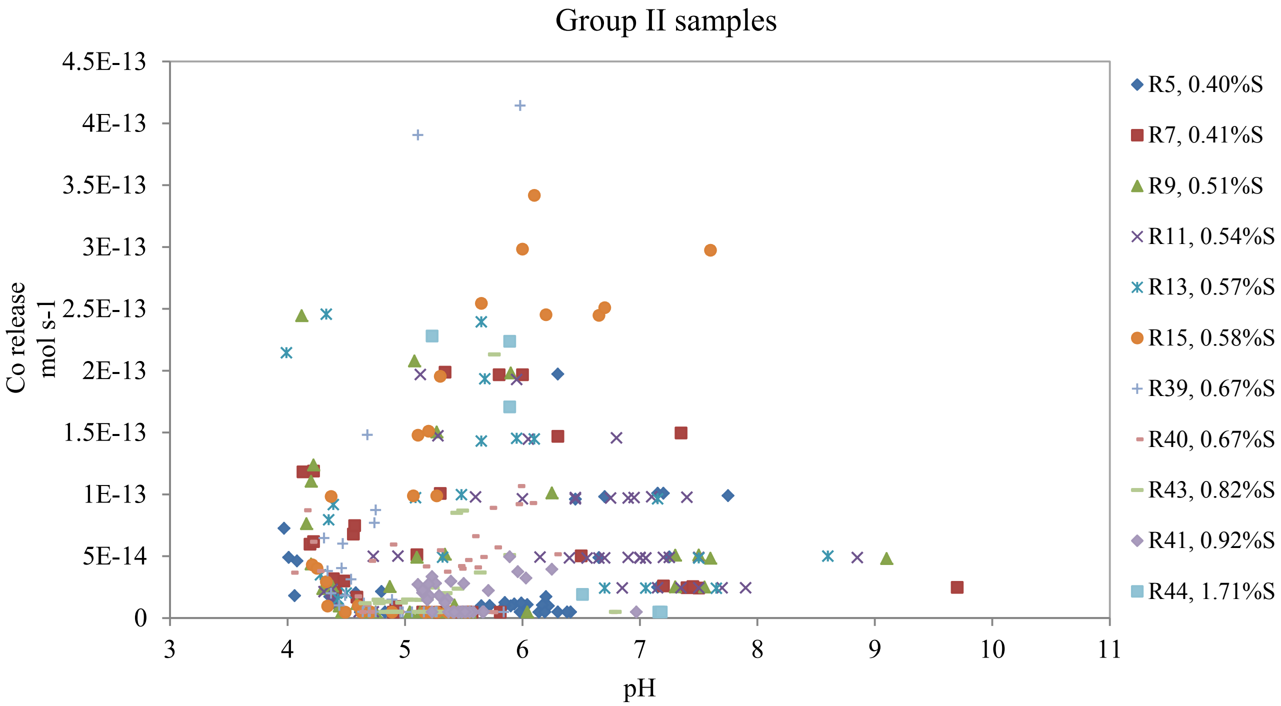

Figure 17. Copper release vs. pH for group II reactors

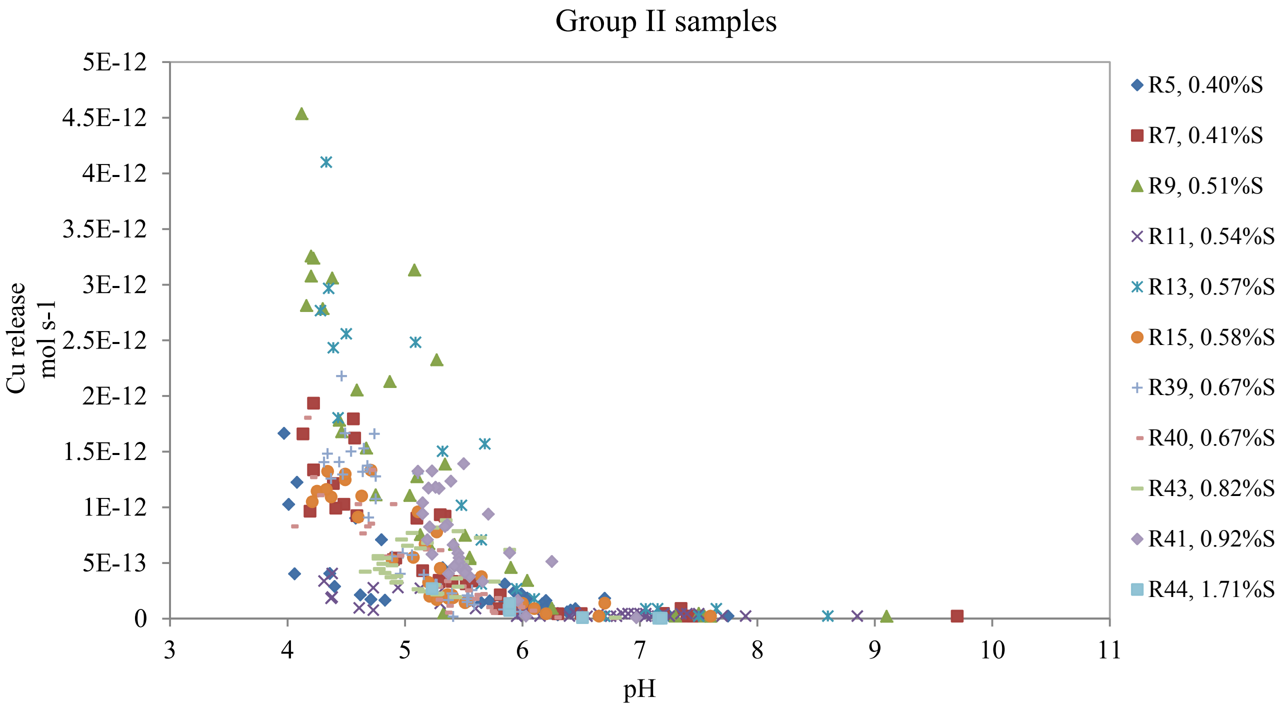

Figure 18. Nickel release vs. pH for group II reactors

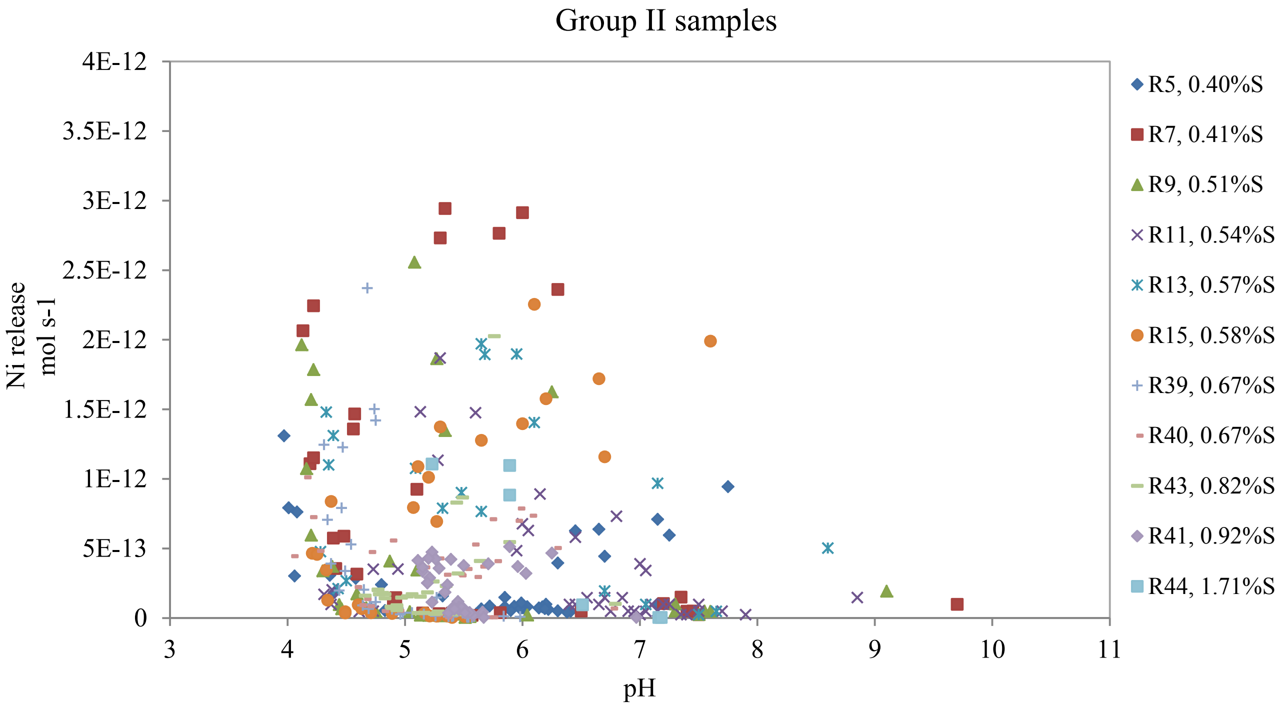

Figure 19. Zinc release vs. pH for group II reactors

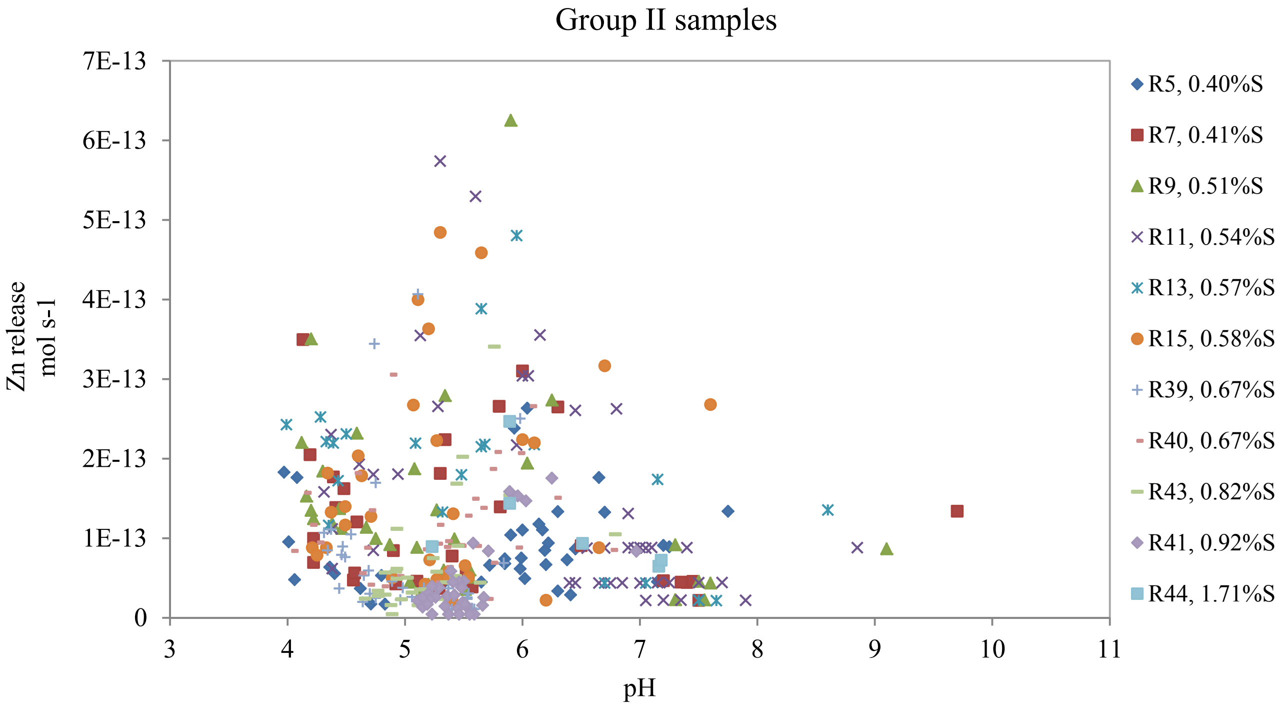

Figure 20. pH vs. sulfur content, period A

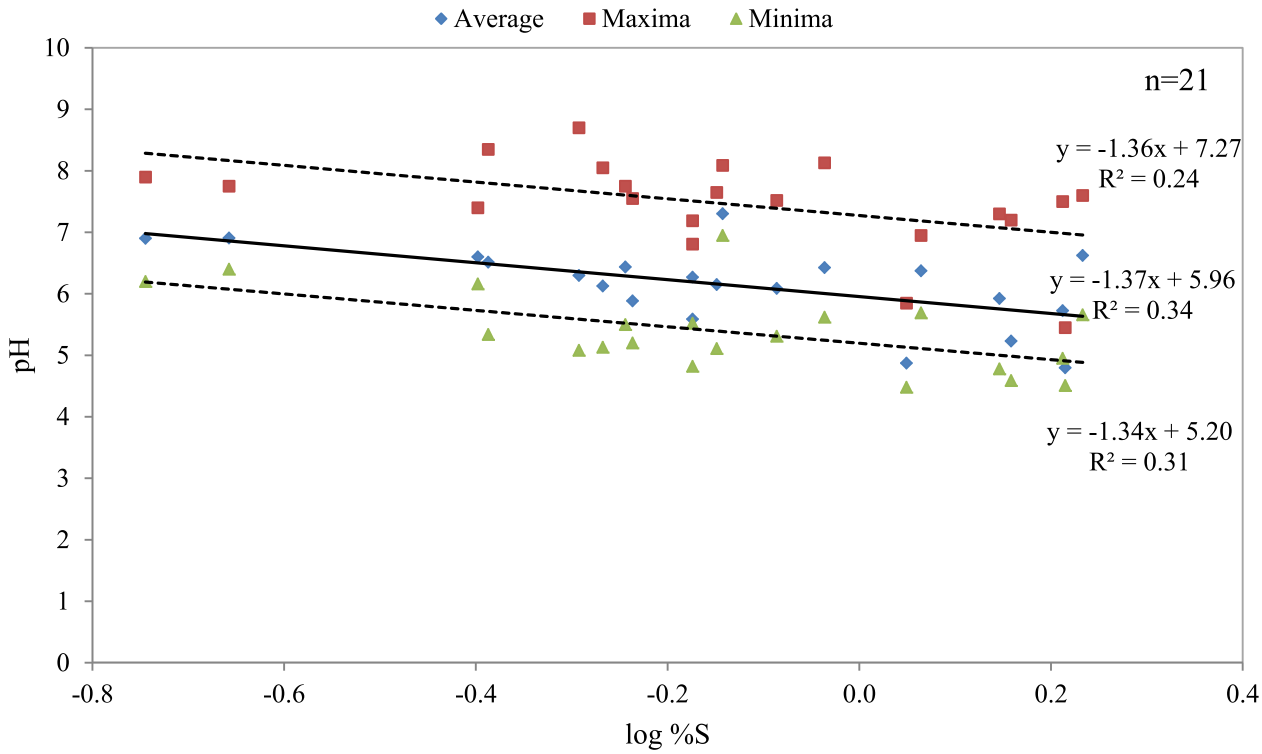

Figure 21. pH vs. sulfur content, period B

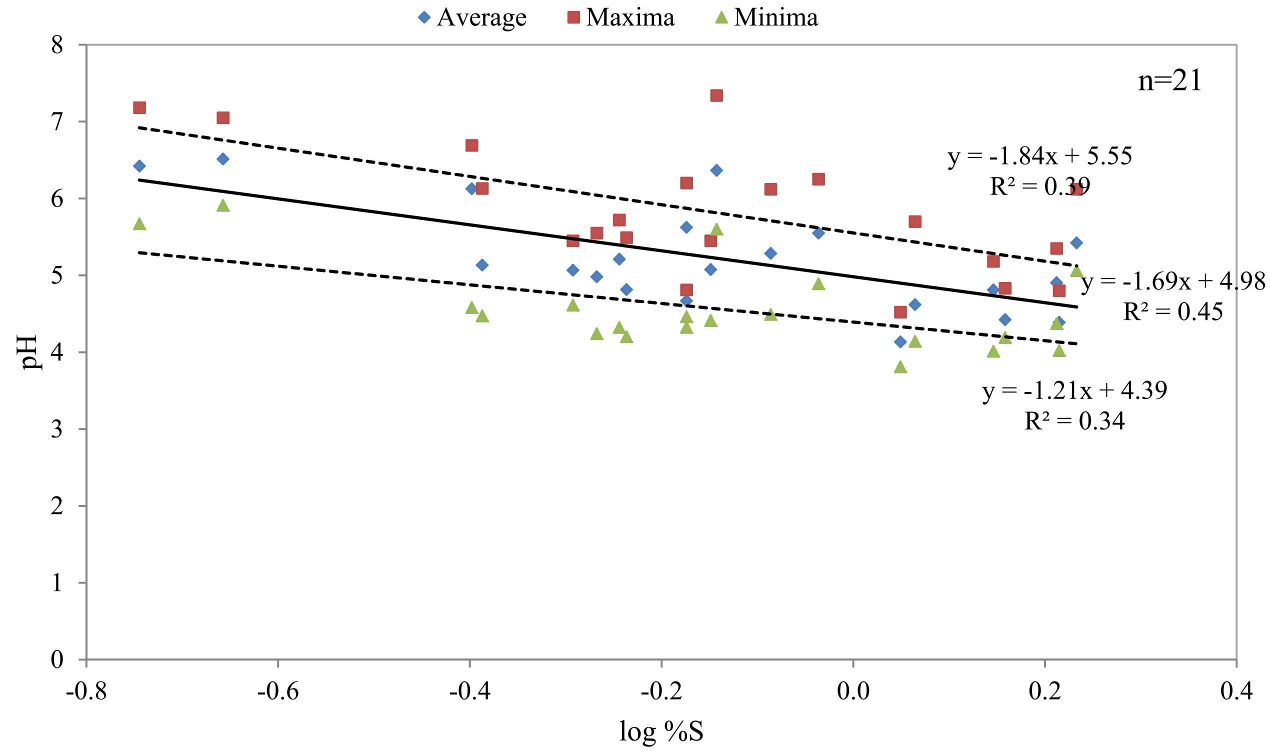

Figure 22. pH vs. sulfur content, period C

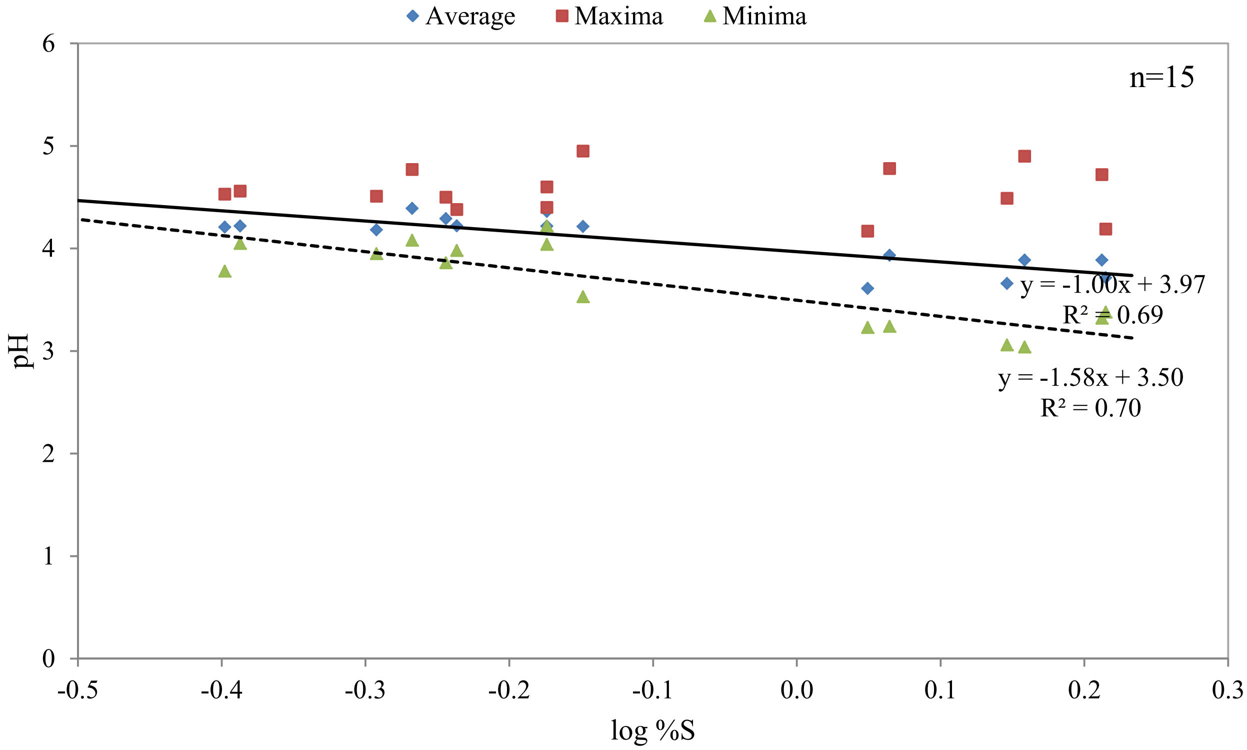

Figure 23. pH vs. sulfur content, period D

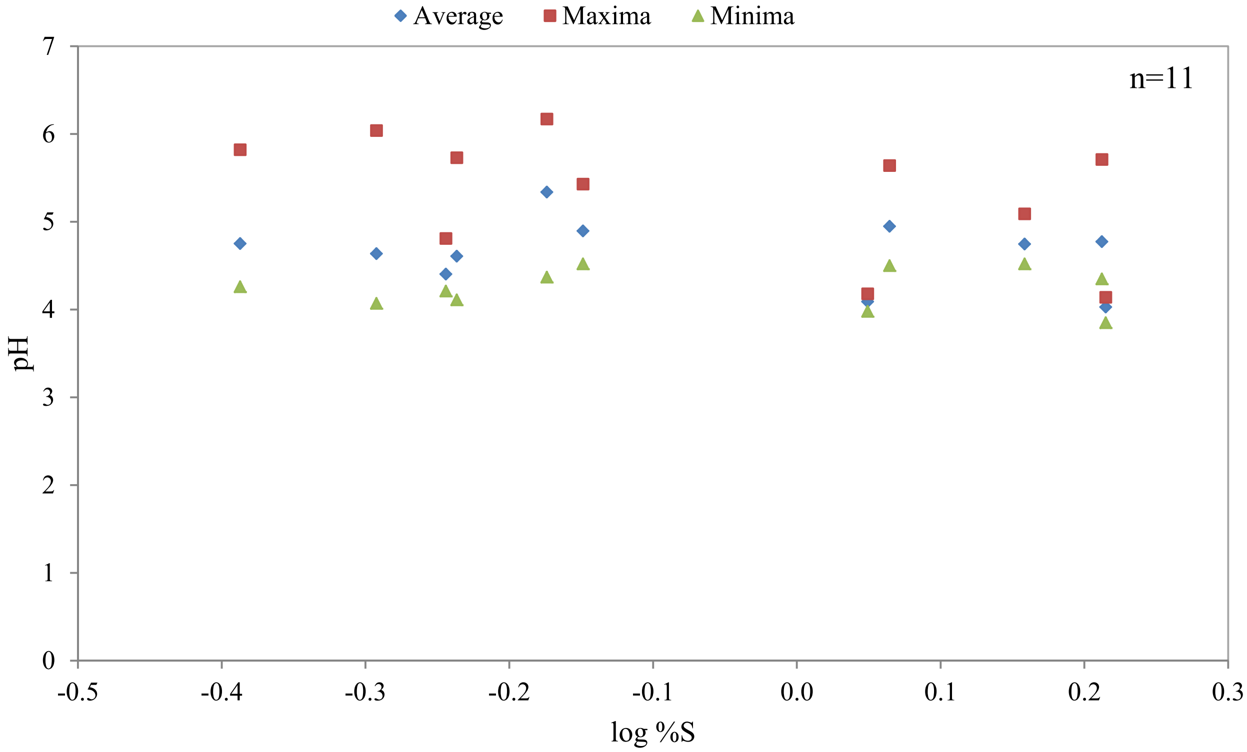

Figure 24. Sulfate release (umol/wk) vs. sulfur content, period A

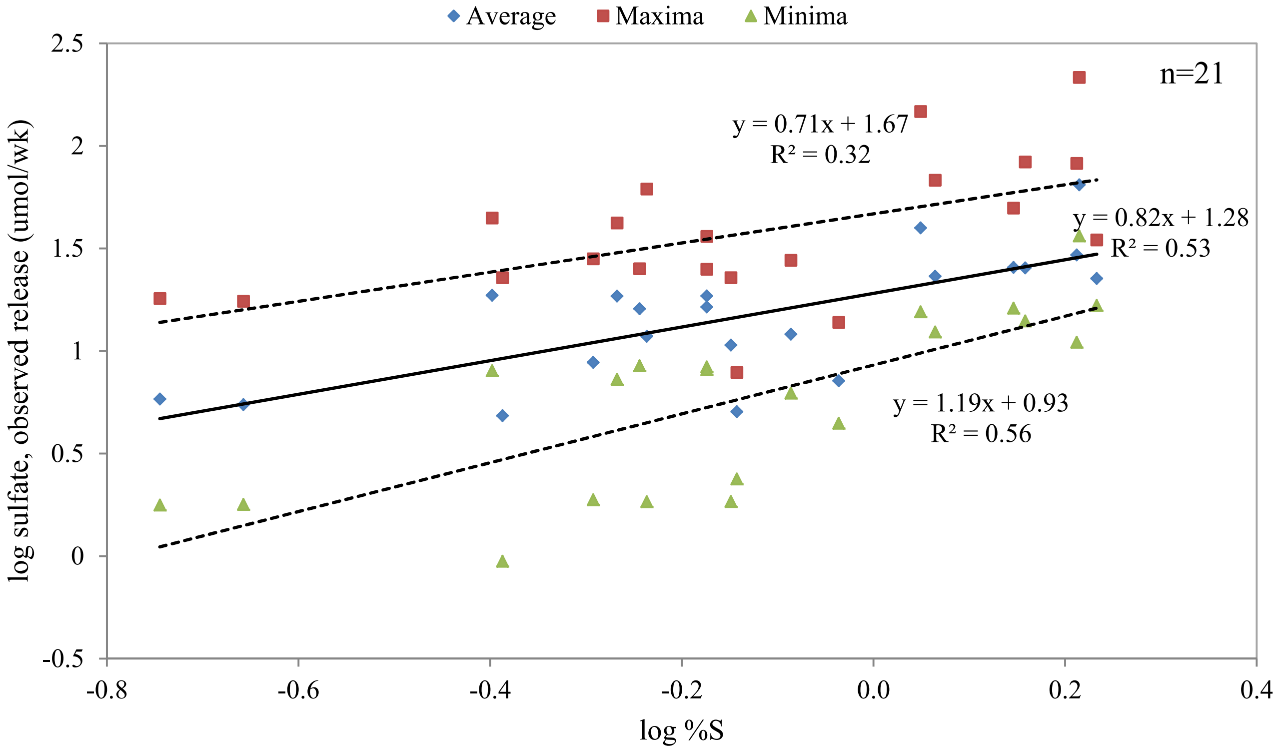

Figure 25. Sulfate release (umol/wk) vs. sulfur content, period B

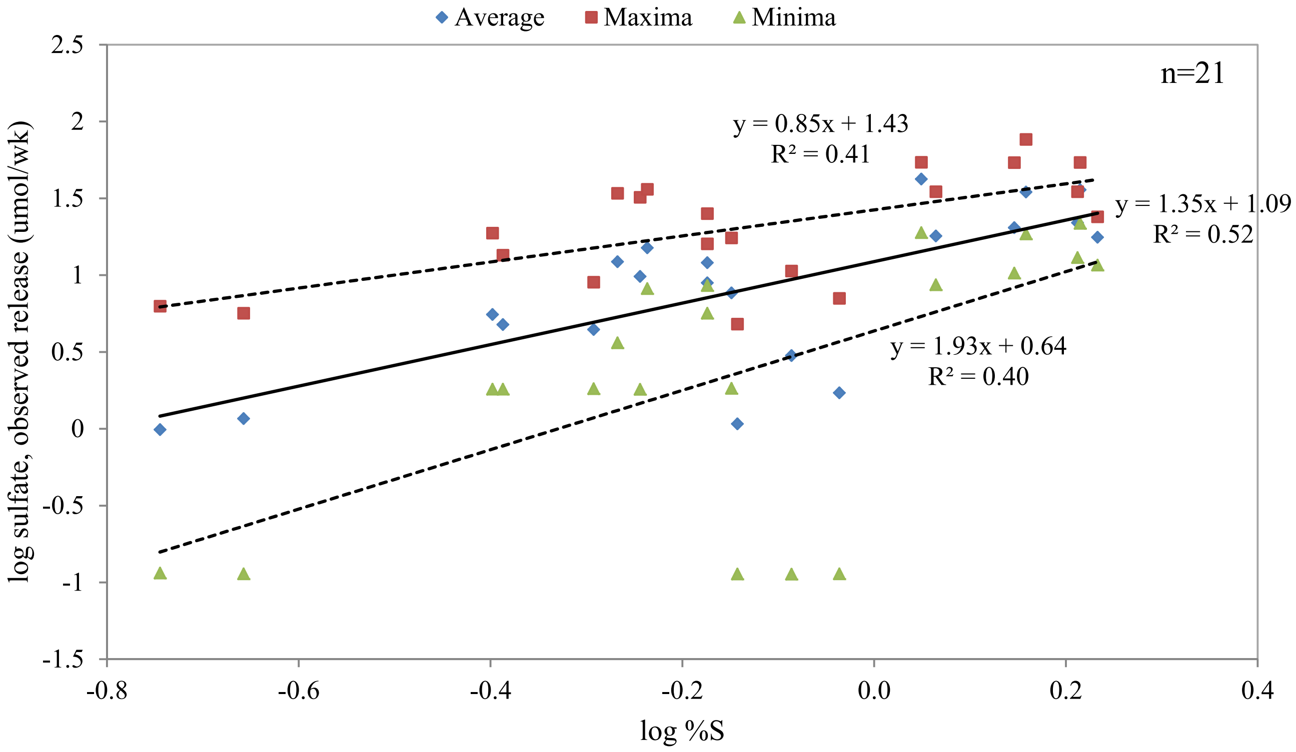

Figure 26. Sulfate release (umol/wk) vs. sulfur content, period C

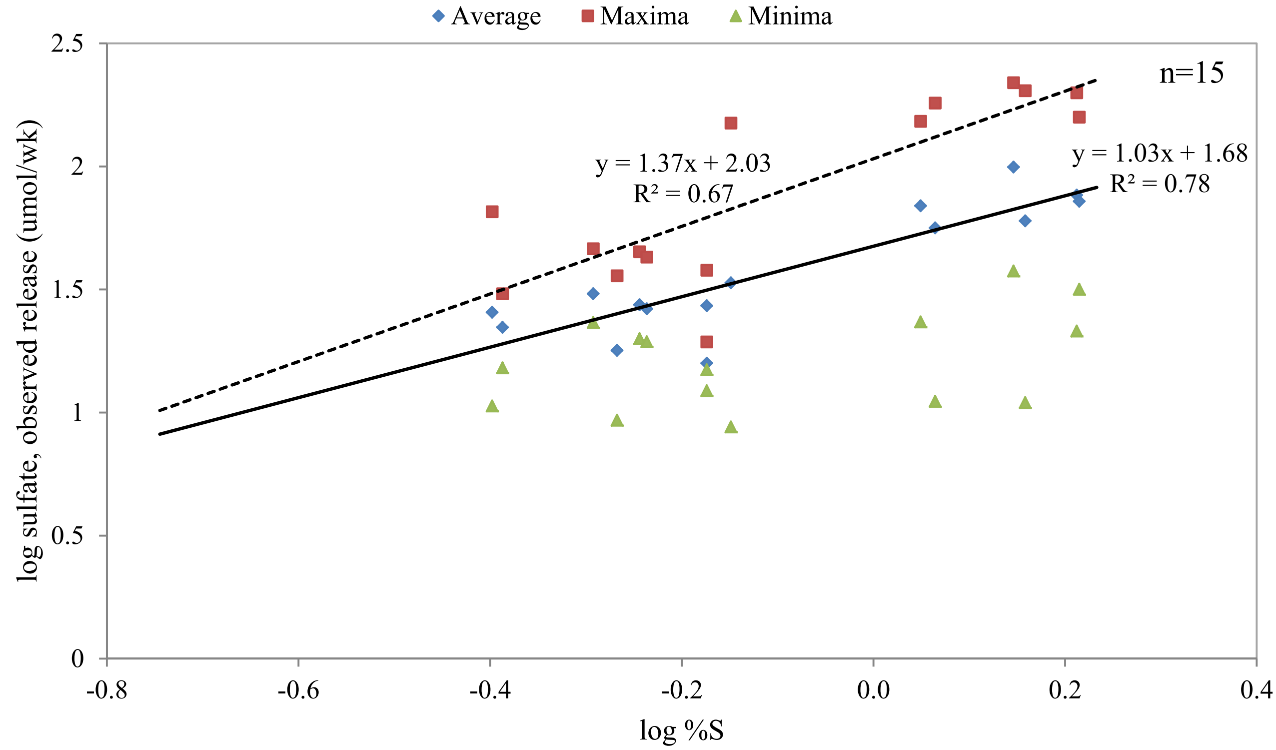

Figure 27. Sulfate release (umol/wk) vs. sulfur content, period D

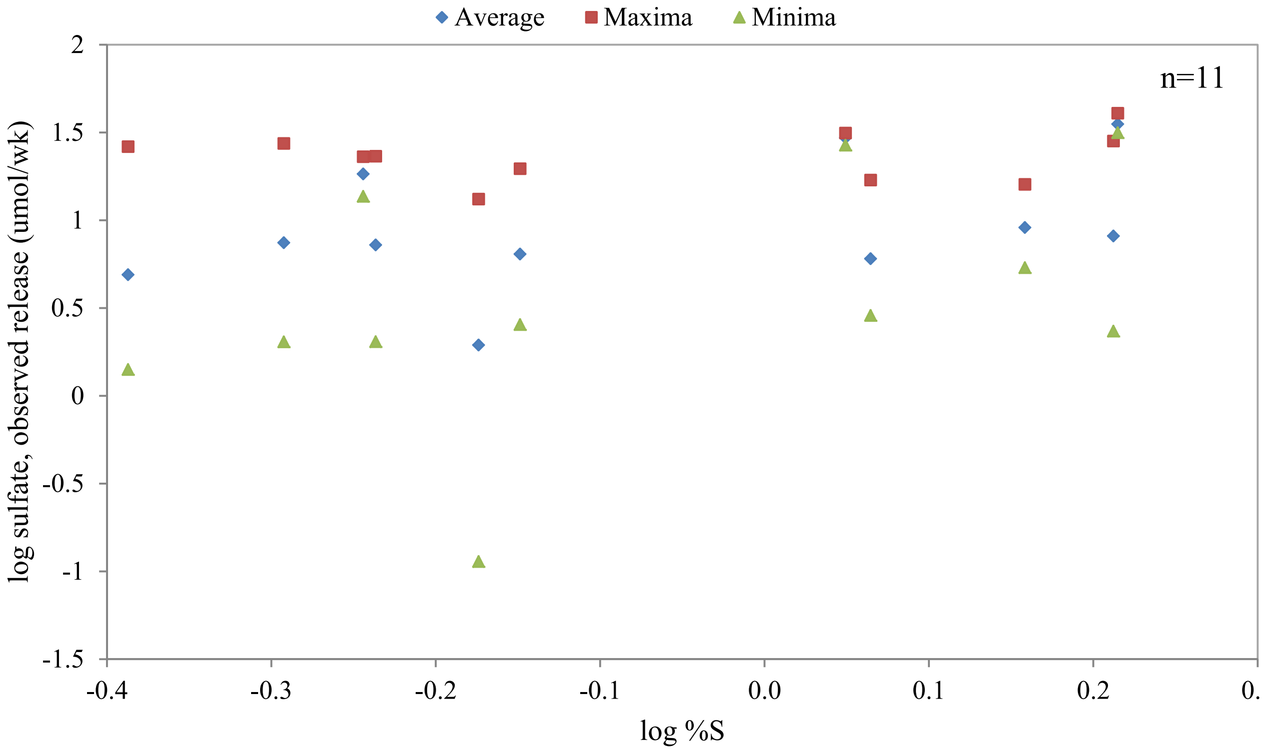

Figure 28. pH vs. sulfate release (umol/wk), period A

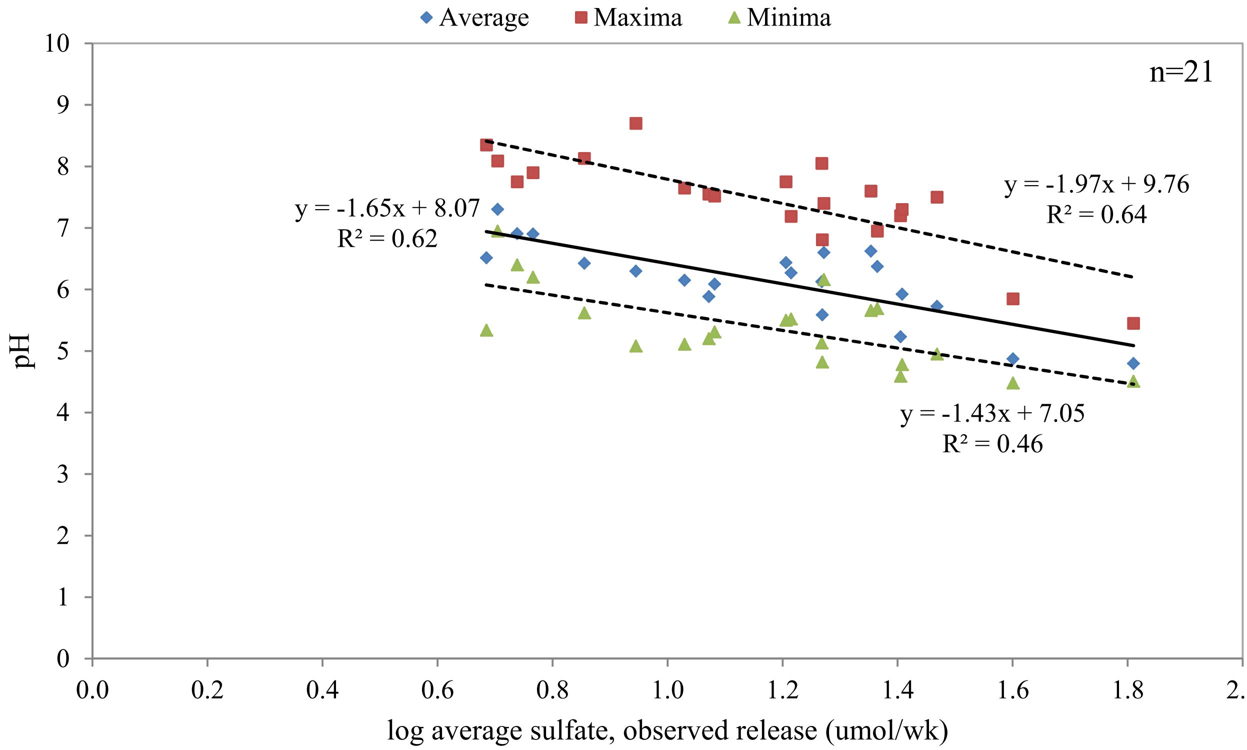

Figure 29. pH vs. sulfate release (umol/wk), period B

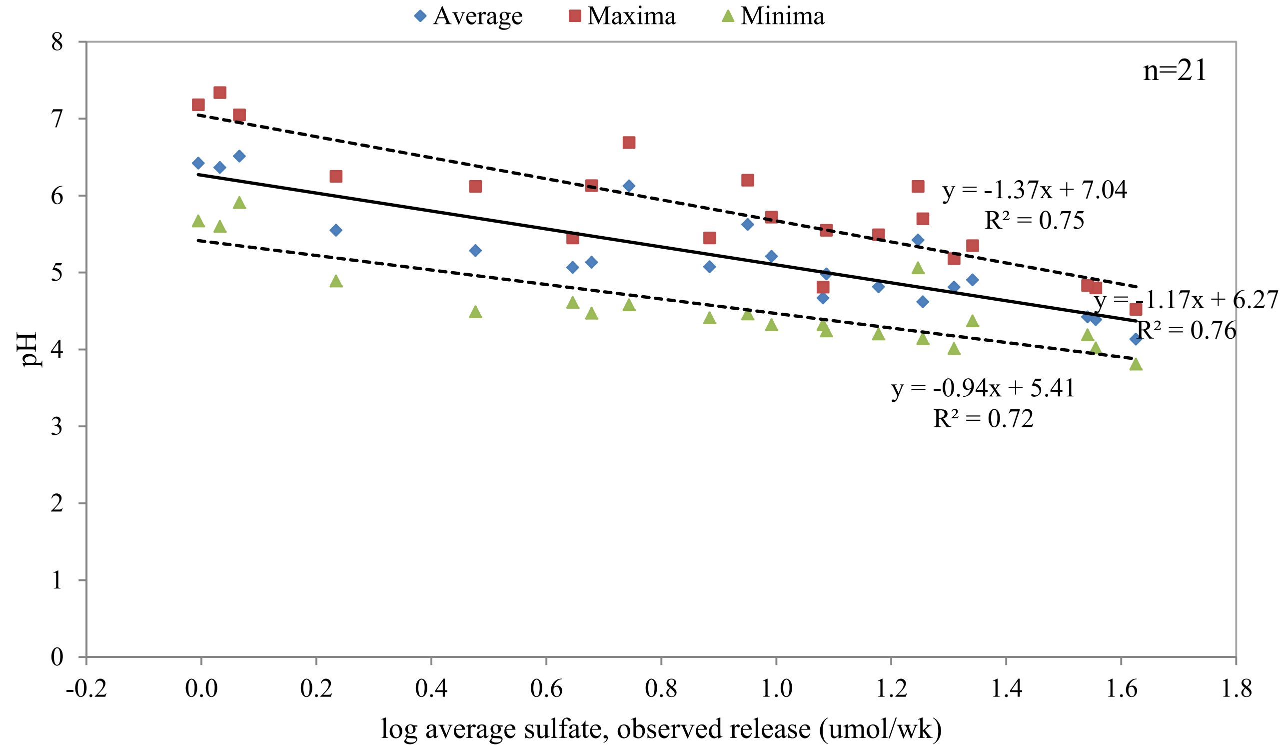

Figure 30. pH vs. sulfate release (umol/wk), period C

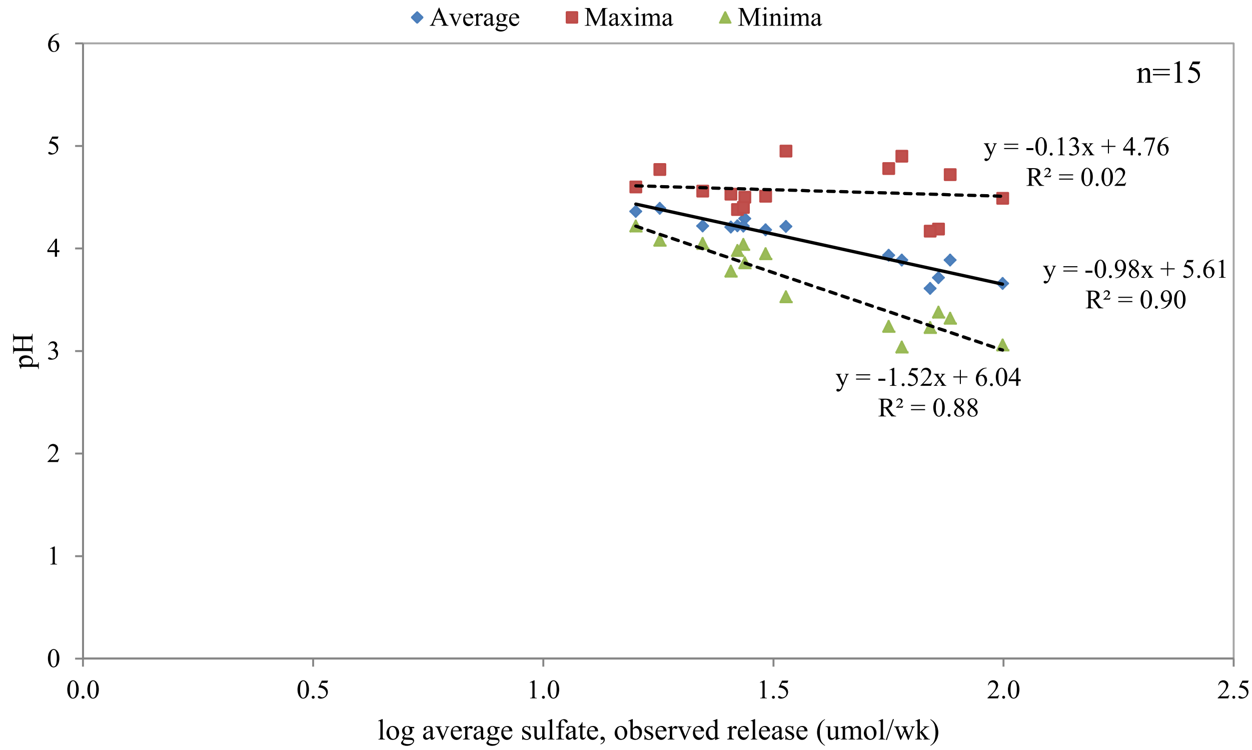

Figure 31. pH vs. sulfate release (umol/wk), period D

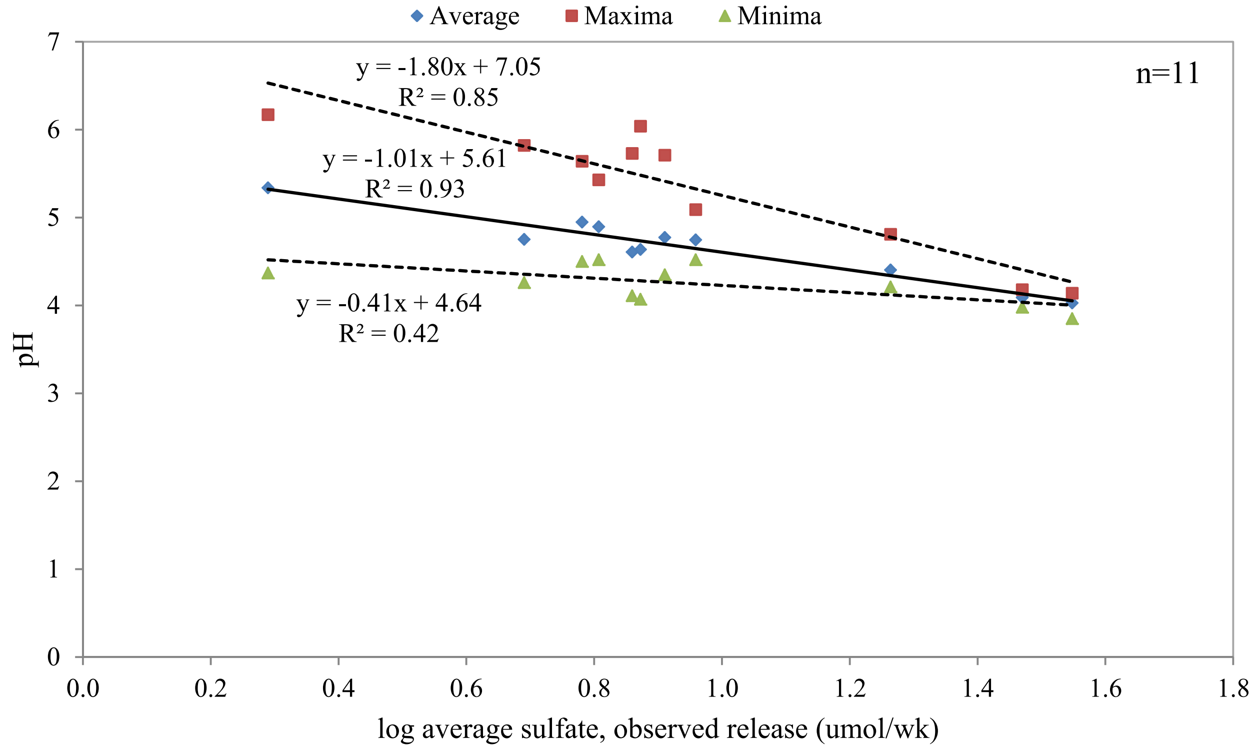

Figure 32. Calcium release vs. sulfate release (umol/wk), period A

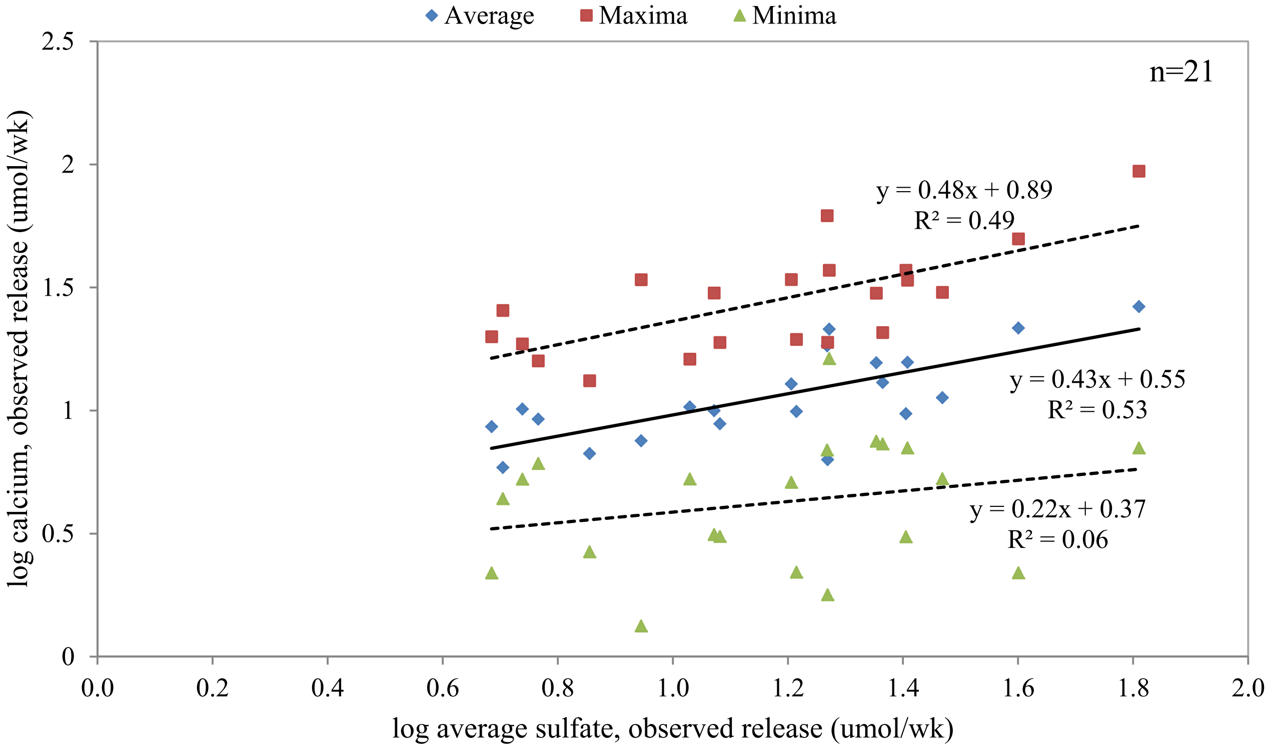

Figure 33. Calcium release vs. sulfate release (umol/wk), period B

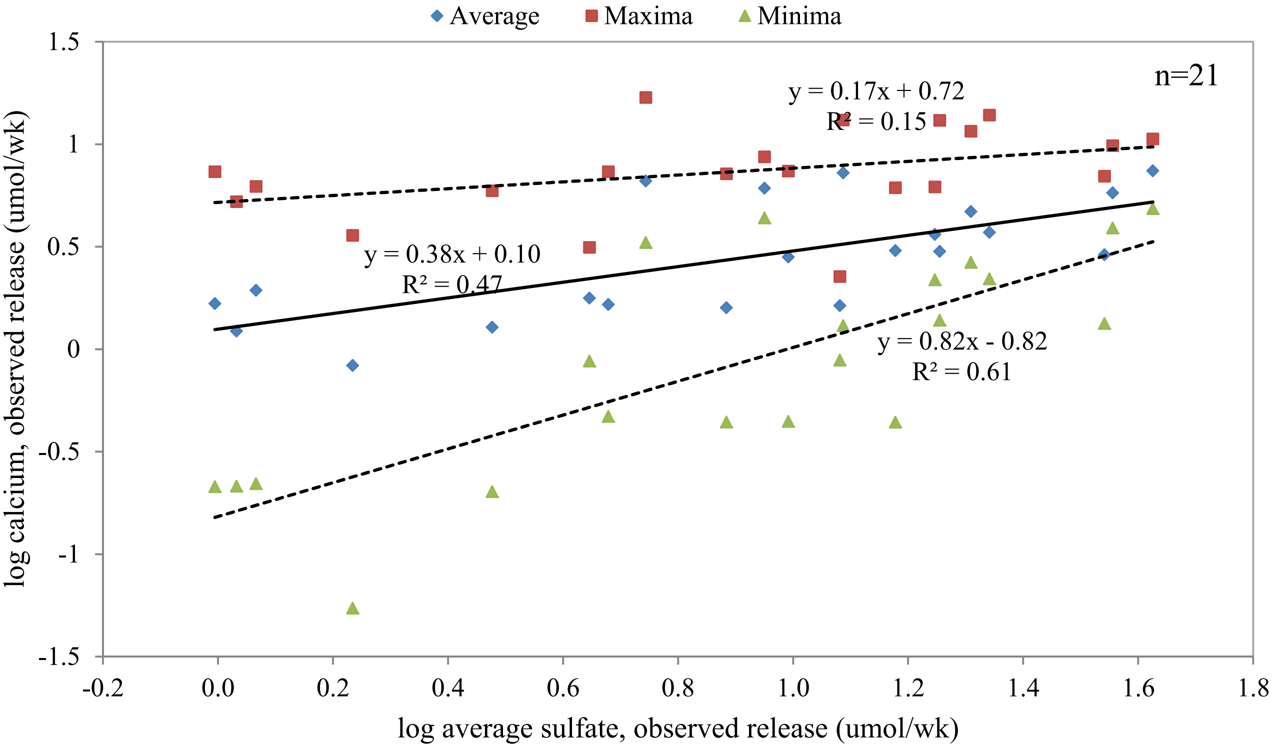

Figure 34. Calcium release vs. sulfate release (umol/wk), period C

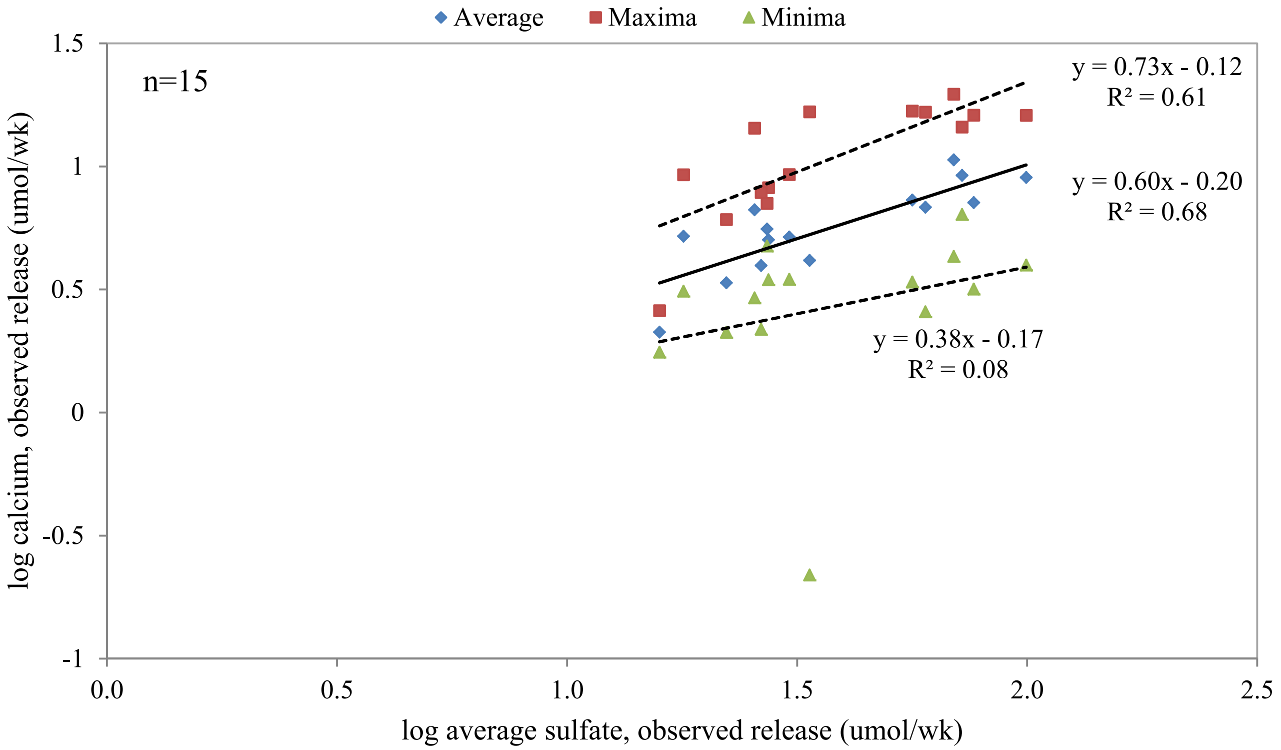

Figure 35. Calcium release vs. sulfate release (umol/wk), period D

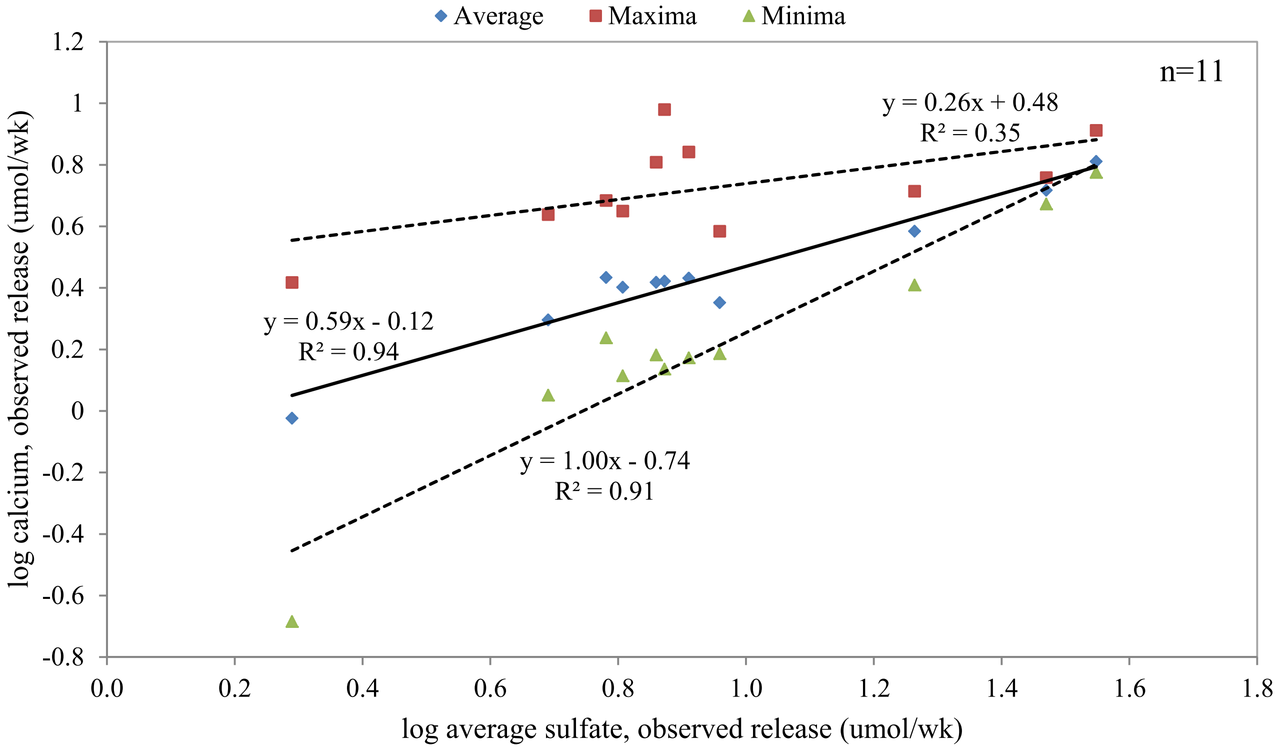

Figure 36. Magnesium release vs. sulfate release (umol/wk), period A

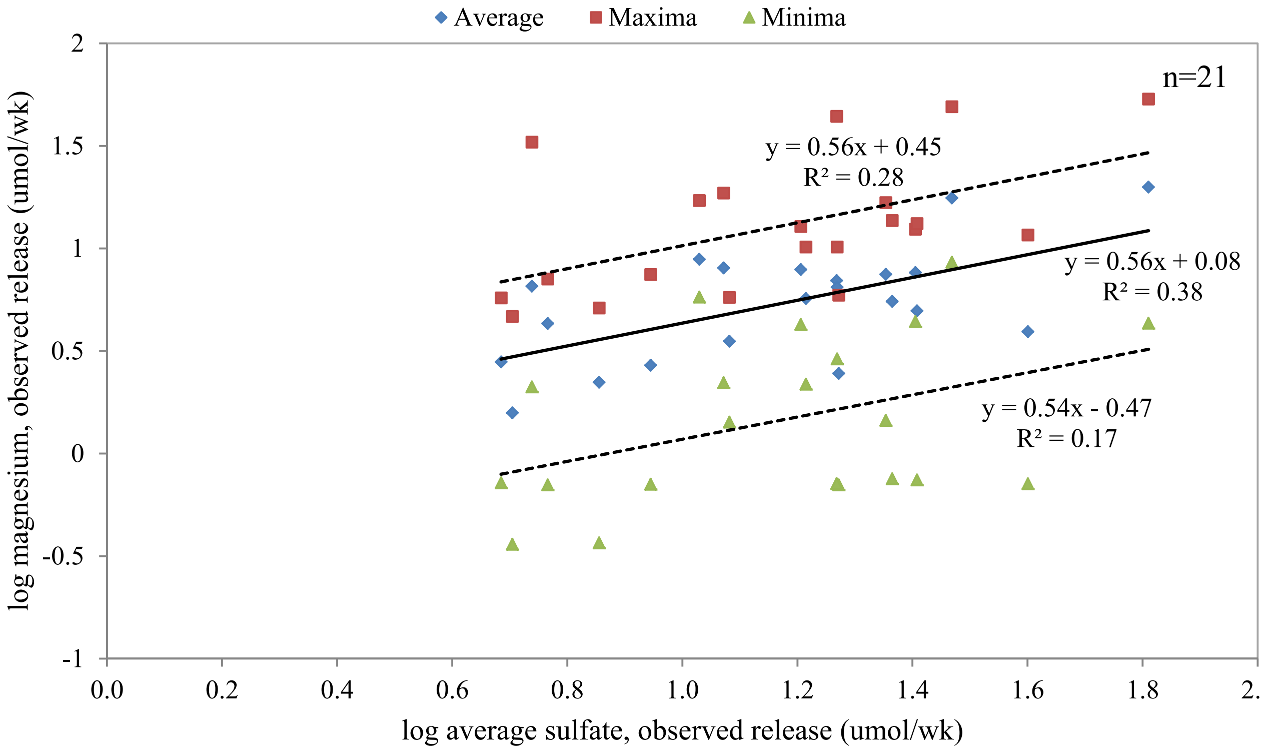

Figure 37. Magnesium release vs. sulfate release (umol/wk), period B

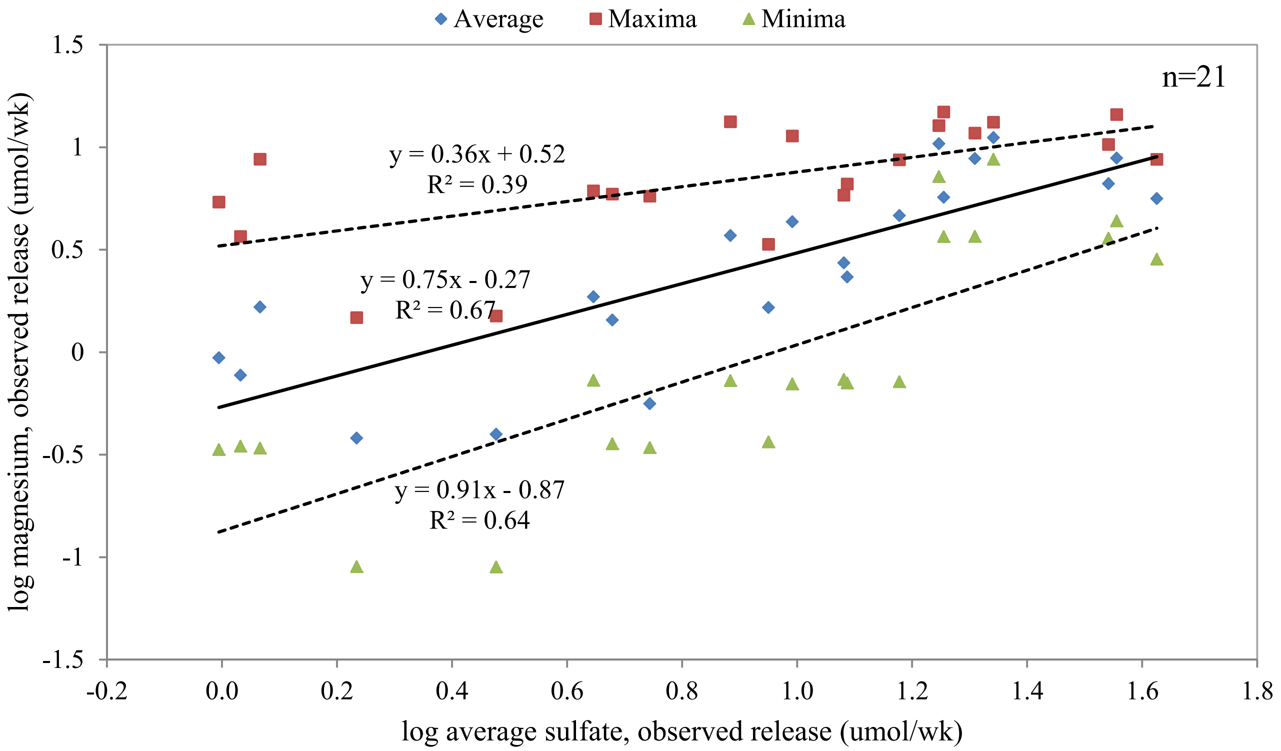

Figure 38. Magnesium release vs. sulfate release (umol/wk), period C

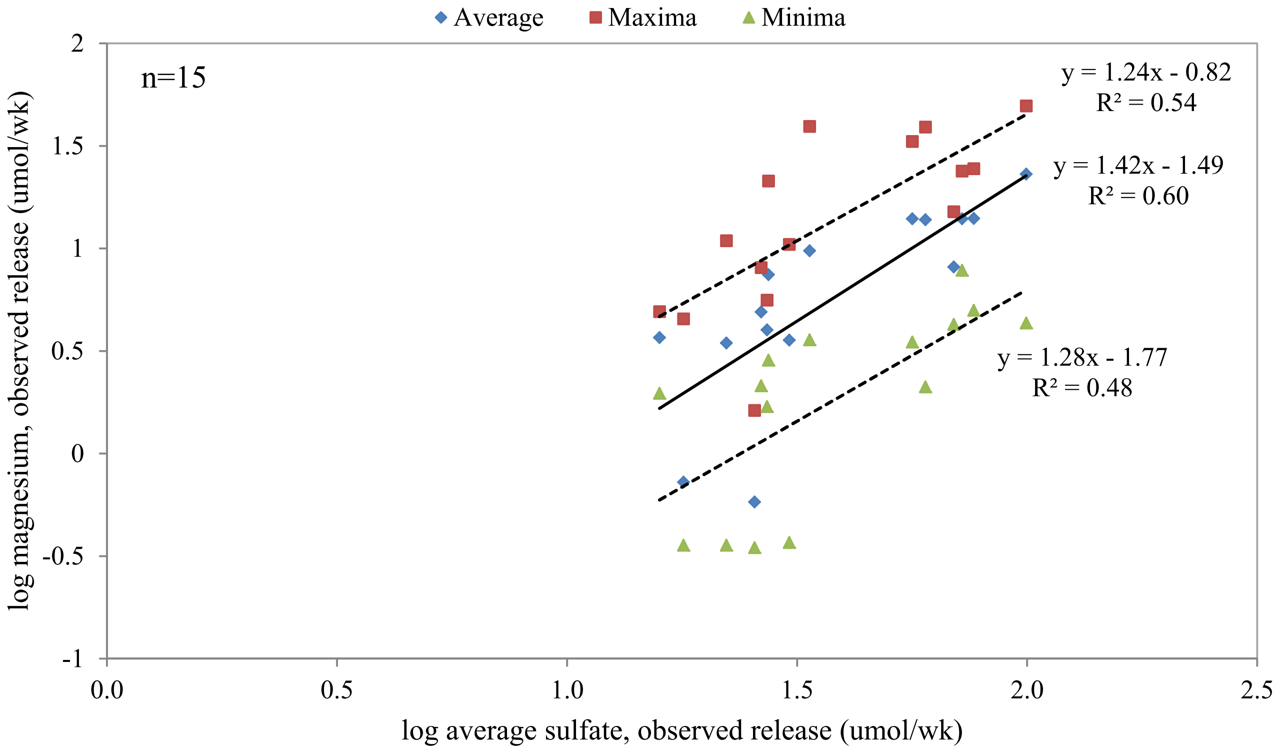

Figure 39. Magnesium release vs. sulfate release (umol/wk), period D

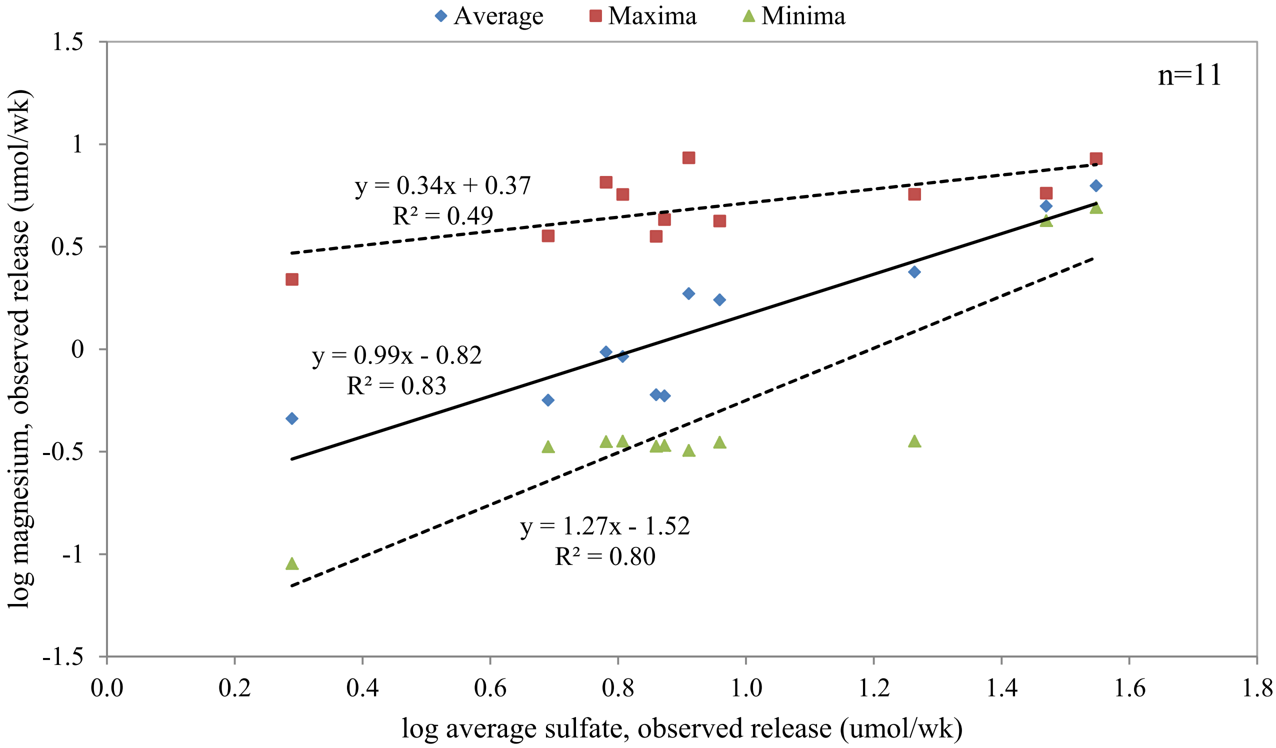

Figure 40. Ca + Mg release vs. sulfate release (umol/wk), period A

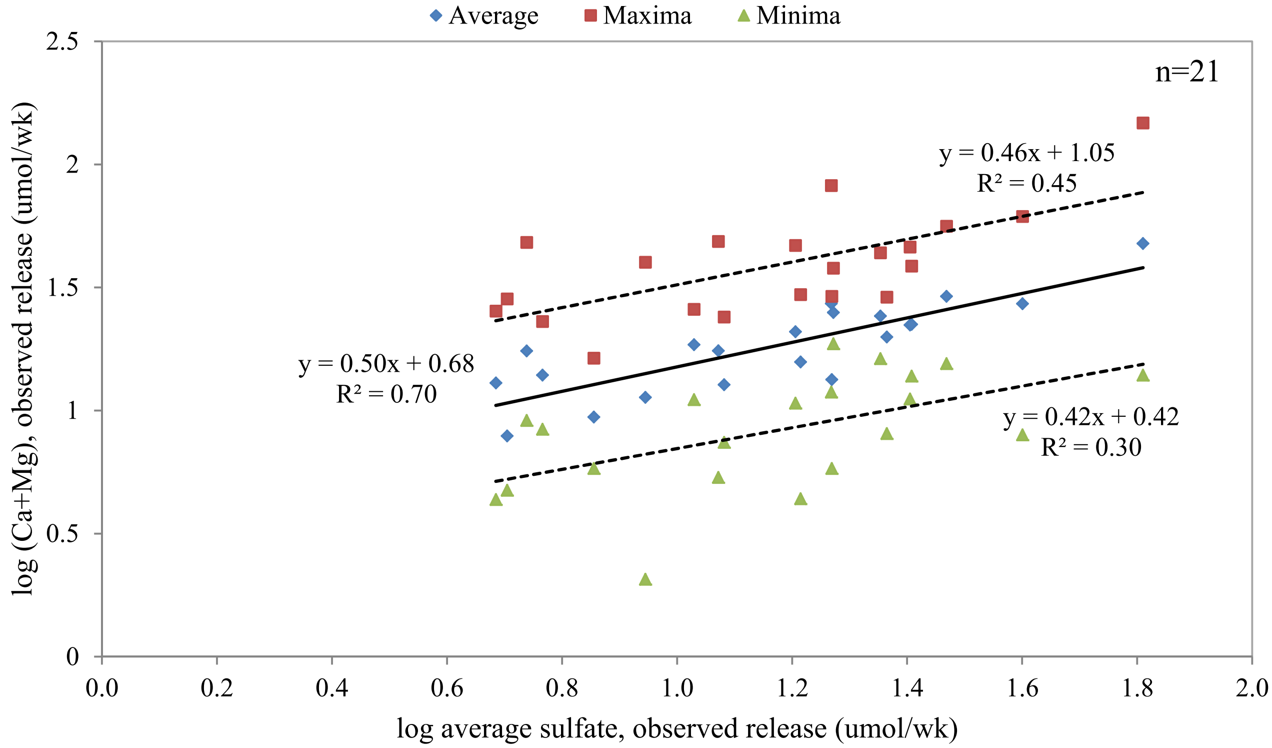

Figure 41. Ca + Mg release vs. sulfate release (umol/wk), period B

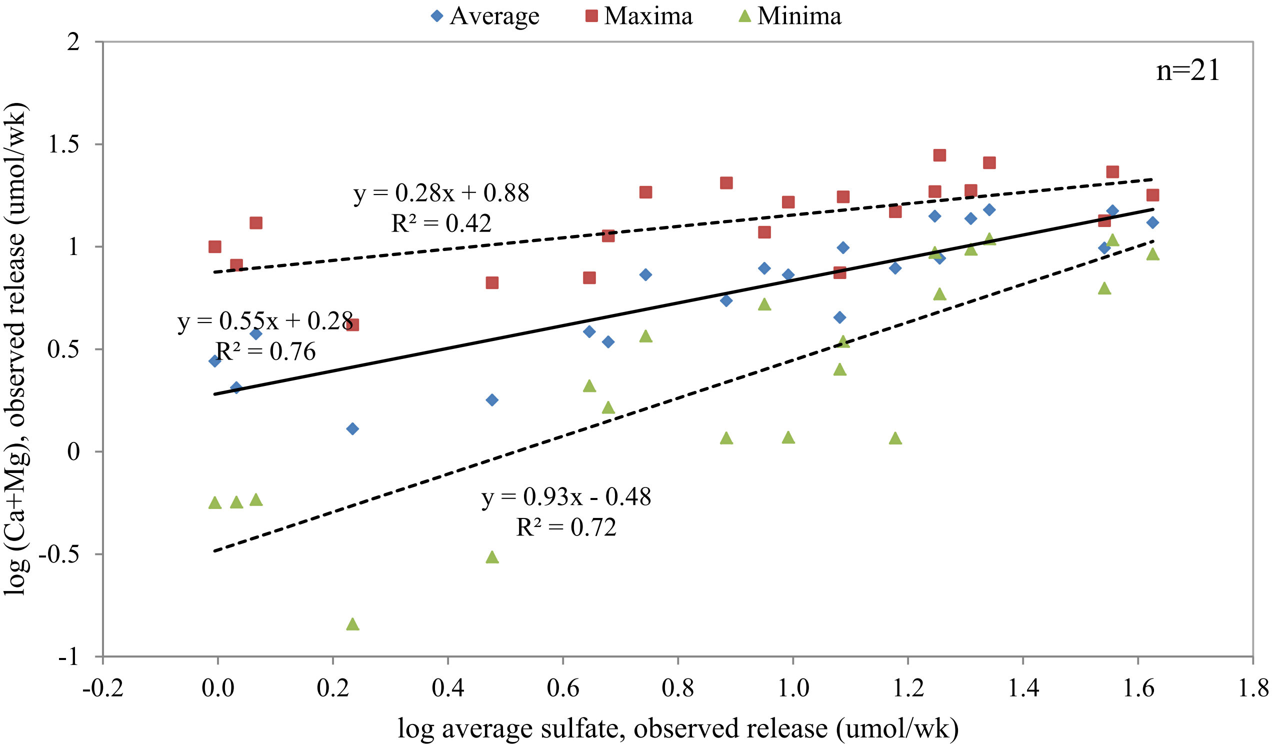

Figure 42. Ca + Mg release vs. sulfate release (umol/wk), period C

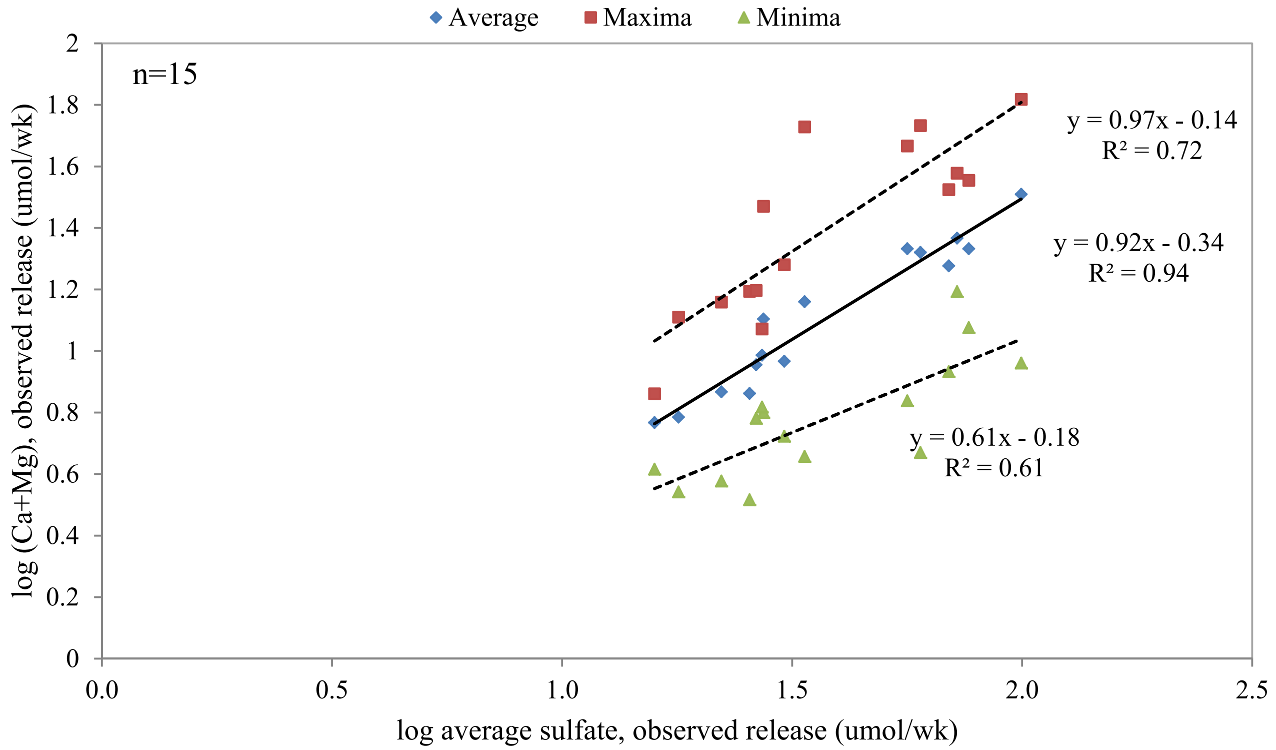

Figure 43. Ca + Mg release vs. sulfate release (umol/wk), period D

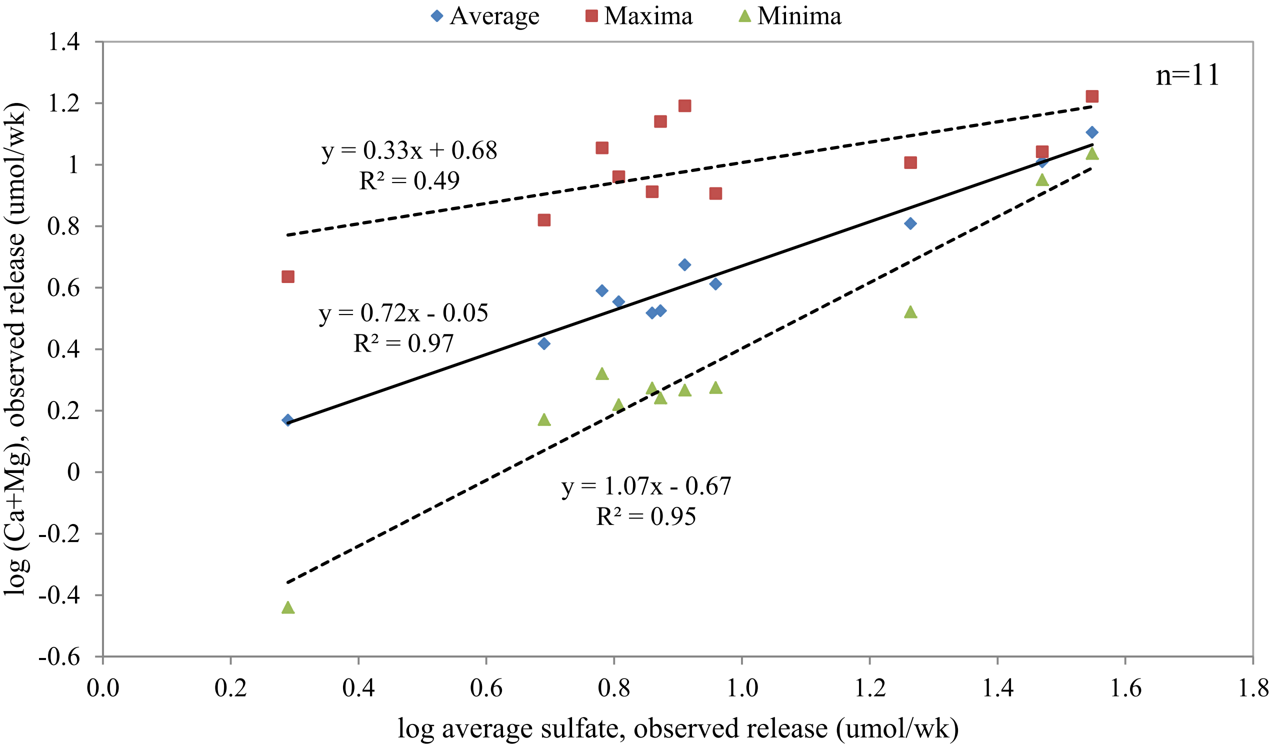

Figure 44. Cobalt composition vs. % sulfur for unleached solids

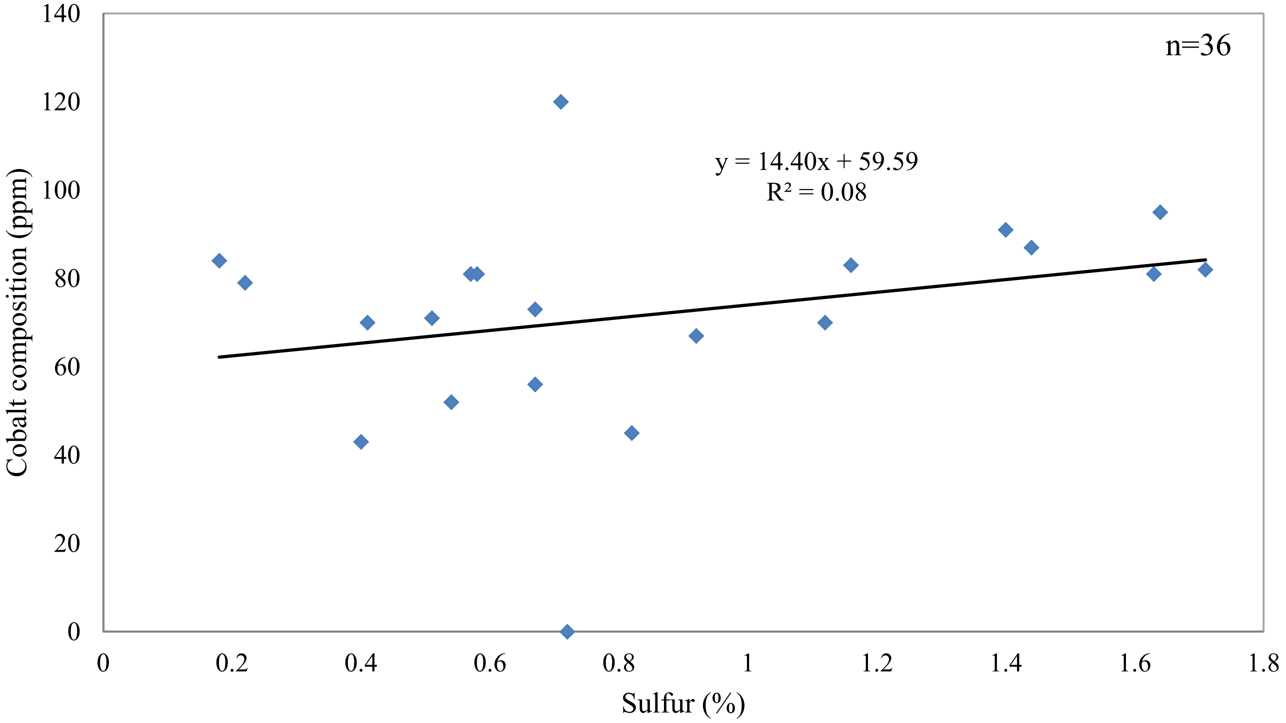

Figure 45. Copper composition vs. % sulfur for unleached solids

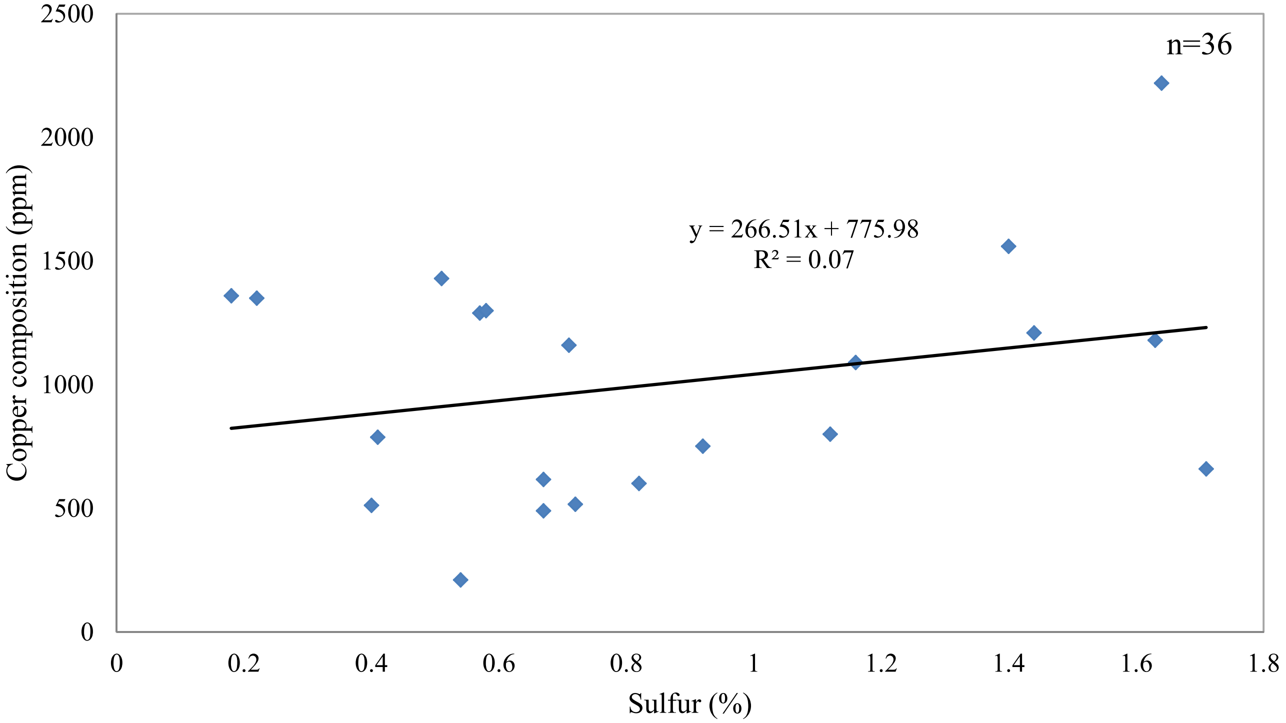

Figure 46. Nickel composition vs. % sulfur for unleached solids

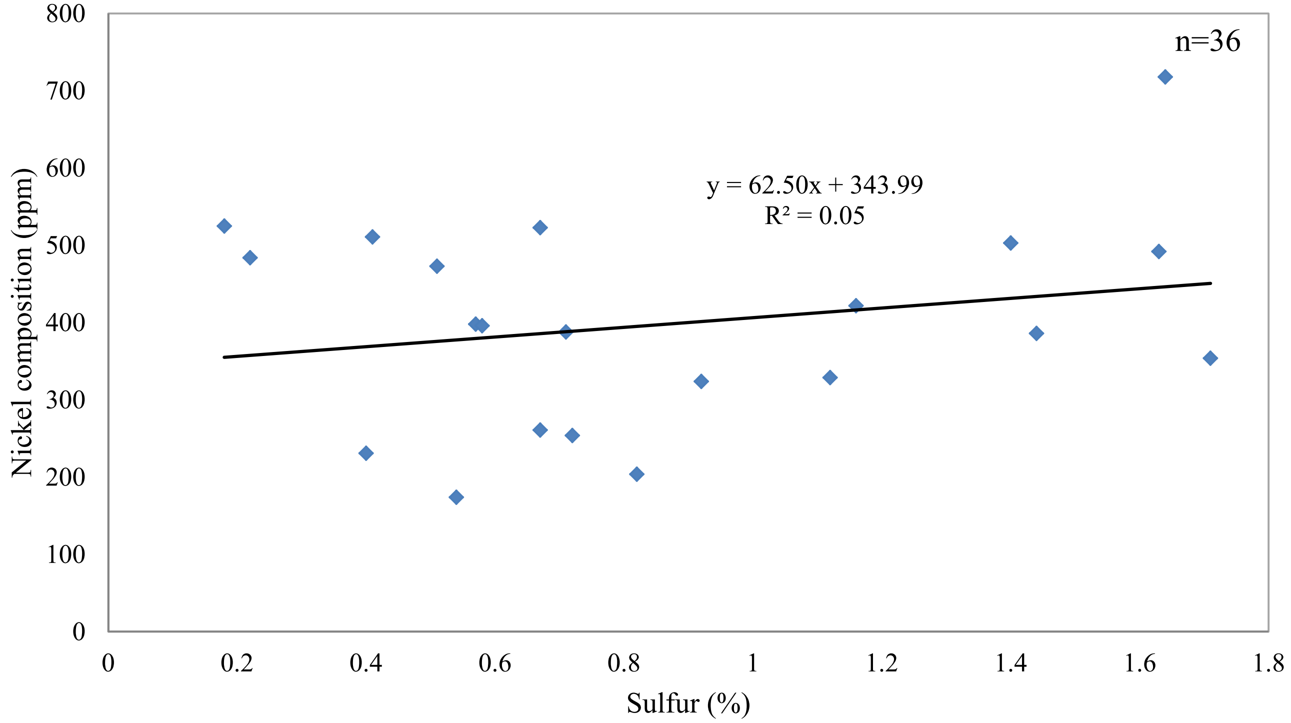

Figure 47. Zinc composition vs. % sulfur for unleached solids

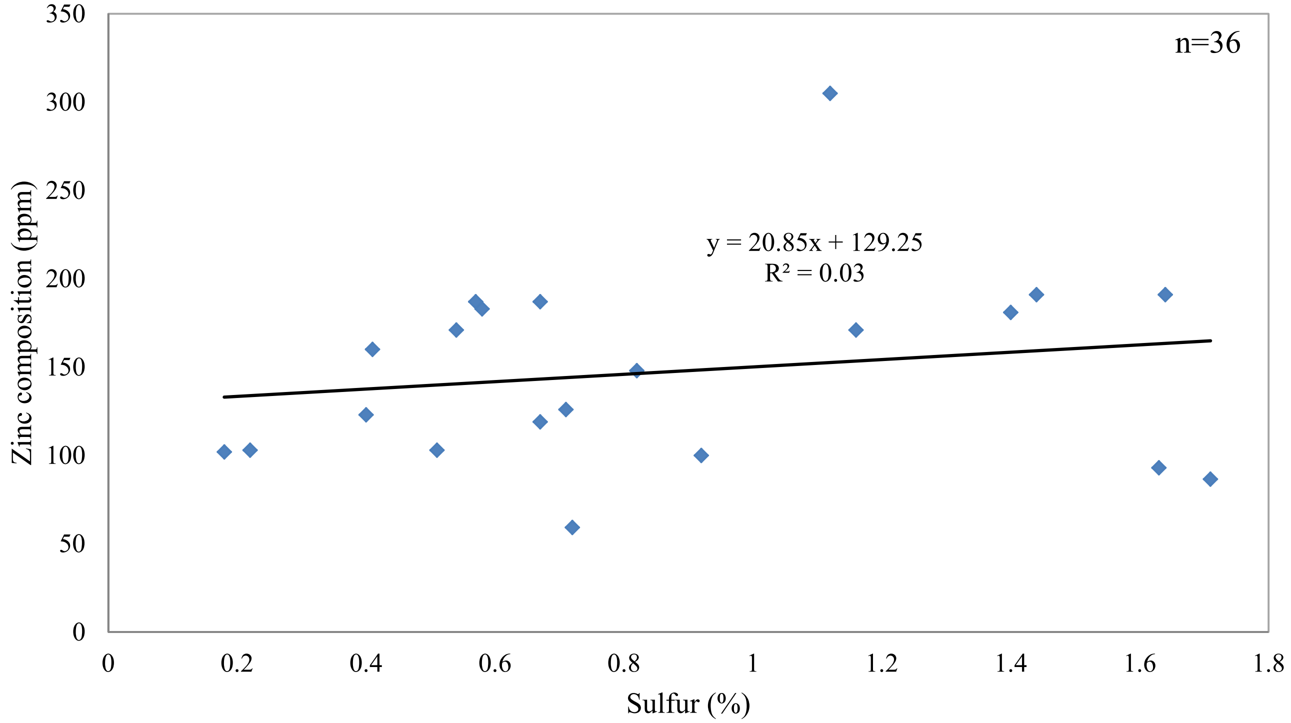

Figure 48. Cobalt concentration vs. minimum pH for all Duluth Complex samples. Metal concentrations plotted are those closest to the week of minimum pH.

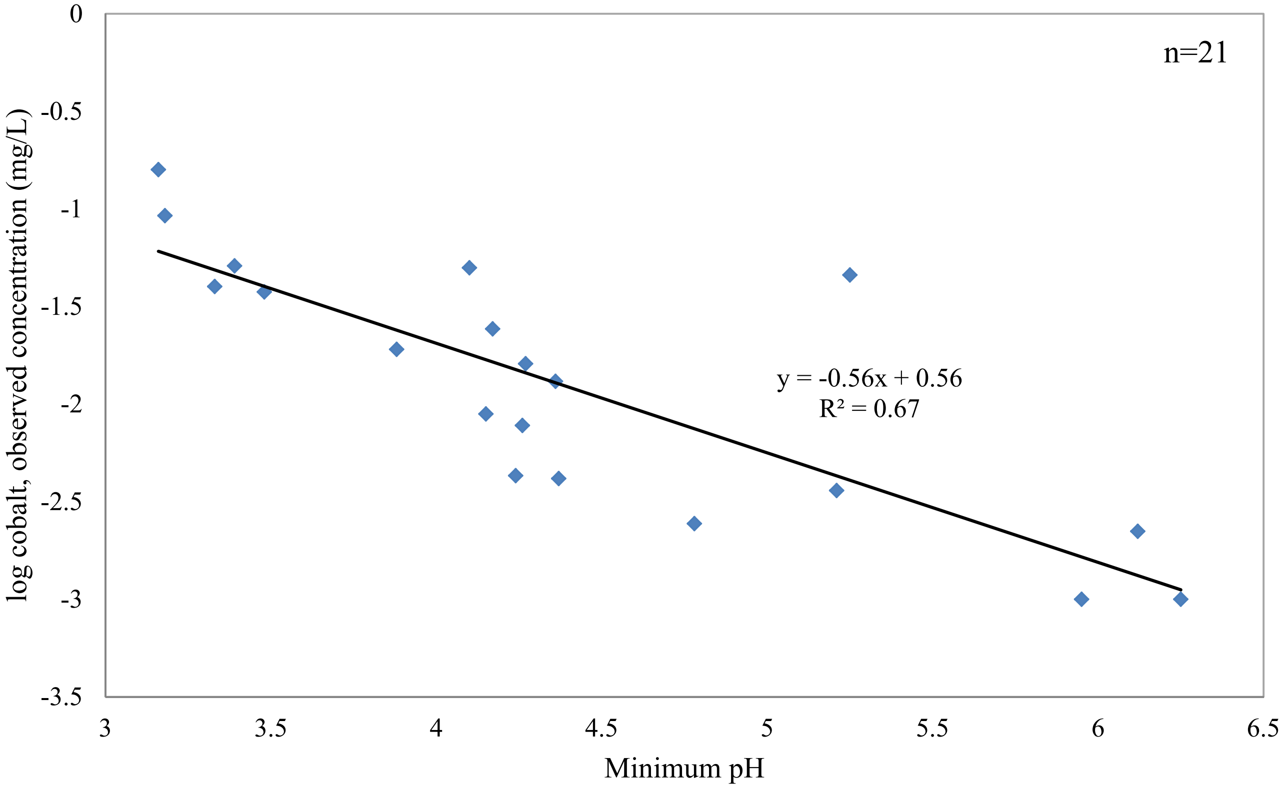

Figure 49. Copper concentration vs. minimum pH for all Duluth Complex samples. Metal concentrations plotted are those closest to the week of minimum pH.

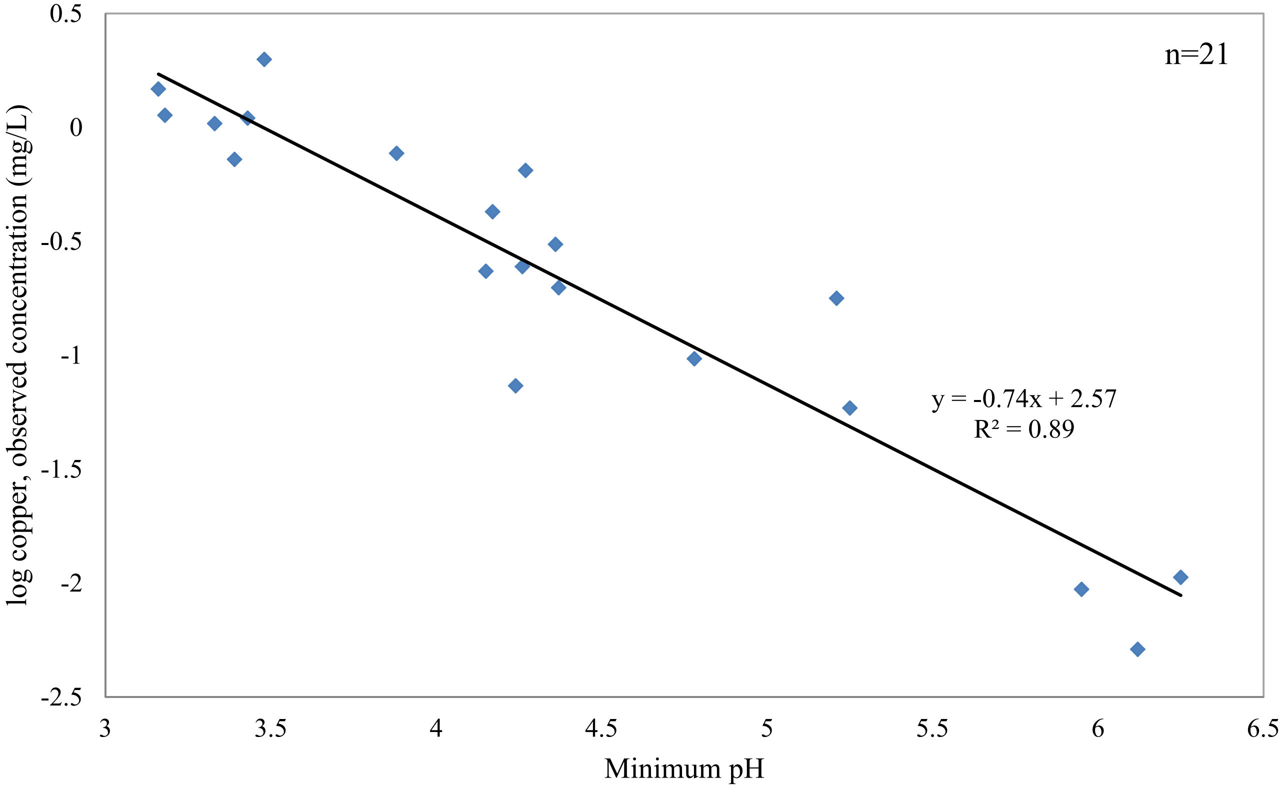

Figure 50. Nickel concentration vs. minimum pH for all Duluth Complex samples. Metal concentrations plotted are those closest to the week of minimum pH.

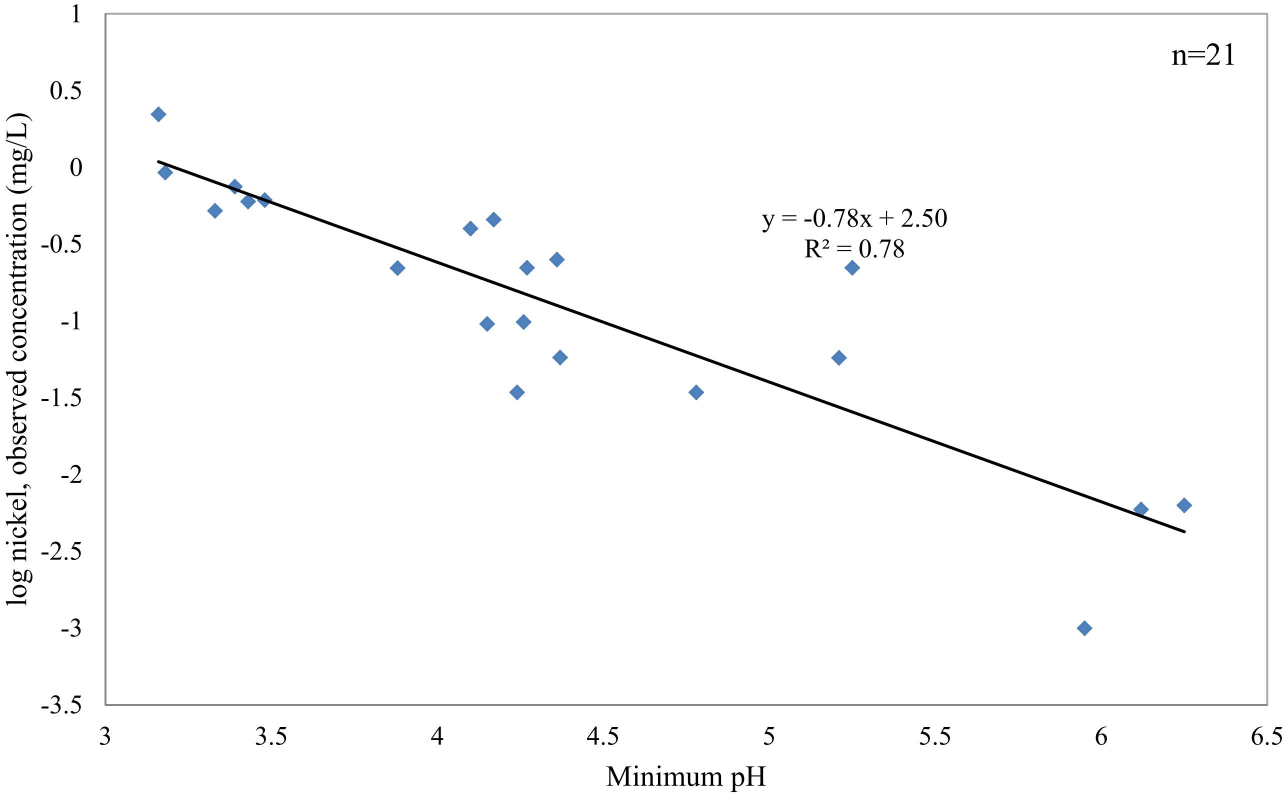

Figure 51. Zinc concentration vs. minimum pH for all Duluth Complex samples. Metal concentrations plotted are those closest to the week of minimum pH.

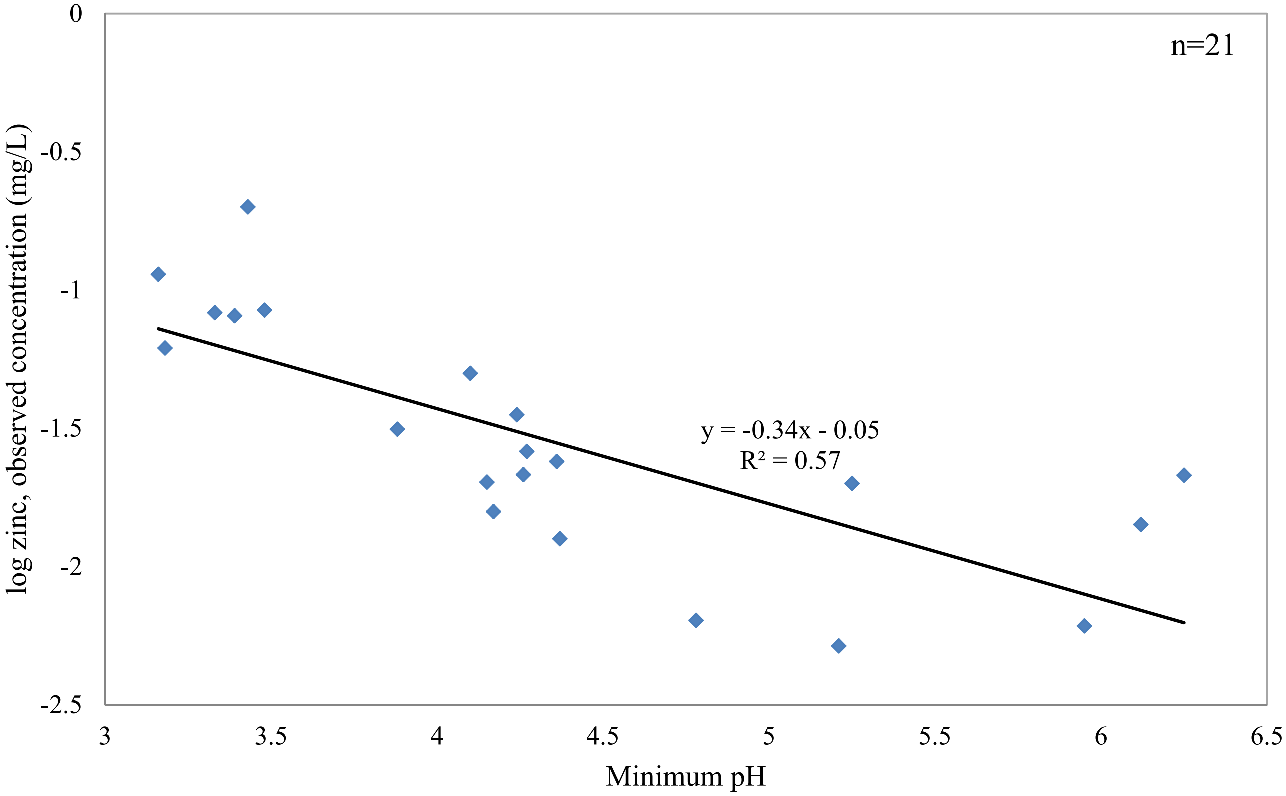

Figure 52. Iron release rate vs. drainage pH, all Duluth Complex samples, entire period of record.

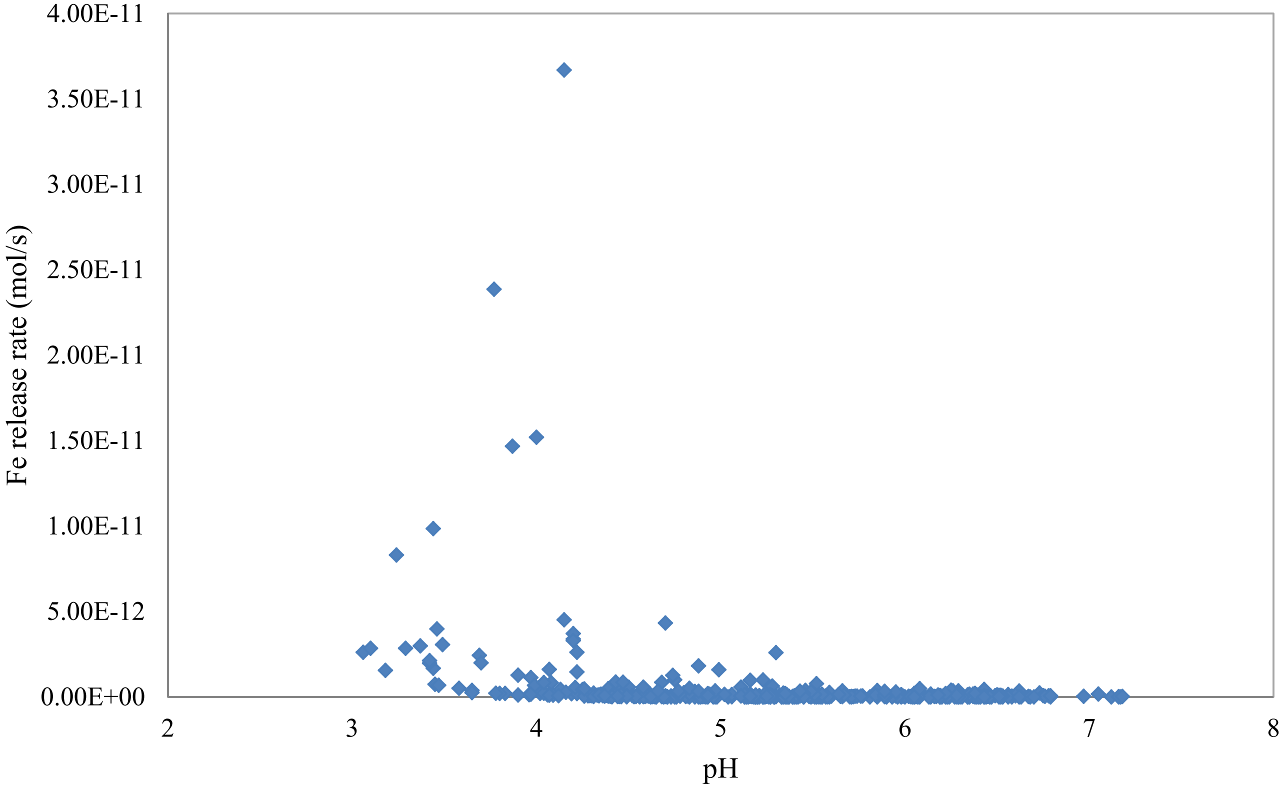

Figure 53. Aluminum release rate vs. drainage pH, all Duluth Complex samples, entire period of record.

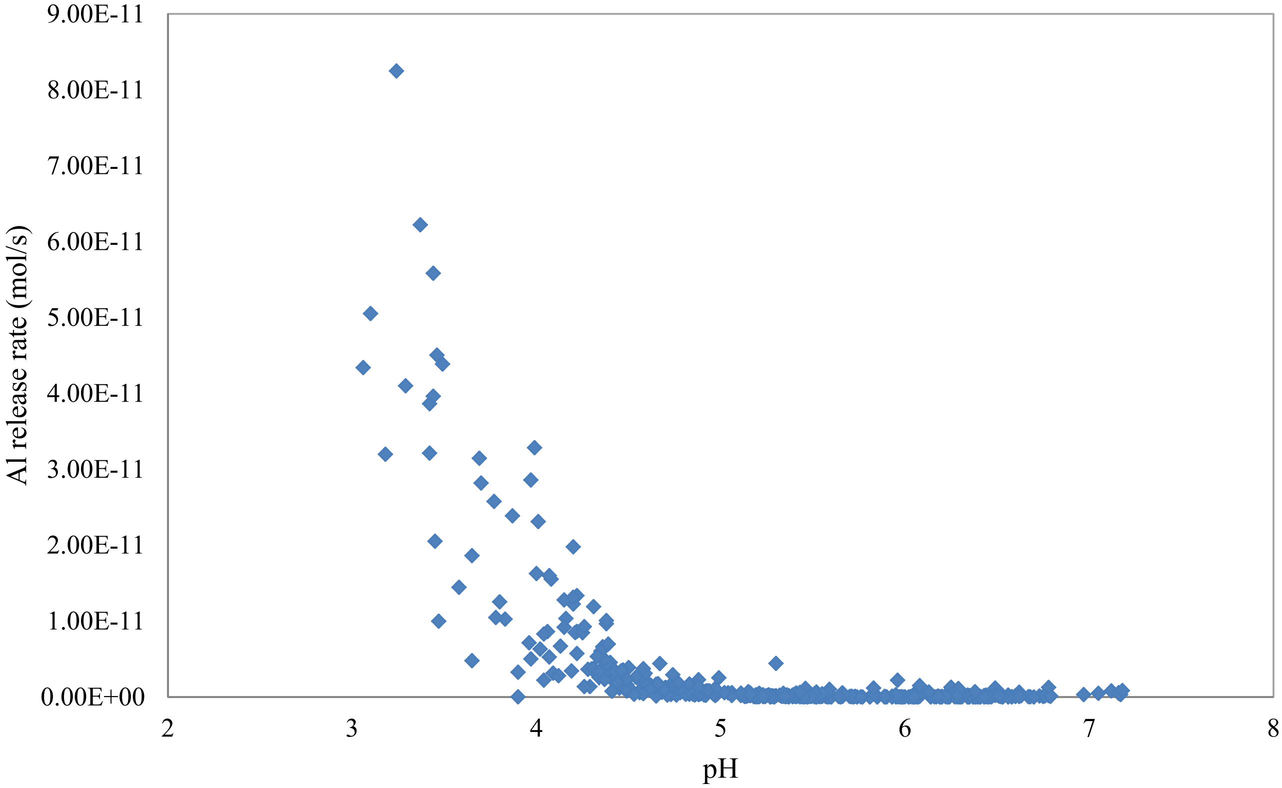

Figure 54. Silicon release rate vs. drainage pH, all Duluth Complex samples, entire period of record.

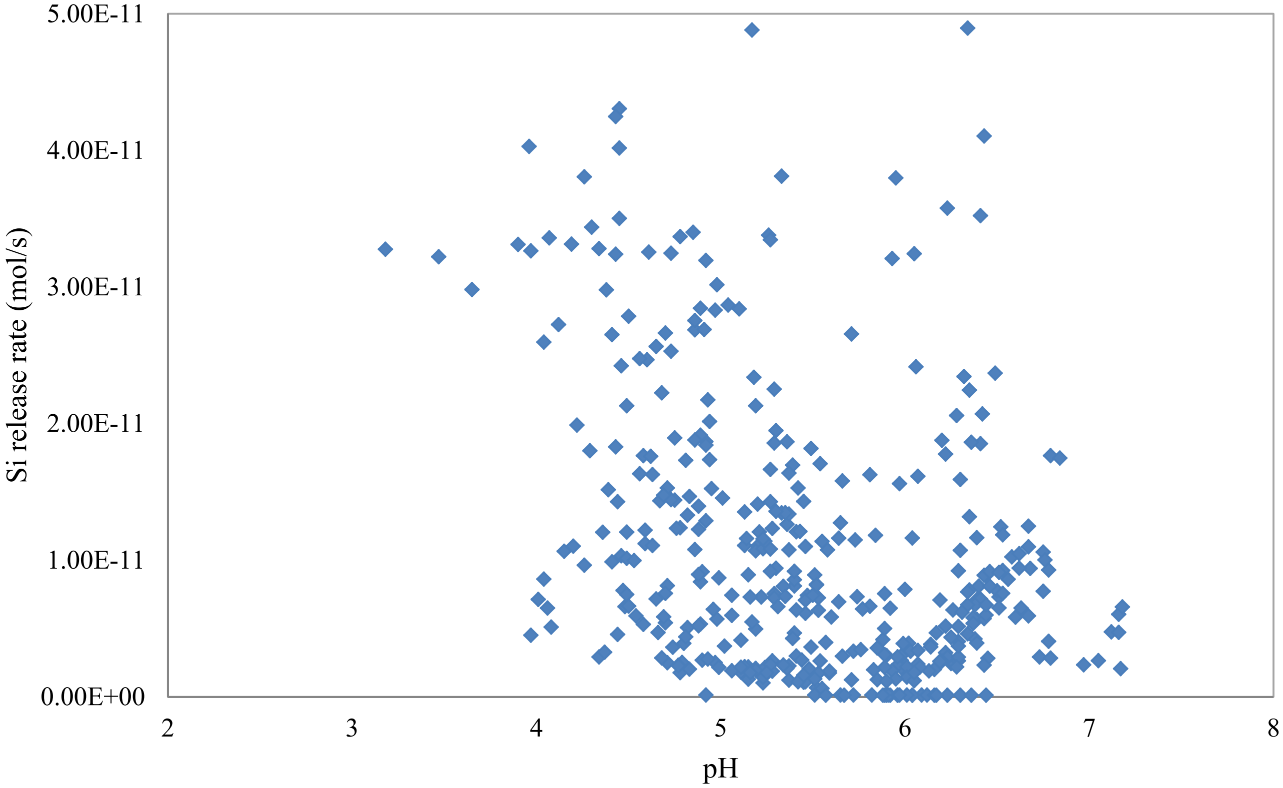

Figure 55. 0.58%S unleached sample (reactors 15 and 16).

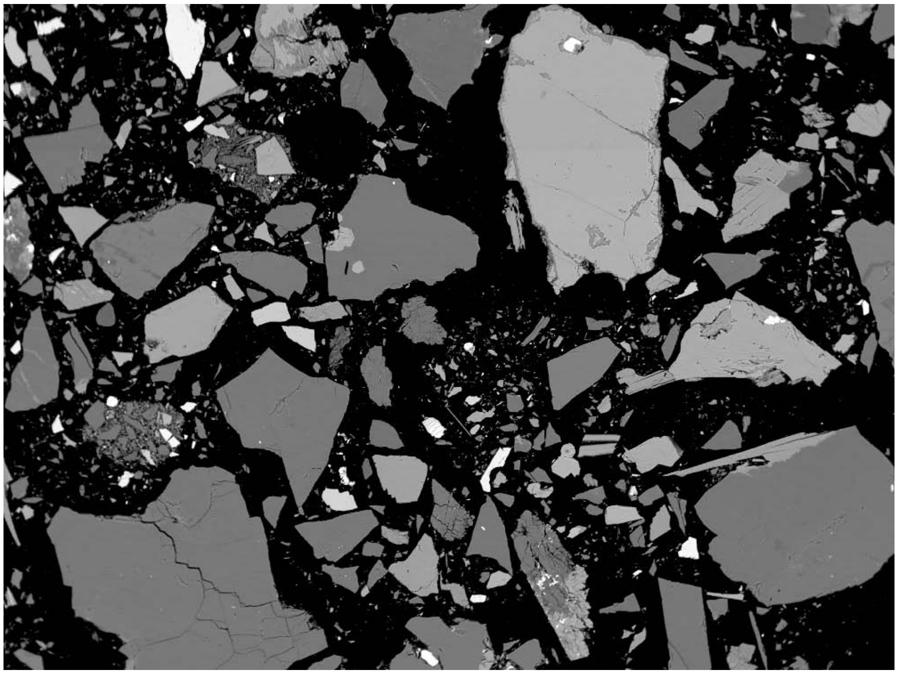

Figure 56. 0.58%S leached sample (reactor 16).

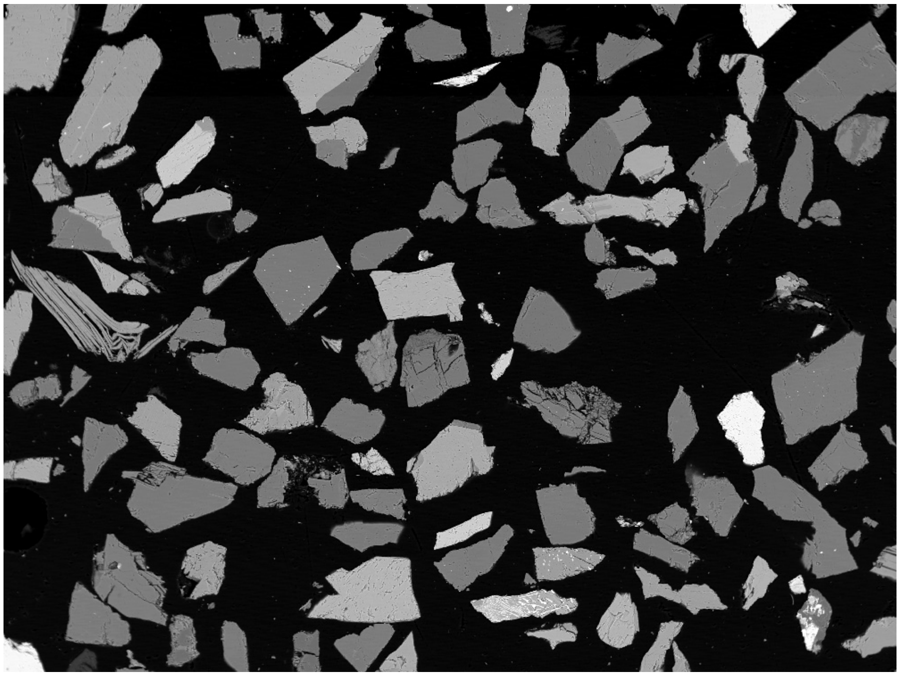

Figure 57. Small particles adhering to mineral grain surfaces as shown by comparison of washed and unwashed grains form unleached (upper) and leached (lower) samples.

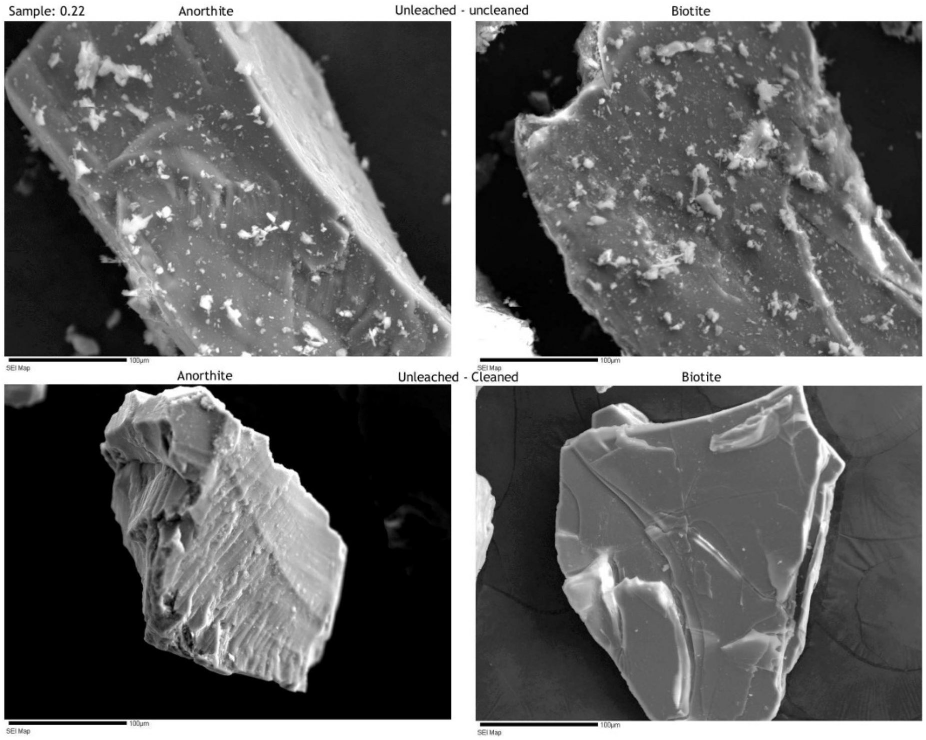

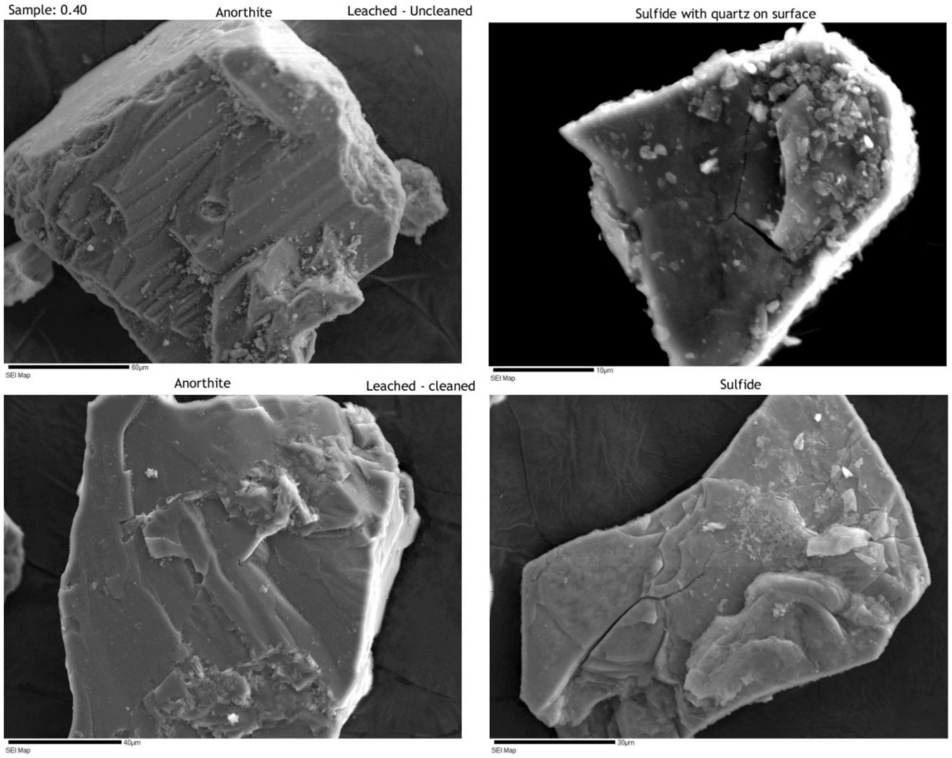

Figure 58. Pyrrhotite grain highly oxidized (dark area, 0.40%S leached sample).

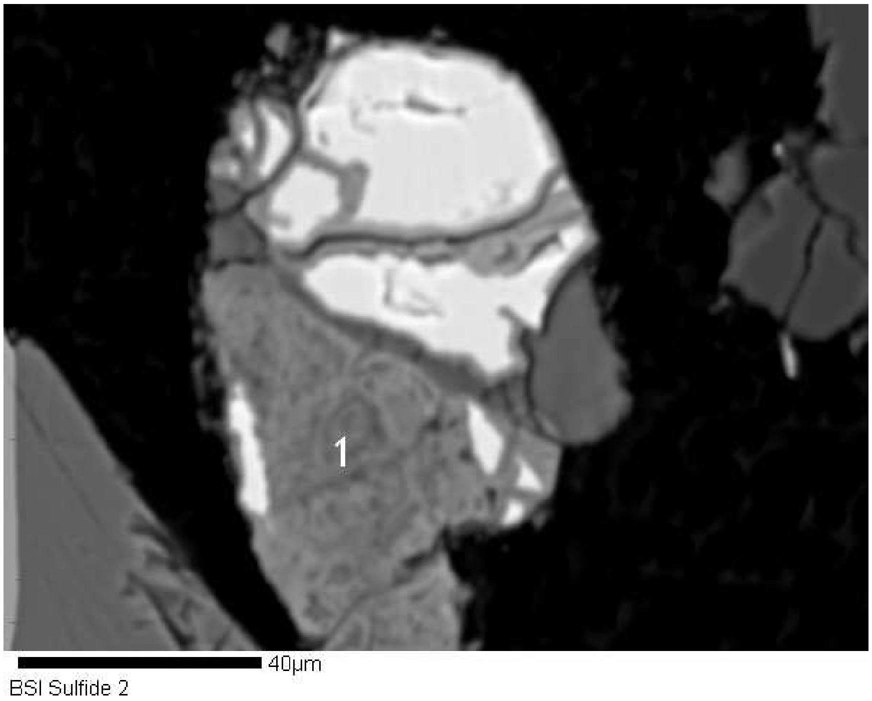

Figure 59. Chalcopyrite grain with thin coating and little oxidation (0.41%S leached sample).

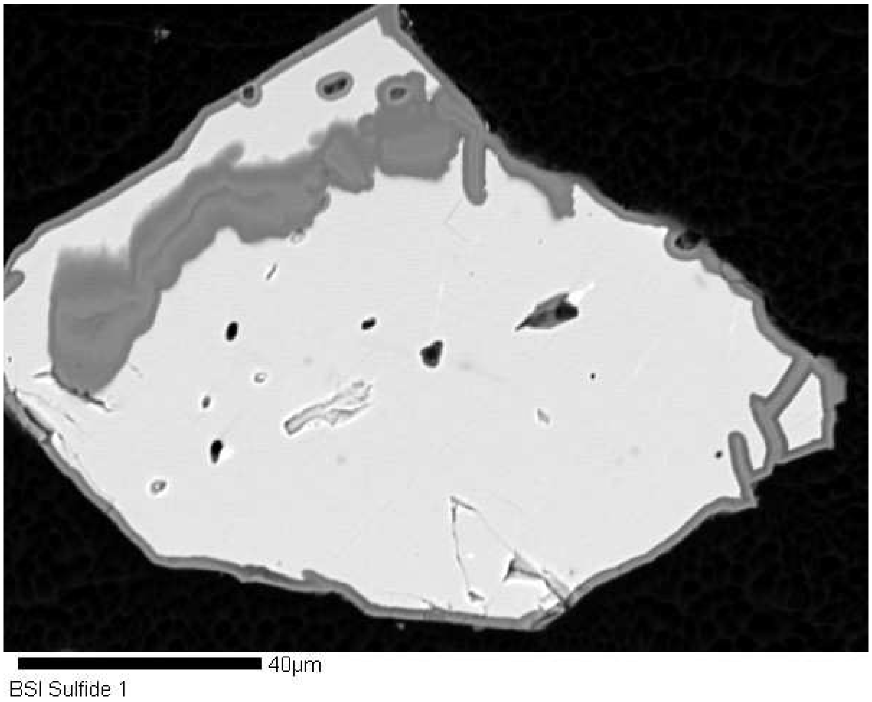

Figure 60. Potential percentage error in point counts. With the number of grains measured in this report (~100), the visual point count method has a 2-σ error level (86.5% confidence) that makes it possible that true values of mineral abundance under 10% could be 60-100% different from estimates. Samples with no grains of a certain mineral detected could have as much as 2% of the sample present as the undetected mineral grains

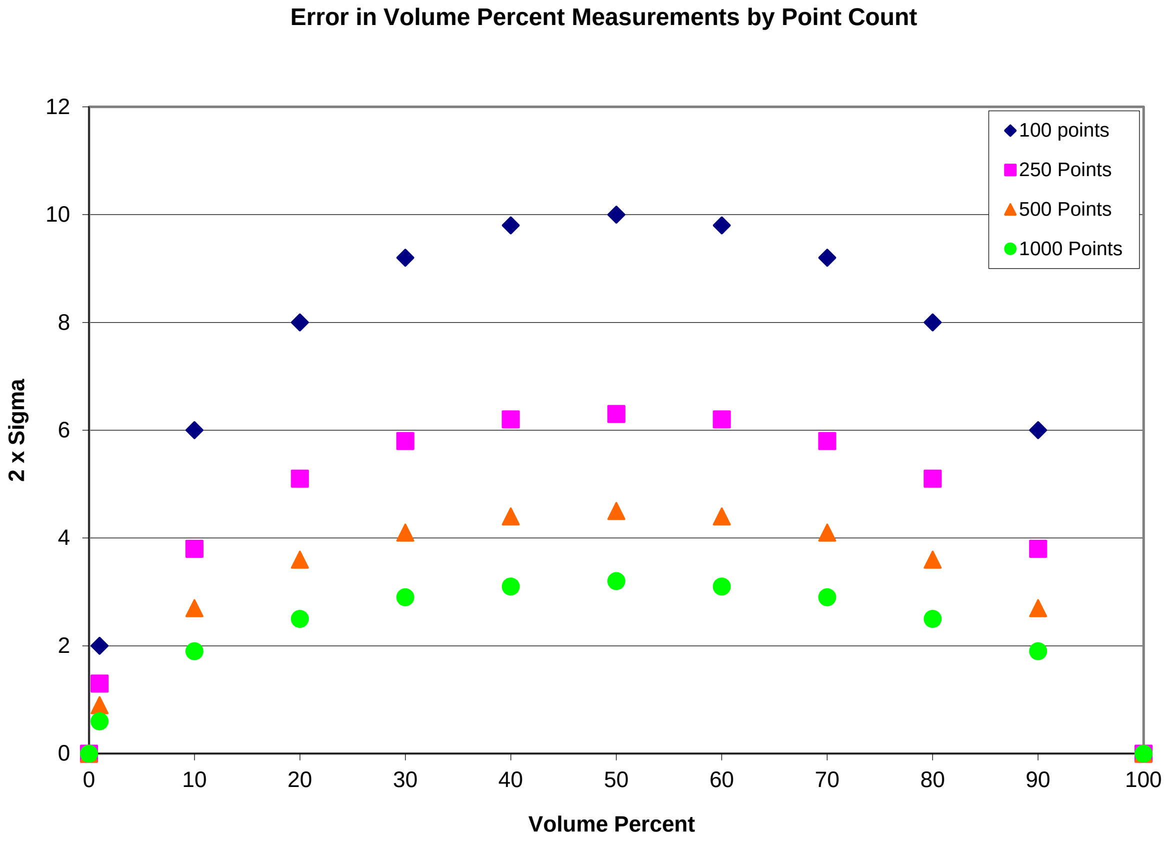

Figure 61. Comparison of neutralization potential calculations for Dunka blast hole samples.

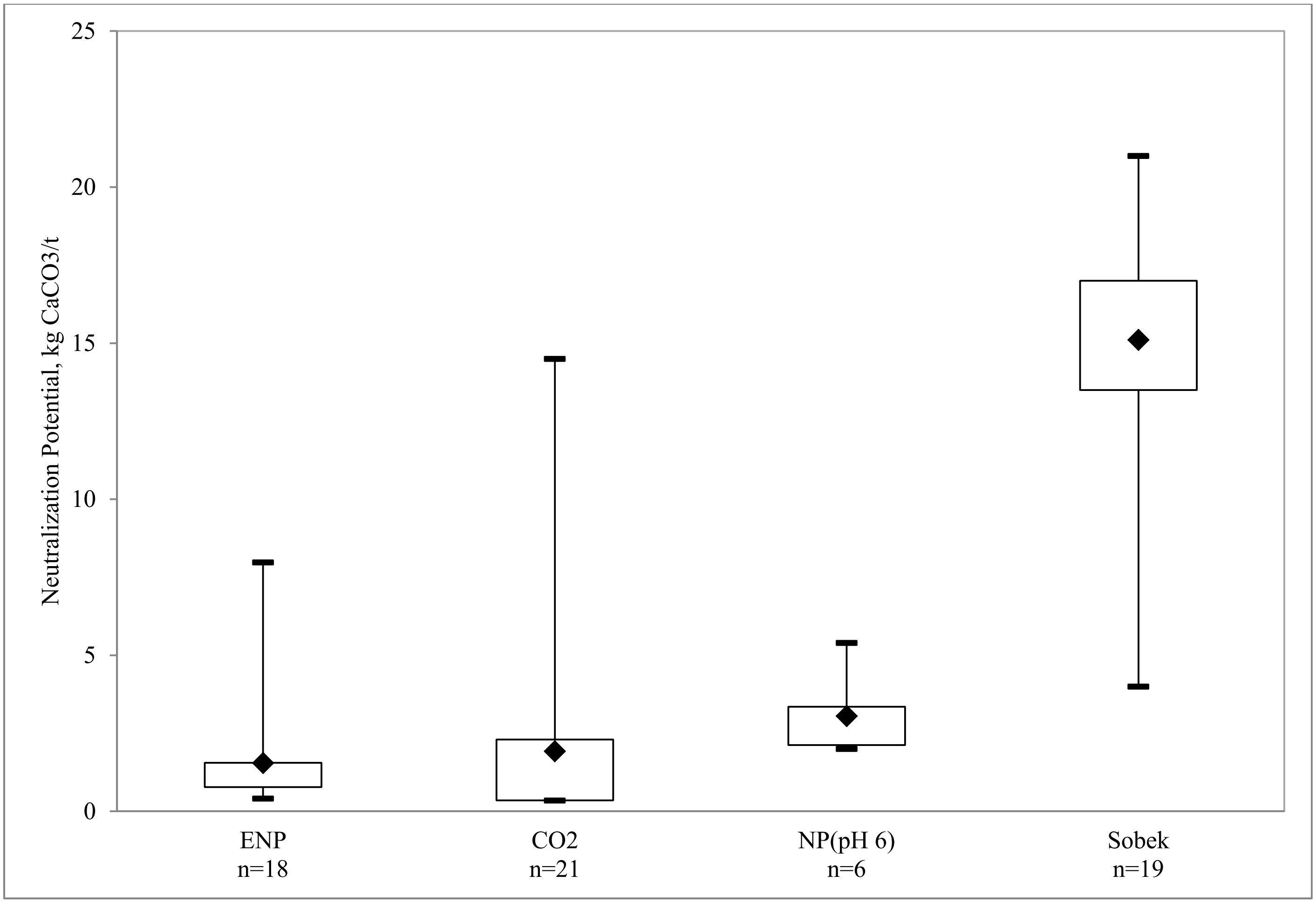

Figure 62. Ratio of calculated: observed nickel release from olivine vs sulfur content. Good correlation with data in periods C and D.

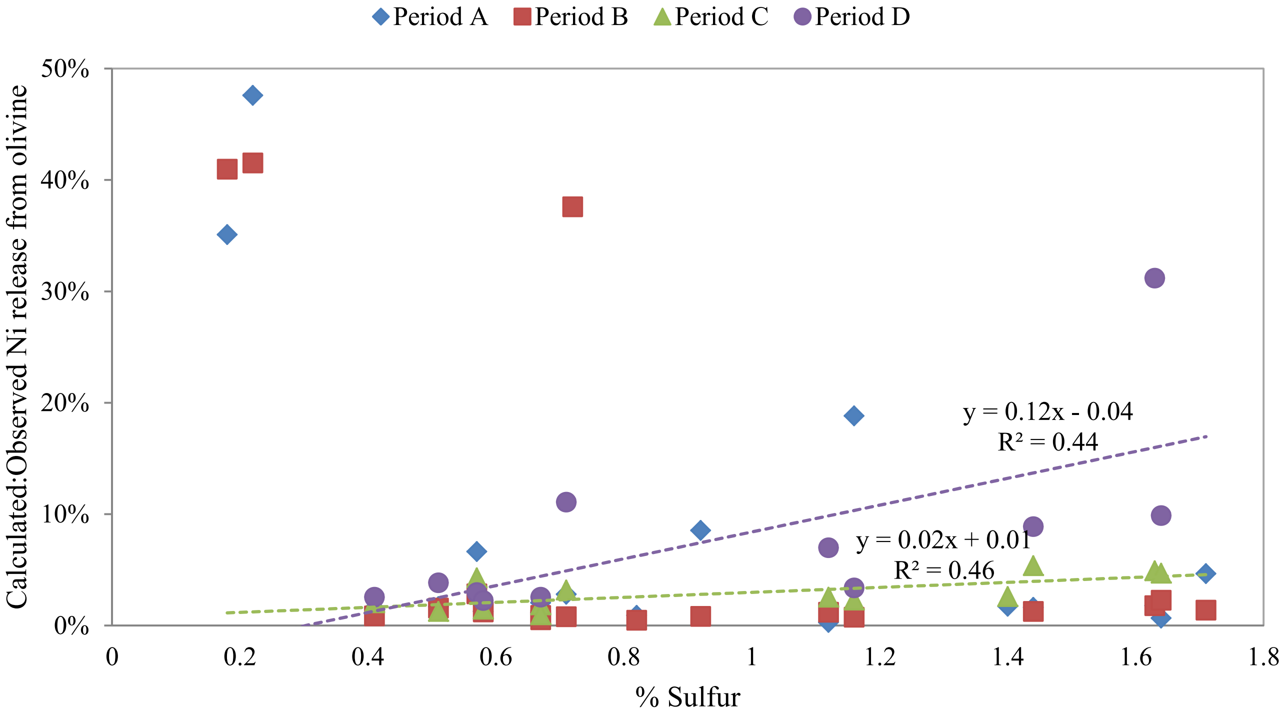

Figure 63. Moles of Nickel / moles of olivine / week vs sulfur content. Good correlation with data in periods B and C.

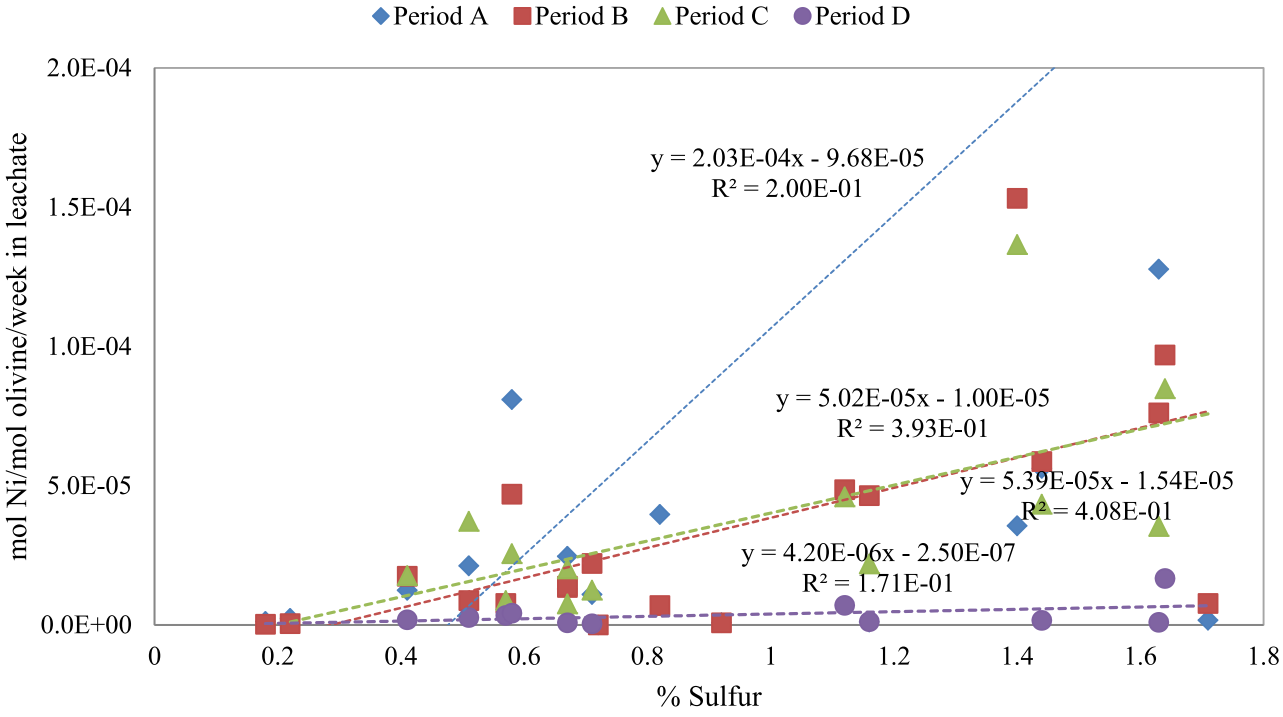

PAGE INTENTIONALLY LEFT BLANK

Figure 64. Ratio of predicted Ni release (based on leachate sulfate) to observed Ni release at days when Ni was sampled. Data for lower dNi/dt are inset.

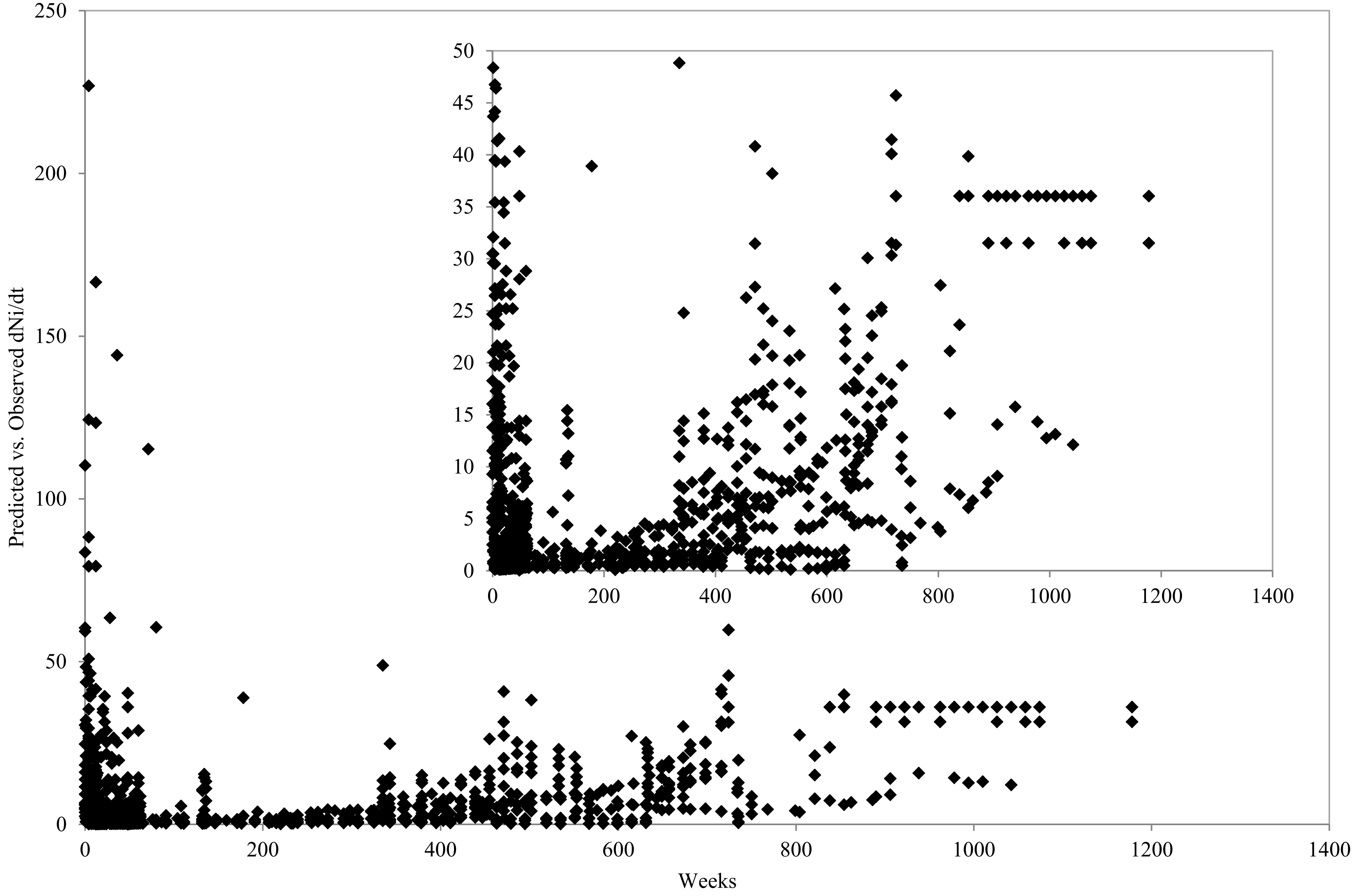

Figure 65. Cumulative probability distribution for ratio of predicted Ni release (based on leachate sulfate) to observed Ni release at days when Ni was sampled. Data compares ratios for each rate period and overall.

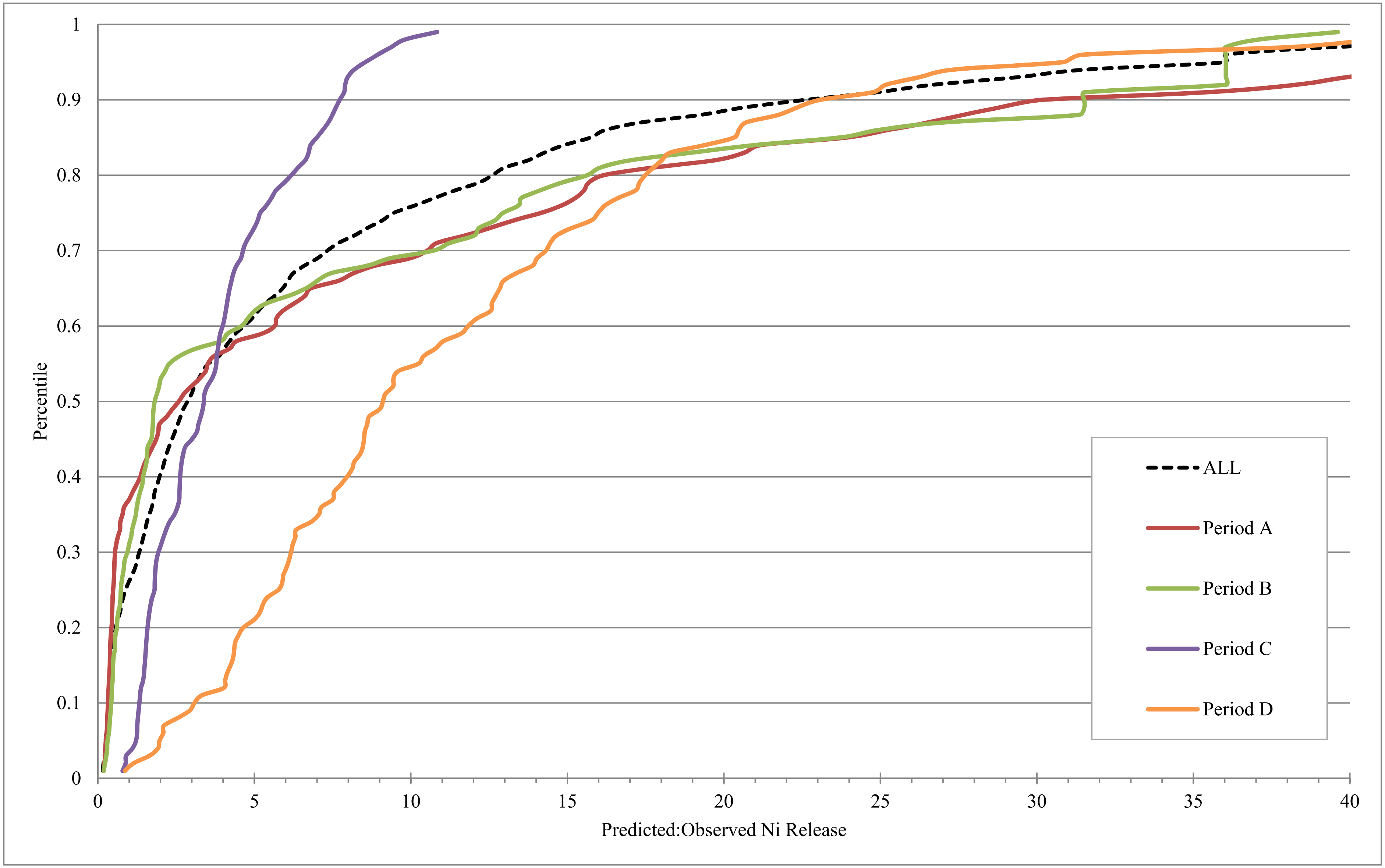

Figure 66. Model illustrating the sequence of oxidation products at the surface of pyrrhotite. Lower panels are at later times. Taken from Belzile et al. 2004.

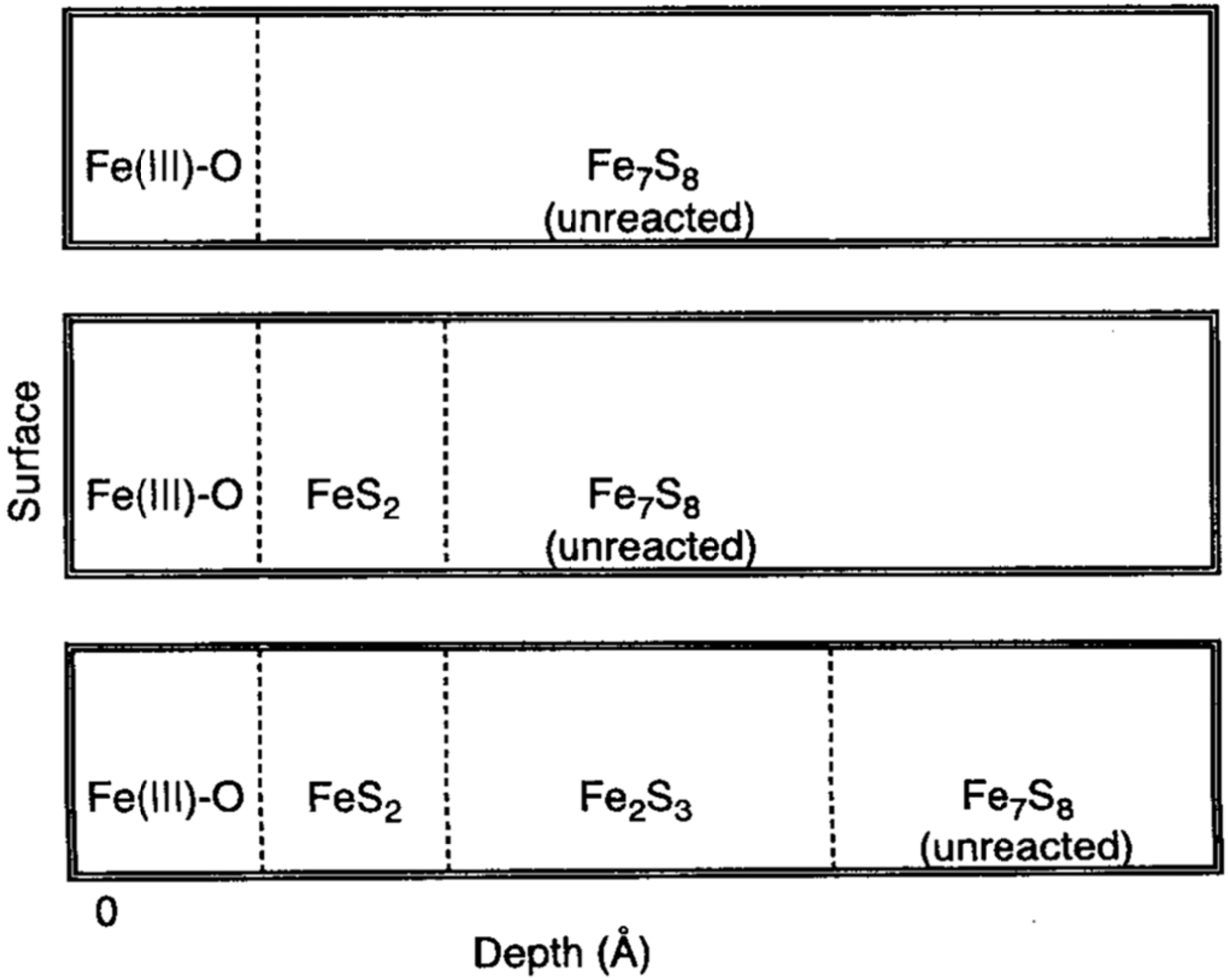

Figure 67. Comparison of modeled pyrrhotite oxidation rates with literature values (excludes R39-44). Calculated pyrrhotite oxidation rates were typically within 1 standard error of the average presented by Janzen et al. (2000). The solid horizontal line represents the mean of 12 reported values and the dashed lines represent one S.E. from the mean. Overall the reported range was from 8.2 x 10^{-12} to 5.9 x 10^{-10} mol m^{-2} s^{-1}.

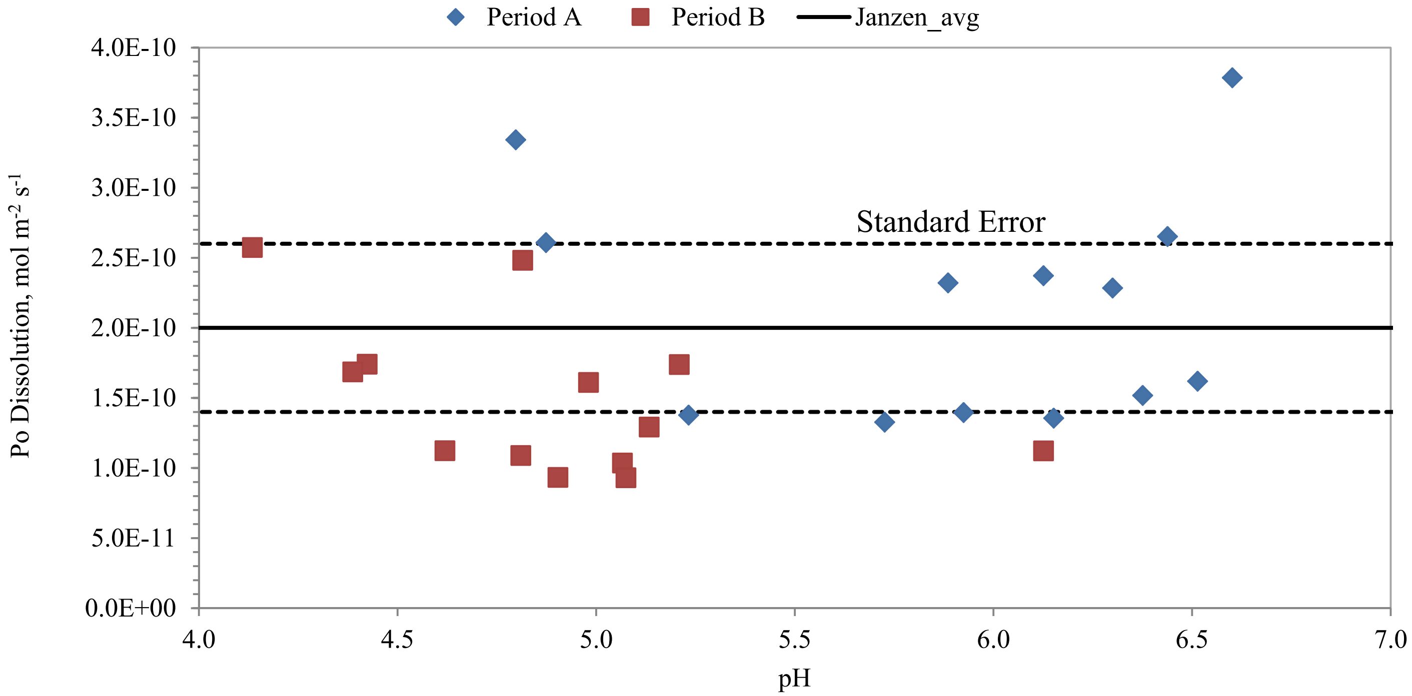

R#	%S	Period A			Period B		
		weeks	Avg pH	Ave po	weeks	Avg pH	Ave po
1[1]	0.18	1-137	6.90	N/A	138-1252	6.42	N/A
3[2]	0.22	1-134	6.91	1.3E-08	135-1252	6.51	3.1E-09
5	0.4	1-140	6.60	3.8E-10	141-769	6.13	1.1E-10
7	0.41	1-129	6.51	1.6E-10	130-351	5.13	1.3E-10
9	0.51	1-140	6.30	2.3E-10	141-277	5.07	1.0E-10
11	0.54	1-137	6.13	2.4E-10	138-278	4.98	1.6E-10
13	0.57	1-103	6.44	2.7E-10	104-294	5.21	1.7E-10
15	0.58	1-101	5.89	2.3E-10	102-217	4.82	2.5E-10
17	0.71	1-100	6.15	1.4E-10	101-274	5.08	9.3E-11
35	1.12	1-127	4.87	2.6E-10	128-214	4.13	2.6E-10
29	1.16	1-38	6.38	1.5E-10	39-189	4.62	1.1E-10
37	1.40	1-74	5.93	1.4E-10	75-209	4.81	1.1E-10
33	1.44	1-76	5.23	1.4E-10	77-212	4.42	1.7E-10
19	1.63	1-66	5.73	1.3E-10	67-155	4.90	9.3E-11
31	1.64	1-64	4.80	3.3E-10	65-228	4.39	1.7E-10

[1] Reactor 1 calculated to have pyrrhotite content less than zero

[2] Data from reactor 3 (0.22%S) omitted from figure due to significantly lower calculated po content

Figure 68. Comparison of plagioclase dissolution rates among models and rate periods (excludes R39-44). See Table 105 for values.

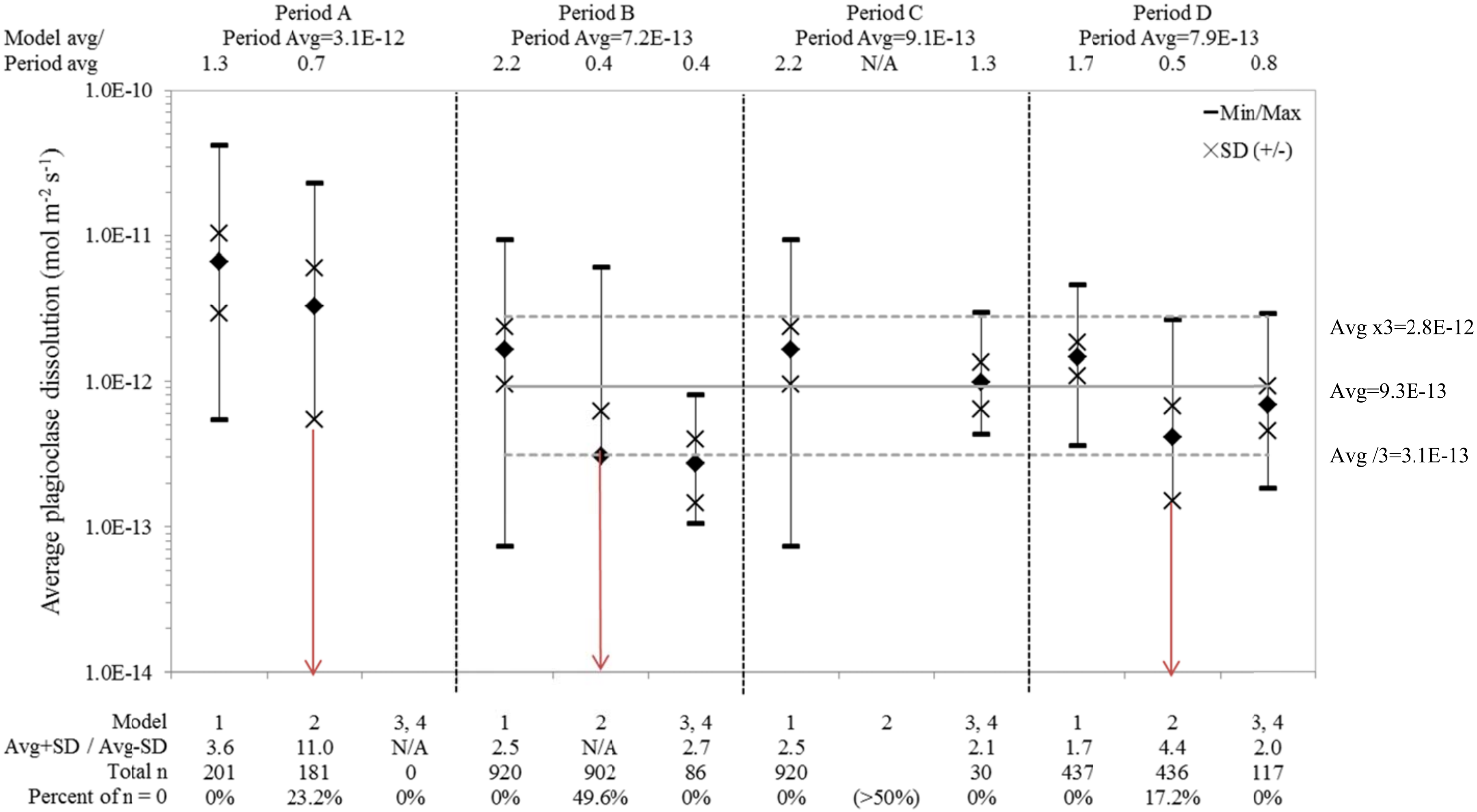

Note: Solid line = average plagioclase dissolution for periods B, C, and D (period A omitted due to initial increase in major cation release). Dashed lines = factor of 3 from average value. Average values from 7 out of 8 model runs during periods B, C, and D were within a factor of 3.

Note: Plagioclase dissolution in Model 1, Period C is calculated in the same manner as Period B. Plagioclase dissolution in Model 4 is the same as in Model 3, and therefore not included in average calculation.

Note: Zero values were calculated in model 2 (17-50% of total values), indicating a calculated absence of plagioclase dissolution (identified by a red arrow).

Figure 69. Comparison of augite dissolution rates among models and rate periods (excludes R39-44). See Table 105 for values.

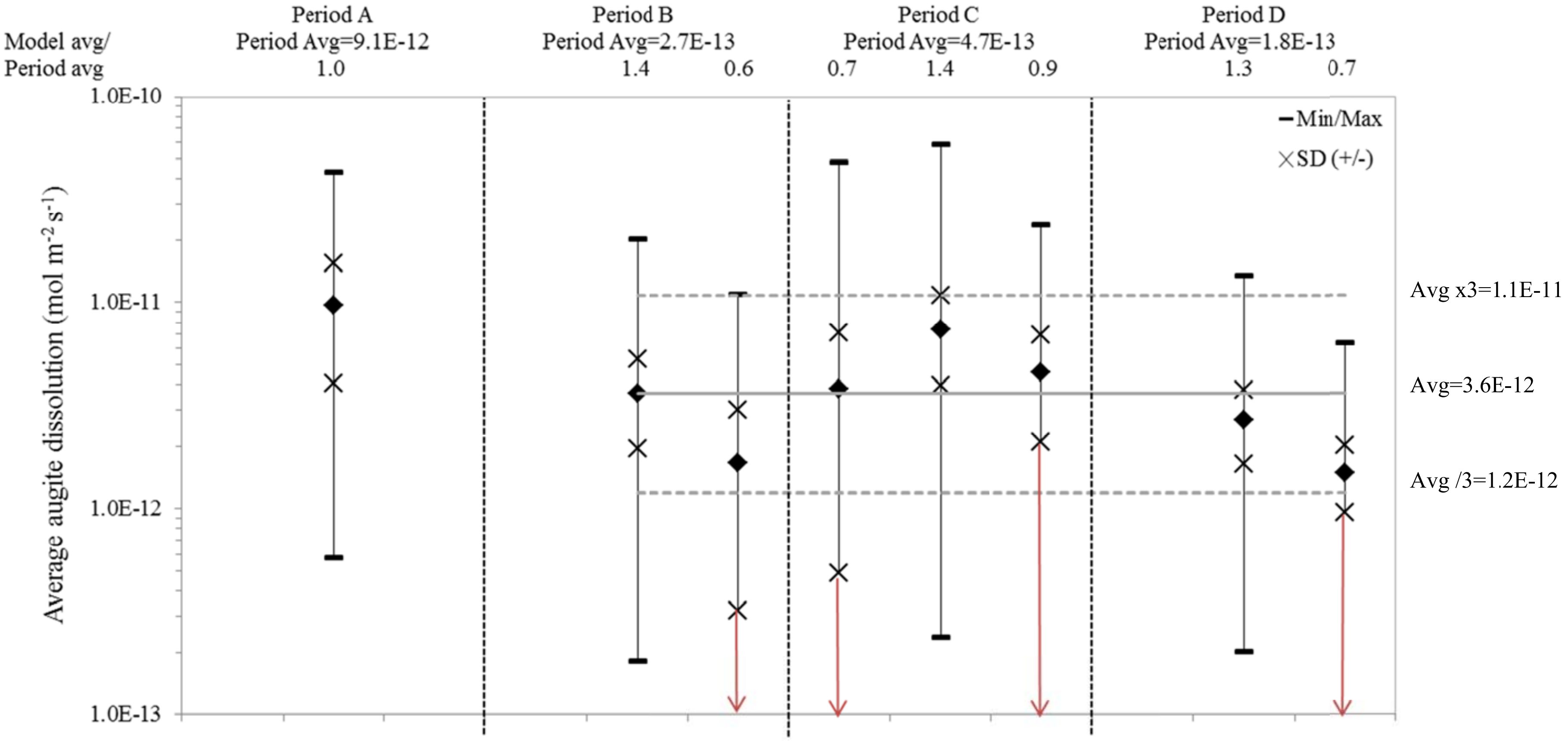

Model	1	2	3, 4	1	2	3, 4	1	2	3, 4	1	2	3, 4
Avg+SD / Avg-SD	N/A	3.8	N/A	N/A	2.7	9.4	14.7	2.7	3.3	N/A	2.3	2.1
Total n	0	201	0	0	920	86	462	462	30	0	437	117
Percent of n = 0	0%	0%	0%	0%	0%	1.2%	18.4%	0%	3.3%	0%	0%	5.1%

Note: Solid line = average augite dissolution for periods B, C, and D (period A omitted due to initial increase in major cation release). Dashed lines = factor of 3 from average value. Average values from all model runs during periods B, C, and D were within a factor of 3.

Note: Augite dissolution in Model 4 is the same as in Model 3, and therefore not included in average calculation.

Note: Range in average dissolution rates with no lower tail occurred when the average – standard deviation < 0.

Note: Zero values were calculated in model 1 (18% of total values) and models 3, 4 (1-5% of total values), indicating a calculated absence of augite dissolution (identified by a red arrow).

Figure 70. Comparison of hypersthene dissolution rates among models and rate periods (excludes R39-44). See Table 105 for values.

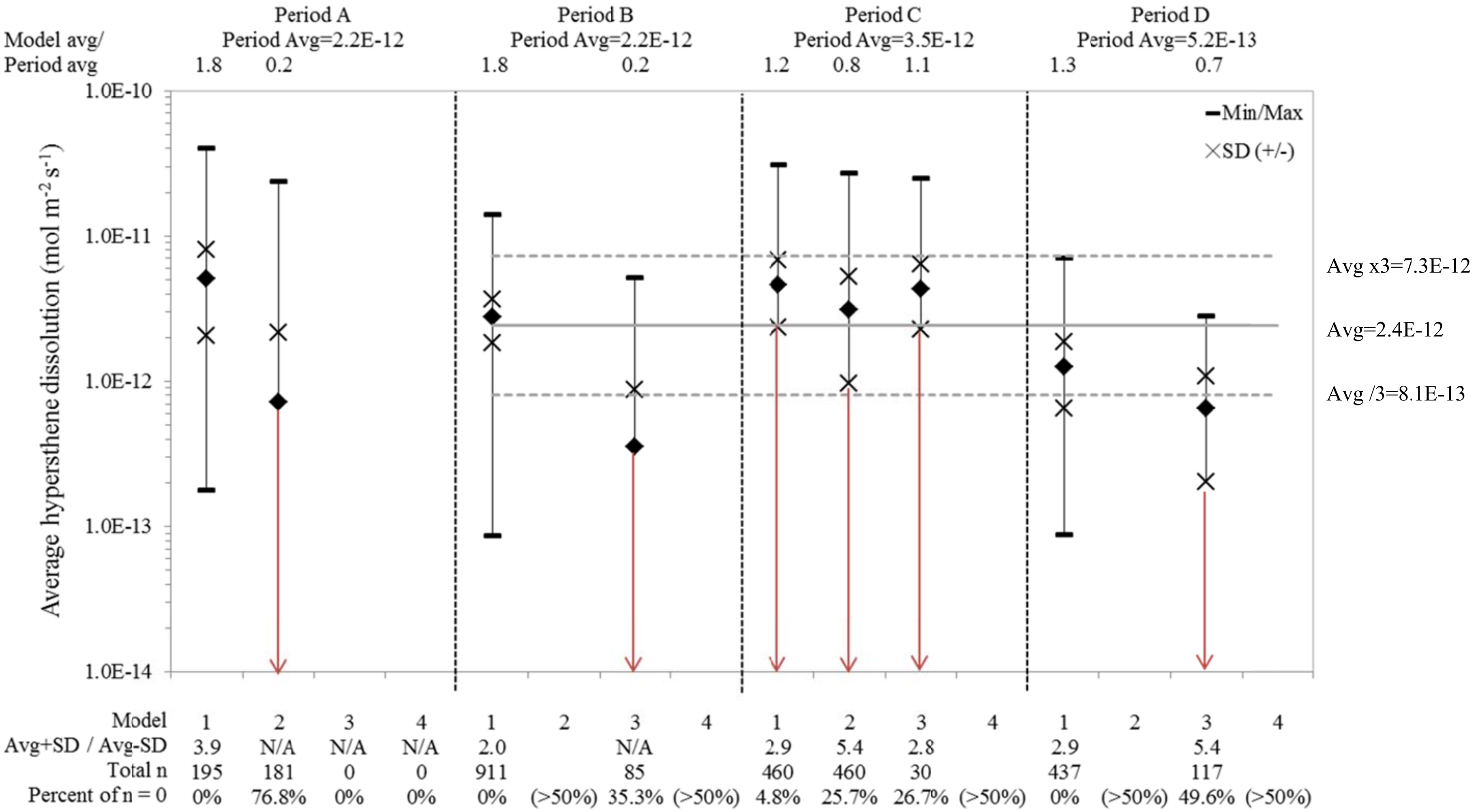

Note: Solid line = average hypersthene dissolution for periods B, C, and D (period A omitted due to initial increase in major cation release). Dashed lines = factor of 3 from average value. Average values from 5 out of 7 model runs during periods B, C, and D were within a factor of 3.

Note: Range in average dissolution rates with no lower tail occurred when the average – standard deviation < 0.

Note: Zero values were calculated in model 2 (26-77% of total values) and model 3 (27-50% of total values) indicating a calculated absence of hypersthene dissolution (identified by a red arrow). Zero values were calculated in model 1, only during period C (5% of the total values).

Figure 71. Comparison of olivine dissolution rates among models and rate periods (excludes R39-44). See Table 105 for values.

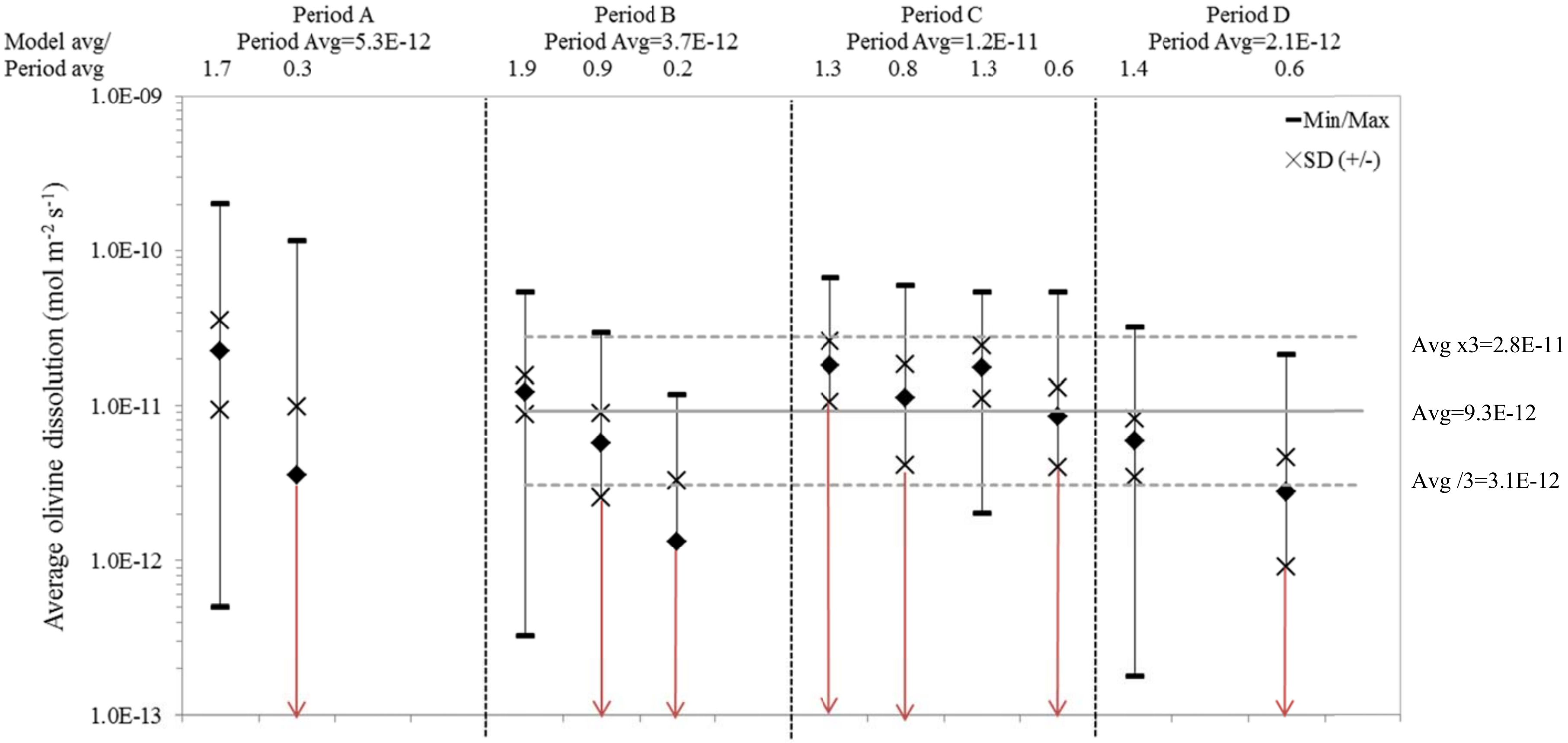

Model	1	2	3	4	1	2	3	4	1	2	3	4	1	2	3	4
Avg+SD / Avg-SD	3.8	N/A	N/A	N/A	1.8	3.5	N/A		2.4	4.5	2.2	3.2	2.4		5.1	
Total n	158	147	0	0	746	738	66		399	399	21	21	428		114	
Percent of n = 0	0%	73.5%	0%	0%	0%	40.7%	19.7%	(>50%)	3.3%	14.3%	0%	42.9%	0%	(>50%)	48.2%	(>50%)

Note: Solid line = average olivine dissolution for periods B, C, and D (period A omitted due to initial increase in major cation release). Dashed lines = factor of 3 from average value. Average values from 7 out of 9 model runs during periods B, C, and D were within a factor of 3.

Note: Range in average dissolution rates with no lower tail occurred when the average – standard deviation < 0.

Note: Zero values were calculated in model 2 (14-74% of total values), model 3 (20-48% of total values), and model 4 (43% of total values) indicating a calculated absence of olivine dissolution (identified by a red arrow). Zero values were calculated in model 1, only during period C (3% of the total values).

Figure 72. Comparison of biotite dissolution rates among models and rate periods (excludes R39-44). See Table 105 for values.

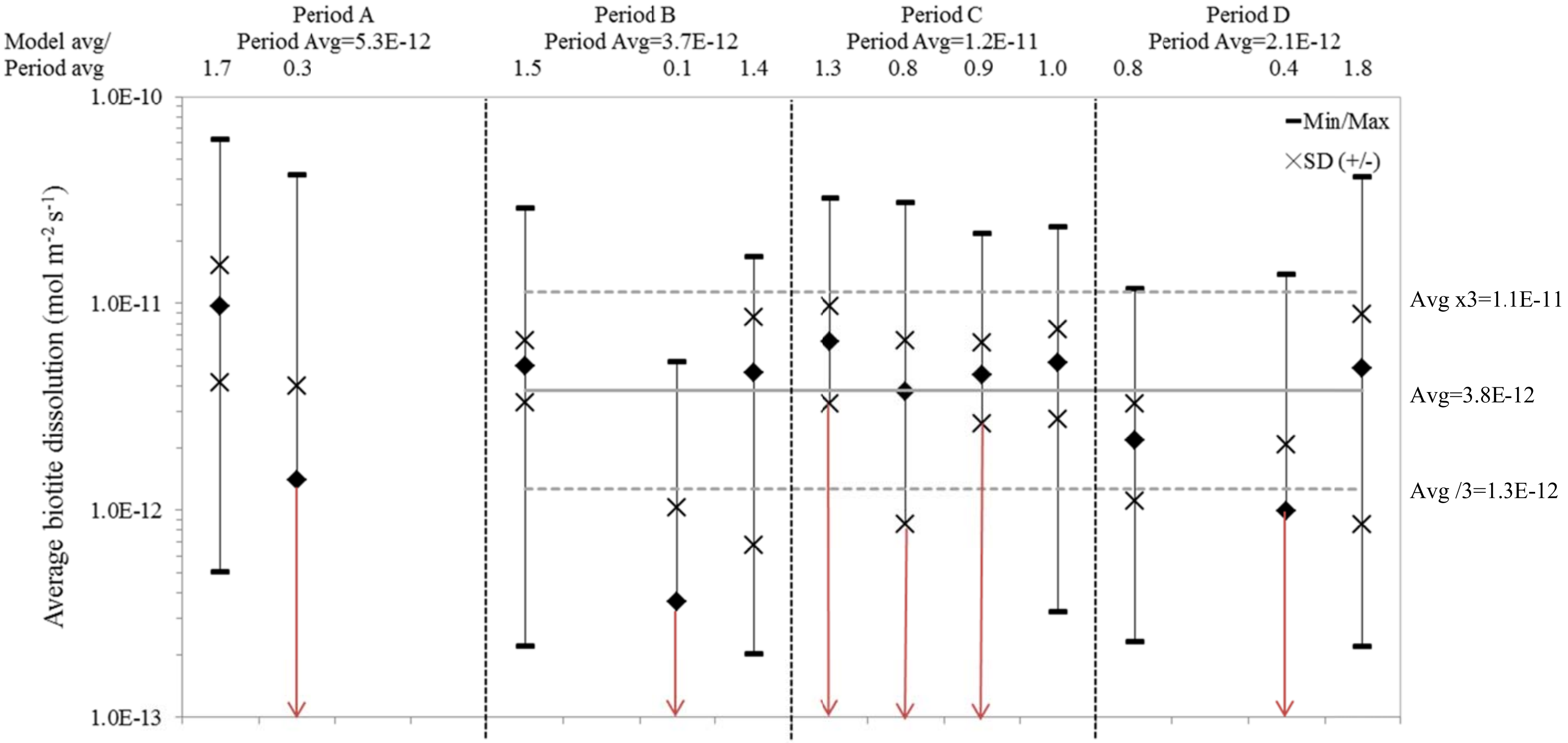

Model	1	2	3	4	1	2	3	4	1	2	3	4	1	2	3	4
Avg+SD / Avg-SD	3.7	N/A	N/A	N/A	1.8		N/A	12.7	3.0	7.8	2.5	2.7	3.0		N/A	10.4
Total n	162	149	0	0	797		85	83	360	360	24	24	368		100	92
Percent of n = 0	0%	74.5%	0%	0%	0%	(>50%)	35.3%	0%	5.8%	31.4%	33.3%	0%	0%	(>50%)	49.0%	0%

Note: Solid line = average biotite dissolution for periods B, C, and D (period A omitted due to initial increase in major cation release). Dashed lines = factor of 3 from average value. Average values from 8 out of 10 model runs during periods B, C, and D were within a factor of 3.

Note: Range in average dissolution rates with no lower tail occurred when the average – standard deviation < 0.

Note: Zero values were calculated in model 2 (31-75% of total values) and model 3 (33-49% of total values) indicating a calculated absence of biotite dissolution (identified by a red arrow). Zero values were calculated in model 1, only during period C (6% of the total values).

Figure 73. Comparison of plagioclase dissolution rates from samples with differing mineralogy.

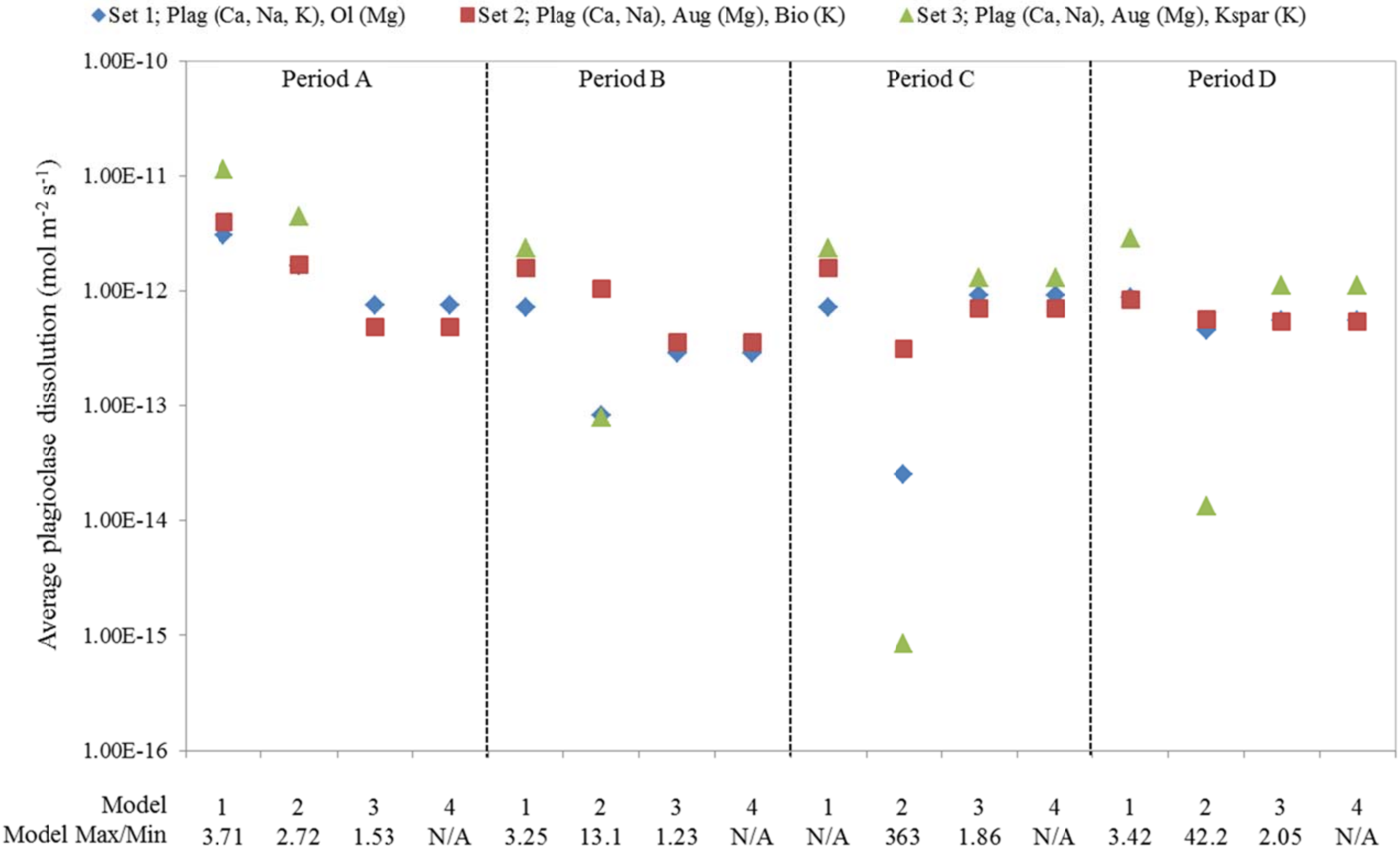

Note: Plagioclase dissolution in Model 1, Period C is the same as Period B. Plagioclase dissolution in Model 4 is the same as in Model 3.

Mineralogical breakdown of cations present (%) for specific samples (see Table U for full mineralogical breakdown)

Set	%S	Reactor	Calcium				Magnesium					Sodium		Potassium			
			Plag	Augite	Prehnite	Amphibole	Augite	Hyper	Olivine	Biotite	Amphibole	Plag	K-Spar	Plag	Biotite	K-Spar	Amphibole
1	0.72	42	94.09	5.91			4.90	10.17	84.93			100.00		100.00			
	1.16	29	76.36	23.64			17.72	31.30	50.98			100.00		100.00			
2	0.67	40	68.15	31.85			25.90	44.55	15.03	14.52		99.44	0.56	15.02	68.73	16.25	
	0.82	43	66.52	33.48			29.18	52.09	11.23	7.50		100.00		33.24	66.76		
3	1.40	37	60.97	29.45	8.15	1.44	34.57	33.96	29.37		2.10	97.59	2.41	30.83		67.72	1.45
	1.64	31	61.29	35.95	2.76		36.46	41.43	13.93	8.18		97.39	2.61	15.08	23.74	61.18	

Figure 74. Comparison of augite dissolution rates from samples with differing mineralogy.

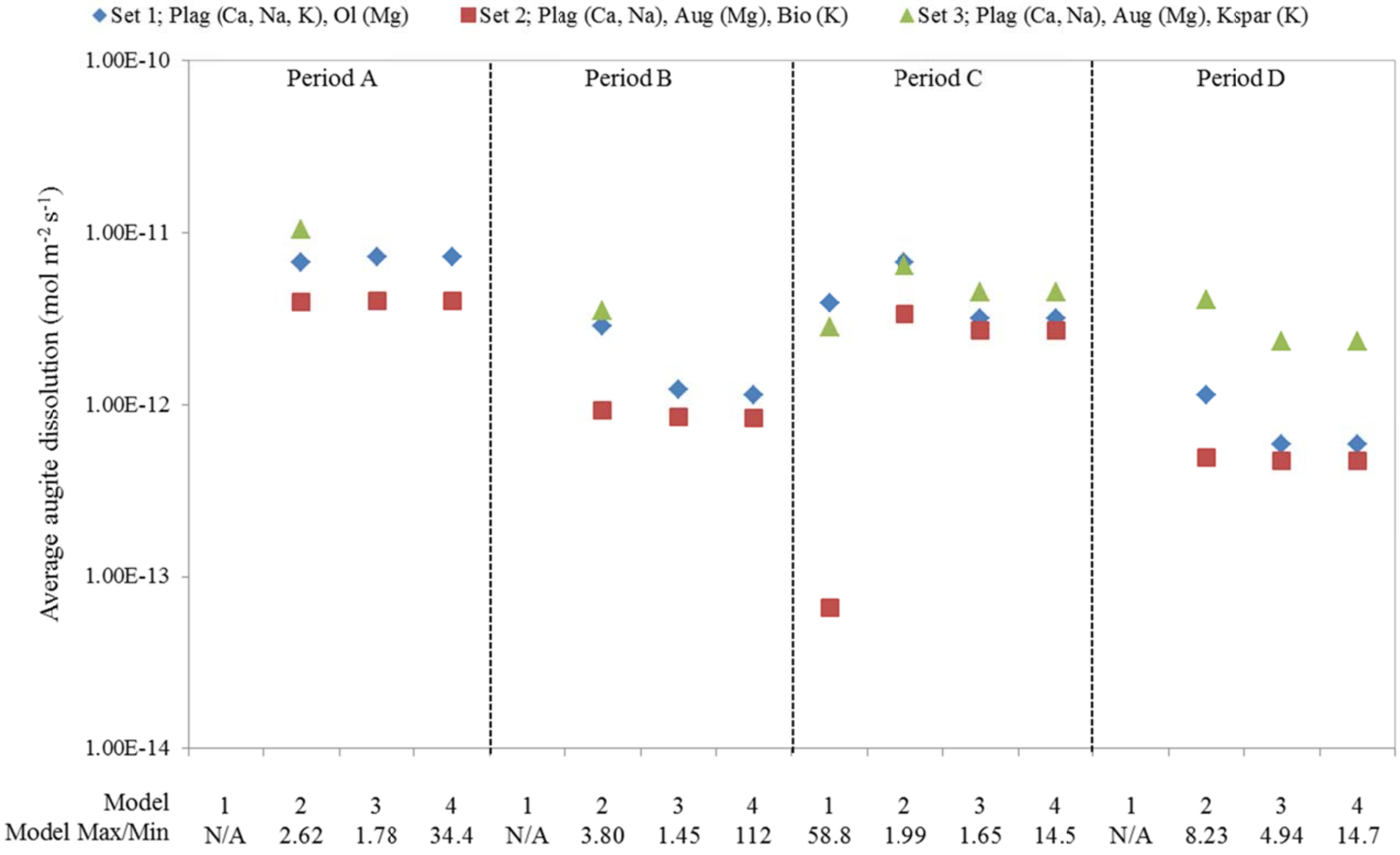

Mineralogical breakdown of cations present (%) for specific samples (see Table U for full mineralogical breakdown)

Set	%S	Reactor	Calcium				Magnesium					Sodium		Potassium			
			Plag	Augite	Prehnite	Amphibole	Augite	Hyper	Olivine	Biotite	Amphibole	Plag	K-Spar	Plag	Biotite	K-Spar	Amphibole
1	0.72	42	94.09	5.91			4.90	10.17	84.93			100.00		100.00			
	1.16	29	76.36	23.64			17.72	31.30	50.98			100.00		100.00			
2	0.67	40	68.15	31.85			25.90	44.55	15.03	14.52		99.44	0.56	15.02	68.73	16.25	
	0.82	43	66.52	33.48			29.18	52.09	11.23	7.50		100.00		33.24	66.76		
3	1.40	37	60.97	29.45	8.15	1.44	34.57	33.96	29.37		2.10	97.59	2.41	30.83		67.72	1.45
	1.64	31	61.29	35.95	2.76		36.46	41.43	13.93	8.18		97.39	2.61	15.08	23.74	61.18	

Figure 75. Comparison of hypersthene dissolution rates from samples with differing mineralogy.

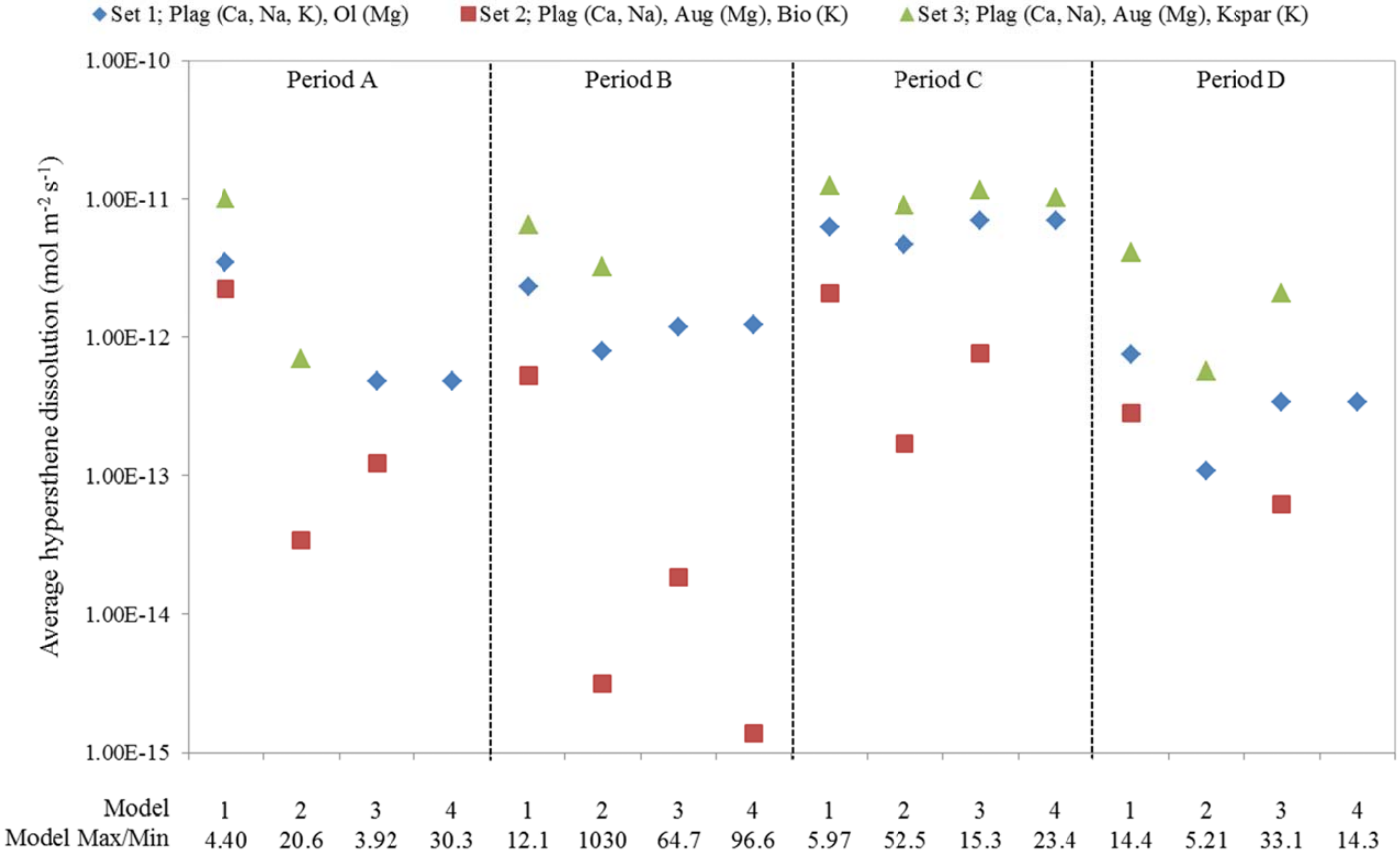

Mineralogical breakdown of cations present (%) for specific samples (see Table U for full mineralogical breakdown)

Set	%S	Reactor	Calcium				Magnesium					Sodium		Potassium			
			Plag	Augite	Prehnite	Amphibole	Augite	Hyper	Olivine	Biotite	Amphibole	Plag	K-Spar	Plag	Biotite	K-Spar	Amphibole
1	0.72	42	94.09	5.91			4.90	10.17	84.93			100.00		100.00			
	1.16	29	76.36	23.64			17.72	31.30	50.98			100.00		100.00			
2	0.67	40	68.15	31.85			25.90	44.55	15.03	14.52		99.44	0.56	15.02	68.73	16.25	
	0.82	43	66.52	33.48			29.18	52.09	11.23	7.50		100.00		33.24	66.76		
3	1.40	37	60.97	29.45	8.15	1.44	34.57	33.96	29.37		2.10	97.59	2.41	30.83		67.72	1.45
	1.64	31	61.29	35.95	2.76		36.46	41.43	13.93	8.18		97.39	2.61	15.08	23.74	61.18	

Figure 76. Comparison of olivine dissolution rates from samples with differing mineralogy.

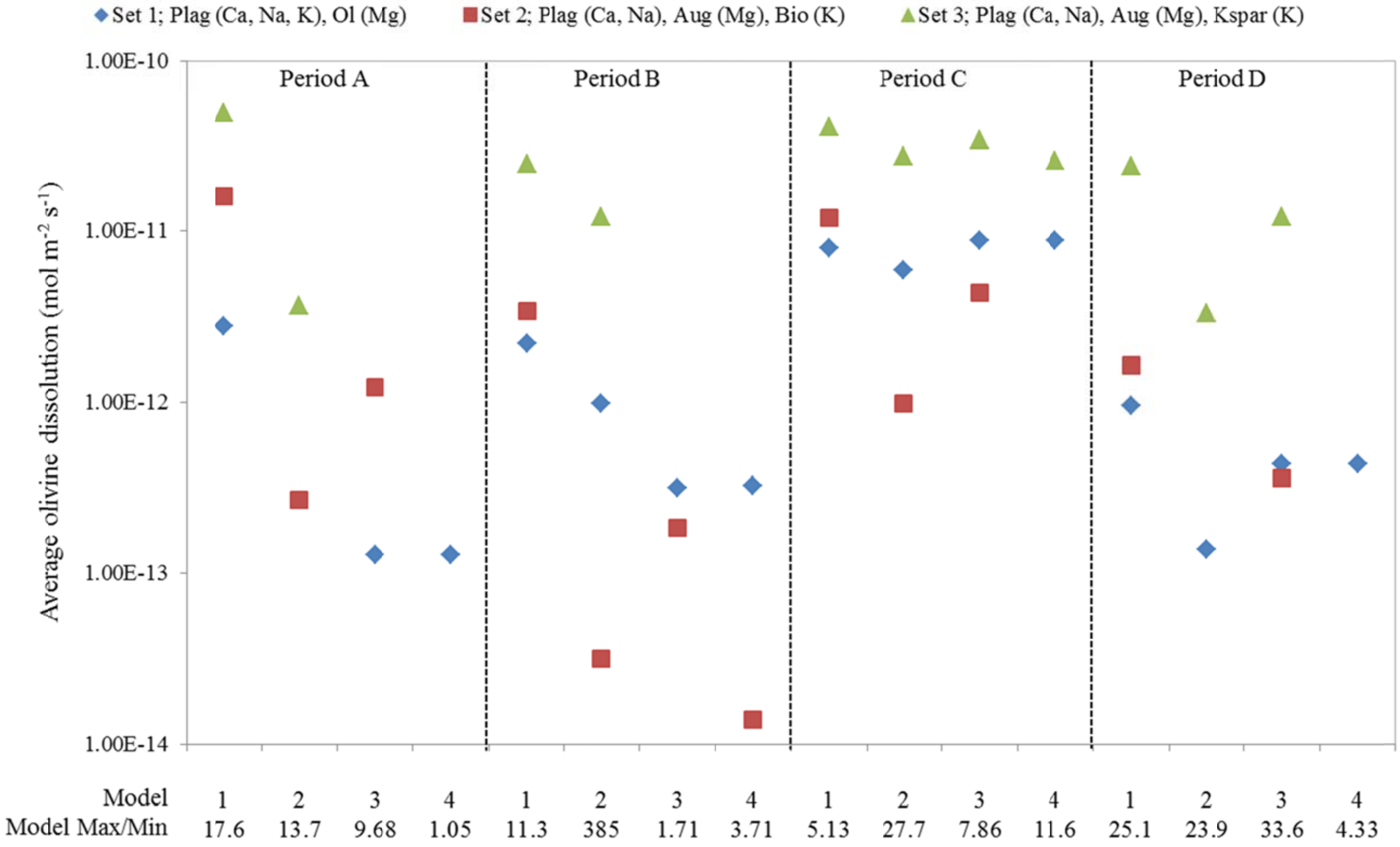

Mineralogical breakdown of cations present (%) for specific samples (see Table U for full mineralogical breakdown)

Set	%S	Reactor	Calcium				Magnesium					Sodium		Potassium			
			Plag	Augite	Prehnite	Amphibole	Augite	Hyper	Olivine	Biotite	Amphibole	Plag	K-Spar	Plag	Biotite	K-Spar	Amphibole
1	0.72	42	94.09	5.91			4.90	10.17	84.93			100.00		100.00			
	1.16	29	76.36	23.64			17.72	31.30	50.98			100.00		100.00			
2	0.67	40	68.15	31.85			25.90	44.55	15.03	14.52		99.44	0.56	15.02	68.73	16.25	
	0.82	43	66.52	33.48			29.18	52.09	11.23	7.50		100.00		33.24	66.76		
3	1.40	37	60.97	29.45	8.15	1.44	34.57	33.96	29.37		2.10	97.59	2.41	30.83		67.72	1.45
	1.64	31	61.29	35.95	2.76		36.46	41.43	13.93	8.18		97.39	2.61	15.08	23.74	61.18	

Figure 77. Comparison of biotite dissolution rates from samples with differing mineralogy.

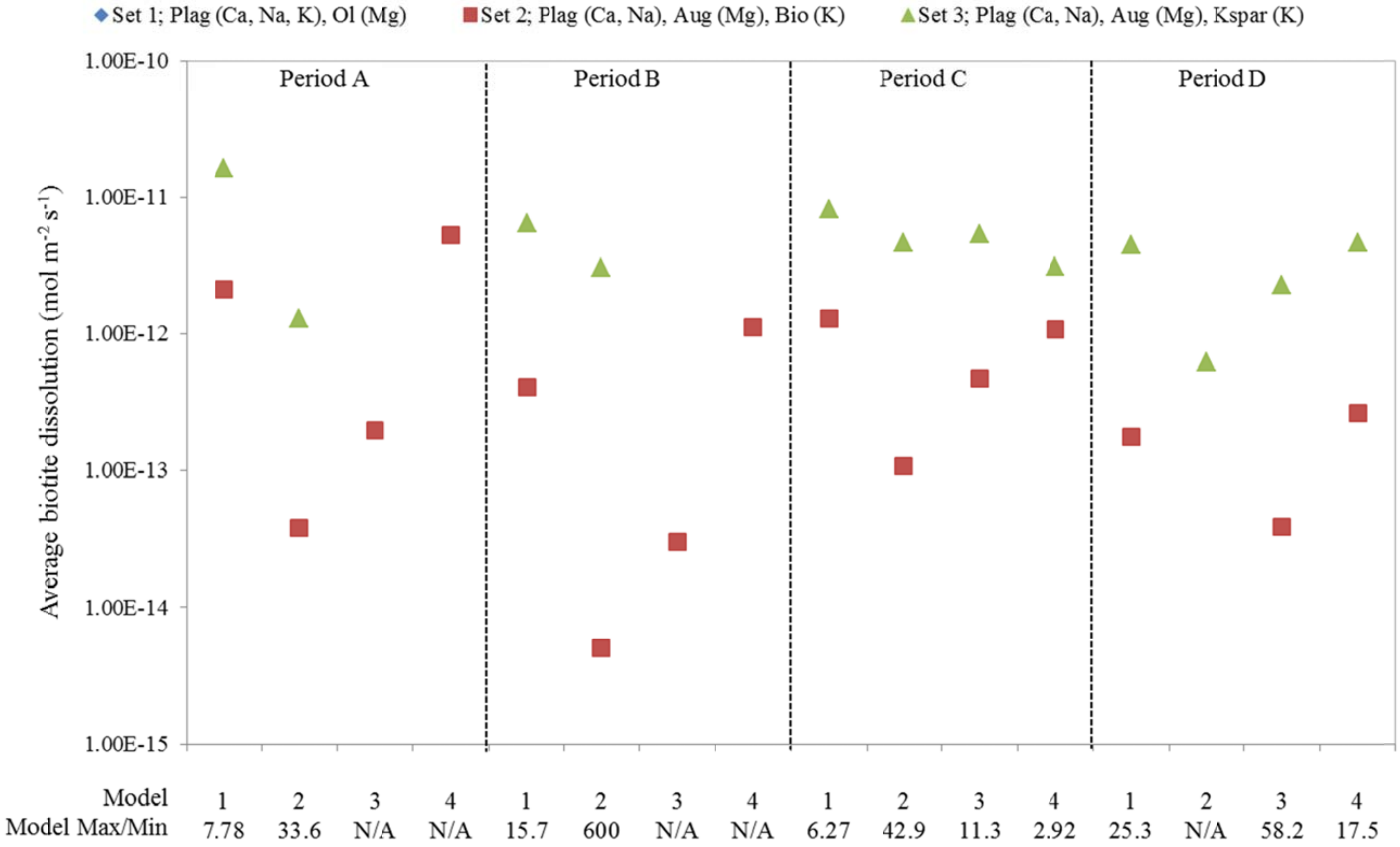

Mineralogical breakdown of cations present (%) for specific samples (see Table U for full mineralogical breakdown)

Set	%S	Reactor	Calcium				Magnesium					Sodium		Potassium			
			Plag	Augite	Prehnite	Amphibole	Augite	Hyper	Olivine	Biotite	Amphibole	Plag	K-Spar	Plag	Biotite	K-Spar	Amphibole
1	0.72	42	94.09	5.91			4.90	10.17	84.93			100.00		100.00			
	1.16	29	76.36	23.64			17.72	31.30	50.98			100.00		100.00			
2	0.67	40	68.15	31.85			25.90	44.55	15.03	14.52		99.44	0.56	15.02	68.73	16.25	
	0.82	43	66.52	33.48			29.18	52.09	11.23	7.50		100.00		33.24	66.76		
3	1.40	37	60.97	29.45	8.15	1.44	34.57	33.96	29.37		2.10	97.59	2.41	30.83		67.72	1.45
	1.64	31	61.29	35.95	2.76		36.46	41.43	13.93	8.18		97.39	2.61	15.08	23.74	61.18	

Figure 78. Below are the equations to determine coefficients for the dissolution rates of plagioclase based on percent anorthite (%An) in the acidic range (pH<4.4). The equation was generated from data in Palandri and Kharaka (2004) and is in the form: log(rate) = log K – n*pH.

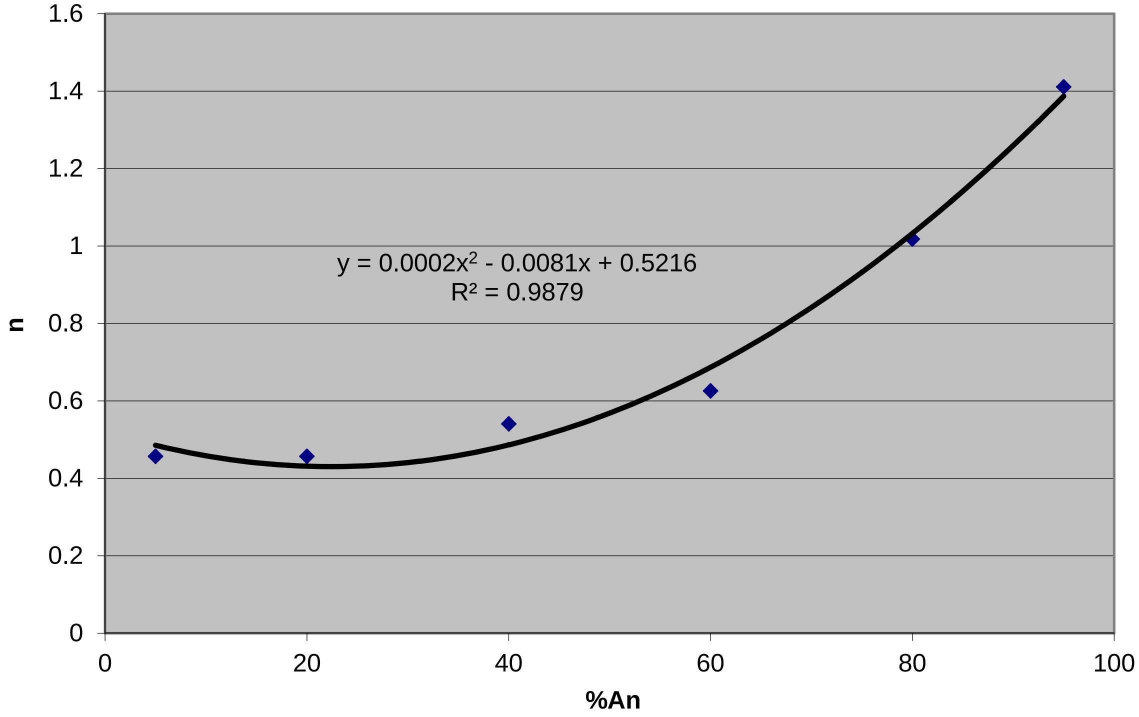

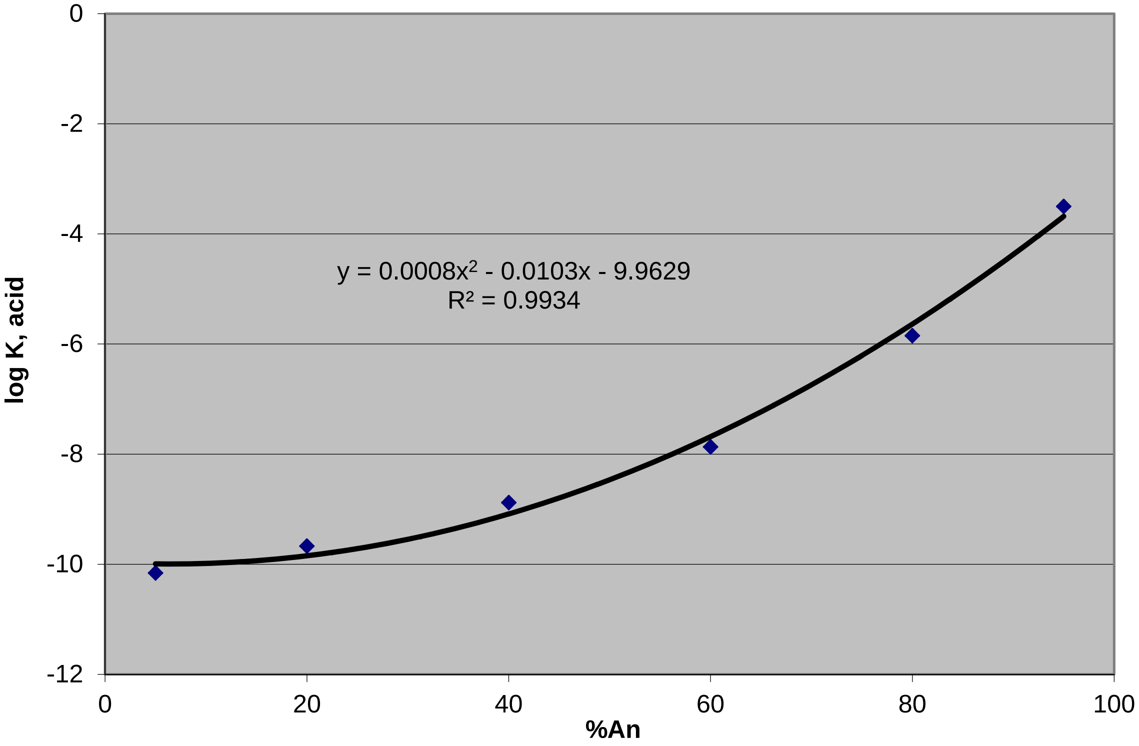

Figure 79. Below are the equations to determine coefficients for the dissolution rates of plagioclase based on percent anorthite (%An) in the neutral range (pH≥4.4). The equation was generated from data in Palandri and Kharaka (2004) and is in the form: log(rate) = log K.

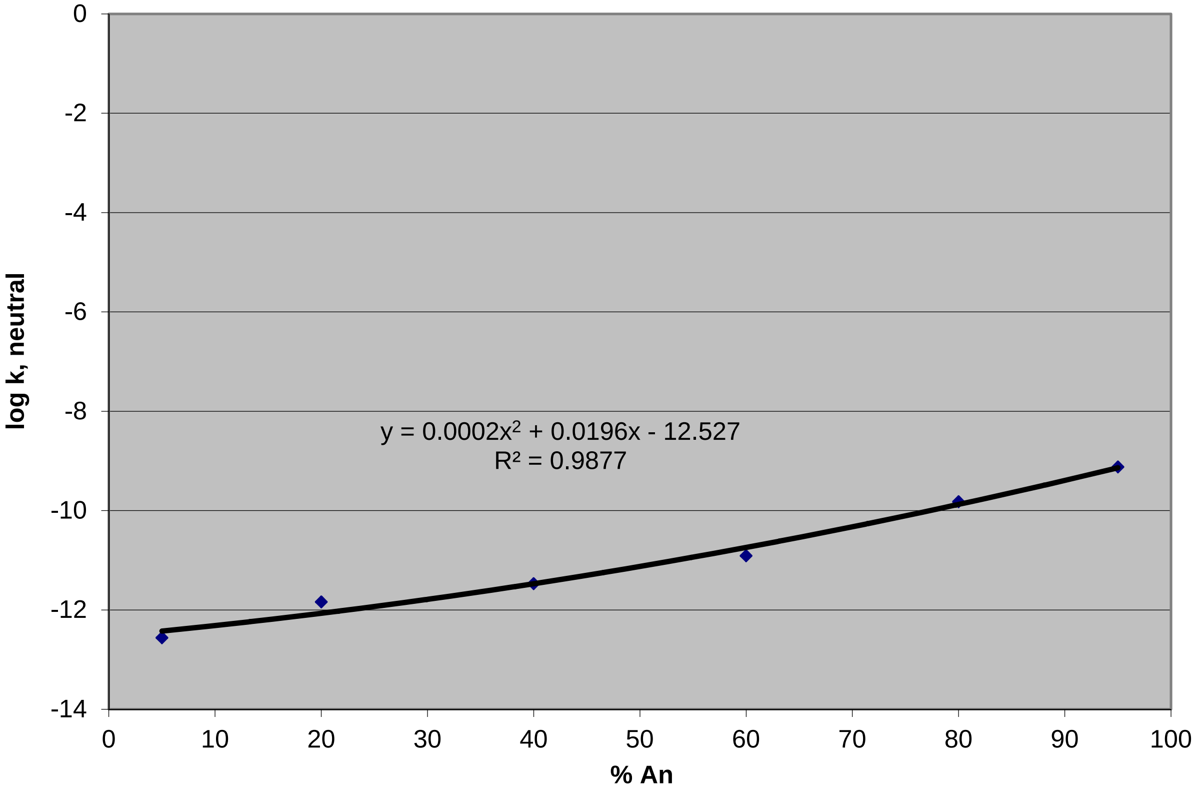

Figure 80. Modeled plagioclase dissolution rates (mol m^{-2} s^{-1}) vs drainage pH. Average plagioclase dissolution rates for each reactor are plotted for each rate period (Table 52-56) as a function of average pH for each of the four silicate dissolution models (Table 27). Palandri and Kharaka acidic+neutral rates for labradorite and andesine are plotted for comparative purposes (Table 73).

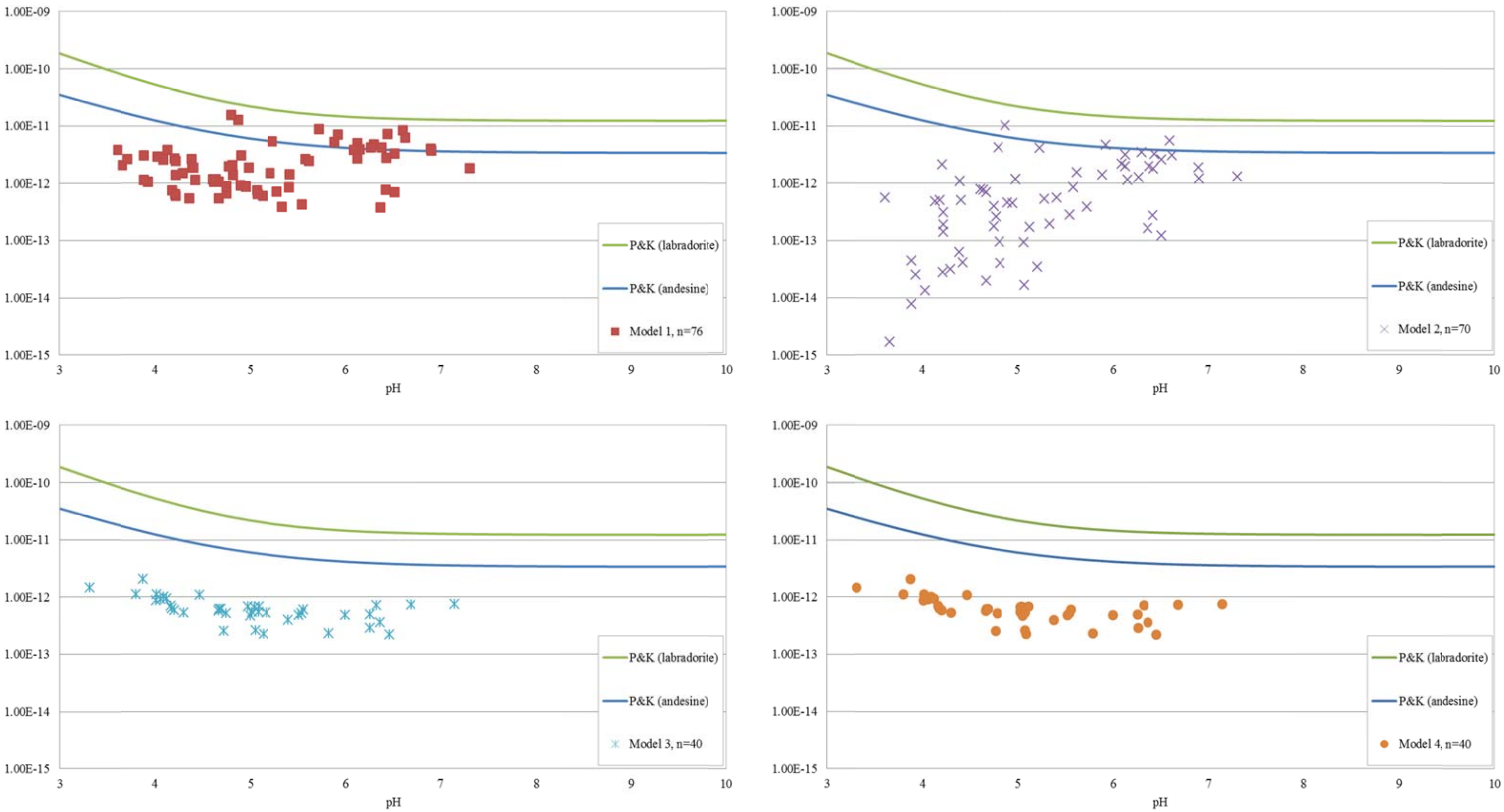

Figure 81. Modeled augite dissolution rates vs drainage pH. Average augite dissolution rates for each reactor are plotted for each rate period (Tables 52-56) as a function of average pH for each of the four silicate dissolution models (Table 27). Palandri and Kharaka acidic+neutral rates for augite are plotted for comparative purposes (Table 76).

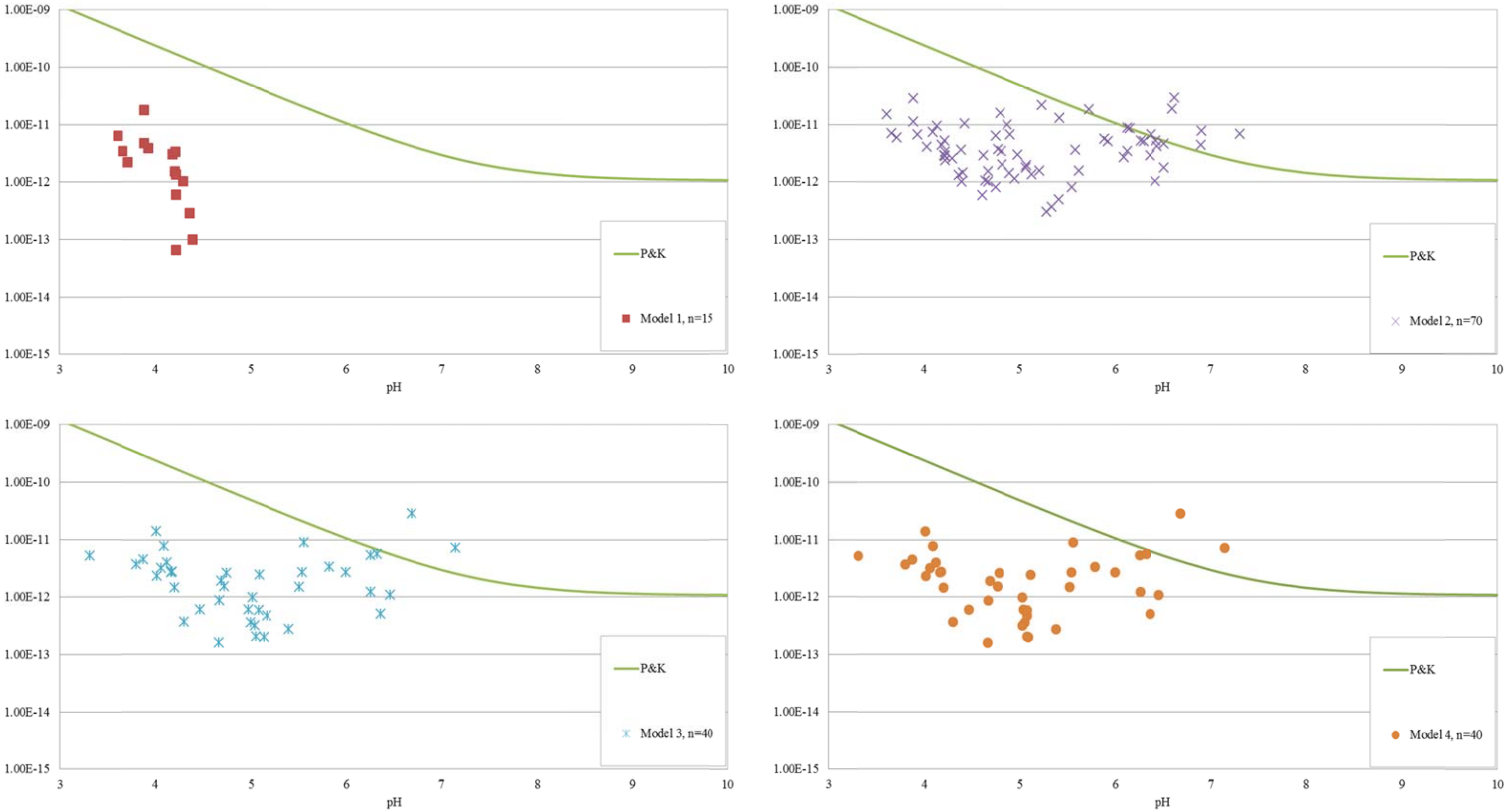

Figure 82. Modeled olivine dissolution rates vs drainage pH. Average olivine dissolution rates for each reactor are plotted for each rate period (Tables 52-56) as a function of average pH for each of the four silicate dissolution models (Table 27). Palandri and Kharaka acidic+neutral rates for forsterite and fayalite are plotted for comparative purposes (Table 74).

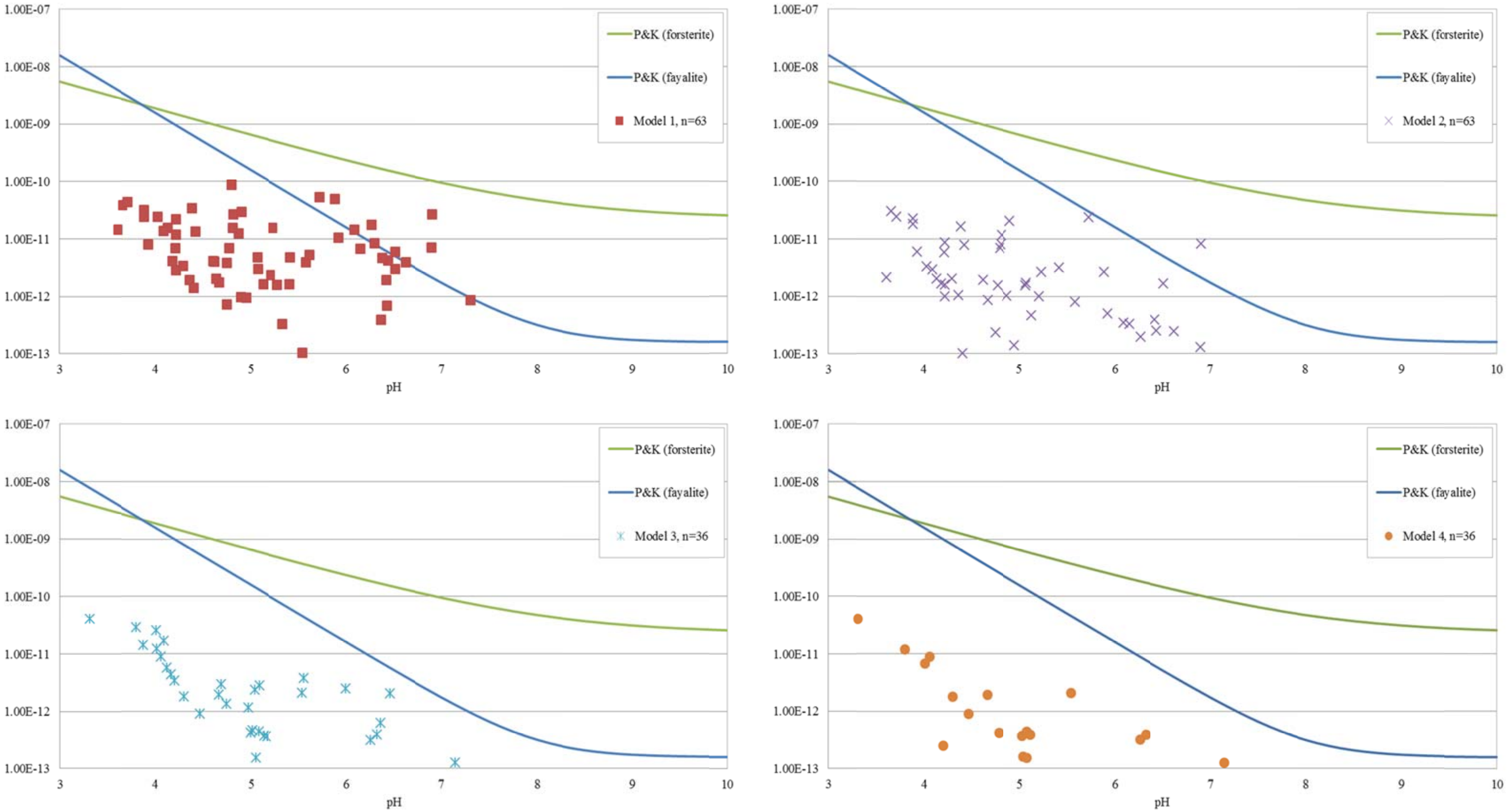

Figure 83. Modeled hypersthene dissolution rates vs drainage pH. Average hypersthene dissolution rates for each reactor are plotted for each rate period (Tables 52-56) as a function of average pH for each of the four silicate dissolution models (Table 27). Palandri and Kharaka acidic+neutral rates for bronzite are plotted for comparative purposes (Table 75).

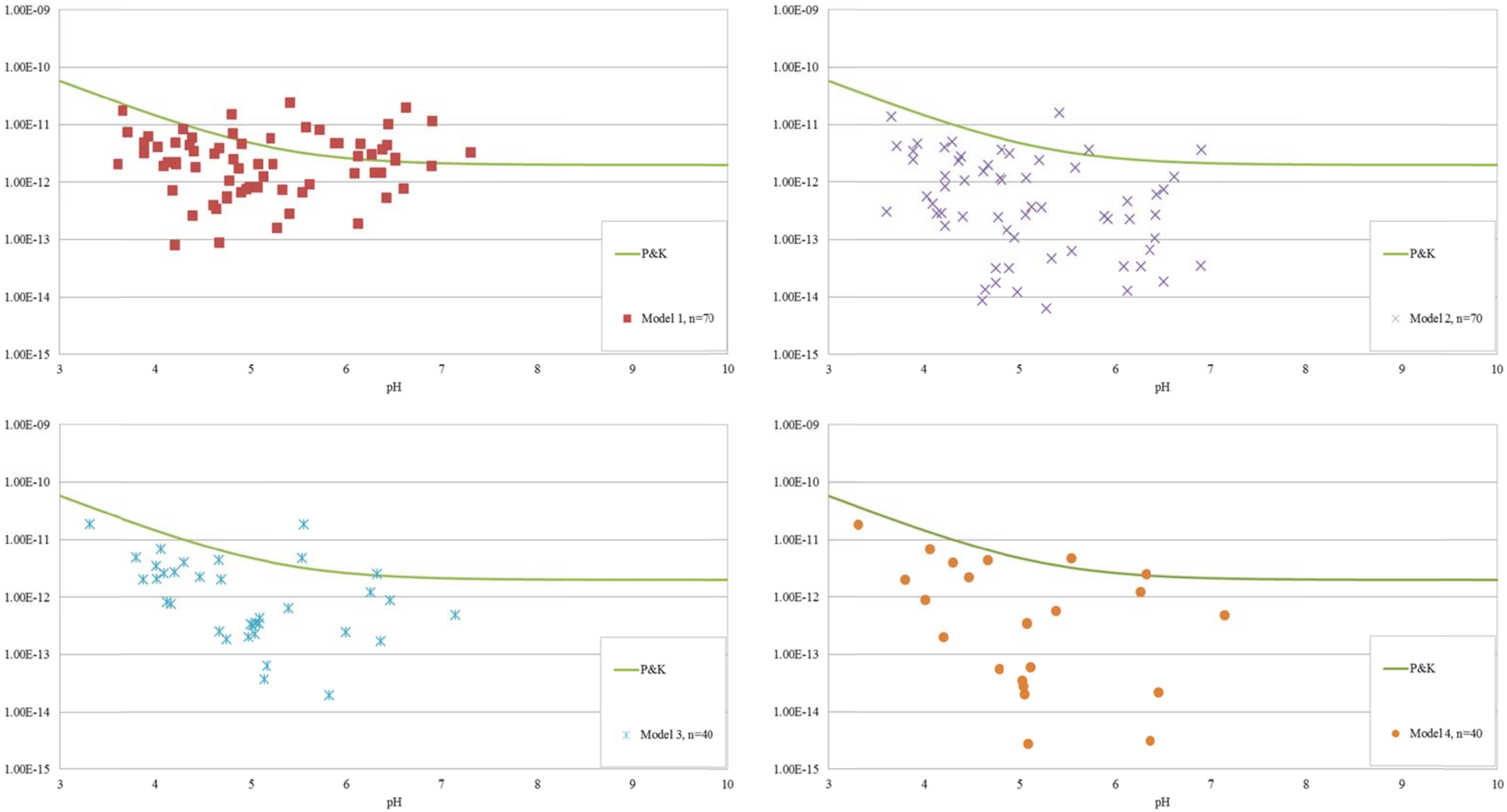

Figure 84. Modeled biotite dissolution rates vs drainage pH. Average biotite dissolution rates for each reactor are plotted for each rate period (Tables 52-56) as a function of average pH for each of the four silicate dissolution models (Table 27). Palandri and Kharaka acidic+neutral rates for biotite are plotted for comparative purposes (Table 77).